# UNIVERSIDAD COMPLUTENSE DE MADRID

FACULTAD DE MEDICINA


# TESIS DOCTORAL

La Galectina-3 promueve la activación del estrés de retículo endoplásmico a través de la disminución de let-7f-5p: relevancia en el daño renal post-infarto de miocardio en el contexto de la obesidad

Galectin-3 promotes endoplasmic reticulum stress via let-7f-5p down regulation: Relevance in renal damage post-myocardial infarction in the context of obesity

MEMORIA PARA OPTAR AL GRADO DE DOCTORA

PRESENTADA POR

Beatriz Delgado Valero

DIRIGIDA POR

María Victoria Cachofeiro Ramos

Ernesto Martínez Martínez

**UNIVERSIDAD COMPLUTENSE DE MADRID**

FACULTAD DE MEDICINA

Programa de Doctorado en Investigación Biomédica


# TESIS DOCTORAL

## La Galectina-3 promueve la activación del estrés de retículo endoplásmico a través de la disminución de let-7f-5p: Relevancia en el daño renal post-infarto de miocardio en el contexto de la obesidad.

## Galectin-3 promotes endoplasmic reticulum stress via let-7f-5p downregulation: Relevance in renal damage post-myocardial infarction in the context of obesity.

Memoria presentada por **Beatriz Delgado Valero**, para optar al grado de doctor por la Universidad Complutense de Madrid.

Directores

Dra. María Victoria Cachofeiro Ramos

Dr. Ernesto Martínez Martínez

Madrid 2024

**UNIVERSIDAD COMPLUTENSE DE MADRID**
FACULTAD DE MEDICINA


# TESIS DOCTORAL

## LA GALECTINA-3 PROMUEVE LA ACTIVACIÓN DEL ESTRÉS DE RETÍCULO ENDOPLÁSMICO A TRAVÉS DE LA DISMINUCIÓN DE LET-7F-5P: RELEVANCIA EN EL DAÑO RENAL POST-INFARTO DE MIOCARDIO EN EL CONTEXTO DE LA OBESIDAD.

## GALECTIN-3 PROMOTES ENDOPLASMIC RETICULUM STRESS VIA LET-7F-5P DOWNREGULATION: RELEVANCE IN RENAL DAMAGE POST-MYOCARDIAL INFARCTION IN THE CONTEXT OF OBESITY.

MEMORIA PARA OPTAR AL GRADO DE DOCTORA
PRESENTADA POR

**Beatriz Delgado Valero**

Directores
Dra. María Victoria Cachofeiro Ramos
Dr. Ernesto Martínez Martínez

Madrid 2024

**UNIVERSIDAD COMPLUTENSE DE MADRID**

FACULTAD DE MEDICINA

Programa de Doctorado en Investigación Biomédica


# TESIS DOCTORAL

## La Galectina-3 promueve la activación del estrés de retículo endoplásmico a través de la disminución de let-7f-5p: Relevancia en el daño renal post-infarto de miocardio en el contexto de la obesidad.

## Galectin-3 promotes endoplasmic reticulum stress via let-7f-5p downregulation: Relevance in renal damage post-myocardial infarction in the context of obesity.

Memoria presentada por **Beatriz Delgado Valero**, para optar al grado de doctor por la Universidad Complutense de Madrid.

Directores

Dra. María Victoria Cachofeiro Ramos

Dr. Ernesto Martínez Martínez

Madrid 2024

UNIVERSIDAD COMPLUTENSE MADRID

# DECLARACIÓN DE AUTORÍA Y ORIGINALIDAD DE LA TESIS PRESENTADA PARA OBTENER EL TÍTULO DE DOCTOR

D./Dña. Beatriz Delgado Valero,
estudiante en el Programa de Doctorado en Investigación Biomédica,
de la Facultad de Medicina de la Universidad Complutense de Madrid, como autor/a de la tesis presentada para la obtención del título de Doctor y titulada:

La Galectina-3 promueve la activación del estrés de retículo endoplásmico a través de la disminución de let-7f-5p: Relevancia en el daño renal post-infarto de miocardio en el contexto de la obesidad.

y dirigida por: Dra. María Victoria Cachofeiro Ramos y Dr. Ernesto Martínez Martínez.

**DECLARO QUE:**

La tesis es una obra original que no infringe los derechos de propiedad intelectual ni los derechos de propiedad industrial u otros, de acuerdo con el ordenamiento jurídico vigente, en particular, la Ley de Propiedad Intelectual (R.D. legislativo 1/1996, de 12 de abril, por el que se aprueba el texto refundido de la Ley de Propiedad Intelectual, modificado por la Ley 2/2019, de 1 de marzo, regularizando, aclarando y armonizando las disposiciones legales vigentes sobre la materia), en particular, las disposiciones referidas al derecho de cita.

Del mismo modo, asumo frente a la Universidad cualquier responsabilidad que pudiera derivarse de la autoría o falta de originalidad del contenido de la tesis presentada de conformidad con el ordenamiento jurídico vigente.

En Madrid, a 28 de junio de 2024

Firmado por Beatriz Delgado Valero el día 28/06/2024 con un certificado emitido por AC FNMT Usuarios

Fdo.: _____

Esta DECLARACIÓN DE AUTORÍA Y ORIGINALIDAD debe ser insertada en la primera página de la tesis presentada para la obtención del título de Doctor.

# *Agradecimientos*

Estas líneas están dedicadas a todas las personas que han hecho posible que hoy esté donde estoy. Aunque las palabras que aquí escriba se quedarán cortas para expresar lo mucho que os agradezco a quienes me habéis acompañado y apoyado en estos años, espero que al menos reflejen una parte de la profunda gratitud que siento. Sin vosotros no lo habría conseguido.

Si a alguien he de dedicar el primer agradecimiento es a mis directores de tesis, a vosotros **Victoria y Ernesto** por acogerme en la pequeña gran familia que habéis ido formando. No sé cómo aunar en unas pocas líneas lo mucho que me habéis aportado, gracias de corazón por vuestros consejos y por ser un apoyo en el que recaer en todos esos momentos en los que lo he necesitado. Gracias por haber estado ahí en un periodo que siempre recordaré de crecimiento profesional y personal, apenas reconozco en mí a aquella chica que apareció totalmente desorientada por el despacho de Victoria para hacer un TFG. De vosotros he aprendido no solo el valor de la perseverancia sino también a no perder mis principios no importa cuál sea el obstáculo. Ambos sois un ejemplo de esfuerzo, constancia, dedicación y liderazgo que combinado con vuestra cercanía, bondad y sentido del humor hacen de vosotros un claro ejemplo a seguir, no os imagináis lo mucho que me alegro de haber podido dar mis primeros pasos en ciencia bajo vuestra tutela.

Agradezco al **Instituto de Salud Carlos III – Fondo Europeo de Desarrollo Regional (FEDER)** por financiar esta investigación (PI18/00257; PI21/0431 y CIBERCV). También agradecer al Instituto de Salud Carlos III por el contrato predoctoral (P-FIS; FI/00277) del que he sido beneficiaria durante esta tesis y por la beca de movilidad (M-AES; MV22/00069) que hizo posible la realización de la estancia internacional en Seúl, Corea del Sur.

Muchos han sido los compañeros que han formado parte del laboratorio y a los que me gustaría agradecer por, de una forma u otra, contribuir a la realización de esta tesis, pero por si alguien he de comenzar es por ti **Sara**. Desde el primer

momento quedó demostrado que tú y yo nos llevaríamos bien, tanto que muchas veces hemos bromeado que fuimos separadas al nacer por lo mucho que nos parecemos en forma de ser y gustos, pero lo que no supe prever es que te convertirías en una de mis mejores amigas y que tenerte a mi lado (literal y metafóricamente) me ayudaría a afrontar y superar tantísimos obstáculos a nivel personal y profesional durante estos años. Gracias por andar este camino junto a mí, por siempre sacarme una sonrisa y, sobre todo, por ser como eres.

A **Ana y Yaiza** por todos esos momentos de risas, cotilleos, viajes y consejos, vuestra amistad es una de las mejores cosas que me llevo de estos años. Al dúo mitocondria, aka **María y Alejandro**, por haber aportado en la última fase de esta tesis un poco de alegría y aire fresco a becarios, nunca perdáis esa chispa ni dejéis de crecer, muchísima suerte. A todos vosotros, gracias por ayudarme a crecer y por aguantarme día a día, trabajar con vosotros ha sido un auténtico privilegio.

No se me olvidan las primeras dos personas que durante el TFG me acogieron y enseñaron tantísimo gracias, **Raquelita y Gema** entre otras cosas por hacerme salir del cascarón. Tampoco puedo dejar de mencionar a muchos otros compañeros que han pasado por el laboratorio, como **Amanda, Isa, Francisco, Álvaro, Ainara, Darío, Lucía, Rocío o Leonor**, gracias también a vosotros.

A **Chema**, por tus consejos, ayuda, apoyo y confianza, pero también por todos esos momentos en las comidas en los que me contagiaste risas y canciones. Me alegro muchísimo de haber podido trabajar con alguien como tú.

A **Virginia y Avelina** por su ayuda tanto en el laboratorio como en prácticas. A **Raquel Rodrigues** y a toda la gente del **Departamento de Fisiología** por vuestros consejos y por hacerme sentir tan a gusto estos años.

A **Natalia, Ernesto, Amaya, Mattie, Lara, Miriam y a toda la gente de Navarrabiomed** por enseñarme tanto y hacerme sentir como uno más durante mi estancia con vosotros. Pero sobre todo gracias a ti **Eva**, por ser una de las

personas más buenas y capaces que he conocido. Desde el primer día me recibiste con los brazos abiertos, me cuidaste y guiaste sin reservas independientemente de lo ocupada que estuvieses, de ti he aprendido mucho (no solo de los miRNAs) y sin dudarlo diré que lo mejor de aquella estancia fue poder conocerte personalmente y trabajar mano a mano contigo.

I would also like to thank **Cecilia, Mikael, Dayoon, Chaerin**, and all the members of the Luterion family for treating me so well and always offering your help when I needed it. It is because of you all that my experience in Seoul was far better than I could have ever wished for. 진심으로 감사드립니다.

Sin embargo, esta tesis también es consecuencia del apoyo de muchas otras personas que, sin entender del todo en qué consiste esto de la investigación, han sido siempre mi lugar seguro.

A mi familia y amigos, sin cuyo aliento constante no habría podido llegar a donde estoy hoy. En especial **a mis padres, a mi hermana, a mis tías Asun y Maribel y a mi pequeño Merlinchi** por siempre brindarme vuestro amor y apoyo incondicional y por perdonar mis cambios de humor consecuencia del estrés durante estos años. Vosotros sois mi fuente de fuerza y mi ancla.

Gracias a mis abuelos por enseñarme con inquebrantable paciencia y por acompañarme en cada paso de este viaje (del que sin duda se alegrarían de verme completar). A pesar de que vuestra ausencia se siente en cada logro, vuestro amor perdurará siempre en mi corazón.

Finalmente, gracias también a **Dani**, por su amor y apoyo a lo largo de estos años, por haber estado siempre a mi lado dándome ánimos y haciéndome feliz en cada paso de este camino.

**Muchas gracias a todos por formar parte de mi vida y por ayudarme a alcanzar este logro.**

# *Abbreviations*

| | |
|---|---|
| ·OH | Hydroxyl radical |
| 4-HNE | 4-Hydroxynonenal. |
| 4-PBA | 4-Phenylbutiric Acid. |
| A.U. | Arbitraty units. |
| ADHF | Acute decompensated heart failure |
| AKI | Acute kidney injury |
| AKT | Protein Kinase B. |
| Ang II | Angiotensin II. |
| APES | 3-Aminopropyltriethoxysilane |
| AT1R | AngiotensIn type 1 receptor |
| ATF4 | Activating Transcription Factor 4. |
| ATF6α | Activating Transcription Factor 6 Alpha. |
| ATF6β | Activating Transcription Factor 6 Beta. |
| BiP | Binding Immunoglobulin Protein. |
| BIRC2 | Baculoviral IAP Repeat Containing 2. |
| BMI | Body mass index. |
| BSA | Bovine Serum Albumin. |
| BUN | Blood urea nitrogen |
| CCL-2 | C-C Motif Chemokine Ligand 2. |
| cDNA | Complementary DNA. |
| CFU | Colony formation units. |
| CHOP | CCAAT-Enhancer-Binding Homologous Protein. |
| CKD | Chronic kidney disease |
| Col I | Collagen Type I. |
| Col IV | Collagen Type IV. |
| CRS | Cardiorenal syndrome |
| CT | Cycle threshold |
| CT | Control |

| | |
|---|---|
| CTGF | Connective Tissue Growth Factor. |
| CVD | Cardiovascular disease |
| DAMPs | Damage-associated molecular patterns |
| DHE | Dihydroethidium. |
| ECM | Extracelular matrix |
| EDD | End-Diastolic Diameter. |
| EDS | End-Systolic Diameter. |
| EDV | End-Diastolic Volume. |
| EF | Ejection fraction |
| ER | Endoplasmic Reticulum. |
| ERK | Extracellular Signal-Regulated Kinases. |
| ESRD | End-stage renal disease |
| FBS | Fetal Bovine Serum. |
| FFA | Free Fatty Acids. |
| FN | Fibronectin. |
| Gal-3 | Galectin 3. |
| GAPDH | Glyceraldehyde-3-Phosphate Dehydrogenase. |
| GFR | Glomerular filtration rate |
| $H_2O_2$ | Hydrogen peroxide |
| HF | Heart failure |
| HFD | High Fat Diet. |
| HK-2 | Human kidney proximal tubule epithelial cells. |
| HPRT | Hypoxanthine Phosphoribosyltransferase. |
| I/R | Ischemia-reperfusion |
| IL | Interleukin |
| iNTC | Inhibitor non-target control. |
| IRE1 | Inositol-Requiring 1 |
| IVT | Interventricular Septum. |

| | |
|---|---|
| IVT | Interventricular septum |
| KIM1 | Kidney Injury Molecule 1. |
| KO | Knock out |
| LAD | Left Anterior Descendent Coronary Artery. |
| LATS1 | Large Tumor Suppressor Kinase 1. |
| LV | Left Ventricle. |
| LVEDV | Left Ventricle End-Diastolic Volume. |
| LVEF | Left Ventricular Ejection Fraction. |
| LVESV | Left Ventricle End-Systolic Volume. |
| LVH | Left ventricular hypertrohy |
| MCP | Modified Citrus Pectin. |
| MI | Myocardial Infarction. |
| miR | MicroRNA |
| MMP | Matrix Metalloproteinase. |
| mNTC | Mimic Non-Target Control. |
| MOB1A/B | MOB Kinase Activator 1A/B. |
| MRI | Magnetic Resonance Imaging. |
| MST1/2 | Macrophage Stimulating 1/2. |
| MUT | Mutant. |
| NFκB | Nuclear Factor-κB. |
| NGAL | Neutrophil Gelatinase Associated Lipocalin. |
| NOX | NADPH oxidases |
| $O_2^{\bullet-}$ | Superoxide anion |
| OPN | Osteopontin. |
| PA | Palmitic Acid. |
| PAMPs | Pathogen-associated molecular patterns. |
| PBS | Phosphate Buffered Saline. |
| PBST | Phosphate Buffered Saline with tween. |

| | |
|---|---|
| PCR | Polimerase Chain Reaction. |
| PDGF | Platelet-derived growth factor |
| PDIA6 | Protein Disulfide Isomerase Family A Member 6. |
| pDNA | Plasmidic DNA. |
| PERK | PKR-like ER kinase |
| PWT | Posterior Wall Thickness. |
| RAAS | Renin-Angiotensin-Aldosterone System |
| RISC | RNA-induced silencing |
| RNS | Reactive species derived from nitrogen |
| ROS | Reactive oxygen species. |
| RT | Retrotranscription |
| SAV | Salvador Family WW Domain Containing Protein 1. |
| SBP | Systolic Blood Pressure. |
| Scr | Scramble. |
| SCr | Serum creatinine levels. |
| SD | Standard Deviation. |
| SDS | Sodium dodecyl sulphate. |
| SEM | Standard Error of The Mean. |
| SLUG | Snail Family Transcriptional Repressor 2. |
| SNAIL | Snail Family Transcriptional Repressor 1. |
| SNS | Sympathetic nervous system |
| SNX | Subtotal nephrectomy |
| SOD | Superoxide dismutase |
| sXBP1 | Spliced X-Box Binding Protein 1. |
| TAZ | Transcriptional Coactivator With PDZ-Binding Motif. |
| TBARS | Thiobarbituric Acid Reactive Substances. |
| TEAD1 | TEA Domain Transcription Factor 1. |
| TFBs | Murine Renal Interstitial Fibroblast Cell Line. |

| | |
|---|---|
| TGF-β | Transforming Growth Factor Beta. |
| TIMPs | Tissue inhibitors of metalloproteinase |
| TN | Tunicamycin. |
| TNF $\alpha$ | Tumour Necrosis Factor Alpha. |
| TTE | Transthoracic Echocardiography. |
| tXBP1 | Total X-Box Binding Protein 1. |
| UNX | Unilateral nephrectomy |
| UPR | Unfolded protein response |
| usXBP1 | Un-spliced X-Box Binding Protein 1. |
| UTR | Untranslated region |
| UUO | Unilateral uretral obstruction |
| WT | Wild Type. |
| YAP1 | Yes1 Associated Transcriptional Regulator. |
| $\alpha$-SMA | Alpha 2 Smooth Muscle Actin. |

# *Index*

# *Resumen*

El síndrome cardiorrenal (SCR) representa una compleja interacción patológica entre el corazón y los riñones, donde una lesión aguda o crónica en uno de ellos induce el daño agudo o crónico en el otro. De los cinco subtipos, el tipo 1 de SCR (SCR-1), que se caracteriza por una lesión aguda renal como consecuencia del empeoramiento de la función cardiaca [1], tiene la mayor incidencia entre los pacientes diagnosticados con SCR [2, 3]. Además, el desarrollo de SCR-1 en pacientes se asocia con un aumento de los tiempos de hospitalización y con peor pronóstico clínico [4, 5].

Aunque se cree que los factores de riesgo tradicionales, como son la hipertensión, la obesidad o la diabetes, están implicados en la patología compartida del corazón y los riñones, en el SCR-1 abordar únicamente estos factores ha mostrado resultados insatisfactorios [6], lo cual sugiere la necesidad de evaluar factores de riesgo no convencionales, así como otros mecanismos subyacentes que podrían ser relevantes en la fisiopatología del daño renal inducido por el SCR.

Esta tesis tiene como objetivo explorar los mecanismos subyacentes y las posibles estrategias terapéuticas para manejar el daño renal en el contexto del SCR, con un interés especial en la fibrosis debido a su importante implicación en la progresión del daño cardiorrenal y en el fallo orgánico [7]. Entre los mecanismos que podrían contribuir al daño renal en el SCR, nos hemos enfocado en si el estrés de retículo endoplásmico (ERE), la Galectina-3 (Gal-3) y las modificaciones post-transcripcionales mediadas por microRNAs podrían participar en el remodelado renal y en sus alteraciones funcionales.

Para ello, se utilizó un modelo de 4 semanas de infarto de miocardio (IM) mediante la ligadura de la arteria coronaria descendente anterior izquierda en ratas macho Wistar que se comparó con un grupo de animales control que fueron sometidos a una operación simulada. De forma similar a lo observado en los pacientes con IM, además de hipertrofia y disfunción cardiaca, las ratas con IM mostraron un aumento en el marcador de daño renal agudo NGAL a nivel

circulante y renal. Tras 4 semanas del IM los animales presentaron fibrosis renal, estrés oxidativo e inflamación, así como también mostraban un incremento en los niveles de Gal-3 y una activación del ERE sin cambios en los niveles de creatinina sérica.

Un estudio *in-vitro* realizado en fibroblastos renales murinos reveló el papel mediador del ERE en los efectos perjudiciales del ácido palmítico (AP) y la Angiotensina II (Ang II), ya que la presencia del inhibidor farmacológico del ERE, ácido 4-fenilbutírico (4-PBA; 4 μM) fue capaz de prevenir la up-regulación en la matriz extracelular, la producción de anión superóxido y los marcadores inflamatorios inducidos tanto por AP (50-200 μM) como por Ang II ($10^{-8}$ a $10^{-6}$ M). Todo ello respalda el posible papel del ERE en las alteraciones renales asociadas al IM.

Dado que tanto el IM como la obesidad pueden inducir alteraciones estructurales y funcionales a nivel cardiaco y a nivel renal, desarrollamos un modelo animal de obesidad e IM para el cual ratas Wistar macho fueron alimentadas con una dieta alta en grasas (HFD) durante 10 semanas. El IM se indujo como está previamente descrito [8] a las seis semanas de evolución una vez se observaron diferencias en el peso corporal. Además, para poder evaluar el posible papel de la Gal-3 y el ERE en el daño renal asociado con el IM en el contexto de la obesidad, desde el día de la cirugía en adelante se administraron diferentes tratamientos: un inhibidor de la actividad de la Gal-3 (MCP; 100 mg/Kg/día); un inhibidor del estrés del ER (4-PBA; 500 mg/Kg/día) o vehículo. Para este modelo también se definió un grupo de ratas con operación simulada y dieta estándar como control.

Primero, evaluamos la posible implicación de la Gal-3 en las consecuencias renales del IM en el contexto de la obesidad y observamos que a nivel renal los animales HFD-IM, a pesar de la ausencia de alteraciones en los niveles de creatinina sérica, presentaron un incremento en la expresión renal de NGAL que la inhibición farmacológica de la Gal-3 fue capaz de prevenir. Este efecto

protector del MCP se acompañaba además de una reducción en la fibrosis renal, el estrés oxidativo y la inflamación, lo cual demuestra la implicación de la Gal-3 en las alteraciones renales en este contexto patológico.

Además, el MCP previno no solo la disminución renal en la expresión del microRNA let-7f-5p en los animales HFD-IM, sino también la modulación de varías de las vías de señalización en las que este microRNA podría estar implicado según las predicciones *in-silico*, como la activación del ERE y la vía de señalización Hippo. Estudios *in-vitro* posteriores nos permitieron confirmar que Gal-3 induce la regulación negativa temprana del let-7f-5p, que se acompañaba de la activación del ERE y la modulación de la vía Hippo en células epiteliales tubulares.

También hemos demostrado que, aunque la activación del ERE no tiene efectos moduladores en la expresión del let-7f-5p, la sobreexpresión de este microRNA en las células renales mejoró los efectos perjudiciales de la activación del ERE a través de la interacción directa con uno de sus genes diana, ATF6β. Adicionalmente observamos que los niveles de ATF6β en los animales HFD-IM se correlacionaban con los niveles de Gal-3, NGAL, matriz extracelular, ERE y de marcadores de la vía Hippo, lo cual muestra la posible implicación del ERE en las alteraciones renales del contexto patológico de IM y obesidad conjunta. De hecho, a pesar de no observarse modulaciones en los niveles del let-7f-5p, el tratamiento con el inhibidor farmacológico del ERE fue capaz de prevenir no solo el aumento en NGAL, sino también la fibrosis renal, el estrés oxidativo, la inflamación y la modulación de la vía Hippo que se observó en los animales HFD-IM, demostrando que el ERE es un mediador downstream del efecto perjudicial de la regulación negativa del let-7f-5p en este contexto patológico.

Considerando todos estos resultados las conclusiones de este estudio son las siguientes:

1. Las alteraciones renales observadas en animales con infarto de miocardio se acompañaron por una regulación al alza de Gal-3 y por la activación del estrés del retículo endoplásmico.

2. Gal-3 participa en el daño renal asociado al infarto de miocardio en el contexto de la obesidad promoviendo la fibrosis renal, el estrés oxidativo y un ambiente proinflamatorio.

3. El infarto de miocardio en el contexto de la obesidad activa el estrés del retículo endoplásmico, lo que promueve la fibrosis renal, el estrés oxidativo y un ambiente proinflamatorio.

4. El infarto de miocardio y la obesidad están asociados con cambios en el patrón de microRNAs.

5. La regulación negativa de microRNA let-7f-5p surge como un mediador potencial de los efectos perjudiciales renales de Gal-3 a través de la activación del estrés del retículo endoplásmico y la vía de señalización Hippo.

En conjunto, Gal-3, el estrés del retículo endoplásmico y let-7f-5p emergen como tres dianas farmacológicas diferentes para el manejo de las complicaciones renales asociadas con el síndrome cardiorrenal en el contexto del infarto de miocardio y la obesidad.

# *Summary*

Cardiorenal syndrome (CRS) represents a complex pathological interaction between the heart and the kidneys, where acute or chronic injury in one of them induces acute or chronic damage in the other. Out of the five subtypes, CRS type 1 (CRS-1), which is characterized by the worsening of cardiac function leading to acute kidney injury [1], is known to have the highest incidence among the CRS diagnosed patients [2, 3]. Moreover, development of CRS-1 is known to increase hospitalization times and complicate clinical outcome in patients [4, 5].

Although traditional cardiovascular risk factors such as hypertension, obesity or diabetes are believed to be implicated in the shared pathology of the heart and the kidneys, targeting only these factors in CRS-1 has shown unsatisfactory results [6], suggesting the need to assess non-conventional risk factors and other underlying mechanisms that could be relevant in the pathophysiology of CRS-induced renal damage.

This thesis aims to explore the underlying mechanisms and potential therapeutic strategies for managing renal damage in the context of CRS, with a special interest in fibrosis due to its key implication in cardiorenal damage progression and organ failure [7]. Among the suggested mechanisms that could contribute to CRS-induced renal damage, we focused on whether endoplasmic reticulum (ER) stress, Galectin-3 (Gal-3) and microRNA-mediated post-transcriptional modulations could participate in the renal remodelling and functional alterations.

For this purpose, a 4-week model of myocardial infarction (MI) by ligation of the left anterior descendent coronary artery in male Wistar rats was used and compared to a group of control animals that underwent Sham operation. Similar to what was observed in patients with MI, apart from cardiac hypertrophy and dysfunction, MI rats showed an increase in the kidney injury marker NGAL at circulating and renal level. 4-weeks post-MI animals presented renal fibrosis,

oxidative stress and inflammation accompanied by enhanced levels of Gal-3 and ER stress activation with no modulation in the serum creatinine levels.

An *in-vitro* study performed in renal fibroblasts revealed that ER stress mediates the deleterious effects of palmitic acid (PA) and angiotensin II (Ang II), as the presence of the ER stress inhibitor 4-phenylbutyric acid (4-PBA; 4 μM) was able to prevent the up-regulation in extracellular matrix, superoxide anion production and inflammatory markers induced by both PA (50-200 μM) and Ang II ($10^{-8}$ to $10^{-6}$ M). This supports the potential role of ER stress on renal alterations associated with MI.

Given that both MI and obesity can induce structural and functional alterations at both cardiac and renal level, we developed an animal model of concomitant obesity and MI, for which male Wistar rats were fed a high-fat diet (HFD) for 10 weeks and, MI was induced as previously described [8] at six weeks once a difference in body weight was observed. Furthermore, in order to evaluate the role of Gal-3 and ER stress in the renal damage linked to MI in the context of obesity, different treatments were administered from the day of the surgery onward: A Gal-3 inhibitor (MCP; 100 mg/Kg/day); an ER stress inhibitor (4-PBA; 500 mg/Kg/day) or vehicle. A group of rats with sham operation and normal diet were defined as control.

First, we assessed the potential involvement of Gal-3 in the renal consequences of MI in the context of obesity and observed that at renal level HFD-MI animals, despite the absence of alterations in creatinine serum levels, presented a renal increase in NGAL expression that the pharmacological inhibition of Gal-3 by MCP was able to prevent. This protective effect of MCP was accompanied by a reduction in renal fibrosis, oxidative stress and inflammation which demonstrates the implication of Gal-3 in the renal alterations of this pathological context.

In addition, MCP was able to prevent not only the renal decrease in the expression of microRNA let-7f-5p in HFD-MI but also the modulation of several in-silico predicted pathways for let-7f-5p actions such as ER stress activation and the Hippo signalling pathway. Moreover, subsequent in-vitro studies allowed us to confirm that Gal-3 induces the early downregulation of let-7f-5p, which was accompanied by the activation of ER stress and the modulation of the Hippo pathway in tubular epithelial cells.

We also demonstrated that although ER stress activation has no modulatory effects on let-7f-5p expression, overexpression of this microRNA in renal epithelial cells improved the deleterious effects of ER stress activation through direct interaction with its target gene ATF6β. Furthermore, ATF6β levels in the obese infarcted animals directly correlated to Gal-3, NGAL, extracellular matrix, ER stress and Hippo pathway markers which show the possible implication of ER stress in the renal alterations of the pathological context of concomitant obesity and MI. In fact, despite no modulation in the let-7f-5p levels were observed, treatment with a pharmacological inhibitor of ER stress prevented not only NGAL increase but also the renal fibrosis, oxidative stress, inflammation and Hippo pathway modulation seen in HFD-MI animals, demonstrating ER stress is a downstream mediator of deleterious effect of the downregulation of let-7f-5p in this pathological context.

Considering all these results, the conclusions of this study are as follows:

1. The renal alterations observed in animals with myocardial infarction were accompanied by an upregulation of Gal-3 and the activation of endoplasmic reticulum stress.
2. Gal-3 participates in the renal damage associated with myocardial infarction in the context of obesity by promoting renal fibrosis, oxidative stress and a proinflammatory environment.

3. Myocardial infarction in the context of obesity activates endoplasmic reticulum stress, which promotes renal fibrosis, oxidative stress and a proinflammatory environment.

4. Myocardial infarction and obesity are associated with changes in the microRNA pattern.

5. Downregulation of microRNA let-7f-5p appears as a potential mediator of the renal deleterious effects of Gal-3 through the activation of endoplasmic reticulum stress and the Hippo signalling pathway.

Altogether, Gal-3, endoplasmic reticulum stress and let-7f-5p emerges as three different pharmacological targets for the management of the renal complications associated with cardiorenal syndrome in the context of myocardial infarction and obesity.

# *Graphical abstract*

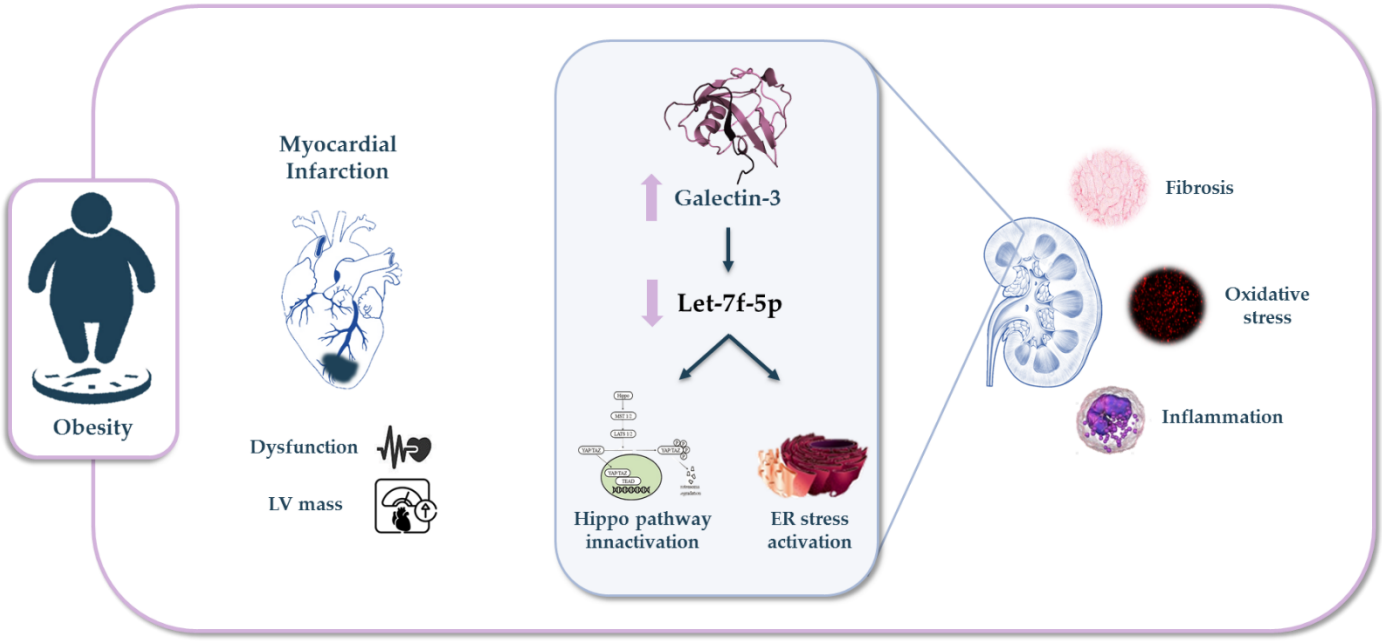


*Obesity predisposes the appearance of cardiovascular diseases such as myocardial infarction, which promotes cardiac and renal alterations. Our findings portray not only the renal consequences associated with obesity and myocardial infarction-induced cardiorenal syndrome type 1 but also reveal the implication and targeting relevance of the Galectin-3/Let-7f-5p/Endoplasmic reticulum (ER) stress axis as a means to alleviating the renal damage in such pathological context.*

# *Introduction*

Clinically, it is well known that the shared pathology of the heart and kidneys has a strong impact on the clinical outcome, as it is associated with increased morbidity and mortality rates [9, 10]. The existence of a relationship between the heart and the kidney was first described in the 19th century by Robert Bright, who reported structural changes in the heart in patients with advanced kidney disease [11]. Since then, new discoveries have given insight into the interaction between heart and kidney diseases in terms of shared risk factors (such as hypertension, obesity, diabetes and atherosclerosis) and pathophysiological pathways involved in each [12, 13].

The classic definition of Cardiorenal syndromes (CRS) was proposed in 2010 by The Acute Dialysis Quality Initiative as a term that gathers the "disorders of the heart and kidneys whereby acute or chronic dysfunction in one organ may induce acute or chronic dysfunction of the other" [1]. Also, there is further classification into different subtypes within the term according to the primary organ dysfunction and to whether it is an acute or chronic situation [1]. However, the appearance of risk factors that can affect both the heart and the kidney complicate the clinical outcome, and with it the causal relationship of one to the other.

Although CRS prevalence depends directly on demographic factors such as age distribution, access to healthcare and main comorbidities, it is generally considered that out of the five different types, Type 1 has the highest incidence among the CRS diagnosed patients [2, 3].

## I. CRS classification

### 1. CRS type 1 or acute cardio-renal syndrome

CRS type 1 (CRS-1) is characterized by the worsening of cardiac function leading to acute kidney injury (AKI) and/or dysfunction of both organs [1]. Around 25-30% of patients with acute decompensated heart failure (ADHF) present AKI,

often after ischemic or non-ischemic heart disease [14, 15]. Patients that develop CRS-1 have higher morbi-mortality and lengthier hospitalization [4, 16]. CRS-1 has a complex pathophysiology, with hemodynamic and non-hemodynamic alterations for which the treatments show no improvements [17, 18], thus demonstrating the need to discover and understand the mechanisms involved.

Faced with a drop in blood pressure levels due to the development of heart failure (HF), the kidney responds to the decrease in cardiac output by retaining sodium and water. Nevertheless, it has been demonstrated that an elevation of the central venous pressure can result in impairment of renal function and congestion of the kidneys [19]. In this context, neurohormonal activation through the Renin-Angiotensin-Aldosterone System (RAAS) also has an important role, as it is both an initially compensatory mechanism for the decrease in volume consequence of the ventricular injury, and a long-term initiator of cardiovascular and renal dysfunction [19, 20]. Other non-hemodynamic mechanisms such as inflammation and oxidative stress have been established as common pathways for cellular dysfunction in heart and kidney failure (Figure 1) [2, 19, 21].

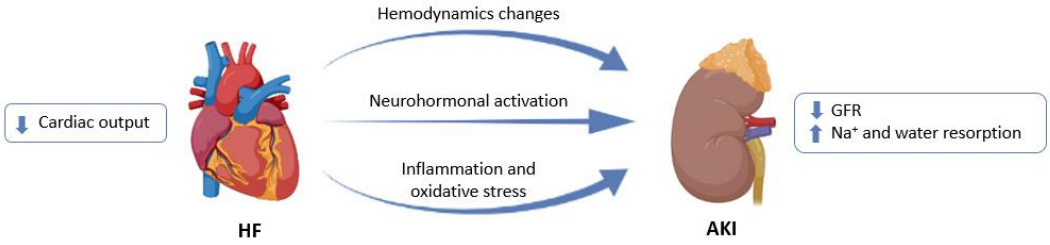


**Figure 1.** Schematic representation of Cardiorenal syndrome type 1. GFR: glomerular filtration rate. Figure adapted from Delgado-Valero B. et al., *cells* 2021 [22].

## 2. CRS type 2 or chronic cardio-renal syndrome

CRS type 2 is defined as chronic cardiac dysfunction that leads to progressive appearance of renal impairment which promotes the development of chronic

kidney disease (CKD) [23, 24]. CKD was defined in 2012 by The Kidney Disease: Improving Global Outcomes (KDIGO) as an abnormality in kidney function or structure that is present for more than 3 months and has implications in health. It is classified based on cause, GFR of <60 ml/min per 1.73 $m^2$ and the degree of albuminuria [25]. Albuminuria evaluation in addition to GFR has proven to positively influence nephrological care [26, 27]. A meta-analysis by Damman et al. showed that almost a third (32%) of the total of 1 million HF patients studied presented CKD, and 23% had worsening renal function [28], confirming that renal dysfunction is an important contributor to the comorbidities in HF.

The pathological process implicated in CKD secondary to HF is consequence of the renal response to preserve the glomerular filtration rate (GFR) (Figure 2). The combination of renal congestion, hypoperfusion and the increased right atrium pressure promotes renal dysfunction in HF patients [18, 23]. It has been suggested that the correct diagnosis of this CRS should be based on HF aetiology, HF with preserved ejection fraction (HFpEF) or with reduced ejection fraction (HFrEF), and on biochemical parameters of renal dysfunction such as high creatinine levels [29, 30]. However, as the interactions between the heart and kidney are bidirectional, is not always easy to assess the inciting event from the secondary damage, thus making it difficult to differentiate CRS type 2 patients from CRS type 4 ones [18, 29].

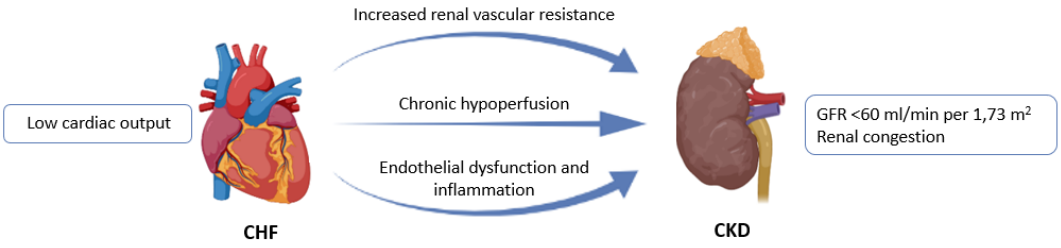


**Figure 2.** Schematic representation of Cardiorenal syndrome type 2. GFR: glomerular filtration rate. Figure adapted from Delgado-Valero B. et al., *cells* 2021 [22].

### 3. CRS type 3 or acute reno-cardiac syndrome

CRS type 3 occurs when there is an acute worsening of kidney function secondary to AKI, ischemia or glomerulonephritis that leads to acute heart injury and/or dysfunction (Figure 3) [18, 23]. AKI may produce cardiac events as a consequence of the fluid overload, hyperkalaemia or metabolic acidosis, but the exact cause of the damage is difficult to establish, as there are shared comorbidities and variability in the risk factors for AKI [18, 23, 31].

There are multiple definitions of AKI according to urine output and serum creatinine levels (SCr), all of which have limitations in their clinical application [32, 33]. It is due to the differing definitions of AKI that make it difficult to identify this type of CRS. Despite the lacking criteria, the incidence of AKI is increasing in hospitalized patients, and is associated with an 86% increased risk of cardiovascular mortality and a 38% increased risk of major cardiovascular events [3].

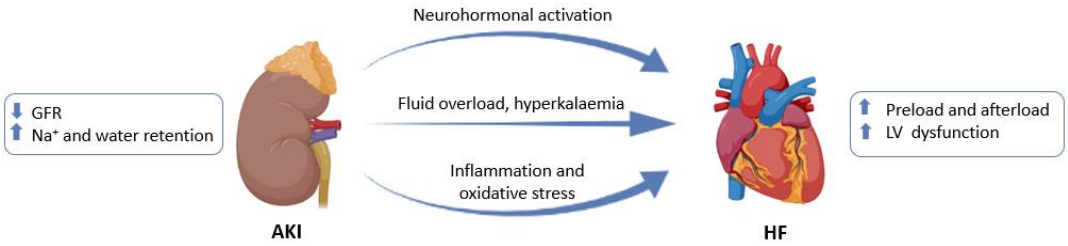


**Figure 3.** Schematic representation of Cardiorenal syndrome type 3. GFR: glomerular filtration rate; LV: left ventricle. Figure adapted from Delgado-Valero B. et al., *cells* 2021 [22].

### 4. CRS type 4 or chronic reno-cardiac syndrome

CRS type 4 is characterized by cardiovascular damage in patients with CKD at any stage [18]. It is well established that renal dysfunction is an independent risk factor for cardiovascular disease (CVD), with the risk for myocardial infarction (MI) and sudden death being higher in CKD patients [34, 35]. Numerous studies have found there is an independent association between the severity of CKD,

evaluated by the degree of decline in kidney function, and the subsequent cardiac events [12, 35], which could suggest that CKD likely accelerates the risk and development of CVD. Statistics show that 37% of patients with healthy kidney function suffer from CVD, whereas in CKD patients, the percentage is increased to 63-75% depending on the reduction in kidney function [36].

CKD has been demonstrated to be associated with inflammation and other cardiovascular factors such as hypertension, activation of RAAS and volume overload, that usually go in parallel with a decline in GFR (Figure 4) [12, 37]. Pressure and volume overload in CKD patients leads to left ventricular hypertrophy (LVH), which is a common feature that is accompanied by fibrosis and other histological changes. These structural changes consequently cause diastolic dysfunction and increased oxygen demand and could also explain these patients' predispositions to arrhythmias and sudden death [35, 38].

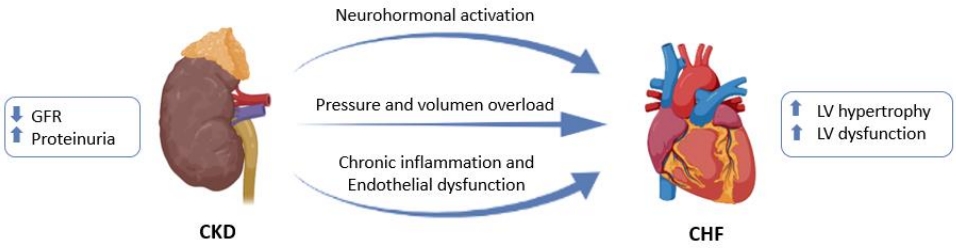


**Figure 4.** Schematic representation of Cardiorenal syndrome type 4. GFR: glomerular filtration rate; LV: left ventricle. Figure adapted from Delgado-Valero B. et al., *cells* 2021 [22].

### 5. CRS type 5 or secondary cardiorenal syndrome

CRS type 5 (CRS-5) represents simultaneous injury and/or dysfunction of the heart and kidneys as a result of a systemic condition such as sepsis, drug toxicity, lupus, cirrhosis or amyloidosis (Figure 5) [33, 39]. Although many pathways have been proposed, it is challenging to identify the mechanisms that are involved in

CRS-5 due to the multitude of contributing factors and the sequence of organ involvement [39].

CRS-5 has been divided into four stages according to severity: hyperacute (0-72 h after diagnosis), acute (3-7 days), subacute (7-30 days) and chronic (beyond 30 days) [33, 40]. The existing studies of CRS-5 are usually those of hyperacute or acute stages, as these evaluate the effects of sepsis. Sepsis, defined as a life-threatening organ dysfunction caused by deregulated host response to infection [41], is one of the most common causes of death among hospitalized patients, among whom the prevalence of CRS-5 is high [1, 42].

In early stages of sepsis microcirculatory changes are developed despite normal systemic hemodynamic [43]. Those alterations, along with inflammation, are important in the cardiac and renal dysfunction given in this type of CRS [44]. For instance, the increase in pro-inflammatory cytokines during sepsis and the decrease in renal blood flow lead to tubular necrosis, reduction in GFR and severe kidney failure [45, 46]. Sepsis is also related to autonomic nervous system dysfunction and RAAS activation [33, 39]. This complex environment makes differentiating between the cardiorenal crosstalk effects and sepsis effects very difficult.

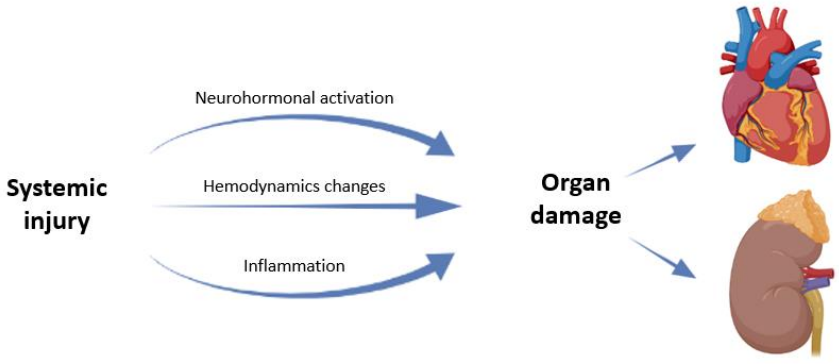


**Figure 5.** Schematic representation of Cardiorenal syndrome type 5. Figure adapted from Delgado-Valero B. et al., *cells* 2021 [22].

## II. Animal models of CRS

In addition to the hemodynamic and neuro-hormonal factors, many pathophysiological mechanisms have been speculated to have a role in the complexity of CRS; however, its implications have not been fully identified [47].

Most of the available information on CRS has been obtained from epidemiological and clinical data, yet the observational character and the design of most clinical studies makes it challenging to study the underlying pathophysiological changes and to assess new therapeutic approaches [48, 49]. Therefore, as further research is needed to obtain mechanistic insight into the pathophysiology of CRS that allows us to evaluate possible treatments for it, numerous animal models have been developed. The existing animal models for CRS study can be differentiated into i) animal models of CRS with primary cardiac injury, ii) animal models of CRS with primary renal disease and iii) animal models of CRS with renal and cardiac damage.

Out of the designed animal models, a vast majority is based on the use of rodents due to the accessibility in terms of housing conditions and availability. Induction of cardiac dysfunction in rodents can be done in various ways, as depicted in Table 1; however, the most commonly used methodology consists of ligation of the left coronary artery to induce MI [50]. The main advantage of this animal model is the similarity to the pathophysiological alterations in the human, as not only the hemodynamic and neurohormonal changes, but also the decrease in cardiac output resembles those observed in patients [48, 50]. The applicability of these animal models has proved effective for example in the assessment of the beneficial effects of RAAS blockade, which is considered a gold-standard in the treatment of cardiovascular alterations, as it was first evaluated in animals with MI and then confirmed in clinical trials [51, 52].

**Table 1.** Animal models of CRS with primary cardiac injury

| Model | Pathophysiological changes | CRS type | References |
|---|---|---|---|
| Myocardial infarction (MI) | Decreased cardiac output and blood pressure<br>Systemic inflammation and ROS production<br>Cardiac remodelling<br>RAAS and SNS activation<br>Decreased GFR<br>Tubulointerstitial injury | CRS-1 or CRS-2 depending on evolution time | Mouse [53, 54] and rat [8] |
| Cardiac ischemia-reperfusion (I/R) | ATP depletion, $Ca^{2+}$ and $Na^{+}$ overload<br>Systemic inflammation and ROS production<br>Cardiac remodelling<br>Decrease in cardiac function<br>Ventricular arrhythmias<br>RAAS and SNS activation<br>Tubular and glomerular injury without GFR loss | Mainly CRS-1 | Rat [55], Pig [56] |
| CA/CPR | Acute HF and cardiogenic shock<br>Ischemic injury to brain, heart, and kidneys<br>Oxidative stress and inflammation<br>Decreased GFR and increased sCr | CRS-1 or CRS-2 depending on evolution time | Mouse [57, 58], rat [59] |
| Hypertension-induced HF | Increased cardiac workload<br>Decreased cardiac output<br>Cardiac remodelling<br>RAAS and SNS activation<br>Renal hypoperfusion<br>Hypertensive organ failure | CRS-1 or CRS-2 depending on evolution time | Rat [60, 61] |
| Transverse aortic constriction | Pressure overload<br>Decreased cardiac output<br>Cardiac remodelling and dysfunction<br>RAAS and SNS activation<br>Renal hypoperfusion<br>Tubulointerstitial injury | CRS-1 or CRS-2 depending on evolution time | Mouse [62-64] |
| Rapid ventricular pacing | HF by impaired contractility<br>Reduced cardiac output<br>Cardiac remodelling<br>RAAS and SNS activation<br>Renal hypoperfusion<br>Tubulointerstitial injury | CRS-1 or CRS-2 depending on evolution time | Dogs [65], pigs [66] |
| Mitral valve regurgitation | LV volume overload<br>Decreased cardiac output<br>Cardiac remodelling and HF<br>RAAS and SNS activation<br>Renal hypoperfusion | CRS-1 or CRS-2 depending on evolution time | Rats [67] |
| Doxorubicin | Cardiotoxicity, congestive HF<br>Cardiac remodelling<br>RAAS and SNS activation<br>Systemic inflammation and ROS production<br>Mitochondrial dysfunction<br>Renal hypoperfusion and nephrotoxicity<br>Glomerular and tubulointerstitial injury | CRS-1 or CRS-2 depending on evolution time | Rats [68, 69] |

RAAS: Renin angiotensin aldosterone system; SNS: Sympathetic nervous system; GFR: Glomerular filtration rate; CRS: Cardiorenal syndrome; CA/CPR: Cardiac arrest/Cardiopulmonary resuscitation; HF: Heart failure; sCr: serum creatinine; ROS: reactive oxygen species.

On the other hand, out of the various animal models available to induce renal failure (Table 2), the most used animal design involves nephrectomies, which consist of the removal of part of the kidney tissue. This procedure eventually alters the function and/or structure of the heart. Unilateral nephrectomy (UNX) consists of the removal of one of the kidneys which leads to mild renal function impairment whereas in subtotal nephrectomy (SNX), also called subnephrectomy, the removal of 5/6 of renal tissue generates severe dysfunction that eventually translates into uremia and complications similar to the ones observed in CKD patients [48, 70].

**Table 2.** Animal models for cardiorenal syndrome of primary renal injury.

| Model | Pathophysiological changes | CRS type | References |
|---|---|---|---|
| SNX | Hypertension, albuminuria<br>Decreased GFR<br>Glomerulosclerosis, tubular atrophy, fibrosis<br>RAAS and SNS activation<br>Uraemic cardiomyopathy<br>Diastolic dysfunction<br>Cardiovascular remodelling | CRS-3 or CRS-4 depending on evolution time | Mouse [70], Rat [71, 72] |
| UNX | Hypertension, albuminuria<br>Decreased GFR<br>Glomerulosclerosis, tubular atrophy, fibrosis<br>RAAS and SNS activation<br>Uraemic cardiomyopathy<br>Diastolic dysfunction<br>Cardiovascular remodelling | CRS-3 or CRS-4 depending on evolution time | Mouse [70], Rat [73, 74] |
| Renal ischemia-reperfusion (I/R) | Increased sCr<br>Glomerular and tubular injury, fibrosis<br>RAAS and SNS activation<br>Systemic inflammation and ROS production<br>Decrease in cardiac function<br>Cardiovascular remodelling<br>Ventricular arrhythmias | CRS-3 | Mouse [75, 76], rat [77] |
| Unilateral uretral obstruction (UUO) | Hydronephrosis<br>Glomerular and tubular injury, fibrosis<br>Decreased GFR<br>Systemic inflammation and ROS production<br>RAAS and SNS activation<br>Cardiovascular remodelling<br>Impairment of cardiac function | CRS-3 or CRS-4 depending on evolution time | Mouse [78, 79], Rat [80] |
| Diet or treatment (Adenine/oxalate/cisplatin) | Nephrotoxicity<br>Increased sCr, proteinuria<br>Glomerulosclerosis, tubular atrophy, fibrosis<br>Cardiac dysfunction<br>Cardiac remodelling | CRS-3 or CRS-4 | Mouse [81-83], rats [84, 85] |
| Alport syndrome knockout models | Cachexia, hematuria<br>Increased sCr, proteinuria<br>Glomerulosclerosis, tubular atrophy, fibrosis<br>Fluid overload and hypertension<br>Cardiac dysfunction<br>Cardiac remodelling (cardiomyopathy) | CRS-4 | Mouse [86, 87] |

SNX: Subtotal nephrectomy; GFR: Glomerular filtration rate; RAAS: Renin angiotensin aldosterone system; CRS: Cardiorenal syndrome; UNX: Unilateral nephrectomy; I/R: ischemia reperfusion; sCr: serum creatinine; ROS: reactive oxygen species.

The aforementioned models are "single hit" approaches based in the induction of a primary damage followed by an evolution period in which the alterations to the secondary organ can be developed. However, "multifactorial hit" animal models in which the injury to both the heart and the kidneys is simultaneous have been proposed (Table 3). Depending on the CRS type of interest the procedure done to one of the organs can be followed by another procedure to the secondary one, for example, animals that undergo a UNX followed by MI after 1 week can be used as a model of CRS-3 whereas a model of CRS-1 could be MI followed by UNX [70, 88]. In general, the damage seen in animal models of simultaneous cardiorenal injury is more severe in a shorter progression period than that of the models of damage induction to only one organ.

**Table 3.** Animal models for cardiorenal syndrome of simultaneous cardiac and renal injury.

| Model | Pathophysiological changes | References |
|---|---|---|
| Double ischemia-reperfusion injury | Increased HF<br>Renal hypoperfusion<br>Volume and pressure overload<br>Increased sCr<br>Inflammation and oxidative stress<br>Decrease in cardiac and renal function<br>Cardiac and renal remodelling | Rat [55, 89] |
| MI + UNX<br>or<br>UNX + MI | Accelerated cardiac and renal remodelling and dysfunction due to the pathophysiological changes explained in both models individually | Rat [90, 91] |
| MI + SNX<br>or<br>SNX + MI | Accelerated cardiac and renal remodelling and dysfunction due to the pathophysiological changes explained in both models individually | Rat [92-94] |
| UNX, SNX or adenine supplementation + hyperlipidemia | Hypercholesterolemia and atherogenesis<br>Hypertension<br>Renal dysfunction and remodelling<br>Cardiac dysfunction and remodelling | Mouse [88, 95] |
| UNX or SNX + hypertension | Increased cardiac workload<br>Decreased cardiac output<br>Renal hypoperfusion<br>Renal dysfunction and remodelling<br>Cardiac dysfunction and remodelling<br>RAAS and SNS activation<br>Hypertensive organ failure | Mouse [73, 88] |
| Doxorubicin + SNX or renal I/R | Dilated cardiomyopathy<br>Nephro and cardiotoxicity<br>Increased oxidative stress<br>Inflammation and mitochondrial injury<br>Renal dysfunction and remodelling (Fibrosis, tubular injury) | Rat [96, 97] |
| CKD + mineral bone disorder | Renal impairment and remodelling<br>Mineral balance disturbance<br>Alterations in circulating levels of FGF23<br>Deficiency in Vitamin D and klotho<br>Anemia<br>Cardiac dysfunction and remodelling (LVH, fibrosis)<br>Possible sudden cardiac death | Mouse [98], Rat [70, 99] |

HF: heart failure; sCr: serum creatinine; MI: myocardial infarction; UNX: Unilateral nephrectomy; SNX: Subtotal nephrectomy; RAAS: Renin angiotensin aldosterone system; SNS: Sympathetic nervous system; I/R: ischemia reperfusion.

## III. Pathophysiology of CRS

The joint discoveries made in both preclinical and clinical studies have allowed us to reach a deeper understanding of the pathophysiology of CRS. Currently it is well known that due to the essential role of both the heart and kidney in the maintenance of cardiovascular homeostasis, initial organ damage during a disease state such as CRS can induce structural remodelling and functional alterations in the other.

### 1. Renal alterations associated to heart failure

As explained before, CRS-1 and CRS-2 are characterized by progressive kidney damage due to HF. Over 50% of HF patients have been reported to have renal insufficiency. Indeed, even a modest reduction in renal function is associated with higher mortality rate in CVD patients [30, 100]. The most currently used diagnostic measurements for renal damage are GFR, albuminuria, serum creatinine levels and urinary output.

The systolic blood pressure and effective arterial volume are reduced once HF develops, which translates to a decrease in renal blood flow as well as GFR [30]. In order to preserve adequate blood flow, the kidneys autoregulate through different mechanisms, including sympathetic nervous system (SNS) and RAAS activation, which would act as vasoconstrictors of the afferent and the efferent arterioles [30, 101]. In the long term this activation of the neurohormonal axis could result in podocyte injury [102, 103], mesangial expansion [104], tubular and glomerular damage and kidney dysfunction [105, 106], which are often associated with CKD and end-stage renal disease (ESRD).

It is common to use the term kidney failure in a clinical setting to refer to a situation where there is a persistent decrease in estimated GFR in the short term [107]. Another important concept is worsening renal function, which is

considered to appear in those patients in which the serum creatinine levels increase by 25% compared to the basal levels or the estimated GFR decreases by more than 20% in a period of around 25 weeks [108, 109]. AKI is characterized by a rapid loss of kidney function that can happen in HF patients when diuresis decreases < 0.5 ml/kg/h in 6-12 hours or the basal serum creatinine levels increases ≥ 0.3 mg/dl for more than 24 hours [109].

In addition to traditional markers of decreased glomerular filtration and kidney damage, such as creatinine and albuminuria respectively [27], other markers such as cystatin C [110] and blood urea nitrogen (BUN) [2, 109, 111] have been proposed as possible specific biomarkers of tubular damage. One of them is Neutrophil Gelatinase Associated Lipocalin (NGAL), a small glycoprotein expressed in renal and other cell types to which different functions have been attributed [112]. Its involvement in renal pathologies and its role as a biomarker comes from its rapid release in response to tubular lesion and its presence in plasma, serum and urine, making it easy to quantify [112, 113]. Another proposed molecule is Kidney injury molecule-1 (KIM-1), a transmembrane glycoprotein expressed in low levels in healthy kidneys. Briefly, after tubular damage KIM-1 cleavage allows its secretion by the injured cells to the tubule lumen, resulting in detection in the urine, to where it is excreted [114, 115]. Moreover, its role as a biomarker has proved to be associated with inflammation and fibrosis in the injured kidney, which would help monitor the degree of tubular damage [115, 116]. Interleukin-18 (IL-18) is a proinflammatory cytokine that is expressed in activated macrophages, renal epithelial cells, and others [117]. Urinary IL-18 is considered to be a marker of both short- and long-term injury in AKI, as it increases within 6 hours of the insult or at least a day before serum creatinine increase [117, 118].

## 2. Obesity, myocardial infarction, and CRS

As previously reported, the highest prevalence among the diagnosed patients with CRS can be found in those with CRS-1. The characteristical worsening of cardiac function can be seen in CRS-1 patients due to different insults, such as acute HF, cardiogenic shock, or acute coronary syndrome such as MI [1]. Moreover, acute HF and AKI stand as two of the most common complications in hospitalized patients with MI, whose mortality has been shown to escalate alongside AKI's severity. It has been shown that CRS-1 incidence rate in acute coronary syndrome is that of 9-19%, and of approximately 16% in patients with MI [119, 120].

MI, commonly known as heart attack, is a serious pathological condition that usually happens due to the obstruction of a coronary artery. As a consequence of the interruption of blood flow to a specific area of the heart, the lack of oxygen leads to tissue damage and death. Each year MI is developed in approximately 7 million individuals worldwide [121], with individuals over 65 years old being a higher risk. Furthermore, MI development is usually concomitant to the presence of obesity, a well-known risk factor that contributes to not only the occurrence of adverse cardiovascular events, but also plays an important role in other co-morbidities such as hypertension, atherosclerosis, or diabetes [122, 123].

In 2018, a consensus by *The Obesity Society* [124] defined obesity as a "multi-causal chronic disease resulting from long-term positive energy balance with development of excess adiposity that over time leads to structural abnormalities and functional impairments". Although obesity is related to an increase in body weight, it is important to also assess body fat distribution independently of total adiposity, as visceral deposition of fat pockets has been proven to correlate with higher all-cause mortality [125, 126].

While generalised obesity is usually evaluated using the body mass index (BMI) in adult population (Table 4), adding other anthropometric indicators such as waist circumference or waist-to-hip ratio into the patient evaluation provides important information about visceral adiposity, usually referred to as central obesity [127]. In the last decades, a high increase in the prevalence of central obesity has been seen, reaching 41.5% of the global population [128], becoming an epidemic that needs to be targeted to reduce the health burden it entails.

**Table 4**. World Health Organization (WHO) criteria for BMI-based classification of obesity.

| Classification | BMI values ($Kg/m^2$) |
|---|---|
| Underweight | < 18.5 |
| Normal weight | 18.5 – 24.9 |
| Overweight | 25.0 – 29.9 |
| Class I obesity | 30.0 – 34.9 |
| Class II obesity | 35.0 – 39.9 |
| Class III obesity | ≥ 40 |

Extensive epidemiological and clinical data has shown the existing association between central obesity and cardiorenal and metabolic diseases such as MI [129, 130], hypertension [131], type 2 diabetes [132, 133], as well as with their complications such as HF, MI, atrial fibrillation, CKD and respiratory diseases [134, 135]. In recent years, the implication of obesity and metabolic syndrome in the development of both cardiac and renal diseases has been coined as "cardiorenal metabolic syndrome", which is applied to pathological contexts of adiposity-related CRS [13, 136]. In this sense, multiple studies have postulated neurohormonal, hemodynamic, inflammatory, and fibrotic responses as the main obesity- induced modulations that could lead to cardiorenal damage [136].

While some consider obesity to be a risk factor for the development of CVD due to its interaction with comorbidities such as hypertension or dyslipidaemia, others consider obesity to be an independent factor for the development of CVD

[137, 138], which remains the leading cause of death globally. Moreover, the high prevalence of overweight and obesity among patients with MI [139] and its association with CVD-mortality [140] make of vital importance the study of its interaction. Although there are numerous underlying mechanisms that could explain the cardiovascular consequences of obesity, it is well known that, the presence of ectopic fat deposits in the vessels, pericardium and epicardium in obese patients is associated with important cardiovascular complications such as increased blood pressure, systemic inflammation, atherosclerosis, insulin resistance and dyslipidaemia [137, 141]. For example, the cytokines and adipokines from epicardial adipose tissue generate an atherogenic environment that could lead to coronary artery obstruction and secondary development of ischemic cardiomyopathy [142]. In the atherogenic process the ingestion of cholesterol by macrophage foam cells and its deposition in the vasculature wall leads to fatty streak development, narrowing the vessel lumen and impeding appropriate blood flow, possibly blocking irrigation to the heart, and leading to cardiac cell death and MI [137, 143].

Furthermore, due to the increase in adipose tissue in obese individuals, several adaptations such as hemodynamic overload, RAAS hyperactivation, SNS activation and higher cardiac output are needed to reach the increased metabolic needs [144]. Because of the sustenance of those adaptations, structural alterations in the heart can occur, LV hypertrophy being the main complication as it could lead to diastolic and systolic dysfunction and therefore to higher risk of cardiovascular events [145, 146].

In addition, in the past years numerous studies have linked obesity and CKD, considering it an important risk factor, as up to a 25% of overweight patients end up developing CKD [147]. Current hypotheses explain the increased risk of CKD development in obese patients due to the changes in hemodynamic, as the hypervolemia, RAAS and SNS activation and systemic inflammation also impair

renal function [148, 149]. However, other aspects of obesity such as ectopic fat deposits, metabolic syndrome, insulin resistance and hyperlipidaemia have been seen to affect the kidney [150, 151]. The deposits of fat not only in the subcutaneous area of the abdomen but also in and around the kidneys can physically compress the kidneys, which raises renal interstitial pressure, compromising tubular blood flow and increases reabsorption of sodium by the tubular cells, all of which can lead to RAAS activation and to the declining of renal function [152, 153]. Along with it, inflammation, oxidative stress and fibrosis within the renal parenchyma leads to some of the most common alterations seen in the kidneys of obese patients, such as podocyte hypertrophy, renal oxidative stress, mesangial expansion, fibrosis, glomerular hyperfiltration and increased renal reabsorption of sodium by the tubular cells [148].

### 3. Fibrosis

A common structural alteration observed in both heart and kidney remodelling in CRS is fibrosis, which is also considered a key contributor to the progression of cardiac and renal failure [7, 154]. Fibrosis is an important process that can be contemplated as aberrant extracellular matrix (ECM) deposition consequence of the misbalance between ECM production and degradation [22]. The fibrotic response to injury can be classified into reparative, when the scar is necessary to stabilize the tissue defect, or reactive, when the mechanical stress and the hormonal mediators facilitates the expansion of connective tissue in a remote non-injured zone, compromising the correct function of the organ [155, 156]. The main fibrosis effectors are the fibroblasts and myofibroblasts, both of which are responsible for the synthesis and accumulation of interstitial ECM proteins. While fibroblasts are mesenchymal cells ubiquitous in tissues and organs, myofibroblasts are differentiated cells that are rarely found in non-pathological environments [157]. The fibrotic scar composition is similar amongst different

tissues, predominantly formed by collagens type I, III, IV and fibronectin, proteoglycans and laminin [158, 159].

As a response to the damaged heart in cardiac ischemia, myocardial remodelling occurs through the secretion of ECM components by the myofibroblasts. Histopathologically, there are three types of cardiac fibrosis: replacement fibrosis, interstitial fibrosis and perivascular fibrosis. Replacement fibrosis provides structural support, as it consists of the removal of necrotic tissue and generation of a fibrotic scar within the infarcted zone that compensates cardiomyocyte loss [160, 161]. On the other hand, the widespread deposition of ECM proteins in the endo and perimysium of remote areas of the infarct is what is known as interstitial fibrosis [7]. The term perivascular fibrosis is used to describe the increase of connective tissue around the cardiac microvasculature [162], both of which are types of fibrotic lesions that could not be consequence of cardiomyocyte death but of myocardial damage.

The remodelling that follows after MI happens in different phases that partially overlap. First there is cell death and inflammatory response (inflammatory phase), secondly the resolution of inflammation and fibroblast proliferation (proliferative or reparative phase) and lastly, the scar formation and maturation (maturation or remodelling phase) [161]. During the proliferative phase, which usually coexists with the inflammatory and reparative phases, there is an increase in the number of fibroblasts that will adopt proliferative, secretory, and migratory myofibroblast phenotype through epithelial-mesenchymal transition [157]. Following the proliferative phase of cardiac repair, when the scar has been synthesized, there begins a long process known as maturation in which an organized fibrotic state is formed due to ECM crosslinking by lysyl oxidase activity [159, 163] and scar reinforcement by other components of the ECM such as the proteoglycan decorin [164, 165]. Also, during the maturation phase the activated fibroblasts go through apoptosis and senescence [166]. The presence of

a mature fibrotic scar ultimately leads to an increased ventricular stiffness that compromises cardiac output and alters the relaxation and contractile ventricular capacity. In addition to the impaired cardiac contractility, fibrosis also interferes with the normal electrical signals within the heart which predisposes to arrhythmias and fibrillation [167, 168]. Overall, fibrosis has thus been proposed as a risk factor in HF as it predisposes to ventricular systolic and diastolic dysfunction, cardiomyocyte hypertrophy and sudden cardiac death, thereby increasing mortality [168, 169].

At renal level, acute injuries that happen due to the rapid decrease in kidney function can facilitate the transition into CKD. CKD is an irreversible damage characterized by the loss of functional nephrons and by the deposition of connective tissue in the kidney that ends up creating a common fibrotic phenotype independently of the initial damage [170, 171]. This happens since tubulointerstitial diseases lead to glomerular injury, and glomerular lesions produce tubulointerstitial damage. Fibrosis is a common manifestation of functional alterations that spreads in response to sustained inflammation and epithelial damage [172]. Among the events that induce fibrosis both diabetes and hypertension are considered to be the leading causes of CKD [173, 174], as they elevate the glomerular pressure which gradually leads to glomerular damage, endothelial dysfunction [175, 176] and other structural changes such as alterations of the glomerular basement membrane, decrease in podocyte number and mesangial distension [176-178]. As a result of such damage, the renal tissue would start a response that resembles wound healing in other tissues. The scar created in the early stage is potentially reversible but with the progression of the damage, the cross-linking of the ECM proteins makes it stiff and resistant to proteolysis [179, 180].

During chronic injury to the kidney, the excessive accumulation of connective tissue and expansion of interstitial fibroblasts during the reparative stage of the

fibrotic scar can happen in all compartments of the kidney, including the glomeruli, usually termed glomerulosclerosis, and the tubules, which is referred to as tubulointerstitial fibrosis [181-183]. Such deposition of fibrotic matrix alters organ structure and function which could further damage kidney function, as it impairs blood flow in this region of the parenchyma [182, 184]. The fibrotic wound is not the only structural change involved as it is usually associated with tubular atrophy, tubular dilation and inflammatory cell infiltration [185-187]. Indeed, as the loss of renal cells and its replacement by ECM are common sequelae of renal damage, expansion of cortical fibrosis is considered one of the best histologic predictors of kidney dysfunction loss in CKD along with tubular atrophy (IFTA parameter) [181, 185]. It is also one of the most common features assessed in biopsies in predicting a progression to ESRD [181, 183].

Even though chronic damage to the kidney will naturally converge into histological and functional alterations that are common and lead to glomerulosclerosis and fibrosis, it is important to understand that the fibrotic progression is different depending on where it begins. In glomerular damage the progression starts with an injury within the Bowman's Capsule that initially leads to glomerular hyperfiltration for a long period of time until it progresses to decrease the total GFR. This reduction in the blood flow results in tubular hypoxia and epithelial cell death, normally referred to as tubule atrophy [188, 189]. In these circumstances, the inflammation initiated by the damaged tubular cells propitiates the formation of a fibrotic scar to fill the void created by epithelial cell death [190, 191]. To form that scar, resident fibroblasts differentiate to myofibroblast phenotype, which can synthesize different ECM proteins. Among the ECM components produced by myofibroblasts in order to form the fibrotic scar, the main ones in the kidney are collagen type I, III and IV, as well as fibronectin [192-194]. During tubule atrophy the tubular basement membrane remains, thereby separating the cell death from the interstitium but disappears

after the cell-free tubule collapses, at which point we could talk of complete loss of the nephron [195, 196].

Epithelial damage is heterogeneous in tubular injury, which can be caused by many factors such as hemodynamic, inflammatory, toxin-related or metabolic alterations. Some cells will instantly go through necrosis or apoptosis, whereas others will survive with different levels of injury, these being the ones that could proliferate and replace the lost cells of the tubular epithelium [197]. In the cases in which the tubules do not recover, inflammation signalling activates and with it the fibroblasts differentiate into myofibroblasts that will lead to tubulointerstitial fibrosis and tubular atrophy [172, 198]. Tubulointerstitial fibrosis is the deposition of ECM proteins in the space between the tubular basement membrane and the peritubular capillaries [192], which impairs renal tubule function and blood flow and induces ischemic injury in the nephrons of the fibrotic wound [198, 199].

Inflammation and oxidative stress serve as the initial response to injury, although its long-term progression could damage organ structure and function [200]. Inflammation is a common process in fibroproliferative diseases that leads to the infiltration of immune cells and to the release of pro-inflammatory mediators that have an important role in tissue damage and could either stimulate or inhibit fibrosis [201, 202]. An appropriate level of cytokines and growth factors that mediates the cellular responses is key in normal wound healing. Among the many growth factors involved, transforming growth factor β (TGF-β) is considered to be a prototypic profibrotic cytokine that has a central role in organ fibrosis as it binds to its receptors causing the phosphorylation of SMADs, which modulate the expression of the target genes. TGF-β can also activate SMAD-independent pathways in what is called non-canonical signalling [203, 204]. Among the many TGF-β mediated responses are cell proliferation and differentiation, ECM production and immune modulation [204]. Through its

canonical signalling pathway, TGF-β1 is able to trigger glomerulosclerosis, interstitial fibrosis and inflammation propitiates renal damage progression into ESRD [205, 206]. In fact, renal biopsies have proven the strong correlation between TGF-β, fibrosis and worse renal outcomes [207]. Another important mediator that is known to work synergically with TGF-β is the connective tissue growth factor (CTGF), a downstream factor of TGF-β that has been reported to promote fibrosis in different organs such as heart and kidney [208, 209]. CTGF promotes the TGF-β-induced excessive ECM production and fibroblast proliferation, and its expression appears to correlate with the degree of fibrosis [203, 210].

As previously said, the degree of fibrosis is regulated by a dynamic balance between production and breakdown of ECM. The degradation of the ECM components is performed by the matrix metalloproteinases (MMPs), whose activity is controlled by the tissue inhibitors of MMPs (TIMPs) in order to maintain the ECM homeostasis [156, 180]. MMPs can be classified according to substrate specificity into collagenases such as MMP-1, MMP-8 and MMP-13, gelatinases such as MMP-2 and MMP-9, membrane MMPs such as MMP-14 and stromelysins such as MMP-3, MMP-10 and MMP-11 [211]. Interestingly, due to its participation in different signalling pathways, MMP regulatory properties are usually bidirectional, as they can have both inhibitory and stimulatory effects on fibrosis. For example, the most frequently studied MMPs in HF and kidney damage are MMP-2 and MMP-9, out of which MMP-9 is believed to have a profibrotic effect [212, 213] whereas MMP-2 has antifibrotic effects in the advanced stages of CKD and profibrotic ones in the early stages [214, 215].

## IV. Mechanisms involved in CRS-induced renal damage and fibrosis progression

Although traditional cardiovascular risk factors, such as hypertension, obesity and diabetes are common among CKD patients, targeting only these factors in the clinical setting has yielded unsatisfactory results, suggesting the relevance of other underlying pathways [6]. Consequently, a growing number of studies have emphasized the importance of researching non-conventional risk factors and other mechanisms that could intervene in the pathophysiology of CRS-induced renal damage.

Furthermore, and as already mentioned, fibrosis is considered a key contributor to the progression of cardiac and renal failure in all types of CRS. Therefore, it is mandatory to understand the mechanisms involved in fibrosis progression which could determine potential therapeutic targets. Despite the efforts to acquire insight into the process, the mechanisms involved in fibrosis are not fully established, and the current therapies, despite being slightly successful, have important side effects that lead to its discontinuation [216, 217]. Hence, this makes it crucial to have a comprehensive understanding of the pathophysiological mechanisms underlying not only renal damage but specifically fibrosis as well.

### 1. Galectin-3

Galectins are a family of 15 small soluble β-galactoside-binding lectins involved in cell-to-cell and cell-to-matrix interactions, as well as in other biological functions such as development, tissue regeneration or regulation of inflammatory responses [218, 219]. Galectin-3 (Gal-3) is a 29 to 35 kDa chimera-type galectin that is present in the heart, kidneys, lungs, blood, and digestive track. Moreover, multiple cell types express Gal-3, such as epithelial, endothelial, immune, inflammatory cells and fibroblasts [220]. Gal-3 is synthetized in the

cytoplasm as a consequence of RAAS activation, expressed in the nucleus, mitochondria, cell surface or secreted into the extracellular space, however, depending on its cellular location Gal-3 can exert different functions in several biological processes, its proinflammation and profibrotic actions being the main contribution to pathophysiology [218, 219]. Although the proposed functions of Gal-3 are ample, it has been widely described that the extracellular Gal-3 acts as an adhesion molecule for cell-to-cell or cell-to-matrix, whereas intracellular Gal-3 is involved in cellular functions such as cell growth, proliferation, differentiation and apoptosis [218, 219]. Given its regulatory effects and its broad distribution in the human body, multiple studies have suggested its utility as a prognostic or diagnostic marker for various pathological conditions such as CVDs [221, 222], kidney disease [223, 224], diabetes [225] and neurodegenerative diseases [226], all of which have been associated with an increase in Gal-3 levels.

The implication of Gal-3 in these pathologies due to its role as a regulator of the inflammatory response depends on the environment, as it can have proinflammatory or anti-inflammatory effects. Gal-3 plays a part in PAMP recognition as it can bind to the exposed glycans in the pathogen surfaces [227, 228]. Moreover, its secretion, which usually happens during monocyte differentiation to macrophages, contributes to macrophage migration into injury sites, neutrophil adhesion and mast cells activation [229]. In those cases, in which inflammation is not resolved in a prolonged period, Gal-3 displays DAMP-like properties, enhancing the transition into chronic inflammation and promoting aberrant tissue repair, fibrinogenesis and organ failure [220].

Numerous *in-vivo* studies have demonstrated the relationship between Gal-3 expression and the presence of a fibrotic lesion in the heart, kidney, liver and lungs, as Gal-3 plays a crucial role in the initial stage of tissue repair by promoting the release of inflammatory mediators such as TGF-β or IL-1, the activation of myofibroblasts and collagen deposition [230-233]. At the heart, Gal-3 is

considered an important contributor to cardiac remodeling and HF development, as it mediates both the inflammatory and fibrotic response to injury. In animal models, the intraperitoneal injection of recombinant Gal-3 in healthy rats proved to increase the myocardial fibrosis, as well as the ventricular remodeling and the induction of HF [230, 234]. On the contrary, targeted inhibition of Gal-3 in a model of MI proved effective in slowing the collagen deposition and ventricular remodeling in the heart [235].

Given that Gal-3 expression is mainly found in the distal and collecting tubules in the mature kidney (although during regeneration it can temporally be expressed in the proximal tubules) [223, 236], several studies focus on the tubular effects of Gal-3. At renal level, Gal-3 has been reported to play an important role in CKD development and progression, as an increase in Gal-3 levels directly associates with a decrease in the GFR and with higher levels of renal interstitial fibrosis, tubular atrophy, and proteinuria [231, 237, 238]. Furthermore, AKI patients present higher levels of Gal-3 than those who do not develop AKI, therefore suggesting it could also be an early biomarker for AKI diagnosis. Also, in different animal models of AKI induced by I/R or hypertension, the pharmacological inhibition of Gal-3 activity by *modified citrus pectin* (MCP) significantly decreased renal dysfunction, renal tubular injury, and the release of inflammatory mediators such as IL-6 or TNF-$\alpha$ [223, 239]. Additionally, studies in Gal-3 KO mice with cisplatin-induced AKI showed that Gal-3 may act as a negative regulator of autophagy, as the absence of Gal-3 in the animal was associated with increased autophagic flux in the animal model of tubular necrosis [240]. Based on all the data that support the relevance of Gal-3 in both the heart and the kidney pathophysiology, several studies have suggested that Gal-3 could be used as a marker of CRS development, possibly acting as a therapeutic target for the treatment of CRS complications [241, 242].

## 2. Inflammation

Inflammation can be defined as a defensive immune response that is triggered by damage to a tissue. The acute inflammatory response can be initiated as a consequence of an infection in which the pattern recognition receptors in the innate immune cells interact with the pathogen-associated molecular patterns (PAMPs), or due to the damage-associated molecular patterns (DAMPs) that are released during physical injury [243]. Acute inflammatory response is characterized by vasodilation, vascular leak and leukocyte emigration and, shortly after its induction, secretion of cytokines and chemokines will happen in order to recruit the immune cells to the damaged or infected region. Among the cells recruited, neutrophils are the first to migrate as a means to engulf the pathogens and secrete pro-inflammatory mediators and vasoactive substances [244, 245].

In a normal inflammatory response, the activity is temporally restricted, as it resolves once the threat has been dealt with. However, the presence of a prolonged low-grade activity leads to chronic inflammation, which is characterized by the activation of different immune components that lead to major alterations in tissues, increasing the risk of diseases [246]. The clinical consequences of chronic inflammation include diabetes [247], hypertension [248], CVDs [249], CKD [250] and metabolic syndrome [251] among others.

Inflammation is known to have an important role in the development and progression of chronic diseases. For example, CKD progression into ESRD is characterized by chronic inflammation in the renal parenchyma that results in excessive ECM deposition and loss of renal function [250, 252]. Moreover, since both chronic HF and CKD are associated with chronic inflammation response characterized by an increase in the circulating inflammatory mediators, this process has become of interest in the understanding of CRS. In fact, studies have

shown that macrophage infiltration in the renal parenchyma and proinflammatory cytokine expression can be seen 3 days post-MI [252].

At renal level, the kidneys can modulate the inflammatory response as they are responsible not only for the clearing of cytokines and PAMPs, but also are involved in sustaining peripheral tolerance to harmless antigens through resident dendritic cells and subtype M2 macrophages. However, the implication of the kidneys in the maintenance of the immune system homeostasis renders them more susceptible to inflammation-related damage [250]. Independent of the original cause, experimental models and human biopsies have shown that cells such as neutrophils and macrophages infiltrate both the glomeruli and tubulointerstitial space during renal inflammation in order to remove the cell and matrix components that were damaged during the insult [253, 254]. In general, M1 macrophages generate the initial response in the diseased organ by generation of pro-inflammatory cytokines such as tumour necrosis factor $\alpha$ (TNF-$\alpha$) and interleukin-1 (IL-1), whereas M2 macrophages propitiate tissue repair by secretion of immunosuppressive cytokines such as IL-10 during the repair phase. Due to a persistent lesion, macrophage polarization into M2 phenotype promotes fibrosis, as the production of cytokines, chemokines and growth factors can alter the ECM balance between production and degradation [255, 256].

It is well established that RAAS activation and the SNS promotes the inflammatory response both in the heart and kidneys. Angiotensin II (Ang II), one of the main effectors of RAAS activation, induces endothelial dysfunction, upregulation of adhesion molecules and fibrosis [257, 258]. These Ang II effects are accompanied by recruitment of infiltrating cells and by the increase in proinflammatory cytokines via de angiotensin type 1 (AT1) receptor in cardiorenal disease [259]. It has been proved that Ang II produces the accumulation of macrophage in the kidney [260], and it was shown in a murine unilateral uretral obstruction (UUO) model that macrophage's AT1 receptor

activation impedes polarization towards the M1 phenotype and ameliorates kidney fibrosis [261]. This shows that an increase in M1 macrophage differentiation makes organs more susceptible to damage, whereas M2 phenotype decreases injury [250, 262]. Nevertheless, neurohormonal activation is not the only proposed source of inflammation in CRS. Both animal and human studies have shown that congestion may lead to endothelial activation and peripheral release of proinflammatory mediators, as venous congestion itself causes inflammatory response activation in cells [263].

Chronic unresolved inflammation induces intrarenal changes in the microvasculature that damages renal structure and function, thereby leading to CKD, a state characterized by progressive renal fibrosis. In previous studies it was reported that circulating levels of fibrinogen, IL-1, TNF-$\alpha$ and a decrease in serum albumin were associated with loss of kidney function, linking the progression of CKD to the inflammatory response [250, 264]. Systemic inflammation and function decline can alter the structure of the kidney, creating an environment in which epithelial damage increases and the factors released by infiltrating macrophages lead into fibrotic expansion [265]. Indeed, macrophage depletion has proved to reduce renal fibrosis in an animal model of MI [266].

In renal fibrosis, the first process involved is the injury itself, followed by persistent inflammation, a trigger that is needed to activate the wound-healing process; however, if not eliminated quickly, the inflammatory cells could increase the response leading to the abnormal wound healing and scarring characteristic of fibrosis. Within the wound-healing mechanism that is activated after injury, the first response is coagulation in which activated platelets release platelet-derived growth factor (PDGF) that act as chemoattractant for inflammatory cells and TGF-β1, which is one of the main drivers of fibrosis, as it stimulates ECM synthesis by the fibroblasts of the tissue that was damaged [267, 268]. In the tubulointerstitium, pro-inflammatory cytokines such as IL-6, TNF-$\alpha$ and IL-1β

promote further inflammatory cell infiltration, propitiating activation of profibrotic cells to differentiate into myofibroblasts and local secretion of fibrotic mediators [269, 270]. This situation will lead to overproduction and deposition of ECM proteins, disruption of tissue integrity and progressive decline in function. Finally, glomerulosclerosis and tubular atrophy will happen in the latest stages [201, 250].

### 3. Oxidative stress

Oxidative stress is a general concept that describes the imbalance between the production of reactive oxygen species (ROS) and the antioxidant defences. ROS could be either free radicals, which are species with an unpaired electron, or non-free radical oxygenated molecules such as hydrogen peroxide ($H_2O_2$), superoxide anion ($O_2^{\bullet -}$) and hydroxyl radical (·OH). Other reactive species derived from nitrogen (RNS) or sulphur do exist, but they are less abundant [271, 272].

Even in basal conditions, aerobic metabolism involves ROS production, thus making $O_2^{\bullet -}$ and $H_2O_2$ physiological intracellular metabolites. In low quantities ROS act as signalling molecules involved in different pathways such as cell proliferation, apoptosis and gene expression [271, 273]. However, the fact that an important increase in oxidants could target almost all substrates implies the impairment and alteration of all biomolecules, resulting in cell damage and death [271, 274]. ROS can damage proteins and nucleic acids [275, 276] but, among all the molecules to undergo oxidation polyunsaturated fatty acids are the most susceptible, leading to an increase in the markers of lipid peroxidation such as malondialdehyde or 4-hydroxynonenal (4-HNE) [277].

The endogenous sources of prooxidant species include organelles where there is high oxygen use, such as the mitochondria, peroxisomes due to the fatty acid β-oxidation and the endoplasmic reticulum (ER) [271], although the mitochondria seem to be the major source of ROS production, as around 95% of the breathed

oxygen is reduced in the mitochondrial electron chain. Specifically, there are two major sites in the electron transport chain, the NADH dehydrogenase (complex I) and the ubiquinone cytochrome c reductase (complex III), which transfer electrons to coenzyme Q or ubiquinone, creating reduced forms that will ultimately transfer electrons to the molecular oxygen, generating superoxide radical [278]. Through the action of mitochondrial superoxide dismutase (SOD) the $O_2^{\bullet-}$ is converted to $H_2O_2$, which can be detoxified by the catalase and glutathione peroxidase [271]. In the outer mitochondrial membrane, the monoamine oxidases are another source of ROS that is not related to respiration [279]. In this case, the bivalent reduction of oxygen produces $H_2O_2$. In order to regulate the levels of ROS, the sources colocalize with the antioxidant response, among which there are enzymes like the SOD, the catalase and glutathione peroxidase, as well as non-enzymatic antioxidants such as vitamin C and E, bilirubin or reduced coenzyme Q [271, 280].

Both inflammation and oxidative stress are related to the initiation and progression of chronic diseases such as diabetes, hypertension, CVDs or CKD [271, 281]. The heart and the kidneys are considered two of the most energy-demanding organs in the human body, rendering them highly susceptible to damage due to ROS [282]. At renal level, ROS have an important role in the regulation of kidney function, making it vulnerable to redox imbalances, as free radicals can affect different structures such as the glomerulus, the basement membrane, and the endothelium, which can in turn trigger other mechanisms as inflammation or fibrosis that then exacerbate the progression to CKD [283]. It is known that under chronic damage the inflammatory and hypoxic environment propitiates ROS formation and fibrosis by fibroblast activation and proliferation into myofibroblasts [284, 285]. Although the deleterious effects of oxidative stress in the renal tissue are well documented, the specific pathways that lead to such alterations are not clear, as it can be attained through different mechanisms such

as uremic toxin-induced endothelial nitric oxide synthase (eNOS) uncoupling, antioxidant losses, mitochondrial dysfunction, increased NADPH oxidases activity and others [283, 286].

Assessment of renal damage induced by CKD has proven the importance of the increase in activity of transcription factors such as TGF-β1 in the nephrons [287], which has been closely linked to ROS-induced activation of NF-κB, a factor that has damaging effects on the renal cells via inflammation and apoptosis enhancement [288]. The link between ROS and TGF-β1 is well established, as ROS production and enhanced ROS formation leads to higher activation and expression of TGF-β1 [289, 290]. One of the possible explanations for this link resides in the action of an important ROS source, such as the different NADPH oxidases (NOX). In normal conditions, the NOX-derived ROS act as modulators of cell growth, proliferation, differentiation, and apoptosis, but once it is uncontrolled oxidative stress damages the DNA, proteins and lipids inducing organ damage and fibrosis [291, 292]. Multiple studies have shown the effectiveness of NOX-4 and NOX-5 inhibition in inflammation, tubular damage and fibrosis amelioration in kidney injury [293, 294], while different studies in the heart have shown that both NOX-2 and NOX-4 mediate the oxidative stress and cardiac injury following I/R [295, 296]. Indeed, NOX-4 is considered to be a well-recognized mediator of the transition from fibroblast to myofibroblast, and its inhibition in *in-vitro* studies in renal cells proved to prevent ROS production and myofibroblast differentiation, which would translate into a decrease in fibrosis during damage [297, 298].

Multiple factors seem to participate in order to produce the characteristic multiorgan dysfunction of CRS, among which the increase in proinflammatory cytokines, the dysregulation of apoptosis and the increase in oxidative stress have been proposed as key elements of this complex pathophysiology [299-301]. Different animal models have shown that an increase in oxidative stress plays a

pivotal role in cardiac and renal damage independently of the CRS type depicted through activation of the inflammatory response [70, 299, 302]. This can also be seen in patients with CRS, who presented an increase in ROS and RNS that was accompanied by higher inflammatory cytokines such as IL-6 [21].

### 4. Endoplasmic reticulum stress

The endoplasmic reticulum (ER) is an essential organelle for calcium homeostasis, lipid biosynthesis and protein synthesis and post-translational modifications. To ensure correct protein folding, ER lumen balance between unfolded and misfolded proteins and the capability to handle it must be maintained. Such homeostasis could be altered by both physiological and pathological entities, such as inflammatory cytokines, protein demand and mutant protein expression, which translates into what is called ER stress [303, 304].

In response to ER stress, the unfolded protein response (UPR, depicted in Figure 6) is initiated by at least one of three different pathways: the ER transmembrane proteins Activating Transcription Factor 6 (ATF6), Inositol-Requiring 1 (IRE1) or PKR-like ER kinase (PERK). In unstressed conditions, the chaperone Immunoglobin Binding Protein (BiP) binds to the luminal domain of ATF6, IRE1 and PERK, keeping them inactive. In ER stress conditions, BiP dissociates from the three regulators, activating the UPR. In this sense, BiP is considered a marker of ER stress activation. Although initially UPR is considered to be a beneficial adaptive response, the UPR pathways guide the damaged cells to apoptosis, inflammation and the consequent tissue injury if it fails to restore homeostasis [303-305].

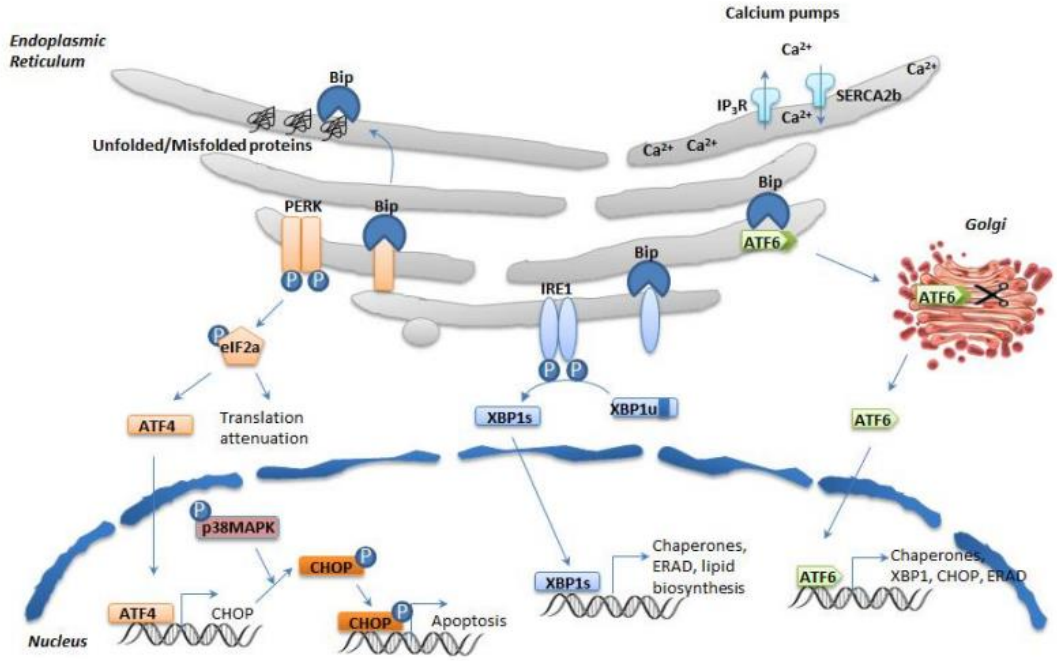


**Figure 6.** Schematic representation of the unfolded protein response (UPR) taken from Ghemrawi, R et al. review paper [306].

Different pathologies, such as diabetes mellitus [307], obesity [308], CVD [309] and CKD [310, 311], have been associated with ER stress. In CRS the activation of ER stress in the heart and kidney could be induced by different situations such ischemia, ischemia-reperfusion injury (IRI) or nephrotoxicity that generate disturbances such as hypoxia, increase ROS production, ATP shortage, inflammation, hemodynamic changes and RAAS activation, all of which lead to ER homeostasis disruption [90, 312, 313]. While the insult is maintained, cell survival is compromised by these pathophysiological mediators, which directly induce a disturbance in protein folding due to the increased biosynthesis demand. As a result of the prolonged UPR activation, ER stress-mediated apoptotic cell death is triggered in the myocardium and/or renal parenchyma, followed by the consequent activation of pro-inflammatory and pro-fibrotic pathways that would generate a fibrotic wound that will eventually culminate in the loss of renal function [303, 312, 314].

At renal level, ER stress is considered a critical mechanism involved in AKI to CKD progression, mainly due to its link to fibrosis [315]. As ER stress inhibition has proved to ameliorate the fibrotic progression, it has been suggested that its blockade could be a new therapeutic approach for fibrosis [316, 317]. One of the possible ways in which ER stress could lead to fibrosis is through fibroblast differentiation and collagen formation by TGF-β upregulation, as activation of both PERK and IRE1 has been seen to increase TGF-β expression [318, 319]. ER stress activation of fibroblasts during injury at the wounded site triggers their differentiation into myoblasts so as to restore the area by ECM protein synthesis and secretion [320]. Different *in-vitro* studies have described ER-mediated differentiation in different cell types such as renal cells [321, 322], cardiac cells [323], adipocytes [324], plasma cells [325] and others [320, 326].

## 5. MicroRNAs

MicroRNAs are small non-coding RNAs of 18 to 25 nucleotides in length that are highly conserved. MicroRNAs, also called miRNAs, function as post-transcriptional regulators of the genetic expression by their attachment to the 3' untranslated region (UTR) of the target mRNA coding sequence [327]. Since their discovery in 1993 [328] more than 2000 miRNAs have been identified in humans (https://www.mirbase.org/browse/results/?organism=hsa) [329], having a role as epigenetic modulators in pathophysiological processes such as proliferation, differentiation, angiogenesis, and apoptosis among others, which have important roles in the development of many diseases [330]. Accordingly, the regulatory function of microRNAs has attracted great interest as potential diagnostic markers and/or therapeutic targets for an ample spectrum of diseases. However, its application in the clinical setting has yet to be viable due to the intrinsic complexity of the microRNA-based regulatory networks, as not only is a single miRNA able to regulate multiple target mRNAs, but a single mRNA can be target of several miRNAs [329].

In brief, the canonical miRNA-target interaction is based on the recognition and complementary union between the miRNA and the 3'UTR region of the target mRNA (depicted in figure 7). In order to create the duplex structure with the mRNA, the microRNA contains 2-8 nucleotides at the 5'-end, usually referred to as the "seed region", and which will reverse-complement with the mRNA [331]. The complementarity between the microRNA and its target is a determinant factor for the subsequent post-transcriptional regulation. The existence of perfect complementarity leads to the degradation of the target mRNA via the RNA-induced silencing (RISC) complex, whereas the presence of mismatches between the seed region and the 3'UTR region of the mRNA will induce the silencing of the target due to RISC repression of the translation [331]. Although most functional target sites for miRNA binding are found in the 3'UTR, other sites have been discovered in the coding sequence (CDS), the 5'UTR, or even in the promoter regions of the genes [332, 333]. Moreover, certain studies have found that nuclear microRNA-gene promoter binding could have regulatory functions other than post-transcriptional gene silencing, as its interaction could exert regulatory effects in the transcription both as an activator or as a silencer depending on the motif/region and epigenetic status of the promoter [334].

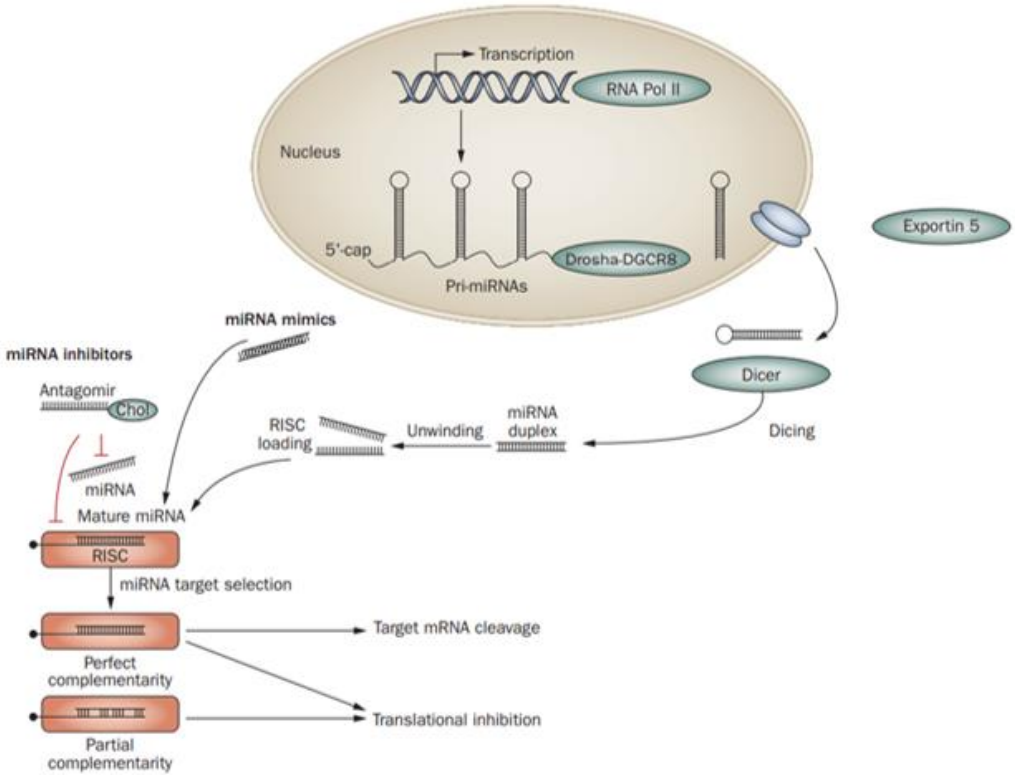


**Figure 7.** Schematic representation of the biogenesis and mechanism of action of microRNAs modified from Lorenzen, JM et al. 2011 [335].
miRNA transcripts originate as pri-miRNAs in the nucleus, undergoing processing by the Drosha protein to form a hairpin. These precursors are then transported into the cytoplasm by exportin 5 action and further processed by Dicer to form miRNA-miRNA duplexes that will later be unwound. The mature miRNA guide strand is then integrated into the RISC complex for the post-transcriptional regulation of the target mRNA, which will lead to either degradation or translational inhibition. In order to modulate the miRNA expression, inhibitors such as antagomirs or enhancers such as double-stranded mimics have proven successful.

In pathological conditions, dysregulation of microRNA expression could happen through various processes such as amplification, deletion or mutations to the miRNA codifying gene, epigenetic modifications, malfunctions in the biogenesis process or changes in the miRNA transcriptional regulation [336]. Due to such sensitive machinery, microRNA changes in expression could possibly inform of the presence of pathological environments even before the start of the symptomatology. Numerous microRNAs have been recognized for their crucial functions in heart [337, 338] and kidney diseases [339, 340]. Also, in CRS the modulation in the expression of several microRNAs has been reported for both the acute and chronic subtypes of CRS [341, 342].

In recent years, the necessity for new antifibrotic therapies and the promising role of microRNAs have opened a new prospective approach to the fibrotic treatment. Various studies have shown that microRNAs can regulate fibrosis in both CKD [343] and CVDs [344], although the specific modulation varies depending on which one we focus on. Some microRNAs such as miR-21 or miR-132 are known to have pro-fibrotic effects, whereas others like the miR-29 or the miR-200 family have an anti-fibrotic role in kidney disease [343, 344].

For example, hsa-miR-21-5p, which is highly expressed in the heart and kidneys, has been linked to worse outcomes in patients but also has been proposed as a useful biomarker of cardiorenal damage. This microRNA is considered to play an important role in both the CVDs, CKD and CRS, as it has been reported in all types of CRS [345]. Due to its implication in the fibrotic pathways, miR-21-5p is known to be involved in cardiac remodeling and regeneration, as well as in the progression of AKI to CKD; therefore, its suppression could act as a therapeutic approach for CRS. It has been shown that CKD patients present an increase of miR-21-5p levels that directly correlates with lower GFR [346]. In these patients, this microRNA seems to inhibit Smad7, enhancing the TGF-β1 signalling pathway which will lead to inflammation and renal fibrosis [347, 348]. Furthermore, there is a positive loop between TGF-β1 and miR-21. TGF-β1 can increase miR-21-5p expression in the mesangial cells, leading to the activation of the phosphoinositide 3-kinase/protein kinase B (PI3K/AKT) pathway, which results in ECM deposition and mesangial hypertrophy [349].

Although the trigger for microRNA modulation in a pathology cannot always be determined, it is known that both miR-21 and miR-29 expression can change due to the RAAS activation, a common mechanism in CRS. Ang II infusion in tubular epithelial cells has proven to downregulate the levels of miR-29 and upregulate those of miR-21, which translated into TGF-β mediated fibrosis [350]. These are only some examples, as modulation in multiple microRNAs have been associated

with fibrosis [343, 344] and the CRS pathological context [351, 352]. Although data seems to suggest that microRNAs could be useful as biomarkers or therapeutic targets for the cardiorenal damage, there is still confounding data about its application in the clinical setting, mainly due to both the complexity of the CRS pathology and of the microRNA regulatory network. Therefore, monitoring microRNA expression in genome-wide analysis could help distinguish microRNA dysregulations associated with diagnosis and/or prognosis in CRS-induced fibrosis. In this context, the Let-7 family, one of the largest most conserved microRNA families across different species, could be of interest.

Since its discovery in the year 2000, the Let-7 family, which in humans is constituted by 10 mature microRNAs (let-7a, b, c, d, e, f, g, i, and miR-98 and miR-202), has been studied in a wide range of diseases, being considered the 5$^{th}$ most abundant within the myocardial tissue [353]. Although initially it was considered a developmental regulator and tumoral suppressor [354, 355], current knowledge has linked the members of this family to many cardiovascular alterations such as arrhythmia [356], angiogenesis [357], cardiac hypertrophy [358, 359] and hypertension, among others. It is important to note that all microRNA expression must be understood as organ and pathology dependent. For example, cardiac diseases are usually associated with the upregulation of this family [360, 361], while vascular injuries are characterized by a marked downregulation of the let-7 family [353, 362]; however, each member can have different impact on the same processes.

# *Hypothesis and objectives*

## I. Hypothesis

Galectin-3, through the activation of endoplasmic reticulum stress, plays an important role in the renal alterations associated with cardiorenal syndrome type 1 in the context of obesity and myocardial infarction.

**Hypothesis foundation**

1. Patients with renal damage and cardiac dysfunction show worse outcomes than those with normal renal function.

2. Myocardial infarction promotes cardiac and renal fibrosis, which translates into functional alterations.

3. Obesity promotes cardiac and renal fibrosis, which translates into functional alterations.

4. Obesity exponentially increases the risk of developing myocardial infarction.

5. Fibrosis is a key factor in the progression of cardiorenal damage; however, there are no pharmacological treatments capable of reversing fibrotic processes.

6. Galectin-3 is a profibrotic and proinflammatory factor that is increased in patients with myocardial infarction and obesity.

7. Endoplasmic reticulum stress is activated at cardiac level in myocardial infarction and obesity and promotes an increase in extracellular matrix accumulation.

8. Myocardial infarction and obesity modulate the expression of microRNAs, post-transcriptional regulators of gene expression that are involved in various physiological and pathological processes, making them potential therapeutic targets for different diseases.

## II. General objectives

The overall aim of this study was to assess the impact of myocardial ischemia on renal damage in the presence or absence of obesity, as well as the role of Galectin-3 in this pathological context.

**Specific objectives**

1. To characterize the renal alterations, including renal function, fibrosis, inflammation, endoplasmic reticulum stress and oxidative stress, in an animal model of myocardial infarction as well as the possible mechanisms involved.

2. To evaluate the involvement of Galectin-3 in the previously mentioned renal alterations in a pathological context of myocardial ischemia and obesity.

3. To assess the role of endoplasmic reticulum stress in the previously mentioned renal alterations in a pathological context of myocardial ischemia and obesity.

4. To analyze the possible interaction between Galectin-3 and endoplasmic reticulum stress in renal damage in a pathological context of myocardial ischemia and obesity.

5. To characterize the plasmatic microRNA pattern in a pathological context of myocardial ischemia and obesity as well as their possible involvement in the associated damage through *in-vitro* studies.

# *Material and methods*

## I. Animal studies

The animal Care and Use Committee of Universidad Complutense de Madrid approved all the experimental procedures (PROEX 121/18) according to the Spanish Policy for Animal Protection RD53/2013, which meets the European Union Directive2010/63/UE.

### 1. Animal model of myocardial infarction.

Male Wistar rats between 320-350 g (Envigo RMS, S.L., Barcelona, Spain) with myocardial infarction (MI) were used and compared with animals subjected to SHAM operation.

MI was induced by ligation of the left anterior descendent (LAD) coronary artery in anesthetized (2% isofluorane), intubated and ventilated (Inspiraasv, Harvard Instruments) rats that were placed on an adjustable heating pad to maintain the temperature at 37˚C. The heart was exposed through the fourth intercostal space separated with an adjustable micro-retractor (Medicon eG, Tuttlingen, Germany) and the LAD was ligated using a 4/0 silk suture (Lorca Marín, S.A., Murcia, Spain), 1 mm distal to left atrial appendage. SHAM operation consisted of the same surgical procedure without the fastening of the suture passing the LAD. These animals were included as the reference group (CT). Buprenorphine (0.05 mg/kg; Ecuphar Veterinaria, Barcelona, Spain) was provided via intramuscular injection every 8 hours for 48 hours after the surgery. After recovery, the animals were kept in collective cages with free access to food and water in the animal facility of the Universidad Complutense de Madrid.

### 2. Animal model of myocardial infarction and obesity.

Male wistar rats of 150 g (Envigo RMS, S.L., Barcelona, Spain) were fed either a high fat diet (HFD, 35% fat; Envigo Teklad ref no. TD.03307.PWD, Haslett, MI,

U.S.A) or a standard diet (5,3% fat; LasVendi ref no. LASQCdiet® Rod18-A, Germany) for a period of 10 weeks. At the sixth week, once a significant difference in body weight was observed between the groups, MI was induced following the same procedure as in the previously described animal model.

Animals were weighted once a week to control body weight evolution. Both the food and drink intake were checked periodically throughout the experimental period. Animals were divided in three groups and treated with:

1. Vehicle. The vehicle used was filtered and sterilized drinking water provided by the animal facility.

2. Galectin-3 activity inhibitor MCP (*modified citrus pectin*; 100 mg/kg/day) in the drinking water for 4 weeks post-surgery. The dose of inhibitor was based on previous data [239].

3. Endoplasmic reticulum (ER) stress inhibitor 4-PBA (*4-phenylbutiric acid*; 500 mg/kg/day) via intraperitoneal injection and in the drinking water for 4 weeks after the surgery. The dose of this inhibitor was based on the literature [363].

**3. Systolic Blood Pressure (SBP).**

Systolic blood pressure (SBP) was indirectly determined at the end of the study by tail-cuff plethysmography (Narco Bio-Systems, Huston, TX, U.S.A.) in unrestrained rats. Prior to the final measurements, simulations of the procedure were conducted to habituate the animals to the procedure and to avoid distortions in the experimental data. The rats were kept for 30 min at 37°C and, after that time, blood pressure was measured 8 consecutive times, considering its arithmetic mean as the final SBP value. All the measurements were obtained during the morning hours (between 10 a.m. and 12 a.m.).

**4. Evaluation of cardiac structure and function.**

These measurements were obtained in the last week of the protocol. To study the cardiac structure and function, animals were anesthetized with 2% isoflurane and transthoracic echocardiography (TTE) was performed with a Vivid-I (General Electric Healthcare, Boston, MA, U.S.A.) connected to a 12 MHz transducer and by magnetic resonance imaging (MRI). Then, 2D-guided M-mode recording made were made from short-axis to measure the left ventricular (LV) chamber end-diastolic dimensions, interventricular septum (IVT), and posterior wall thickness (PWT). The mean measurements from several consecutive beats were used for the data analysis.

Diastolic function was assessed by early and late transmitral peak diastolic flow velocity (E and A waves) and ratio between E-waves and A-wave (E/A ratio) was calculated. End-diastolic diameter (EDD) and end-systolic diameter (EDS) were used to calculate the left ventricular ejection fraction (LVEF) in percentage according to the Teicholz Formula:

$$(EDD^3\ x\ 7)/(2.4 + EDD)$$

The infarct size and LV mass were defined by MRI, performed with the Biospec BMT 47/40 spectrometer (Bunker, Ettlingen, Germany) located at the CAI Center of the Universidad Complutense de Madrid. Infarct size was measured by late gadolinium enhancement.

**5. Euthanasia.**

Animals were euthanized by decapitation using a guillotine after body weight measurement. Blood was collected either in a tube containing the anticoagulant EDTA to obtain the plasma or without anticoagulant to attain serum. Afterwards, the tubes were centrifuged at 3000 rpm for 15 min to collect and aliquot the supernatant, which was then stored at -80°C.

The kidneys were removed carefully from the animals, the blood was eliminated and the decapsulated kidneys were weighted separately before carving the medulla portion. The left kidney was cut in several pieces, and immediately frozen in liquid nitrogen and stored at -80°C for molecular biology studies. For histological studies, a cross section of the right kidney was stored in 4% (w/v) formaldehyde and another cross section was placed in 30% (w/v) sucrose solution for approximately 4 hours before embedding it in the tissue freezing medium (OCT), freezing it in liquid nitrogen and storing it at -80 °C.

Fat pockets such as epididymal, mesenteric, lumbar, and brown fat were also extracted and weighted after removal of blood clots. The adiposity index was calculated by the following formula:

$$\frac{fat\ deposits\ sum\ (g)}{body\ weight\ (g) - fat\ pad\ weight\ (g)}\ x\ 100$$

Fat deposit sum being the sum of epididymal, mesenteric and lumbar fat.

**6. Circulating parameters.**

The collected blood samples during the euthanasia were used to study the circulating concentrations of various analytes through ELISA kits. The kits are based in precoated 96-well plates for a specific antibody in which standards and samples are incubated in order to obtain a colorimetric reaction that can be measured in a spectrophotometer to know each sample concentration for the evaluated protein.

In this sense, Angiotensin II (Ang II; Abbexa, Cambridge, UK; Ref: abx052349) and thiobarbituric acid reactive substances (TBARS; Sigma Aldrich, Missouri, U.S.A.; Ref: MAK085) levels, were measured following the instructions of the manufacturer and densitometries have been expressed in arbitrary units (A.U.).

### 6.1. Palmitic Acid.

In order to measure palmitic acid (PA), aliquots of 100 µl of plasma were transferred to Eppendorf tubes and mixed with 10 µl of standard mixture. The lipids were then extracted with hexane/isopropanol, 3:2 v/v at a 1:10 sample/solvent ratio. The tubes were vortexed and maintained at −20˚C for 10 min, then centrifuged at 14.000 g at 4˚C for 5 min. The supernatant was collected, transferred to glass tubes, and dried under nitrogen flow. Then, 1 ml of 80% methanol was added, and the tubes were thoroughly mixed.

The liquid chromatography-tandem mass spectrometry (LC-MS/MS) system comprised a Shimadzu UHPLC Nexera X2 system hyphenated to a triple quadrupole mass spectrometer LCMS-8030 (Shimadzu Corporation, Kyoto, Japan). The mass spectrometer was operated with an electrospray ionization (ESI) source in negative mode. The desolvation line and heat block temperatures were set at 250 and 400˚C, respectively. The interface voltage was maintained at 3.5 kV. Nitrogen was used as nebulizing and drying gas at a flow of 1.5 and 15 l/min, respectively. Argon was used as collision gas at 230 kPa.

### 6.2. Creatinine.

Plasma creatinine levels were measured using spectrophotometric techniques in an autoanalyzer (Vitros 5600, Diagnostics Ortho Clinical, Johnson & Jonson, New Brunswick, NJ, U.S.A.).

### 6.3. Microarray.

In order to quantify miRNAs expression in the plasma of the animals from the SHAM and HFD-MI groups, a Human PCR panel from Exiqon was used. For that purpose, 10 ng of the isolated miRNA samples from each group were divided into pools of 6 animals each. 30 ng of total RNA from each pool was employed for cDNA synthesis with miRCURY LNA™ Universal RT microRNA PCR System (Exiqon/Qiagen; Hilden, Germany) following the manual's instructions.

Reverse transcription reaction efficiency and polymerase chain reaction (PCR) inhibitors presence were checked with UniSp6 and Cel-miR-39-3p, respectively. PCR determinations were then performed using the Serum/Plasma focus microRNA PCR Panel V4.M (Exiqon/Qiagen; Hilden, Germany; Ref: 339325) which allows for the analysis of 179 microRNAs. The amplification was performed in an ABI 7900HT qPCR instrument (Life Technologies Ltd.) in 384-well plates. The amplification curves were analysed using the SDS v.2.4 software (Life Technologies Ltd.) with manual baseline/threshold settings to determine the threshold cycles (Ct). Blank controls consisting in a qPCR reaction where the sample was replaced by water were included to assess the presence of contamination. Out of the initial panel of 179 analysed microRNAs, 28 were eliminated since they were not expressed in any of the samples. Data was normalized using miR-23a-3p as reference control, which was previously selected from a panel screening of stably expressed miRNAs. Fold changes were calculated using $2^{-\Delta\Delta Cq}$ method.

**7. Histological and morphological evaluations.**

Renal samples were fixed in formaldehyde 4% for at least 24 hours before its dehydration with increasing solutions of ethyl alcohol and a final step of xylol. Once completely dehydrated, the tissue was embedded in liquid paraffin (56 °C). The tissue paraffin blocks were cut with a microtome (Leica 1512, IMEB INC, CH, U.S.A.) in 4 μm-thick sections.

For each sample stained, 15 fields all through the cortex with a 20X objective under transmitted light microscopy were evaluated (Leica DM 2000; Leica AG, Germany). Quantification was performed by the image analyser (Leica Q550 IWB).

### 7.1. Haematoxylin-Eosin staining.

In order to evaluate glomerular area, previously deparaffined and rehydrated kidney sections were stained with haematoxylin for 15 min and eosin for 2 min. Once stained, slides were dehydrated and mounted using entellan™ and coverslips.

### 7.2. Picrosirius Red staining.

The area of interstitial, glomerular and perivascular fibrosis was detected with picrosirius red staining, which dye the collagen fibres red and the rest of the tissue a light pink colour. After deparaffination and rehydration of the kidney sections, phosphomolybdic acid 0.2% was used for 2 min in order to allow the dye to penetrate the tissue. Slides were then embedded in picrosirius red for 1 hour. Once stained, slides were dehydrated and mounted using entellan™ and coverslips.

## 8. In situ detection of superoxide anion ($O_2^{\cdot-}$) levels.

The oxidative fluorogenic dye dihydroethidium (DHE) was used to detect the superoxide anion ($O_2^{\cdot-}$) levels in the kidney samples previously embedded in OCT. Sections of 14 μm thickness were cut using a cryostat and place onto microscope slides treated with 3-Aminopropyltriethoxysilane (APES). The day of the experiment, slides were placed at 37°C for a minimum of 1 hour to fix the sample, preventing its detachment from the glass. After that, Krebs-HEPES buffer (composition in the annex VI.2.) was used for 30 min to wash the slides, and then, they were incubated with DHE ($2x10^{-6}$ M) for 30 min at 37°C in a dark humidified chamber. The reaction between superoxide anions and DHE generates its oxidation into ethidium which binds to the nuclear DNA. This causes a red fluorescence signal in the nucleus of the cells; whose intensity depends on the levels of $O_2^{\cdot-}$.

One tissue section per animal was photographed in 10-12 fields using a 40x objective (Leica DMI 3000; Ex 561 nm, Em 610 nm). The microscope and camera conditions were kept constants for all preparations and the fluorescence intensity was quantified with Leica application suite (Leica microsystems, Wetzlar, Germany).

## 9. Gene expression.

### 9.1. RNA extraction.

50 mg of renal tissue was pulverized using liquid nitrogen (N2) and then, 900 µl of Trizol reagent (Fisher Scientific, Waltham, MA, U.S.A.) were added to each sample and kept at -80˚C for at least 12 hours.

On the day of the extraction, tissue was homogenized using 50 mg of 0.5 mm Zirconium oxide beads and the Next Advance Storm Bullet Blender (Scientific Instrument Services, MA, U.S.A.) according to the user guide. Chloroform was then added and centrifuged in order to separate the homogenate into phases. The upper aqueous phase is transferred into a different Eppendorf and isopropanol is added to precipitate the extracted RNA after centrifugation (same volume than the aqueous phase obtained). After washing with cold ethanol (70° and prepared in RNase/DNase free water) and leaving to dry, the obtained pellet was resuspended with 200 µl RNase/DNase free water (Fisher Scientific, Waltham, MA, U.S.A.).

RNA concentration was quantified measuring the sample absorbance at 260 and 280 nm. The sample's purity was assessed by the 260/280 and 260/230 ratio, considering optimal values those close to 2. All these quantifications were done with Implen™ NanoPhotometer N6O (Fisher Scientific, Waltham, MA, U.S.A.).

### 9.2. Reverse transcription.

1.5 µg of the extracted RNA was reverse transcribed into complementary DNA (cDNA) using the High-Capacity cDNA Reverse Transcription Kit (Thermo Fisher Scientific Inc, Waltham, MA, U.S.A.) in a total volume of 20 µl. The reaction was done in a thermocycler with a first step of 10 min at 25˚C, followed by 120 min at 37˚C, a third step of 5 min and 85˚C and then conserved at 4˚C until its dilution to 5 ng/µl and storage at -20˚C.

### 9.3. Real-time RT-PCR.

Quantitative PCR analysis was performed with SYBR green PCR technology in a Quant Studio 3 (QS3) Real-Time PCR instrument with Quant Studio Design & Analysis Desktop Software (Applied Biosystems, Waltham, MA, U.S.A.).

Per sample, PCR reaction mix was prepared by adding: 6 µl of cDNA at 5 ng/µl, 7.5 µl of 2x SYBRGreen PCR Master Mix and 1.5 µl of forward and reverse primer mix at 10 µM (Sequences shown in Table 5). In order to quantify the mRNA levels in each sample the $2^{-\Delta\Delta Cq}$ method was used, which can be defined as the difference between the normalized cycle threshold (CT) of an experimental group and the normalized CTs of the control group.

In these experiments, data was normalized to the housekeeping genes hypoxanthine phosphoribosyltransferase (HPRT) and 18S, two genes whose expressions are not altered in the experimental conditions.

**Table 5.** Rat primer sequences.

| Gene | Temperature | Forward Primer | Reverse primer |
|---|---|---|---|
| *Atf4* | 60 ˚C | AATGGATGACCTGGAAACCA | TCTTGGACTAGAGGGGCAAA |
| *Atf6α* | 60 ˚C | TCTCTTCTCCTCGGTCCACA | AGCTGTCGCCATACAAGGAA |
| *Atf6β* | 60 ˚C | TCCAGATCACTGTGGGCTCT | CCTCGGAGTTGACAGAGGAAG |
| *Bip* | 60 ˚C | TGGGTACATTTGATCTGACTGGA | CTCAAAGGTGACTTCAATCTGGG |
| *Col1a1* | 62 ˚C | GCCTCCCAGAACATCACCTA | ATGTCTGTCTTGCCCCAAGT |
| *Col4a1* | 62 ˚C | GCCAAGTGTGCATGAGAAGA | AGCGGGGTGTGTTAGTTACG |
| *Ctgf* | 60 ˚C | GAGTCGTCTCTGCATGGTCA | CCACAGAACTTAGCCCGGTA |
| *Fn1* | 62 ˚C | GGGGTCACGTACCTCTTCAA | TGGAGGTTAGTGGGAGCATC |
| *Gal-3* | 60 ˚C | AGCCCAACGCAAACAGTATC | GGCTTCAACCAGGACCTGTA |
| *Il-6* | 62 ˚C | GCCCTTCAGGAACAGCTATG | GTCTCCTCTCCGGACTTGTG |
| *Kim1* | 60 ˚C | GTGAGTGGACCAGGCACACA | AATCCCTTGATCCATTGTTTTCTT |
| *Lats1* | 62 ˚C | GAAGTGCTACTACGGACAGGATA | GACTGAGCTTGGCTTGAGGT |
| *Ngal* | 60 ˚C | CGATGAACTGAAGGAGCGAT | TCTGGCAACAGGAAAGATGG |
| *Ccl-2* | 60 ˚C | TTCCTTATTGGGGTCAGCAC | CAGTTAATGCCCCACTCACC |
| *Opn* | 60 ˚C | ATGAGACTGGCAGTGGTT | GCTTTCATTGGAGTTGCT |
| *Slug* | 62 ˚C | CCCAACTACAGCGAACTGGA | GCATGGGGTAGCTCTCACAG |
| *Snail* | 62 ˚C | AGTTGTCTACCGACCTTGCG | TGCAGCTCGCTATAGTTGGG |
| *Tead1* | 62 ˚C | TGTCAAATTCTGGGCGGACT | ATCGGCCATTCTCGAACCTC |
| *Tgf-β* | 62 ˚C | CAGAAGTTGGCATGGTAGCC | TGCTTCAGCTCCACAGAGAA |
| *Tnfα* | 62 ˚C | ACTCGAGTGACAAGCCCGTA | GATAAGGTACAGCCCATCTGC |
| *Yap1* | 62 ˚C | GTTCGAGCTCACTCGTCTCC | ATATTCCGTATTGCCTGCCGAA |
| *sXbp1* | 60 ˚C | CTGAGTCCGAATCAGGTGCAG | ATCCATGGGAAGATGTTCTGG |
| *usXbp1* | 60 ˚C | CAGCACTCAGACTACGTGCG | ATCCATGGGAAGATGTTCTGG |
| *tXbp1* | 60 ˚C | TGGCCGGGTCTGCTGAGTCCG | ATCCATGGGAAGATGTTCTGG |
| *α-Sma* | 62 ˚C | GAAGGAATAGCCACGCTCAG | TGTGCTGGACTCTGGAGATG |
| *18S* | 60 ˚C | CATTCGAACGTCTGCCCTAT | GTTTCTCAGGCTCCCTCTCC |
| *Hprt* | 62 ˚C | AGGACCTCTCGAAGTGT | ATTCAAATCCCTGAAGTACTCAT |

*Atf4*: Activating transcription factor 4; Atf6*α*: Activating transcription factor 6 alpha; *Atf6β*: Activating transcription factor 6 beta; *Bip:* Binding immunoglobulin protein; *Col1a1*: Collagen type I alpha 1 chain; *Col4a1*: Collagen type IV alpha 1 chain; *Ctgf*: Connective tissue growth factor; *Fn1*: Fibronectin 1; *Gal-3*: Galectin-3; *Il-6*: Interleukin 6; *Kim1*: Kidney injury molecule 1; *Lats1*: Large tumor suppressor kinase 1; *Ngal*: Neutrophil gelatinase associated lipocalin; *Ccl-2*: C-C motif chemokine ligand 2; *Opn*: Osteopontin; *Slug*: Snail family transcriptional repressor 2; *Snail*: Snail family transcriptional repressor 1; *Tead1*: TEA domain transcription factor 1; *Tgf-β:* Transforming growth factor beta; *Tnf α*: Tumor necrosis factor alpha; *Yap1*: Yes1 associated transcriptional regulator; *sXbp1*: spliced X-Box binding protein 1; usXbp1: unspliced X-Box binding protein 1; *tXbp1*: total X-Box binding protein 1; *α-Sma*: Alpha 2 smooth muscle actin; *Hprt*: Hypoxanthine Phosphoribosyltransferase.

### 9.4. MicroRNA analyses in tissue samples.

To analyse the content of target microRNAs in tissue samples we used Taqman PCR Technology. All microRNA assays were purchased from Applied Biosystems (Waltham, Massachusetts, U.S.A.). In brief, specific microRNA primers were used to reverse transcribe total RNA and the RT products were amplified by using TaqMan probes and appropriate master mixes thereafter.

Instead of random hexamers or oligo dTs, specific microRNA assay primers (Table 6) were employed for the reverse transcription of 10 ng of total RNA using the TaqMan™ MicroRNA Reverse Transcription Kit (Applied Biosystems, Waltham, Massachusetts, U.S.A.; Ref: 4366596). Such system enhances the efficiency and specificity of the ulterior qPCR analyses. The RT reaction was done in a thermocycler following the provider's recommendations. Briefly, a first step of 30 min at 16˚C was followed by 30 min at 42˚C, a third step of 5 min at 85˚C and then conserved at 4˚C until its 2-fold dilution.

**Table 6.** MicroRNA TaqMan assays from Applied Biosystems (Ref: 4427975) used for microRNA expression studies.

| Gene Name | Reference sequence | Assay ID |
|---|---|---|
| snRNU6 | NR_004394 | ID 001973 |
| let-7f-5p | NR_029483 | ID 000382 |
| miR-17-5p | NR_029487 | ID 002308 |
| miR-144-5p | NR_031890 | ID 464811 |
| miR-339-3p | NR_031784 | ID 002059 |
| miR-485-3p | NR_032132 | ID 462841 |

Downstream quantitative PCR (qPCR) amplifications were performed using a TaqMan® Universal PCR Master Mix, no AmpErase® UNG (Applied Biosystems, Waltham, Massachusetts, U.S.A.) combined with the specific microRNA primers and Taqman probe mixtures for each miRNA of interest. The

reaction was done in a Quant Studio 3 (QS3) Real-Time PCR instrument with Quant Studio Design & Analysis Desktop Software (Applied Biosystems, Waltham, MA, U.S.A.) following the manufacturer's indications. In brief, the thermal cycler with an initial hold stage of 2 min at 50°C, followed by 10 min at 95°C for polymerase activation. The cycling stage of the PCR is divided into a denaturing step of 15 seconds at 95°C; the annealing and extension step consisted on 40 cycles of 60°C for 60 seconds.

In order to quantify mRNA levels in each sample the $2^{-\Delta\Delta Cq}$ method was used as per the MIQE guidelines [364]. RNU6-1 (codifying for U6 snRNA) was used as reference gene to normalize miRNA readouts for rat samples and *in-vitro* studies.

## 10. Protein measurements.

### 10.1. Protein extraction

100 mg of renal tissue was pulverized using liquid nitrogen ($N_2$) and then homogenized with 300 µl of Lysis buffer (composition in the annex VI.1.1.) with the T10 Basic Ultra Turrax homogenizer (IKA-Werke, Staufen, Germany). The homogenate was incubated for 30 min on ice and centrifuged at 13.000 rpm for 12 min at 4°C. The supernatant was collected and stored at -80°C until use.

Protein quantification was done following the Bradford protein colorimetric assay. In brief, the Coomasie brilliant blue dye binds to the proteins resulting in a shift from orange (absorbance at 460 nm) to blue (absorbance at 610 nm), having its greatest difference peak of absorbance at 595 nm. Development of colour in Coomasie dye-based protein assays is due to the presence of basic amino acids in the proteins in an acidic environment. Two-fold dilutions of bovine serum albumin (BSA; 2mg/mL) were used to prepare standard curves. The lysis buffer was tested to rule out any background effect on our readouts.

### 10.2. Western blot

Aliquots of 40 μg of renal proteins were denatured by heating at 95 °C for 5 min in presence of β-mercaptoethanol. Sodium dodecyl sulphate (SDS)-PAGE on polyacrylamide Criterion™ TGX™ Precast Gels (Bio-Rad, California, U.S.A.) were submerged in running buffer (composition in Annex VI.1.) in order to separate the proteins according to molecular weight via electrophoresis. After sample and protein marker loading, an electric current of 100 mA for approximately one hour was applied. After the electrophoresis, the separated proteins were transferred to Transblot® Turbo™ Midisize Nitrocellulose (Bio-Rad, California, U.S.A.) with the Transblot® Turbo™ Transfer System. Transfer buffer composition is detailed in the annex VI.1.

For immunodetection, the nitrocellulose membranes were blocked with 7.5% non-fat dry milk in PBST for 1 hour at room temperature and slow agitation. Each primary and secondary antibody incubation conditions are detailed in Table 7. The chemiluminescence signal was detected using ECL (Millipore, Burlington, MA, U.S.A). Several proteins were analysed in the same membrane after embedding it for 7 minutes in stripping buffer in fast agitation (Thermo Scientific, Waltham, MA, U.S.A.). The results are expressed as fold-change relative to the control condition in arbitrary densitometric units.

**Table 7.** Immunodetection conditions for the proteins measured by western blot.

| Antibody | Molecular weight | Dilution | Secondary antibody and dilution | Commercial reference |
|---|---|---|---|---|
| **Primary antibodies** | | | | |
| 4-HNE | 65 kDa | 1:250 | α- Rabbit (1:1000) | Abcam |
| ATF4 | 39 kDa | 1:1000 | α- Rabbit (1:1000) | Proteintech |
| ATF6α | 90 kDa | 1:250 | α- Mouse (1:250) | Santa Cruz Biotechnology |
| BiP | 78 kDa | 1:1000 | α- Mouse (1:1000) | BD bioscience |
| Catalase | 64 kDa | 1:500 | α- Mouse (1:5000) | Santa Cruz Biotechnology |
| CHOP | 30 kDa | 1:500 | α- Mouse (1:500) | Cell Signalling |
| Collagen I | 115 kDa | 1:500 | α- Rabbit (1:1000) | Calbiochem |
| Collagen IV | 180 kDa | 1:500 | α- Mouse (1:1000) | Santa Cruz Biotechnology |
| CTGF | 37 kDa | 1:500 | α- Rabbit (1:1000) | Sigma Aldrich |
| Fibronectin | 260 kDa | 1:500 | α- Mouse (1:500) | Millipore |
| Galectin 3 | 30 kDa | 1:500 | α- Mouse (1:500) | Santa Cruz Biotechnology |
| pAKT | 60 kDa | 1:1000 | α- Rabbit (1:1000) | Cell Signalling |
| PDIA6 | 48 kDa | 1:500 | α- Rabbit (1:500) | Abcam |
| pERK1/2 | 42-44 kDa | 1:1000 | α- Rabbit (1:1000) | Cell Signalling |
| pNFkB | 60 kDa | 1:1000 | α- Rabbit (1:1000) | Abcam |
| pYAP1 | 65 kDa | 1:500 | α- Rabbit (1:500) | Invitrogen |
| TGF-β | 25 kDa | 1:500 | α- Mouse (1:500) | Santa Cruz Biotechnology |
| Total AKT | 60 kDa | 1:1000 | α- Rabbit (1:1000) | Cell Signalling |
| Total ERK1/2 | 42-44 kDa | 1:1000 | α- Rabbit (1:1000) | Thermo fisher |
| Total NFkB | 60 kDa | 1:1000 | α- Rabbit (1:1000) | Abcam |
| Total YAP1 | 65 kDa | 1:500 | α- Rabbit (1:500) | Invitrogen |
| α-SMA | 42 kDa | 1:500 | α- Rabbit (1:1000) | GeneTex |
| β-actin (Constitutive) | 42 kDa | 1:5000 | α- Mouse (1:5000) | Sigma Aldrich |
| GAPDH (Constitutive) | 37 kDa | 1:5000 | α- Rabbit (1:5000) | Cell Signalling |
| **Secondary antibodies** | | | | |
| α- Mouse | - | - | - | GE Healthcare |
| α- Rabbit | - | - | - | Cytiva |

4-HNE: 4-Hydroxynonenal; ATF4: Activating transcription factor 4; ATF6α: Activating transcription factor 6 alpha; BiP: Binding immunoglobulin protein; CHOP: CCAAT-enhancer-

binding protein homologous protein; CTGF: Connective tissue growth factor; pAKT: Phosphorilated Protein kinase B; PDIA6: Protein disulfide isomerase family A member 6; pERK1/2: Phosphorilated extracellular signal-regulated kinases 1/2; pNFkB: Phosphorilated nuclear factor-κB; pYAP1: Phosphorilated Yes1 associated transcriptional regulator; TGF-β: Transforming growth factor beta; α-SMA: Alpha 2 smooth muscle actin; GAPDH: Glyceraldehyde-3-phosphate dehydrogenase.

### 10.3. Zymography

20 µg of tissue protein lysates prepared with loading dye buffer ((0.8% SDS, 5% glycerol, 0.002% bromophenol blue, 32 mM Tris-HCl pH 6.8) were loaded into 10% SDS polyacrylamide gels containing 0.14% gelatine. After electrophoresis at 70 mA (performed as described in section I.10.2.), gels were rinsed 3 times for 10 min with 2.5% Triton X-100 solution to re-naturalize the metalloproteinases. Afterwards, gels were incubated overnight at 37°C in a buffer that contains 1M Tris-HCl, pH 7.5 with 10 mM CaCl2 and 50 mM NaCl to promote gelatine degradation by the metalloproteinases. Gels were stained with Coomassie blue R250 at room temperature and then washed with a discolouring buffer (10% acetic acid, 40% methanol and 50% distilled water) to identify the metalloproteinases (MMPs) proteolytic activity. Fold changes in band densitometries have been expressed in arbitrary units (A.U.).

## II. Clinical study

### 1. Clinical cohort.

The "Third Universal Definition of Myocardial Infarction" [365] defines an acute myocardial infarction (MI) as an increase in biomarkers in the presence of ischemia, ST-T changes, the appearance of new Q waves and identification of alterations of local contraction by image technique or intracoronary thrombus detected by angiography. Patients who suffered a first MI were recruited from

the Cardiology Department of Hospital Clínico San Carlos, Madrid, Spain. Exclusion criteria were previous MI or myocardial revascularization, hemodynamic instability 12 h previous revascularization, severe chronic kidney disease with a creatinine clearance < 30 ml/min/1.7m$^2$.

Twenty-four to forty-eight hours after hospital admission for MI, patients underwent transthoracic echocardiographic and at the same time blood samples were collected. A group of healthy volunteers (n =12) were recruited from staff of the hospital. The study protocol was approved by the ethics committee (18/195-E) and all participants signed the informed consent. The present study was conducted in compliance with Good Clinical Practice Guidelines and the ethical principles stated in the Declaration of Helsinki.

**2. Echocardiography.**

Echocardiographic studies were performed by expert cardiovascular imaging cardiologists with the ultrasound system Vivid® (GE Healthcare, Waukesha, WI, U.S.A.), equipped with a 2.5 MHz transductor. Image processing was conducted using Echopack software v.201 (General Electric Healthcare, Boston, MA, U.S.A.).

TTE images and chamber quantifications such as left ventricular dimensions, volumes and systolic and diastolic function were acquired according to the American Society of Echocardiography and the European Society of Cardiovascular Imaging [366, 367].

Traditional TTE planes were utilized, such as the parasternal long axis for the measurement of the left ventricle (LV) wall thickness to calculate ventricular mass.

Furthermore, two-chamber (2C), three-chamber (3C), and four-chamber (4C) apical planes were obtained to measure LV end-diastolic (EDV) and end-systolic (ESV) volumes. Systolic function was classified by the LV ejection fraction (LVEF),

which was determined by the ratio of LV end-diastolic volume (LVEDV) to LV end-systolic volume (LVESV), both obtained from the apical 4C and apical 2C planes using the following formula:

$$LVEF = (LVEDV - LVESV)/LVEDV$$

For diastolic function, early and late transmitral peak diastolic flow velocity (E and A waves) were evaluated. The E/A ratio, derived from these measurements, was also calculated. Diastolic function was also evaluated by peak E-wave velocity by the peak e' velocity (E/e') ratio obtained by means of tissue Doppler imaging in both lateral and septal segments of the mitral annulus.

**3. Circulating parameters.**

Blood samples were obtained following the clinical protocol approved by the Hospital Clínico San Carlos. Each patient was identified at the hospital with a code that was used as identification for each tube. Serum concentration of Neutrophil gelatinase-associated lipocalin (NGAL; R&D systems, Minneapolis, U.S.A.) and other analytes were analysed according to the manufacturer's instructions.

## III. *In-silico* analysis

In order to understand microRNA-dependent regulation and its possible association with a specific pathology, bioinformatic/computational tools were used. These programs' predictions and analysis are based on algorithms that integrate different criteria, such as miRNA complementarity, binding energy or stability of the miRNA:mRNA duplex. Given the variances among the available tools, consensus among the scientific community dictates that several prediction parameters must be used in order to validate a target.

In this study, *in-silico* identification of possible let-7f-5p targets was carried out via the open-access prediction tools TargetScan, TarBase, microT-CDS and miRWalk 2.0, as well as miRPath to assess the potentially regulated signaling pathways. Results from these analyses predicted the union of let-7f-5p to the 3'UTR sequence of 3007 targets with a threshold set to 0.5 and the implication of said microRNA in 30 KEGG pathways. An extensive revision of the literature identified for potential targets in fibrosis and endoplasmic reticulum stress such as *Atf4*, *Atf6β*, *Eif2ak1*, *Col 1a1*, *Col 4a1* and *Fn1*. However, given the results obtained in the *in-vitro* experiments, further luciferase assays were carried out only on *Atf6β* to evaluate its possible role as a let-7f-5p target (Figure 8).

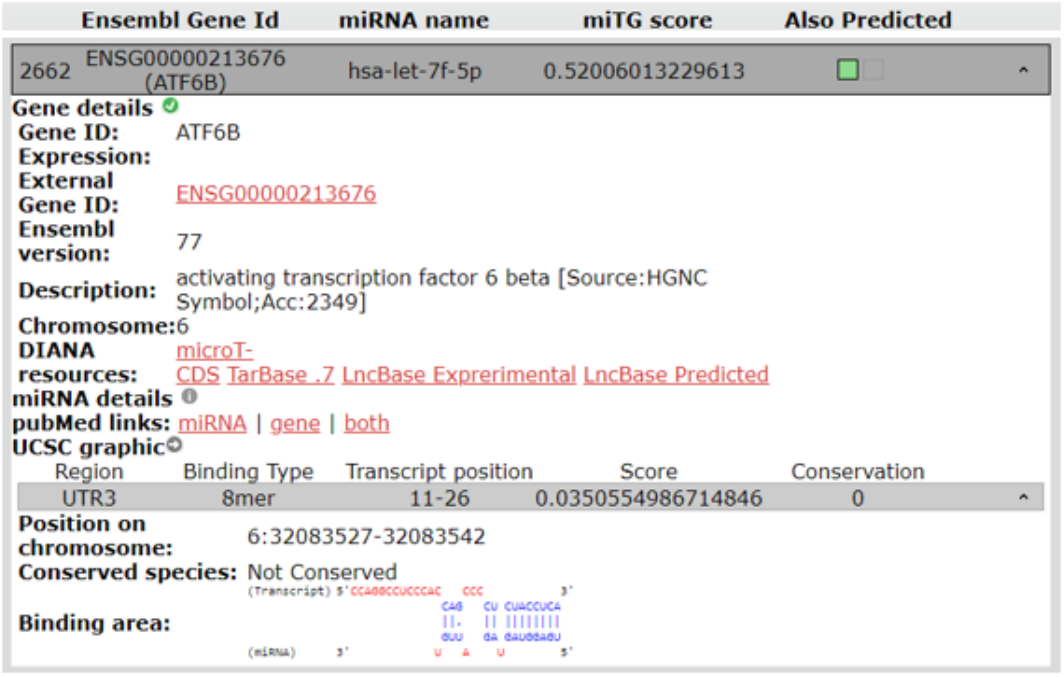


**Figure 8**. DIANA-tools prediction of let-7f-5p interaction to *Atf6β*'s gen 3'UTR region.

## IV. *In-vitro* cell culture studies

### 1. Renal fibroblasts.

For this study murine renal interstitial fibroblast (TFBs) was used. This cell line was originally isolated from SJL mouse kidney and was a generous gift from Dr. A.C. Ucero. Cells were seeded in T75 tissue culture flasks pretreated with poly-l-lysine (0.1 mg/ml; Sigma Aldrich, Missouri, U.S.A.) and grown as a monolayer culture in RPMI 1640 medium supplemented as described in annex VI.3. Complete medium was changed every 1-2 days to remove non-adhered cells until flask confluence reached 80-90%, at which point, cells were passaged with 1x trypsin. For all the assays, cells were maintained at a constant temperature of 37°C, 95% sterile air and 5% $CO_2$ in a saturation humidified incubator.

#### 1.1. Immunocytochemistry.

To characterize the cells and confirm their fibroblast phenotype, we performed an immunocytochemistry for vimentin. For that purpose, cells were seeded in 4 well chambers and fixated with Merckofix (Merck KGaA, Darmstadt, Germany). After fixation, cells were permeabilized in the dark for at least 30 min with Triton-X-100 and incubated overnight at 4°C with vimentin's primary antibody (1:100 dilution in a mix of 65% PBS, 30% Triton-X-100 and 5% FBS; GeneTex, California, U.S.A.). After 3 PBS washes of 10 min each, cells were incubated for 1 hour at room temperature with a fluorescein-conjugated anti-rabbit (1:200 dilution in a mix of 97.5% PBS and 2.5% FBS; Vector laboratories, Newark, U.S.A.) as a secondary antibody. Cell nucleus was dyed using 4',6-diamidin-2-fenilindol (DAPI; 1:100 dilution in PBS; Sigma-Aldrich, Missouri, U.S.A.). Images were obtained using a 40x objective in a Leica DMI 3000B fluorescence microscope.

### 1.2. *In-vitro* studies.

ECM, oxidative stress, ER stress and inflammation were evaluated under the following conditions.

#### 1.2.1. Palmitic acid.

In order to choose the appropriate dose for the studies, cells were seeded and, after 24 hours in medium without serum, stimulated with 50, 100 or 200 μM of palmitic acid conjugated to 10% free fatty acids (FFA)-free BSA as a carrier. Finally, the dose of 100 μM of palmitic acid was used in all analyses in the presence or absence of the ER stress inhibitor 4-PBA at 2 or 4 μM.

#### 1.2.2. Angiotensin II.

The dose of Ang II was determined after a dose-response assay in which seeded cells were stimulated with $10^{-8}$ - $10^{-6}$M of Ang II. In order to determine the effect of ER stress on the Ang II effects, the dose of $10^{-6}$M was used in the presence or absence of the ER stress inhibitor 4-PBA at 4 μM.

The possible intracellular pathways by which Ang II exerts it effects was assessed via a time-response study in which cells were treated with $10^{-6}$M Ang II for 5, 10, 15, 30 and 60 min. Chemical inhibition of NFkB, AKT and ERK1/2 was obtained by addition of BAY11-7082, LY294002 and PD98059 (all at $10^{-6}$ M and purchased from Sigma-Aldrich, Missouri, U.S.A.) in Ang II treated cells for 24 hours.

### 2. Renal epithelial cells.

Epithelial cells of the human renal proximal tubule cell line HK-2 (ATCC, Manassas, VA, U.S.A.) were maintained in RPMI 1640 medium supplemented as described in annex VI.3. The cells were seeded in T75 tissue culture flasks and

grown as a monolayer. Complete medium was changed every 1-2 days to remove non-adhered cells until flask confluence reached 80-90%, at which point cells were passaged with 1x trypsin. For all the assays, cells were maintained at a constant temperature of 37°C, 95% sterile air and 5% $CO_2$ in a saturation humidified incubator.

### 2.1. *In-vitro* stimulation.

#### 2.1.1. Galectin-3.

In order to determine Gal-3 effects, including its possible role in modulating microRNAs, a dose and time response experiment was performed. Once the seeded cells reached a confluence of 80%, they were put in starvation media for 24 hours. After said time, cells were stimulated with $10^{-8}$ - $10^{-6}$M Gal-3 for 3, 6, 12 or 24 hours to determine dose-dependent renal injury marker levels. Once dose of $10^{-6}$M Gal-3 was selected, cells were stimulated for 3, 6, 12 or 24 hours in order to assess the miRNA modification timeframe.

#### 2.1.2. Tunicamycin.

Appropriate timing and dosage of the pharmacological ER stress activator tunicamycin (TN) was determined after a time and dose-response assay in which seeded cells were stimulated with 1.5 µg/µl for 3, 6 or 12 hours.

The dose of 1.5 µg/µl with a 12-hour stimulation was used in all analyses in the presence (mimic) or absence (mNTC; mimic Non-Target Control) of the let-7f-5p agomiR. AgomiR incubation was carried out as described in section IV.2.2 followed by the 12-hour stimulation with tunicamycin.

### 2.2. Let-7f-5p agomiR and antagomir studies.

HK-2 were seeded at 21500 cells/cm$^2$ in RPMI 1640 media (12 multi-well plates). After 24 hours, let-7f-5p antagomiR or agomiR experiments were conducted by transiently transfecting 25 nM let-7f-5p antago-miR (inhibitor), let-7f-5p ago-miR (mimic) or appropriate scramble (Scr) controls. Scramble sequences were purchased from Thermo Fisher (mirVana™ miRNA Mimic, Negative Control #1, Ref: 4464058; mirVana™ miRNA Inhibitor, Negative Control #1, Ref: 4464076, Invitrogen, Thermo Fisher, UK) to be comparable with the chemistry of the antago- and ago-miR-let-7f-5p used.

Lipofectamine RNAiMAX (Invitrogen, Thermo Fisher, Waltham, MA, U.S.A.) was used following the manufacturer's protocols. 3 µL of lipofectamine RNAiMAX and ago- or antago-miR (25 nM) were diluted into 50 µL Opti-MEM® I Reduced Serum Medium (GibcoTM, Thermo Fisher Scientific, Waltham, MA, U.S.A.), incubated for 5 min and combined (20 min) to form transfection lipocomplexes; after 20 min incubation, 100 µL of the lipocomplexes were inoculated into 500 µL final volume and incubated for 6 hours, at 37 °C, 5 % $CO_2$. Experiments started 24 hours after transfecting the cell target to allow for the miRNA targets regulation.

### 2.3. Prediction of microRNA targets and enrichment analyses

Online tools miRPath v.3 [368] and miRPath v4.0 [369] were used to identify the KEGG pathways relevant to our experimental pathological model. In brief, hsa-let-7f-5p was inputted in Tarbase, Target Scan and microT-CDS to search for relevant pathways and its interaction among databases. After an extensive revision of the literature, ECM-receptor interaction (hsa04512), Hippo signaling pathway (hsa04390) and Protein processing in endoplasmic reticulum (hsa04141) were selected for further analyses (Table 8).

Only for ECM-receptor interaction was there found a predicted pathway interaction, including COL1A1, COL1A2 or COL4A1, among Tarbase and microT-CDS. Nevertheless because of the potentially relevant contribution of 'Hippo signaling pathway' and 'Protein processing in endoplasmic reticulum' (both predicted by TarBase v8.0) on the development of kidney damage, ATF4, ATF6B, YAP1, TEAD1, LATS1 were additionally explored as hsa-let-7f-5p target mRNAs. Moreover, term-centric analysis of 'ECM-receptor interaction', 'Hippo signaling pathway', 'Protein processing in endoplasmic reticulum' and 'TGFB-signalling pathway (hsa04350) in miRPath v4.0 [369] evidenced hsa-let-7f-5p as one major regulator of the last three pathways (merged p-value = 5.44e-7, merged FDR = 0.0000207) just after hsa-miR-27a-3p [370-372], hsa-miR-497-5p and hsa-miR-203a-3p [373].

**Table 8.** *In-silico* prediction of let-7f-5p targets and enrichment analysis.

| | | | |
|---|---|---|---|
| **Protein processing in endoplasmic reticulum; TGF-beta signaling pathway; Hippo signaling pathway** (term-centric analysis) | | | |
| **p-value** 0,00000000709 | **FDR** 3,17E-07 | **Target Genes** 2165 | |
| **Gene names** | n/a | | |
| **Prediction tool** | MirPath v4.0; Term-centric analysis (Tarbase v8.0), miRNA ID MIMAT0000067, hsa-let-7f-5p | | |
| **ECM-receptor interaction** (hsa04512) | | | |
| **p-value** 3,17E-16 | **FDR** n/a | **Target Genes** 18 | |
| **Gene names** | THBS2, COL3A1, HSPG2, LAMC3, ITGAV, COL4A2, COL5A1, **COL1A1**, COL1A2, LAMC1**, FN1, COL4A1**, ITGB6, ITGA7, COL4A6, COL5A2 | | |
| **Prediction tool** | Tarbase; microT-CDS | | |
| **Hippo signaling pathway** (hsa04390) | | | |
| **p-value** 5,10E-05 | **FDR** 0,0031 | **Target Genes** 40 | |
| **Gene names** | BIRC3, CTNNA1, GLI2, ACTB, SMAD7, FZD3, TGFBR1, YWHAE, CCND1, **BIRC2**, BMP5, PPP2CA, MOB1A, ID2, CCND2, BMP2, AMOT, **LATS1**, LLGL1, APC, **YAP1**, CSNK1D, WNT9A, LIMD1, PARD3, TCF7L2, DVL3, TGFBR2, YWHAZ, BTRC, YWHAG, SMAD1, PPP1CA, MOB1B, FZD8, FZD2, ACTG1, **TEAD1**, BMPR2, CSNK1E | | |
| **Prediction tool** | MirPath v4.0; Tarbase; microT-CDS | | |
| **Protein processing in endoplasmic reticulum** (hsa04141) | | | |
| **p-value** 0,00039 | **FDR** 0,011 | **Target Genes** 41 | |
| **Gene names** | SEC63, CUL1, DNAJA2, SEL1L, EIF2AK1, EDEM2, DNAJB11, HSP90AB1, UBXN8, MAPK8, UBE2D3, HSPA8, SEC24A, EDEM3, FBXO6, RPN2, HSPH1, SIL1, **ATF4**, EIF2AK4, PRKCSH, UBE4B, UBQLN1, OS9, DERL1, PREB, SEC31A, HSP90B1, PDIA3, BCL2, SEC24C, YOD1, NPLOC4, UBE2G2, UBQLN2, ERO1A, UBE2J1, **ATF6B**, DDOST | | |
| **Prediction tool** | MirPath v4.0; Tarbase; microT-CDS | | |
| **TGF-beta signaling pathway** (hsa04350) | | | |
| **p-value** 0,0011 | **FDR** 0,037 | **Target Genes** 25 | |
| **Gene names** | MAPK1, SMAD7, TGFBR1, BMP5, PPP2CA, SMAD5, ACVR2B, ID2, ACVR1C, BMP2, E2F5, ACVR1B, THBS1, TGFBR2, FBN1, SMAD1, ID4, RGMB, RPS6KB2, TGIF1, SP1, TFDP1, BMPR2, E2F4 | | |
| **Prediction tool** | MirPath v4.0; Tarbase; microT-CDS | | |

FDR: false discovery rate method, as a correction for multiple hypothesis testing; n/a: not applicable.

## 2.4. Cloning methods and luciferase assay.

The luciferase reporter assay is an effective method to study the effects of a microRNA in the genetic expression of a possible target gene. This quantitative assay is based on the luciferase, an oxidative enzyme that allows bioluminescence as a consequence of the oxidation of its substrate, luciferin, in the presence of oxygen [374].

Luciferase reporter vectors were prepared containing the *in-silico* predicted sequence of miRNA:target complementary hybridation (see section III) to validate that any regulation seen in ago/antagomir experiments is the result of the miRNA:mRNA target binding. The 3'UTR sequence of the mRNA target was subcloned downstream of the firefly luciferase gene; a Renilla *sp* luciferase was used as internal control for all luminescence readouts normalization.

### 2.4.3. 3'-UTR luciferase constructs and molecular cloning of DNA.

As a previous step of the luciferase assay, we performed bioinformatic searches that allows to *in-silico* predict the putative 3'UTR target binding of our microRNA, let-7f-5p (has-let-7f-5p, MIMAT0000067), within the mRNA targets.

UCSC Genome Browser was consulted to obtain the 3'UTR oligonucleotide sequences for the gene ATF6β. A mutated version of the ATF6β sequence was also cloned to confirm the specificity of the miRNA:mRNA complementarity and ulterior expression regulation. A pmiRGLO Dual Luciferase miRNA Target Expression Vector (Promega, Wisconsin, U.S.A.; Depicted in Figure 9) was used as backbone plasmid for the cloning.

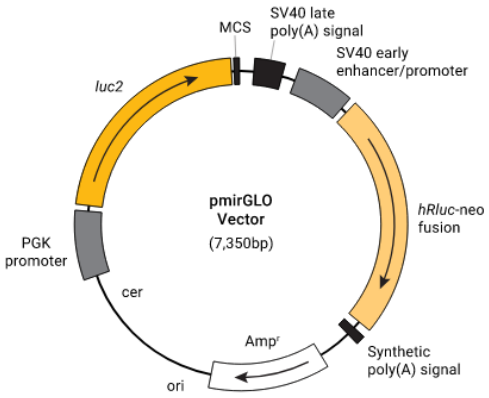


**Figure 9**. Schematic representation of the pmiRGlo Dual-Luciferase Expression Vector from Promega, in which **luc2** is the firefly luciferase reporter gene and **hRluc-neo** is the renilla firefly control reporter gene. **MCS** is the multiple cloning site, the section in which restriction enzymes activity generates the linearization of the vector needed for the ligation of the annealed oligos. **AmpR** is a gene that allows ampicillin resistance, needed as the selective antibiotic in the bacterial transformation.

## Insert design and preparation

The *in-silico* predicted 3'UTR of the target mRNA containing the binding site of let-7f-5p was designed to contain *Pme*I (GTTT/AAAC) and *Sal*I (G/TCGAC) endonuclease restriction sites 5' and 3' ends, respectively (sequences listed in Table 9). An additional *Not*I (GC/GGCCGC) restriction site was added to further confirm oligonucleotide cloning into pmiRGLO Vector. As pmiRGlo has a *Not*I site outside of the multicloning site, a positive construct containing our insert would produce two *Not*I cuts visible by agarose gel electrophoresis.

**Table 9.** Design of 3′UTR oligonucleotide sequences for target cloning inserts.

| **ATF6β sequence cloning design** | |
|---|---|
| 5′ – AAACTAGCGGCCGCCCAGGCCTCCCACCAGCCCCTCTACCTCAATCAG -3′ | |
| 3′ – TTTGATCGCCGGCGGGTCCGGAGGGTGGTCGGGGAGATGGAGTTAGTCAGCT -5′ | |
| **ATF6β WT** (Wild type) | |
| Forward primer | AAACTAGCGGCCGCCCAGGCCTCCCACCAGCCCCTCTACCTCAATCAG |
| Reverse primer | TCGACTGATTGAGGTAGAGGGGCTGGTGGGAGGCCTGGGCGGCCGCTAGTTT |
| **ATF6β MUT** (mutant) | |
| Forward primer | AAACTAGCGGCCGCCCAGGCCTCCCACCAGCCCCTATTGCTAAATCAG |
| Reverse primer | TCGACTGATTTAGCAATAGGGGCTGGTGGGAGGCCTGGGCGGCCGCTAGTTT |

Orange coloured letters show the **let-7f-5p binding site to the gene** according to the *in-silico* prediction.
Red coloured letters show the endonuclease restriction site of the ***Pme*I** (GTTT/AAAC) restriction enzyme.
Blue coloured letters show the endonuclease restriction site of the ***Not*I** (GC/GGCCGC) restriction enzyme.
Green coloured letters show the endonuclease restriction site of the ***Sal*I** (G/TCGAC) restriction enzyme.

The designed complementary oligos (HPLC purified, prepared in 10 mM Tris-HCl buffer to a final concentration of 100 μM) were diluted to 1 ng/μl and subsequently annealed at 40 ng/μl each in pmiRGlo annealing buffer, for example, 2 μl of 1 ng/μl forward oligo, 2 μl of 1 ng/μl reverse oligo and 46 μl of the pmiRGlo annealing buffer. The annealing was conducted in a thermal cycler set at 90°C for 3 min followed by a slow cooling down in a water bath set at 37°C for 15 min.

In order to linearize the vector, the pmiRGlo backbone (5-10 μg) was double-digested in a final volume of 20 μl, with 1U *Pme*I-HF and 1U *Sal*I-HF (New England Biosciences, Ipswich, U.S.A.) in 1x FastDigest Green buffer for 1 hour, 37°C. Digestion products were then electrophoresed into 1% agarose gel in 1x TAE, which separates the linearized and non-linearized vectors according to its molecular weight. This method allows us to isolate and purify only the products that were properly linearized and therefore containing cohesive ends for Pme*I* and *Sal*I. Bands were excised with a clean scalpel under UV light irradiation and

isolated using the Silica Bead DNA gel extraction kit (Thermo Fisher Scientific, Waltham, MA, U.S.A.) by following the manufacturer's instructions.

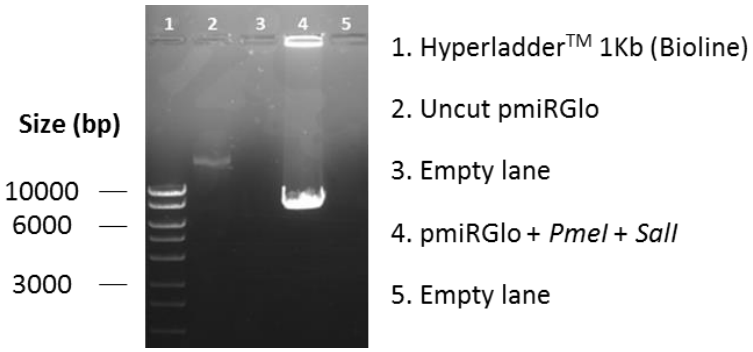


**Figure 10**. Representative transilluminator picture of double digestion products for pmiRGlo linearization via usage of Pme*I* and Sal*I* endonucleases.

### Ligation of the insert

The annealed oligos (insert) were ligated to a molar ratio 1:1 (insert:DNA). In order to do that, the annealing product was diluted 1/200 in nuclease free water (0.2 ng/μl) and 285 pg (1 μl) were ligated with 50 ng of the linearized pmiRGlo in 1.1 μl 10x T4 Ligase buffer (containing 0.5 mM ATP) and 1 μl T4 ligase (1U) (both purchased from Thermo Scientific, Waltham, MA, U.S.A.). A final volume of 11 μl was achieved with nuclease free water. The ligation reaction was conducted for 1 hour at room temperature (approximately 20°C). The amount of insert was calculated as follows:

$$ng\ insert = (molar\ ratio\ insert/pDNA\ x\ ng\ pDNA)x\ (bp\ insert/bp\ pDNA)$$

Where "bp" stands for base pairs.

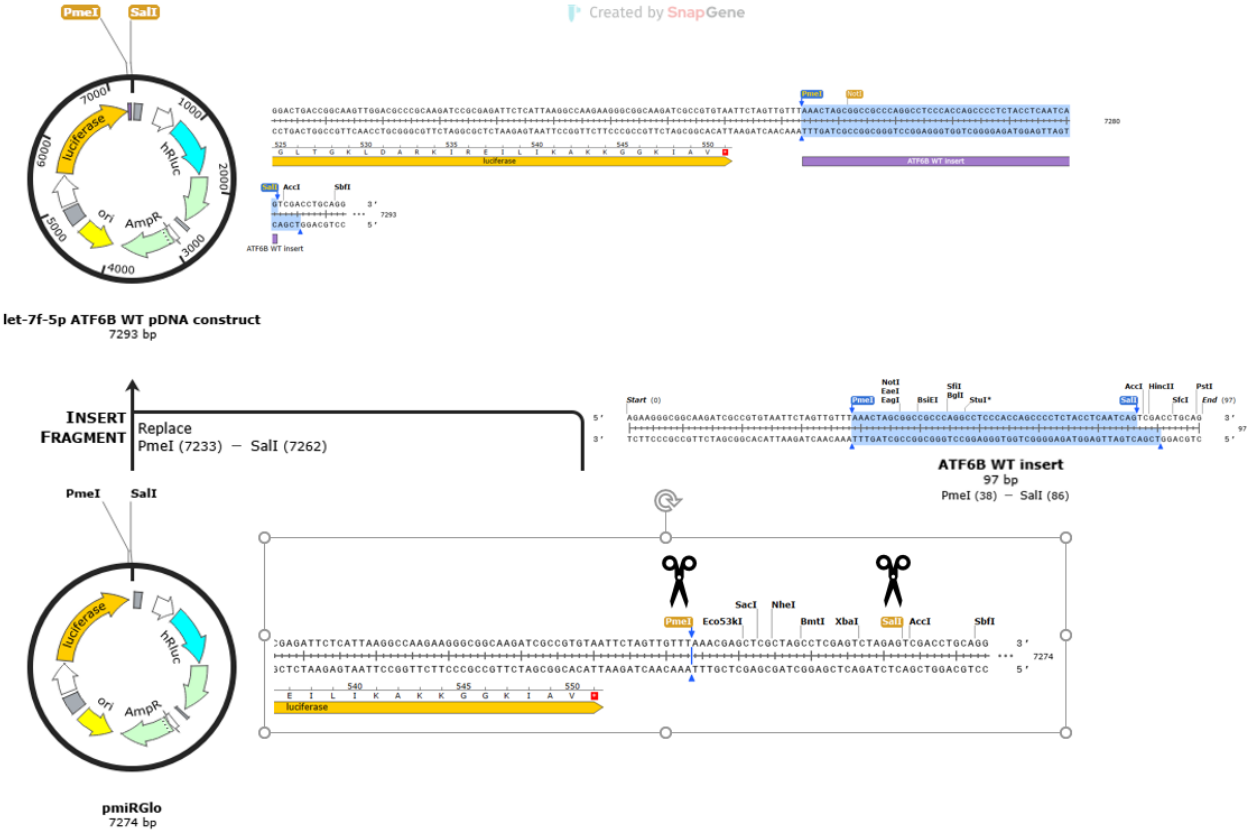


**Figure 11**. Schematic representation of the cloning workflow followed for pATF6β plasmid design. The 3'UTR ATF6β wild type sequence was inserted into a pmiRGlo vector, specifically in the region between the Pme*I* and Sal*I* restriction sites, downstream of the Firefly luciferase reporter gene. Image obtained with SnapGene® software.

### 2.4.4. Transformation and plasmid preparations.

*E. coli* JM109 strain was transformed with the plasmid DNA constructs by heat shock transformation by which 1.5 µL of the ligation product were added to 15 µL JM109 *E. coli* competent cells (Promega, Wisconsin, U.S.A.). Briefly, transformation was carried out at 42 °C for 45s, followed by 2 min on ice. The transformation product was then 10-fold diluted in SOC media (New England Biosciences, Ipswich, U.S.A.) and incubated for 1 hour in agitation before platting into selective LB-Agar (100 µg/ml ampicillin; composition in annex VI.4.) and further expanded into mini or midi format, as appropriate. Because the plasmid backbone contains a β-lactamase gene as an antibiotic, only the successfully

transformed bacteria were Amp resistant and, therefore underwent colonies formation.

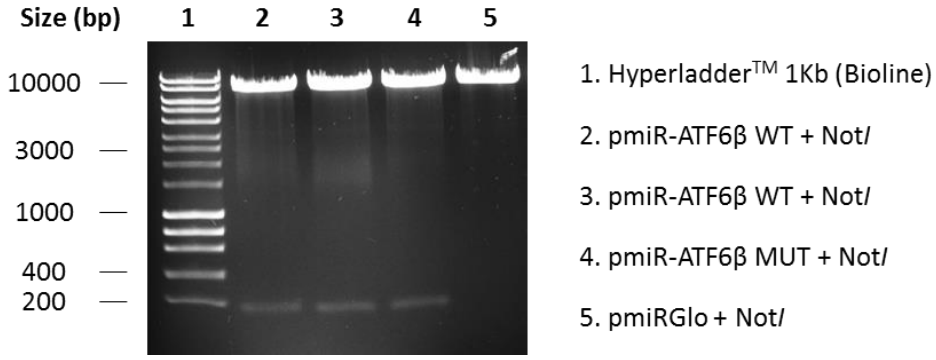


**Figure 12**. Representative transilluminator picture of digestion products for pATF6β (pDNA) to validate ATF6β insert ligation into the pmiRGlo vector.

Up to 10 colony formation units (CFU) of the transformed bacteria were then screened to confirm successful insert recombination with the pmiRGlo backbone. Randomly selected CFUs (n=10) were picked and separately grown in 3-5 ml of selection Amplicillin LB-Broth media (composition in annex VI.4.) overnight (16 hours) in an orbital shaker (250 rpm). Plasmid DNA minipreps were undertaken following the manufacturer's instructions. Isolated pDNAs were then single digested with 1U Not*I*-HF (New England Biosciences, Ipswich, U.S.A.) and electrophoresed in 1.2% agarose gel prepared in 1X TAE buffer to validate insert ligation into the backbone. The expected results were: i) a single band corresponding to the linearized pDNA construct if the ligation did not work or ii) two bands if the insert was properly ligated into the backbone, then generating a second Not*I* site.

Positive CFUs were further expanded into 50 ml for midi endotoxin free plasmid preparations (Merck/Sigma-Aldrich, Cambridge, UK). Removal of JM109 endotoxins was fundamental to maximise the ulterior efficiency of plasmid transfections in HK-2 cells, as well as to guarantee survival and minimize the inflammatory responses to the plasmids. Such endotoxin-free pDNAs were later

ethanol-concentrated under the flow laminar hood to ensure sterility, and their concentrations were quantified with a Nanodrop Spectrophotometer (Implen™ NanoPhotometer N6O; Fisher Scientific, Waltham, MA, U.S.A.).

### 2.4.5. Transient transfection and luciferase assay.

Luciferase plasmid construct preparations were co-transfected with Scr or let-7f-5p mimic/inhibitor in 80% confluent HK-2 cell monolayers (96 multi-well plates). Luciferase plasmid constructs (0.12 µg) were co-diluted with 35 ng (25 nM final concentration) of agomiR-let-7f-5p/agomiR scramble in 5 µL Opti-MEM® I Reduced Serum Medium (GibcoTM, Thermo Fisher Scientific, Waltham, MA, U.S.A.) and 0.145 µL Reagent Plus (1:1 with pDNA/miR diluted). Lipofectamine LTX (0.22 µL) (Invitrogen/ Thermo Fisher Scientific, Waltham, MA, U.S.A.) was also diluted in 5 µL Opti-MEM®. Both preparations were incubated separately for 5 min at 20 °C, mixed into the same tube and incubated for further 20 min. 10 µL of the lipocomplexes were inoculated in 100 µL final volume and were incubated for 5h, at 37°C, 5% $CO_2$. The lipocomplexes media was replaced by complete media and luciferase assays were performed after 36 h using a Dual-Glo® Luciferase Assay System (Promega, Wisconsin, U.S.A.) following the manufacturer's instructions. Luminiscence readouts were sequentially obtained in a GloMax® Discover plate reader (Promega, Wisconsin, U.S.A.).

Firefly luminescence (FLuc) readouts were normalized to Renilla *sp.* Luminescence (RLuc). An additional normalization to the control condition (agomiR Scr) in each experiment was performed to avoid data heterogeneity between experiments. Empty pmiRGLO control (*e.g.,* pmiRGlo with no insert) was additionally transfected with and without agomiRs to rule out any confounding off-target binding of let-7f-5p to the backbone. Each experiment was conducted in at least 4 technical replicates per condition. The data are plotted as relative luminescence units (RLU) of the experimental condition, normalized to

the control condition. RLUs from technical replicates and condition were averaged. The averages were then compared for appropriate statistical analysis.

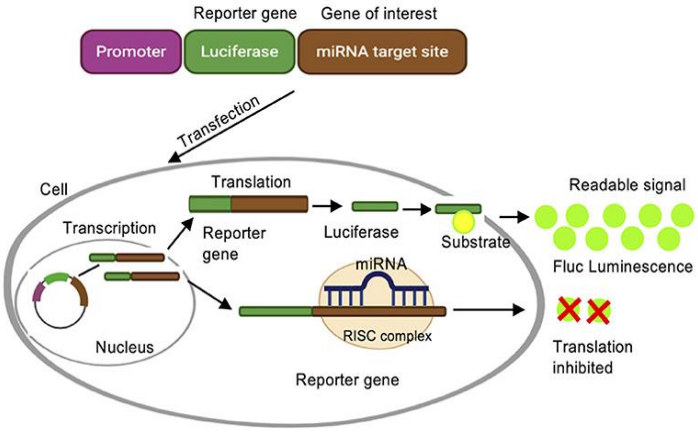


**Figure 13**. Luciferase reporter assay representation taken from Siddika & Heinemann, 2021 [375]. This assay can be used to validate miRNA binding sites to a target gene by fusing the target 3'UTR of a target mRNA to the luciferase reporter gene. If the microRNA binds to the UTR of the gene, the RISC complex interferes with the translation of the reporter gene, consequently the production of luciferase will decrease. If the microRNA and the inserted gene do not interact the production of luciferase enzyme allows the emission of light as a consequence of the oxidation of the substrate.

## 3. Sample processing in the *in-vitro* studies.

### 3.1. RNA isolation and gene expression analyses in cultured cells.

For RNA extraction, 750 µl of Trizol reagent (Fisher Scientific, Waltham, MA, U.S.A.) were added to each well from a 6-well plate before freezing at -80°C. On the day of the extraction chloroform was added and centrifuged to separate the homogenate into phases. The upper aqueous phase was transferred into a different Eppendorf and isopropanol is added to precipitate the isolated RNA after centrifugation. After washing with cold ethanol and leaving to dry, the obtained pellet was resuspended with 200 µl RNase/DNase free water (Fisher Scientific, Waltham, MA, U.S.A.).

RNA concentration was quantified as described in section I.9.1. Both retrotranscription and Real-time RT-PCR were performed as described in

sections I.9.2 and I.9.3 respectively. In the *in-vitro* experiments, data was normalized to the housekeeping genes hypoxanthine phosphoribosyltransferase (HPRT) and glyceraldehyde-3-phosphate dehydrogenase (GAPDH). Primers used in both the TFB murine, and the HK-2 human cell lines are listed in Table 10 and Table 11, respectively.

**Table 10.** Mouse primer sequences.

| Gene | Temperature | Forward Primer | Reverse primer |
|---|---|---|---|
| *Ccl-2* | 60 ˚C | AGGTCCCTGTCATGCTTCTG | TCTGGACCCATTCCTTCTTG |
| *Col1a1* | 62 ˚C | ACTGGTACATCAGCCCGAAC | TACTCGAACGGGAATCCATC |
| *Il-6* | 60 ˚C | CTCTGGGAAATCGTGGAAATG | AAGTGCATCATCGTTGTTCATACA |
| *Ngal* | 60 ˚C | GGACCAGGGCTGTCGCTACT | GGTGGCCACTTGCACATTGT |
| *Opn* | 60 ˚C | GGCTGGTGCCTGACCCATC | TTCATTGGAATTGCTTGGAAGA |
| *Hprt* | 62 ˚C | TCTAACTTTAACTGGAAAGAATGTC | TCCTTTTCACCAGCAAGCT |

*Ccl-2*: C-C motif chemokine ligand 2; *Col1a1*: Collagen type I alpha 1 chain; *Il-6*: Interleukin 6; *Ngal*: Neutrophil gelatinase associated lipocalin; *Opn*: Osteopontin; *Hprt*: Hypoxanthine Phosphoribosyltransferase.

**Table 11.** Human primer sequences.

| Gene | Temperature | Forward Primer | Reverse primer |
|---|---|---|---|
| *Atf4* | 60 ˚C | GTCCCTCCAACAACAGCAAG | TACCCAACAGGGCATCCAAG |
| *Atf6α* | 62 ˚C | TTCAGTCTCGTCTCCTCGGT | ATCTTCCTTCAGTGGCTCCG |
| *Atf6β* | 62 ˚C | GGAGGTGCTCCATGTGAAGA | AGGCCTCAGAGTTGACGGAA |
| *BiP* | 60 ˚C | AACCGCTGAGGCTTATTTGG | AACCGCTGAGGCTTATTTGG |
| *Birc2* | 60 ˚C | GGGCCGTATCTCCTTGTCG | TGCAGGGGGACAAAATAGGG |
| *Chop* | 60 ˚C | TTGCCTTTCTCCTTCGGGAC | TGATTCTTCCTCTTCATTTCCAGG |
| *Col1a1* | 62 ˚C | GGACACAGAGGTTTCAGTGGT | CACCATCATTTCCACGAGCA |
| *Ctgf* | 62 ˚C | CTCGCGGCTTACCGACTG | GGCTCTGCTTCTCTAGCCTG |
| *Lats1* | 62 ˚C | CAGCAGCTGCCAGACCTATT | CACTTTCTCCTAGTGGCGGG |
| *Ngal* | 62 ˚C | ACAGGGAGTACTTCAAGATCAC | GGTCGATTGGGACAGGGAAG |
| *Snail* | 62 ˚C | CCTGTCTGCGTGGGTTTTTG | ACCTGGGGGTGGATTATTGC |
| *Slug* | 62 ˚C | TTGGAGCAGTTTTTGCACTG | TCGGACCCACACATTACCTT |
| *Tead1* | 62 ˚C | ACTTCCCTTCCCTTTCGGTTT | CGTCTTGCCTGTCCTGAGTT |
| *Tgf-β* | 62 ˚C | TACCTGAACCCGTGTTGCTC | CCGGTAGTGAACCCGTTGAT |
| *Yap1* | 62 ˚C | CTGCCCGACTCCTTCTTCAA | CCAACTGCAGAGAAGCTGGA |
| *Gapdh* | 62 ˚C | ACCAGCCCCAGCAAGAGCACAAG | TTCAAGGGGTCTACATGGCAACTG |
| *Hprt* | 62 ˚C | TTGCTTTCCTTGGTCAGGCA | ATCCAACACTTCGTGGGGTC |

*Atf4*: Activating transcription factor 4; Atf6*α*: Activating transcription factor 6 alpha; *Atf6β*: Activating transcription factor 6 beta; *Bip:* Binding immunoglobulin protein; *Birc2:* Baculoviral IAP Repeat containing 2; *Chop*: CCAAT-enhancer-binding protein homologous protein; *Col1a1*: Collagen type I alpha 1 chain; *Ctgf*: Connective tissue growth factor; *Lats1*: Large tumor suppressor kinase 1; *Ngal*: Neutrophil gelatinase associated lipocalin; *Snail*: Snail family transcriptional repressor 1; *Slug*: Snail family transcriptional repressor 2; *Tead1*: TEA domain transcription factor 1; *Tgf-β:* Transforming growth factor beta; *Yap1*: Yes1 associated transcriptional regulator; *Gapdh*: Glyceraldehyde-3-phosphate dehydrogenase; *Hprt*: Hypoxanthine Phosphoribosyltransferase.

### 3.2. MicroRNA levels evaluation.

For microRNA evaluation, RNA of the *in-vitro* assays was extracted using column-based methods. For that purpose, we used the miRNeasy micro kit (Quiagen, Hilden, Germany), which combines phenol/guanidine-based lysis and silica membrane-based purification of the total RNA (< 200 bp RNAs), including microRNAs.

In brief, for RNA extraction 500 µl of QIAzol Lysis Reagent was added to each well from a 12-well plate before freezing at -80˚C. As the user guide dictates, on the day of the extraction after addition of chloroform and centrifugation, the upper aqueous phase is transferred into a different Eppendorf and ethanol is added. Each sample is then moved into the RNeasy Mini Spin column and centrifuged; this way the RNA will bind to the silica membrane, allowing washing off the phenols and other possible contaminants without disrupting or diminishing the yield of RNA. Lastly, the purified RNA was eluted in 35 µl RNase-free milliQ water. The RNA yields were quantified by spectrophotometry at 260 nm. Sample purity was considered appropriate when the 260/280 ratio which informs of proteins or inorganic contaminants, and the 260/230 ratio that shows contaminants such as phenol or carbohydrates was ≥ 1.70. All these quantifications were done with Implen™ NanoPhotometer N6O (Fisher Scientific, Waltham, MA, U.S.A.).

MicroRNA reverse transcription and qPCR was done using Taqman MicroRNA assay kits as described in section I.9.4.

### 3.3. Protein processing.

For protein extraction, confluent cells seeded in 6-well plates were trypsinized and transferred to an Eppendorf for its centrifugation at 4000 rpm for 5 min at 4 ˚C. Pellet was then resuspended with 75 µl of Lysis buffer (composition in the annex VI.1.1.) and incubated for 30 min on ice with vortexing every 5 min. The samples were centrifuged at 13000 rpm for 12 min at 4˚C thereafter. The supernatant was collected and stored at -80˚C until use.

Protein quantification was done by the Bradford protein assay as specified in section I.10.1. Aliquots of 20 µg of the extracted cellular proteins were prepared by denaturation at 95˚C for 5 min in presence of β-mercaptoethanol. Samples

were electrophoresed in SDS-PAGE and transferred into nitrocellulose membranes as indicated in section I.10.2.

### 3.4. Superoxide anion production evaluation.

Evaluation of the cellular production of superoxide anion was performed using the DHE technique.

For this assessment, cells were seeded in 48-well plates in the presence of poly-l-lysin for the TFB cells. Once the desired confluence was reached, cells were put in the starvation media for 24 hours. After the 24 hours passed, cells were pretreated with the ER stress inhibitor 4-PBA for 30 min prior to their stimulation with either palmitic acid or Ang II at the doses described on sections IV.1.2.1 and IV.1.2.2 for 24 hours.

Cells were then incubated with $10^{-5}$ M DHE for 30 min at 37°C in a dark humidified chamber. Afterwards, cells were washed with room temperature PBS and sample fluorescence intensity was then analysed using a 40x objective in a fluorescence microscope Leica DMI 3000. The microscope and camera conditions were kept constant for all preparations and the fluorescence intensity was quantified with Leica application suite (Leica microsystems, Wetzlar, Germany). For each experimental condition, $150 - 200$ cells were analysed.

## V. Statistical analysis.

### 1. Experimental model data analysis.

Results from continuous variables of experimental data are expressed as mean ± standard error of the mean (SEM). The normality of distributions was verified by

the Kolmogorov-Smirnov test, and Levene's test was used to assess the equality of variances.

Unpaired Student's t test was performed to determine significant differences between two sets of data or by Mann-Whitney U test in case of nonparametric distribution. One-way ANOVA was used to evaluate differences among several groups. Newman-Keuls test was used as a post hoc test for differences in means, whereas Dunnet test was used for dose-dependent studies. Two-way ANOVA was used and followed by Bonferroni tests to compare quantitative variable changes according to the levels of two categorical variables. Pearson correlation analysis was applied to examine the association among different variables.

A value of $P<0.05$ was used as the cut-off value for defining statistical significance. Data analysis was performed using the statistical program GraphPad Prism 8 (San Diego, CA, U.S.A.).

**2. Clinical data analysis.**

Continuous variables are expressed as mean ± standard deviation (SD). Normality of distributions was verified by the Kolmogorov-Smirnov test. Categorical variables are expressed in absolute values and percentages. Levene's test was used to assess the equality of variances and a Student's t test was performed to determine if two sets of data were significantly different from each other. A value of $P<0.05$ was used as the cut-off value for defining statistical significance. Data analysis was performed using the statistical program SPSS 22.0 (SPSS Inc., Chicago, Il, U.S.A.).

# VI. Annex

## 1. Protein analysis.

### 1.1. Extraction buffer.

| | |
|---|---|
| Complete Lysis-M reagent (Roche, Ref: 04719956001) ……... | 10 ml |
| Complete Tablets (protease inhibitor cocktail; Roche, Ref: 05892970001) …...… | 1 tablet |

### 1.2. Running buffer.

| | |
|---|---|
| Tris …… | 50 mM |
| Glycine ……. | 192 mM |
| SDS ……... | 0.3% |

### 1.3. Transfer buffer.

| | |
|---|---|
| 5x transfer buffer (Bio-Rad) ….. | 200 ml |
| Ethanol ……. | 200 ml |
| Distilled water …… | 600 ml |

### 1.4. PBS.

| | | |
|---|---|---|
| NaCl ……. | 140 mM | pH = 7.4 |
| KCl …… | 3 mM | |
| $Na_2HPO_4$ ……. | 9 mM | |
| $KH_2PO_4$ …… | 2mM | |

## 2. Superoxide anion detection.

### 2.1. KHB-HEPES.

| | | |
|---|---|---|
| $CaCl_2 \bullet 2H_2O$ ……..……. | 2 mM | pH = 7.4 |
| NaCl ……. | 130 mM | |
| KCl ……...…… | 5.6 mM | |
| $MgCl_2 \bullet 6H_2O$ ……..…… | 250 µM | |
| Hepes ……...…… | 8.4 mM | |
| Glucose …… | 10 mM | |

## 3. Cell culture.

### 3.1. RPMI full media supplementation.

| | |
|---|---|
| FBS …..……..... | 10% |
| L-Glutamine …….. | 1% |
| Penicillin/Streptomycin …… | 1% |

## 4. Bacterial growth and maintenance.

### 4.1. LB agar.

| | |
|---|---|
| LB media (Invitrogen, Ref: 22700025) ..... | 32 g |
| Distilled water …….…….... | 1 L |
| Ampicillin …… | 100 µg/ml |

### 4.2. LB broth base.

| | |
|---|---|
| LB media (Invitrogen, Ref: 12780052) ..... | 20 g |
| Distilled water …….…….... | 1 L |
| Ampicillin …… | 100 µg/ml |

# *Results*

## I. Clinical characteristics of patients who suffered a first myocardial infarction.

The mean age of patients with myocardial infarction (MI) was significantly higher than that of control subjects. Control group had almost 50% of female participants whereas MI patients were only males (Table 12). All MI patients had associated comorbidities that were only present in 8.3% of the control subjects, with the most prevalent being hypertension and dyslipidemia. Patients with hypertension were treated with angiotensin converting enzyme inhibitors or angiotensin II type 1 receptor antagonists whereas dyslipidemia patients were place on statins (Table 12).

Body mass index (BMI) was higher in MI patients than in non-MI subjects. Even though plasma creatinine values were within normal range in both groups of patients, MI patients presented renal alterations characterized by higher plasma levels of creatinine and NGAL, an acute marker of renal injury (Table 12).

**Table 12**. Clinical characteristics, cardiac function and circulating markers in control subjects and patients who suffered a myocardial infarction.

| | Control Subjects (n = 12) | MI Patients (n = 12) | P Value |
|---|---|---|---|
| Women (%) | 41 | 0 | < 0.0001 |
| Age (years) | 41.6 ± 4.1 | 54.8 ± 6.8 | < 0.0001 |
| LVEF (%) | 75.2 ± 4.2 | 62.7 ± 5.6 | < 0.0001 |
| E/A ratio | 1.5 ± 0.3 | 0.9 ± 0.4 | 0.0002 |
| E/e' ratio | 6.7 ± 1.4 | 8.1 ± 1.9 | 0.0433 |
| BMI (kg/m$^2$) | 23.04 ± 2.01 | 26.4 ± 2.1 | 0.005 |
| Hypertension (n (%)) | 1 (8.33%) | 6 (50%) | 0.0813 |
| Dyslipemia (n (%)) | 0 (0%) | 5 (41.6%) | 0.0435 |
| Plasma creatinine (mg/dl) | 0.73 ± 0.11 | 0.88 ± 0.17 | 0.0119 |
| NGAL (pg/ml) | 61941 ± 14695 | 87873 ± 24419 | 0.0046 |

Data is expressed as means ± SD, number, or percentage of patients. LVEF: left ventricle ejection fraction; E/A ratio: early to late diastolic transmitral flow velocity ratio; E/e' ratio: E

to early diastolic mitral annular tissue velocity ratio; BMI: body mass index; NGAL: neutrophil gelatinase-associated lipocalin.

## II. Renal consequences of myocardial infarction in rats.

Due to the obtained data in the patients, we explored the possible renal alterations in a MI animal model. Rats subjected to coronary artery ligation presented several cardiac structural and functional alterations in the absence of modifications in the blood pressure and body weight. At structural level, the heart of MI animals presented cardiac fibrosis and hypertrophy evaluated by collagen volume fraction and left ventricular (LV) mass respectively. The structural modifications were accompanied by alterations in the systolic and diastolic function, as these animals presented a reduction in LV ejection fraction (LVEF) and E/A ratio when compared to the control group (Table 13).

**Table 13**. Impact of myocardial infarction on general characteristics, cardiac function and infarct size in rats subjected to myocardial infarction (MI) or to a sham operation (Sham) after 4 weeks of evolution.

| | Sham | MI |
|---|---|---|
| Body weight (g) | 396.2 ± 10.8 | 394.8 ± 9.7 |
| SBP (mmHg) | 127.72 ± 2.7 | 132.6 ± 1.3 |
| LV mass (g) | 0.287 ± 0.061 | 0.42 ± 0.015*** |
| Cardiac fibrosis (%) | 2.088 ± 0.082 | 4.013 ± 0.197*** |
| LVEF (%) | 84.81 ± 1.112 | 69.72 ± 3.163*** |
| E/A ratio | 1.595 ± 0.21 | 0.996 ± 0.075** |
| Infarct size/LV mass (%) | - | 18.1 ± 2.9 |
| Creatinine (mg/dl) | 0.43 ± 0.021 | 0.46 ± 0.018 |

Data is expressed as means ± SEM of 8-10 animals. SBP: systolic blood pressure; LV: left ventricle; LVEF: left ventricle ejection fraction. **p < 0.01; ***p < 0.001 versus Sham group.

Similar to what we observed in the patients, the creatinine serum levels were similar between both groups of animals (Table 13); however, infarcted animals presented a renal increase in the acute injury markers NGAL and KIM-1 (Figure

14A), suggesting kidney damage in the absence of functional alterations. Furthermore, infarcted animals also presented an increase in the expression levels of the profibrotic and proinflammatory mediator Gal-3 (Figure 14B).

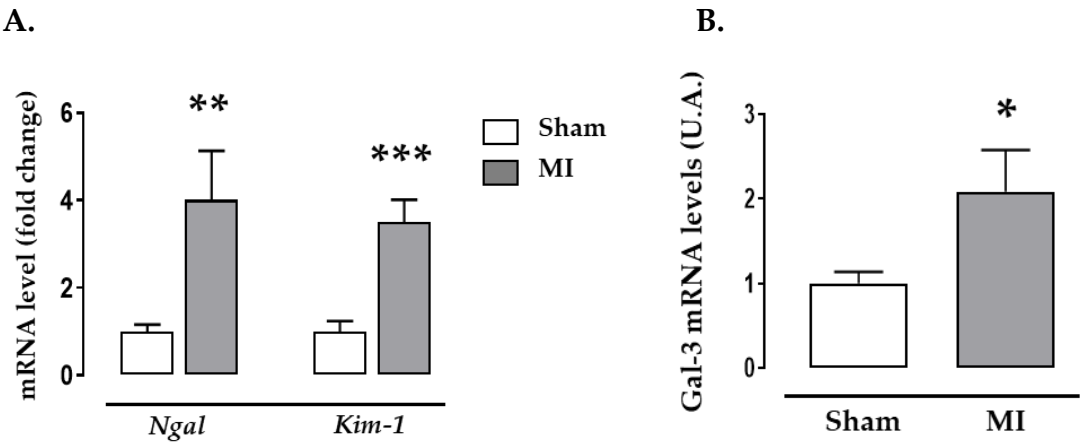


**Figure 14. Impact of MI on (A) renal injury markers** NGAL and KIM-1 and **(B)** profibrotic mediator Gal-3 mRNA levels in kidneys from rats subjected to myocardial infarction (MI) or to a sham operation (Sham). Bar graphs represent the mean ± SEM of 8-10 animals normalized to hypoxanthine-guanine phosphoribosyltransferase (HPRT). **p < 0.01; ***p < 0.001 versus Sham group.

### 1. Effects on renal fibrosis.

Histological assessment of the interstitial collagen levels showed that animals subjected to MI presented an increase in renal fibrosis without changes in the glomerular area when compared to the Sham group (Figure 15A-B). This demonstrates that MI induces structural modifications within the kidney that are prior to the occurrence of functional alterations.

The presence of renal interstitial fibrosis was accompanied by enhanced levels of the extracellular matrix protein collagen type I. Complementary analysis revealed that MI animals also showed a non-significant increase in the marker of activated fibroblast $\alpha$-SMA, as well as elevated protein levels of the profibrotic mediator TGF-$\beta$ without modification in CTGF (Figure 15C).

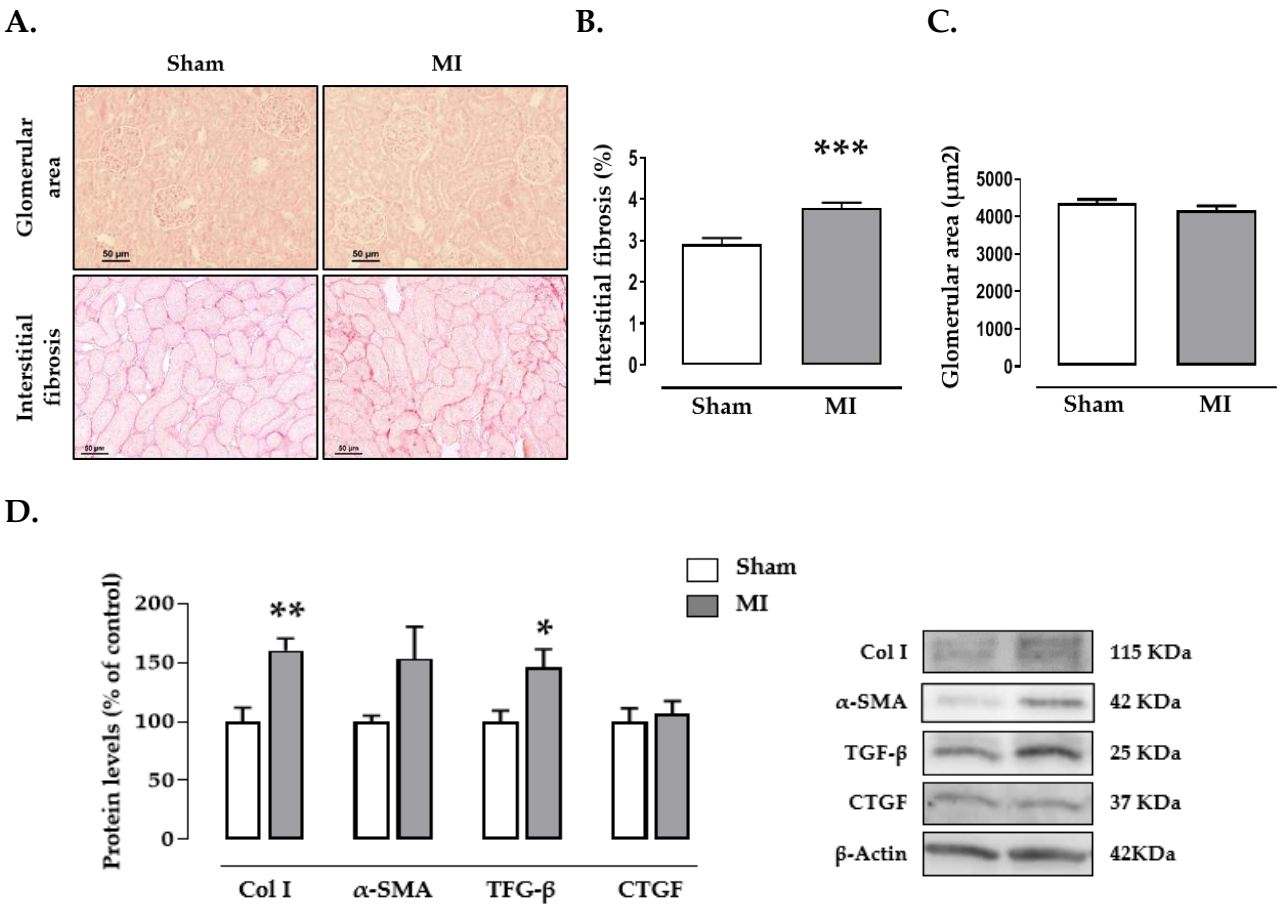


**Figure 15. Impact of MI on renal fibrosis.** **(A)** Representative microphotographs (20x magnification) of renal cortex sections staining with haematoxylin-eosin for glomerular area analysis or picrosirius red for fibrosis analysis. Quantification of **(B)** interstitial fibrosis and (C) glomerular area. **(D)** Protein levels of collagen type I, alpha-smooth muscle actin (α-SMA), transforming factor-beta (TGF-β) and connective tissue growth factor (CTGF) in the kidneys from rats subjected to myocardial infarction (MI) or to a sham operation (Sham). Bar graphs represent the mean ± SEM of 8-10 animals normalized to β-actin. *p < 0.05; **p < 0.01; ***p < 0.001 versus Sham group.

## 2. Effects on oxidative stress and inflammation.

The presence of oxidative stress was evaluated in the infarcted and sham group of animals at both circulating and renal levels. MI animals presented higher circulating levels of Thiobarbituric acid reactive substances (TBARS), an end-product of lipid peroxidation (Figure 16A). As shown in Figure 16B, there was an increase in fluorescence intensity in the infarcted animals that shows higher presence of superoxide anion in this group as compared to non-infarcted animals. This prooxidant scenario was confirmed by 4-HNE, another major end-

product of lipid peroxidation that was enhanced after MI at renal level (Figure 16C).

MI induced not only a prooxidant environment in the kidney of the animals but also a pro-inflammatory scenario characterized by an increase in the proinflammatory cytokines IL-6 and TNF-α (Figure 16D).

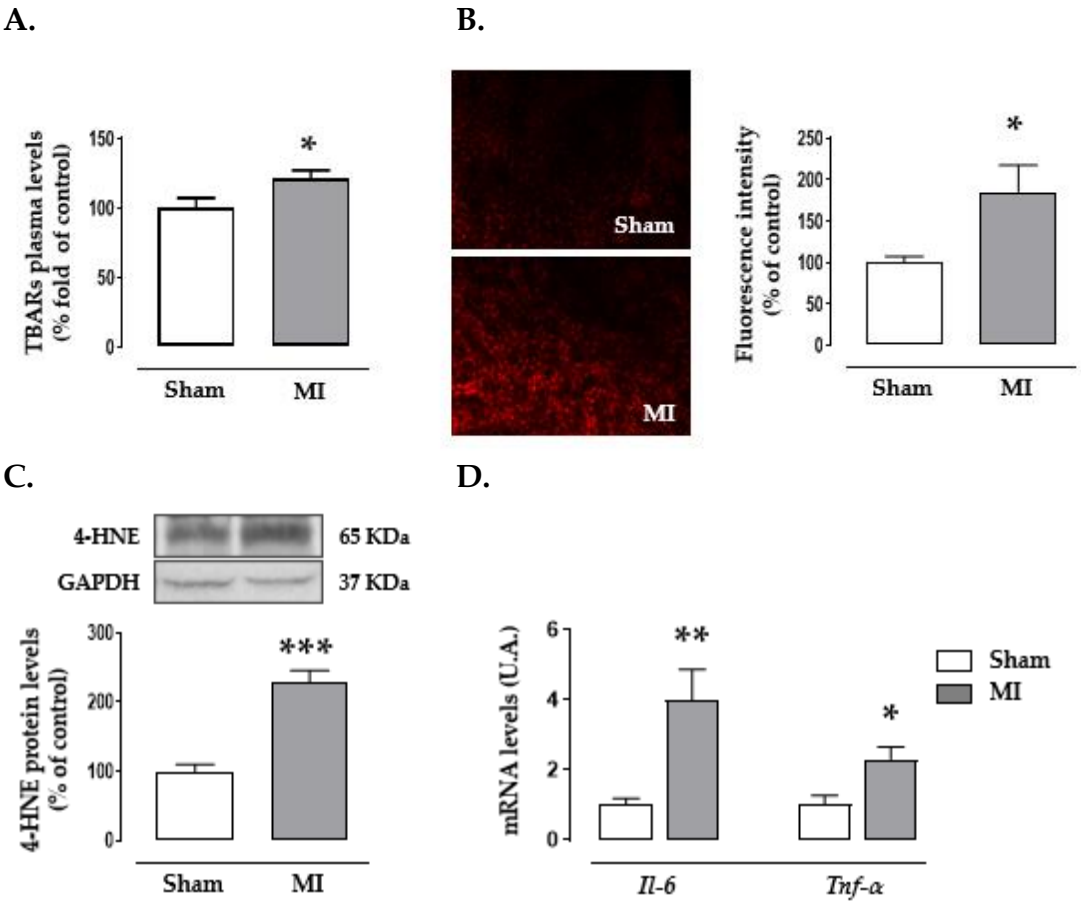


**Figure 16**. **Impact of MI on renal oxidative stress and inflammation**. (**A**) Thiobarbituric acid reactive substances (TBARS) plasmatic levels. (**B**) Representative images and quantification of renal cortex sections labelled with the oxidative dye dihydroethidium (40X magnification). **(C)** Protein levels of 4-hydroxynonenal (4-HNE). **(D)** mRNA levels of Interleukin-6 (IL-6) and tumor necrosis factor-alpha (TNF-α) in kidneys from rats subjected to myocardial infarction (MI) or to a sham operation (Sham). Bar graphs represent the mean ± SEM of 8-10 animals normalized to β-actin for protein or HPRT for cDNA. *p < 0.05; **p < 0.01; ***p < 0.001 versus Sham group.

### 3. Effects on the endoplasmic reticulum stress.

Different proteins were measured in order to appraise the possible activation of ER stress in this pathological context. 4 weeks after MI, animals presented a renal up-regulation of two markers of ER stress, BiP and PDIA6, as compared with control ones (Figures 17A-B). Additional analysis of the different pathways involved in the ER stress activation showed that ATF6$\alpha$ protein levels were enhanced in absence of CHOP protein modifications in the MI animals (Figures 17C-D).

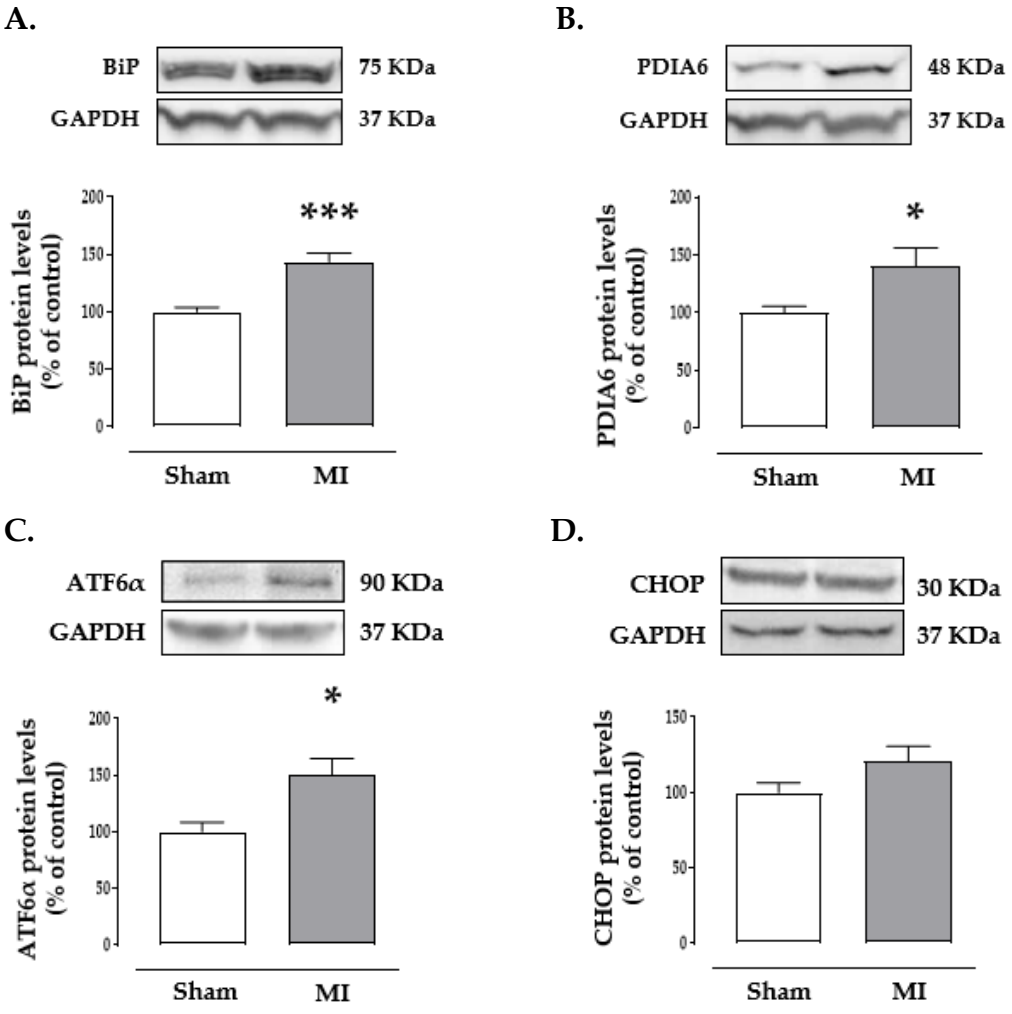


**Figure 17**. **MI induces renal ER stress activation**. Renal protein levels of (**A**) Immunoglobulin binding protein (BIP). (**B**) Protein disulfide isomerase family A member 6 (PDIA6). (**C**) Activating transcription factor 6-alpha (ATF6-$\alpha$) and (**D**) CCAAT-enhancer-binding homologous protein (CHOP) in kidneys from rats subjected to myocardial infarction (MI) or to a sham operation (Sham). Bar graphs represent the mean ± SEM of 8-10 animals normalized to

glyceraldehyde-3-phosphate dehydrogenase (GAPDH). *p < 0.05; ***p < 0.001 versus Sham group.

Interestingly, we observed a positive correlation between ER stress activation, evaluated by the protein levels of BiP, PDIA6 and CHOP, and both interstitial fibrosis and Collagen type I protein levels (Figure 18). These correlations suggest the possible implication of ER stress in the development of a renal fibrotic wound in animals with MI.

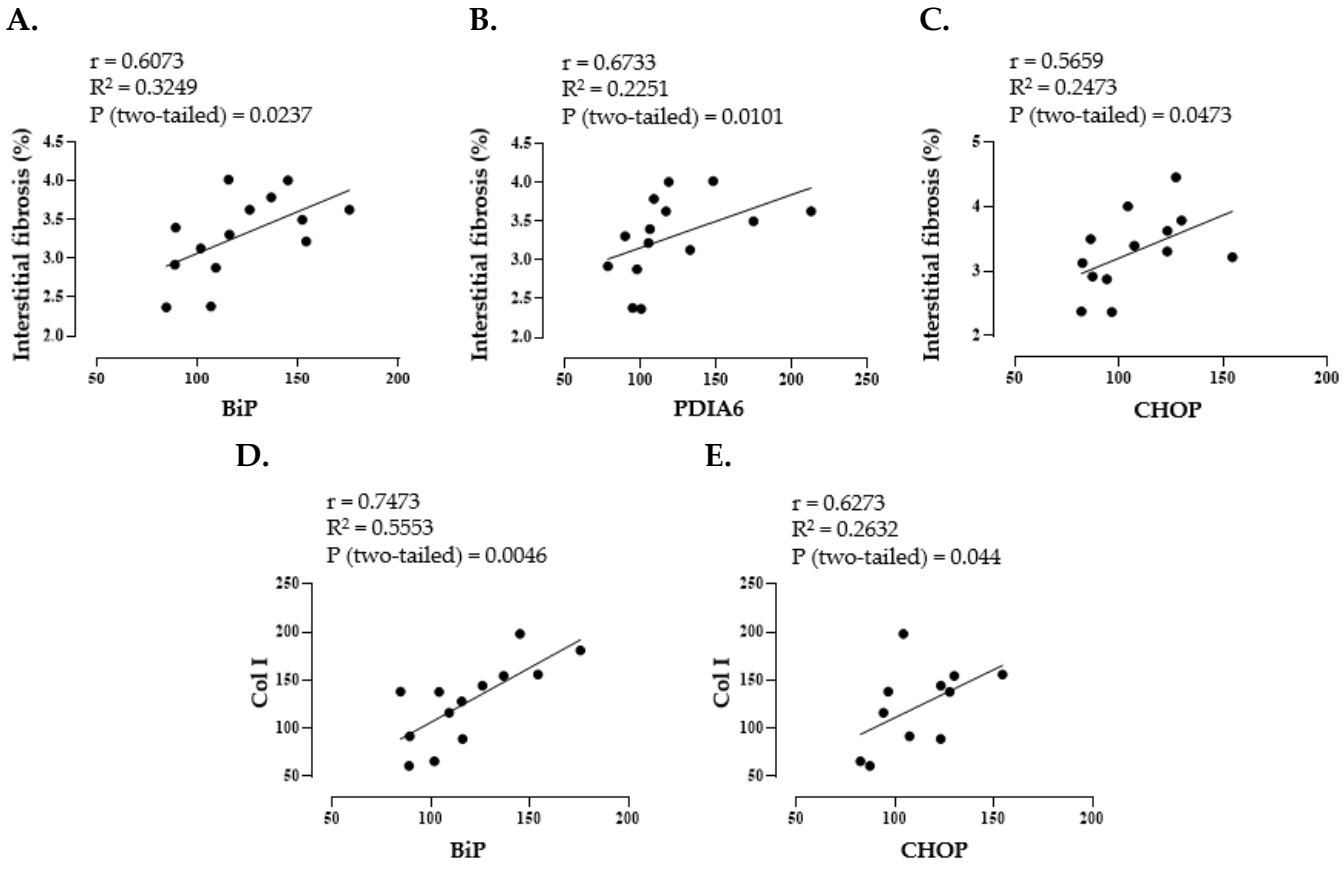


**Figure 18. ER stress correlations in the animal model of MI**. Correlation between the renal levels of interstitial fibrosis and (**A**) Immunoglobulin binding protein (BIP), (**B**) Protein disulfide isomerase family A member 6 (PDIA6) or (**C**) CCAAT-enhancer-binding homologous protein (CHOP). Correlation between renal protein levels of collagen I (Col I) and (**D**) BiP or (**E**) CHOP from from rats subjected to myocardial infarction (MI) or to a sham operation (Sham).

Along with fibrosis, oxidative stress, inflammation and ER stress activation, infarcted animals presented higher circulating levels of two well-known

deleterious effectors, which could participate in renal damage. Compared to the control group, animals with MI presented a slight increase of palmitic acid (PA; 48.04 ± 6.42 for Sham vs. 58.92 ± 4.18 μM for MI) and a significant increment of angiotensin II plasmatic levels ($p < 0.001$) (Figure 19).

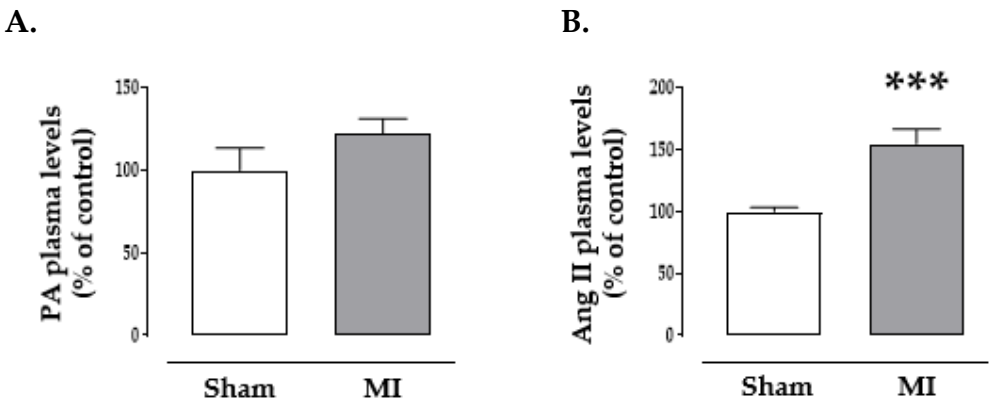


**Figure 19. Impact of MI on Palmitic Acid (PA) and Angiotensin II (Ang II) circulating levels** in rats subjected to myocardial infarction (MI) or to a sham operation (Sham). Bar graphs represent the mean ± SEM of 8-10 animals normalized to glyceraldehyde-3-phosphate dehydrogenase (GAPDH). ***$p < 0.001$ versus Sham group.

### 3.1. Palmitic acid activation of ER stress in renal fibroblasts.

Previous studies have shown that PA activates ER stress and inflammation in podocytes [376]. The presence of different concentrations of PA (50-200 μM) in the culture medium for 24 hours resulted in the activation of ER stress, as evidenced by the increase in PDIA6 protein levels and the upregulation of two downstream ER stress proteins, ATF6$\alpha$ and CHOP (Figure 20). Interestingly, PA-treated cells exhibited elevated levels of collagen I at the dose of 100 μM of PA (Figure 21A) and increased levels of the profibrotic mediator TGF-β independently of the PA dose (Figure 21B). This profibrotic response to PA was accompanied by heightened production of superoxide anion, reaching its maximum effect at the dose of 100 μM of PA after 24 hours of stimulation (Figure 21C).

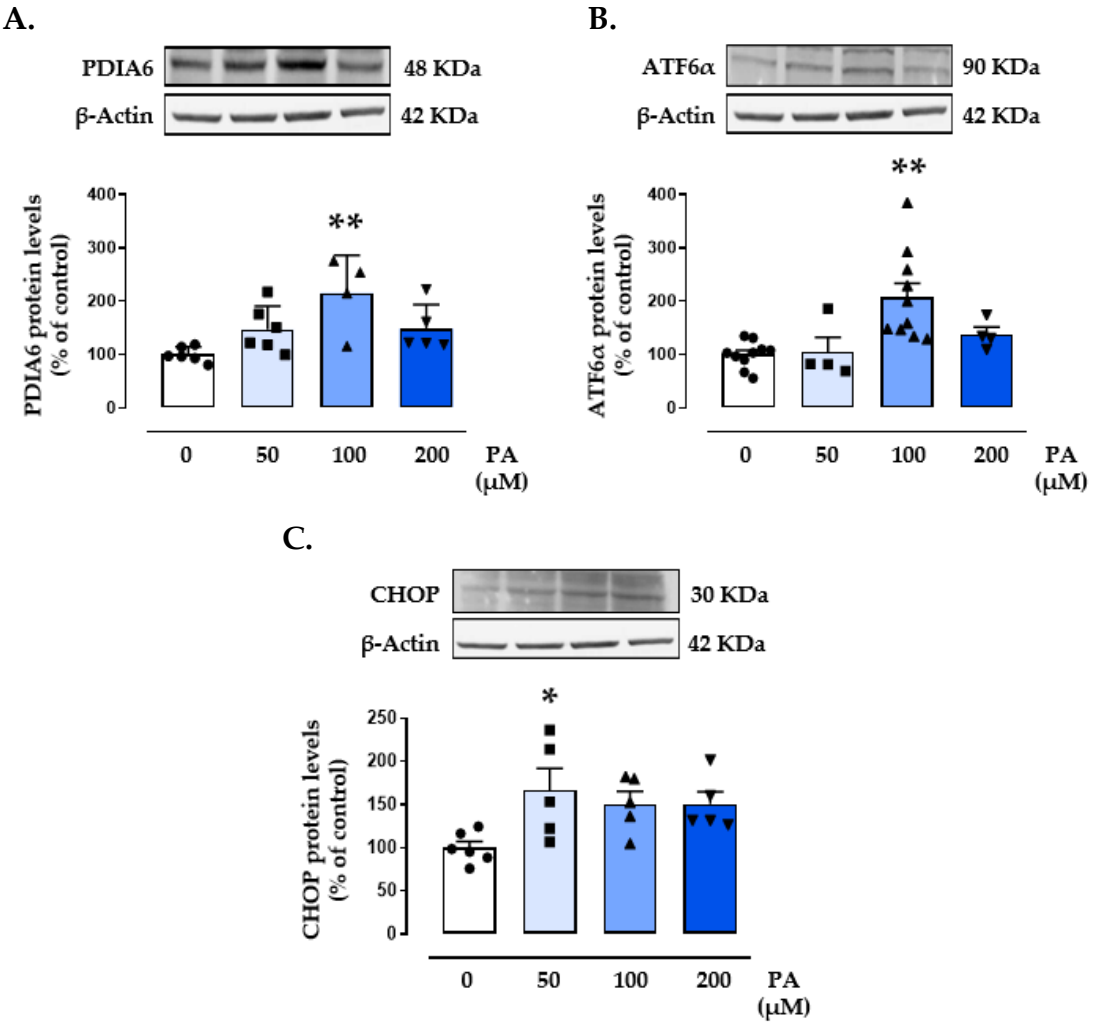


**Figure 20**. **Palmitic Acid (PA) effects on endoplasmic reticulum stress.** Protein levels of **(A)** protein disulfide isomerase family A member 6 (PDIA6); (**B**) activating transcription factor 6-alpha (ATF6α) and (**C**) CCAAT-enhancer-binding homologous protein (CHOP) in renal fibroblasts (TFBs) stimulated with palmitic acid (PA; 50-200 μM) for 24 hours. Bar graphs represent the mean ± SEM of 4-6 assays normalized to β-actin. *$p < 0.05$; **$p < 0.01$ versus control cells.

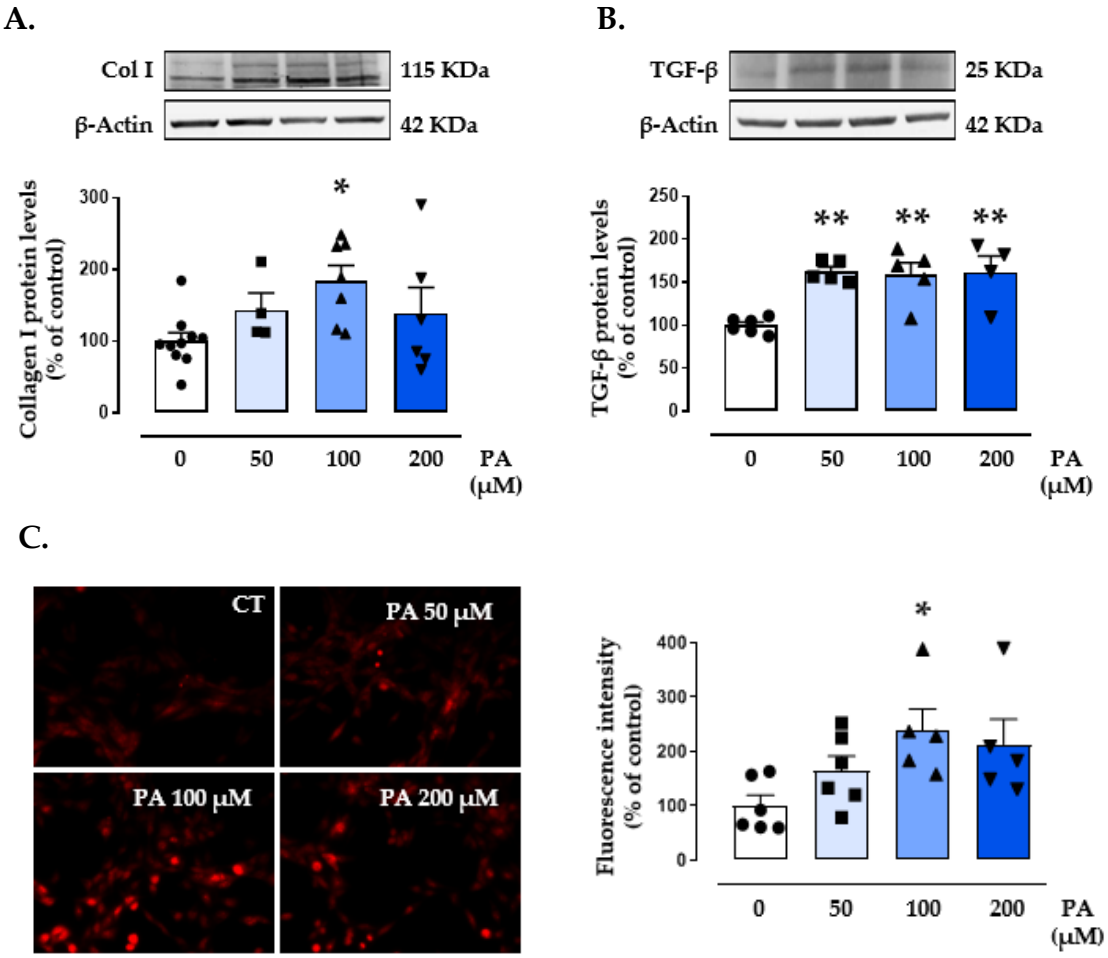


**Figure 21**. **Palmitic Acid (PA) effects on extracellular matrix proteins and superoxide anion production.** Protein levels of **(A)** collagen I and (**B**) transforming growth factor beta (TGF-β), (**C**) representative microphotographs and quantification of cells labeled with the oxidative dye dihydroethidium (40X magnification) in renal fibroblasts (TFBs) stimulated with palmitic acid (PA; 50-200 μM) for 24 hours. Bar graphs represent the mean ± SEM of 4-6 assays normalized to β-actin. *$p < 0.05$; **$p < 0.01$ versus control cells.

### 3.1.1. ER stress plays a pivotal role in mediating the prooxidant, profibrotic and proinflammatory effects of palmitic acid.

To investigate the potential involvement of ER stress in the prooxidant and profibrotic effects of PA, TFBs were exposed to 100 μM dose of PA for 24 hours in the presence or absence of the pharmacological inhibitor of ER stress, 4-PBA.

The results revealed that 4-PBA effectively prevented the PA-induced increase in superoxide anion production at both the 2 μM and the 4 μM doses of 4-PBA (Figure 22A-B). Subsequently, the 4 μM dose of 4-PBA was used for further experiments. At this concentration, the pharmacological treatment successfully inhibited the activation of ER stress, thereby preventing the upregulation of BiP, PDIA6 and ATF6*α* protein levels induced by PA (Figure 22C-E), showing the efficiency of 4-PBA.

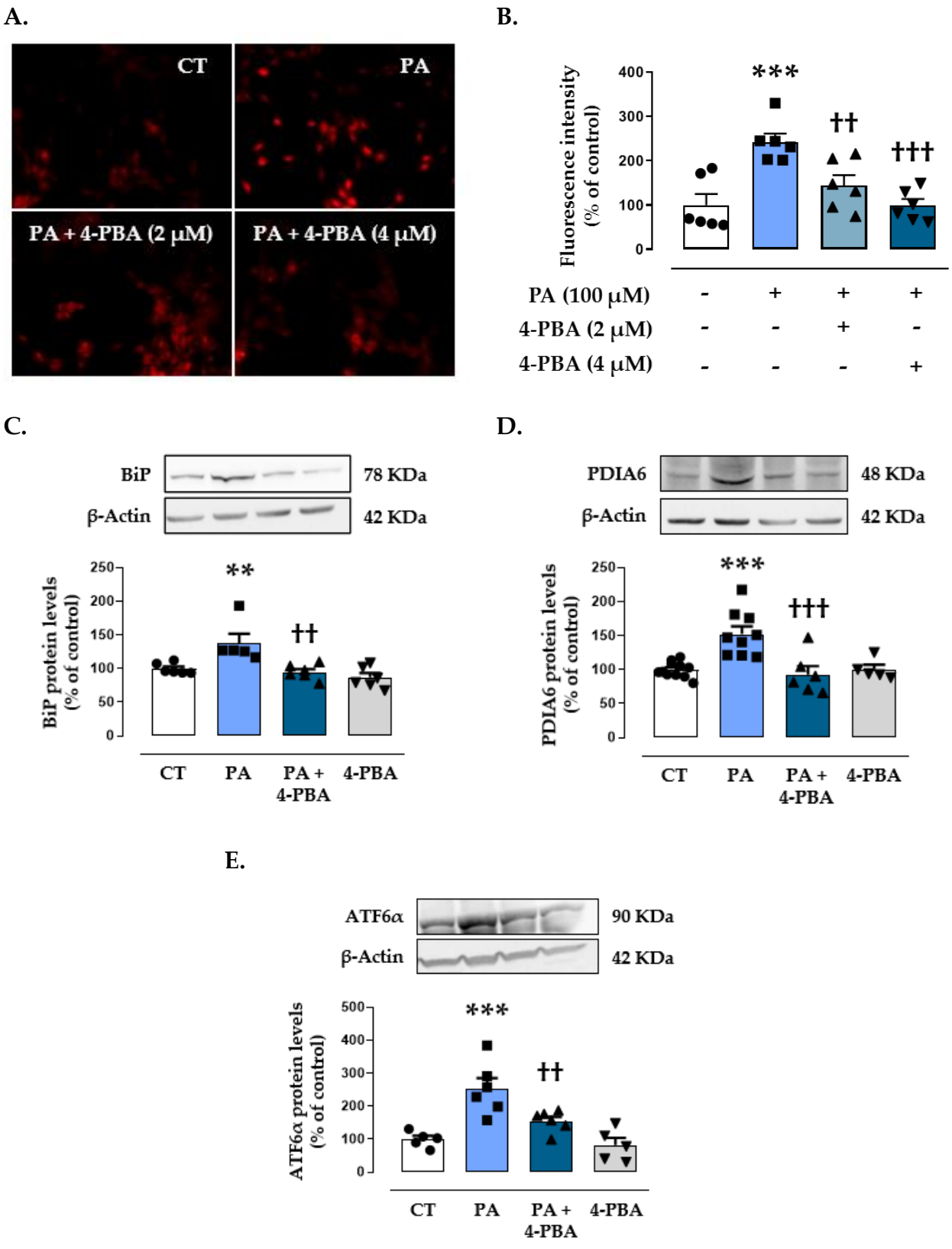


**Figure 22. Endoplasmic reticulum stress mediates the prooxidant effects of palmitic acid in renal fibroblasts. (A-B)** Representative microphotographs and quantification of cells labeled with the oxidative dye dihydroethidium (40X magnification) in renal fibroblasts (TFBs) stimulated with palmitic acid (PA; 100 μM) and treated with 4-phenylbutyrate acid (4-PBA; 2-4 μM) for 24 hours. Protein levels of (**C**) immunoglobin binding protein (BiP); (**D**) protein

disulfide isomerase family A member 6 (PDIA6) and (**E**) activating transcription factor 6 alpha (ATF6$\alpha$) in TFBs stimulated with palmitic acid (PA; 100 µM) and treated with 4-PBA (4 µM) for 24 hours. Bar graphs represent the mean ± SEM of 4-6 assays normalized to β-actin. **p < 0.01; ***p < 0.001 versus control cells. †† p< 0.01; ††† p < 0.001 versus PA-treated cells.

Moreover, 4-PBA demonstrated the ability to counteract the increase in extracellular matrix proteins generated by PA after a 24-hour treatment. TFBs treated with the pharmacological inhibitor of ER stress were resistant to the PA-induced increase in TGF-β (Figure 23) and exhibited hindered collagen I production at mRNA levels (Figure 23). Additionally, cells treated with PA (100 µM) showed an elevation in proinflammatory markers, including IL-6, CCL-2 and osteopontin (OPN). The pharmacological inhibition of ER stress effectively prevented the PA-triggered proinflammatory response in renal fibroblasts. These protective effects of 4-PBA were associated with the prevention of the upregulation in the acute kidney injury marker, NGAL, induced by PA in renal cells (Figure 23).

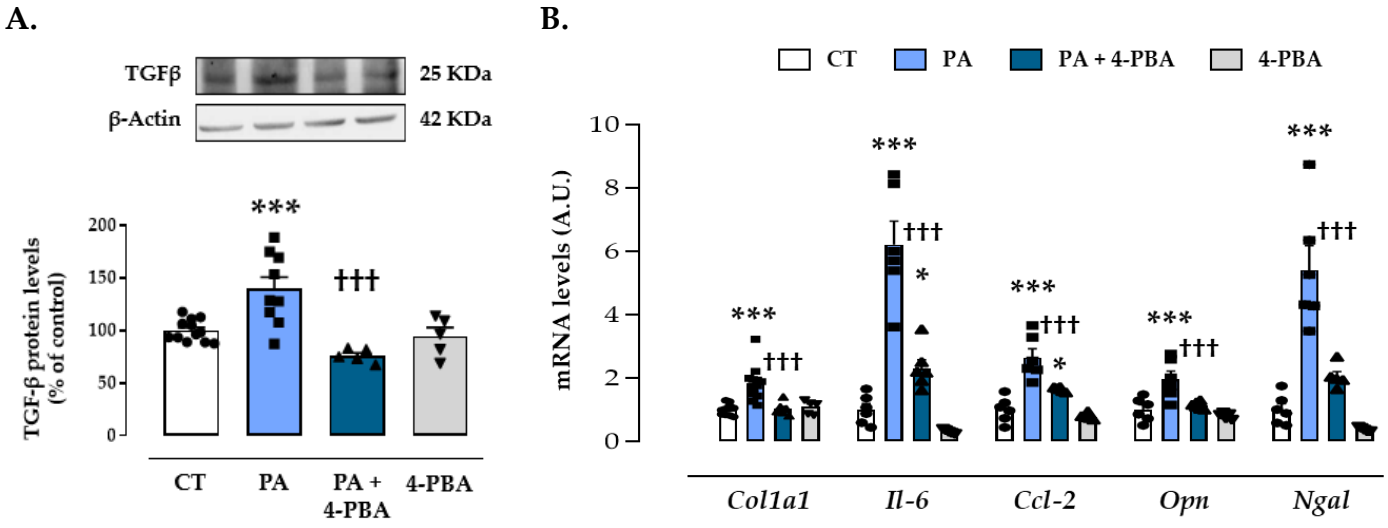


**Figure 23. Endoplasmic reticulum stress mediates the profibrotic and proinflammatory effects of palmitic acid in renal fibroblasts.** (**A**) transforming growth factor beta (TGF-β) protein expression; (**B**) collagen I mRNA expression, interleukin-6 (IL-6), C-C motif chemokine ligand 2 (CCL-2), osteopontin (OPN) and neutrophil gelatinase-associated lipocalin (NGAL) mRNA expression in renal fibroblasts (TFBs) stimulated with palmitic acid (PA; 100 µM) and treated with 4-phenylbutyrate acid (4-PBA; 4 µM) for 24 hours. Bar graphs represent the mean

± SEM of 4-6 assays normalized to β-actin for protein or HPRT for cDNA. *p < 0.05; ***p < 0.001 versus control cells. ††† p < 0.001 versus PA-treated cells.

### 3.2. Angiotensin II activation of ER stress in renal fibroblasts.

We examined the potential involvement of ER stress in a well-established profibrotic factor at renal level. Angiotensin II (Ang II) induced ER stress in a dose-dependent manner as evidenced by elevated protein levels of BiP, PDIA6, CHOP and ATF6$\alpha$ after 24 hours of stimulation in TFBs (Figure 24).

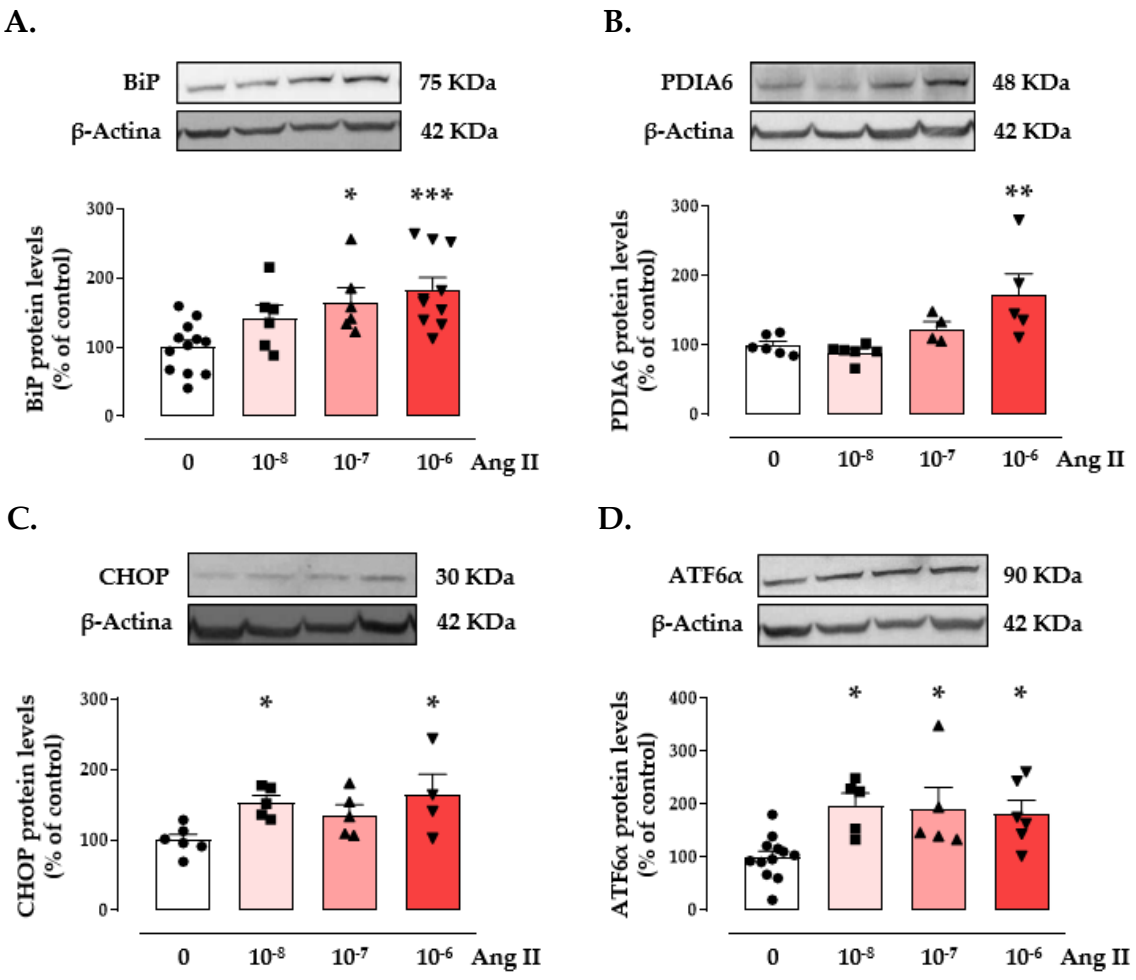


**Figure 24. Angiotensin II induces endoplasmic reticulum stress activation in renal fibroblasts.** Protein levels of (A) immunoglobulin binding protein (BiP); (B) protein disulfide isomerase family A member 6 (PDIA6); (C) CCAAT-enhancer-binding homologous protein (CHOP) and (D) activating transcription factor 6 alpha (ATF6$\alpha$) in renal fibroblasts (TFBs) stimulated with Angiotensin II (Ang II; $10^{-8}$- $10^{-6}$M) for 24 hours. Bar graphs represent the

mean ± SEM of 4-6 assays normalized to β-actin. *p < 0.05; **p < 0.01; ***p < 0.001 versus control cells.

Subsequent experiments were performed with the dose of $10^{-6}$M Ang II in the presence or absence of 4-PBA at 4 μM. The pharmacological inhibitor of ER stress successfully prevented the increase in superoxide anion production induced by Ang II (Figure 25A-B). Additionally, it mitigated the elevation of collagen I and Gal-3 as well as the mRNA levels of the proinflammatory markers IL-6, CCL-2 and OPN in Ang II-treated cells (Figure 25 C).

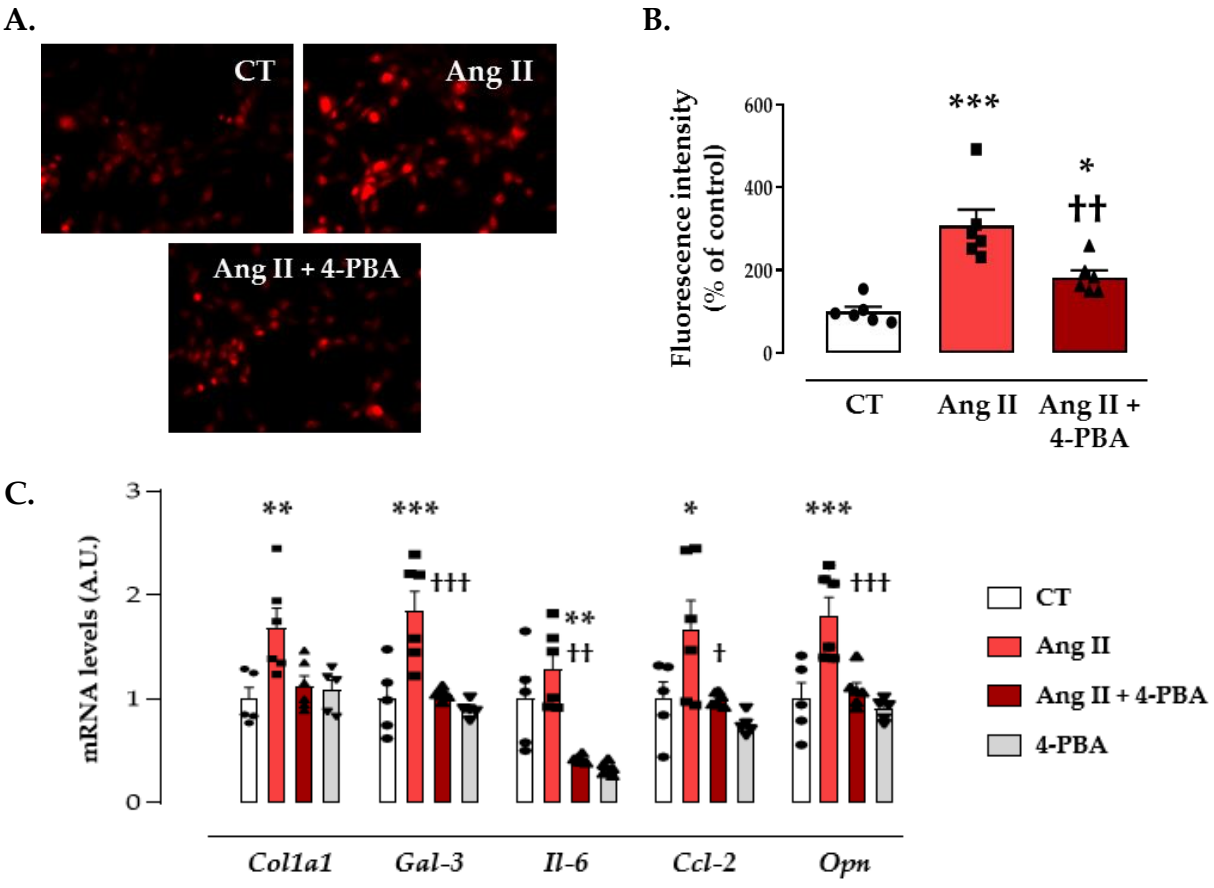


**Figure 25. Endoplasmic reticulum stress mediates the prooxidant, profibrotic and proinflammatory effects of Angiotensin II in renal fibroblasts. (A-B)** Representative microphotographs and quantification of cells labelled with the oxidative dye dihydroethidium (40X magnification). mRNA levels of (**C**) Collagen I, interleukin 6 (IL-6), C-C motif chemokine ligand 2 (CCL-2) and osteopontin (OPN) in TFBs stimulated with Angiotensin II (Ang II; $10^{-6}$M) and treated with 4-PBA (4 μM) for 24 hours. Bar graphs represent the mean ± SEM of 4-6 assays normalized to HPRT for cDNA. *p < 0.05; **p < 0.01; ***p < 0.001 versus control cells. † p < 0.05; †† p < 0.01; ††† p < 0.001 versus Ang II-treated cells.

The potential intracellular pathways through which Ang II exerts its fibrotic effects in renal fibroblasts were also examined. Ang II at $10^{-6}$ M induced NFκB phosphorylation within 10 minutes of stimulation (Figure 26A), Akt phosphorylation at 60 minutes (Figure 26B) and increased protein levels of ERK phosphorylation at 5 and 10 minutes (Figure 26C). The addition of LY294002, a specific inhibitor of the PI3K/Akt pathway, did not alter the elevation in collagen I protein levels caused by Ang II (Figure 26D). Conversely, the presence of BAY11-7082 and PD98059, the specific inhibitors of the NFκB pathway and ERK1/2, respectively, prevented the profibrotic effects of Ang II in renal cells (Figure 26D).

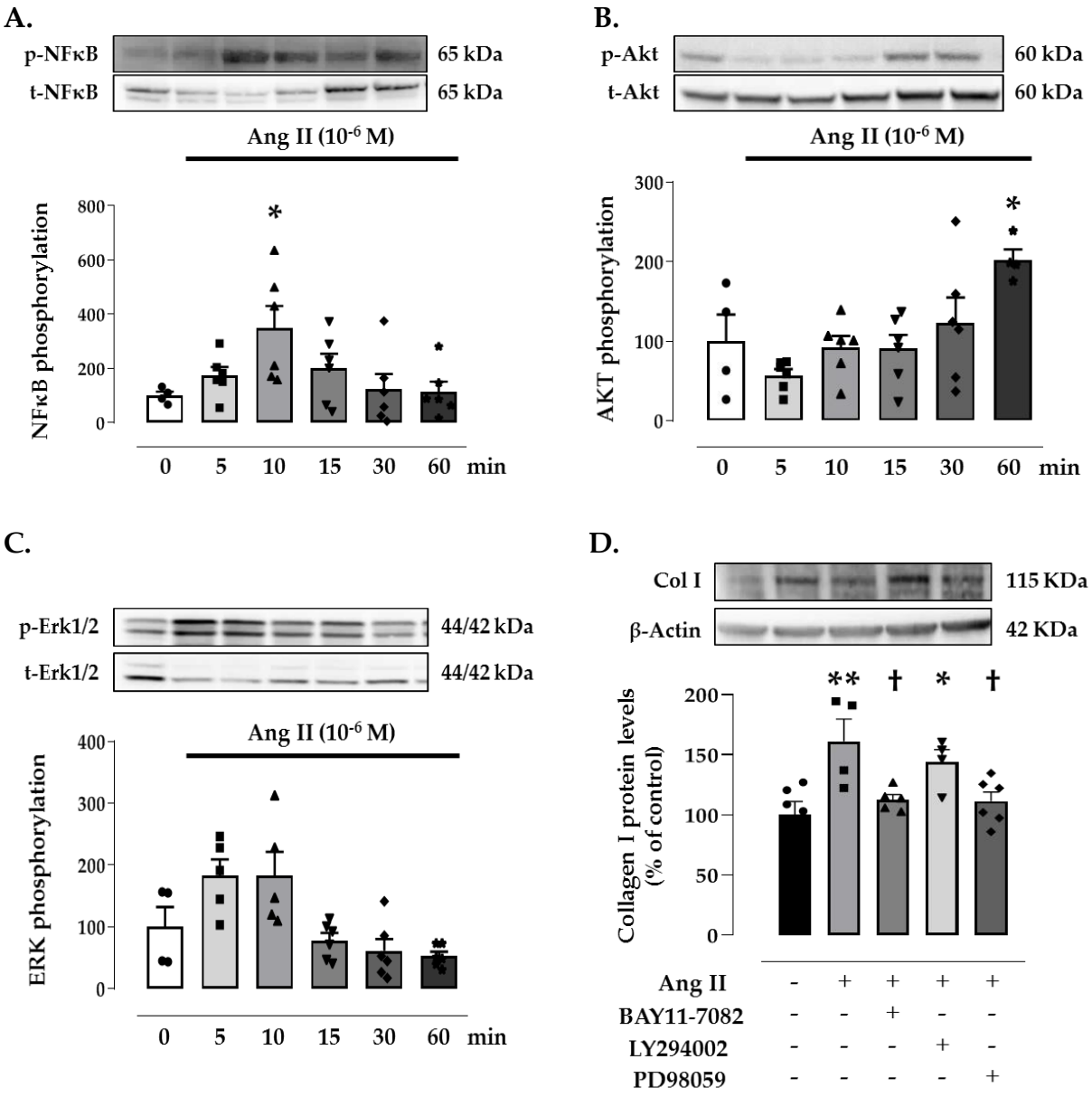


**Figure 26. NFκB and ERK 1/2 mediate the profibrotic effects of Angiotensin II in renal fibroblasts**. Phosphorilation of **(A)** nuclear factor-**κB** (p-NFκB); **(B)** protein kinase B (p-Akt) and **(C)** extracellular signal-regulated kinases 1/2 (p-ERK1/2) in renal fibroblasts (TFBs) stimulated with Angiotensin II (Ang II; $10^{-6}$M) for 5-60 minutes. **(D)** Effects of the NFκB inhibitor BAY11-7082 ($10^{-6}$M), the Akt inhibitor LY294002 ($10^{-6}$M) or the ERK1/2 inhibitor PD98059 ($10^{-6}$M) on collagen type I protein synthesis in renal fibroblasts (TFBs) stimulated with Ang ($10^{-6}$M) for 24 hours. Bar graphs represent the mean ± SEM of 4-6 assays normalized to total NFκB, total Akt, total ERK1/2 or β-actin. *$p < 0.05$; **$p < 0.01$ versus control cells. † $p < 0.05$ versus Ang II-treated cells.

## III. Renal consequences of myocardial infarction in the context of obesity.

Rats on a high-fat diet (HFD) exhibited an increase in body weight and a higher adiposity index that the control animals which were fed a standard diet (Table 14). Obese animals that underwent coronary artery ligation exhibited cardiac functional alterations such as a decrease in systolic and diastolic function compared with the control group in the absence of modifications in systolic blood pressure. Additionally, structural modifications including cardiac hypertrophy and interstitial fibrosis were observed (Table 14).

In this context, the pharmacological inhibition of Gal-3 by *modified citrus pectin* (MCP) was able to ameliorate the alterations observed in functional parameters as well as in cardiac hypertrophy and fibrosis in absence of effects on body weight or adiposity index (Table 14).

**Table 14**. Effect of Galectin-3 inhibition on HFD-MI induced alterations after 4 weeks of treatment. Rats fed a normal diet were subjected to a sham operation (Sham) whereas rats fed a high fat diet (HFD) were subjected to myocardial infarction (MI) in the presence or absence of *modified citrus pectin* (MCP).

| | Sham | HFD-MI | HFD-MI MCP |
|---|---|---|---|
| Body weight (g) | 356.1 ± 6.15 | 394.8 ± 9.7 ** | 407.5 ± 11.55 ** |
| Adiposity index (%) | 4.57 ± 0.41 | 10.82 ± 0.86 *** | 10.50 ± 0.73 *** |
| LVEF (%) | 80.95 ± 0.99 | 70.147 ± 1.02 ** | 75.349 ± 3.5 |
| E/A ratio | 0.96 ± 0.04 | 0.79 ± 0.05 * | 0.975 ± 0.029 # |
| SBP (mmHg) | 124.3 ± 1.704 | 129.5 ± 1.708 | 129.9 ± 0.911 |
| Relative heart weight (g/cm tibia) | 0.243 ± 0.004 | 0.264 ± 0.005 * | 0.275 ± 0.007 ** |
| Cardiac fibrosis (%) | 1.856 ± 0.15 | 5.124 ± 0.42 *** | 3.146 ± 0.14 ** ### |
| Creatinine (mg/dl) | 0.31 ± 0.014 | 0.31 ± 0.01 | 0.29 ± 0.02 |

Data is expressed as means ± SEM of 8-10 animals. SBP: systolic blood pressure; LV: left ventricle; LVEF: left ventricle ejection fraction. *p < 0.05; **p < 0.01; ***p < 0.001 versus Sham group. #p < 0.05; ##p < 0.01; ###p < 0.001 versus HFD-MI group.

### 1. Effects of Galectin-3 inhibition on renal fibrosis in MI obese animals.

Despite the well-known profibrotic role of Gal-3 in different pathological contexts, including obesity and MI, the underlying mechanisms are not totally defined. To investigate the potential involvement of Gal-3 in the renal consequences of MI in the context of obesity, a group of animals was treated with the Gal-3 activity inhibitor MCP.

At renal level, despite the absence of alterations in creatinine serum levels, HFD-MI animals presented a renal increase in NGAL mRNA levels in comparison to the control group, effect that the treatment with MCP was able to prevent (Figure 27A). The protective effect of MCP on NGAL renal levels was accompanied by a reduction in both Gal-3 gene and protein levels, as illustrated in Figure 27B.

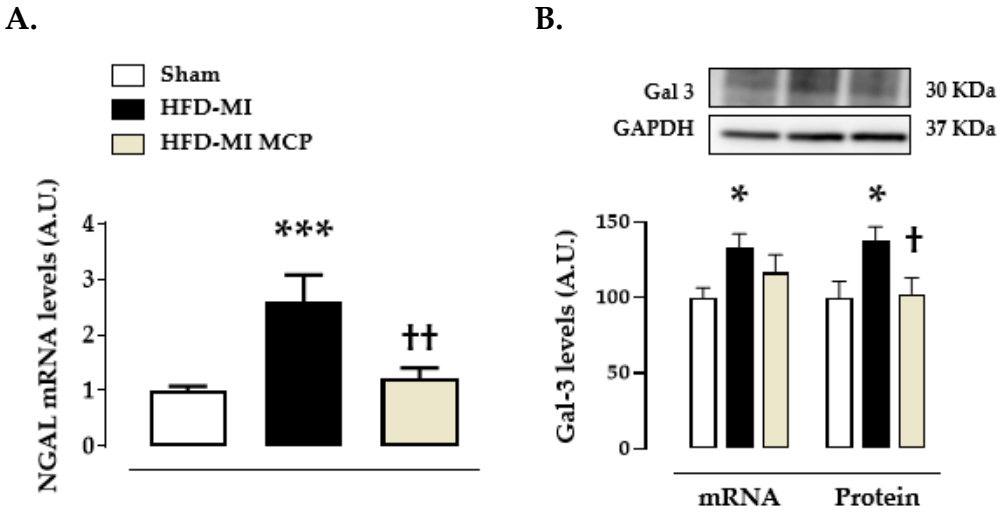


**Figure 27. Beneficial effect of MCP on NGAL and Galectin-3 renal levels in HFD-MI animals. (A)** mRNA levels of neutrophil gelatinase-associated lipocalin (NGAL), (**B**) mRNA and protein levels of Galectin-3 (Gal-3) in kidneys from rats fed a high fat diet (HFD) and subjected to myocardial infarction (MI) in the presence or absence of modified citrus pectin (MCP) treatment. Bar graphs represent the mean ± SEM of 8-10 animals normalized to glyceraldehyde-3-phosphate dehydrogenase (GAPDH) for protein or hypoxanthine-guanine phosphoribosyltransferase (HPRT). *p < 0.05; ***p < 0.001 versus Sham animals. † p < 0.05; †† p < 0.01 versus HFD-MI group.

At structural level, HFD-MI animals exhibited similar glomerular area to sham animals regardless of MCP treatment (Figure 28A-B). Nevertheless, obese-

infarcted animals displayed not only glomerular but also interstitial and perivascular fibrosis, as illustrated in Figures 28A-E. Additional analysis showed that the observed renal fibrosis resulted from a reduction in the matrix metalloproteinase 2 (MMP-2) activity (Figure 29A) and an increase in Collagen type IV and fibronectin, along with an elevation of the profibrotic mediators TGF-β and $\alpha$-SMA protein levels (Figure 29C). Similar findings were observed at the mRNA levels (Figure 29B). The pharmacological inhibition of Gal-3 activity successfully normalized all these outcomes except for the fibronectin protein levels. Notably, matrix metalloproteinase 9 (MMP-9) activity and collagen type I protein levels remained unchanged in all studied groups (Figures 29 A, C).

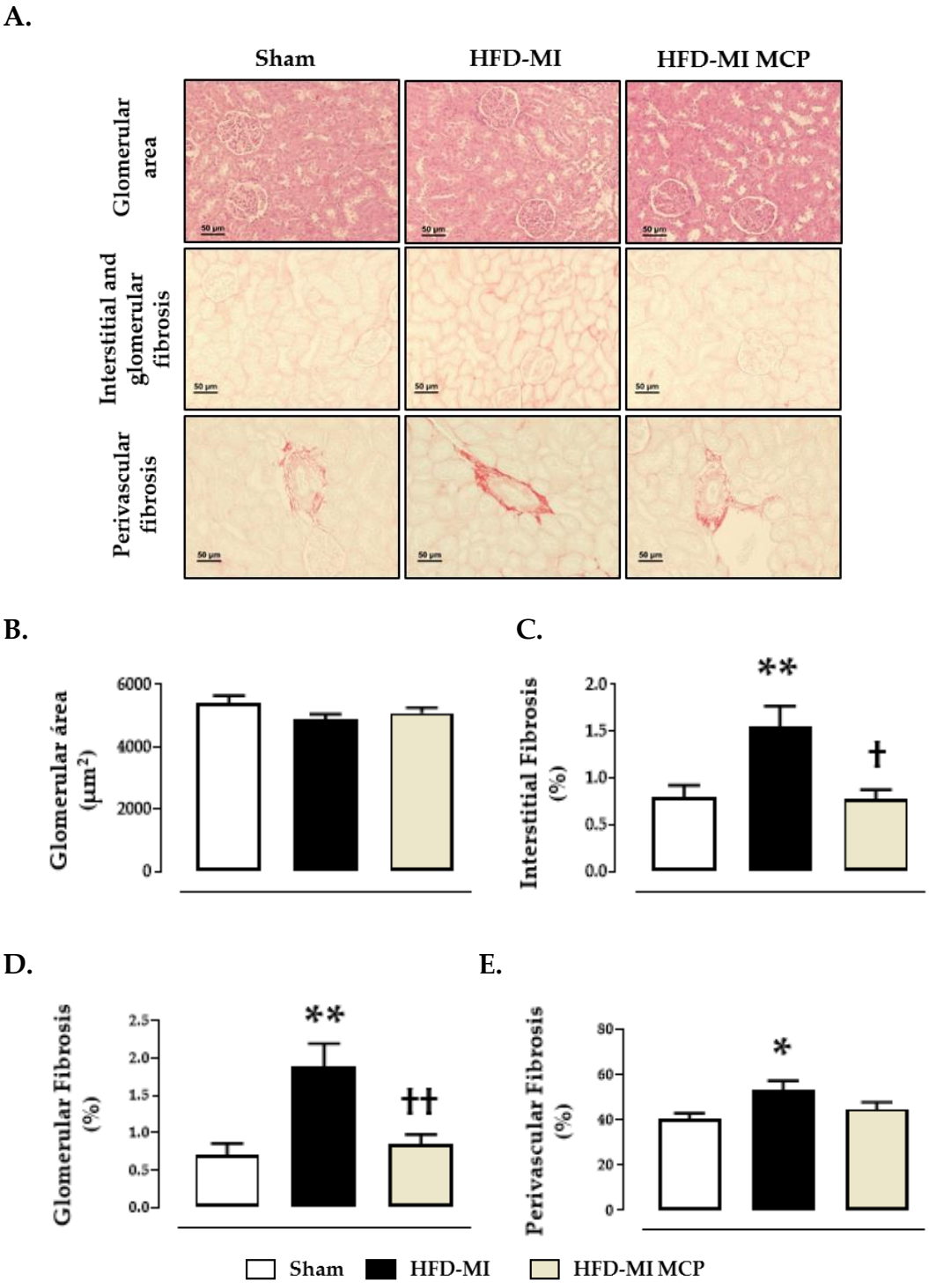


**Figure 28. Effect of Galectin-3 inhibition on renal fibrosis in HFD-MI animals. (A)** Representative microphotographs (20x magnification) of renal cortex sections staining with haematoxylin-eosin for glomerular area analysis or picrosirius red for fibrosis analysis. Quantification of **(B)** glomerular area, (**C**) interstitial fibrosis, (**D**) glomerular fibrosis and **(E)** perivascular fibrosis in kidneys from rats fed a high fat diet (HFD) and subjected to myocardial infarction (MI) in the presence or absence of modified citrus pectin (MCP) treatment. Bar graphs represent the mean ± SEM of 8-10 animals. *$p < 0.05$; **$p < 0.01$ versus Sham animals. † $p < 0.05$; †† $p < 0.01$ versus HFD-MI group.

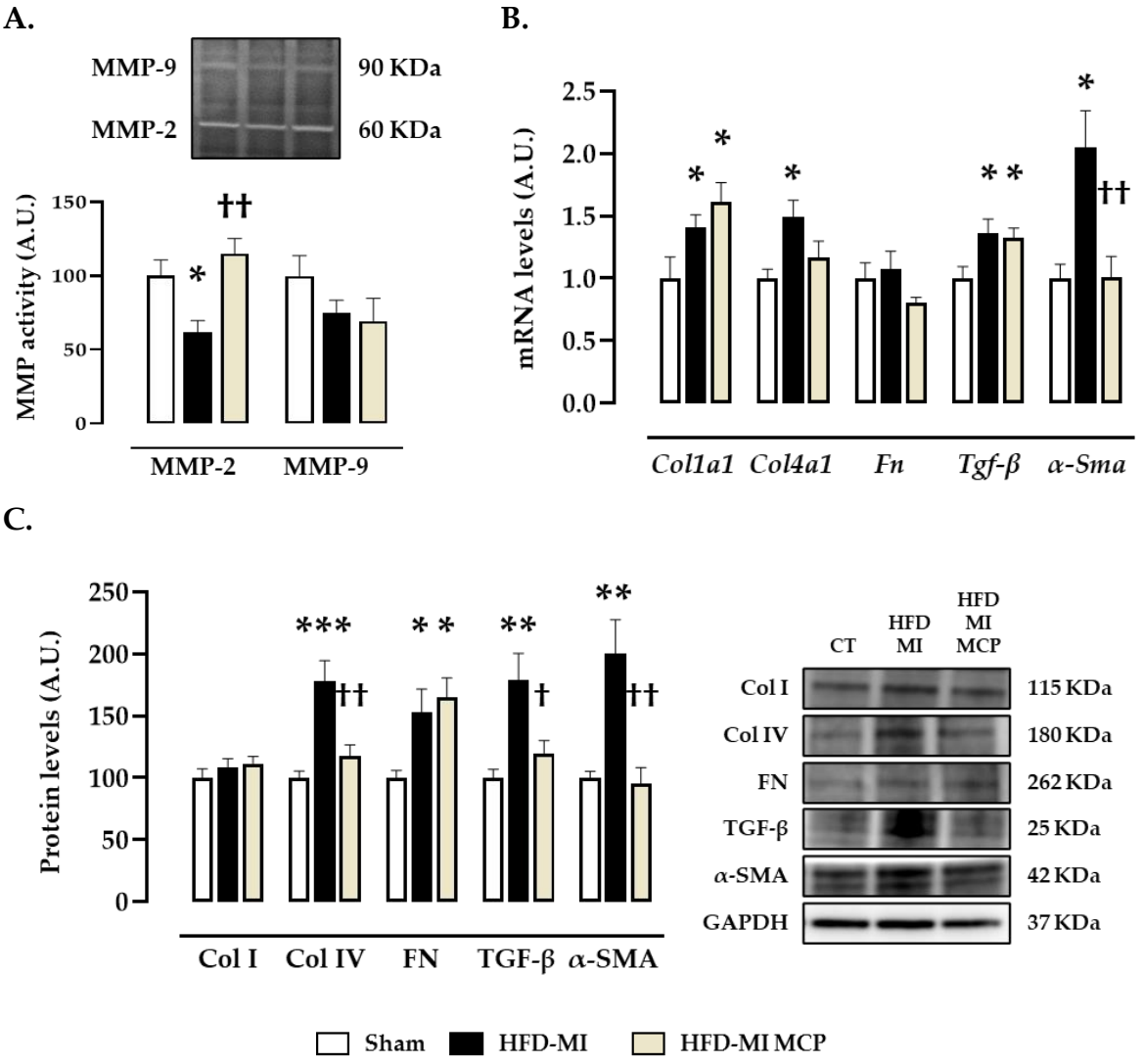


**Figure 29. Effect of Galectin-3 inhibition on extracellular matrix synthesis and degradation in HFD-MI animals. (A)** Matrix metalloproteinase 2 (MMP-2) and 9 (MMP-9) renal activity reduction in HFD-MI animals. **(B)** renal mRNA and **(C)** protein levels of collagen type I, collagen type IV, fibronectin (FN), transforming growth factor beta (TGF-β) and alpha-smooth muscle actin (α-SMA) in in kidneys from rats fed a high fat diet (HFD) and subjected to myocardial infarction (MI) in the presence or absence of modified citrus pectin (MCP) treatment. Bar graphs represent the mean ± SEM of 8-10 animals normalized to glyceraldehyde-3-phosphate dehydrogenase (GAPDH) for protein or hypoxanthine-guanine phosphoribosyltransferase (HPRT). *p < 0.05; **p < 0.01; ***p < 0.001 versus Sham animals. † p < 0.05; †† p < 0.01 versus HFD-MI group.

**2. Effects of Galectin-3 inhibition on renal oxidative stress and inflammation in MI obese animals.**

As depicted in Figure 30A-B, HFD-MI animals presented higher levels of superoxide anions indicated by a renal elevation in the fluorescence intensity as compared to control animals. This prooxidant environment seems to be due to an increase in the production of ROS without modifications in the antioxidant defence, evaluated by catalase protein levels (Figure 30C).

The mentioned prooxidant environment was accompanied by an inflammatory response characterized by elevated levels of proinflammatory cytokines such as OPN, IL-6 and TNF-$\alpha$ without modifications in CCL-2 mRNA levels as compared with control group (Figure 30D). MCP treatment was able to mitigate the increase in superoxide anions and proinflammatory markers in the kidney of the obese infarcted animals.

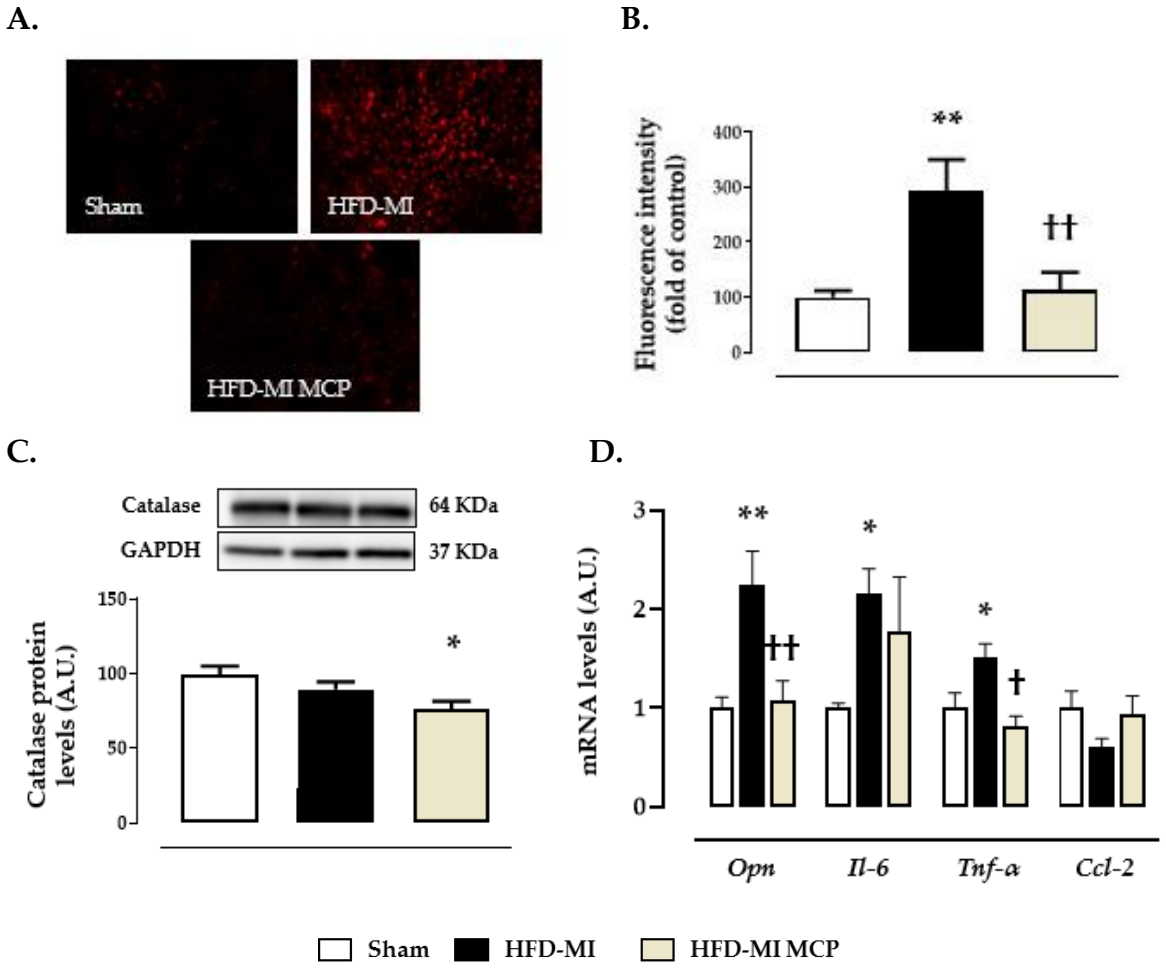


**Figure 30. Effect of Galectin-3 inhibition on oxidative stress and inflammation in HFD-MI animals. (A-B)** Representative microphotographs and quantification of renal cortex sections labelled with the oxidative dye dihydroethidium (40X magnification). **(C)** Renal protein levels of catalase and **(D)** Renal mRNA levels of osteopontin (OPN), interleukin-6 (IL-6), tumor necrosis factor-alpha (TNF-$\alpha$), C-C motif chemokine ligand 2 (CCL-2) in kidneys from rats fed a high fat diet (HFD) and subjected to myocardial infarction (MI) in the presence or absence of modified citrus pectin (MCP) treatment. Bar graphs represent the mean ± SEM of 8-10 animals normalized to glyceraldehyde-3-phosphate dehydrogenase (GAPDH) for protein or hypoxanthine-guanine phosphoribosyltransferase (HPRT). *p < 0.05; **p < 0.01 versus Sham animals. † p < 0.05; †† p < 0.01 versus HFD-MI group.

### 3. Galectin-3 downregulates microRNA let-7f-5p in MI obese animals.

In order to further comprehend the mechanisms contributing to renal damage in concomitant obesity and MI, plasma samples from Sham and HFD-MI animals were screened to identify microRNAs relevant to this pathological context. Out of 179 microRNAs examined, 151 were detected in the microarray. 47 of the

detected microRNAs presented significant alterations between the control and HFD-MI group. Specifically, 36 microRNAs were decreased while 11 presented an increase of more than two-fold (Figure 31). Among them, the 5 most differentially expressed microRNAs between the two groups were selected for further analysis, being let-7f-5p, miR-17-5p, miR-144-5p and miR-339-3p down-regulated and miR-485-3p up-regulated (Table 15).

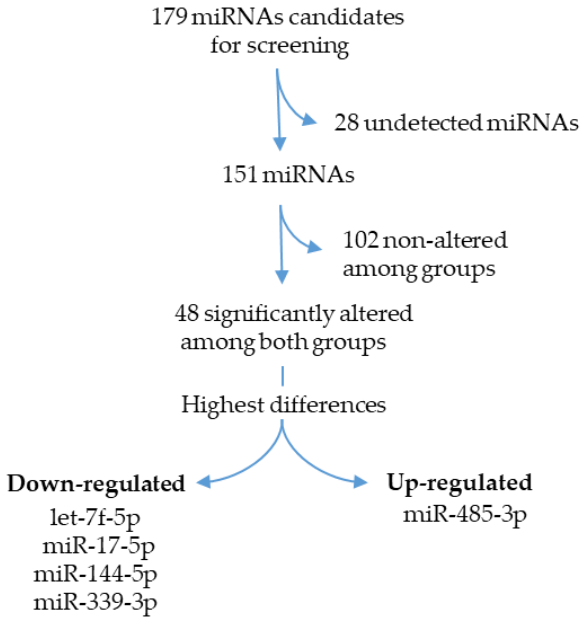


**Figure 31.** Visual representation in the form of a flow chart delineating the sequential approach for microRNA selection.

**Table 15**. microRNA expression in plasma samples from sham and HFD-MI animals.

| | Ct Values | | Fold-change (CT/HFD-MI) | Fold-regulation |
|---|---|---|---|---|
| | Sham | HFD-MI | | |
| let-7f-5p | 29.3 | 31.97 | 0.3763 | -2.6574 |
| miR-17-5p | 32.3 | 35 | 0.3686 | -2.7132 |
| miR-144-5p | 32.37 | 34.64 | 0.4965 | -2.0139 |
| miR-339-3p | 29.73 | 35 | 0.0621 | -16.1113 |
| miR-485-3p | 35 | 33.78 | 5.579 | 5.579 |

Next, we verified the expression of these microRNAs in the renal samples from our *in-vivo* model in order to assess whether the circulating levels mirror the

expression of these microRNAs at tissue level and to also explore the potential influence of Gal-3 inhibition on them. The obese animals with MI showed a decrease in all the five microRNAs (Figure 32A-E), however, Gal-3 inhibition had a significant effect only on the let-7f-5p levels (Figure 32A), showing that in this pathological scenario Gal-3 could exert its effects through the downregulation of let-7f-5p.

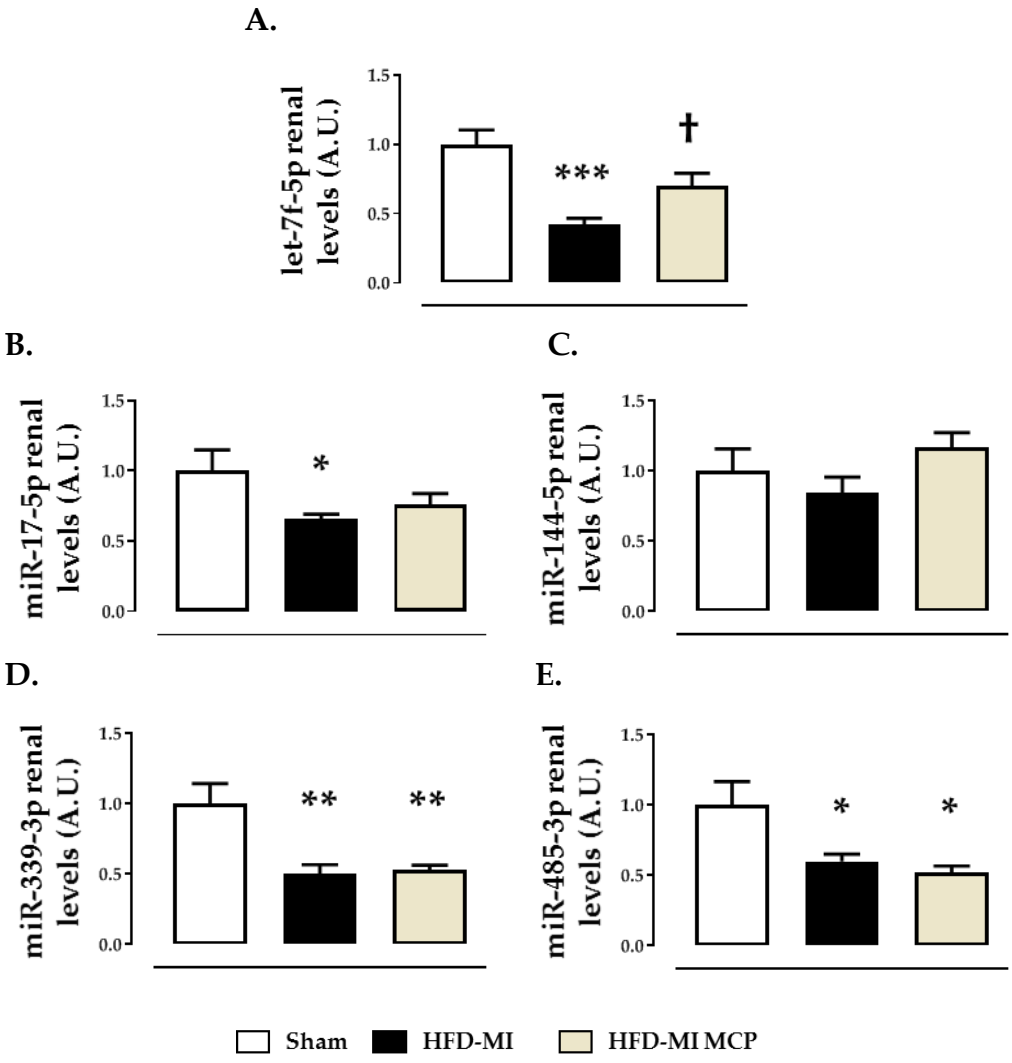


**Figure 32. Effect of Galectin-3 inhibition on microRNA renal expression in HFD-MI animals.** Renal expression levels of **(A)** let-7f-5p; **(B)** miR-17-5p; **(C)** miR-144-5p; **(D)** miR-339-3p and **(E)** miR-485-3p in kidneys from rats fed a high fat diet (HFD) and subjected to myocardial infarction (MI) in the presence or absence of modified citrus pectin (MCP) treatment. Bar graphs represent the mean ± SEM of 8-10 animals normalized to U6 gene for cDNA. *p < 0.05; **p < 0.01; ***p < 0.001 versus Sham animals. † p < 0.05 versus HFD-MI group.

To investigate whether let-7f-5p might function as a potential mediator of Gal-3, tools such as mirWalk 2.0 [377] and tarbase v.7 [378] were used to *in-silico* predict relevant pathways and targets potentially regulated by this microRNA in our animal model. Figure 33 illustrates the Log 10 (p-values) of the significantly enriched pathways identified through mirPath v.3 and v4.0 [368, 369]. Interestingly, out of the prediction analysis of let-7f-5p revealed ECM-receptor interaction as the most significant pathway. The fact that, the pharmacological inhibition of Gal-3 prompted the recovery of let-7f-5p levels, which was accompanied by a reduction in renal fibrosis in MCP-treated rats that suggests let-7f-5p may serve as a novel mediator of the profibrotic actions of Gal-3 in HFD-MI animals.

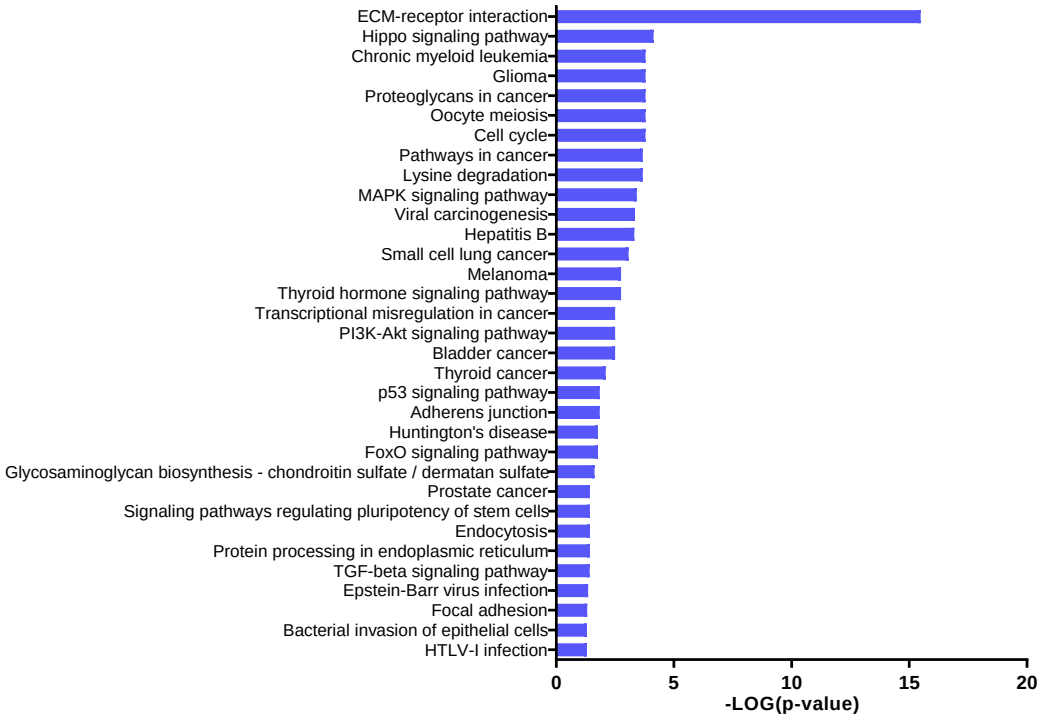


**Figure 33.** Target genes and pathway prediction analysis of let-7f-5p. Figure represents the Log 10 (p-values) of the significantly enriched pathways identified through mirPath v.3 and Tarbase.

Furthermore, the predictive analysis of let-7f-5p indicated potential involvement in protein processing within the endoplasmic reticulum, particularly targeting ATF4 and ATF6β genes, as well as the Hippo signalling pathway, which emerged

as other potential mechanisms associated with the actions of let-7f-5p. In this context, HFD-MI animals presented ER stress, as evidenced by elevated levels of BiP protein and mRNA levels (Figure 34A-B). Treatment with MCP was able to mitigate this upregulation in the ER stress marker as well as in PDIA6 protein levels. The ER stress response in the non-treated animals was characterized by an elevation in ATF6β, ATF4, ATF6α and CHOP levels (Figure 34), as well as an increase in the total levels of XBP1 non-dependent of modulations in its splicing (Figure 34C). Pharmacological inhibition of Gal-3 not only prevented the increase in ATF6β but also attenuated the activation of the other downstream effectors associated with ER stress.

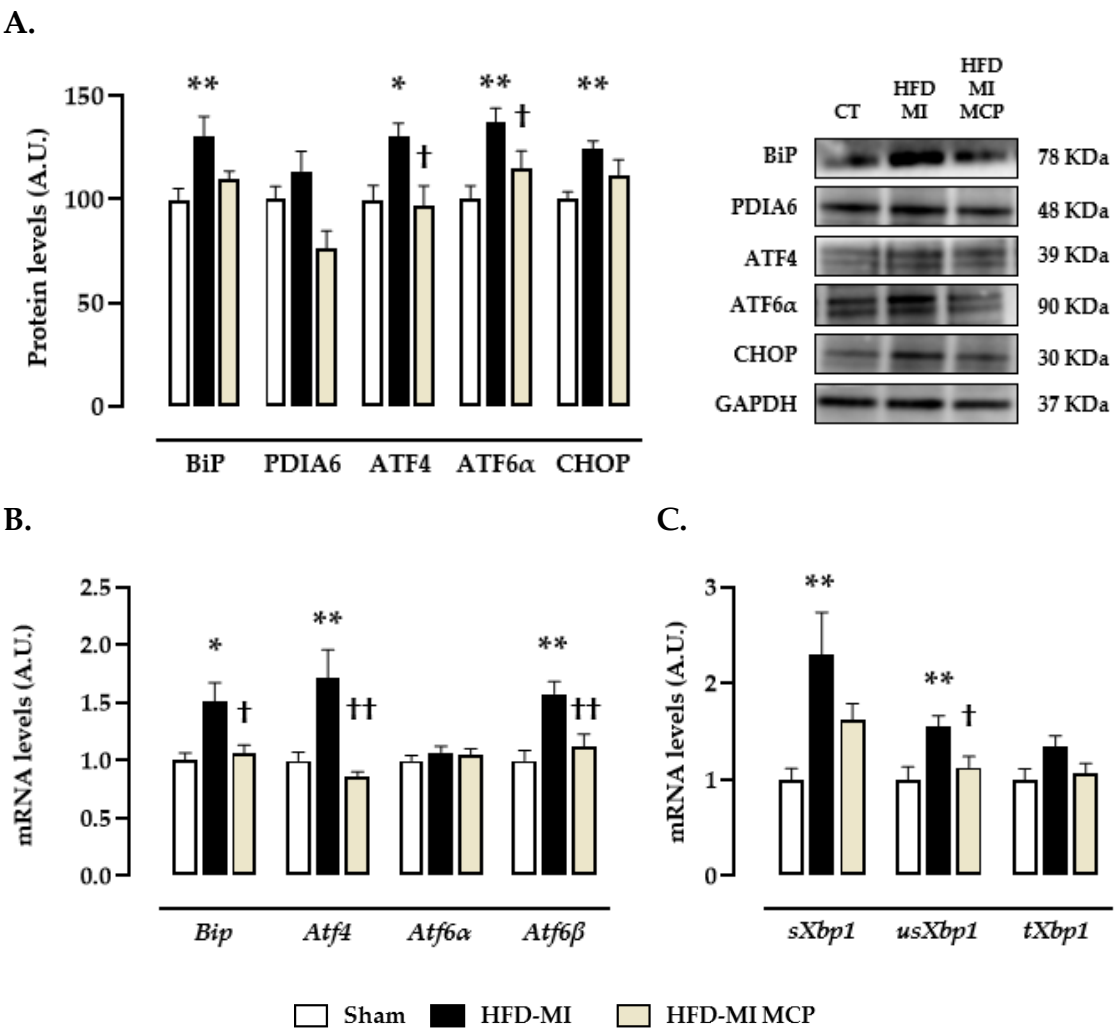


**Figure 34. Effect of Galectin-3 inhibition on endoplasmic reticulum stress in HFD-MI animals. (A)** Renal protein levels and **(B)** mRNA levels of immunoglobulin binding protein

(BiP), protein disulfide isomerase family A member 6 (PDIA6), activating transcription factor 4 (ATF4), activating transcription factor 6 alpha (ATF6$\alpha$), CCAAT-enhancer-binding homologous protein (CHOP) and activating transcription factor 6 beta (ATF6$\beta$). X-Box binding protein 1 (XBP1) mRNA levels in its **(C)** spliced form (sXBP1), unspliced form (usXBP1) and total levels (tXBP1) in kidneys from rats fed a high fat diet (HFD) and subjected to myocardial infarction (MI) in the presence or absence of modified citrus pectin (MCP) treatment. Bar graphs represent the mean ± SEM of 8-10 animals normalized to glyceraldehyde-3-phosphate dehydrogenase (GAPDH) for protein or hypoxanthine-guanine phosphoribosyltransferase (HPRT). *$p < 0.05$; **$p < 0.01$ versus Sham animals. † $p < 0.05$; †† $p < 0.01$ versus HFD-MI group.

In relation to the Hippo signalling pathway, the main effectors and target genes of this pathway were evaluated. Kidney samples from the HFD-MI group of animals had higher gene expression of LATS1, YAP1 and TEAD1 (Figure 35A) as well as an upregulation of the main target genes of this pathway (Figure 35B) when compared to the control group, confirming the activation of the Hippo-YAP pathway in this context.

As the Hippo pathway limits YAP1 function via phosphorylation of serine residues [379], western blot assessment of the protein levels of YAP1 and its phosphorylated form (pYAP1) was performed. HFD-MI animals presented a decrease in the pYAP1/tYAP1 ratio (Figure 35C), suggesting that in this pathological context, YAP1 is exerting its role as a transcriptional coactivator of the target genes. MCP successfully prevented the increase in mRNA levels of LATS1, YAP1 and TEAD1, as well as the decrease in YAP1 phosphorylation, confirming the role of Gal-3 in the activation of this signalling pathway.

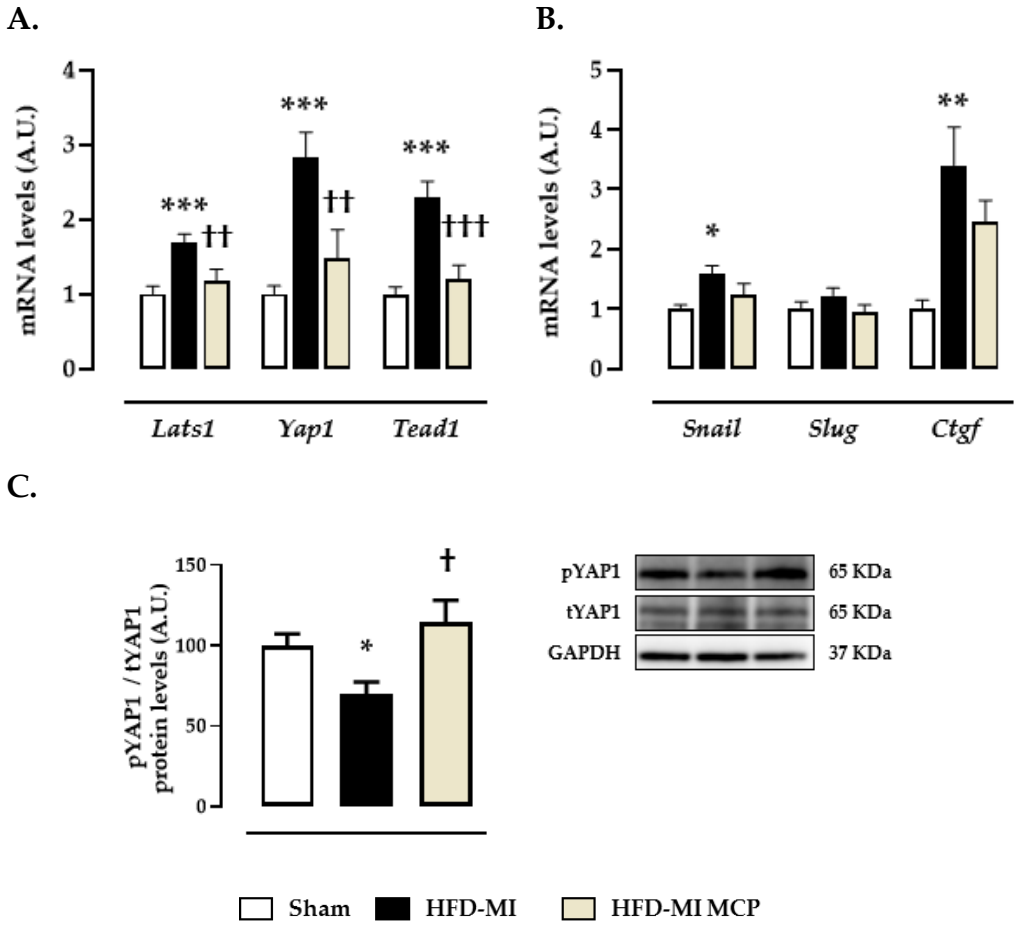


**Figure 35. Effect of Galectin-3 inhibition on the Hippo signalling pathway in HFD-MI animals. (A)** Renal mRNA levels of large tumor suppressor kinase 1 (LATS1), Yes1 associated transcriptional regulator (YAP1) and TEA domain transcription factor 1 (TEAD1). **(B)** Renal mRNA levels of Snail family transcriptional repressor 1 (SNAIL), Snail family transcriptional repressor 2 (SLUG) and connective tissue growth factor (CTGF). **(C)** Renal phosphorylated and total YAP1 protein levels (pYAP/tYAP1 ratio) in kidneys from rats fed a high fat diet (HFD) and subjected to myocardial infarction (MI) in the presence or absence of modified citrus pectin (MCP) treatment. Bar graphs represent the mean ± SEM of 8-10 animals normalized to glyceraldehyde-3-phosphate dehydrogenase (GAPDH) for protein or hypoxanthine-guanine phosphoribosyltransferase (HPRT). *p < 0.05; **p < 0.01; ***p < 0.001 versus Sham animals. † p < 0.05; †† p < 0.01; ††† p < 0.001 versus HFD-MI group.

### 4. Galectin-3 downregulates let-7f-5p, activates ER stress and modulates the Hippo-YAP pathway in HK-2 cells.

To assess the direct impact of Gal-3 on let-7f-5p, a dose and time response experiment was conducted in human epithelial cells from the kidney proximal tubule (HK-2 cell line). In this experiment, the effect of Gal-3 on the acute injury marker NGAL was used to select the dose of $10^{-6}$ M for future experiments, as the

only significant changes in its expression were seen in cells treated with that concentration after a 6-hour stimulation (Figure 36).

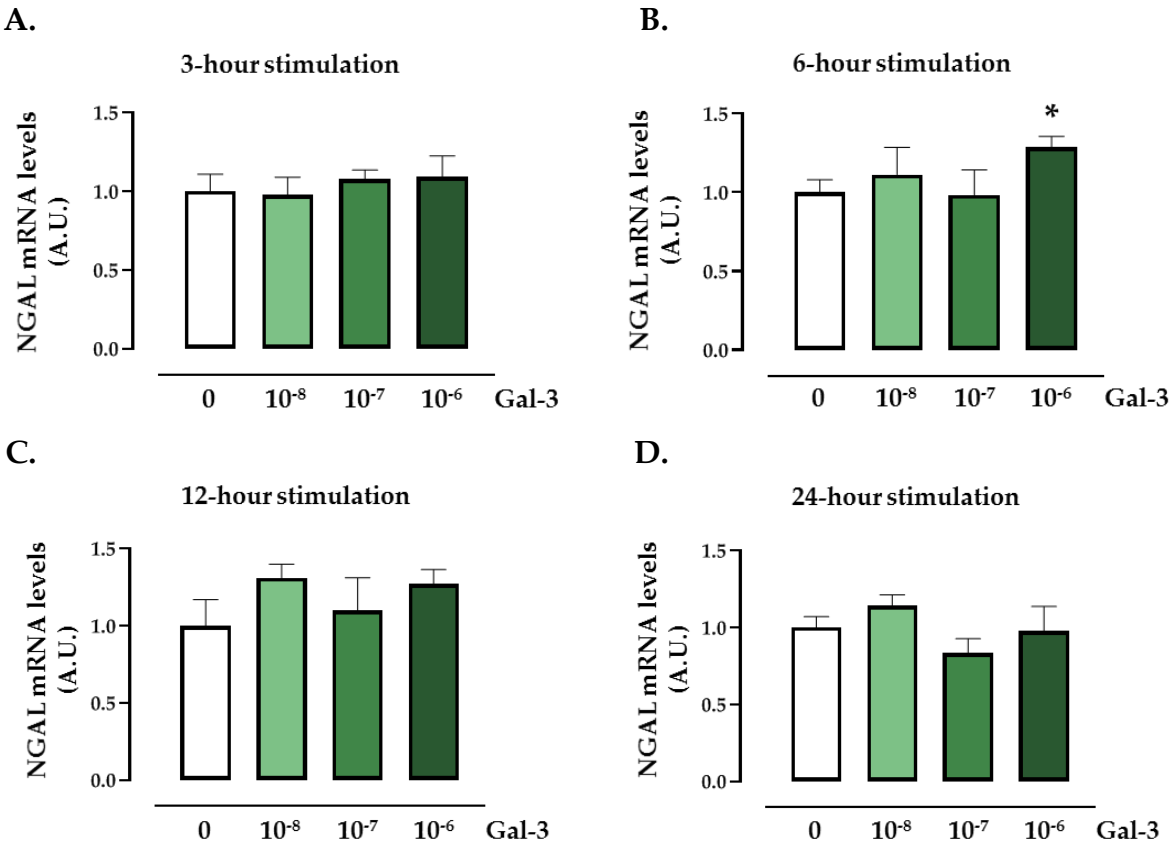


**Figure 36. Galectin-3 induces NGAL expression in a time-dependent pattern in renal epithelial cells.** Neutrophil gelatinase-associated lipocalin (NGAL) mRNA levels in HK-2 cells stimulated with Galectin-3 (Gal-3; $10^{-8}$- $10^{-6}$M) after **(A)** 3-hour stimulation, **(B)** 6-hour stimulation, **(C)** 12-hour stimulation and **(D)** 24-hour stimulation. Bar graphs represent the mean ± SEM of 4-6 assays normalized to glyceraldehyde-3-phosphate dehydrogenase (GAPDH). *$p < 0.05$ versus control cells.

Next, to investigate the potential involvement of Gal-3 in let-7f-5p modulation, ER stress and the Hippo-YAP pathway, we stimulated HK-2 cells with Gal-3 ($10^{-6}$M) at different times (3-24 hours). We confirmed that Gal-3 induces an early reduction in let-7f-5p mRNA expression after 3 hours of stimulation (Figure 37 A) that was accompanied by a tendency of increment in Collagen type I and TGF-β (Figure 37B-C).

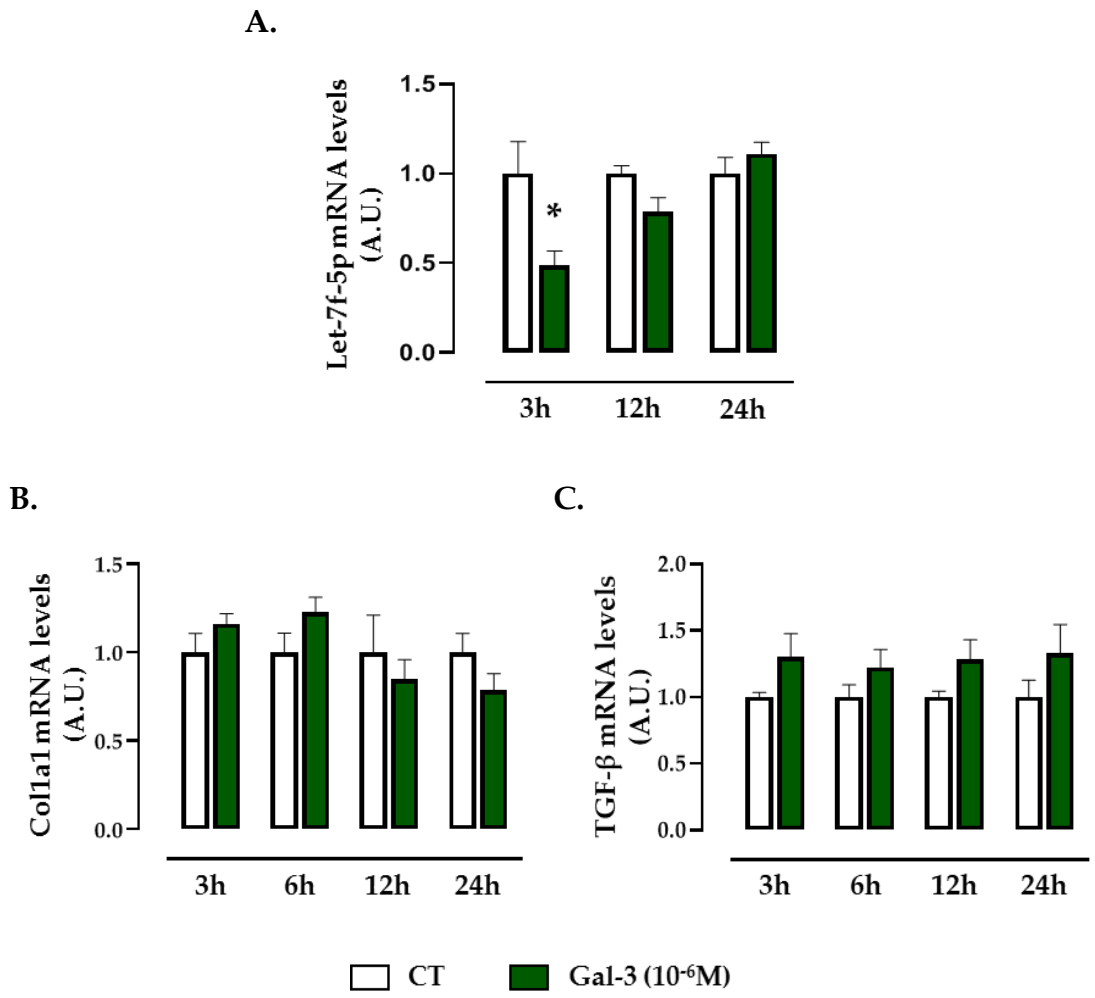


**Figure 37. Galectin-3 down-regulates let-7f-5p and modulates extracellular matrix in renal epithelial cells.** mRNA levels of **(A)** let-7f-5p, **(B)** collagen type I and, **(C)** transforming growth factor beta (TGF-β) in HK-2 cells stimulated with Galectin-3 (Gal-3; $10^{-6}$M) for 3-24 hours. Bar graphs represent the mean ± SEM of 4-6 assays normalized to U6 for the microRNA or glyceraldehyde-3-phosphate dehydrogenase (GAPDH) for cDNA. *$p < 0.05$ versus control cells.

These modulations in the microRNA and the ECM were concomitant with the activation of ER stress, characterized by enhanced expression of BiP, ATF4, ATF6$\alpha$, ATF6β and CHOP (Figure 38). Additionally, Gal-3 also modulated the Hippo-YAP pathway, as evidenced by the increased levels of the effectors LATS1, YAP1 and TEAD1, and the target genes SNAIL, SLUG, CTGF and BIRC2 (Figure 39).

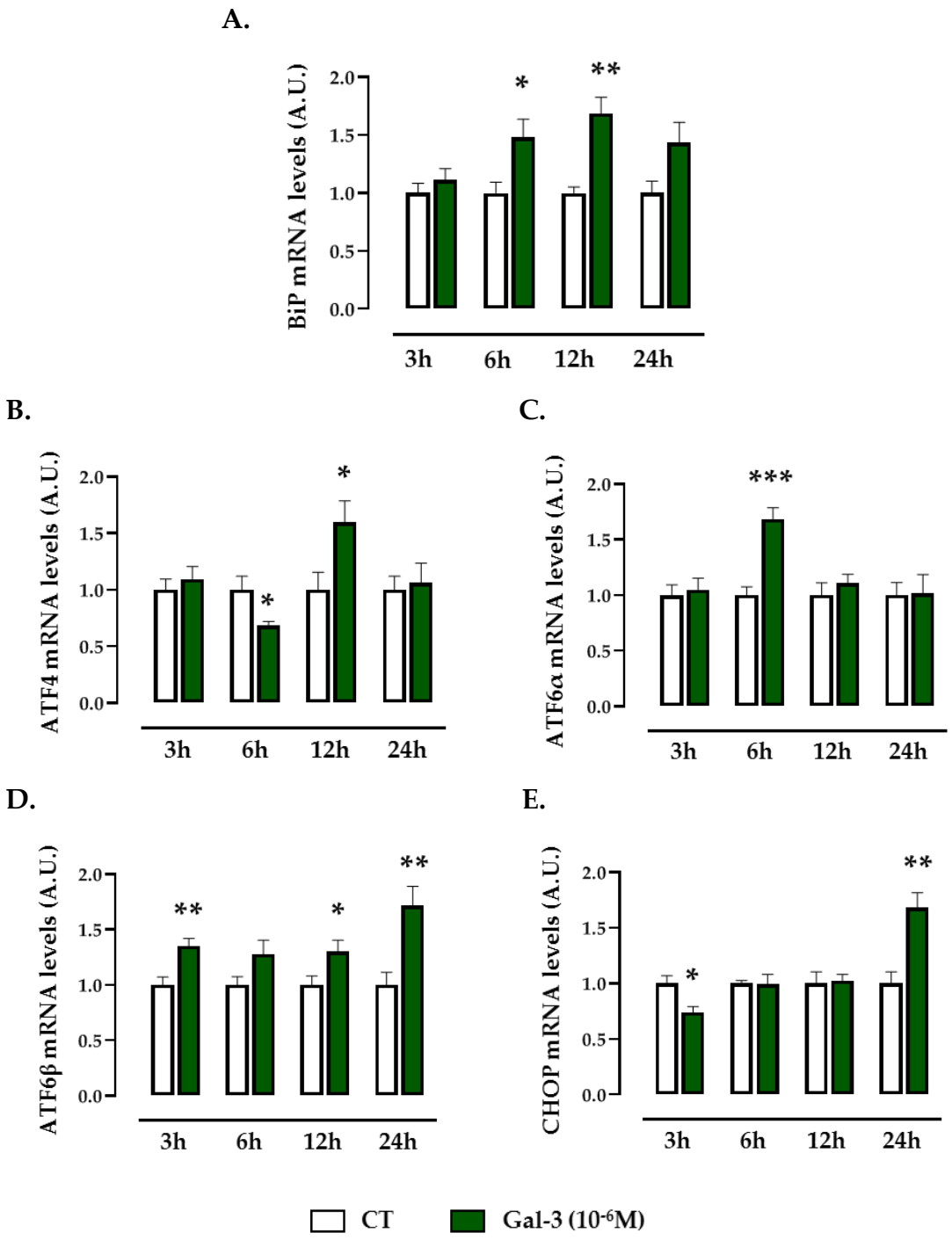


**Figure 38. Galectin-3 activates endoplasmic reticulum stress in renal epithelial cells.** mRNA levels of **(A)** Immunoglobulin binding protein (BIP), **(B)** Activating transcription factor 4 (ATF4), **(C)** Activating transcription factor 6-alpha (ATF6$\alpha$), **(D)** Activating transcription factor 6-beta (ATF6$\beta$) and **(E)** CCAAT-enhancer-binding homologous protein (CHOP) in HK-2 cells stimulated with Galectin-3 (Gal-3; $10^{-6}$M) for 3-24 hours. Bar graphs represent the mean ± SEM of 4-6 assays normalized to glyceraldehyde-3-phosphate dehydrogenase (GAPDH). *p < 0.05; **p < 0.01; ***p < 0.001 versus control cells.

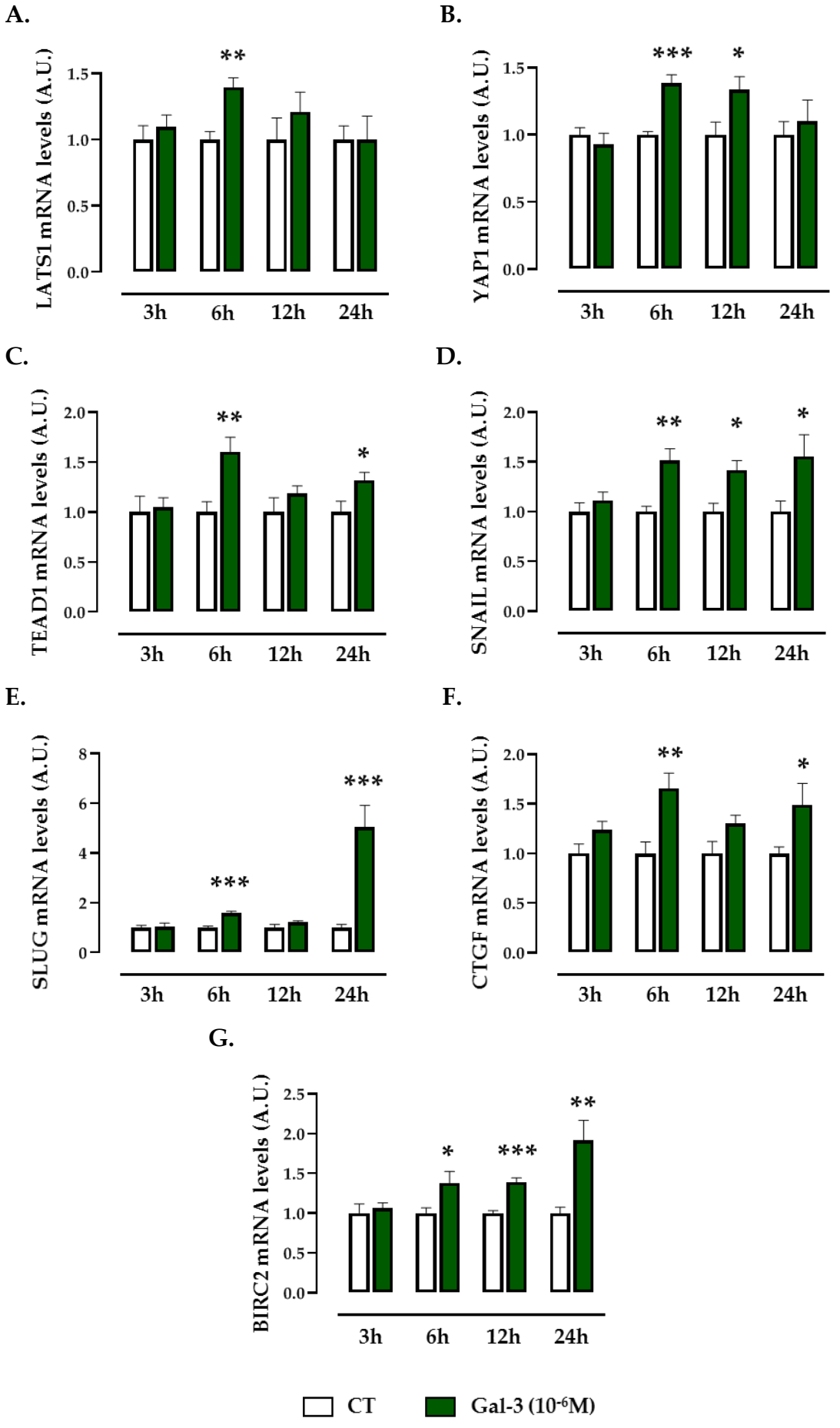
A.
LATS1 mRNA levels (A.U.)
1.5
1.0
0.5
0.0
**
3h
6h
12h
24h
B.
YAP1 mRNA levels (A.U.)
***
*
C.
TEAD1 mRNA levels (A.U.)
2.0
**
*
D.
SNAIL mRNA levels (A.U.)
E.
SLUG mRNA levels (A.U.)
8
6
4
2
0
***
F.
CTGF mRNA levels (A.U.)
G.
BIRC2 mRNA levels (A.U.)
2.5
CT
Gal-3 (10-6M)

**Figure 39. Galectin-3 modulates the Hippo signalling pathway in renal epithelial cells.** mRNA levels of **(A)** Large tumor suppressor kinase 1 (LATS1), **(B)** Yes1 associated transcriptional regulator (YAP1), **(C)** TEA domain transcription factor 1 (TEAD1), **(D)** Snail family transcriptional repressor 1 (SNAIL), **(E)** Snail family transcriptional repressor 2 (SLUG), **(F)** connective tissue growth factor (CTGF) and **(G)** Baculoviral IAP Repeat Containing 2 (BIRC2) in HK-2 cells stimulated with Galectin-3 (Gal-3; $10^{-6}$M) for 3-24 hours. Bar graphs represent the mean ± SEM of 4-6 assays normalized to glyceraldehyde-3-phosphate dehydrogenase (GAPDH). *p < 0.05; **p < 0.01; ***p < 0.001 versus control cells.

## 5. Let-7f-5p contributes to the activation of ER stress and modulates ECM components.

In order to go in depth about the implications of let-7f-5p as a mediator of the Gal-3 effects in the kidney, several genetic modulation experiments were performed. First, transfection with a mimic (agomir) or an inhibitor (antagomir) construct in basal conditions was conducted. As expected, as shown in Figure 40A, agomir transfection induced an important increase in the let-7f-5p mRNA levels whereas the antagomir decreased its levels (Figure 40B), demonstrating the effectiveness of both constructs.

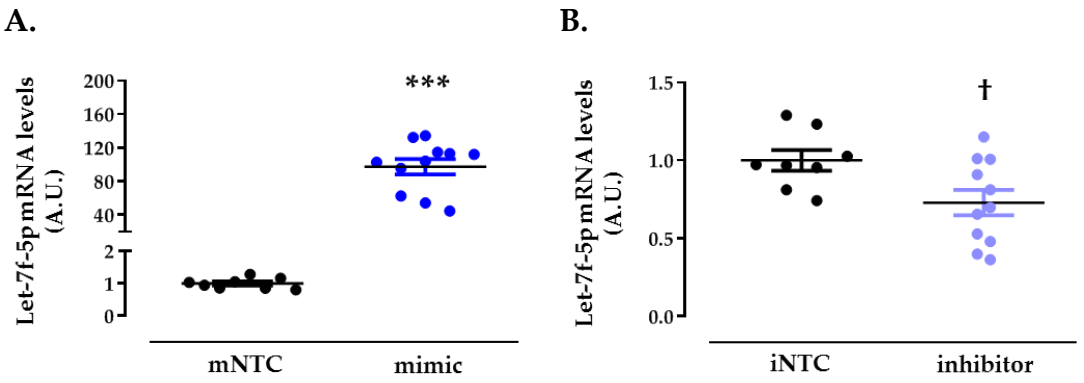


**Figure 40.** Effects of **(A)** mimic or **(B)** inhibitor transfection on let-7f-5p mRNA levels in non-stimulated HK-2 cells. Transfected cells with a mNTC (mimic Non-Target Control) or with a iNTC construct (inhibitor non-target control) were used as control cells. Scatter plots represent the mean ± SEM of 10-12 assays normalized to U6. ***p < 0.001 versus mNTC cells. † p < 0.05 versus iNTC cells.

Neither of the transfected constructs were able to modulate the gene expression of Gal-3 (Figure 41A), demonstrating that let-7f-5p is a downstream target of Gal-

3. Also, we demonstrated that transfection with either the mimic or the inhibitor did not change mRNA levels of the acute injury marker NGAL (Figure 41B). However, lower levels of let-7f-5p were associated with higher expression of ER stress marker BiP and the ECM component collagen type I, as well as with a tendency to increase levels of ATF6β (Figure 41C-E).

In basal conditions, cells transfected with the mimic construct showed a declining tendency in mRNA levels of both BiP and ATF6β, as well a significant decrease in collagen type IV levels (Figure 41F). All these data suggest the implication of let-7f-5p in both the ER stress activation and the ECM production.

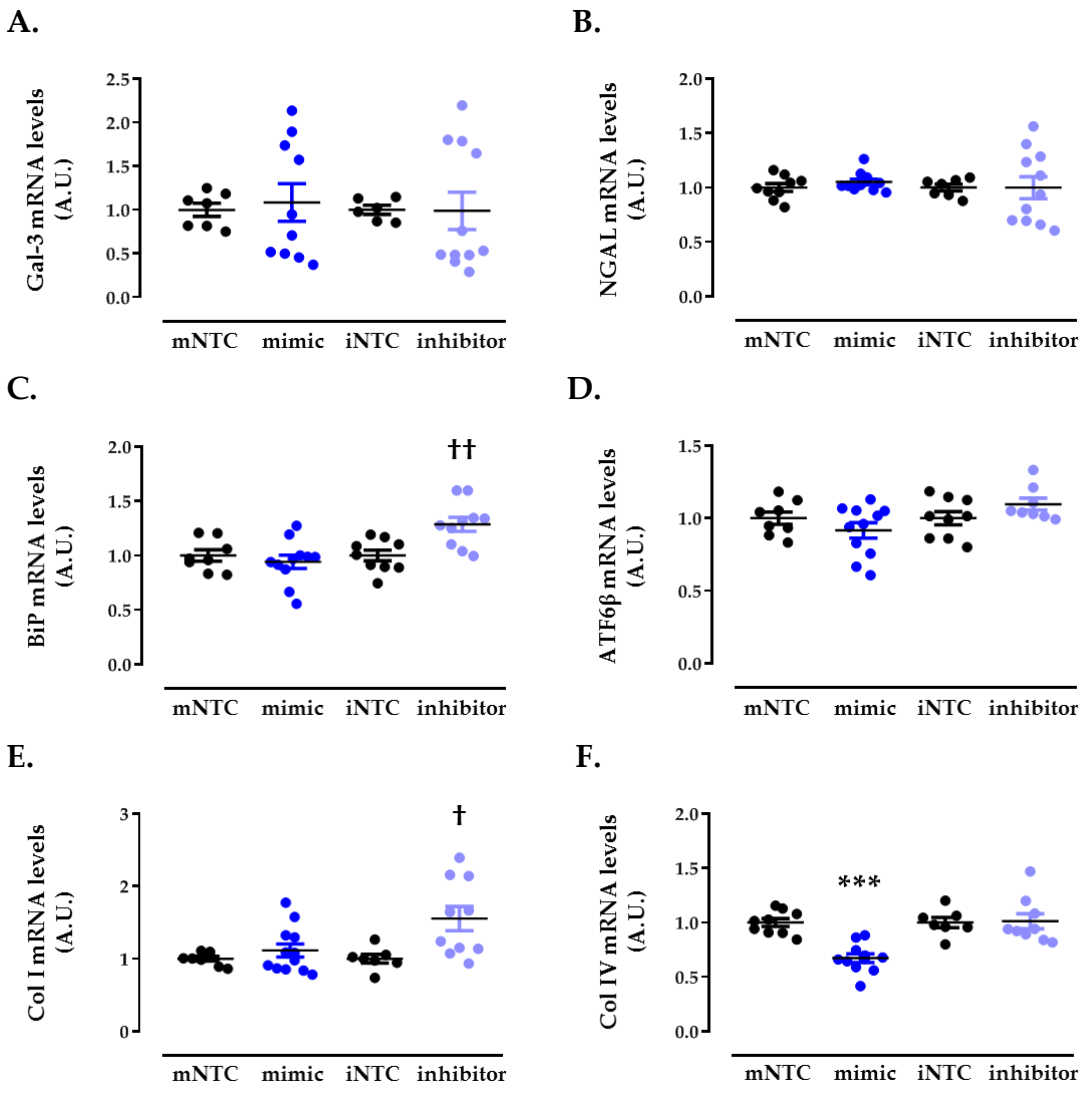

**Figure 41.** Effects of mimic or inhibitor transfection on **(A)** Galectin-3 (Gal-3), **(B)** Neutrophil gelatinase-associated lipocalin (NGAL), **(C)** Immunoglobulin binding protein (BIP), **(D)** Activating transcription factor 6-beta (ATF6β), **(E)** Collagen type I and **(F)** collagen type IV mRNA levels in non-stimulated HK-2 cells. Transfected cells with a mNTC (mimic Non-Target Control) or with an iNTC construct (inhibitor non-target control) were used as control cells. Scatter plots represent the mean ± SEM of 10-12 assays normalized to hypoxanthine-guanine phosphoribosyltransferase (HPRT). ***p < 0.001 versus mNTC cells. † p < 0.05 versus iNTC cells.

### 6. Effects of ER stress activation on let-7f-5p, ECM and the Hippo pathway.

Based on the *in-silico* predictions, ER stress could play an important role in Gal-3 and let-7f-5p induced renal damage. In order to evaluate the implications of ER stress activation, a time response study was performed in HK-2 cells treated with the pharmacological inductor of ER stress, tunicamycin, at 1.5 µg/µl, dose that was based on previous data from our group [380].

As expected, tunicamycin induced ER stress activation, as the dose of 1.5 µg/µl induced an important increase in the ER stress marker BiP at all time points (Figure 42A). We confirmed the effectiveness of tunicamycin with the downstream target ATF6$\alpha$ (Figure 42B).

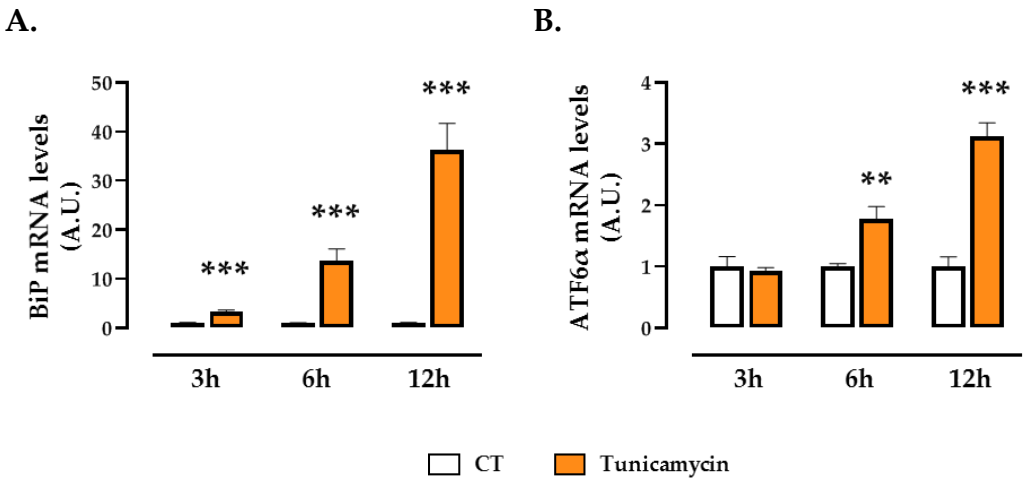


**Figure 42. Tunicamycin effectiveness in ER stress activation.** mRNA levels of (A) Immunoglobulin binding protein (BIP), **(B)** Activating transcription factor 6-alpha (ATF6$\alpha$) in HK-2 cells stimulated with tunicamycin (TN; 1.5 µg/µl) for 3-12 hours. Bar graphs represent

the mean ± SEM of 4-6 assays normalized to hypoxanthine-guanine phosphoribosyltransferase (HPRT). **p < 0.01; ***p < 0.001 versus control cells.

Next, we evaluated the possible implication of ER stress activation in the expression of the microRNA, in the ECM production and in the Hippo pathway. We observed no significant alterations in the expression of let-7f-5p that was accompanied by an increase in collagen type I and the Hippo pathway effectors YAP1 and TEAD1, mainly after 12-hour stimulation (Figure 43).

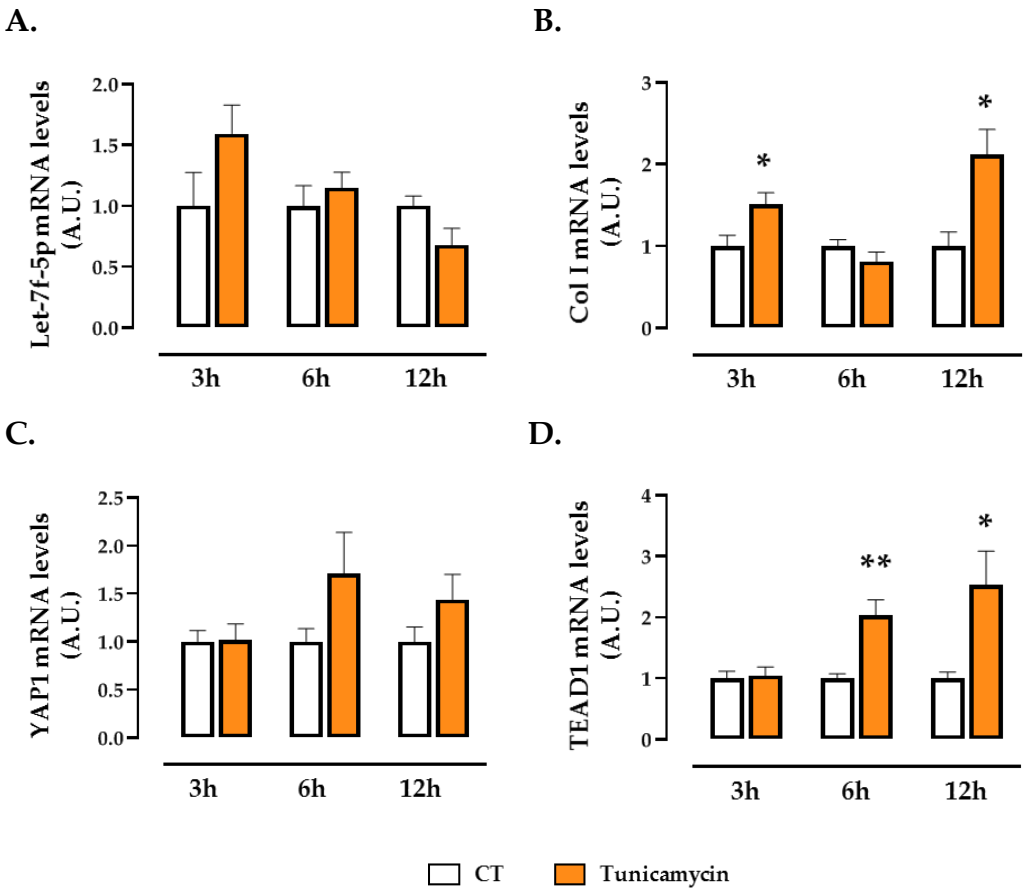


**Figure 43. Tunicamycin modulation of let-7f-5p, the ECM and the Hippo-YAP pathway in renal epithelial cells.** mRNA levels of **(A)** let-7f-5p, **(B)** collagen type I, **(C)** Yes1 associated transcriptional regulator (YAP1), **(D)** TEA domain transcription factor 1 (TEAD1) in HK-2 cells stimulated with tunicamycin (TN; 1.5 µg/µl) for 3-12 hours. Bar graphs represent the mean ± SEM of 4-6 assays normalized to U6 for the microRNA or hypoxanthine-guanine phosphoribosyltransferase (HPRT) for cDNA. *p < 0.05; **p < 0.01 versus control cells.

### 7. The downregulation of let-7f-5p contributes to the modulation of the Hippo-YAP pathway through ER stress activation.

Bearing in mind the fact that let-7f-5p is downregulated in the pathological context and that the *in-silico* studies predicted the possible implication of let-7f-5p on the activation of ER stress and the Hippo pathway, an increase in its expression could potentially play a beneficial role. In order to confirm that hypothesis, HK-2 cells were stimulated with the pharmacological activator of ER stress, Tunicamycin (TN; 1.5µg/µl), for 12 hours in presence (mimic) or absence (mNTC) of the let-7f-5p agomir.

We confirmed that the pharmacological activation of ER stress did not modify the levels of let-7f-5p mRNA in HK-2 cells (Figure 44) but as expected, increased the expression of the ER stress marker BiP, along with other ER stress genes such as ATF4, ATF6$\alpha$, ATF6$\beta$ and CHOP (Figure 45). Let-7f-5p mimic transfection modulated ATF4 and prevented the increase in ATF6$\beta$ mRNA levels (Figure 45D).

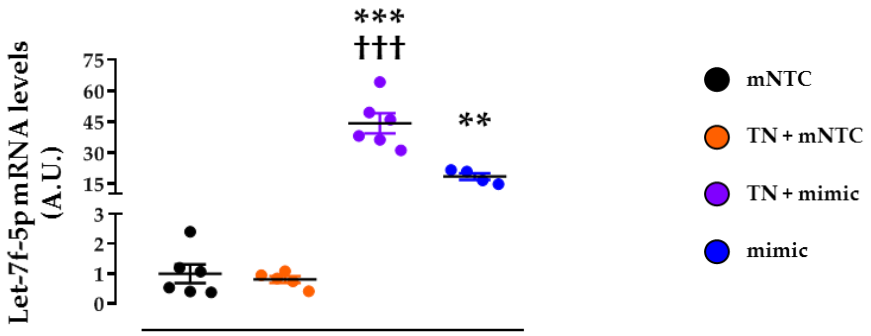


**Figure 44. Tunicamycin does not induce modification in the expression of let-7f-5p in renal epithelial cells**. Let-7f-5p mRNA levels in in HK-2 cells stimulated with tunicamycin (TN; 1.5 µg/µl) for 12 hours in the presence or absence of a mimic or a mNTC (mimic non-target control) construct. Scatter plots represent the mean ± SEM of 4-6 assays normalized to U6. **p < 0.01, ***p < 0.001 versus mNTC cells. ††† p < 0.001 versus TN + mNTC cells.

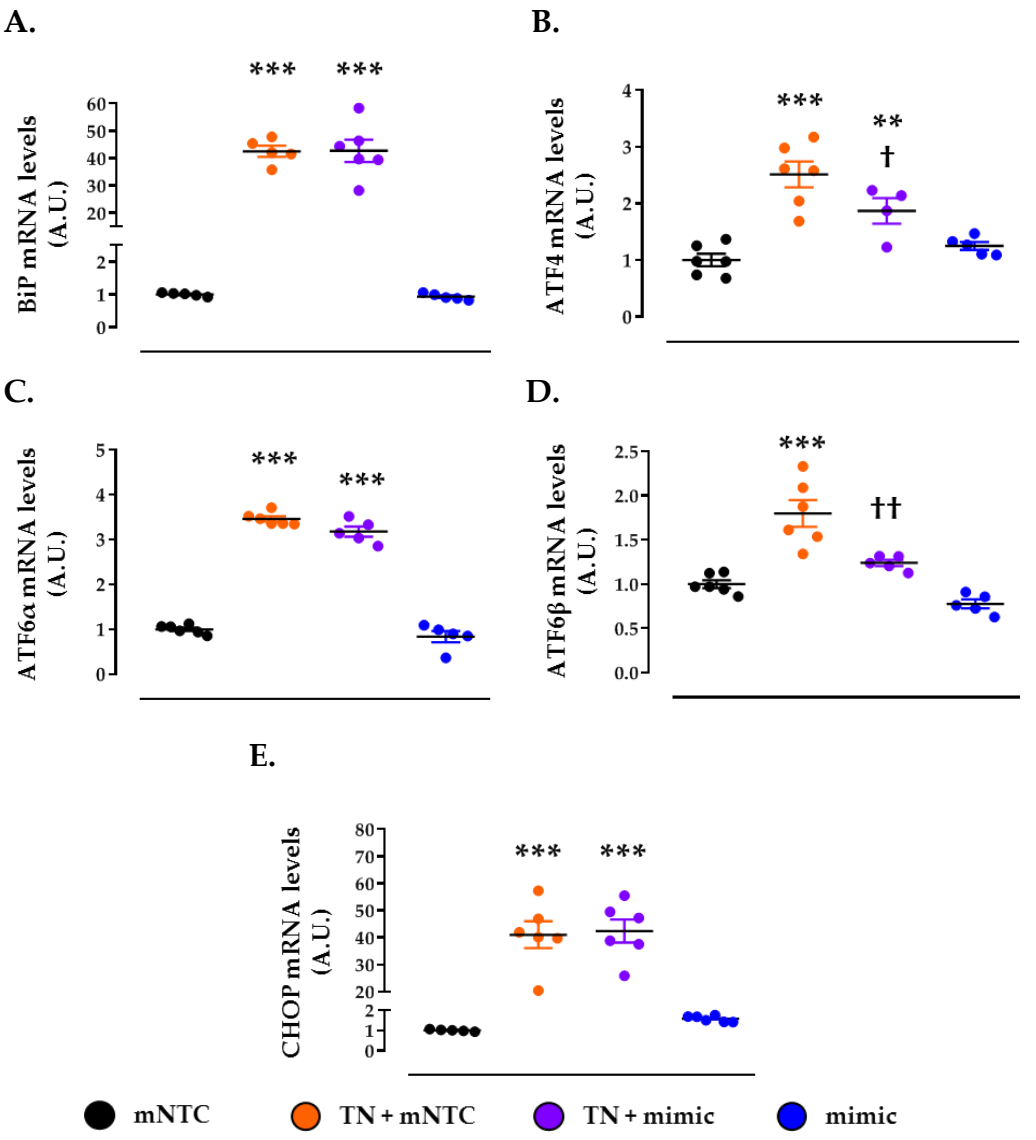


**Figure 45. Tunicamycin activates endoplasmic reticulum stress in renal epithelial cells.** mRNA levels of **(A)** Immunoglobulin binding protein (BIP), **(B)** Activating transcription factor 4 (ATF4), **(C)** Activating transcription factor 6-alpha (ATF6α), **(D)** Activating transcription factor 6-beta (ATF6β) and **(E)** CCAAT-enhancer-binding homologous protein (CHOP) in HK-2 cells stimulated with tunicamycin (TN; 1.5 μg/μl) for 12 hours in the presence or absence of a mimic or a mNTC (mimic non-target control) construct. Scatter plots represent the mean ± SEM of 4-6 assays normalized to hypoxanthine-guanine phosphoribosyltransferase (HPRT). **p < 0.01, ***p < 0.001 versus mNTC cells. † p < 0.05, †† p < 0.01 versus TN + mNTC cells.

To explore the potential of ATF6β as a direct target gene of let-7f-5p, luciferase assays were conducted. As shown in Figure 46, HK-2 cells co-transfected with the wild-type ATF6β plasmid construct and let-7f-5p mimic exhibited a reduction in relative luciferase activity as compared to cells co-transfected with the same

plasmid construct but a let-7f-5p scramble. This decrease indicates the direct interaction between let-7f-5p and ATF6β, demonstrating its role as a direct target of this microRNA and its involvement in ER stress activation specifically through ATF6β.

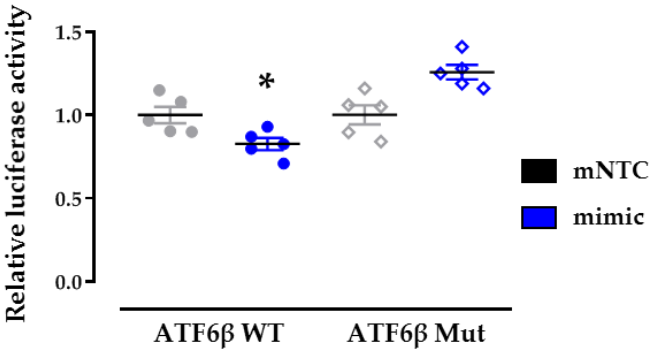


**Figure 46. ATF6β is a direct target of let-7f-5p.** Firefly relative luciferase activity from HK-2 cells transfected with a plasmid construct that contains either the ATF6β wild type (WT) or the ATF6β mutant (Mut) sequences in the presence of a let-7f-5p mimic or its negative control (mNTC). Scatter plots represent the mean ± SEM of 5 assays normalized to renilla luciferase activity. *$p < 0.05$ versus mNTC co-transfected cells.

Considering these findings, we evaluated the possible relevance of ATF6β in the animal model. The data showed a negative correlation between let-7f-5p and the target gene (Figure 47A). Interestingly, ATF6β was also correlated with the levels of Gal-3 and of NGAL (Figure 47B-C), as well as with mediators of renal fibrosis, ER stress and the Hippo pathway such as collagen I, collagen IV, BiP, ATF6α and YAP1 (Figure 47D-H). All these correlations suggest the possible involvement of ER stress in the renal alterations associated with MI in the context of obesity.

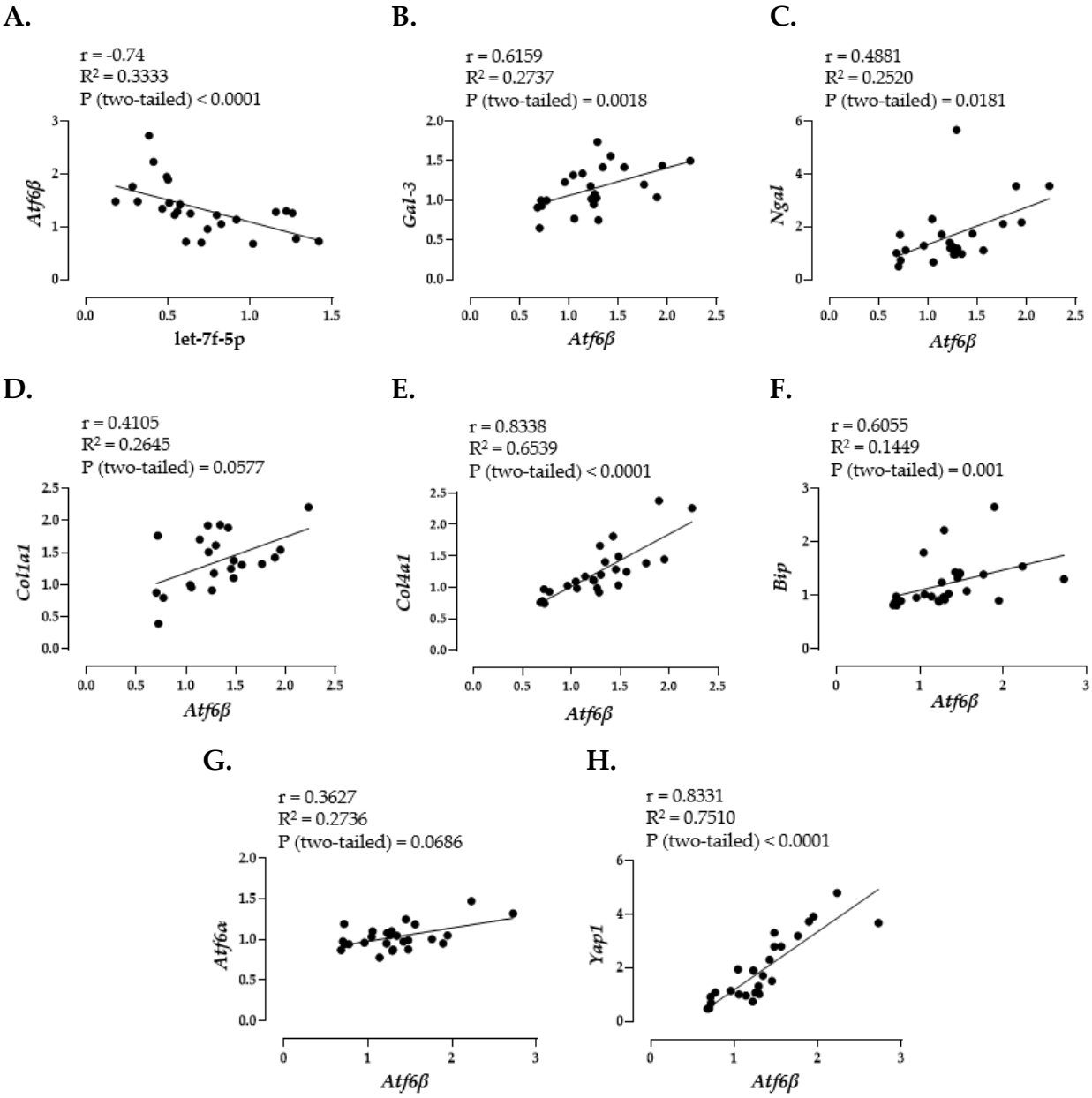


**Figure 47. ATF6β correlations in the animal model of obesity and MI.** Correlation between Activating transcription factor 6-beta (ATF6β) and **(A)** let-7f-5p, **(B)** Galectin-3 (Gal-3), **(C)** Neutrophil gelatinase-associated lipocalin (NGAL), **(D)** Collagen type I, **(E)** Collagen type IV, **(F** Immunoglobulin binding protein (BIP), **(G)** Activating transcription factor 6-alpha (ATF6α) or **(H)** Yes1 associated transcriptional regulator (YAP1).

Furthermore, let-7f-5p rescue in HK-2 cells resulted in a reduction of the elevated expression of Collagen type I observed in the tunicamycin treated cells (Figure 48A) but did not change the rise in the profibrotic mediator TGF-β or the injury marker NGAL (Figure 48B-C).

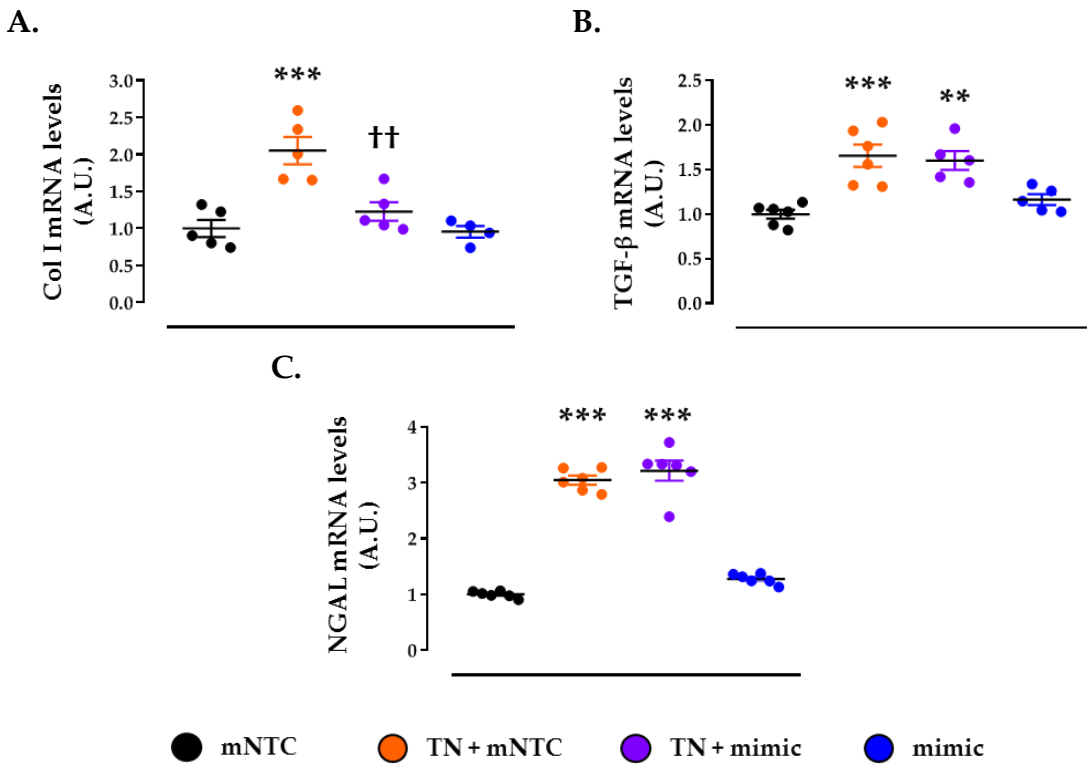


**Figure 48. Let-7f-5p overexpression prevents tunicamycin-induced increase in ECM in renal epithelial cells.** mRNA levels of **(A)** Collagen type I, **(B)** Collagen type IV and **(C)** Neutrophil gelatinase-associated lipocalin (NGAL) in HK-2 cells stimulated with tunicamycin (TN; 1.5 µg/µl) for 12 hours in the presence or absence of a mimic or a mNTC (mimic non-target control) construct. Scatter plots represent the mean ± SEM of 4-6 assays normalized to hypoxanthine-guanine phosphoribosyltransferase (HPRT). **p < 0.01, ***p < 0.001 versus mNTC cells. †† p < 0.01 versus TN + mNTC cells.

Regarding the Hippo signalling pathway, activation of ER stress led to a decrease in the kinase LATS1 that was accompanied by an increase in the expression of YAP1 and TEAD1 (Figure 49A-C). Treatment with tunicamycin resulted in a decrease in phosphorylated YAP1 protein levels (Figure 49D), demonstrating that ER stress activation inhibits the Hippo-YAP pathway, thereby enhancing the transcription of target genes. Moreover, cells stimulated with tunicamycin presented elevated mRNA levels in target genes of this pathway such as SLUG and BIRC2 (Figure 50B-C) with no alterations in SNAIL and a decrease in CTGF (figure 50 A, D), demonstrating the involvement of ER stress in the Hippo-YAP pathway. In this context, upregulation of let-7f-5p was able to modulate not only YAP1 expression and its phosphorylation but also the mRNA levels of the target gene SLUG.

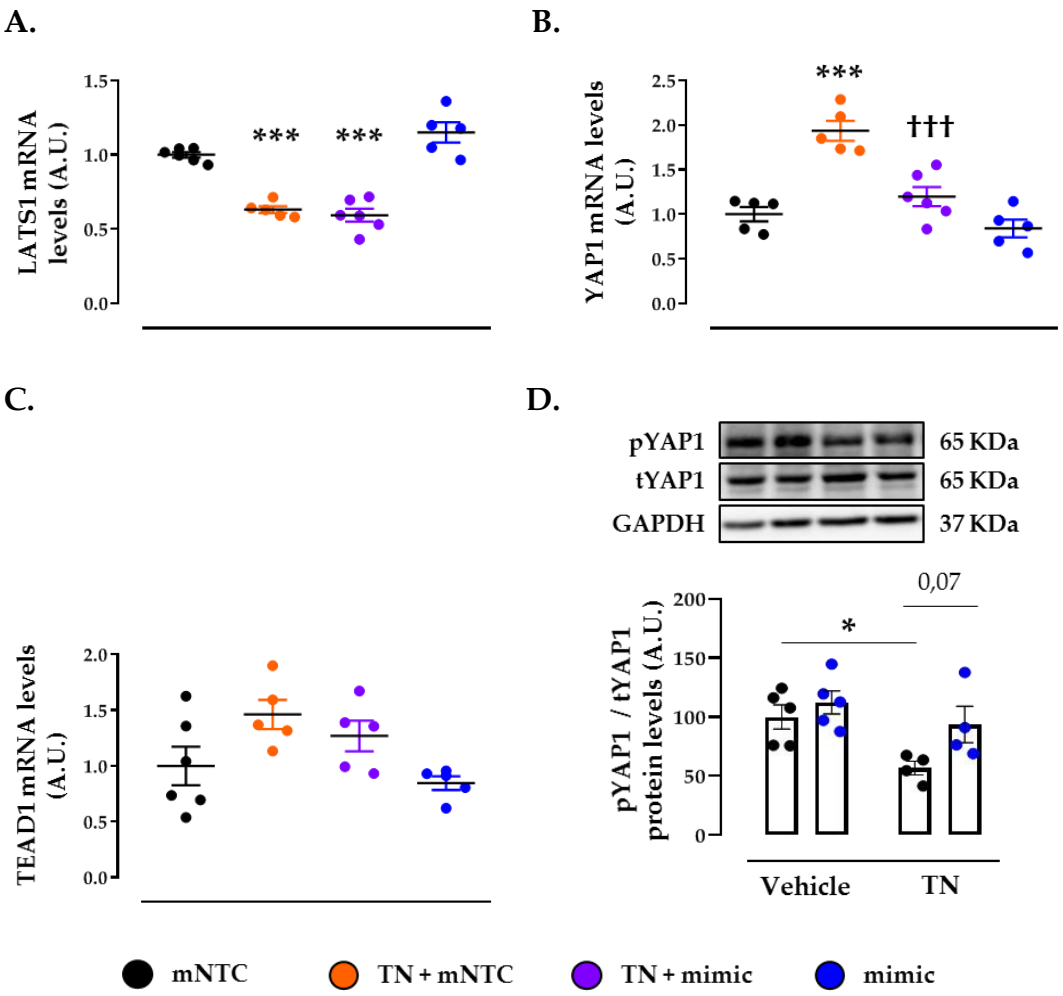


**Figure 49. Let-7f-5p overexpression reverts the tunicamycin-induced modulations in the hippo pathway effectors in renal epithelial cells.** mRNA levels of **(A)** Large tumor suppressor kinase 1 (LATS1), **(B)** Yes1 associated transcriptional regulator (YAP1) and **(C)** TEA domain transcription factor 1 (TEAD1). **(D)** phosphoryalated and total YAP1 protein levels (pYAP/tYAP1 ratio) in HK-2 cells stimulated with tunicamycin (TN; 1.5 µg/µl) for 12 hours in the presence or absence of a mimic or a mNTC (mimic non-target control) construct. Scatter plots represent the mean ± SEM of 4-6 assays normalized to hypoxanthine-guanine phosphoribosyltransferase (HPRT). *p < 0.05, ***p < 0.001 versus mNTC cells. ††† p < 0.001 versus TN + mNTC cells.

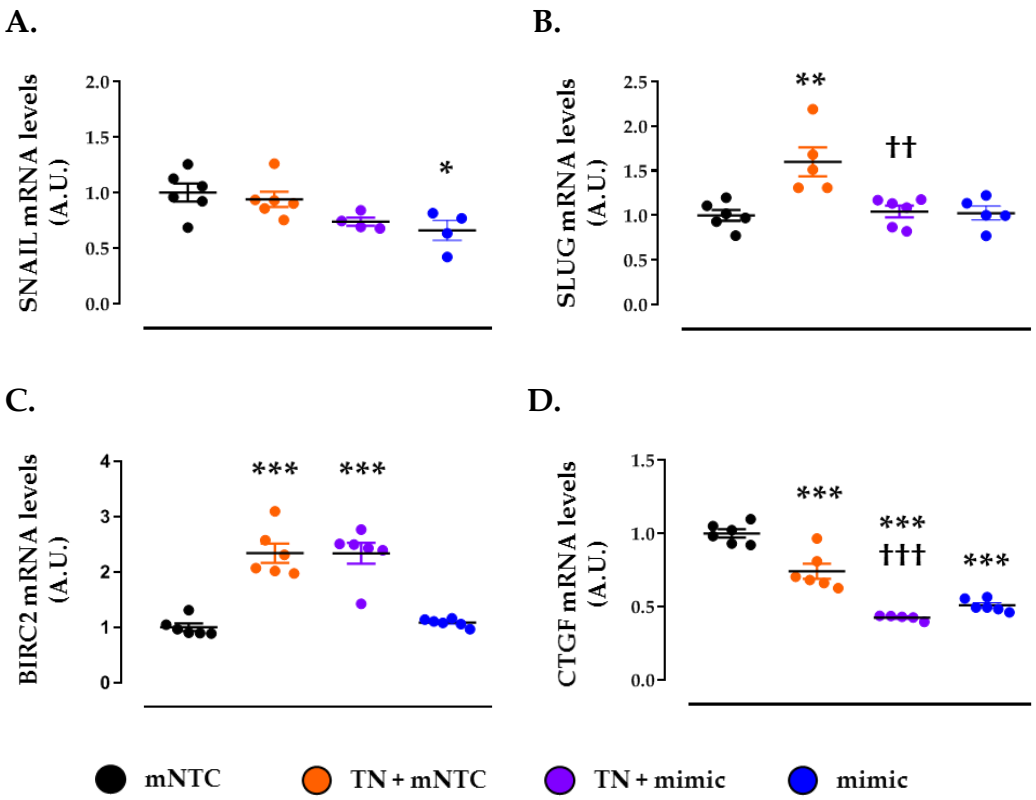


**Figure 50. Let-7f-5p overexpression effects in the tunicamycin-induced modulations in the hippo pathway target genes in renal epithelial cells.** mRNA levels of **(A)** Snail family transcriptional repressor 1 (SNAIL), **(B)** Snail family transcriptional repressor 2 (SLUG), **(C)** Baculoviral IAP Repeat Containing 2 (BIRC2) and **(D)** connective tissue growth factor (CTGF) in HK-2 cells stimulated with tunicamycin (TN; 1.5 µg/µl) for 12 hours in the presence or absence of a mimic or a mNTC (mimic non-target control) construct. Scatter plots represent the mean ± SEM of 4-6 assays normalized to hypoxanthine-guanine phosphoribosyltransferase (HPRT). *p < 0.05, **p < 0.01, ***p < 0.001 versus mNTC cells. †† p < 0.01, ††† p < 0.001 versus TN + mNTC cells.

Although functional protein association networks and enrichment analysis by String [381] or cytoscape [382] show two distinct clusters between the regulated targets (Figure 51), the previous results suggest that let-7f-5p acts as the link between ER stress and Hippo pathway as well as the development of fibrotic phenotypes.

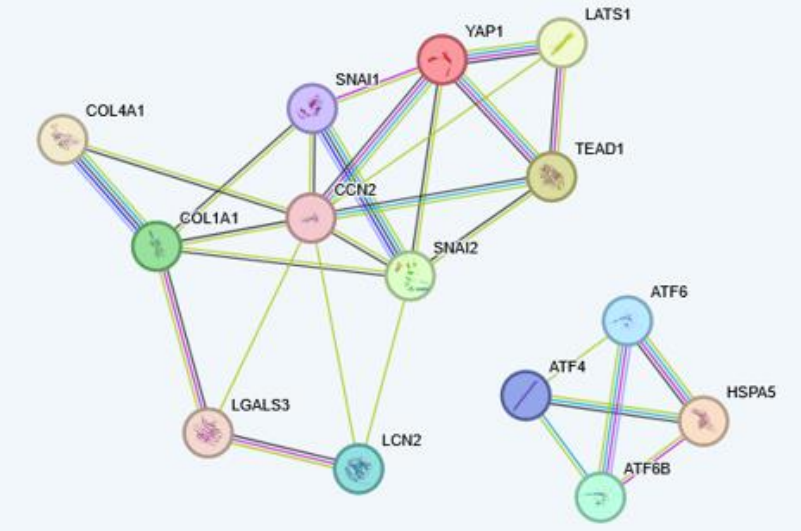


**Figure 51.** String interaction network of let-7f-5p regulated genes points to two independent signalling clusters, Hippo/ECM/Gal-3 and the ER stress pathways. Genes included in the analysis: Atf4, Atf6, Atf6b, Col1a1, Col4a1, Ccn2 (CTGF), Hspa5 (BiP), Lats1, Lcn2 (NGAL), Snai1 (SNAIL), Snai2 (SLUG), Tead1, Yap1, Lgals3 (Gal-3)

### 8. Effects of ER stress inhibition in MI obese animals.

Based on the earlier findings that suggests ER stress activation might play an important role in the renal damage via the interaction of let-7f-5p and ATF6β, we explored whether the pharmacological inhibition of ER stress could improve the renal deleterious consequences of myocardial infarction in the context of obesity.

First, we observed that similarly to what was seen in the MCP treated animals, the treatment with the inhibitor of ER stress improved the structural and functional cardiac alterations present in the HFD-MI but did not have any effect on the adiposity index or the body weight (Table 16). Regarding renal function none of the groups presented any alterations in the creatinine serum levels as compared to control animals (Table 16).

**Table 16**. Effect of ER stress inhibition on HFD-MI induced alterations after 4 weeks of treatment. Rats fed a normal diet were subjected to a sham operation (Sham) whereas rats fed a high fat diet (HFD) were subjected to myocardial infarction (MI) in the presence or absence of 4-phenylbutyric acid (4PBA).

| | Sham | HFD-MI | HFD-MI 4PBA |
|---|---|---|---|
| Body weight (g) | 356.1 ± 6.15 | 394.8 ± 9.7 ** | 395.9 ± 4.99 *** |
| Adiposity index (%) | 4.57 ± 0.41 | 10.82 ± 0.86 *** | 10.37 ± 0.46 *** |
| LVEF (%) | 80.95 ± 0.99 | 70.147 ± 1.02 ** | 75.66 ± 1.81 # |
| E/A ratio | 0.96 ± 0.04 | 0.79 ± 0.05 * | 1.102 ± 0.08 ## |
| SBP (mmHg) | 124.3 ± 1.704 | 129.5 ± 1.708 | 126.2 ± 2.25 |
| Relative heart weight (g/cm tibia) | 0.242 ± 0.004 | 0.257 ± 0.005 * | 0.234 ± 0.005 ## |
| Cardiac fibrosis (%) | 1.856 ± 0.15 | 4.989 ± 0.39 *** | 3.12 ± 0.136 ###** |
| Creatinine (mg/dl) | 0.31 ± 0.014 | 0.31 ± 0.01 | 0.29 ± 0.088 |

Data is expressed as means ± SEM of 8-10 animals. SBP: systolic blood pressure; LV: left ventricle; LVEF: left ventricle ejection fraction. *p < 0.05; **p < 0.01; ***p < 0.001 versus Sham group. #p < 0.05; ##p < 0.01; ###p < 0.001 versus HFD-MI group.

As we had previously described, animals fed a high fat diet followed by MI presented ER stress activation, evidenced by elevated levels of protein and mRNA of the marker BiP and the mediators ATF6β, ATF4, ATF6α and CHOP. This activation of ER stress was effectively mitigated by the administration of the pharmacological inhibitor 4PBA, as illustrated in Figure 52A-B. Additionally, 4PBA was able to prevent the renal increase in the mRNA levels of the spliced and unspliced forms of XBP1 observed in the non-treated animals (Figure 52C).

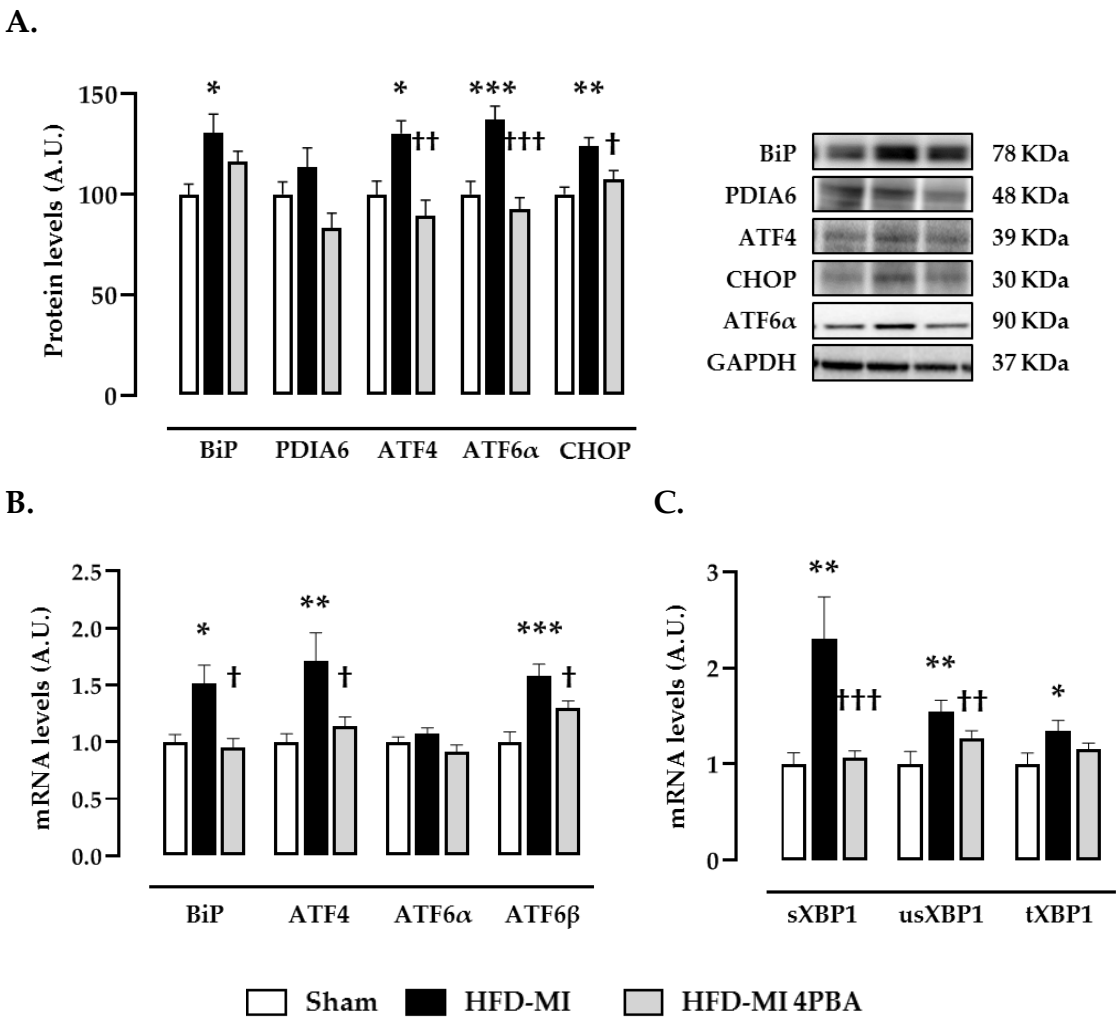


**Figure 52. Effect of 4PBA in the prevention of the renal increase in ER stress markers in HFD-MI animals. (A)** Renal protein levels and **(B)** mRNA levels of immunoglobulin binding protein (BiP), protein disulfide isomerase family A member 6 (PDIA6), activating transcription factor 4 (ATF4), activating transcription factor 6 alpha (ATF6α), CCAAT-enhancer-binding homologous protein (CHOP) and activating transcription factor 6 beta (ATF6β). X-Box binding protein 1 (XBP1) mRNA levels in its **(C)** spliced form (sXBP1), unspliced form (usXBP1) and total levels (tXBP1) in kidneys from rats fed a high fat diet (HFD) and subjected to myocardial infarction (MI) in the presence or absence of 4-phenylbutyric acid (4PBA) treatment. Bar graphs represent the mean ± SEM of 8-10 animals normalized to glyceraldehyde-3-phosphate dehydrogenase (GAPDH) for protein or hypoxanthine-guanine phosphoribosyltransferase (HPRT). *p < 0.05; **p < 0.01; ***p < 0.001 versus Sham animals. † p < 0.05; †† p < 0.01; ††† p < 0.001 versus HFD-MI group.

Besides its effectivity in ER stress inactivation, treatment with 4PBA was also able to prevent the upregulation of the acute injury marker NGAL observed in the HFD-MI animals (Figure 53A). However, the inhibition of ER stress in the obese animals with MI did not modulate the decline in let-7f-5p mRNA levels observed

in the untreated animals (Figure 53B), therefore demonstrating that ER stress acts as a downstream mediator of the microRNA actions.

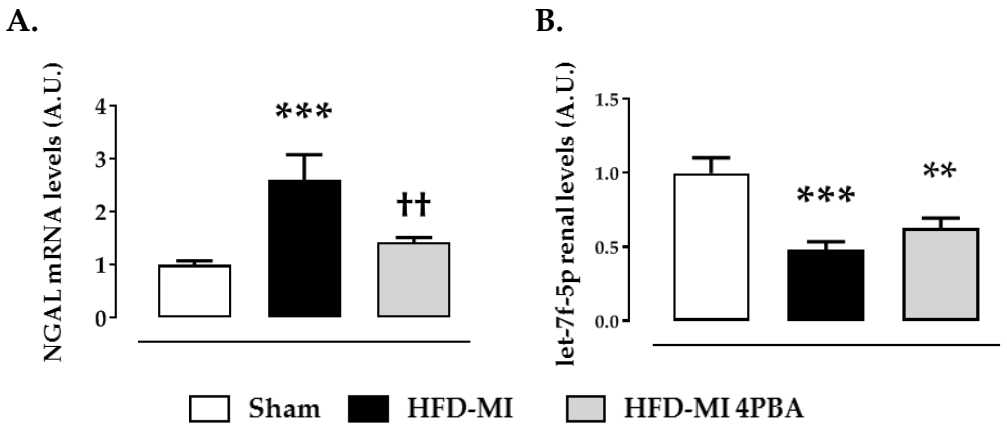


**Figure 53. Effect of ER stress inhibition in the renal expression of NGAL and let-7f-5p.** mRNA levels of (**A**) mRNA levels of neutrophil gelatinase-associated lipocalin (NGAL) and (**B**) let-7f-5p in kidneys from rats fed a high fat diet (HFD) and subjected to myocardial infarction (MI) in the presence or absence of 4-phenylbutyric acid (4PBA) treatment. Bar graphs represent the mean ± SEM of 8-10 animals normalized U6 for the microRNA or hypoxanthine-guanine phosphoribosyltransferase (HPRT) for cDNA. **p < 0.01; ***p < 0.001 versus Sham animals. †† p < 0.01 versus HFD-MI group.

### 9. Effects of ER stress inhibition on renal fibrosis in MI obese animals.

At structural level, regardless of the 4PBA treatment, HFD-MI animals presented similar glomerular area (Figure 54A-B). Nonetheless, the presence of the pharmacological inhibitor of ER stress was able to prevent the renal structural alterations present in the non-treated animals such as the glomerular, interstitial, and perivascular fibrosis (Figure 54A, C-E).

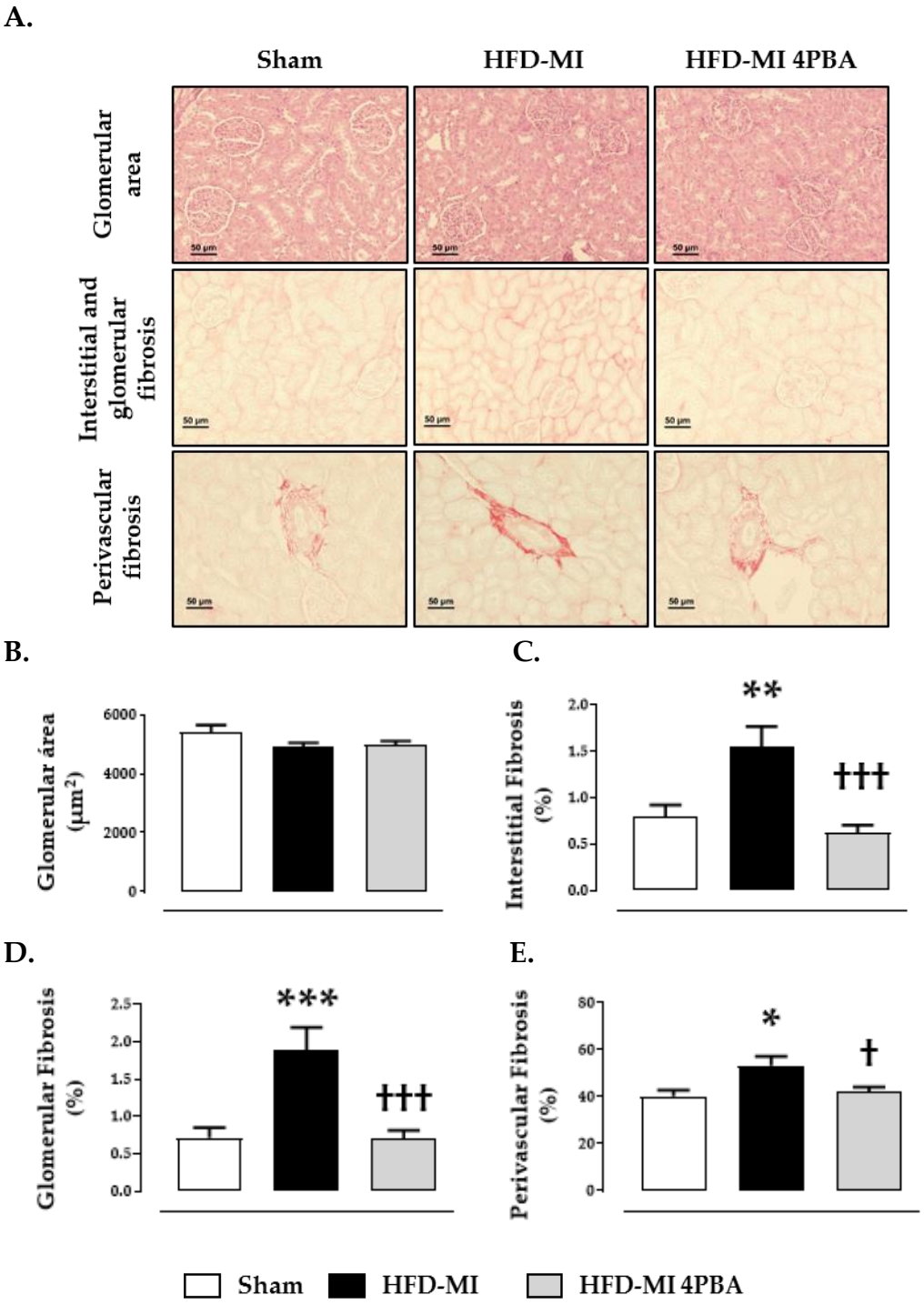


**Figure 54. Effect of ER stress inhibition on renal fibrosis. (A)** Representative microphotographs (20x magnification) of renal cortex sections staining with haematoxylin-eosin for glomerular area analysis or picrosirius red for fibrosis analysis. Quantification of **(B)** glomerular area, (**C**) interstitial fibrosis, (**D**) glomerular fibrosis and **(E)** perivascular fibrosis in kidneys from rats fed a high fat diet (HFD) and subjected to myocardial infarction (MI) in the presence or absence of 4-phenylbutyric acid (4PBA) treatment. Bar graphs represent the mean ± SEM of 8-10 animals. *p < 0.05; **p < 0.01 versus Sham animals. † p < 0.05; †† p < 0.01 versus HFD-MI group.

Further analysis revealed that obese animals with MI presented not only a renal decrease in MMP-2 activity (Figure 55A) but also an exacerbation of the genetic expression and protein levels of Collagen type IV, along with an elevation in TGF-β, fibronectin and α-SMA (Figure 55B, C). In this pro-fibrotic context, the beneficial effects of ER stress inhibition can be attributed to a decline in the ECM components synthesis and not to an increase in ECM degradation, as 4PBA did not modulate the decrease in MMP activity seen in the untreated animals (Figure 55).

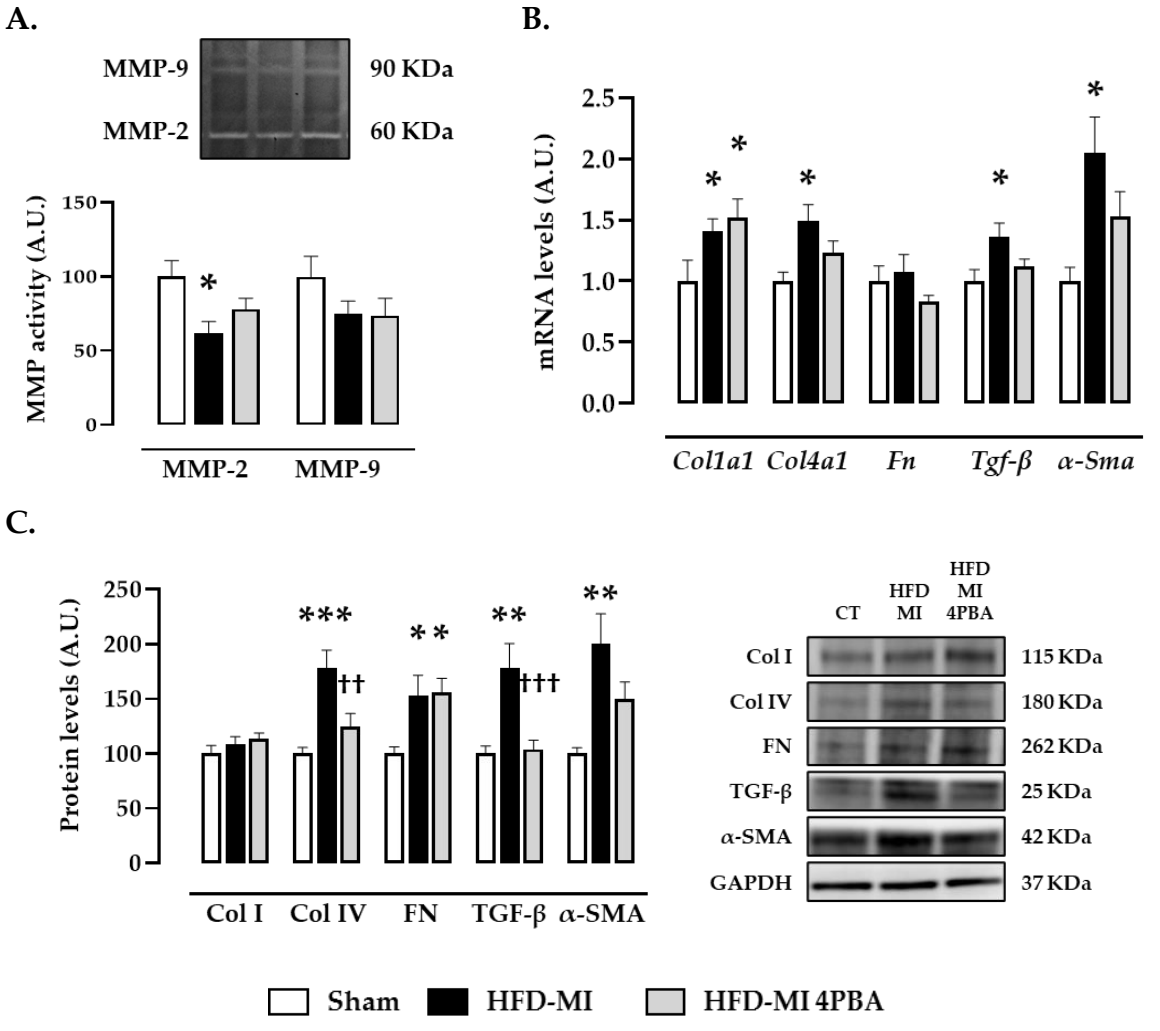


**Figure 55. Effect of ER stress inhibition on extracellular matrix synthesis and degradation in HFD-MI animals. (A)** Matrix metalloproteinase 2 (MMP-2) and 9 (MMP-9) renal activity reduction in HFD-MI animals. **(B)** Renal mRNA and **(C)** protein levels of collagen type I, collagen type IV, fibronectin (FN), transforming growth factor beta (TGF-β) and alpha-smooth muscle actin (α-SMA) in in kidneys from rats fed a high fat diet (HFD) and subjected to

myocardial infarction (MI) in the presence or absence of 4-phenylbutyric acid (4PBA) treatment. Bar graphs represent the mean ± SEM of 8-10 animals normalized to glyceraldehyde-3-phosphate dehydrogenase (GAPDH) for protein or hypoxanthine-guanine phosphoribosyltransferase (HPRT) for cDNA. *p < 0.05; **p < 0.01; ***p < 0.001 versus Sham animals. †† p < 0.01; ††† p < 0.001 versus HFD-MI group.

### 10. Effects of ER stress inhibition on renal oxidative stress, inflammation, and the Hippo-YAP pathway in MI obese animals.

As shown in Figure 56A-B, obese animals with MI had an increase in fluorescence intensity at renal level, indicating higher presence of superoxide anions. Interestingly, lower presence of superoxide anions was observed in the obese infarcted animals treated with the inhibitor of ER stress activation despite the absence of changes in the antioxidant defence, evaluated by catalase protein levels (Figure 56C). This prooxidant milieu was concomitant with an inflammatory response characterized by an elevation in the mRNA levels of proinflammatory cytokines such as OPN, IL-6 and TNF-$\alpha$ without changes in CCL-2 expression that the treatment with 4PBA was able to blunt (Figure 56D).

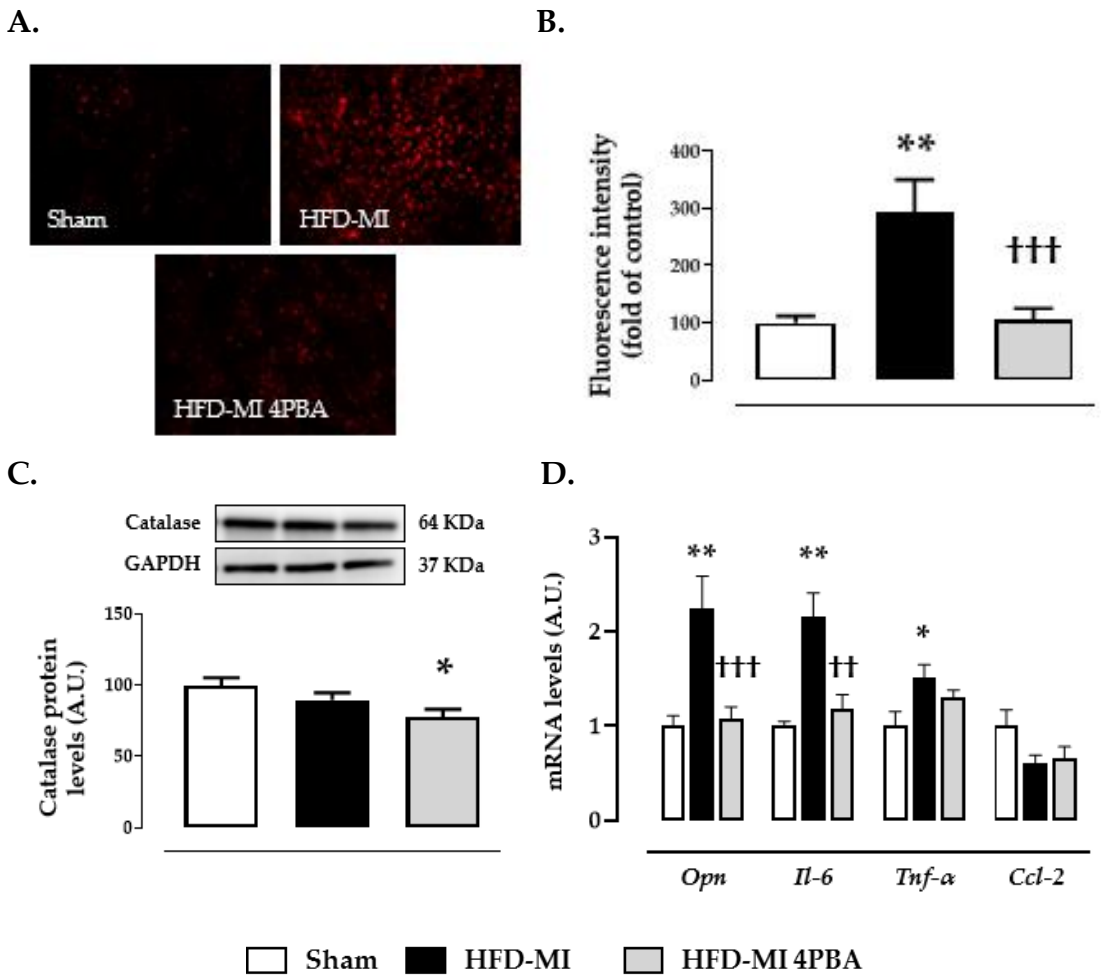


**Figure 56. Effect of ER stress inhibition on extracellular matrix synthesis and degradation in HFD-MI animals. (A-B)** Representative microphotographs and quantification of renal cortex sections labelled with the oxidative dye dihydroethidium (40X magnification). **(C)** Renal protein levels of catalase and **(D)** renal mRNA levels of osteopontin (OPN), interleukin-6 (IL-6), tumor necrosis factor-alpha (TNF-$\alpha$) and C-C motif chemokine ligand 2 (CCL-2) in kidneys from rats fed a high fat diet (HFD) and subjected to myocardial infarction (MI) in the presence or absence of 4-phenylbutyric acid (4PBA) treatment. Bar graphs represent the mean ± SEM of 8-10 animals normalized to glyceraldehyde-3-phosphate dehydrogenase (GAPDH) for protein or hypoxanthine-guanine phosphoribosyltransferase (HPRT) for cDNA. *$p < 0.05$; **$p < 0.01$ versus Sham animals. †† $p < 0.01$; ††† $p < 0.001$ versus HFD-MI group.

Regarding the Hippo pathway, despite no significant effect on the pathway effectors (Figure 57A), ER stress inhibition induced an increase in the phosphorylation of YAP1 protein (Figure 57C) that could explain the decrease in transcription of the target gene CTGF, and the tendency observed in SLUG (Figure 57B).

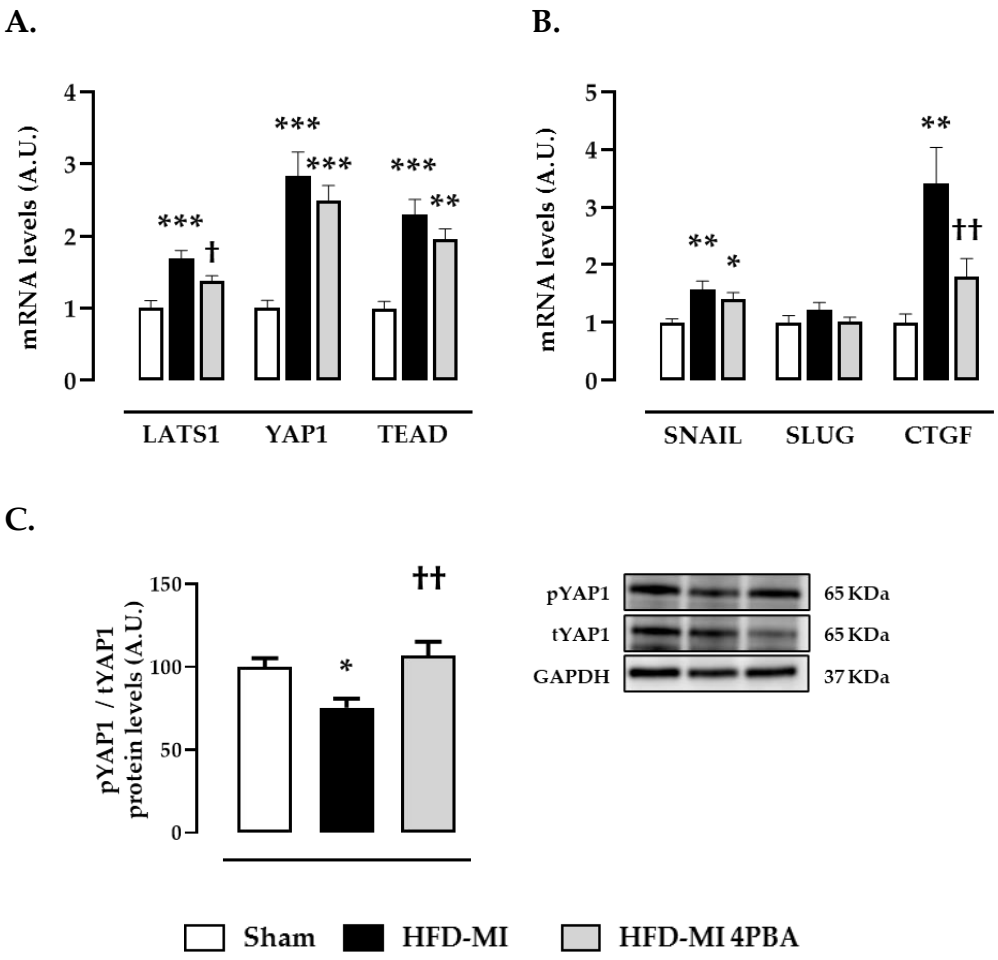


**Figure 57. Effect of ER stress inhibition on the Hippo signalling pathway in HFD-MI animals. (A)** Renal mRNA levels of large tumor suppressor kinase 1 (LATS1), Yes1 associated transcriptional regulator (YAP1) and TEA domain transcription factor 1 (TEAD1). **(B)** Renal mRNA levels of Snail family transcriptional repressor 1 (SNAIL), Snail family transcriptional repressor 2 (SLUG) and connective tissue growth factor (CTGF). **(C)** Renal phosphorylated and total YAP1 protein levels (pYAP/tYAP1 ratio in kidneys from rats fed a high fat diet (HFD) and subjected to myocardial infarction (MI) in the presence or absence of 4-phenylbutyric acid (4PBA) treatment. Bar graphs represent the mean ± SEM of 8-10 animals normalized to glyceraldehyde-3-phosphate dehydrogenase (GAPDH) for protein or hypoxanthine-guanine phosphoribosyltransferase (HPRT) for cDNA. *p < 0.05; **p < 0.01; ***p < 0.001 versus Sham animals. † p < 0.05; †† p < 0.01; ††† p < 0.001 versus HFD-MI group.

# *Discussion*

The shared pathology of the heart and kidneys significantly influences clinical outcomes, as it has been widely observed that the development of renal alterations in patients with cardiovascular diseases is associated with worse prognosis and higher mortality [9, 10, 383]. These circumstances are usually referred to as cardiorenal syndrome, a term that gathers the disorders of the heart and kidneys, whereby acute or chronic dysfunction in one organ may induce dysfunction in the other [1]. Out of the five different types of CRS, CRS-1, also known as acute cardiorenal syndrome, is the most prevalent among CRS diagnosed patients [3, 384]. CRS-1, characterized by AKI due to a deterioration in cardiac function, has a complex pathophysiology that combines hemodynamic and non-hemodynamic alterations over which treatments show no improvement, therefore demonstrating the importance of exploring the involved mechanisms in order to understand and assess new therapeutic targets.

Although deterioration in cardiac function can happen in a wide range of diseases, the high incidence of MI worldwide [121] and its close association with renal damage and widespread risk factors such as obesity and hypertension [123, 385] make MI a relevant clinical problem in the context of CRS. Moreover, early detection of renal damage in MI patients is considered compulsory, as MI patients with renal alterations experience poorer outcomes and lengthier hospitalizations [4, 16]. In line with this, we have observed that patients with MI presented higher plasma levels of the acute injury marker NGAL, confirming the impact of MI in the early damage of the renal tissue. In the clinical setting, serum levels of NGAL are known to correlate with the severity of renal damage even with normal creatinine levels [386], having been suggested as an important biomarker in CRS diagnosis. Similarly, the *in-vivo* results herein presented show that MI animals present an increase in NGAL and KIM-1 renal levels that is accompanied by interstitial fibrosis and ECM overexpression in the kidney cortex without changes in the renal function or in the glomerular area, therefore

suggesting that fibrosis development is an early alteration in the renal injury 4 weeks post-MI.

Renal fibrosis development is a common structural alteration that is considered a key factor in CRS progression, as it has been associated with renal impairment and transition into irreversible damage such as CKD [154, 170]. Despite its importance in CKD, current pharmacological approaches only ameliorate fibrosis progression, not being able to revert renal fibrosis [387, 388], therefore making it necessary to further understand the involved mechanisms. Whilst multiple mechanisms have been suggested to possibly play a part in fibrosis, we have confirmed the implication of Gal-3 in this context, as its pharmacological inhibition by MCP prevented not only the interstitial, glomerular and perivascular fibrosis at least, in part, by the amelioration of the imbalance in ECM production and degradation observed in obese infarcted animals. These results are coherent with the renal distribution of Gal-3, which has been described to be predominantly found in the distal and collecting tubules of the kidney [223, 236], regions included in the fibrotic area observed. Additionally, these results agree with previous studies that showed the profibrotic role of Gal-3 in the kidney, as it has been reported that inhibition of Gal-3 in animals with nephropathies ameliorated renal interstitial fibrosis, cell apoptosis, ECM protein synthesis and, therefore, kidney injury progression [225, 389]. Moreover, an increase in Gal-3 has also been previously described to induce renal fibrosis through the epithelial-mesenchymal transition [239, 390], an important mechanism known to promote myofibroblast upsurge [157]. These results suggest the potential therapeutic relevance of Gal-3 in the progression of fibrosis in CRS-1; however, other mechanisms have been associated with this pathological context.

Multiple studies have suggested that inflammation and oxidative stress are highly involved in the progression of renal failure independently of the initial damage, as both the inflammatory and hypoxic environment propitiate fibroblast

activation and proliferation, promoting fibrosis in the affected tissues [391, 392]. In the cardiorenal axis the implication of inflammation has been widely proven in experiments where macrophage depletion [393] and inhibition of inflammatory mediators such as IL-6 or the NF-KB signalling was effective in the reduction of cardiac and renal fibrosis in CRS animal models [94, 394]. Moreover, inflammatory markers IL-6, TNF-$\alpha$ and C-reactive protein are well known predictors of cardiovascular mortality in CKD, having considered biomarkers of the severity of inflammation and progression of the disease [395, 396]. In line with this, kidneys from infarcted animals in our animal model of CRS-1 presented an increase in proinflammatory markers IL-6 and TNF-$\alpha$ as well as an upsurge in superoxide anion levels and two end-products of lipid peroxidation, confirming not only the presence a proinflammatory environment, but also a prooxidant one at renal level 4 weeks post-MI.

This concomitance of inflammation and oxidative stress reinforce the theory that both processes are intimately linked to the development of organ damage and fibrosis in the CRS [391, 397]. The renal increase in superoxide anion and consequent formation of lipid-peroxidation products 4-HNE and TBARS observed in our animal model of MI demonstrates the implication of oxidative stress in the CRS, results that are in agreement with previous studies that showed CRS-1 is associated not only with an increase in ROS levels but also, with higher expression of NOX2 and the apoptosis rate in the kidneys from animals subjected to MI [398].

Over the past few years, it has been suggested that development of fibrosis and organ damage in the CRS pathological context can be triggered by metabolic changes other than inflammation and oxidative, for example by ER stress activation. In CRS, pathophysiological changes in the haemodynamics and in the components of the RAAS can alter the balance between the unfolded and misfolded proteins due to the increased biosynthesis demand leading to ER stress

and compromising cell survival, allowing the formation of a fibrotic wound [303, 399, 400]. In our study we observed not only that ER stress is activated at renal level 4 weeks post-MI, but also that it correlates with tubulointerstitial fibrosis, showing the possible role of ER stress in renal ECM production in CRS-1. Accordingly, other studies have associated ER stress to myocardial or renal fibrosis, however, the studies did not represent a pathological context of CRS. For example, pharmacological inhibition of ER stress proved effective in the reduction of collagen IV and fibronectin levels in both the renal tissue of a murine model of diabetic kidney disease and in tunicamycin-treated renal cells [322]. Also, in a model of renal I/R injury genetic disruption of ATF6$\alpha$, a downstream mediator of UPR cascade prevented collagen I upregulation and promoted a reduction in tubulointerstitial fibrosis [401]. Similarly, we have observed that renal fibrosis was accompanied by renal increase in the protein levels of ATF6$\alpha$ after MI without modifications in CHOP, a previously described mediator of apoptosis [402].

ATF6$\alpha$ has been identified as a crucial regulator of lipid metabolism, as its depletion decreases lipid accumulation in the kidneys of mice after I/R injury [401]. The relationship between ER stress and PA-induced lipotoxicity has been previously demonstrated by both Martínez-García et al., who observed that PA accumulation in intracellular lipid droplets was associated with insulin resistance and ER stress in podocytes [376], and Hamada et al who proved ER stress activation in PA-stimulated tubular epithelial cells [403]. However, the specific effects of PA on renal fibroblast, the main cell type responsible for ECM production and fibrosis development, was not previously assessed. In this study we have confirmed the role of PA on ER stress activation in renal fibroblasts, and we also proved that PA exerts profibrotic, prooxidant and proinflammatory actions in renal cells, confirming its detrimental role. Since the pharmacological inhibition of ER stress by 4-PBA was able to prevent all these modifications, it

seems ER stress activation plays an important role in the PA effects seen in renal fibroblasts.

4-PBA, a chemical chaperone that enhances protein folding and can stabilize misfolded proteins in the ER lumen, is an FDA-approved drug for urea cycle enzyme deficiencies due to its function as an ammonia scavenger [404]; however, it has also shown promising results in the treatment of cystic fibrosis with few side effects such as headache and nausea [405, 406]. In addition to the previously described benefits of 4-PBA, in the current study we also show the beneficial effects of this drug on Ang II-induced inflammation, ECM and ROS production in renal fibroblasts. Similarly to what was previously reported in podocytes [407], macrophages [408] and mesangial cells [409], we observed that Ang II is able to induce ER stress in renal fibroblasts. In fact, previous studies have reported that blockade of Ang II type I receptor (AT1R) with Valsartan was able to prevent ER stress activation by PA in renal cells [410].

As has been previously mentioned, RAAS also promotes renal alterations. In this sense, Ang II has been linked to several pathologies such as MI and CKD, as it exerts hemodynamic and neurohormonal effects that can impair cardiovascular and renal damage [411, 412], making treatment against the main effector of the RAAS one of the standard clinical procedures for preserving cardiorenal function [413]. High levels of Ang II are known to promote sarcolemic permeability, cell death and increased vascular permeability due to endothelial cell damage, all of which leads to the replacement of injured tissue by fibrotic one. Accordingly, *in-vitro* studies have demonstrated that AT1R blockade or inhibition of the Angiotensin Converting Enzyme improves glomerular damage and inflammatory infiltration in the kidneys [414, 415], with some improvement in fibrosis [387, 416].

Furthermore, once RAAS is activated, Ang II can promote the progression of organ fibrosis, inflammation and hypertrophy due to its implication in Gal-3

expression and secretion [417]. It is known that an increase in Ang II levels promotes the secretion of aldosterone, which then interacts with the mineralocorticoid receptor (MR), activating it and triggering its translocation to the nucleus, where it can bind to the promoter region of target genes such as the gene encoding Gal-3 to act as recruitment factor that propitiates target transcription [418-420]. As previously mentioned, the upregulation of Gal-3 can then contribute to fibrosis in the context of cardiorenal injury [421].

In addition, Ang II can also exert detrimental effects due to the chronic activation of mechanisms such as inflammation, ER stress and oxidative stress, which can trigger the fibrotic response affecting organ function [422, 423]. With our results, we confirmed that Ang II stimulation leads to higher genetic expression of Gal-3 in renal fibroblasts, a process that seems to be mediated by ER stress activation. In a study from Bezerra Lins et al. in male Wistar rats demonstrated that sustained administration of Ang II induced ER stress and oxidative stress, whereas treatment with the AT1R inhibitor, losartan, reduced both ER and oxidative stress markers, as well as prevented the decline in renal function [313]. In our animal model of MI, we observed higher plasmatic levels of Ang II in infarcted animals as compared to control ones. Moreover, our results also show that NFκB and ERK1/2 pathways mediate the profibrotic effects of Ang II. Overall, we corroborated the profibrotic, proinflammatory and prooxidant effects of Ang II in renal fibroblasts, alterations that seem to be mediated by ER stress activation since i) Ang II was able to induce ER stress and ii) 4-PBA prevented the increase in Collagen I, superoxide anions, inflammatory markers and Gal-3 in Ang II-treated fibroblasts.

As previously mentioned, MI development is usually concomitant to the presence of obesity, an important risk factor for cardiovascular events that has also proven to correlate with higher all-cause mortality rates, which can also modulate prognosis in CRS. In recent years, researchers have realized the need

to differentiate between adiposity-related CRS and non-adiposity related CRS, giving those pathological contexts in which obesity is implicated the term "cardiorenal metabolic syndrome" [13]. Although multiple pathophysiological pathways such as haemodynamic impairment, insulin resistance, inflammation, endothelial dysfunction and oxidative stress have been suggested to play a role in the development of cardiorenal metabolic diseases, other mechanisms are yet to be assessed.

As Gal-3 is an independent predictor of all-cause mortality in heart failure that has also been associated with renal function impairment, it could be an interesting potential biomarker as an early predictor of CRS or as a prognostic value in patients with CRS. In the context of renal and cardiac physiopathology, Gal-3 mediated profibrotic and proinflammatory signalling cascades in cells such as macrophages, fibroblasts or endothelial cells result in the development of chronic inflammation, fibrosis, and other mechanisms like oxidative stress, consequently leading to organ dysfunction. In fact, several studies that demonstrated the direct association between the Gal-3 levels, CRS-1 development, and mortality in patients with HF, have suggested it could possibly be due to Gal-3 implication in inflammation and fibrosis [421, 424, 425]. Further studies in animal models of cardiac [426, 427] and renal injury [225, 239] have proven that Gal-3 modulation *via* depletion or pharmacological inhibition is an effective therapeutic approach for the reduction of renal fibrosis, inflammation, and oxidative stress. Our data adds a cardiorenal perspective into the previously reported proinflammatory effects of Gal-3 and in the relationship between Gal-3 and oxidative stress, as our results show that along with its beneficial effects in the normalization of fibrosis, MCP treatment was also able to blunt the increase in pro-inflammatory cytokines OPN and TNF-$\alpha$ and the upsurge in superoxide anions in the kidneys from obese MI animals.

In recent years the aberrant expression of microRNAs, small non-coding RNAs that act as post-transcriptional regulators, has been linked to a great variety of processes involved in the development of many diseases [330, 338, 340]. MicroRNAs are of great clinical interest due to their potential role as diagnostic markers and/or therapeutic targets for a wide range of illnesses. Due to the sensitive machinery that regulates microRNA expression and functionality, changes in the expression of a specific microRNA could inform of the presence of a pathological environment prior to the start of symptoms [329]. Thanks to the results of a microarray done in plasma samples, we were able to focus on five microRNAs whose expression was significantly modulated as a consequence of MI in the context of obesity. Specifically, we observed concomitant obesity and MI were associated with the upregulation of miR-485-3p and with the downregulation of let-7f-5p, miR-17-5p, miR-144-5p and miR-339-3p, which have been linked to obesity, cardiac and/or renal diseases [428-431]. Further studies done to assess whether the circulating levels mirror the tissue expression of these microRNAs and the potential influence of Gal-3 on them demonstrated that obese animals with MI presented a renal decrease in all the five microRNAs but that Gal-3 inhibition only had significant effects on the let-7f-5p levels.

Similar to other members of the let-7 family, modulation in the let-7f expression has been associated with multiple cardiovascular diseases. A 2019 study by Chen-Yun et al. showed a significant downregulation in the circulating levels of let-7f in samples from ST elevation MI (STEMI) patients, as well as in the infarct area from both pig and mice 24 h after the ligation of the coronary artery, although normal levels of let-7f were found after 6 days post-MI [432]. Inhibition of let-7f by adenovirus exacerbated cardiomyocyte apoptosis and induced cardiac hypertrophy with worsened LVEF, whereas its overexpression improved cardiac function and reduced the fibrotic scaring, suggesting the possible cardioprotective role of this microRNA in the pathological context of MI [432].

Let-7f downregulation in STEMI patients was also evaluated in a different study that demonstrated its potential diagnostic value to distinguish between STEMI and takotsubo cardiomyopathy, a clinically indistinguishable pathology from acute MI that presents a significant upregulation of this microRNA when compared to STEMI [433]. Conversely, other studies have demonstrated that an upregulation in the circulating levels of let-7f can be useful to differentiate between spontaneous coronary artery dissection and atherothrombotic acute MI [434].

Although not many studies have assessed let-7f levels in kidney diseases other than cancer, some have suggested its possible implication in renal damage. Ichii et al., have reported let-7f as one of the most abundantly expressed microRNAs within the glomerulus of mice and have shown it is significantly downregulated in both early and late glomerulonephritis [435]. In addition, sequencing results have suggested that modulations in the urinary exosome-derived microRNA pattern can indicate the presence of renal damage in cats, let-7f being one of the proposed microRNAs due to its downregulated expression in animals with kidney disease when compared to healthy ones [436]. Given the importance of ischemic injury to the kidney, other studies assessed microRNA profiles in both normoxic and hypoxic conditions and found that under 10-days hypoxic exposure, let-7f renal expression tended to decrease, reduction that was potentiated with δ-opioid receptor activation [437].

Along with its implication in cardiovascular and kidney diseases, the let-7 family has proven to be associated with changes in the lipid profile, insulin resistance [438] and body weight, as its overexpression leads to a decrease in fat mass and body size. In fact, knockdown of the let-7 family in diet-induced obesity improved insulin sensitivity and prevented ectopic fat deposition in mice [439]. Different murine models of diet-induced obesity have demonstrated that obesity is associated with a decrease in let-7f-5p circulating levels, whereas low-fat fed

animals present an up-regulation of this microRNA [428, 440]. Moreover, switching the obese animals to a low-fat feeding not only decrease body weight and adiposity but also reversed the downregulation of let-7f-5p [440]. In the clinical setting, studies done in a cohort of patients with both obesity and type 2 diabetes that underwent bariatric surgery showed that the decrease in BMI was accompanied by changes in the microRNA circulating pattern after 21 days of intervention. In that cohort let-7f-5p had the second largest increase after bariatric surgery and was significantly expressed in the pituitary gland, which could contribute to hormone release control [441]. The recovery of this microRNA levels after bariatric surgery could be due to the reduction in visceral adipose tissue, whose let-7f expression levels are known to be associated with obesity and type 2 diabetes possibly through the regulation of the vascular endothelial growth factor (VEGF) pathways, WNT signalling, and inflammation [442].

In accordance with the above, our data demonstrates that the concomitance of obesity and MI does also show a marked downregulation in the circulating levels of let-7f-5p that was also observed in the kidney cortex of the animals. In our data, in-silico target prediction identified ECM-receptor interaction, protein processing within the endoplasmic reticulum and the Hippo-signalling pathway as potentially regulated pathways by let-7f-5p, all of which were significantly modulated in obese animals with MI at renal level. Furthermore, the pharmacological inhibition of Gal-3 both recovered let-7f-5p levels and attenuated cortical fibrosis, ER stress and Hippo-signalling at renal level, suggesting let-7f-5p downregulation might mediate Gal-3 renal consequences through the modulation of the aforementioned signalling pathways in the pathological scenario of obesity and MI.

The Hippo pathway (depicted in Figure 58) is a well-conserved kinase cascade that has a crucial role in adult organ size regulation, tissue regeneration and tumour formation due to its implication in cell proliferation, differentiation and

apoptosis [443, 444]. Both intracellular and extracellular inputs such as metabolic state, ROS levels, cell-cell contact, matrix stiffness, mechanical cues and hormonal signals can activate the core kinase cascade of the Hippo pathway [444-446]. When the Hippo pathway is active MST1/2 and its cofactor SAV get phosphorylated, allowing them to phosphorylate downstream proteins LATS1/2 and MOB1A/B. Consequently, the phosphorylated LATS1/2 further phosphorylates the main effectors of this signalling pathway, YAP and TAZ, preventing their translocation to the nucleus and contributing to its cytoplasmic sequestration and degradation which hinders cell proliferation and organ growth. On the contrary, inhibition of this pathway results in dephosphorylation of the upstream kinases, allowing active YAP/TAZ to enter the nucleus, where they will interact with the transcription factor TEAD, mediating transcription of target genes involved in cell cycle, migration and cell fate such as CTGF, BIRC or SNAIL which can promote epithelial-mesenchymal transition, cell proliferation and tissue growth [443, 447].

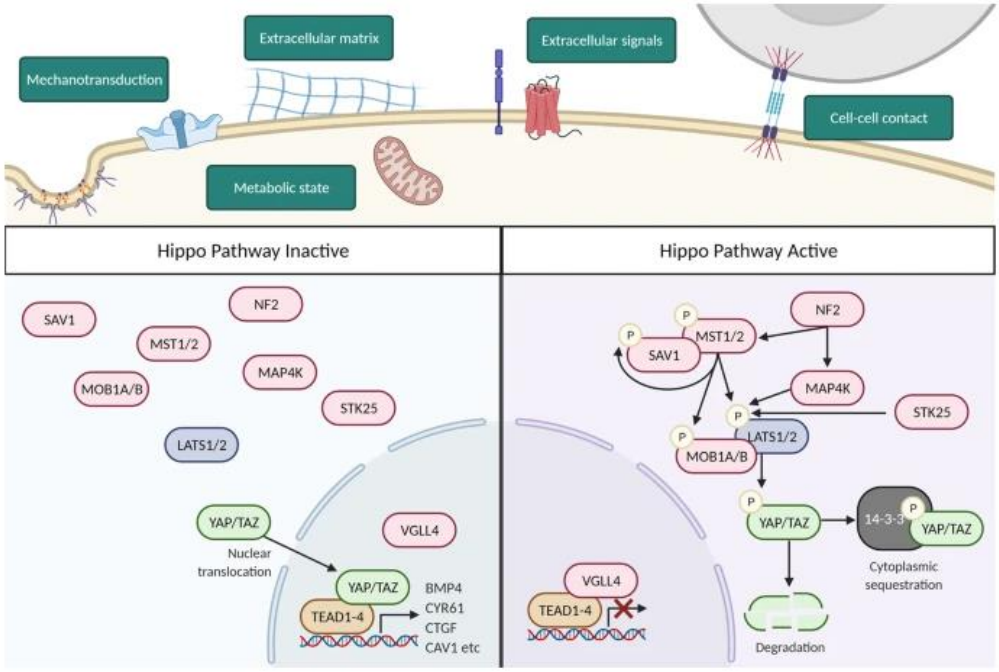


**Figure 58.** Schematic representation of the Hippo signalling pathway and its activation inputs taken from Riley, SE et al. review paper [445].

Dysregulation of the Hippo signalling pathway has been associated to multiple disorders, from cancer [448] to cardiovascular [446, 449], renal [450, 451] and hepatic [452] diseases among others. Several studies have found that the loss of any component of the Hippo kinase cascade results in cell proliferation, resistance to apoptosis and organ overgrowth [453], although depending on the organ, the modulation of this cascade seems to have different roles in remodelling and fibrinogenesis. As an example, in the developing kidneys LATS deletion translates into increased fibrosis and myofibroblast presence [454], whereas YAP/TAZ deletion disrupts cortical fibroblast and myofibroblast development [455], therefore suggesting an anti-fibrotic role of the active Hippo pathway. However, in the developing heart the same genetic deletion blunts cardiac fibroblast proliferation which results in spontaneous transition into myofibroblast phenotype, leading to organ damage due to a persistent pro-fibrotic and pro-inflammatory environment [456]. Although the role of the Hippo signalling pathway has been widely described in both cardiac and kidney injuries, current bibliography shows only one study that has assessed its involvement in the CRS pathological context. Specifically, in a murine model of CRS-3, ROS-induced Hippo pathway activation seems to mediate cardiac dysfunction in AKI animals [300]. In contrast, our data in an animal model of CRS-1 demonstrates that the renal inactivation of the Hippo signalling pathway in the obese MI animals, characterized by decreased levels of YAP phosphorylation and increased expression of the pathway target genes, seems to be triggered by the increase in Gal-3 levels, possibly *via* the downregulation of let-7f-5p. The possible role of let-7f-5p in the Hippo pathway was only previously suggested in colitis-associated cancer [457], whereas our results add a different pathological perspective where Gal-3 might act as the trigger for let-7f-5p alteration and consequent Hippo pathway modulation.

Although previous reports have demonstrated the complex interplay between Gal-3 and microRNAs, showing that Gal-3 is a target of a wide range of microRNAs involved in pathological mechanisms such as tumour progression [458, 459], inflammation [460], cardiomyocyte injury [370] and fibrosis [461], few studies have demonstrated the role of Gal-3 over microRNA expression. The results herein presented demonstrated for the first time the direct involvement of Gal-3 in let-7f-5p modulation, as Gal-3 stimulation induces an early downregulation of let-7f-5p expression in renal epithelial cells. In addition to the changes in the microRNA we confirmed that Gal-3 enhances the expression of ECM components, ER stress mediators and Hippo pathway effectors and targets, possibly through the decrease in let-7f-5p levels, as our miRNA transfection studies in non-stimulated cells corroborated that let-7f-5p is a downstream target gene of Gal-3 that directly contributes to ER stress activation and ECM modulation.

Further *in-vitro* validation confirmed ER stress acts as a downstream mediator of let-7f-5p actions, as pharmacological activation of ER stress did not significantly modify the expression of this microRNA but let-7f-5p overexpression did modulate the levels of ATF4 and prevent the increase in ATF6β mRNA levels, two of the let-7f-5p predicted target genes. In fact, the results from luciferase assay show the direct interaction between let-7f-5p and ATF6β, demonstrating its role as a direct target of this microRNA and its involvement in ER stress activation, specifically through ATF6β.

ATF6β is a member of the ATF/cAMP response element-binding (CREB) family of transcription factors which play an important role in the UPR. Most studies focused on the implication of another member of this family, ATF6$\alpha$, whereas ATF6β has been poorly studied. Although both members are functionally associated with ER stress and cell viability, isoform-specific rates of generation and degradation regulate the levels of both ATF6$\alpha$ and ATF6β during the ER

stress response, leading to a competition for binding to ER stress elements such as BiP, which translates into differential gene expression regulation depending on which member conforms the transcriptional complexes [462]. Despite its high degree of homology to ATF6α, due to structural differences among both isoforms ATF6β exhibits lower transcriptional activity but higher stability than those of ATF6α [462, 463]. Surprisingly, although ATF6β has been described as a weak transcription factor that inhibits ATF6α in the heart, both genetic deletion of ATF6α or ATF6β induces a similar reduction in the cardiac hypertrophy induced by pressure overload in mice, suggesting both isoforms upregulate the same set of genes, serving the same functional role in the UPR signalling [464]. Despite the obvious functional redundancy between ATF6α and ATF6β, several studies have demonstrated that they also have different functions, as ATF6β but not ATF6α modulates Wfs1 transcription in the pancreatic cells and Plgf in placental ones [465]. In our results, ATF6β correlated not only with let-7f-5p but also with the levels of Gal-3, which could add isoform specificity to the results of a previous study by Macke et al. that reported ATF6 depletion induces a decrease in Gal-3 expression [466]. Furthermore, ATF6β also correlated to the levels of NGAL, renal fibrosis and even the Hippo-signalling pathway, suggesting the possible involvement of ATF6β in the renal alterations associated with cardiorenal syndrome in the context of MI and obesity.

In addition to the positive correlation between ATF6β and the Hippo pathway, we demonstrated the direct involvement of ER stress activation in the Hippo pathway inactivation in renal epithelial cells. These results are in agreement with previous studies that also showed an association between UPR and the Hippo pathway, mainly through YAP1 involvement [467, 468]. For example, in a study regarding liver tumorigenesis, the authors demonstrated that pharmacological inhibition of ER stress was associated with activated Hippo pathway, which translated into decreased liver overgrowth. They also reported that YAP acts as

a switch between the pro-apoptotic and pro-survival UPR responses. In cells under ER stress conditions, YAP activation increased ATF6 cleavage and ER size to promote cell survival, whereas cells undergoing chronic ER stress showed activation of the Hippo signalling, which translates into decreased UPR and increased cell death due to YAP degradation [453]. Moreover, we confirmed that in this context an upregulation of let-7f-5p reverts Tunicamycin-induced inactivation of the Hippo pathway, therefore enhancing target gene transcription, which suggest that let-7f-5p could act as a connector between ER stress and the Hippo signalling pathway.

Considering the previous data that suggested the implication of ER stress activation in the renal damage via the interaction of let-7f-5p and ATF6β, we decided to assess whether the pharmacological inhibition of ER stress could improve renal deleterious consequences of MI in the context of obesity. Similarly to what was previously observed in other animal models of renal injury [469-471], inhibition of ER stress in our animal model of CRS-1 proved effective in reducing the severity of renal damage and cardiac alterations. Treatment with 4-PBA, while effective in ER stress mitigation, also proved to decrease the upregulation of the acute injury marker NGAL seen in the non-treated animals. Moreover, this animal model allowed us to further confirm the downstream role of ER stress in regard to let-7f-5p, as neither tunicamycin stimulation in cells nor ER stress inhibition in the animals modulated this microRNA expression. 4-PBA pharmacological inhibition of ER stress also demonstrated beneficial effects in terms of prevention of the glomerular, interstitial and perivascular fibrosis, renal oxidative stress and inflammation observed in obese infarcted animals, demonstrating concomitant MI and obesity activate ER stress, which promotes fibrosis, oxidative stress and inflammation in the kidney. Although functional protein association networks and enrichment analysis show the Hippo pathway and ER stress form two distinct clusters, we suggested that they could be linked

by let-7f-5p actions. Data from this animal model reveals that ER stress inhibition propitiates YAP1 phosphorylation and a decrease in Hippo pathway target genes transcription, which combined with our *in-vitro* results in tunicamycin-treated cells, clearly demonstrates the direct link between both pathways.

Therefore, our findings portray not only the renal consequences associated with obesity and MI-induced cardiorenal syndrome but also reveal the implication and targeting relevance of the Gal-3/let-7f-5p/ER stress axis as a means to alleviating the described renal damage in such pathological context.

## I. Limitations

While this study provides valuable insights into the renal consequences associated with obesity and MI-induced cardiorenal syndrome and the implication of certain mechanisms, some limitations should be acknowledged.

Regarding the clinical study, the fact that the average age of the MI patients is significantly higher than that of the control subjects could be a bias for the interpretation of the results. However, we have adjusted for age in our statistical analysis through a multiple logistic regression, ensuring that the impact of the different parameters considered are evaluated independently of age-related effect, which reinforces the results' validity despite this potential limitation. Furthermore, taking into account that the average age at which most MI occur in Spain is around 68 years old and the fact that the cohort of MI patients presented in this thesis is below such age, we do not consider it to be the most determining factor.

Due to time constraints, certain experiments that could have provided additional insights were not included in this study. While the conducted in-vitro experiments offer valuable data and support the primary conclusions, further

analysis could have confirmed the suggested mediatory role of let-7f-5p of the renal deleterious effects of Gal-3. These additional studies are recommended for future research to build upon the current results

# *Conclusions*

1. The renal alterations observed in animals with myocardial infarction were accompanied by an upregulation of Galectin-3 and the activation of endoplasmic reticulum stress.
2. Galectin-3 participates in the renal damage associated with myocardial infarction in the context of obesity by promoting renal fibrosis, oxidative stress and a proinflammatory environment.
3. Myocardial infarction in the context of obesity activates endoplasmic reticulum stress, which promotes renal fibrosis, oxidative stress and a proinflammatory environment.
4. Myocardial infarction and obesity are associated with changes in the microRNA the modulation of the microRNA pattern.
5. Downregulation of microRNA let-7f-5p appears as a potential mediator of the renal deleterious effects of Gal-3 through the activation of endoplasmic reticulum stress and the Hippo signalling pathway.

Altogether, Galectin-3, endoplasmic reticulum stress and let-7f-5p emerges as three different pharmacological targets for the management of the renal complications associated with cardiorenal syndrome in the context of myocardial infarction and obesity.

# *Bibliography*

[1] C. Ronco *et al.*, "Cardio-renal syndromes: report from the consensus conference of the acute dialysis quality initiative," *Eur Heart J,* vol. 31, no. 6, pp. 703-11, Mar 2010, doi: 10.1093/eurheartj/ehp507.

[2] A. Dutta, S. Saha, A. Bahl, A. Mittal, and T. Basak, "A comprehensive review of acute cardio-renal syndrome: need for novel biomarkers," *Front Pharmacol,* vol. 14, p. 1152055, 2023, doi: 10.3389/fphar.2023.1152055.

[3] J. Uduman, "Epidemiology of Cardiorenal Syndrome," *Adv Chronic Kidney Dis,* vol. 25, no. 5, pp. 391-399, Sep 2018, doi: 10.1053/j.ackd.2018.08.009.

[4] G. R. Shroff, P. D. Frederick, and C. A. Herzog, "Renal failure and acute myocardial infarction: clinical characteristics in patients with advanced chronic kidney disease, on dialysis, and without chronic kidney disease. A collaborative project of the United States Renal Data System/National Institutes of Health and the National Registry of Myocardial Infarction," *Am Heart J,* vol. 163, no. 3, pp. 399-406, Mar 2012, doi: 10.1016/j.ahj.2011.12.002.

[5] Y. Yang *et al.*, "Predictors of mortality in heart failure with reduced ejection fraction: interaction between diabetes mellitus and impaired renal function," *Int Urol Nephrol,* vol. 55, no. 9, pp. 2285-2293, Sep 2023, doi: 10.1007/s11255-023-03525-0.

[6] L. P. Gregg and S. S. Hedayati, "Management of Traditional Cardiovascular Risk Factors in CKD: What Are the Data?," *Am J Kidney Dis,* vol. 72, no. 5, pp. 728-744, Nov 2018, doi: 10.1053/j.ajkd.2017.12.007.

[7] T. Chiuariu *et al.*, "Cardiac and Renal Fibrosis, the Silent Killer in the Cardiovascular Continuum: An Up-to-Date," *J Cardiovasc Dev Dis,* vol. 11, no. 2, Feb 16 2024, doi: 10.3390/jcdd11020062.

[8] B. Delgado-Valero *et al.*, "Role of endoplasmic reticulum stress in renal damage after myocardial infarction," *Clin Sci (Lond),* vol. 135, no. 1, pp. 143-159, Jan 15 2021, doi: 10.1042/CS20201137.

[9] M. Cobo Marcos *et al.*, "Prevalence and clinical profile of kidney disease in patients with chronic heart failure. Insights from the Spanish cardiorenal registry," *Rev Esp Cardiol (Engl Ed),* vol. 77, no. 1, pp. 50-59, Jan 2024, doi: 10.1016/j.rec.2023.05.003.

[10] Q. Li *et al.*, "Effect of kidney disease on all-cause and cardiovascular mortality in patients undergoing coronary angiography," *Ren Fail,* vol. 45, no. 1, p. 2195950, Dec 2023, doi: 10.1080/0886022X.2023.2195950.

[11] "Cases and Observations Illustrative of Renal Disease, Accompanied with the Secretion of Albuminous Urine," *Med Chir Rev,* vol. 25, no. 49, pp. 23-35, Jul 1 1836. [Online]. Available: https://www.ncbi.nlm.nih.gov/pubmed/29918407.

[12] S. Vondenhoff, S. J. Schunk, and H. Noels, "Increased cardiovascular risk in patients with chronic kidney disease," *Herz,* vol. 49, no. 2, pp. 95-104, Mar 2024, doi: 10.1007/s00059-024-05235-4. Erhohtes kardiovaskulares Risiko bei Patienten mit chronischer Niereninsuffizienz.

[13] S. Al-Chalabi, A. A. Syed, P. A. Kalra, and S. Sinha, "Mechanistic Links between Central Obesity and Cardiorenal Metabolic Diseases," *Cardiorenal Med,* vol. 14, no. 1, pp. 12-22, 2024, doi: 10.1159/000535772.

[14] J. J. Chen *et al.*, "Acute Kidney Disease After Acute Decompensated Heart Failure," *Kidney Int Rep,* vol. 7, no. 3, pp. 526-536, Mar 2022, doi: 10.1016/j.ekir.2021.12.033.

[15] K. W. Prins, T. Thenappan, J. S. Markowitz, and M. R. Pritzker, "Cardiorenal Syndrome Type 1: Renal Dysfunction in Acute Decompensated Heart Failure," *J Clin Outcomes Manag,* vol. 22, no. 10, pp. 443-454, Sep 2015. [Online]. Available: https://www.ncbi.nlm.nih.gov/pubmed/27158218.

[16] I. Leontsinis *et al.*, "Cardiorenal multimorbidity in hospitalized cardiology patients: The Hellenic Cardiorenal Morbidity Snapshot (HECMOS) study," *Hellenic J Cardiol,* vol. 74, pp. 8-17, Nov-Dec 2023, doi: 10.1016/j.hjc.2023.03.006.

[17] D. Seckinger, O. Ritter, and D. Patschan, "Risk factors and outcome variables of cardiorenal syndrome type 1 from the nephrologist's perspective," *Int Urol Nephrol,* vol. 54, no. 7, pp. 1591-1601, Jul 2022, doi: 10.1007/s11255-021-03036-w.
[18] C. Ronco, A. Bellasi, and L. Di Lullo, "Cardiorenal Syndrome: An Overview," *Adv Chronic Kidney Dis,* vol. 25, no. 5, pp. 382-390, Sep 2018, doi: 10.1053/j.ackd.2018.08.004.
[19] Z. Abassi, E. E. Khoury, T. Karram, and D. Aronson, "Edema formation in congestive heart failure and the underlying mechanisms," *Front Cardiovasc Med,* vol. 9, p. 933215, 2022, doi: 10.3389/fcvm.2022.933215.
[20] M. K. Ames, C. E. Atkins, and B. Pitt, "The renin-angiotensin-aldosterone system and its suppression," *J Vet Intern Med,* vol. 33, no. 2, pp. 363-382, Mar 2019, doi: 10.1111/jvim.15454.
[21] G. M. Virzi *et al.*, "Oxidative stress: dual pathway induction in cardiorenal syndrome type 1 pathogenesis," *Oxid Med Cell Longev,* vol. 2015, p. 391790, 2015, doi: 10.1155/2015/391790.
[22] B. Delgado-Valero, V. Cachofeiro, and E. Martinez-Martinez, "Fibrosis, the Bad Actor in Cardiorenal Syndromes: Mechanisms Involved," *Cells,* vol. 10, no. 7, Jul 19 2021, doi: 10.3390/cells10071824.
[23] R. Raina, N. Nair, R. Chakraborty, L. Nemer, R. Dasgupta, and K. Varian, "An Update on the Pathophysiology and Treatment of Cardiorenal Syndrome," *Cardiol Res,* vol. 11, no. 2, pp. 76-88, Apr 2020, doi: 10.14740/cr955.
[24] J. C. Harrison *et al.*, "A Clinically Relevant Functional Model of Type-2 Cardio-Renal Syndrome with Paraventricular Changes consequent to Chronic Ischaemic Heart Failure," *Sci Rep,* vol. 10, no. 1, p. 1261, Jan 27 2020, doi: 10.1038/s41598-020-58071-x.
[25] P. E. Stevens, A. Levin, and M. Kidney Disease: Improving Global Outcomes Chronic Kidney Disease Guideline Development Work Group, "Evaluation and management of chronic kidney disease: synopsis of the kidney disease: improving global outcomes 2012 clinical practice guideline," *Ann Intern Med,* vol. 158, no. 11, pp. 825-30, Jun 4 2013, doi: 10.7326/0003-4819-158-11-201306040-00007.
[26] M. Murton *et al.*, "Burden of Chronic Kidney Disease by KDIGO Categories of Glomerular Filtration Rate and Albuminuria: A Systematic Review," *Adv Ther,* vol. 38, no. 1, pp. 180-200, Jan 2021, doi: 10.1007/s12325-020-01568-8.
[27] C. D. Chu *et al.*, "Albuminuria testing and nephrology care among insured US adults with chronic kidney disease: a missed opportunity," *BMC Prim Care,* vol. 23, no. 1, p. 299, Nov 24 2022, doi: 10.1186/s12875-022-01910-9.
[28] K. Damman, M. A. Valente, A. A. Voors, C. M. O'Connor, D. J. van Veldhuisen, and H. L. Hillege, "Renal impairment, worsening renal function, and outcome in patients with heart failure: an updated meta-analysis," *Eur Heart J,* vol. 35, no. 7, pp. 455-69, Feb 2014, doi: 10.1093/eurheartj/eht386.
[29] R. De Vecchis and C. Baldi, "Cardiorenal syndrome type 2: from diagnosis to optimal management," *Ther Clin Risk Manag,* vol. 10, pp. 949-61, 2014, doi: 10.2147/TCRM.S63255.
[30] S. Y. Jang and D. H. Yang, "Prognostic and Therapeutic Implications of Renal Insufficiency in Heart Failure," *Int J Heart Fail,* vol. 4, no. 2, pp. 75-90, Apr 2022, doi: 10.36628/ijhf.2021.0039.
[31] S. M. Bagshaw *et al.*, "Cardiorenal syndrome type 3: pathophysiologic and epidemiologic considerations," *Contrib Nephrol,* vol. 182, pp. 137-57, 2013, doi: 10.1159/000349971.
[32] L. Di Lullo, P. B. Reeves, A. Bellasi, and C. Ronco, "Cardiorenal Syndrome in Acute Kidney Injury," *Semin Nephrol,* vol. 39, no. 1, pp. 31-40, Jan 2019, doi: 10.1016/j.semnephrol.2018.10.003.

[33] U. Kumar, N. Wettersten, and P. S. Garimella, "Cardiorenal Syndrome: Pathophysiology," *Cardiol Clin,* vol. 37, no. 3, pp. 251-265, Aug 2019, doi: 10.1016/j.ccl.2019.04.001.
[34] L. Di Lullo *et al.*, "Pathophysiology of the cardio-renal syndromes types 1-5: An uptodate," *Indian Heart J,* vol. 69, no. 2, pp. 255-265, Mar-Apr 2017, doi: 10.1016/j.ihj.2017.01.005.
[35] J. Jankowski, J. Floege, D. Fliser, M. Bohm, and N. Marx, "Cardiovascular Disease in Chronic Kidney Disease: Pathophysiological Insights and Therapeutic Options," *Circulation,* vol. 143, no. 11, pp. 1157-1172, Mar 16 2021, doi: 10.1161/CIRCULATIONAHA.120.050686.
[36] K. Matsushita, S. H. Ballew, A. Y. Wang, R. Kalyesubula, E. Schaeffner, and R. Agarwal, "Epidemiology and risk of cardiovascular disease in populations with chronic kidney disease," *Nat Rev Nephrol,* vol. 18, no. 11, pp. 696-707, Nov 2022, doi: 10.1038/s41581-022-00616-6.
[37] C. Xu, G. Tsihlis, K. Chau, K. Trinh, N. M. Rogers, and S. M. Julovi, "Novel Perspectives in Chronic Kidney Disease-Specific Cardiovascular Disease," *Int J Mol Sci,* vol. 25, no. 5, Feb 24 2024, doi: 10.3390/ijms25052658.
[38] S. H, S. A. B, V. Moger, and M. Swamy, "Cardiorenal syndrome type 4: A study of cardiovascular diseases in chronic kidney disease," *Indian Heart J,* vol. 69, no. 1, pp. 11-16, Jan-Feb 2017, doi: 10.1016/j.ihj.2016.07.006.
[39] R. L. Mehta *et al.*, "Cardiorenal syndrome type 5: clinical presentation, pathophysiology and management strategies from the eleventh consensus conference of the Acute Dialysis Quality Initiative (ADQI)," *Contrib Nephrol,* vol. 182, pp. 174-94, 2013, doi: 10.1159/000349970.
[40] M. Prastaro *et al.*, "Cardiorenal syndrome: Pathophysiology as a key to the therapeutic approach in an under-diagnosed disease," *J Clin Ultrasound,* vol. 50, no. 8, pp. 1110-1124, Oct 2022, doi: 10.1002/jcu.23265.
[41] M. Singer *et al.*, "The Third International Consensus Definitions for Sepsis and Septic Shock (Sepsis-3)," *JAMA,* vol. 315, no. 8, pp. 801-10, Feb 23 2016, doi: 10.1001/jama.2016.0287.
[42] S. Vallabhajosyula *et al.*, "Clinical profile and outcomes of acute cardiorenal syndrome type-5 in sepsis: An eight-year cohort study," *PLoS One,* vol. 13, no. 1, p. e0190965, 2018, doi: 10.1371/journal.pone.0190965.
[43] H. Wang, H. Ding, Z. Y. Wang, and K. Zhang, "Research progress on microcirculatory disorders in septic shock: A narrative review," *Medicine (Baltimore),* vol. 103, no. 8, p. e37273, Feb 23 2024, doi: 10.1097/MD.0000000000037273.
[44] A. Kotecha, S. Vallabhajosyula, H. H. Coville, and K. Kashani, "Cardiorenal syndrome in sepsis: A narrative review," *J Crit Care,* vol. 43, pp. 122-127, Feb 2018, doi: 10.1016/j.jcrc.2017.08.044.
[45] A. Balkrishna *et al.*, "Sepsis-mediated renal dysfunction: Pathophysiology, biomarkers and role of phytoconstituents in its management," *Biomed Pharmacother,* vol. 165, p. 115183, Sep 2023, doi: 10.1016/j.biopha.2023.115183.
[46] S. Peerapornratana, C. L. Manrique-Caballero, H. Gomez, and J. A. Kellum, "Acute kidney injury from sepsis: current concepts, epidemiology, pathophysiology, prevention and treatment," *Kidney Int,* vol. 96, no. 5, pp. 1083-1099, Nov 2019, doi: 10.1016/j.kint.2019.05.026.
[47] P. Hatamizadeh, "From cardiorenal syndrome to nephrocardiology: The journey of exploring the interconnection between nephrology and cardiovascular medicine," *Trends Cardiovasc Med,* Mar 22 2024, doi: 10.1016/j.tcm.2024.03.002.
[48] T. D. Hewitson, S. G. Holt, and E. R. Smith, "Animal Models to Study Links between Cardiovascular Disease and Renal Failure and Their Relevance to Human Pathology," *Front Immunol,* vol. 6, p. 465, 2015, doi: 10.3389/fimmu.2015.00465.

[49] T. Georgopoulou *et al.*, "Cardiorenal Syndrome: Challenges in Everyday Clinical Practice and Key Points towards a Better Management," *J Clin Med,* vol. 12, no. 12, Jun 18 2023, doi: 10.3390/jcm12124121.
[50] M. Kumar *et al.*, "Animal models of myocardial infarction: Mainstay in clinical translation," *Regul Toxicol Pharmacol,* vol. 76, pp. 221-30, Apr 2016, doi: 10.1016/j.yrtph.2016.03.005.
[51] B. I. Levy and J. J. Mourad, "Renin Angiotensin Blockers and Cardiac Protection: From Basis to Clinical Trials," *Am J Hypertens,* vol. 35, no. 4, pp. 293-302, Apr 2 2022, doi: 10.1093/ajh/hpab108.
[52] M. A. Pfeffer, J. M. Pfeffer, C. Steinberg, and P. Finn, "Survival after an experimental myocardial infarction: beneficial effects of long-term therapy with captopril," *Circulation,* vol. 72, no. 2, pp. 406-12, Aug 1985, doi: 10.1161/01.cir.72.2.406.
[53] P. Ranganathan *et al.*, "MicroRNA-150 deletion in mice protects kidney from myocardial infarction-induced acute kidney injury," *Am J Physiol Renal Physiol,* vol. 309, no. 6, pp. F551-8, Sep 15 2015, doi: 10.1152/ajprenal.00076.2015.
[54] X. Fan *et al.*, "Interleukin-10 attenuates renal injury after myocardial infarction in diabetes," *J Investig Med,* vol. 70, no. 5, pp. 1233-1242, Jun 2022, doi: 10.1136/jim-2021-002008.
[55] S. Yu *et al.*, "Establishment and assessment of a preclinical model of acute kidney injury induced by contrast media combined acute myocardial ischemia reperfusion surgery," *Exp Ther Med,* vol. 26, no. 1, p. 321, Jul 2023, doi: 10.3892/etm.2023.12020.
[56] S. Y. Duan, C. Y. Xing, B. Zhang, and Y. Chen, "Detection and evaluation of renal biomarkers in a swine model of acute myocardial infarction and reperfusion," *Int J Clin Exp Pathol,* vol. 8, no. 7, pp. 8336-47, 2015. [Online]. Available: https://www.ncbi.nlm.nih.gov/pubmed/26339403.
[57] K. Matsushita *et al.*, "The acute kidney injury to chronic kidney disease transition in a mouse model of acute cardiorenal syndrome emphasizes the role of inflammation," *Kidney Int,* vol. 97, no. 1, pp. 95-105, Jan 2020, doi: 10.1016/j.kint.2019.06.022.
[58] R. Wakasaki *et al.*, "Glomerular filtrate proteins in acute cardiorenal syndrome," *JCI Insight,* vol. 4, no. 4, Feb 21 2019, doi: 10.1172/jci.insight.122130.
[59] L. Tian *et al.*, "Renoprotective effects of levosimendan on acute kidney injury following cardiac arrest via anti-inflammation, anti-apoptosis, and ERK activation," *FEBS Open Bio,* vol. 11, no. 8, pp. 2236-2244, Aug 2021, doi: 10.1002/2211-5463.13227.
[60] G. Youcef *et al.*, "Simultaneous characterization of metabolic, cardiac, vascular and renal phenotypes of lean and obese SHHF rats," *PLoS One,* vol. 9, no. 5, p. e96452, 2014, doi: 10.1371/journal.pone.0096452.
[61] S. Montoro-Molina *et al.*, "The Long-Term Study of Urinary Biomarkers of Renal Injury in Spontaneously Hypertensive Rats," *Kidney Blood Press Res,* vol. 46, no. 4, pp. 502-513, 2021, doi: 10.1159/000516843.
[62] L. Bosch *et al.*, "The transverse aortic constriction heart failure animal model: a systematic review and meta-analysis," *Heart Fail Rev,* vol. 26, no. 6, pp. 1515-1524, Nov 2021, doi: 10.1007/s10741-020-09960-w.
[63] F. A. Kamal, J. G. Travers, A. E. Schafer, Q. Ma, P. Devarajan, and B. C. Blaxall, "G Protein-Coupled Receptor-G-Protein betagamma-Subunit Signaling Mediates Renal Dysfunction and Fibrosis in Heart Failure," *J Am Soc Nephrol,* vol. 28, no. 1, pp. 197-208, Jan 2017, doi: 10.1681/ASN.2015080852.
[64] S. L. Young *et al.*, "Sotagliflozin, a Dual SGLT1/2 Inhibitor, Improves Cardiac Outcomes in a Normoglycemic Mouse Model of Cardiac Pressure Overload," *Front Physiol,* vol. 12, p. 738594, 2021, doi: 10.3389/fphys.2021.738594.
[65] T. Ichiki, B. K. Huntley, G. J. Harty, S. J. Sangaralingham, and J. C. Burnett, Jr., "Early activation of deleterious molecular pathways in the kidney in experimental heart

failure with atrial remodeling," *Physiol Rep,* vol. 5, no. 9, May 2017, doi: 10.14814/phy2.13283.

[66] Y. Xie *et al.*, "[Effect of catheter-based renal sympathetic denervation in pigs with rapid pacing induced heart failure]," *Zhonghua Xin Xue Guan Bing Za Zhi,* vol. 42, no. 1, pp. 48-52, Jan 2014. [Online]. Available: https://www.ncbi.nlm.nih.gov/pubmed/24680270.

[67] K. Rafiq *et al.*, "Renal sympathetic denervation suppresses de novo podocyte injury and albuminuria in rats with aortic regurgitation," *Circulation,* vol. 125, no. 11, pp. 1402-13, Mar 20 2012, doi: 10.1161/CIRCULATIONAHA.111.064097.

[68] S. Jichova *et al.*, "Kidney Response to Chemotherapy-Induced Heart Failure: mRNA Analysis in Normotensive and Ren-2 Transgenic Hypertensive Rats," *Int J Mol Sci,* vol. 22, no. 16, Aug 6 2021, doi: 10.3390/ijms22168475.

[69] W. Xing *et al.*, "Cardiorenal Protective Effect of Costunolide against Doxorubicin-Induced Toxicity in Rats by Modulating Oxidative Stress, Inflammation and Apoptosis," *Molecules,* vol. 27, no. 7, Mar 25 2022, doi: 10.3390/molecules27072122.

[70] C. V. C. Junho, J. Frisch, J. Soppert, J. Wollenhaupt, and H. Noels, "Cardiomyopathy in chronic kidney disease: clinical features, biomarkers and the contribution of murine models in understanding pathophysiology," *Clin Kidney J,* vol. 16, no. 11, pp. 1786-1803, Nov 2023, doi: 10.1093/ckj/sfad085.

[71] R. Mohamed, S. M. Elshazly, O. E. Nafea, and D. M. Abd El Motteleb, "Comparative cardioprotective effects of carvedilol versus atenolol in a rat model of cardiorenal syndrome type 4," *Naunyn Schmiedebergs Arch Pharmacol,* vol. 394, no. 10, pp. 2117-2128, Oct 2021, doi: 10.1007/s00210-021-02130-1.

[72] V. Koch *et al.*, "Impact of Homoarginine on Myocardial Function and Remodeling in a Rat Model of Chronic Renal Failure," *J Cardiovasc Pharmacol Ther,* vol. 27, p. 10742484211054620, Jan-Dec 2022, doi: 10.1177/10742484211054620.

[73] N. Muromachi *et al.*, "Cardiorenal damages in mice at early phase after intervention induced by angiotensin II, nephrectomy, and salt intake," *Exp Anim,* vol. 73, no. 1, pp. 11-19, Feb 14 2024, doi: 10.1538/expanim.23-0071.

[74] A. S. Lee *et al.*, "Electronegative LDL-mediated cardiac electrical remodeling in a rat model of chronic kidney disease," *Sci Rep,* vol. 7, p. 40676, Jan 17 2017, doi: 10.1038/srep40676.

[75] C. V. C. Junho *et al.*, "Klotho relieves inflammation and exerts a cardioprotective effect during renal ischemia/reperfusion-induced cardiorenal syndrome," *Biomed Pharmacother,* vol. 153, p. 113515, Sep 2022, doi: 10.1016/j.biopha.2022.113515.

[76] C. V. C. Junho, L. Gonzalez-Lafuente, J. A. Navarro-Garcia, E. Rodriguez-Sanchez, M. S. Carneiro-Ramos, and G. Ruiz-Hurtado, "Unilateral Acute Renal Ischemia-Reperfusion Injury Induces Cardiac Dysfunction through Intracellular Calcium Mishandling," *Int J Mol Sci,* vol. 23, no. 4, Feb 18 2022, doi: 10.3390/ijms23042266.

[77] O. Dilken, C. Ince, A. Kapucu, P. M. Heeman, and B. Ergin, "Furosemide exacerbated the impairment of renal function, oxygenation and medullary damage in a rat model of renal ischemia/reperfusion induced AKI," *Intensive Care Med Exp,* vol. 11, no. 1, p. 25, May 1 2023, doi: 10.1186/s40635-023-00509-3.

[78] K. Homma, Y. Enoki, S. Uchida, K. Taguchi, and K. Matsumoto, "A combination of 5/6-nephrectomy and unilateral ureteral obstruction model accelerates progression of remote organ fibrosis in chronic kidney disease," *FASEB Bioadv,* vol. 5, no. 10, pp. 377-394, Oct 2023, doi: 10.1096/fba.2023-00045.

[79] N. Florens, R. K. Kasam, V. Rudman-Melnick, S. C. Lin, V. Prasad, and J. D. Molkentin, "Interleukin-33 Mediates Cardiomyopathy After Acute Kidney Injury by Signaling to Cardiomyocytes," *Circulation,* vol. 147, no. 9, pp. 746-758, Feb 28 2023, doi: 10.1161/CIRCULATIONAHA.122.063014.

[80] Y. Chang *et al.*, "Eplerenone Prevents Cardiac Fibrosis by Inhibiting Angiogenesis in Unilateral Urinary Obstruction Rats," *J Renin Angiotensin Aldosterone Syst,* vol. 2022, p. 1283729, 2022, doi: 10.1155/2022/1283729.
[81] M. A. Fuchs *et al.*, "Fibroblast Growth Factor (FGF) 23 and FGF Receptor 4 promote cardiac metabolic remodeling in chronic kidney disease," *Res Sq,* Dec 23 2023, doi: 10.21203/rs.3.rs-3705543/v1.
[82] S. R. Mulay *et al.*, "Oxalate-induced chronic kidney disease with its uremic and cardiovascular complications in C57BL/6 mice," *Am J Physiol Renal Physiol,* vol. 310, no. 8, pp. F785-F795, Apr 15 2016, doi: 10.1152/ajprenal.00488.2015.
[83] J. Xu, B. Zhang, Z. Chu, F. Jiang, and J. Han, "Wogonin Alleviates Cisplatin-induced Cardiotoxicity in Mice Via Inhibiting Gasdermin D-mediated Pyroptosis," *J Cardiovasc Pharmacol,* vol. 78, no. 4, pp. 597-603, Jun 16 2021, doi: 10.1097/FJC.0000000000001085.
[84] T. Crestani *et al.*, "A Sodium Oxalate-Rich Diet Induces Chronic Kidney Disease and Cardiac Dysfunction in Rats," *Int J Mol Sci,* vol. 22, no. 17, Aug 26 2021, doi: 10.3390/ijms22179244.
[85] D. D. Santos *et al.*, "Effect of modified citrus pectin on galectin-3 inhibition in cisplatin-induced cardiac and renal toxicity," *Toxicology,* vol. 504, p. 153786, May 2024, doi: 10.1016/j.tox.2024.153786.
[86] S. Nikolaou and C. Deltas, "A Comparative Presentation of Mouse Models That Recapitulate Most Features of Alport Syndrome," *Genes (Basel),* vol. 13, no. 10, Oct 18 2022, doi: 10.3390/genes13101893.
[87] K. Yousefi *et al.*, "Osteopontin Promotes Left Ventricular Diastolic Dysfunction Through a Mitochondrial Pathway," *J Am Coll Cardiol,* vol. 73, no. 21, pp. 2705-2718, Jun 4 2019, doi: 10.1016/j.jacc.2019.02.074.
[88] J. Soppert *et al.*, "A systematic review and meta-analysis of murine models of uremic cardiomyopathy," *Kidney Int,* vol. 101, no. 2, pp. 256-273, Feb 2022, doi: 10.1016/j.kint.2021.10.025.
[89] P. H. Sung *et al.*, "Combined levosimendan and Sacubitril/Valsartan markedly protected the heart and kidney against cardiorenal syndrome in rat," *Biomed Pharmacother,* vol. 148, p. 112745, Apr 2022, doi: 10.1016/j.biopha.2022.112745.
[90] Z. Dong *et al.*, "Myocardial infarction worsens glomerular injury and microalbuminuria in rats with pre-existing renal impairment accompanied by the activation of ER stress and inflammation," *Mol Biol Rep,* vol. 41, no. 12, pp. 7911-21, Dec 2014, doi: 10.1007/s11033-014-3685-5.
[91] S. Liu *et al.*, "Subtotal nephrectomy accelerates pathological cardiac remodeling post-myocardial infarction: implications for cardiorenal syndrome," *Int J Cardiol,* vol. 168, no. 3, pp. 1866-80, Oct 3 2013, doi: 10.1016/j.ijcard.2012.12.065.
[92] R. Watanabe *et al.*, "Angiotensin II receptor blocker irbesartan attenuates cardiac dysfunction induced by myocardial infarction in the presence of renal failure," *Hypertens Res,* vol. 39, no. 4, pp. 237-44, Apr 2016, doi: 10.1038/hr.2015.141.
[93] S. J. Kim, S. K. Kwon, H. Y. Kim, S. M. Kim, J. W. Bae, and J. K. Choi, "DPP-4 inhibition enhanced renal tubular and myocardial GLP-1 receptor expression decreased in CKD with myocardial infarction," *BMC Nephrol,* vol. 20, no. 1, p. 75, Mar 1 2019, doi: 10.1186/s12882-019-1243-z.
[94] N. R. Oosterhuis *et al.*, "Targeting multiple pathways reduces renal and cardiac fibrosis in rats with subtotal nephrectomy followed by coronary ligation," *Acta Physiol (Oxf),* vol. 220, no. 3, pp. 382-393, Jul 2017, doi: 10.1111/apha.12829.
[95] J. Wollenhaupt *et al.*, "Pro-oxidative priming but maintained cardiac function in a broad spectrum of murine models of chronic kidney disease," *Redox Biol,* vol. 56, p. 102459, Oct 2022, doi: 10.1016/j.redox.2022.102459.

[96] D. M. Furcea *et al.*, "(18)F-FDG PET/MRI Imaging in a Preclinical Rat Model of Cardiorenal Syndrome-An Exploratory Study," *Int J Mol Sci,* vol. 23, no. 23, Dec 6 2022, doi: 10.3390/ijms232315409.
[97] J. H. Dominguez, D. Xie, and K. J. Kelly, "Cardiac effects of renal ischemia," *Am J Physiol Renal Physiol,* vol. 324, no. 1, pp. F64-F74, Jan 1 2023, doi: 10.1152/ajprenal.00183.2022.
[98] A. Zaloszyc, J. Bernardor, J. Bacchetta, G. Laverny, and C. P. Schmitt, "Mouse Models of Mineral Bone Disorders Associated with Chronic Kidney Disease," *Int J Mol Sci,* vol. 24, no. 6, Mar 10 2023, doi: 10.3390/ijms24065325.
[99] A. Verhulst, E. Neven, and P. C. D'Haese, "Characterization of an Animal Model to Study Risk Factors and New Therapies for the Cardiorenal Syndrome, a Major Health Issue in Our Aging Population," *Cardiorenal Med,* vol. 7, no. 3, pp. 234-244, Jun 2017, doi: 10.1159/000462984.
[100] M. Szlagor, J. Dybiec, E. Mlynarska, J. Rysz, and B. Franczyk, "Chronic Kidney Disease as a Comorbidity in Heart Failure," *Int J Mol Sci,* vol. 24, no. 3, Feb 3 2023, doi: 10.3390/ijms24032988.
[101] J. A. Borovac, D. D'Amario, J. Bozic, and D. Glavas, "Sympathetic nervous system activation and heart failure: Current state of evidence and the pathophysiology in the light of novel biomarkers," *World J Cardiol,* vol. 12, no. 8, pp. 373-408, Aug 26 2020, doi: 10.4330/wjc.v12.i8.373.
[102] L. Erichsen, C. Thimm, M. Bohndorf, M. S. Rahman, W. Wruck, and J. Adjaye, "Activation of the Renin-Angiotensin System Disrupts the Cytoskeletal Architecture of Human Urine-Derived Podocytes," *Cells,* vol. 11, no. 7, Mar 24 2022, doi: 10.3390/cells11071095.
[103] I. Bensaada *et al.*, "Calpastatin prevents Angiotensin II-mediated podocyte injury through maintenance of autophagy," *Kidney Int,* vol. 100, no. 1, pp. 90-106, Jul 2021, doi: 10.1016/j.kint.2021.02.024.
[104] X. Ding, J. Lv, J. Luan, and J. Zhang, "Calycosin may Alleviate Ang II-Induced Pro-proliferative Effects on Glomerular Mesangial Cells via Partially Inhibiting Autophagy and ERK Signaling Pathway," *Biol Pharm Bull,* vol. 43, no. 12, pp. 1893-1898, Dec 1 2020, doi: 10.1248/bpb.b20-00520.
[105] D. Aggarwal and G. Singh, "Effects of single and dual RAAS blockade therapy on progressive kidney disease transition to CKD in rats," *Naunyn Schmiedebergs Arch Pharmacol,* vol. 393, no. 4, pp. 615-627, Apr 2020, doi: 10.1007/s00210-019-01759-3.
[106] Y. Fan *et al.*, "Sirt6-mediated Nrf2/HO-1 activation alleviates angiotensin II-induced DNA DSBs and apoptosis in podocytes," *Food Funct,* vol. 12, no. 17, pp. 7867-7882, Sep 7 2021, doi: 10.1039/d0fo03467c.
[107] L. A. Inker *et al.*, "A meta-analysis of GFR slope as a surrogate endpoint for kidney failure," *Nat Med,* vol. 29, no. 7, pp. 1867-1876, Jul 2023, doi: 10.1038/s41591-023-02418-0.
[108] A. Shirakabe *et al.*, "Worsening renal function definition is insufficient for evaluating acute renal failure in acute heart failure," *ESC Heart Fail,* vol. 5, no. 3, pp. 322-331, Jun 2018, doi: 10.1002/ehf2.12264.
[109] W. Mullens *et al.*, "Evaluation of kidney function throughout the heart failure trajectory - a position statement from the Heart Failure Association of the European Society of Cardiology," *Eur J Heart Fail,* vol. 22, no. 4, pp. 584-603, Apr 2020, doi: 10.1002/ejhf.1697.
[110] S. Chen *et al.*, "Predictive effect of estimated glomerular filtrate rate by creatinine or cystatin C on mortality in patients with coronary artery disease," *Ren Fail,* vol. 46, no. 1, p. 2327494, Dec 2024, doi: 10.1080/0886022X.2024.2327494.
[111] B. Richter *et al.*, "Blood urea nitrogen has additive value beyond estimated glomerular filtration rate for prediction of long-term mortality in patients with acute myocardial

infarction," *Eur J Intern Med,* vol. 59, pp. 84-90, Jan 2019, doi: 10.1016/j.ejim.2018.07.019.
[112] M. Buonafine, E. Martinez-Martinez, and F. Jaisser, "More than a simple biomarker: the role of NGAL in cardiovascular and renal diseases," *Clin Sci (Lond),* vol. 132, no. 9, pp. 909-923, May 16 2018, doi: 10.1042/CS20171592.
[113] I. Merdler *et al.*, "Neutrophil Gelatinase-Associated Lipocalin for the Early Prediction of Acute Kidney Injury in ST-Segment Elevation Myocardial Infarction Patients Treated with Primary Percutaneous Coronary Intervention," *Cardiorenal Med,* vol. 10, no. 3, pp. 154-161, 2020, doi: 10.1159/000506378.
[114] R. N. Moresco, G. V. Bochi, C. S. Stein, J. A. M. De Carvalho, B. M. Cembranel, and Y. S. Bollick, "Urinary kidney injury molecule-1 in renal disease," *Clin Chim Acta,* vol. 487, pp. 15-21, Dec 2018, doi: 10.1016/j.cca.2018.09.011.
[115] M. M. Al-Bataineh *et al.*, "KIM-1-mediated anti-inflammatory activity is preserved by MUC1 induction in the proximal tubule during ischemia-reperfusion injury," *Am J Physiol Renal Physiol,* vol. 321, no. 2, pp. F135-F148, Aug 1 2021, doi: 10.1152/ajprenal.00127.2021.
[116] R. Zhou *et al.*, "Bi-functional KIT-PR1P peptides combine with VEGF to protect ischemic kidney in rats by targeting to Kim-1," *Regen Ther,* vol. 25, pp. 162-173, Mar 2024, doi: 10.1016/j.reth.2023.12.014.
[117] D. Szumilas, A. J. Owczarek, A. Brzozowska, Z. I. Niemir, M. Olszanecka-Glinianowicz, and J. Chudek, "The Value of Urinary NGAL, KIM-1, and IL-18 Measurements in the Early Detection of Kidney Injury in Oncologic Patients Treated with Cisplatin-Based Chemotherapy," *Int J Mol Sci,* vol. 25, no. 2, Jan 16 2024, doi: 10.3390/ijms25021074.
[118] A. A.-S. RM, M. A. Mohanad, N. J. Khudhair, and R. A.-M. MA, "Using urinary Interleukin-18 as a potential marker for early detection of acute kidney injury in intensive care unit," *Saudi J Kidney Dis Transpl,* vol. 32, no. 2, pp. 341-347, Mar-Apr 2021, doi: 10.4103/1319-2442.335445.
[119] C. S. She, Y. L. Deng, G. Q. Huang, C. Cheng, and F. J. Zhang, "Risk Factors and Outcome Variables of Cardiorenal Syndrome Type 1 in Acute Myocardial Infarction Patients," *Int J Gen Med,* vol. 15, pp. 1565-1573, 2022, doi: 10.2147/IJGM.S350361.
[120] Y. Hua, W. Zhang, and X. Li, "The Value of Soluble ST2 in Predicting Cardiorenal Syndrome Type 1 in Acute Myocardial Infarction Patients," *Heart Surg Forum,* vol. 26, no. 5, pp. E584-E591, Oct 25 2023, doi: 10.59958/hsf.6669.
[121] N. Salari *et al.*, "The global prevalence of myocardial infarction: a systematic review and meta-analysis," *BMC Cardiovasc Disord,* vol. 23, no. 1, p. 206, Apr 22 2023, doi: 10.1186/s12872-023-03231-w.
[122] B. Cui *et al.*, "Disease-specific mortality and major adverse cardiovascular events after bariatric surgery: a meta-analysis of age, sex, and BMI-matched cohort studies," *Int J Surg,* vol. 109, no. 3, pp. 389-400, Mar 1 2023, doi: 10.1097/JS9.0000000000000066.
[123] R. K. Akyea, G. Ntaios, and W. Doehner, "Obesity, metabolic health and clinical outcomes after incident cardiovascular disease: A nationwide population-based cohort study," *J Cachexia Sarcopenia Muscle,* vol. 14, no. 6, pp. 2653-2662, Dec 2023, doi: 10.1002/jcsm.13340.
[124] A. M. Jastreboff, C. M. Kotz, S. Kahan, A. S. Kelly, and S. B. Heymsfield, "Obesity as a Disease: The Obesity Society 2018 Position Statement," *Obesity (Silver Spring),* vol. 27, no. 1, pp. 7-9, Jan 2019, doi: 10.1002/oby.22378.
[125] R. Abdi Dezfouli, N. Mohammadian Khonsari, A. Hosseinpour, S. Asadi, H. S. Ejtahed, and M. Qorbani, "Waist to height ratio as a simple tool for predicting mortality: a systematic review and meta-analysis," *Int J Obes (Lond),* vol. 47, no. 12, pp. 1286-1301, Dec 2023, doi: 10.1038/s41366-023-01388-0.
[126] A. Jayedi, S. Soltani, M. S. Zargar, T. A. Khan, and S. Shab-Bidar, "Central fatness and risk of all cause mortality: systematic review and dose-response meta-analysis of 72

prospective cohort studies," *BMJ,* vol. 370, p. m3324, Sep 23 2020, doi: 10.1136/bmj.m3324.
[127] I. Sommer *et al.*, "The performance of anthropometric tools to determine obesity: a systematic review and meta-analysis," *Sci Rep,* vol. 10, no. 1, p. 12699, Jul 29 2020, doi: 10.1038/s41598-020-69498-7.
[128] M. C. S. Wong *et al.*, "Global, regional and time-trend prevalence of central obesity: a systematic review and meta-analysis of 13.2 million subjects," *Eur J Epidemiol,* vol. 35, no. 7, pp. 673-683, Jul 2020, doi: 10.1007/s10654-020-00650-3.
[129] Z. Sedaghat, S. Khodakarim, S. A. Nejadghaderi, and S. Sabour, "Association between metabolic syndrome and myocardial infarction among patients with excess body weight: a systematic review and meta-analysis," *BMC Public Health,* vol. 24, no. 1, p. 444, Feb 12 2024, doi: 10.1186/s12889-024-17707-7.
[130] D. H. Lan *et al.*, "Impact of Obesity on Microvascular Obstruction and Area at Risk in Patients After ST-Segment-Elevation Myocardial Infarction: A Magnetic Resonance Imaging Study," *Diabetes Metab Syndr Obes,* vol. 15, pp. 2207-2216, 2022, doi: 10.2147/DMSO.S369222.
[131] Z. Zhang *et al.*, "Secular trends of population-attributable fractions of obesity for hypertension among US population by sex and race/ethnicity: Analysis from NHANES 1999-2018," *Prev Med Rep,* vol. 41, p. 102719, May 2024, doi: 10.1016/j.pmedr.2024.102719.
[132] A. Emamian, M. H. Emamian, H. Hashemi, and A. Fotouhi, "The association of ALT to HDL-C ratio with type 2 diabetes in 50-74 years old adults: a population-based study," *Sci Rep,* vol. 14, no. 1, p. 9390, Apr 24 2024, doi: 10.1038/s41598-024-60092-9.
[133] O. T. Gupta and R. K. Gupta, "The Expanding Problem of Regional Adiposity: Revisiting a 1985 Diabetes Classic by Ohlson et al," *Diabetes,* vol. 73, no. 5, pp. 649-652, May 1 2024, doi: 10.2337/dbi24-0021.
[134] Z. Zhou *et al.*, "Are people with metabolically healthy obesity really healthy? A prospective cohort study of 381,363 UK Biobank participants," *Diabetologia,* vol. 64, no. 9, pp. 1963-1972, Sep 2021, doi: 10.1007/s00125-021-05484-6.
[135] R. Sarzani *et al.*, "Adipocentric origin of the common cardiometabolic complications of obesity in the young up to the very old: pathophysiology and new therapeutic opportunities," *Front Med (Lausanne),* vol. 11, p. 1365183, 2024, doi: 10.3389/fmed.2024.1365183.
[136] F. Pazos, "Range of adiposity and cardiorenal syndrome," *World J Diabetes,* vol. 11, no. 8, pp. 322-350, Aug 15 2020, doi: 10.4239/wjd.v11.i8.322.
[137] T. M. Powell-Wiley *et al.*, "Obesity and Cardiovascular Disease: A Scientific Statement From the American Heart Association," *Circulation,* vol. 143, no. 21, pp. e984-e1010, May 25 2021, doi: 10.1161/CIR.0000000000000973.
[138] C. Cercato and F. A. Fonseca, "Cardiovascular risk and obesity," *Diabetol Metab Syndr,* vol. 11, p. 74, 2019, doi: 10.1186/s13098-019-0468-0.
[139] J. Zhu, X. Su, G. Li, J. Chen, B. Tang, and Y. Yang, "The incidence of acute myocardial infarction in relation to overweight and obesity: a meta-analysis," *Arch Med Sci,* vol. 10, no. 5, pp. 855-62, Oct 27 2014, doi: 10.5114/aoms.2014.46206.
[140] Z. Sedaghat *et al.*, "The effect of obesity phenotype changes on cardiovascular outcomes in adults older than 40 years in the prospective cohort of the Tehran lipids and glucose study (TLGS): joint model of longitudinal and time-to-event data," *BMC Public Health,* vol. 24, no. 1, p. 1126, Apr 23 2024, doi: 10.1186/s12889-024-18577-9.
[141] A. Chait and L. J. den Hartigh, "Adipose Tissue Distribution, Inflammation and Its Metabolic Consequences, Including Diabetes and Cardiovascular Disease," *Front Cardiovasc Med,* vol. 7, p. 22, 2020, doi: 10.3389/fcvm.2020.00022.

[142] V. Patel and J. Patel, "Cellular cross talk between epicardial fat and cardiovascular risk," *J Basic Clin Physiol Pharmacol,* vol. 33, no. 6, pp. 683-694, Nov 1 2022, doi: 10.1515/jbcpp-2022-0230.
[143] A. Le, H. Peng, D. Golinsky, M. Di Scipio, R. Lali, and G. Pare, "What Causes Premature Coronary Artery Disease?," *Curr Atheroscler Rep,* vol. 26, no. 6, pp. 189-203, Jun 2024, doi: 10.1007/s11883-024-01200-y.
[144] C. Koliaki, S. Liatis, and A. Kokkinos, "Obesity and cardiovascular disease: revisiting an old relationship," *Metabolism,* vol. 92, pp. 98-107, Mar 2019, doi: 10.1016/j.metabol.2018.10.011.
[145] J. A. Henry *et al.*, "Changes in epicardial and visceral adipose tissue depots following bariatric surgery and their effect on cardiac geometry," *Front Endocrinol (Lausanne),* vol. 14, p. 1092777, 2023, doi: 10.3389/fendo.2023.1092777.
[146] J. Opio *et al.*, "Overweight or obesity increases the risk of cardiovascular disease among older Australian adults, even in the absence of cardiometabolic risk factors: a Bayesian survival analysis from the Hunter Community Study," *Int J Obes (Lond),* vol. 47, no. 2, pp. 117-125, Feb 2023, doi: 10.1038/s41366-022-01241-w.
[147] S. Nawaz *et al.*, "Obesity and chronic kidney disease: A current review," *Obes Sci Pract,* vol. 9, no. 2, pp. 61-74, Apr 2023, doi: 10.1002/osp4.629.
[148] A. Stasi *et al.*, "Obesity-Related Chronic Kidney Disease: Principal Mechanisms and New Approaches in Nutritional Management," *Front Nutr,* vol. 9, p. 925619, 2022, doi: 10.3389/fnut.2022.925619.
[149] R. Lengton *et al.*, "Hypertension and diabetes, but not leptin and adiponectin, mediate the relationship between body fat and chronic kidney disease," *Endocrine,* Apr 16 2024, doi: 10.1007/s12020-024-03811-6.
[150] S. Yang, J. Ling, S. Zhang, Y. Li, and G. Yang, "Metabolic dysfunction, rather than obesity, is a risk factor for chronic kidney disease in Chinese population," *Aging Male,* vol. 27, no. 1, p. 2335158, Dec 2024, doi: 10.1080/13685538.2024.2335158.
[151] M. M. Ali, S. Parveen, V. Williams, R. Dons, and G. I. Uwaifo, "Cardiometabolic comorbidities and complications of obesity and chronic kidney disease (CKD)," *J Clin Transl Endocrinol,* vol. 36, p. 100341, Jun 2024, doi: 10.1016/j.jcte.2024.100341.
[152] Z. Gai, T. Wang, M. Visentin, G. A. Kullak-Ublick, X. Fu, and Z. Wang, "Lipid Accumulation and Chronic Kidney Disease," *Nutrients,* vol. 11, no. 4, Mar 28 2019, doi: 10.3390/nu11040722.
[153] S. H. Hammoud, I. AlZaim, Y. Al-Dhaheri, A. H. Eid, and A. F. El-Yazbi, "Perirenal Adipose Tissue Inflammation: Novel Insights Linking Metabolic Dysfunction to Renal Diseases," *Front Endocrinol (Lausanne),* vol. 12, p. 707126, 2021, doi: 10.3389/fendo.2021.707126.
[154] H. Mao *et al.*, "Noninvasive Assessment of Renal Fibrosis of Chronic Kidney Disease in Rats by [(68)Ga]Ga-FAPI-04 Small Animal PET/CT and Biomarkers," *Mol Pharm,* vol. 20, no. 5, pp. 2714-2725, May 1 2023, doi: 10.1021/acs.molpharmaceut.3c00163.
[155] R. T. Cowling, D. Kupsky, A. M. Kahn, L. B. Daniels, and B. H. Greenberg, "Mechanisms of cardiac collagen deposition in experimental models and human disease," *Transl Res,* vol. 209, pp. 138-155, Jul 2019, doi: 10.1016/j.trsl.2019.03.004.
[156] S. Ravassa *et al.*, "Cardiac Fibrosis in heart failure: Focus on non-invasive diagnosis and emerging therapeutic strategies," *Mol Aspects Med,* vol. 93, p. 101194, Oct 2023, doi: 10.1016/j.mam.2023.101194.
[157] M. D'Urso and N. A. Kurniawan, "Mechanical and Physical Regulation of Fibroblast-Myofibroblast Transition: From Cellular Mechanoresponse to Tissue Pathology," *Front Bioeng Biotechnol,* vol. 8, p. 609653, 2020, doi: 10.3389/fbioe.2020.609653.
[158] X. Zhao, J. Chen, H. Sun, Y. Zhang, and D. Zou, "New insights into fibrosis from the ECM degradation perspective: the macrophage-MMP-ECM interaction," *Cell Biosci,* vol. 12, no. 1, p. 117, Jul 27 2022, doi: 10.1186/s13578-022-00856-w.

[159] R. B. Diller and A. J. Tabor, "The Role of the Extracellular Matrix (ECM) in Wound Healing: A Review," *Biomimetics (Basel),* vol. 7, no. 3, Jul 1 2022, doi: 10.3390/biomimetics7030087.
[160] N. G. Frangogiannis, "Cardiac fibrosis: Cell biological mechanisms, molecular pathways and therapeutic opportunities," *Mol Aspects Med,* vol. 65, pp. 70-99, Feb 2019, doi: 10.1016/j.mam.2018.07.001.
[161] A. C. Silva, C. Pereira, A. Fonseca, O. P. Pinto-do, and D. S. Nascimento, "Bearing My Heart: The Role of Extracellular Matrix on Cardiac Development, Homeostasis, and Injury Response," *Front Cell Dev Biol,* vol. 8, p. 621644, 2020, doi: 10.3389/fcell.2020.621644.
[162] K. Ytrehus, J. S. Hulot, C. Perrino, G. G. Schiattarella, and R. Madonna, "Perivascular fibrosis and the microvasculature of the heart. Still hidden secrets of pathophysiology?," *Vascul Pharmacol,* Apr 27 2018, doi: 10.1016/j.vph.2018.04.007.
[163] H. Schilter *et al.*, "The lysyl oxidase like 2/3 enzymatic inhibitor, PXS-5153A, reduces crosslinks and ameliorates fibrosis," *J Cell Mol Med,* vol. 23, no. 3, pp. 1759-1770, Mar 2019, doi: 10.1111/jcmm.14074.
[164] A. D. Theocharis, D. Manou, and N. K. Karamanos, "The extracellular matrix as a multitasking player in disease," *FEBS J,* vol. 286, no. 15, pp. 2830-2869, Aug 2019, doi: 10.1111/febs.14818.
[165] C. K. Nagaraju *et al.*, "Global fibroblast activation throughout the left ventricle but localized fibrosis after myocardial infarction," *Sci Rep,* vol. 7, no. 1, p. 10801, Sep 7 2017, doi: 10.1038/s41598-017-09790-1.
[166] X. Fu *et al.*, "Specialized fibroblast differentiated states underlie scar formation in the infarcted mouse heart," *J Clin Invest,* vol. 128, no. 5, pp. 2127-2143, May 1 2018, doi: 10.1172/JCI98215.
[167] X. Bi *et al.*, "Collagen Cross-Linking Is Associated With Cardiac Remodeling in Hypertrophic Obstructive Cardiomyopathy," *J Am Heart Assoc,* vol. 10, no. 1, p. e017752, Jan 5 2021, doi: 10.1161/JAHA.120.017752.
[168] A. Gonzalez, B. Lopez, S. Ravassa, G. San Jose, and J. Diez, "The complex dynamics of myocardial interstitial fibrosis in heart failure. Focus on collagen cross-linking," *Biochim Biophys Acta Mol Cell Res,* vol. 1866, no. 9, pp. 1421-1432, Sep 2019, doi: 10.1016/j.bbamcr.2019.06.001.
[169] N. N. Shah *et al.*, "Galactin-3 and soluble ST2 as complementary tools to cardiac MRI for sudden cardiac death risk stratification in heart failure: A review," *JRSM Cardiovasc Dis,* vol. 9, p. 2048004020957840, Jan-Dec 2020, doi: 10.1177/2048004020957840.
[170] M. A. Martinez-Rojas *et al.*, "A short treatment with resveratrol after a renal ischaemia-reperfusion injury prevents maladaptive repair and long-term chronic kidney disease in rats," *J Physiol,* vol. 602, no. 8, pp. 1835-1852, Apr 2024, doi: 10.1113/JP285979.
[171] T. H. Yeh, K. C. Tu, H. Y. Wang, and J. Y. Chen, "From Acute to Chronic: Unraveling the Pathophysiological Mechanisms of the Progression from Acute Kidney Injury to Acute Kidney Disease to Chronic Kidney Disease," *Int J Mol Sci,* vol. 25, no. 3, Feb 1 2024, doi: 10.3390/ijms25031755.
[172] R. Huang, P. Fu, and L. Ma, "Kidney fibrosis: from mechanisms to therapeutic medicines," *Signal Transduct Target Ther,* vol. 8, no. 1, p. 129, Mar 17 2023, doi: 10.1038/s41392-023-01379-7.
[173] P. Dube *et al.*, "Novel Model of Oxalate Diet-Induced Chronic Kidney Disease in Dahl-Salt-Sensitive Rats," *Int J Mol Sci,* vol. 24, no. 12, Jun 13 2023, doi: 10.3390/ijms241210062.
[174] L. Sequira, A. R. Prabhu, S. M. S, S. Prasad Nagaraju, and S. N. B, "Effectiveness of a Disease Management Program (DMP) in controlling the progression of Chronic Kidney

Disease among hypertensives and diabetics," *F1000Res,* vol. 11, p. 1111, 2022, doi: 10.12688/f1000research.123787.3.
[175] S. Hu, X. Hang, Y. Wei, H. Wang, L. Zhang, and L. Zhao, "Crosstalk among podocytes, glomerular endothelial cells and mesangial cells in diabetic kidney disease: an updated review," *Cell Commun Signal,* vol. 22, no. 1, p. 136, Feb 19 2024, doi: 10.1186/s12964-024-01502-3.
[176] Z. Wang *et al.*, "Mitochondria-Derived Reactive Oxygen Species Contribute to Synergistic Interaction of Diabetes and Hypertension in Causing Chronic Kidney Injury," *Am J Physiol Renal Physiol,* Jan 25 2024, doi: 10.1152/ajprenal.00320.2023.
[177] W. Kriz, T. Wiech, and H. J. Grone, "Mesangial Injury and Capillary Ballooning Precede Podocyte Damage in Nephrosclerosis," *Am J Pathol,* vol. 192, no. 12, pp. 1670-1682, Dec 2022, doi: 10.1016/j.ajpath.2022.08.007.
[178] V. T. N. Stefansson *et al.*, "Molecular programs associated with glomerular hyperfiltration in early diabetic kidney disease," *Kidney Int,* vol. 102, no. 6, pp. 1345-1358, Dec 2022, doi: 10.1016/j.kint.2022.07.033.
[179] X. Zhang *et al.*, "Lysyl oxidase promotes renal fibrosis via accelerating collagen cross-link driving by beta-arrestin/ERK/STAT3 pathway," *FASEB J,* vol. 36, no. 8, p. e22427, Aug 2022, doi: 10.1096/fj.202200573R.
[180] G. Narayanan *et al.*, "Molecular Phenotyping and Mechanisms of Myocardial Fibrosis in Advanced Chronic Kidney Disease," *Kidney360,* vol. 4, no. 11, pp. 1562-1579, Nov 1 2023, doi: 10.34067/KID.0000000000000276.
[181] B. Ginley *et al.*, "Automated Computational Detection of Interstitial Fibrosis, Tubular Atrophy, and Glomerulosclerosis," *J Am Soc Nephrol,* vol. 32, no. 4, pp. 837-850, Apr 2021, doi: 10.1681/ASN.2020050652.
[182] S. Panizo *et al.*, "Fibrosis in Chronic Kidney Disease: Pathogenesis and Consequences," *Int J Mol Sci,* vol. 22, no. 1, Jan 2 2021, doi: 10.3390/ijms22010408.
[183] A. Denic *et al.*, "Prognostic Implications of a Morphometric Evaluation for Chronic Changes on All Diagnostic Native Kidney Biopsies," *J Am Soc Nephrol,* vol. 33, no. 10, pp. 1927-1941, Oct 2022, doi: 10.1681/ASN.2022030234.
[184] A. Bohle, S. Mackensen-Haen, and H. von Gise, "Significance of tubulointerstitial changes in the renal cortex for the excretory function and concentration ability of the kidney: a morphometric contribution," *Am J Nephrol,* vol. 7, no. 6, pp. 421-33, 1987, doi: 10.1159/000167514.
[185] M. T. Eadon *et al.*, "Kidney Histopathology and Prediction of Kidney Failure: A Retrospective Cohort Study," *Am J Kidney Dis,* vol. 76, no. 3, pp. 350-360, Sep 2020, doi: 10.1053/j.ajkd.2019.12.014.
[186] F. Wang *et al.*, "Renal tubular dilation and fibrosis after unilateral ureter obstruction revealed by relaxometry and spin-lock exchange MRI," *NMR Biomed,* vol. 34, no. 8, p. e4539, Aug 2021, doi: 10.1002/nbm.4539.
[187] K. G. Burfeind, Y. Funahashi, A. C. Munhall, M. Eiwaz, and M. P. Hutchens, "Natural Killer Lymphocytes Mediate Renal Fibrosis Due to Acute Cardiorenal Syndrome," *Kidney360,* vol. 5, no. 1, pp. 8-21, Jan 1 2024, doi: 10.34067/KID.0000000000000305.
[188] A. Chagnac, B. Zingerman, B. Rozen-Zvi, and M. Herman-Edelstein, "Consequences of Glomerular Hyperfiltration: The Role of Physical Forces in the Pathogenesis of Chronic Kidney Disease in Diabetes and Obesity," *Nephron,* vol. 143, no. 1, pp. 38-42, 2019, doi: 10.1159/000499486.
[189] J. Dong *et al.*, "The profiles of biopsy-proven renal tubulointerstitial lesions in patients with glomerular disease," *Ann Transl Med,* vol. 8, no. 17, p. 1066, Sep 2020, doi: 10.21037/atm-20-1669.
[190] K. Sun, Q. Xie, and C. M. Hao, "Mechanisms of Scarring in Focal Segmental Glomerulosclerosis," *Kidney Dis (Basel),* vol. 7, no. 5, pp. 350-358, Sep 2021, doi: 10.1159/000517108.

[191] L. Chan, Y. Danyi, and C. Chen, "A new index for the outcome of focal segmental glomerulosclerosis," *Sci Rep,* vol. 14, no. 1, p. 8278, Apr 9 2024, doi: 10.1038/s41598-024-59007-5.
[192] R. D. Bulow and P. Boor, "Extracellular Matrix in Kidney Fibrosis: More Than Just a Scaffold," *J Histochem Cytochem,* vol. 67, no. 9, pp. 643-661, Sep 2019, doi: 10.1369/0022155419849388.
[193] G. A. Muller and H. P. Rodemann, "Characterization of human renal fibroblasts in health and disease: I. Immunophenotyping of cultured tubular epithelial cells and fibroblasts derived from kidneys with histologically proven interstitial fibrosis," *Am J Kidney Dis,* vol. 17, no. 6, pp. 680-3, Jun 1991, doi: 10.1016/s0272-6386(12)80351-9.
[194] H. P. Rodemann and G. A. Muller, "Characterization of human renal fibroblasts in health and disease: II. In vitro growth, differentiation, and collagen synthesis of fibroblasts from kidneys with interstitial fibrosis," *Am J Kidney Dis,* vol. 17, no. 6, pp. 684-6, Jun 1991, doi: 10.1016/s0272-6386(12)80352-0.
[195] S. Kurata *et al.*, "Immunoglobulin G deposition on proximal tubules and the tubular basement membrane in acute tubular injury complicated with focal segmental glomerulosclerosis (FSGS): A possible prediction tool for subclinical FSGS," *Ann Diagn Pathol,* vol. 66, p. 152154, Oct 2023, doi: 10.1016/j.anndiagpath.2023.152154.
[196] J. Wang *et al.*, "Combining Clinical Parameters and Acute Tubular Injury Grading Is Superior in Predicting the Prognosis of Deceased-Donor Kidney Transplantation: A 7-Year Observational Study," *Front Immunol,* vol. 13, p. 912749, 2022, doi: 10.3389/fimmu.2022.912749.
[197] T. Nadasdy, Z. Laszik, K. E. Blick, L. D. Johnson, and F. G. Silva, "Proliferative activity of intrinsic cell populations in the normal human kidney," *J Am Soc Nephrol,* vol. 4, no. 12, pp. 2032-9, Jun 1994, doi: 10.1681/ASN.V4122032.
[198] Z. Peng *et al.*, "Is the proximal tubule the focus of tubulointerstitial fibrosis?," *Heliyon,* vol. 9, no. 2, p. e13508, Feb 2023, doi: 10.1016/j.heliyon.2023.e13508.
[199] G. Fortrie, H. R. H. de Geus, and M. G. H. Betjes, "The aftermath of acute kidney injury: a narrative review of long-term mortality and renal function," *Crit Care,* vol. 23, no. 1, p. 24, Jan 24 2019, doi: 10.1186/s13054-019-2314-z.
[200] N. Ren, W. F. Wang, L. Zou, Y. L. Zhao, H. Miao, and Y. Y. Zhao, "The nuclear factor kappa B signaling pathway is a master regulator of renal fibrosis," *Front Pharmacol,* vol. 14, p. 1335094, 2023, doi: 10.3389/fphar.2023.1335094.
[201] X. M. Meng, "Inflammatory Mediators and Renal Fibrosis," *Adv Exp Med Biol,* vol. 1165, pp. 381-406, 2019, doi: 10.1007/978-981-13-8871-2_18.
[202] M. A. Sikking, S. Stroeks, F. Marelli-Berg, S. R. B. Heymans, B. Ludewig, and J. A. J. Verdonschot, "Immunomodulation of Myocardial Fibrosis," *JACC Basic Transl Sci,* vol. 8, no. 11, pp. 1477-1488, Nov 2023, doi: 10.1016/j.jacbts.2023.03.015.
[203] A. B. Reiss, B. Jacob, A. Zubair, A. Srivastava, M. Johnson, and J. De Leon, "Fibrosis in Chronic Kidney Disease: Pathophysiology and Therapeutic Targets," *J Clin Med,* vol. 13, no. 7, Mar 25 2024, doi: 10.3390/jcm13071881.
[204] Z. Deng *et al.*, "TGF-beta signaling in health, disease, and therapeutics," *Signal Transduct Target Ther,* vol. 9, no. 1, p. 61, Mar 22 2024, doi: 10.1038/s41392-024-01764-w.
[205] Q. Dan Hu *et al.*, "Btg2 Promotes Focal Segmental Glomerulosclerosis via Smad3-Dependent Podocyte-Mesenchymal Transition," *Adv Sci (Weinh),* vol. 10, no. 32, p. e2304360, Nov 2023, doi: 10.1002/advs.202304360.
[206] P. C. Tang *et al.*, "TGF-beta1 Signaling: Immune Dynamics of Chronic Kidney Diseases," *Front Med (Lausanne),* vol. 8, p. 628519, 2021, doi: 10.3389/fmed.2021.628519.
[207] S. G. Mansour, J. Puthumana, S. G. Coca, M. Gentry, and C. R. Parikh, "Biomarkers for the detection of renal fibrosis and prediction of renal outcomes: a systematic review," *BMC Nephrol,* vol. 18, no. 1, p. 72, Feb 20 2017, doi: 10.1186/s12882-017-0490-0.

[208] L. Mao, L. Liu, T. Zhang, X. Wu, T. Zhang, and Y. Xu, "MKL1 mediates TGF-beta-induced CTGF transcription to promote renal fibrosis," *J Cell Physiol,* vol. 235, no. 5, pp. 4790-4803, May 2020, doi: 10.1002/jcp.29356.
[209] T. Nakayama *et al.*, "Vaccination against connective tissue growth factor attenuates the development of renal fibrosis," *Sci Rep,* vol. 12, no. 1, p. 10933, Jun 29 2022, doi: 10.1038/s41598-022-15118-5.
[210] K. Frazier, S. Williams, D. Kothapalli, H. Klapper, and G. R. Grotendorst, "Stimulation of fibroblast cell growth, matrix production, and granulation tissue formation by connective tissue growth factor," *J Invest Dermatol,* vol. 107, no. 3, pp. 404-11, Sep 1996, doi: 10.1111/1523-1747.ep12363389.
[211] G. A. Cabral-Pacheco *et al.*, "The Roles of Matrix Metalloproteinases and Their Inhibitors in Human Diseases," *Int J Mol Sci,* vol. 21, no. 24, Dec 20 2020, doi: 10.3390/ijms21249739.
[212] H. Wang *et al.*, "MMP-9-positive neutrophils are essential for establishing profibrotic microenvironment in the obstructed kidney of UUO mice," *Acta Physiol (Oxf),* vol. 227, no. 2, p. e13317, Oct 2019, doi: 10.1111/apha.13317.
[213] Y. Wang *et al.*, "The role of matrix metalloproteinase 9 in fibrosis diseases and its molecular mechanisms," *Biomed Pharmacother,* vol. 171, p. 116116, Feb 2024, doi: 10.1016/j.biopha.2023.116116.
[214] Z. Cheng, X. Zhang, Y. Zhang, L. Li, and P. Chen, "Role of MMP-2 and CD147 in kidney fibrosis," *Open Life Sci,* vol. 17, no. 1, pp. 1182-1190, 2022, doi: 10.1515/biol-2022-0482.
[215] T. Hirata *et al.*, "Knockout of Matrix Metalloproteinase 2 Opposes Hypertension- and Diabetes-induced Nephropathy," *J Cardiovasc Pharmacol,* vol. 82, no. 6, pp. 445-457, Dec 1 2023, doi: 10.1097/FJC.0000000000001473.
[216] M. Zhao *et al.*, "Targeting fibrosis, mechanisms and cilinical trials," *Signal Transduct Target Ther,* vol. 7, no. 1, p. 206, Jun 30 2022, doi: 10.1038/s41392-022-01070-3.
[217] M. J. De Blasio, E. H. Ohlstein, and R. H. Ritchie, "Therapeutic targets of fibrosis: Translational advances and current challenges," *Br J Pharmacol,* vol. 180, no. 22, pp. 2839-2845, Nov 2023, doi: 10.1111/bph.16236.
[218] A. Hara *et al.*, "Galectin-3 as a Next-Generation Biomarker for Detecting Early Stage of Various Diseases," *Biomolecules,* vol. 10, no. 3, Mar 3 2020, doi: 10.3390/biom10030389.
[219] L. An, G. Chang, L. Zhang, P. Wang, W. Gao, and X. Li, "Pectin: Health-promoting properties as a natural galectin-3 inhibitor," *Glycoconj J,* vol. 41, no. 2, pp. 93-118, Apr 2024, doi: 10.1007/s10719-024-10152-z.
[220] A. A. Mansour, F. Krautter, Z. Zhi, A. J. Iqbal, and C. Recio, "The interplay of galectins-1, -3, and -9 in the immune-inflammatory response underlying cardiovascular and metabolic disease," *Cardiovasc Diabetol,* vol. 21, no. 1, p. 253, Nov 19 2022, doi: 10.1186/s12933-022-01690-7.
[221] R. M. Vucic *et al.*, "Galectin-3 as a Prognostic Biomarker in Patients with First Acute Myocardial Infarction without Heart Failure," *Diagnostics (Basel),* vol. 13, no. 21, Oct 31 2023, doi: 10.3390/diagnostics13213348.
[222] J. B. Echouffo-Tcheugui *et al.*, "Galectin-3, Metabolic Risk, and Incident Heart Failure: The ARIC Study," *J Am Heart Assoc,* vol. 13, no. 6, p. e031607, Mar 19 2024, doi: 10.1161/JAHA.123.031607.
[223] H. Sun *et al.*, "A translational study of Galectin-3 as an early biomarker and potential therapeutic target for ischemic-reperfusion induced acute kidney injury," *J Crit Care,* vol. 65, pp. 192-199, Oct 2021, doi: 10.1016/j.jcrc.2021.06.013.
[224] F. Wang *et al.*, "The potential roles of galectin-3 in AKI and CKD," *Front Physiol,* vol. 14, p. 1090724, 2023, doi: 10.3389/fphys.2023.1090724.

[225] H. M. Mahmoud, A. H. Abdel-Razik, M. A. Elrehany, E. M. Othman, and A. A. Bekhit, "Modified Citrus Pectin (MCP) Confers a Renoprotective Effect on Early-Stage Nephropathy in Type-2 Diabetic Mice," *Chem Biodivers,* p. e202400104, Apr 8 2024, doi: 10.1002/cbdv.202400104.
[226] B. M. Lozinski, K. Ta, and Y. Dong, "Emerging role of galectin 3 in neuroinflammation and neurodegeneration," *Neural Regen Res,* vol. 19, no. 9, pp. 2004-2009, Sep 1 2024, doi: 10.4103/1673-5374.391181.
[227] I. C. Weng *et al.*, "Cytosolic galectin-3 and -8 regulate antibacterial autophagy through differential recognition of host glycans on damaged phagosomes," *Glycobiology,* vol. 28, no. 6, pp. 392-405, Jun 1 2018, doi: 10.1093/glycob/cwy017.
[228] C. P. Rezende, P. Brito, T. A. Da Silva, A. M. Pessoni, L. N. Z. Ramalho, and F. Almeida, "Influence of Galectin-3 on the Innate Immune Response during Experimental Cryptococcosis," *J Fungi (Basel),* vol. 7, no. 6, Jun 20 2021, doi: 10.3390/jof7060492.
[229] N. C. Henderson and T. Sethi, "The regulation of inflammation by galectin-3," *Immunol Rev,* vol. 230, no. 1, pp. 160-71, Jul 2009, doi: 10.1111/j.1600-065X.2009.00794.x.
[230] G. Sygitowicz, A. Maciejak-Jastrzebska, and D. Sitkiewicz, "The Diagnostic and Therapeutic Potential of Galectin-3 in Cardiovascular Diseases," *Biomolecules,* vol. 12, no. 1, Dec 29 2021, doi: 10.3390/biom12010046.
[231] S. M. Ou *et al.*, "Urinary Galectin-3 as a Novel Biomarker for the Prediction of Renal Fibrosis and Kidney Disease Progression," *Biomedicines,* vol. 10, no. 3, Mar 2 2022, doi: 10.3390/biomedicines10030585.
[232] D. Ezhilarasan, "Unraveling the pathophysiologic role of galectin-3 in chronically injured liver," *J Cell Physiol,* vol. 238, no. 4, pp. 673-686, Apr 2023, doi: 10.1002/jcp.30956.
[233] J. F. Calver *et al.*, "Defining the mechanism of galectin-3-mediated TGF-beta1 activation and its role in lung fibrosis," *J Biol Chem,* vol. 300, no. 6, p. 107300, Apr 18 2024, doi: 10.1016/j.jbc.2024.107300.
[234] U. C. Sharma *et al.*, "Galectin-3 marks activated macrophages in failure-prone hypertrophied hearts and contributes to cardiac dysfunction," *Circulation,* vol. 110, no. 19, pp. 3121-8, Nov 9 2004, doi: 10.1161/01.CIR.0000147181.65298.4D.
[235] W. Li *et al.*, "Ultrasonic Microbubble Cavitation Deliver Gal-3 shRNA to Inhibit Myocardial Fibrosis after Myocardial Infarction," *Pharmaceutics,* vol. 15, no. 3, Feb 22 2023, doi: 10.3390/pharmaceutics15030729.
[236] D. Vansthertem *et al.*, "Immunohistochemical localization of galectins-1 and -3 and monitoring of tissue galectin-binding sites during tubular regeneration after renal ischemia reperfusion in the rat," *Histol Histopathol,* vol. 25, no. 11, pp. 1417-29, Nov 2010, doi: 10.14670/HH-25.1417.
[237] C. M. Rebholz *et al.*, "Plasma galectin-3 levels are associated with the risk of incident chronic kidney disease," *Kidney Int,* vol. 93, no. 1, pp. 252-259, Jan 2018, doi: 10.1016/j.kint.2017.06.028.
[238] S. M. Ou *et al.*, "Identification of Galectin-3 as Potential Biomarkers for Renal Fibrosis by RNA-Sequencing and Clinicopathologic Findings of Kidney Biopsy," *Front Med (Lausanne),* vol. 8, p. 748225, 2021, doi: 10.3389/fmed.2021.748225.
[239] E. Martinez-Martinez *et al.*, "Galectin-3 pharmacological inhibition attenuates early renal damage in spontaneously hypertensive rats," *J Hypertens,* vol. 36, no. 2, pp. 368-376, Feb 2018, doi: 10.1097/HJH.0000000000001545.
[240] S. Al-Salam, G. S. Jagadeesh, M. Sudhadevi, and J. Yasin, "Galectin-3 and Autophagy in Renal Acute Tubular Necrosis," *Int J Mol Sci,* vol. 25, no. 7, Mar 22 2024, doi: 10.3390/ijms25073604.
[241] E. A. Medvedeva, Berezin, II, and Y. V. Shchukin, "[Galectin-3, Markers of Oxidative Stress and Renal Dysfunction in Patients With Chronic Heart Failure]," *Kardiologiia,* vol.

57, no. 3, pp. 46-50, Mar 2017. [Online]. Available: https://www.ncbi.nlm.nih.gov/pubmed/28762935.
[242] M. Prud'homme *et al.*, "Acute Kidney Injury Induces Remote Cardiac Damage and Dysfunction Through the Galectin-3 Pathway," *JACC Basic Transl Sci,* vol. 4, no. 6, pp. 717-732, Oct 2019, doi: 10.1016/j.jacbts.2019.06.005.
[243] J. Zindel and P. Kubes, "DAMPs, PAMPs, and LAMPs in Immunity and Sterile Inflammation," *Annu Rev Pathol,* vol. 15, pp. 493-518, Jan 24 2020, doi: 10.1146/annurev-pathmechdis-012419-032847.
[244] A. Dahdah *et al.*, "Neutrophil Migratory Patterns: Implications for Cardiovascular Disease," *Front Cell Dev Biol,* vol. 10, p. 795784, 2022, doi: 10.3389/fcell.2022.795784.
[245] L. A. Abdulkhaleq, M. A. Assi, R. Abdullah, M. Zamri-Saad, Y. H. Taufiq-Yap, and M. N. M. Hezmee, "The crucial roles of inflammatory mediators in inflammation: A review," *Vet World,* vol. 11, no. 5, pp. 627-635, May 2018, doi: 10.14202/vetworld.2018.627-635.
[246] D. Furman *et al.*, "Chronic inflammation in the etiology of disease across the life span," *Nat Med,* vol. 25, no. 12, pp. 1822-1832, Dec 2019, doi: 10.1038/s41591-019-0675-0.
[247] S. Tsalamandris *et al.*, "The Role of Inflammation in Diabetes: Current Concepts and Future Perspectives," *Eur Cardiol,* vol. 14, no. 1, pp. 50-59, Apr 2019, doi: 10.15420/ecr.2018.33.1.
[248] L. Xiao and D. G. Harrison, "Inflammation in Hypertension," *Can J Cardiol,* vol. 36, no. 5, pp. 635-647, May 2020, doi: 10.1016/j.cjca.2020.01.013.
[249] M. Y. Henein, S. Vancheri, G. Longo, and F. Vancheri, "The Role of Inflammation in Cardiovascular Disease," *Int J Mol Sci,* vol. 23, no. 21, Oct 26 2022, doi: 10.3390/ijms232112906.
[250] S. P. Kadatane, M. Satariano, M. Massey, K. Mongan, and R. Raina, "The Role of Inflammation in CKD," *Cells,* vol. 12, no. 12, Jun 7 2023, doi: 10.3390/cells12121581.
[251] G. Fahed *et al.*, "Metabolic Syndrome: Updates on Pathophysiology and Management in 2021," *Int J Mol Sci,* vol. 23, no. 2, Jan 12 2022, doi: 10.3390/ijms23020786.
[252] J. H. Greenberg *et al.*, "Plasma Biomarkers of Tubular Injury and Inflammation Are Associated with CKD Progression in Children," *J Am Soc Nephrol,* vol. 31, no. 5, pp. 1067-1077, May 2020, doi: 10.1681/ASN.2019070723.
[253] S. Brandt *et al.*, "Fibrosis and Immune Cell Infiltration Are Separate Events Regulated by Cell-Specific Receptor Notch3 Expression," *J Am Soc Nephrol,* vol. 31, no. 11, pp. 2589-2608, Nov 2020, doi: 10.1681/ASN.2019121289.
[254] Y. Y. Wang *et al.*, "Macrophage-to-Myofibroblast Transition Contributes to Interstitial Fibrosis in Chronic Renal Allograft Injury," *J Am Soc Nephrol,* vol. 28, no. 7, pp. 2053-2067, Jul 2017, doi: 10.1681/ASN.2016050573.
[255] S. Perez and S. Rius-Perez, "Macrophage Polarization and Reprogramming in Acute Inflammation: A Redox Perspective," *Antioxidants (Basel),* vol. 11, no. 7, Jul 19 2022, doi: 10.3390/antiox11071394.
[256] J. Wei, Z. Xu, and X. Yan, "The role of the macrophage-to-myofibroblast transition in renal fibrosis," *Front Immunol,* vol. 13, p. 934377, 2022, doi: 10.3389/fimmu.2022.934377.
[257] E. Cantero-Navarro *et al.*, "Renin-angiotensin system and inflammation update," *Mol Cell Endocrinol,* vol. 529, p. 111254, Jun 1 2021, doi: 10.1016/j.mce.2021.111254.
[258] P. P. Lang *et al.*, "Blockade of intercellular adhesion molecule-1 prevents angiotensin II-induced hypertension and vascular dysfunction," *Lab Invest,* vol. 100, no. 3, pp. 378-386, Mar 2020, doi: 10.1038/s41374-019-0320-z.
[259] K. Panico, M. V. Abrahao, M. Trentin-Sonoda, H. Muzi-Filho, A. Vieyra, and M. S. Carneiro-Ramos, "Cardiac Inflammation after Ischemia-Reperfusion of the Kidney: Role of the Sympathetic Nervous System and the Renin-Angiotensin System," *Cell Physiol Biochem,* vol. 53, no. 4, pp. 587-605, 2019, doi: 10.33594/000000159.

[260] N. P. Rudemiller *et al.*, "C-C Motif Chemokine 5 Attenuates Angiotensin II-Dependent Kidney Injury by Limiting Renal Macrophage Infiltration," *Am J Pathol,* vol. 186, no. 11, pp. 2846-2856, Nov 2016, doi: 10.1016/j.ajpath.2016.07.015.
[261] J. D. Zhang *et al.*, "Type 1 angiotensin receptors on macrophages ameliorate IL-1 receptor-mediated kidney fibrosis," *J Clin Invest,* vol. 124, no. 5, pp. 2198-203, May 2014, doi: 10.1172/JCI61368.
[262] T. Chen, Q. Cao, Y. Wang, and D. C. H. Harris, "M2 macrophages in kidney disease: biology, therapies, and perspectives," *Kidney Int,* vol. 95, no. 4, pp. 760-773, Apr 2019, doi: 10.1016/j.kint.2018.10.041.
[263] V. S. R. Peesapati, M. Sadik, S. Verma, M. A. Attallah, and S. Khan, "Panoramic Dominance of the Immune System in Cardiorenal Syndrome Type I," *Cureus,* vol. 12, no. 8, p. e9869, Aug 19 2020, doi: 10.7759/cureus.9869.
[264] R. L. Amdur *et al.*, "Inflammation and Progression of CKD: The CRIC Study," *Clin J Am Soc Nephrol,* vol. 11, no. 9, pp. 1546-1556, Sep 7 2016, doi: 10.2215/CJN.13121215.
[265] R. Li, Y. Guo, Y. Zhang, X. Zhang, L. Zhu, and T. Yan, "Salidroside Ameliorates Renal Interstitial Fibrosis by Inhibiting the TLR4/NF-kappaB and MAPK Signaling Pathways," *Int J Mol Sci,* vol. 20, no. 5, Mar 4 2019, doi: 10.3390/ijms20051103.
[266] E. Cho *et al.*, "Role of inflammation in the pathogenesis of cardiorenal syndrome in a rat myocardial infarction model," *Nephrol Dial Transplant,* vol. 28, no. 11, pp. 2766-78, Nov 2013, doi: 10.1093/ndt/gft376.
[267] T. T. Ma and X. M. Meng, "TGF-beta/Smad and Renal Fibrosis," *Adv Exp Med Biol,* vol. 1165, pp. 347-364, 2019, doi: 10.1007/978-981-13-8871-2_16.
[268] G. F. Pierce *et al.*, "Platelet-derived growth factor and transforming growth factor-beta enhance tissue repair activities by unique mechanisms," *J Cell Biol,* vol. 109, no. 1, pp. 429-40, Jul 1989, doi: 10.1083/jcb.109.1.429.
[269] X. Wang, J. Chen, J. Xu, J. Xie, D. C. H. Harris, and G. Zheng, "The Role of Macrophages in Kidney Fibrosis," *Front Physiol,* vol. 12, p. 705838, 2021, doi: 10.3389/fphys.2021.705838.
[270] L. M. Black, J. M. Lever, and A. Agarwal, "Renal Inflammation and Fibrosis: A Double-edged Sword," *J Histochem Cytochem,* vol. 67, no. 9, pp. 663-681, Sep 2019, doi: 10.1369/0022155419852932.
[271] K. Jomova *et al.*, "Reactive oxygen species, toxicity, oxidative stress, and antioxidants: chronic diseases and aging," *Arch Toxicol,* vol. 97, no. 10, pp. 2499-2574, Oct 2023, doi: 10.1007/s00204-023-03562-9.
[272] N. Lau and M. D. Pluth, "Reactive sulfur species (RSS): persulfides, polysulfides, potential, and problems," *Curr Opin Chem Biol,* vol. 49, pp. 1-8, Apr 2019, doi: 10.1016/j.cbpa.2018.08.012.
[273] J. Pei *et al.*, "Hydrogen Sulfide Promotes Cardiomyocyte Proliferation and Heart Regeneration via ROS Scavenging," *Oxid Med Cell Longev,* vol. 2020, p. 1412696, 2020, doi: 10.1155/2020/1412696.
[274] S. Yamamoto *et al.*, "Sunitinib with photoirradiation-mediated reactive oxygen species generation induces apoptosis of renal cell carcinoma cells," *Photodiagnosis Photodyn Ther,* vol. 35, p. 102427, Sep 2021, doi: 10.1016/j.pdpdt.2021.102427.
[275] C. L. Hawkins and M. J. Davies, "Detection, identification, and quantification of oxidative protein modifications," *J Biol Chem,* vol. 294, no. 51, pp. 19683-19708, Dec 20 2019, doi: 10.1074/jbc.REV119.006217.
[276] M. Kowalska, T. Piekut, M. Prendecki, A. Sodel, W. Kozubski, and J. Dorszewska, "Mitochondrial and Nuclear DNA Oxidative Damage in Physiological and Pathological Aging," *DNA Cell Biol,* vol. 39, no. 8, pp. 1410-1420, Aug 2020, doi: 10.1089/dna.2019.5347.

[277] B. Wang *et al.*, "ROS-induced lipid peroxidation modulates cell death outcome: mechanisms behind apoptosis, autophagy, and ferroptosis," *Arch Toxicol,* vol. 97, no. 6, pp. 1439-1451, Jun 2023, doi: 10.1007/s00204-023-03476-6.
[278] R. Z. Zhao, S. Jiang, L. Zhang, and Z. B. Yu, "Mitochondrial electron transport chain, ROS generation and uncoupling (Review)," *Int J Mol Med,* vol. 44, no. 1, pp. 3-15, Jul 2019, doi: 10.3892/ijmm.2019.4188.
[279] L. G. Iacovino *et al.*, "Rational Redesign of Monoamine Oxidase A into a Dehydrogenase to Probe ROS in Cardiac Aging," *ACS Chem Biol,* vol. 15, no. 7, pp. 1795-1800, Jul 17 2020, doi: 10.1021/acschembio.0c00366.
[280] J. F. Creeden, D. M. Gordon, D. E. Stec, and T. D. Hinds, Jr., "Bilirubin as a metabolic hormone: the physiological relevance of low levels," *Am J Physiol Endocrinol Metab,* vol. 320, no. 2, pp. E191-E207, Feb 1 2021, doi: 10.1152/ajpendo.00405.2020.
[281] Q. Yan *et al.*, "Targeting oxidative stress as a preventive and therapeutic approach for cardiovascular disease," *J Transl Med,* vol. 21, no. 1, p. 519, Aug 2 2023, doi: 10.1186/s12967-023-04361-7.
[282] Z. Wang *et al.*, "Specific metabolic rates of major organs and tissues across adulthood: evaluation by mechanistic model of resting energy expenditure," *Am J Clin Nutr,* vol. 92, no. 6, pp. 1369-77, Dec 2010, doi: 10.3945/ajcn.2010.29885.
[283] K. Daenen, A. Andries, D. Mekahli, A. Van Schepdael, F. Jouret, and B. Bammens, "Oxidative stress in chronic kidney disease," *Pediatr Nephrol,* vol. 34, no. 6, pp. 975-991, Jun 2019, doi: 10.1007/s00467-018-4005-4.
[284] S. Kumar *et al.*, "HIMF (Hypoxia-Induced Mitogenic Factor)-IL (Interleukin)-6 Signaling Mediates Cardiomyocyte-Fibroblast Crosstalk to Promote Cardiac Hypertrophy and Fibrosis," *Hypertension,* vol. 73, no. 5, pp. 1058-1070, May 2019, doi: 10.1161/HYPERTENSIONAHA.118.12267.
[285] T. He *et al.*, "Resveratrol prevents high glucose-induced epithelial-mesenchymal transition in renal tubular epithelial cells by inhibiting NADPH oxidase/ROS/ERK pathway," *Mol Cell Endocrinol,* vol. 402, pp. 13-20, Feb 15 2015, doi: 10.1016/j.mce.2014.12.010.
[286] H. J. Ho and H. Shirakawa, "Oxidative Stress and Mitochondrial Dysfunction in Chronic Kidney Disease," *Cells,* vol. 12, no. 1, Dec 25 2022, doi: 10.3390/cells12010088.
[287] Y. Uehara *et al.*, "Immunohistochemical Expression of TGF-beta1 in Kidneys of Cats with Chronic Kidney Disease," *Vet Sci,* vol. 9, no. 3, Mar 3 2022, doi: 10.3390/vetsci9030114.
[288] H. Yaribeygi, F. R. Farrokhi, R. Rezaee, and A. Sahebkar, "Oxidative stress induces renal failure: A review of possible molecular pathways," *J Cell Biochem,* vol. 119, no. 4, pp. 2990-2998, Apr 2018, doi: 10.1002/jcb.26450.
[289] J. Chung *et al.*, "Correlation between Oxidative Stress and Transforming Growth Factor-Beta in Cancers," *Int J Mol Sci,* vol. 22, no. 24, Dec 7 2021, doi: 10.3390/ijms222413181.
[290] R. M. Liu and L. P. Desai, "Reciprocal regulation of TGF-beta and reactive oxygen species: A perverse cycle for fibrosis," *Redox Biol,* vol. 6, pp. 565-577, Dec 2015, doi: 10.1016/j.redox.2015.09.009.
[291] H. Buvelot, V. Jaquet, and K. H. Krause, "Mammalian NADPH Oxidases," *Methods Mol Biol,* vol. 1982, pp. 17-36, 2019, doi: 10.1007/978-1-4939-9424-3_2.
[292] N. Wang and C. Zhang, "Oxidative Stress: A Culprit in the Progression of Diabetic Kidney Disease," *Antioxidants (Basel),* vol. 13, no. 4, Apr 12 2024, doi: 10.3390/antiox13040455.
[293] J. C. Jha *et al.*, "Independent of Renox, NOX5 Promotes Renal Inflammation and Fibrosis in Diabetes by Activating ROS-Sensitive Pathways," *Diabetes,* vol. 71, no. 6, pp. 1282-1298, Jun 1 2022, doi: 10.2337/db21-1079.

[294] T. A. Schiffer, L. Carvalho, D. Guimaraes, A. Boeder, P. Wikstrom, and M. Carlstrom, "Specific NOX4 Inhibition Preserves Mitochondrial Function and Dampens Kidney Dysfunction Following Ischemia-Reperfusion-Induced Kidney Injury," *Antioxidants (Basel),* vol. 13, no. 4, Apr 19 2024, doi: 10.3390/antiox13040489.
[295] X. Cai *et al.*, "Targeting NOX 4 by petunidin improves anoxia/reoxygenation-induced myocardium injury," *Eur J Pharmacol,* vol. 888, p. 173414, Dec 5 2020, doi: 10.1016/j.ejphar.2020.173414.
[296] S. S. M. Sofiullah *et al.*, "Natural Bioactive Compounds Targeting NADPH Oxidase Pathway in Cardiovascular Diseases," *Molecules,* vol. 28, no. 3, Jan 20 2023, doi: 10.3390/molecules28031047.
[297] T. He *et al.*, "Resveratrol inhibits renal interstitial fibrosis in diabetic nephropathy by regulating AMPK/NOX4/ROS pathway," *J Mol Med (Berl),* vol. 94, no. 12, pp. 1359-1371, Dec 2016, doi: 10.1007/s00109-016-1451-y.
[298] G. Kern *et al.*, "Tacrolimus increases Nox4 expression in human renal fibroblasts and induces fibrosis-related genes by aberrant TGF-beta receptor signalling," *PLoS One,* vol. 9, no. 5, p. e96377, 2014, doi: 10.1371/journal.pone.0096377.
[299] W. Caio-Silva *et al.*, "Characterization of the Oxidative Stress in Renal Ischemia/Reperfusion-Induced Cardiorenal Syndrome Type 3," *Biomed Res Int,* vol. 2020, p. 1605358, 2020, doi: 10.1155/2020/1605358.
[300] X. Han *et al.*, "Hippo pathway activated by circulating reactive oxygen species mediates cardiac diastolic dysfunction after acute kidney injury," *Biochim Biophys Acta Mol Basis Dis,* vol. 1870, no. 5, p. 167184, Jun 2024, doi: 10.1016/j.bbadis.2024.167184.
[301] G. M. Virzi *et al.*, "Lipopolysaccharide in systemic circulation induces activation of inflammatory response and oxidative stress in cardiorenal syndrome type 1," *J Nephrol,* vol. 32, no. 5, pp. 803-810, Oct 2019, doi: 10.1007/s40620-019-00613-2.
[302] H. Guo *et al.*, "Kidney failure, arterial hypertension and left ventricular hypertrophy in rats with loss of function mutation of SOD3," *Free Radic Biol Med,* vol. 152, pp. 787-796, May 20 2020, doi: 10.1016/j.freeradbiomed.2020.01.023.
[303] M. B. Rowland, P. E. Moore, and R. N. Correll, "Regulation of cardiac fibroblast cell death by unfolded protein response signaling," *Front Physiol,* vol. 14, p. 1304669, 2023, doi: 10.3389/fphys.2023.1304669.
[304] C. Cheng, Y. Yuan, F. Yuan, and X. Li, "Acute kidney injury: exploring endoplasmic reticulum stress-mediated cell death," *Front Pharmacol,* vol. 15, p. 1308733, 2024, doi: 10.3389/fphar.2024.1308733.
[305] A. Read and M. Schroder, "The Unfolded Protein Response: An Overview," *Biology (Basel),* vol. 10, no. 5, Apr 29 2021, doi: 10.3390/biology10050384.
[306] R. Ghemrawi, S. F. Battaglia-Hsu, and C. Arnold, "Endoplasmic Reticulum Stress in Metabolic Disorders," *Cells,* vol. 7, no. 6, Jun 19 2018, doi: 10.3390/cells7060063.
[307] N. Shrestha, E. De Franco, P. Arvan, and M. Cnop, "Pathological beta-Cell Endoplasmic Reticulum Stress in Type 2 Diabetes: Current Evidence," *Front Endocrinol (Lausanne),* vol. 12, p. 650158, 2021, doi: 10.3389/fendo.2021.650158.
[308] B. Baba, M. Caliskan, G. Boyuk, and A. Hacisevki, "Chemical Chaperone PBA Attenuates ER Stress and Upregulates SOCS3 Expression as a Regulator of Leptin Signaling," *Biochemistry (Mosc),* vol. 86, no. 4, pp. 480-488, Apr 2021, doi: 10.1134/S0006297921040088.
[309] A. Ajoolabady *et al.*, "ER Stress in Cardiometabolic Diseases: From Molecular Mechanisms to Therapeutics," *Endocr Rev,* vol. 42, no. 6, pp. 839-871, Nov 16 2021, doi: 10.1210/endrev/bnab006.
[310] R. Zhang, C. Bian, J. Gao, and H. Ren, "Endoplasmic reticulum stress in diabetic kidney disease: adaptation and apoptosis after three UPR pathways," *Apoptosis,* vol. 28, no. 7-8, pp. 977-996, Aug 2023, doi: 10.1007/s10495-023-01858-w.

[311] T. Habshi, V. Shelke, A. Kale, H. J. Anders, and A. B. Gaikwad, "Role of endoplasmic reticulum stress and autophagy in the transition from acute kidney injury to chronic kidney disease," *J Cell Physiol,* vol. 238, no. 1, pp. 82-93, Jan 2023, doi: 10.1002/jcp.30918.
[312] J. G. Dickhout, R. E. Carlisle, and R. C. Austin, "Interrelationship between cardiac hypertrophy, heart failure, and chronic kidney disease: endoplasmic reticulum stress as a mediator of pathogenesis," *Circ Res,* vol. 108, no. 5, pp. 629-42, Mar 4 2011, doi: 10.1161/CIRCRESAHA.110.226803.
[313] B. B. Lins, F. A. M. Casare, F. F. Fontenele, G. L. Goncalves, and M. Oliveira-Souza, "Long-Term Angiotensin II Infusion Induces Oxidative and Endoplasmic Reticulum Stress and Modulates Na(+) Transporters Through the Nephron," *Front Physiol,* vol. 12, p. 642752, 2021, doi: 10.3389/fphys.2021.642752.
[314] Y. Wu, Y. Bai, Y. Feng, Q. Zhang, Z. Diao, and W. Liu, "Renalase Prevents Renal Fibrosis by Inhibiting Endoplasmic Reticulum Stress and Down-Regulating GSK-3beta/Snail Signaling," *Int J Med Sci,* vol. 20, no. 5, pp. 669-681, 2023, doi: 10.7150/ijms.82192.
[315] D. Wu *et al.*, "Research progress on endoplasmic reticulum homeostasis in kidney diseases," *Cell Death Dis,* vol. 14, no. 7, p. 473, Jul 27 2023, doi: 10.1038/s41419-023-05905-x.
[316] H. Sankrityayan, V. Shelke, A. Kale, and A. B. Gaikwad, "Evaluating the potential of tauroursodeoxycholic acid as add-on therapy in amelioration of streptozotocin-induced diabetic kidney disease," *Eur J Pharmacol,* vol. 942, p. 175528, Mar 5 2023, doi: 10.1016/j.ejphar.2023.175528.
[317] S. Shu *et al.*, "Endoplasmic reticulum stress contributes to cisplatin-induced chronic kidney disease via the PERK-PKCdelta pathway," *Cell Mol Life Sci,* vol. 79, no. 8, p. 452, Jul 27 2022, doi: 10.1007/s00018-022-04480-2.
[318] Z. Xiong *et al.*, "The gut microbe-derived metabolite trimethylamine-N-oxide induces aortic valve fibrosis via PERK/ATF-4 and IRE-1alpha/XBP-1s signaling in vitro and in vivo," *Atherosclerosis,* vol. 391, p. 117431, Apr 2024, doi: 10.1016/j.atherosclerosis.2023.117431.
[319] Y. T. Chen *et al.*, "Endoplasmic reticulum protein TXNDC5 promotes renal fibrosis by enforcing TGF-beta signaling in kidney fibroblasts," *J Clin Invest,* vol. 131, no. 5, Mar 1 2021, doi: 10.1172/JCI143645.
[320] E. Turishcheva, M. Vildanova, G. Onishchenko, and E. Smirnova, "The Role of Endoplasmic Reticulum Stress in Differentiation of Cells of Mesenchymal Origin," *Biochemistry (Mosc),* vol. 87, no. 9, pp. 916-931, Sep 2022, doi: 10.1134/S000629792209005X.
[321] C. A. Chen, J. M. Chang, E. E. Chang, H. C. Chen, and Y. L. Yang, "Crosstalk between transforming growth factor-beta1 and endoplasmic reticulum stress regulates alpha-smooth muscle cell actin expression in podocytes," *Life Sci,* vol. 209, pp. 9-14, Sep 15 2018, doi: 10.1016/j.lfs.2018.07.050.
[322] J. Han, X. Pang, X. Shi, Y. Zhang, Z. Peng, and Y. Xing, "Ginkgo Biloba Extract EGB761 Ameliorates the Extracellular Matrix Accumulation and Mesenchymal Transformation of Renal Tubules in Diabetic Kidney Disease by Inhibiting Endoplasmic Reticulum Stress," *Biomed Res Int,* vol. 2021, p. 6657206, 2021, doi: 10.1155/2021/6657206.
[323] Y. Li *et al.*, "4-phenylbutyrate exerts stage-specific effects on cardiac differentiation via HDAC inhibition," *PLoS One,* vol. 16, no. 4, p. e0250267, 2021, doi: 10.1371/journal.pone.0250267.
[324] G. Zhu *et al.*, "GRP78 plays an essential role in adipogenesis and postnatal growth in mice," *FASEB J,* vol. 27, no. 3, pp. 955-64, Mar 2013, doi: 10.1096/fj.12-213330.
[325] B. T. Gaudette, D. D. Jones, A. Bortnick, Y. Argon, and D. Allman, "mTORC1 coordinates an immediate unfolded protein response-related transcriptome in activated B cells

preceding antibody secretion," *Nat Commun,* vol. 11, no. 1, p. 723, Feb 5 2020, doi: 10.1038/s41467-019-14032-1.
[326] B. J. Meijer *et al.*, "Endoplasmic reticulum stress regulates the intestinal stem cell state through CtBP2," *Sci Rep,* vol. 11, no. 1, p. 9892, May 10 2021, doi: 10.1038/s41598-021-89326-w.
[327] S. E. Krown, "Interferons in malignancy: biological products or biological response modifiers?," *J Natl Cancer Inst,* vol. 80, no. 5, pp. 306-9, May 4 1988, doi: 10.1093/jnci/80.5.306.
[328] R. C. Lee, R. L. Feinbaum, and V. Ambros, "The C. elegans heterochronic gene lin-4 encodes small RNAs with antisense complementarity to lin-14," *Cell,* vol. 75, no. 5, pp. 843-54, Dec 3 1993, doi: 10.1016/0092-8674(93)90529-y.
[329] C. Diener, A. Keller, and E. Meese, "Emerging concepts of miRNA therapeutics: from cells to clinic," *Trends Genet,* vol. 38, no. 6, pp. 613-626, Jun 2022, doi: 10.1016/j.tig.2022.02.006.
[330] D. E. Ellakwa *et al.*, "Molecular functions of microRNAs in colorectal cancer: recent roles in proliferation, angiogenesis, apoptosis, and chemoresistance," *Naunyn Schmiedebergs Arch Pharmacol,* Apr 15 2024, doi: 10.1007/s00210-024-03076-w.
[331] C. Diener, A. Keller, and E. Meese, "The miRNA-target interactions: An underestimated intricacy," *Nucleic Acids Res,* vol. 52, no. 4, pp. 1544-1557, Feb 28 2024, doi: 10.1093/nar/gkad1142.
[332] Z. W. Guo, C. Xie, J. R. Yang, J. H. Li, J. H. Yang, and L. Zheng, "MtiBase: a database for decoding microRNA target sites located within CDS and 5'UTR regions from CLIP-Seq and expression profile datasets," *Database (Oxford),* vol. 2015, 2015, doi: 10.1093/database/bav102.
[333] J. P. Broughton, M. T. Lovci, J. L. Huang, G. W. Yeo, and A. E. Pasquinelli, "Pairing beyond the Seed Supports MicroRNA Targeting Specificity," *Mol Cell,* vol. 64, no. 2, pp. 320-333, Oct 20 2016, doi: 10.1016/j.molcel.2016.09.004.
[334] H. Liu, C. Lei, Q. He, Z. Pan, D. Xiao, and Y. Tao, "Nuclear functions of mammalian MicroRNAs in gene regulation, immunity and cancer," *Mol Cancer,* vol. 17, no. 1, p. 64, Feb 22 2018, doi: 10.1186/s12943-018-0765-5.
[335] J. M. Lorenzen, H. Haller, and T. Thum, "MicroRNAs as mediators and therapeutic targets in chronic kidney disease," *Nat Rev Nephrol,* vol. 7, no. 5, pp. 286-94, May 2011, doi: 10.1038/nrneph.2011.26.
[336] A. A. Seyhan, "Circulating microRNAs as Potential Biomarkers in Pancreatic Cancer-Advances and Challenges," *Int J Mol Sci,* vol. 24, no. 17, Aug 28 2023, doi: 10.3390/ijms241713340.
[337] G. Liang, C. Guo, H. Tang, and M. Zhang, "miR-30a-5p attenuates hypoxia/reoxygenation-induced cardiomyocyte apoptosis by regulating PTEN protein expression and activating PI3K/Akt signaling pathway," *BMC Cardiovasc Disord,* vol. 24, no. 1, p. 236, May 5 2024, doi: 10.1186/s12872-024-03900-4.
[338] H. Murase *et al.*, "Plasma microRNA-143 and microRNA-145 levels are elevated in patients with left ventricular dysfunction," *Heart Vessels,* May 8 2024, doi: 10.1007/s00380-024-02410-9.
[339] L. A. Bravo-Vazquez *et al.*, "Exploring the Therapeutic Significance of microRNAs and lncRNAs in Kidney Diseases," *Genes (Basel),* vol. 15, no. 1, Jan 19 2024, doi: 10.3390/genes15010123.
[340] J. Su *et al.*, "MicroRNA-30a inhibits cell proliferation in a sepsis-induced acute kidney injury model by targeting the YAP-TEAD complex," *J Intensive Med,* vol. 4, no. 2, pp. 231-239, Apr 2024, doi: 10.1016/j.jointm.2023.08.004.
[341] K. L. Wu *et al.*, "MicroRNA regulators of vascular pathophysiology in chronic kidney disease," *Clin Chim Acta,* vol. 551, p. 117610, Nov 1 2023, doi: 10.1016/j.cca.2023.117610.

[342] Y. Zong, Y. Hu, M. Zheng, and Z. Wang, "Bioinformatics analysis of the microRNA genes associated with type 2 cardiorenal syndrome," *BMC Cardiovasc Disord,* vol. 24, no. 1, p. 142, Mar 5 2024, doi: 10.1186/s12872-024-03816-z.
[343] A. Gluba-Sagr, B. Franczyk, M. Rysz-Gorzynska, J. Lawinski, and J. Rysz, "The Role of miRNA in Renal Fibrosis Leading to Chronic Kidney Disease," *Biomedicines,* vol. 11, no. 9, Aug 23 2023, doi: 10.3390/biomedicines11092358.
[344] A. C. Improta-Caria, L. F. Rodrigues, V. H. A. Joaquim, R. A. L. De Sousa, T. Fernandes, and E. M. Oliveira, "MicroRNAs regulating signaling pathways in cardiac fibrosis: potential role of the exercise training," *Am J Physiol Heart Circ Physiol,* vol. 326, no. 3, pp. H497-H510, Mar 1 2024, doi: 10.1152/ajpheart.00410.2023.
[345] C. K. Huang, C. Bar, and T. Thum, "miR-21, Mediator, and Potential Therapeutic Target in the Cardiorenal Syndrome," *Front Pharmacol,* vol. 11, p. 726, 2020, doi: 10.3389/fphar.2020.00726.
[346] T. Lange *et al.*, "MiR-21 is up-regulated in urinary exosomes of chronic kidney disease patients and after glomerular injury," *J Cell Mol Med,* vol. 23, no. 7, pp. 4839-4843, Jul 2019, doi: 10.1111/jcmm.14317.
[347] A. Figuer *et al.*, "New mechanisms involved in the development of cardiovascular disease in chronic kidney disease," *Nefrologia (Engl Ed),* vol. 43, no. 1, pp. 63-80, Jan-Feb 2023, doi: 10.1016/j.nefroe.2023.05.014.
[348] L. Liu, L. Liu, R. Liu, J. Liu, and Q. Cheng, "Exosomal miR-21-5p derived from multiple myeloma cells promote renal epithelial-mesenchymal transition through targeting TGF-beta/SMAD7 signalling pathway," *Clin Exp Pharmacol Physiol,* vol. 50, no. 9, pp. 711-718, Sep 2023, doi: 10.1111/1440-1681.13768.
[349] N. Dey, N. Ghosh-Choudhury, B. S. Kasinath, and G. G. Choudhury, "TGFbeta-stimulated microRNA-21 utilizes PTEN to orchestrate AKT/mTORC1 signaling for mesangial cell hypertrophy and matrix expansion," *PLoS One,* vol. 7, no. 8, p. e42316, 2012, doi: 10.1371/journal.pone.0042316.
[350] S. Rajabi *et al.*, "Interaction of estradiol and renin-angiotensin system with microRNAs-21 and -29 in renal fibrosis: focus on TGF-beta/smad signaling pathway," *Mol Biol Rep,* vol. 51, no. 1, p. 137, Jan 18 2024, doi: 10.1007/s11033-023-09127-4.
[351] M. D'Agostino *et al.*, "miRNAs in Uremic Cardiomyopathy: A Comprehensive Review," *Int J Mol Sci,* vol. 24, no. 6, Mar 12 2023, doi: 10.3390/ijms24065425.
[352] R. Ishrat *et al.*, "In Silico Integrative Approach Revealed Key MicroRNAs and Associated Target Genes in Cardiorenal Syndrome," *Bioinform Biol Insights,* vol. 15, p. 11779322211027396, 2021, doi: 10.1177/11779322211027396.
[353] M. H. Bao, X. Feng, Y. W. Zhang, X. Y. Lou, Y. Cheng, and H. H. Zhou, "Let-7 in cardiovascular diseases, heart development and cardiovascular differentiation from stem cells," *Int J Mol Sci,* vol. 14, no. 11, pp. 23086-102, Nov 21 2013, doi: 10.3390/ijms141123086.
[354] B. J. Reinhart *et al.*, "The 21-nucleotide let-7 RNA regulates developmental timing in Caenorhabditis elegans," *Nature,* vol. 403, no. 6772, pp. 901-6, Feb 24 2000, doi: 10.1038/35002607.
[355] Y. Ma, N. Shen, M. S. Wicha, and M. Luo, "The Roles of the Let-7 Family of MicroRNAs in the Regulation of Cancer Stemness," *Cells,* vol. 10, no. 9, Sep 14 2021, doi: 10.3390/cells10092415.
[356] B. M. Navarre *et al.*, "miR Profile of Chronic Right Ventricular Pacing: a Pilot Study in Children with Congenital Complete Atrioventricular Block," *J Cardiovasc Transl Res,* vol. 16, no. 2, pp. 287-299, Apr 2023, doi: 10.1007/s12265-022-10318-w.
[357] S. Aday *et al.*, "Bioinspired artificial exosomes based on lipid nanoparticles carrying let-7b-5p promote angiogenesis in vitro and in vivo," *Mol Ther,* vol. 29, no. 7, pp. 2239-2252, Jul 7 2021, doi: 10.1016/j.ymthe.2021.03.015.

[358] C. Gray, M. Li, R. Patel, C. M. Reynolds, and M. H. Vickers, "Let-7 miRNA profiles are associated with the reversal of left ventricular hypertrophy and hypertension in adult male offspring from mothers undernourished during pregnancy after preweaning growth hormone treatment," *Endocrinology,* vol. 155, no. 12, pp. 4808-17, Dec 2014, doi: 10.1210/en.2014-1567.
[359] Y. Wang *et al.*, "The Human Myotrophin Variant Attenuates MicroRNA-Let-7 Binding Ability but Not Risk of Left Ventricular Hypertrophy in Human Essential Hypertension," *PLoS One,* vol. 10, no. 8, p. e0135526, 2015, doi: 10.1371/journal.pone.0135526.
[360] M. Jiao *et al.*, "Circulating microRNA signature for the diagnosis of childhood dilated cardiomyopathy," *Sci Rep,* vol. 8, no. 1, p. 724, Jan 15 2018, doi: 10.1038/s41598-017-19138-4.
[361] A. Mompeon *et al.*, "Circulating miRNA Fingerprint and Endothelial Function in Myocardial Infarction: Comparison at Acute Event and One-Year Follow-Up," *Cells,* vol. 11, no. 11, Jun 2 2022, doi: 10.3390/cells11111823.
[362] A. Ring *et al.*, "MicroRNAs in peripheral artery disease: potential biomarkers and pathophysiological mechanisms," *Ther Adv Cardiovasc Dis,* vol. 16, p. 17539447221096940, Jan-Dec 2022, doi: 10.1177/17539447221096940.
[363] M. Zhu, M. Guo, L. Fei, X. Q. Pan, and Q. Q. Liu, "4-phenylbutyric acid attenuates endoplasmic reticulum stress-mediated pancreatic beta-cell apoptosis in rats with streptozotocin-induced diabetes," *Endocrine,* vol. 47, no. 1, pp. 129-37, Sep 2014, doi: 10.1007/s12020-013-0132-7.
[364] S. A. Bustin *et al.*, "The MIQE guidelines: minimum information for publication of quantitative real-time PCR experiments," *Clin Chem,* vol. 55, no. 4, pp. 611-22, Apr 2009, doi: 10.1373/clinchem.2008.112797.
[365] K. Thygesen *et al.*, "Third universal definition of myocardial infarction," *Eur Heart J,* vol. 33, no. 20, pp. 2551-67, Oct 2012, doi: 10.1093/eurheartj/ehs184.
[366] S. F. Nagueh *et al.*, "Recommendations for the Evaluation of Left Ventricular Diastolic Function by Echocardiography: An Update from the American Society of Echocardiography and the European Association of Cardiovascular Imaging," *J Am Soc Echocardiogr,* vol. 29, no. 4, pp. 277-314, Apr 2016, doi: 10.1016/j.echo.2016.01.011.
[367] R. M. Lang *et al.*, "Recommendations for cardiac chamber quantification by echocardiography in adults: an update from the American Society of Echocardiography and the European Association of Cardiovascular Imaging," *J Am Soc Echocardiogr,* vol. 28, no. 1, pp. 1-39 e14, Jan 2015, doi: 10.1016/j.echo.2014.10.003.
[368] I. S. Vlachos *et al.*, "DIANA-miRPath v3.0: deciphering microRNA function with experimental support," *Nucleic Acids Res,* vol. 43, no. W1, pp. W460-6, Jul 1 2015, doi: 10.1093/nar/gkv403.
[369] S. Tastsoglou *et al.*, "DIANA-miRPath v4.0: expanding target-based miRNA functional analysis in cell-type and tissue contexts," *Nucleic Acids Res,* vol. 51, no. W1, pp. W154-W159, Jul 5 2023, doi: 10.1093/nar/gkad431.
[370] Z. Song, X. Zhong, Z. Ning, and X. Song, "The Protective Effect of miR-27-3p on Ischemia-Reperfusion-Induced Myocardial Injury Depends on HIF-1alpha and Galectin-3," *J Cardiovasc Transl Res,* vol. 15, no. 4, pp. 772-785, Aug 2022, doi: 10.1007/s12265-021-10203-y.
[371] L. Wu *et al.*, "Involvement of miR-27a-3p in diabetic nephropathy via affecting renal fibrosis, mitochondrial dysfunction, and endoplasmic reticulum stress," *J Cell Physiol,* vol. 236, no. 2, pp. 1454-1468, Feb 2021, doi: 10.1002/jcp.29951.
[372] X. R. Zhao *et al.*, "MicroRNA-27a-3p aggravates renal ischemia/reperfusion injury by promoting oxidative stress via targeting growth factor receptor-bound protein 2," *Pharmacol Res,* vol. 155, p. 104718, May 2020, doi: 10.1016/j.phrs.2020.104718.
[373] J. Chen *et al.*, "MiR-203-3p inhibits the oxidative stress, inflammatory responses and apoptosis of mice podocytes induced by high glucose through regulating Sema3A

expression," *Open Life Sci,* vol. 15, no. 1, pp. 939-950, 2020, doi: 10.1515/biol-2020-0088.
[374] T. Azad, A. Tashakor, and S. Hosseinkhani, "Split-luciferase complementary assay: applications, recent developments, and future perspectives," *Anal Bioanal Chem,* vol. 406, no. 23, pp. 5541-60, Sep 2014, doi: 10.1007/s00216-014-7980-8.
[375] T. Siddika and I. U. Heinemann, "Bringing MicroRNAs to Light: Methods for MicroRNA Quantification and Visualization in Live Cells," *Front Bioeng Biotechnol,* vol. 8, p. 619583, 2020, doi: 10.3389/fbioe.2020.619583.
[376] C. Martinez-Garcia *et al.*, "Renal Lipotoxicity-Associated Inflammation and Insulin Resistance Affects Actin Cytoskeleton Organization in Podocytes," *PLoS One,* vol. 10, no. 11, p. e0142291, 2015, doi: 10.1371/journal.pone.0142291.
[377] C. Sticht, C. De La Torre, A. Parveen, and N. Gretz, "miRWalk: An online resource for prediction of microRNA binding sites," *PLoS One,* vol. 13, no. 10, p. e0206239, 2018, doi: 10.1371/journal.pone.0206239.
[378] I. S. Vlachos *et al.*, "DIANA-TarBase v7.0: indexing more than half a million experimentally supported miRNA:mRNA interactions," *Nucleic Acids Res,* vol. 43, no. Database issue, pp. D153-9, Jan 2015, doi: 10.1093/nar/gku1215.
[379] N. Werneburg, G. J. Gores, and R. L. Smoot, "The Hippo Pathway and YAP Signaling: Emerging Concepts in Regulation, Signaling, and Experimental Targeting Strategies With Implications for Hepatobiliary Malignancies," *Gene Expr,* vol. 20, no. 1, pp. 67-74, Jun 12 2020, doi: 10.3727/105221619X15617324583639.
[380] F. V. Souza-Neto *et al.*, "The Interplay of Mitochondrial Oxidative Stress and Endoplasmic Reticulum Stress in Cardiovascular Fibrosis in Obese Rats," *Antioxidants (Basel),* vol. 10, no. 8, Aug 11 2021, doi: 10.3390/antiox10081274.
[381] D. Szklarczyk *et al.*, "The STRING database in 2023: protein-protein association networks and functional enrichment analyses for any sequenced genome of interest," *Nucleic Acids Res,* vol. 51, no. D1, pp. D638-D646, Jan 6 2023, doi: 10.1093/nar/gkac1000.
[382] P. Shannon *et al.*, "Cytoscape: a software environment for integrated models of biomolecular interaction networks," *Genome Res,* vol. 13, no. 11, pp. 2498-504, Nov 2003, doi: 10.1101/gr.1239303.
[383] M. Beles *et al.*, "Cardio-renal-metabolic syndrome: clinical features and dapagliflozin eligibility in a real-world heart failure cohort," *ESC Heart Fail,* vol. 10, no. 4, pp. 2269-2280, Aug 2023, doi: 10.1002/ehf2.14381.
[384] M. Prothasis *et al.*, "Prevalence, types, risk factors, and outcomes of cardiorenal syndrome in a rural population of central India: A cross-sectional study," *J Family Med Prim Care,* vol. 9, no. 8, pp. 4127-4133, Aug 2020, doi: 10.4103/jfmpc.jfmpc_533_20.
[385] Z. Feng *et al.*, "Combined effect of time in target range and variability of systolic blood pressure on cardiovascular outcomes and mortality in patients with hypertension: A prospective cohort study," *J Clin Hypertens (Greenwich),* vol. 26, no. 6, pp. 714-723, Jun 2024, doi: 10.1111/jch.14816.
[386] R. Singh, J. C. Watchorn, A. Zarbock, and L. G. Forni, "Prognostic Biomarkers and AKI: Potential to Enhance the Identification of Post-Operative Patients at Risk of Loss of Renal Function," *Res Rep Urol,* vol. 16, pp. 65-78, 2024, doi: 10.2147/RRU.S385856.
[387] N. Prakoura, J. Hadchouel, and C. Chatziantoniou, "Novel Targets for Therapy of Renal Fibrosis," *J Histochem Cytochem,* vol. 67, no. 9, pp. 701-715, Sep 2019, doi: 10.1369/0022155419849386.
[388] M. V. Nastase, J. Zeng-Brouwers, M. Wygrecka, and L. Schaefer, "Targeting renal fibrosis: Mechanisms and drug delivery systems," *Adv Drug Deliv Rev,* vol. 129, pp. 295-307, Apr 2018, doi: 10.1016/j.addr.2017.12.019.

[389] H. Y. Li, S. Yang, J. C. Li, and J. X. Feng, "Galectin 3 inhibition attenuates renal injury progression in cisplatin-induced nephrotoxicity," *Biosci Rep,* vol. 38, no. 6, Dec 21 2018, doi: 10.1042/BSR20181803.
[390] Y. Zhao *et al.*, "Mesenchymal Stem Cells Ameliorate Fibrosis by Enhancing Autophagy via Inhibiting Galectin-3/Akt/mTOR Pathway and by Alleviating the EMT via Inhibiting Galectin-3/Akt/GSK3beta/Snail Pathway in NRK-52E Fibrosis," *Int J Stem Cells,* vol. 16, no. 1, pp. 52-65, Feb 28 2023, doi: 10.15283/ijsc22014.
[391] P. Shen, X. Deng, T. Li, X. Chen, and X. Wu, "Demethylzeylasteral protects against renal interstitial fibrosis by attenuating mitochondrial complex I-mediated oxidative stress," *J Ethnopharmacol,* vol. 327, p. 117986, Jun 12 2024, doi: 10.1016/j.jep.2024.117986.
[392] D. Landau *et al.*, "A Nuphar lutea plant active ingredient, 6,6'-dihydroxythiobinupharidine, ameliorates kidney damage and inflammation in a mouse model of chronic kidney disease," *Sci Rep,* vol. 14, no. 1, p. 7577, Mar 30 2024, doi: 10.1038/s41598-024-58055-1.
[393] Z. Hu, J. Zhan, G. Pei, and R. Zeng, "Depletion of macrophages with clodronate liposomes partially attenuates renal fibrosis on AKI-CKD transition," *Ren Fail,* vol. 45, no. 1, p. 2149412, Dec 2023, doi: 10.1080/0886022X.2022.2149412.
[394] H. Tanaka *et al.*, "Interleukin-6 blockade reduces salt-induced cardiac inflammation and fibrosis in subtotal nephrectomized mice," *Am J Physiol Renal Physiol,* vol. 323, no. 6, pp. F654-F665, Dec 1 2022, doi: 10.1152/ajprenal.00396.2021.
[395] J. Tollitt *et al.*, "Does previous stroke modify the relationship between inflammatory biomarkers and clinical endpoints in CKD patients?," *BMC Nephrol,* vol. 23, no. 1, p. 38, Jan 18 2022, doi: 10.1186/s12882-021-02625-2.
[396] L. J. Ward *et al.*, "Coronary artery calcification and aortic valve calcification in patients with kidney failure: a sex-disaggregated study," *Biol Sex Differ,* vol. 14, no. 1, p. 48, Jul 13 2023, doi: 10.1186/s13293-023-00530-x.
[397] Y. Chen *et al.*, "The potential role of hydrogen sulfide in regulating macrophage phenotypic changes via PINK1/parkin-mediated mitophagy in sepsis-related cardiorenal syndrome," *Immunopharmacol Immunotoxicol,* vol. 46, no. 2, pp. 139-151, Apr 2024, doi: 10.1080/08923973.2023.2281901.
[398] X. Duan *et al.*, "Qiliqiangxin Protects against Renal Injury in Rat with Cardiorenal Syndrome Type I through Regulating the Inflammatory and Oxidative Stress Signaling," *Biol Pharm Bull,* vol. 41, no. 8, pp. 1178-1185, 2018, doi: 10.1248/bpb.b17-00930.
[399] A. Kale, H. Sankrityayan, H. J. Anders, and A. B. Gaikwad, "Klotho in kidney diseases: a crosstalk between the renin-angiotensin system and endoplasmic reticulum stress," *Nephrol Dial Transplant,* vol. 38, no. 4, pp. 819-825, Mar 31 2023, doi: 10.1093/ndt/gfab340.
[400] "Chemical chaperon 4-phenylbutric acid improves cardiac function following isoproterenol-induced myocardial infarction in rats," *Iran J Basic Med Sci,* vol. 26, no. 3, pp. 367-373, Mar 2023, doi: 10.22038/IJBMS.2023.68183.14891.
[401] T. M. Jao *et al.*, "ATF6alpha downregulation of PPARalpha promotes lipotoxicity-induced tubulointerstitial fibrosis," *Kidney Int,* vol. 95, no. 3, pp. 577-589, Mar 2019, doi: 10.1016/j.kint.2018.09.023.
[402] J. Zhao *et al.*, "A study on expression of GRP78 and CHOP in neutrophil endoplasmic reticulum and their relationship with neutrophil apoptosis in the development of sepsis," *J Biosci,* vol. 49, 2024. [Online]. Available: https://www.ncbi.nlm.nih.gov/pubmed/38726820.
[403] S. Hamada *et al.*, "Five-Aminolevulinic Acid (5-ALA) Induces Heme Oxygenase-1 and Ameliorates Palmitic Acid-Induced Endoplasmic Reticulum Stress in Renal Tubules," *Int J Mol Sci,* vol. 24, no. 12, Jun 15 2023, doi: 10.3390/ijms241210151.
[404] S. Osaka *et al.*, "A randomized trial to examine the impact of food on pharmacokinetics of 4-phenylbutyrate and change in amino acid availability after a single oral

administration of sodium 4-phenylbutyrarte in healthy volunteers," *Mol Genet Metab,* vol. 132, no. 4, pp. 220-226, Apr 2021, doi: 10.1016/j.ymgme.2021.02.002.

[405] R. C. Rubenstein and P. L. Zeitlin, "A pilot clinical trial of oral sodium 4-phenylbutyrate (Buphenyl) in deltaF508-homozygous cystic fibrosis patients: partial restoration of nasal epithelial CFTR function," *Am J Respir Crit Care Med,* vol. 157, no. 2, pp. 484-90, Feb 1998, doi: 10.1164/ajrccm.157.2.9706088.

[406] P. L. Zeitlin, M. Diener-West, R. C. Rubenstein, M. P. Boyle, C. K. Lee, and L. Brass-Ernst, "Evidence of CFTR function in cystic fibrosis after systemic administration of 4-phenylbutyrate," *Mol Ther,* vol. 6, no. 1, pp. 119-26, Jul 2002, doi: 10.1006/mthe.2002.0639.

[407] V. G. Cardoso *et al.*, "Angiotensin II-induced podocyte apoptosis is mediated by endoplasmic reticulum stress/PKC-delta/p38 MAPK pathway activation and trough increased Na(+)/H(+) exchanger isoform 1 activity," *BMC Nephrol,* vol. 19, no. 1, p. 179, Jul 13 2018, doi: 10.1186/s12882-018-0968-4.

[408] J. Yang, X. Zhang, X. Yu, W. Tang, and H. Gan, "Renin-angiotensin system activation accelerates atherosclerosis in experimental renal failure by promoting endoplasmic reticulum stress-related inflammation," *Int J Mol Med,* vol. 39, no. 3, pp. 613-621, Mar 2017, doi: 10.3892/ijmm.2017.2856.

[409] T. N. Wang *et al.*, "SREBP-1 Mediates Angiotensin II-Induced TGF-beta1 Upregulation and Glomerular Fibrosis," *J Am Soc Nephrol,* vol. 26, no. 8, pp. 1839-54, Aug 2015, doi: 10.1681/ASN.2013121332.

[410] C. Li *et al.*, "Intrarenal renin-angiotensin system mediates fatty acid-induced ER stress in the kidney," *Am J Physiol Renal Physiol,* vol. 310, no. 5, pp. F351-63, Mar 1 2016, doi: 10.1152/ajprenal.00223.2015.

[411] P. Fularski *et al.*, "Unveiling Selected Influences on Chronic Kidney Disease Development and Progression," *Cells,* vol. 13, no. 9, Apr 26 2024, doi: 10.3390/cells13090751.

[412] M. Reina-Couto *et al.*, "Interrelationship between renin-angiotensin-aldosterone system and oxidative stress in chronic heart failure patients with or without renal impairment," *Biomed Pharmacother,* vol. 133, p. 110938, Jan 2021, doi: 10.1016/j.biopha.2020.110938.

[413] D. T. Ilges, M. L. Dermody, C. Blankenship, V. Mansfield, and J. S. Van Tuyl, "Impact of Angiotensin-Converting Enzyme Inhibitors and Angiotensin Receptor Blockers on Renal Function in Type 1 Cardiorenal Syndrome," *J Cardiovasc Pharmacol Ther,* vol. 26, no. 6, pp. 611-618, Nov 2021, doi: 10.1177/10742484211022625.

[414] Z. Wen, M. Cai, Z. Mai, Y. Chen, D. Geng, and J. Wang, "Protection of renal impairment by angiotensin II type 1 receptor blocker in rats with post-infarction heart failure," *Ren Fail,* vol. 35, no. 5, pp. 766-75, 2013, doi: 10.3109/0886022X.2013.780561.

[415] X. Huang, S. M. Hamza, W. Zhuang, W. A. Cupples, and B. Braam, "Angiotensin II and the Renal Hemodynamic Response to an Isolated Increased Renal Venous Pressure in Rats," *Front Physiol,* vol. 12, p. 753355, 2021, doi: 10.3389/fphys.2021.753355.

[416] H. Peng, O. A. Carretero, T. D. Liao, E. L. Peterson, and N. E. Rhaleb, "Role of N-acetyl-seryl-aspartyl-lysyl-proline in the antifibrotic and anti-inflammatory effects of the angiotensin-converting enzyme inhibitor captopril in hypertension," *Hypertension,* vol. 49, no. 3, pp. 695-703, Mar 2007, doi: 10.1161/01.HYP.0000258406.66954.4f.

[417] G. E. Gonzalez *et al.*, "Cardiac-deleterious role of galectin-3 in chronic angiotensin II-induced hypertension," *Am J Physiol Heart Circ Physiol,* vol. 311, no. 5, pp. H1287-H1296, Nov 1 2016, doi: 10.1152/ajpheart.00096.2016.

[418] N. D. Camarda, J. Ibarrola, L. A. Biwer, and I. Z. Jaffe, "Mineralocorticoid Receptors in Vascular Smooth Muscle: Blood Pressure and Beyond," *Hypertension,* vol. 81, no. 5, pp. 1008-1020, May 2024, doi: 10.1161/HYPERTENSIONAHA.123.21358.

[419] M. L. Johansen *et al.*, "The Mineralocorticoid Receptor Antagonist Eplerenone Suppresses Interstitial Fibrosis in Subcutaneous Adipose Tissue in Patients With Type 2 Diabetes," *Diabetes,* vol. 70, no. 1, pp. 196-203, Jan 2021, doi: 10.2337/db20-0394.
[420] E. Martinez-Martinez *et al.*, "Galectin-3 blockade inhibits cardiac inflammation and fibrosis in experimental hyperaldosteronism and hypertension," *Hypertension,* vol. 66, no. 4, pp. 767-75, Oct 2015, doi: 10.1161/HYPERTENSIONAHA.115.05876.
[421] S. Ozyildirim *et al.*, "Galectin-3 as a Biomarker to Predict Cardiorenal Syndrome in Patients with Acute Heart Failure," *Acta Cardiol Sin,* vol. 39, no. 6, pp. 862-870, Nov 2023, doi: 10.6515/ACS.202311_39(6).20230903A.
[422] Z. Xu *et al.*, "Angiotensin II induces kidney inflammatory injury and fibrosis through binding to myeloid differentiation protein-2 (MD2)," *Sci Rep,* vol. 7, p. 44911, Mar 21 2017, doi: 10.1038/srep44911.
[423] Y. Du, J. Han, H. Zhang, J. Xu, L. Jiang, and W. Ge, "Kaempferol Prevents Against Ang II-induced Cardiac Remodeling Through Attenuating Ang II-induced Inflammation and Oxidative Stress," *J Cardiovasc Pharmacol,* vol. 74, no. 4, pp. 326-335, Oct 2019, doi: 10.1097/FJC.0000000000000713.
[424] P. Caravaca Perez *et al.*, "Renal Function Impact in the Prognostic Value of Galectin-3 in Acute Heart Failure," *Front Cardiovasc Med,* vol. 9, p. 861651, 2022, doi: 10.3389/fcvm.2022.861651.
[425] Y. U. Horiuchi *et al.*, "Galectin-3, Acute Kidney Injury and Myocardial Damage in Patients With Acute Heart Failure," *J Card Fail,* vol. 29, no. 3, pp. 269-277, Mar 2023, doi: 10.1016/j.cardfail.2022.09.017.
[426] P. Cassaglia *et al.*, "Genetic Deletion of Galectin-3 Alters the Temporal Evolution of Macrophage Infiltration and Healing Affecting the Cardiac Remodeling and Function after Myocardial Infarction in Mice," *Am J Pathol,* vol. 190, no. 9, pp. 1789-1800, Sep 2020, doi: 10.1016/j.ajpath.2020.05.010.
[427] X. Wang *et al.*, "Inhibition of galectin-3 post-infarction impedes progressive fibrosis by regulating inflammatory profibrotic cascades," *Cardiovasc Res,* vol. 119, no. 15, pp. 2536-2549, Nov 25 2023, doi: 10.1093/cvr/cvad116.
[428] A. Jones *et al.*, "miRNA Signatures of Insulin Resistance in Obesity," *Obesity (Silver Spring),* vol. 25, no. 10, pp. 1734-1744, Oct 2017, doi: 10.1002/oby.21950.
[429] E. C. Willner *et al.*, "Amniotic fluid microRNA profiles in twin-twin transfusion syndrome with and without severe recipient cardiomyopathy," *Am J Obstet Gynecol,* vol. 225, no. 4, pp. 439 e1-439 e10, Oct 2021, doi: 10.1016/j.ajog.2021.06.066.
[430] Y. Xu *et al.*, "circ-AKT3 aggravates renal ischaemia-reperfusion injury via regulating miR-144-5p /Wnt/beta-catenin pathway and oxidative stress," *J Cell Mol Med,* vol. 26, no. 6, pp. 1766-1775, Mar 2022, doi: 10.1111/jcmm.16072.
[431] A. Galluzzo *et al.*, "Identification of novel circulating microRNAs in advanced heart failure by next-generation sequencing," *ESC Heart Fail,* vol. 8, no. 4, pp. 2907-2919, Aug 2021, doi: 10.1002/ehf2.13371.
[432] C. Y. Chen *et al.*, "MicroRNA let-7-TGFBR3 signalling regulates cardiomyocyte apoptosis after infarction," *EBioMedicine,* vol. 46, pp. 236-247, Aug 2019, doi: 10.1016/j.ebiom.2019.08.001.
[433] M. Jaguszewski *et al.*, "A signature of circulating microRNAs differentiates takotsubo cardiomyopathy from acute myocardial infarction," *Eur Heart J,* vol. 35, no. 15, pp. 999-1006, Apr 2014, doi: 10.1093/eurheartj/eht392.
[434] M. Lozano-Prieto *et al.*, "Differential miRNAs in acute spontaneous coronary artery dissection: Pathophysiological insights from a potential biomarker," *EBioMedicine,* vol. 66, p. 103338, Apr 2021, doi: 10.1016/j.ebiom.2021.103338.
[435] O. Ichii *et al.*, "Decreased miR-26a expression correlates with the progression of podocyte injury in autoimmune glomerulonephritis," *PLoS One,* vol. 9, no. 10, p. e110383, 2014, doi: 10.1371/journal.pone.0110383.

[436] O. Ichii *et al.*, "Urinary Exosome-Derived microRNAs Reflecting the Changes in Renal Function in Cats," *Front Vet Sci,* vol. 5, p. 289, 2018, doi: 10.3389/fvets.2018.00289.
[437] X. He *et al.*, "delta-Opioid receptor activation modified microRNA expression in the rat kidney under prolonged hypoxia," *PLoS One,* vol. 8, no. 4, p. e61080, 2013, doi: 10.1371/journal.pone.0061080.
[438] S. Giardina, P. Hernandez-Alonso, A. Diaz-Lopez, A. Salas-Huetos, J. Salas-Salvado, and M. Bullo, "Changes in circulating miRNAs in healthy overweight and obese subjects: Effect of diet composition and weight loss," *Clin Nutr,* vol. 38, no. 1, pp. 438-443, Feb 2019, doi: 10.1016/j.clnu.2017.11.014.
[439] R. J. Frost and E. N. Olson, "Control of glucose homeostasis and insulin sensitivity by the Let-7 family of microRNAs," *Proc Natl Acad Sci U S A,* vol. 108, no. 52, pp. 21075-80, Dec 27 2011, doi: 10.1073/pnas.1118922109.
[440] C. H. Hsieh *et al.*, "Weight-reduction through a low-fat diet causes differential expression of circulating microRNAs in obese C57BL/6 mice," *BMC Genomics,* vol. 16, no. 1, p. 699, Sep 16 2015, doi: 10.1186/s12864-015-1896-3.
[441] S. L. Atkin *et al.*, "Changes in Blood microRNA Expression and Early Metabolic Responsiveness 21 Days Following Bariatric Surgery," *Front Endocrinol (Lausanne),* vol. 9, p. 773, 2018, doi: 10.3389/fendo.2018.00773.
[442] A. M. Gentile *et al.*, "miR-20b, miR-296, and Let-7f Expression in Human Adipose Tissue is Related to Obesity and Type 2 Diabetes," *Obesity (Silver Spring),* vol. 27, no. 2, pp. 245-254, Feb 2019, doi: 10.1002/oby.22363.
[443] I. M. Moya and G. Halder, "Hippo-YAP/TAZ signalling in organ regeneration and regenerative medicine," *Nat Rev Mol Cell Biol,* vol. 20, no. 4, pp. 211-226, Apr 2019, doi: 10.1038/s41580-018-0086-y.
[444] Z. Meng, T. Moroishi, and K. L. Guan, "Mechanisms of Hippo pathway regulation," *Genes Dev,* vol. 30, no. 1, pp. 1-17, Jan 1 2016, doi: 10.1101/gad.274027.115.
[445] S. E. Riley, Y. Feng, and C. G. Hansen, "Hippo-Yap/Taz signalling in zebrafish regeneration," *NPJ Regen Med,* vol. 7, no. 1, p. 9, Jan 27 2022, doi: 10.1038/s41536-022-00209-8.
[446] Q. Xu *et al.*, "The role of angiotensin II activation of yes-associated protein/PDZ-binding motif signaling in hypertensive cardiac and vascular remodeling," *Eur J Pharmacol,* vol. 962, p. 176252, Jan 5 2024, doi: 10.1016/j.ejphar.2023.176252.
[447] H. Kwon, J. Kim, and E. H. Jho, "Role of the Hippo pathway and mechanisms for controlling cellular localization of YAP/TAZ," *FEBS J,* vol. 289, no. 19, pp. 5798-5818, Oct 2022, doi: 10.1111/febs.16091.
[448] J. Taylor, F. Dubois, E. Bergot, and G. Levallet, "Targeting the Hippo pathway to prevent radioresistance brain metastases from the lung (Review)," *Int J Oncol,* vol. 65, no. 1, Jul 2024, doi: 10.3892/ijo.2024.5656.
[449] B. Mohamed, S. A. Ghareib, A. E. Alsemeh, and S. S. El-Sayed, "Telmisartan ameliorates nephropathy and restores the hippo pathway in rats with metabolic syndrome," *Eur J Pharmacol,* vol. 973, p. 176605, Jun 15 2024, doi: 10.1016/j.ejphar.2024.176605.
[450] T. Habshi, V. Shelke, A. Kale, M. Lech, and A. B. Gaikwad, "Hippo signaling in acute kidney injury to chronic kidney disease transition: Current understandings and future targets," *Drug Discov Today,* vol. 28, no. 8, p. 103649, Aug 2023, doi: 10.1016/j.drudis.2023.103649.
[451] S. B. Xu, B. Xu, Z. H. Ma, M. Q. Huang, Z. S. Gao, and J. L. Ni, "Peptide 17 alleviates early hypertensive renal injury by regulating the Hippo/YAP signalling pathway," *Nephrology (Carlton),* vol. 27, no. 8, pp. 712-723, Aug 2022, doi: 10.1111/nep.14066.
[452] M. H. Shihan *et al.*, "AMPK stimulation inhibits YAP/TAZ signaling to ameliorate hepatic fibrosis," *Sci Rep,* vol. 14, no. 1, p. 5205, Mar 3 2024, doi: 10.1038/s41598-024-55764-5.

[453] H. Wu *et al.*, "Integration of Hippo signalling and the unfolded protein response to restrain liver overgrowth and tumorigenesis," *Nat Commun,* vol. 6, p. 6239, Feb 19 2015, doi: 10.1038/ncomms7239.
[454] H. McNeill and A. Reginensi, "Lats1/2 Regulate Yap/Taz to Control Nephron Progenitor Epithelialization and Inhibit Myofibroblast Formation," *J Am Soc Nephrol,* vol. 28, no. 3, pp. 852-861, Mar 2017, doi: 10.1681/ASN.2016060611.
[455] K. A. Drake *et al.*, "Transcription Factors YAP/TAZ and SRF Cooperate To Specify Renal Myofibroblasts in the Developing Mouse Kidney," *J Am Soc Nephrol,* vol. 33, no. 9, pp. 1694-1707, Sep 2022, doi: 10.1681/ASN.2021121559.
[456] Y. Xiao *et al.*, "Hippo pathway deletion in adult resting cardiac fibroblasts initiates a cell state transition with spontaneous and self-sustaining fibrosis," *Genes Dev,* vol. 33, no. 21-22, pp. 1491-1505, Nov 1 2019, doi: 10.1101/gad.329763.119.
[457] G. Chen *et al.*, "Post-transcriptional Gene Regulation in Colitis Associated Cancer," *Front Genet,* vol. 10, p. 585, 2019, doi: 10.3389/fgene.2019.00585.
[458] Y. Wan *et al.*, "Overexpression of miRNA-9 enhances galectin-3 levels in oral cavity cancers," *Mol Biol Rep,* vol. 48, no. 5, pp. 3979-3989, May 2021, doi: 10.1007/s11033-021-06398-7.
[459] D. Bieg, D. Sypniewski, E. Nowak, and I. Bednarek, "MiR-424-3p suppresses galectin-3 expression and sensitizes ovarian cancer cells to cisplatin," *Arch Gynecol Obstet,* vol. 299, no. 4, pp. 1077-1087, Apr 2019, doi: 10.1007/s00404-018-4999-7.
[460] H. Shi *et al.*, "Regulating microglial miR-155 transcriptional phenotype alleviates Alzheimer's-induced retinal vasculopathy by limiting Clec7a/Galectin-3(+) neurodegenerative microglia," *Acta Neuropathol Commun,* vol. 10, no. 1, p. 136, Sep 8 2022, doi: 10.1186/s40478-022-01439-z.
[461] M. Li *et al.*, "Inhibition of Long Noncoding RNA SNHG20 Improves Angiotensin II-Induced Cardiac Fibrosis and Hypertrophy by Regulating the MicroRNA 335/Galectin-3 Axis," *Mol Cell Biol,* vol. 41, no. 9, p. e0058020, Aug 24 2021, doi: 10.1128/MCB.00580-20.
[462] D. J. Thuerauf, M. Marcinko, P. J. Belmont, and C. C. Glembotski, "Effects of the isoform-specific characteristics of ATF6 alpha and ATF6 beta on endoplasmic reticulum stress response gene expression and cell viability," *J Biol Chem,* vol. 282, no. 31, pp. 22865-78, Aug 3 2007, doi: 10.1074/jbc.M701213200.
[463] D. J. Thuerauf, L. Morrison, and C. C. Glembotski, "Opposing roles for ATF6alpha and ATF6beta in endoplasmic reticulum stress response gene induction," *J Biol Chem,* vol. 279, no. 20, pp. 21078-84, May 14 2004, doi: 10.1074/jbc.M400713200.
[464] R. N. Correll, K. M. Grimes, V. Prasad, J. M. Lynch, H. Khalil, and J. D. Molkentin, "Overlapping and differential functions of ATF6alpha versus ATF6beta in the mouse heart," *Sci Rep,* vol. 9, no. 1, p. 2059, Feb 14 2019, doi: 10.1038/s41598-019-39515-5.
[465] L. T. Hien and S. H. Back, "Establishment of a reporter system for monitoring activation of the ER stress transducer ATF6beta," *Biochem Biophys Res Commun,* vol. 558, pp. 1-7, Jun 18 2021, doi: 10.1016/j.bbrc.2021.04.052.
[466] A. J. Macke *et al.*, "Targeting the ATF6-Mediated ER Stress Response and Autophagy Blocks Integrin-Driven Prostate Cancer Progression," *Mol Cancer Res,* vol. 21, no. 9, pp. 958-974, Sep 1 2023, doi: 10.1158/1541-7786.MCR-23-0108.
[467] U. Gopal, Y. Mowery, K. Young, and S. V. Pizzo, "Targeting cell surface GRP78 enhances pancreatic cancer radiosensitivity through YAP/TAZ protein signaling," *J Biol Chem,* vol. 294, no. 38, pp. 13939-13952, Sep 20 2019, doi: 10.1074/jbc.RA119.009091.
[468] S. Hou, L. Wang, and G. Zhang, "Mitofusin-2 regulates inflammation-mediated mouse neuroblastoma N2a cells dysfunction and endoplasmic reticulum stress via the Yap-Hippo pathway," *J Physiol Sci,* vol. 69, no. 5, pp. 697-709, Sep 2019, doi: 10.1007/s12576-019-00685-6.

[469] S. Shu, J. Zhu, Z. Liu, C. Tang, J. Cai, and Z. Dong, "Endoplasmic reticulum stress is activated in post-ischemic kidneys to promote chronic kidney disease," *EBioMedicine,* vol. 37, pp. 269-280, Nov 2018, doi: 10.1016/j.ebiom.2018.10.006.

[470] J. Guo *et al.*, "Chronic Kidney Disease Exacerbates Myocardial Ischemia Reperfusion Injury: Role of Endoplasmic Reticulum Stress-Mediated Apoptosis," *Shock,* vol. 49, no. 6, pp. 712-720, Jun 2018, doi: 10.1097/SHK.0000000000000970.

[471] Z. Mohammed-Ali *et al.*, "Endoplasmic reticulum stress inhibition attenuates hypertensive chronic kidney disease through reduction in proteinuria," *Sci Rep,* vol. 7, p. 41572, Feb 2 2017, doi: 10.1038/srep41572.

# *Appendix*

*Clinical Science* (2021) **135** 143–159
https://doi.org/10.1042/CS20201137

PORTLAND PRESS

Research Article

# Role of endoplasmic reticulum stress in renal damage after myocardial infarction

**Beatriz Delgado-Valero[1], Lucía de la Fuente-Chávez[1], Ana Romero-Miranda[1], María Visitación Bartolomé[2,3], Bunty Ramchandani[4], Fabián Islas[5], María Luaces[5], Victoria Cachofeiro[1,3,*] and Ernesto Martínez-Martínez[1,3,*]**

[1]Departamento de Fisiología, Facultad de Medicina, Universidad Complutense de Madrid-Instituto de Investigación Sanitaria Gregorio Marañón (IiSGM), Madrid, Spain; [2]Departmento de Inmunología, Oftalmología y Otorrinolaringología, Facultad de Psicología, Universidad Complutense Madrid, Spain; [3]Ciber de Enfermedades Cardiovasculares (CIBERCV), Instituto de Salud Carlos III, Madrid, Spain; [4]Servicio de Cirugía Cardiaca Infantil, Hospital La Paz, Madrid, Spain; [5]Servicio de Cardiología, Instituto Cardiovascular, Hospital Clínico San Carlos, Madrid, Spain

**Correspondence:** Victoria Cachofeiro (vcara@ucm.es) or Ernesto Martínez-Martínez (ernmarti@ucm.es)

Myocardial infarction (MI) is associated with renal alterations resulting in poor outcomes in patients with MI. Renal fibrosis is a potent predictor of progression in patients and is often accompanied by inflammation and oxidative stress; however, the mechanisms involved in these alterations are not well established. Endoplasmic reticulum (ER) plays a central role in protein processing and folding. An accumulation of unfolded proteins leads to ER dysfunction, termed ER stress. Since the kidney is the organ with highest protein synthesis fractional rate, we herein investigated the effects of MI on ER stress at renal level, as well as the possible role of ER stress on renal alterations after MI. Patients and MI male Wistar rats showed an increase in the kidney injury marker neutrophil gelatinase-associated lipocalin (NGAL) at circulating level or renal level respectively. Four weeks post-MI rats presented renal fibrosis, oxidative stress and inflammation accompanied by ER stress activation characterized by enhanced immunoglobin binding protein (BiP), protein disulfide-isomerase A6 (PDIA6) and activating transcription factor 6-alpha (ATF6$\alpha$) protein levels. In renal fibroblasts, palmitic acid (PA; 50-200 $\mu$M) and angiotensin II (Ang II; $10^{-8}$ to $10^{-6}$M) promoted extracellular matrix, superoxide anion production and inflammatory markers up-regulation. The presence of the ER stress inhibitor, 4-phenylbutyric acid (4-PBA; 4 $\mu$M), was able to prevent all of these modifications in renal cells. Therefore, the data show that ER stress mediates the deleterious effects of PA and Ang II in renal cells and support the potential role of ER stress on renal alterations associated with MI.

## Introduction

Kidneys and heart are linked since the heart provides nutrients and oxygen to support normal kidney function. Moreover, kidneys regulate fluid, electrolytes and acid-base homeostasis which facilitate heart function [1]. Based on that interaction, Consensus Conference of Acute Dialysis Quality Initiative Group defined cardiorenal syndrome as the different conditions in which kidney and heart dysfunction overlap [2]. The definition of cardiorenal syndrome involves five subtypes, being type 1 defined by renal injury due to a deterioration in cardiac function, the most prevalent in patients diagnosed with cardiorenal syndrome [3].

Several animal models have been described to study cardiorenal syndrome, being myocardial infarction (MI) the most commonly used to evaluate it due to its reproducibility and its relation to human pathophysiology [4]. It has been observed that approximately 20% of MI patients present renal damage which increase mortality as compared with MI patients without renal impairment [5,6]. Experimental studies have

*These authors contributed equally to this work.

Received: 03 September 2020
Revised: 17 December 2020
Accepted: 23 December 2020

Accepted Manuscript online: 23 December 2020
Version of Record published: 08 January 2021

*Clinical Science* (2021) **135** 143–159
https://doi.org/10.1042/CS20201137

demonstrated that MI is associated with development of renal fibrosis accompanied by renal inflammation even in absence of renal dysfunction few weeks post-MI [7]. Chronically, MI is accompanied by renal dysfunction. Although patients with MI usually show a time-course recovery of impaired renal function, an increased mortality rate is observed [5]. Renal fibrosis is a common feature of chronic kidney diseases and plays a critical role in renal dysfunction contributing to mortality complications [8,9]. Renal fibrosis occurs as a consequence in the misbalance between extracellular matrix (ECM) production/degradation. The increase in ECM production could be a trigger for an inflammatory response and myofibroblast proliferation [9]. Several cytokines appear to be major contributors to renal fibrosis as transforming growth factor-beta (TGF-β) which is involved in ECM production, as well as in the inflammatory response. In accordance with that, MI is accompanied by interleukin (IL)-6 overexpression, as well as macrophage infiltration at renal level in rats [6]. The inflammatory response seems to play a critical role in the development of renal fibrosis, since systemic depletion of monocytes/macrophages improves renal fibrosis in an animal model of MI [10]. However, the mechanisms involved in renal fibrosis are not fully established and there is not an effective treatment, with new strategies being mandatory for treating it.

In the last years, it has been described that various types of kidney damage such as kidney aging [11], nephronophthisis [12], diabetic kidney disease [13], acute kidney injury [14] and hypertension-associated kidney disease [15] are associated with endoplasmic reticulum (ER) dysfunction, termed ER stress. ER plays a central role in calcium homeostasis, lipid biosynthesis and protein processing. Different conditions such as high protein demand, viral infections, inflammatory cytokines and mutant protein expression, result in ER stress and the subsequent activation of unfolded protein response (UPR) in order to try to mitigate this pathological situation [16]. UPR response tries to deal with the accumulation of unfolded proteins, activating three different pathways initiated by inositol requiring 1 (IRE1), PKR-like ER kinase (PERK) and activating transcription factor 6 (ATF6) proteins. In unstressed conditions, immunoglobin binding protein (BiP) binds to IRE1, PERK and ATF6 and keep them inactive. Upon undergoing ER stress, BiP dissociates from these master regulators, thereby activating UPR. For this reason, BiP is considered to be a monitor of ER stress [17]. UPR activation is initially considered to be an adaptive response; however, persistent activation of UPR drives damaged cells to apoptosis [18] and is associated with the pathogenesis of a number of diseases.

Therefore, the aim of the present study was to evaluate whether ER stress can participate in the renal fibrosis associated with MI. To achieve this aim, we have evaluated if ER stress is activated at renal level in rats with MI and its association with renal fibrosis. We have also analyzed the impact of the activation of ER stress on ECM components and mediators on renal fibroblasts stimulated with palmitic acid (PA) which has been proven to activate ER stress accompanied by an increase in inflammatory markers in podocytes [19]; however, its effect on renal fibroblasts and the effects of PA on ECM production is not studied. In addition, we used a well-known profibrotic factor such as angiotensin II (Ang II) in renal fibroblasts to study the possible role of ER stress in ECM production.

# Materials and methods

## Subjects

Patients who suffer a first acute myocardial infarction (MI) as defined by "The Third Universal Definition of Myocardial Infarction" [20]: increase in biomarkers in the presence of ischemia, ST-T changes, the appearance of new Q waves, identification of alterations of local contraction by image technique or intracoronary thrombus detected by angiography were recruited from the Cardiology Department of Hospital Clínico San Carlos, Madrid, Spain. The exclusion criterion were a previous MI or myocardial revascularization, hemodynamic instability 12 h previous revascularization, severe chronic kidney disease with a creatinine clearance $<30$ ml/min/1.7m$^2$. Twenty-four to forty-eight hours after hospital admission for MI, patients underwent transthoracic echocardiographic and at the same time blood samples were collected. A group of healthy volunteers were recruited from staff of the hospital. The study protocol was approved by the ethics committee (16/107-E_BS) and all participants signed the informed consent. The present study was conducted in compliance with Good Clinical Practice Guidelines and the ethical principles stated in the Declaration of Helsinki.

## Experimental design and animals

Myocardial infarction was induced in 12-week-old male Wistar rats of 320–350 g (Harlan Ibérica, Barcelona, Spain; $n=8$) anesthetized (2% isofluorane), intubated and ventilated (Inspira Asv, Harvard Instruments) and placed on an adjustable heating pad to maintain a core temperature of 36–37°C by ligation of the left anterior descendent (LAD) coronary artery as previously reported [21]. Rats subjected to Sham operation (the same surgical procedure except that

the suture passing the LAD was not fastened; $n$=8) was included as a reference group (Sham). After surgery, buprenorphine (0.05 mg/kg per 8 h, intramuscular) was given for 48 h. After recovery, the animals were kept in collective cages with free access to food and water in the animal facility of the Universidad Complutense de Madrid. Four-weeks after myocardial infarction, animals were sacrificed. Systolic blood pressure (SBP) was estimated end-of-study through use of a tail-cuff plethysmograph (Narco Bio-Systems) in unrestrained rats. Animals were sacrificed by decapitation. At the end of the experiment, blood was collected in EDTA in food-deprived animals. Kidneys were removed carefully from animals, immediately frozen in liquid nitrogen and stored at −80°C until its use. The Animal Care and Use Committee of Universidad Complutense de Madrid approved all experimental procedures according to the Spanish Policy for Animal Protection RD53/2013, which meets the European Union Directive 2010/63/UE.

## Creatinine measurements

Plasma creatinine levels were measured using spectrophotometric techniques in an autoanalyzer (Vitros 5600, Diagnostics Ortho Clinical, Johnson & Johnson, New Brunswick, NJ, U.S.A.).

## Circulating measurements

Plasma Neutrophil gelatinase-associated lipocalin (NGAL) (R&D Systems; catalogue number: DY1757-05), Ang II (abbex; catalogue number: abx052349) and thiobarbituric acid reactive substances (TBARS) (Sigma Aldrich; catalogue number: MAK085) levels, were measured following the instructions of the manufacturer.

PA was measured as previously reported [22]. Aliquots of 100 μl of plasma were transferred to Eppendorf tubes. The lipids were then extracted with hexane/isopropanol, 3:2 v/v at a 1:10 sample/solvent ratio. The tubes were vortexed and maintained at −20°C for 10 min, then centrifuged at 14,000 ***g*** at 4°C for 5 min. The supernatant was collected, transferred to glass tubes and dried under nitrogen flow. Then, 1 ml of 80% methanol was added, and the tubes were thoroughly mixed.

The liquid chromatography-tandem mass spectrometry (LC-MS/MS) system comprised a Shimadzu UHPLC Nexera X2 system hyphenated to a triple quadrupole mass spectrometer LCMS-8030 (Shimadzu Corporation, Kyoto, Japan). The mass spectrometer was operated with an electrospray ionization (ESI) source in negative mode. The desolvation line and heat block temperatures were set at 250 and 400°C, respectively. The interface voltage was maintained at 3.5 kV. Nitrogen was used as nebulizing and drying gas at a flow of 1.5 and 15 l/min, respectively. Argon was used as collision gas at 230 kPa.

## Morphological and histological evaluation

Renal tissue samples were dehydrated, embedded in paraffin and cut in 4 μm-thick sections that were stained with picrosirius red in order to detect collagen fibers. Other renal tissue samples were embedded in Tissue-Tek® O.C.T™. The area of renal interstitial fibrosis was identified as the ratio of fibrosis or collagen deposition to the total tissue area (after excluding the vessel and glomerular area from the region of interest). For each sample stained with picrosirius red, 30 fields all through the cortex were analysed with a 20× objective under transmitted light microscopy (Leica DM 2000; Leica AG, Germany).

## Cell culture

The renal tube fibroblasts (TFBs) is a murine renal interstitial fibroblast cell line originally isolated from SJL mouse kidney and was a generous gift from Dr Ucero AC. TFBs were maintained in RPMI 1640 medium supplemented with 10% FBS, L-glutamine 1% and penicillin/streptomycin 1%. The cells were seeded in T75 tissue culture flask pretreated with L-polylysine (0.1 mg/ml) and then grown as a monolayer culture. Cells were passaged with 1× trypsin whenever they became confluent. All assays in the present study were done at temperatures of 37°C, 95% sterile air and 5% $CO_2$ in a saturation humidified incubator. Cells were treated with different doses of palmitic acid (PA) with bovine serum albumin (BSA) as a carrier—conjugated to 10% free fatty acids (FFA)-free BSA (PA; 50-200 μM), angiotensin II (Ang II; $10^{-8}$ to $10^{-6}$M) and/or 4-phenylbutyric acid (4-PBA; 2 and 4 μM).

For the intracellular pathways study, cells were treated with Ang II for 5, 10, 15, 30 and 60 min. The following chemical inhibitors were added at $10^{-6}$ M: BAY11-7082 (Sigma Aldrich); LY294002 (Sigma Aldrich) and PD98059 (Sigma Aldrich).

*Clinical Science* (2021) **135** 143–159
https://doi.org/10.1042/CS20201137

## Western blot

Protein extraction was performed from kidneys by mechanic disruption by 0.5 mm zirconium oxide beads in a tissue homogenizer bullet blender (Scientific Instrument Services, MA, U.S.A.) containing 300 μl of lysis buffer (cOmplete Lysis-M; Roche, Risch-Rotkreuz, Suiza, catalogue number 04719956001).

Renal and cellular proteins were separated by SDS-PAGE on polyacrylamide Criterion™ TGX™ Precast Gels (Bio-Rad, California, U.S.A.) and transfered to Hybond-c Extra nitrocellulose membranes (Hybond-P; Amersham Biosciences, Piscataway, NJ). Membranes were probed with primary antibody for α-smooth muscle actin (α-SMA; Biocare medical, California, U.S.A.; dilution 1:200), 4-Hydroxynonenal (4-HNE; Abcam plc, Cambridge, U.K.; dilution 1:250), protein kinase B (Akt, Cell Signaling, Danvers, MA, U.S.A.; dilution 1:1000), Akt, (phospho Ser473, Cell Signaling, Danvers, MA, U.S.A.; dilution 1:1000), activating transcription factor 6-alpha (ATF6α; Santa Cruz, Texas, U.S.A.; dilution 1:250), immunoglobin binding protein (BiP; BD Biosciences, Madrid, Spain; dilution 1:500), CCAAT-enhancer-binding protein homologous protein (CHOP; Cell Signaling Technology, Massachusetts, U.S.A.; dilution 1:500), collagen I (Calbiochem, California, U.S.A.; dilution 1:1000), connective tissue growth factor (CTGF; Sigma-Aldrich, Missouri, U.S.A.; dilution 1:1000), extracellular signal-regulated kinases (Erk1/2, ThermoFisher; Rockford, IL, U.S.A.; dilution 1:1000), Erk1/2 (phospho-p44/42 Thr202/Tyr204, Cell Signaling, Danvers, MA, U.S.A.; dilution 1:1000), nuclear factor-κB p65 (NF-κB, Abcam; Cambridge, U.K.; dilution 1:1000), NF-κB (phospho S536, Abcam; Cambridge, U.K.; dilution 1:1000), protein disulfide-isomerase A6 (PDIA6; Abcam plc, Cambridge, U.K.; dilution 1:1000), transforming growth factor-β (TGF-β; Abcam plc, Cambridge, U.K.; dilution 1:1000), β-actin (Sigma-Aldrich, Missouri, U.S.A.; dilution 1:1000) and glyceraldehyde 3-phosphate dehydrogenase (GAPDH; Cell Signaling Technology, Massachusetts, U.S.A.; dilution 1:5000) as a loading control. Signals were detected using the ECL system (Millipore, Massachusetts; U.S.A.). Results are expressed as an *n*-fold increase over the values of the control group in densitometric arbitrary units.

## Detection of superoxide anion production

The oxidative fluorescent dye dihydroethidium (DHE; $10^{-5}$ M) was used to evaluate superoxide anion ($O^{-2}$) presence at renal level or production in cells as previously described [23]. The fluorescence intensity was determined with Leica application suite (Leica microsystems, Wetzlar, Germany).

## Inmunocytochemistry

Characterization of the cells using immunocytochemistry technical procedure, revealed a consistent expression of vimentin (Supplementary Figure S1) confirming that the cells possessed fibroblasts phenotype. Renal fibroblasts (TFBs) were fixed with Merckofix (Merck KGaA, Darmstadt, Germany) and permeabilized with Triton X-100. Cells were then incubated overnight at 4°C in a solution containing 1:100 antivimentin (GeneTex, California, U.S.A.). After three washings (5 min each) in PBS, the cells were incubated in fluorescein anti-rabbit (Vectastin Vector) 1:200. Images were analysed and photographed at 40× objective with a Leica DMI 3000B microscope.

## Retrotranscription and real-time PCR

Total RNA was isolated using Trizol Reagent (Fisher Scientific, Waltham, MA, U.S.A.) and was reverse transcribed into cDNA using the High-Capacity cDNA Reverse Transcription Kit (Thermo Fisher Scientific Inc, Waltham, MA, U.S.A.). Quantitative PCR analysis was performed with SYBR green PCR technology (Bio-Rad) (Supplementary Tables S1 and S2). Quantification of mRNA levels was performed by real-time PCR using the $\Delta\Delta C_t$ method. Data were normalized to hypoxanthine phosphoribosyltransferase (HPRT).

## Statistical analysis

Continuous variables of patients are expressed as mean ± SD. Categorical variables are expressed in absolute values and percentages. Continuous variables of experimental data are expressed as mean ± SEM. Normality of distributions was verified by means of the Kolmogorov–Smirnov test. Levene's test was used to assess the equality of variances and a Student's *t* test was performed to determine if two sets of data were significantly different from each other. One-way ANOVA was used and followed by Newman–Keuls test or a Dunnett test. Pearson correlation analysis was used to examine association among different variables. A value of $P<0.05$ was used as the cut-off value for defining statistical significance. Data analysis was performed using the statistical program GraphPad Prism 8 (San Diego, CA, U.S.A.).

# Results

## MI is associated with higher NGAL levels in patients

The mean age of patients with MI was higher than that of control subjects (54.8 ± 6.8 vs. 41.6 ± 4.1 years; $P<0.0001$), with there being only males in the group of MI versus 50% in the control one. All MI patients, but only 8.3% of the control subjects, had associated comorbidities, with the most prevalent being hypertension and dyslipidemia. Drug treatment for hypertension included angiotensin converting enzyme inhibitors (or angiotensin II type 1 receptor antagonists), whereas all dyslipidemic patients were placed on statins. Body mass index (BMI) was higher in MI patients than in non-MI subjects (26.4 ± 2.1 vs. 23.04 ± 2.01 kg/m$^2$; $P$=0.005). Plasma creatinine levels in MI patients were higher than those of control subjects (0.88 ± 0.17 vs. 0.73 ± 0.11 mg/dl; $P$=0.0119). Despite the fact that plasma creatinine values were within normal values in both groups, MI group presented an important increase in NGAL, an acute marker of kidney injury, as compared to control subjects (87,873 ± 24,419 vs. 61,941 ± 14,695 pg/ml; $P$=0.0046; Supplementary Table S3).

## MI is associated with renal fibrosis, oxidative stress and inflammation

Animals subjected to ligation of the coronary artery presented several cardiac structural and functional alterations characterized by an increase in left ventricular end-systolic diameter accompanied by a reduction in systolic and diastolic function as compared with Sham group [21]. MI animals also presented an increase in interstitial cardiac fibrosis [21].

As occurs in patients, creatinine serum levels were similar between both groups; however, MI animals presented an increase in two markers of kidney injury NGAL and kidney injury marker-1 (KIM-1), as compared to control animals (Figure 1A). In addition, MI animals showed kidney fibrosis (Figure 1B) which was accompanied by an increase in collagen type I protein levels (Figure 1C). Complementary analysis revealed that the MI group presented a slight increase in α-SMA without signification and enhanced protein levels of the profibrotic mediator TGF-β without modification in CTGF protein levels (Figure 1C).

Oxidative stress was evaluated at renal level in the animals. An increase in TBARs circulating plasma levels was observed in MI animals as compared with control ones (Figure 1D). As shown in Figure 1E, there was an increase in fluorescence intensity in the kidney of MI animals as compared with control ones, suggesting a higher presence of superoxide anion in MI animals. This prooxidant scenario was confirmed by 4-HNE, a major end-product of lipid peroxidation, which was enhanced after MI at renal level (Figure 1F).

MI induced increased levels of pro-inflammatory markers in the kidney, including IL-6 and TNF-α (Figure 1G) mRNA levels as compared with Sham animals.

## Endoplasmic reticulum stress is activated at renal level after MI

At 4 weeks after MI, two markers of ER stress, BiP (Figure 2A) and PDIA6 (Figure 2B) were up-regulated in MI animals as compared with control ones. Analysis of different pathways involved in ER stress activation revealed that ATF6α protein levels were enhanced in MI animals (Figure 2C) in absence of CHOP protein modifications (Figure 2D). This endoplasmic reticulum stress activation was accompanied by a slight increase of PA, which did not reach significant statistically, (Figure 2E) and Ang II plasma levels in MI rats (Figure 2F).

## Activation of ER stress in renal fibroblasts

In order to activate the ER stress in renal tube fibroblasts (TFBs), we exposed the cells to PA that has been demonstrated to activate ER stress accompanied by an increase in inflammatory markers in podocytes [19].

The exposition of TFBs to different doses of PA (50–200 μM) for 24 h was accompanied by activation of ER stress characterized by enhanced PDIA6 protein levels (Figure 3A) and up-regulation of two downstream proteins of ER stress as ATF6α and CHOP (Figure 3B,C). Interestingly, PA-treated cells presented an increase in collagen I protein levels at the dose of 100 μM of PA (Figure 3D) and a protein increase in the profibrotic mediator TGF-β independently of the dose of PA (Figure 3E). This profibrotic effect of PA was accompanied by an enhanced production of superoxide anion production, reaching a maximum effect at 100 μM of PA after 24 h of stimulation (Figure 3F).

## Endoplasmic reticulum stress mediates the prooxidant, profibrotic and proinflammatory effects of PA in renal fibroblasts

In order to explore the possible role of ER stress in the prooxidants and profibrotic effects of PA, TFBs were exposed to PA (100 μM) in presence or absence of the pharmacological inhibitor of ER stress, 4-PBA, for 24 h.

*Clinical Science* (2021) **135** 143–159
https://doi.org/10.1042/CS20201137

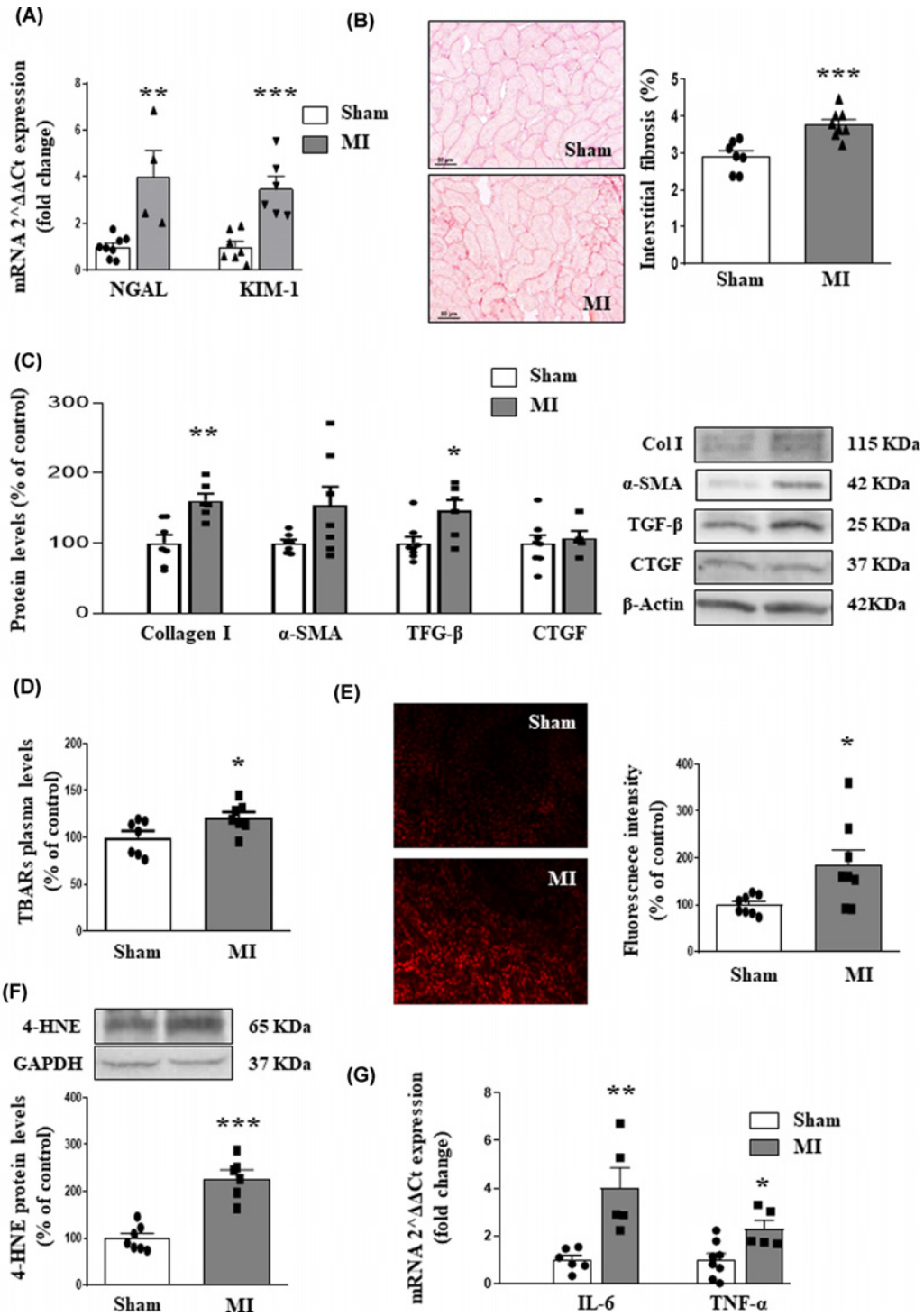


**Figure 1. Impact of MI on renal fibrosis, oxidative stress and inflammation**

(**A**) Neutrophil gelatinase-associated lipocalin (NGAL) and kidney injury marker-1 (KIM-1) mRNA levels. (**B**) Representative microphotographs of renal sections staining with picrosirius red (magnification 20×) and quantification of collagen volume fraction. (**C**) Renal protein levels of collagen type I, alpha-smooth muscle actin (α-SMA), transforming growth factor-beta (TGF-β) and connective tissue growth factor (CTGF). (**D**) Thiobarbituric acid reactive substances (TBARS) plasma. (**E**) Representative images and quantification of renal sections labelled with the oxidative dye hydroethidine (magnification 40×). (**F**) Renal protein levels of 4-hydroxynonenal (4-HNE). (**G**) Renal mRNA levels of interleukin-6 (IL-6) and tumor necrosis factor-alpha (TNF-α) in kidneys from rats after MI or Sham animals. Bar graphs represent the mean ± SEM of 8–10 animals normalized to hypoxanthine-guanine phosphoribosyltransferase (HPRT) or β-actin for cDNA and protein, respectively: *$P<0.05$; **$P<0.01$; ***$P<0.001$ versus Sham group.

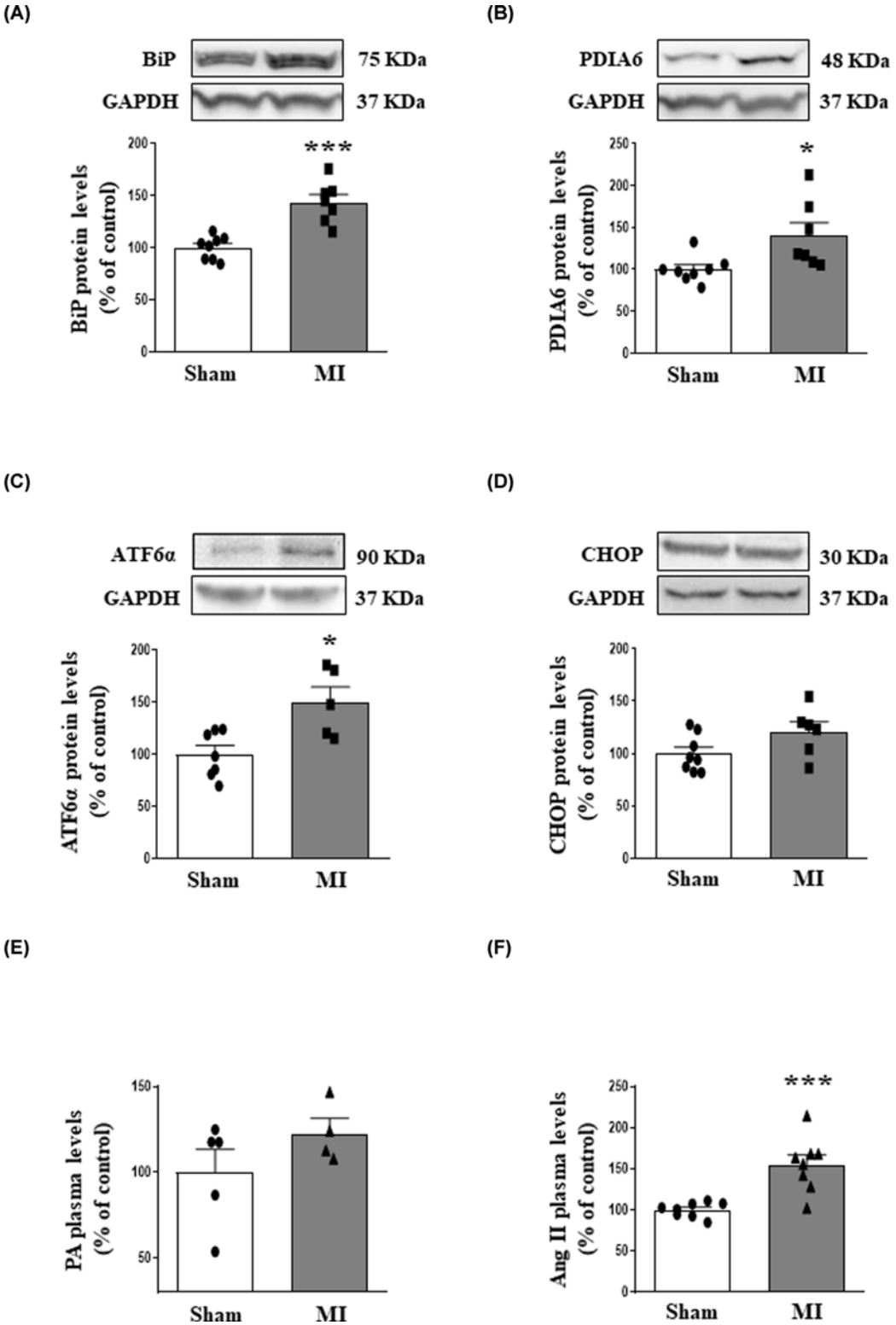


**Figure 2. MI induces endoplasmic reticulum stress at renal level**

Renal protein levels of (**A**) immunoglobulin binding protein (BiP). (**B**) Protein disulfide isomerase family A member 6 (PDIA6). (**C**) Activating transcription factor 6-alpha (ATF6$\alpha$) and (**D**) CCAAT-enhancer-binding protein homologous protein (CHOP) from rats after MI or Sham animals. Plasma levels of (**E**) palmitic acid (PA) and (**F**) Angiotensin II (Ang II) from rats after MI or Sham animals. Bar graphs represent the mean $\pm$ SEM of 8–10 animals normalized to glyceraldehyde-3-phosphate dehydrogenase (GAPDH); $^{*}P<0.05$; $^{***}P<0.001$ versus Sham group.

*Clinical Science* (2021) **135** 143–159
https://doi.org/10.1042/CS20201137

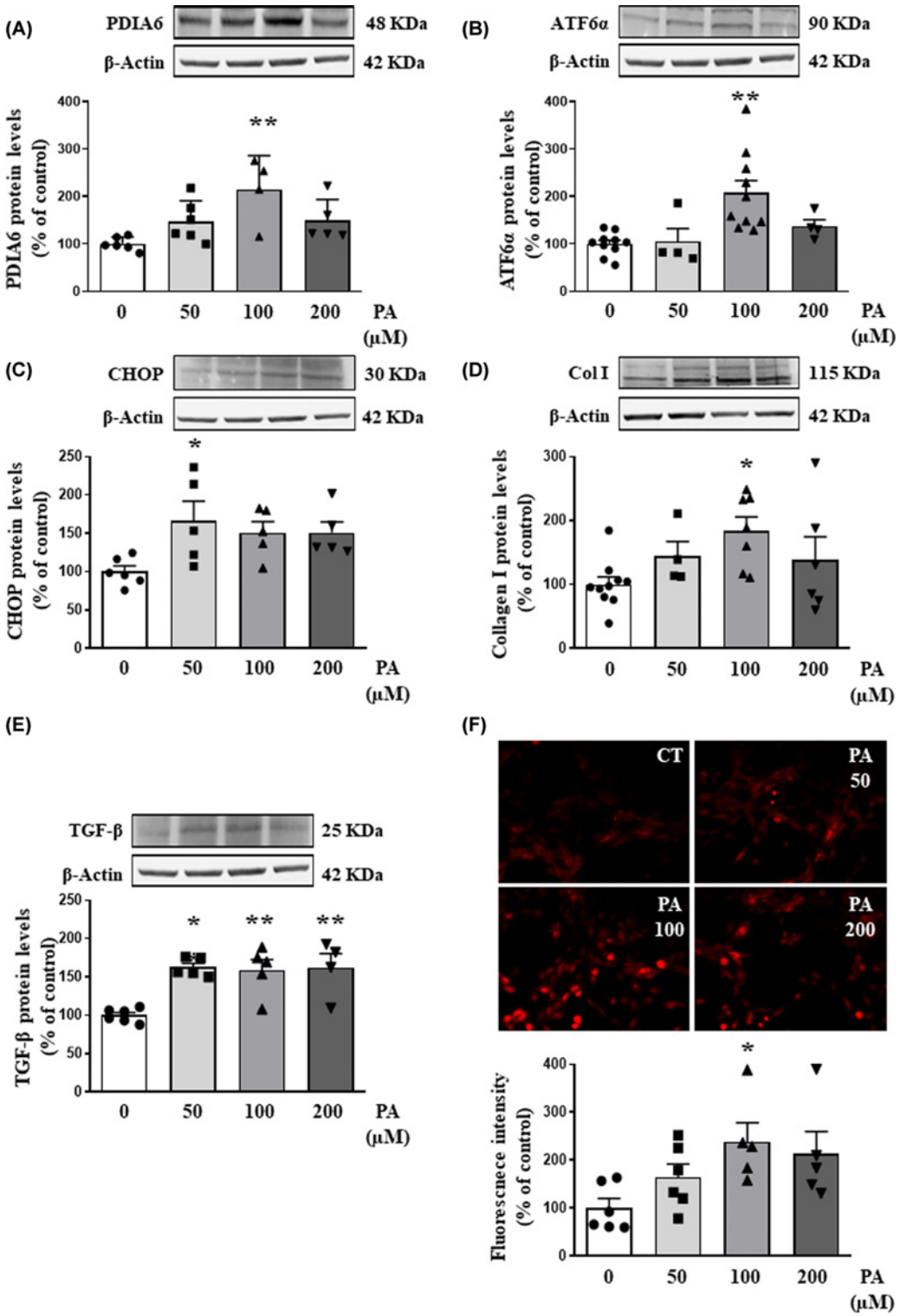


**Figure 3. Palmitic acid (PA) effects on endoplasmic reticulum stress, extracellular matrix proteins and superoxide anion production in renal fibroblasts**

Dose–response (50–200 μM) of PA in renal fibroblasts on (**A**) protein disulfide isomerase family A member 6 (PDIA6); (**B**) activating transcription factor 6-alpha (ATF6α); (**C**) CCAAT-enhancer-binding protein homologous protein (CHOP); (**D**) collagen I; (**E**) transforming growth factor-beta (TGF-β) protein expression and (**F**) representative microphotographs and quantification of cells labeled with the oxidative dye hydroethidine (magnification 40×). Bar graphs represent the mean ± SEM of four to six assays normalized to β-actin; *$P<0.05$, **$P<0.01$ versus control cells.

4-PBA was able to prevent the increase in superoxide anion production induced by PA at two different doses, 2 and 4 μM (Figure 4A). For the next experiments, we used the dose of 4 μM of 4-PBA. At that dose, 4-PBA was able to prevent the activation of ER stress and thus preventing the protein up-regulation of BiP, PDIA6 and ATF6α protein levels induced by PA, showing the efficiency of the treatment (Supplementary Figure S2A–C). In addition, 4-PBA was able to prevent the increase in ECM proteins induced by PA after 24 h of treatment. 4-PBA-treated cells were resistant to the increase in TGF-β (Figure 4B) induced by PA in TFBs. 4-PBA blunted the production of collagen I induced by PA at mRNA levels (Figure 4C).

TFBs treated with PA (100 μM) for 24 h presented and increase in different proinflammatory markers such as IL-6, CCL-2 and osteopontin at mRNA level (Figure 4C). The pharmacological inhibitor of ER stress was able to prevent the proinflammatory response of PA in TFBs (Figure 4C). These effects of 4-PBA were accompanied by a prevention of the up-regulation in the acute kidney injury biomarker, NGAL, induced by PA in the renal cells (Figure 4C).

### Endoplasmic reticulum stress mediates the prooxidant, profibrotic and proinflammatory effects of angiotensin II in renal fibroblasts

We evaluated the possible role of ER stress in a well-known profibrotic factor at renal level. Ang II was able to activate ER stress in a dose dependent-manner characterized by an increase in BiP, PDIA6, CHOP and ATF6α protein levels after 24 h of stimulation (Figure 5A–D). For the next experiments, cells were exposed to Ang II ($10^{-6}$ M) in presence or absence of 4-PBA at 4 μM. The presence of the ER stress inhibitor was able to block the rise in superoxide anion production induced by Ang II (Figure 5E), as well as the increase in collagen I and the inflammatory markers IL-6, CCL-2 and osteopontin at mRNA level in Ang II-treated cells (Figure 5F).

The possible intracellular pathways by which Ang II exerts its profibrotic effects in renal fibroblasts were analysed. Ang II ($10^{-6}$ M) increased NFκB phosphorylation after 10 min of stimulation (Figure 6A), Akt phosphorylation at 60 min (Figure 6B) and enhanced protein levels of ERK phosphorylation at 5 and 10 min (Figure 6C). The presence of LY294002, a specific inhibitor of PI3K/Akt pathway, was not able to modify the increase in collagen I protein levels induced by Ang II (Figure 6D). In contrast, the presence of BAY11-7082, a specific inhibitor of NFκB pathway, or the presence of PD98059, a specific inhibitor of ERK 1/2, prevented the profibrotic effects of Ang II in renal cells (Figure 6D).

## Discussion

The main purpose of the present study was to investigate the role of ER stress in the renal alterations associated with MI. Four weeks post-MI, animals presented renal fibrosis, oxidative stress and inflammation. We show for the first time that these alterations were accompanied by ER stress activation showing its possible role on ECM production. To our knowledge, this is the first study demonstrating that PA is able to exert profibrotic actions as well as ER stress activation. In addition, the pharmacological ER stress inhibition prevented the increase in collagen I, superoxide anion production and inflammatory markers induced by PA or by another profibrotic factor such as Ang II, supporting the role of ER stress in this process. Thus, ER stress emerges as a potential target for treatment of renal fibrosis associated with MI.

Several studies have demonstrated that MI is associated with renal damage [24,25]. This effect was accompanied by the fact that patients with renal alterations experience poor outcomes post-MI [26,27], and make an earlier detection of renal damage in patients mandatory, even in absence of creatinine alterations. Serum NGAL levels have correlated with the severity of renal damage and are associated with an increased risk of mortality in patients [28]. In this line, we have observed an increase in NGAL levels, a marker of acute renal damage, in patients with MI even in the presence of normal creatinine levels. Similarly, 4-week post-MI, animals do not present alterations in creatinine circulating levels as compared with control ones. In fact, serum creatinine levels were not elevated until 60 days post-MI [7]. However, renal NGAL and KIM-1 levels were higher than in Sham rats. This further supports the impact of myocardial ischemia in the kidney.

Renal fibrosis is an alteration that indicates the progression of kidney disease and is related to a decline in renal function in patients and animal models [29]. Different mediators have been postulated as contributors to renal fibrosis with TGF-β being a central one [10]. Our results show an increase in protein levels of this important fibrogenic cytokine in the kidneys of MI animals, which is accompanied by renal fibrosis and collagen I up-regulation. Along with TGF-β and renal fibrosis, oxidative stress and inflammation are other mechanisms described in the progression of renal failure. Our data show that MI animals presented an increase in superoxide anion levels, in 4-HNE, a major end-product of lipid peroxidation, and TBARs confirming oxidative stress at renal level after 4 weeks of MI. A common pathway involved in tissue dysfunction is oxidative stress, which has been associated with different pathologies,

*Clinical Science* (2021) **135** 143–159
https://doi.org/10.1042/CS20201137

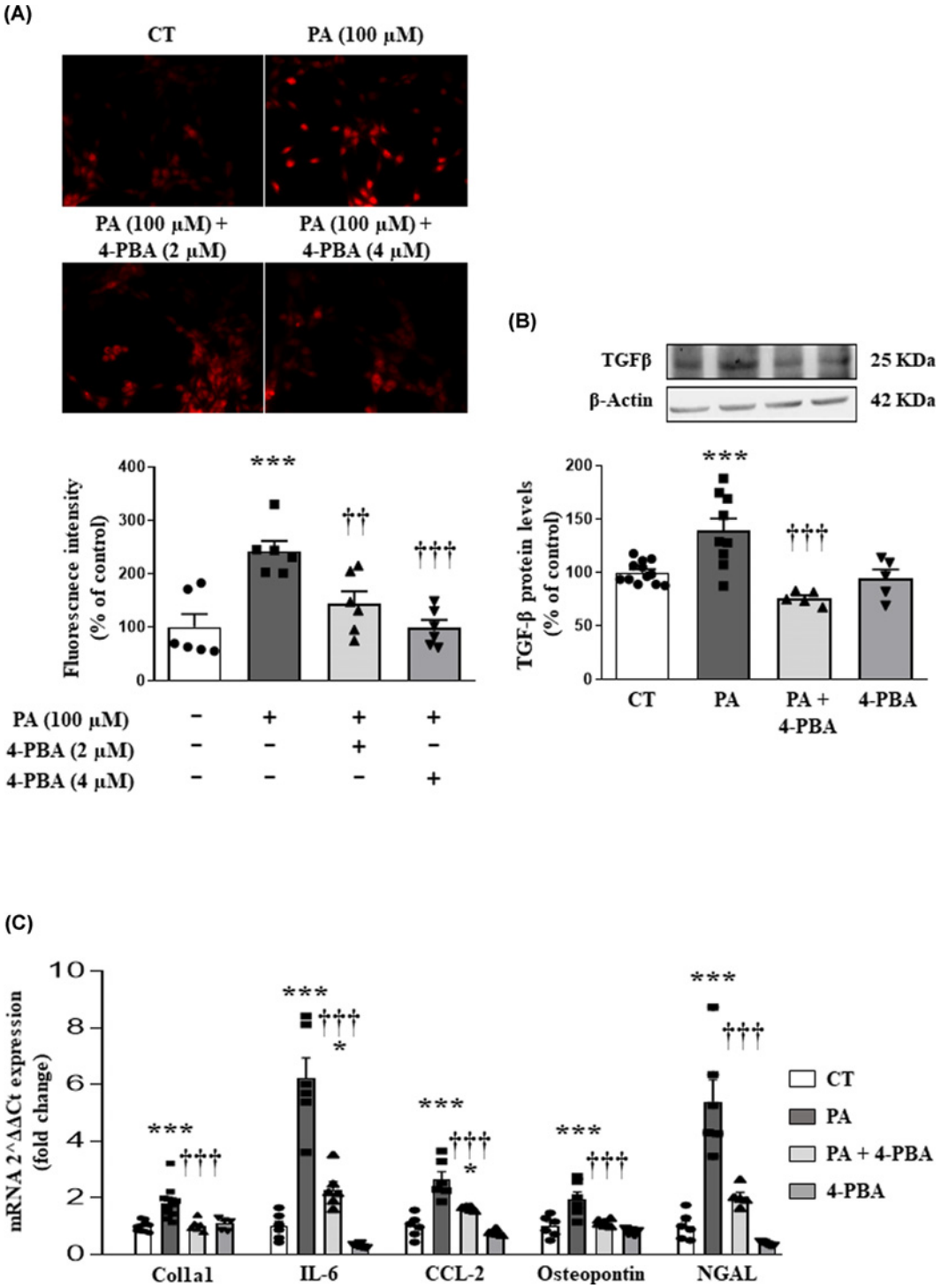


**Figure 4. Endoplasmic reticulum stress mediates the prooxidant, profibrotic and proinflammatory effects of palmitic acid (PA) in renal fibroblasts**

(**A**) Effects of 4-phenylbutyric acid (4-PBA at 2 and 4 μM) on superoxide anion production in renal fibroblasts treated with PA (100 μM) for 24 h. Representative microphotographs and quantification of cells labeled with the oxidative dye hydroethidine (magnification 40×). Effects of 4-PBA (4 μM) on (**B**) transforming growth factor-beta (TGF-β) protein expression; (**C**) collagen I mRNA expression, interleukin-6 (IL-6), C-C motif chemokine ligand 2 (CCL-2), osteopontin and neutrophil gelatinase-associated lipocalin (NGAL) mRNA expression in PA-treated cells (100 μM) for 24 h. Bar graphs represent the mean ± SEM of four to six assays normalized to hypoxanthine-guanine phosphoribosyltransferase (HPRT) or β-actin for cDNA and protein, respectively; *$P<0.05$; ***$P<0.001$ versus control cells; ††$P<0.01$; †††$P<0.001$ versus PA-treated cells.

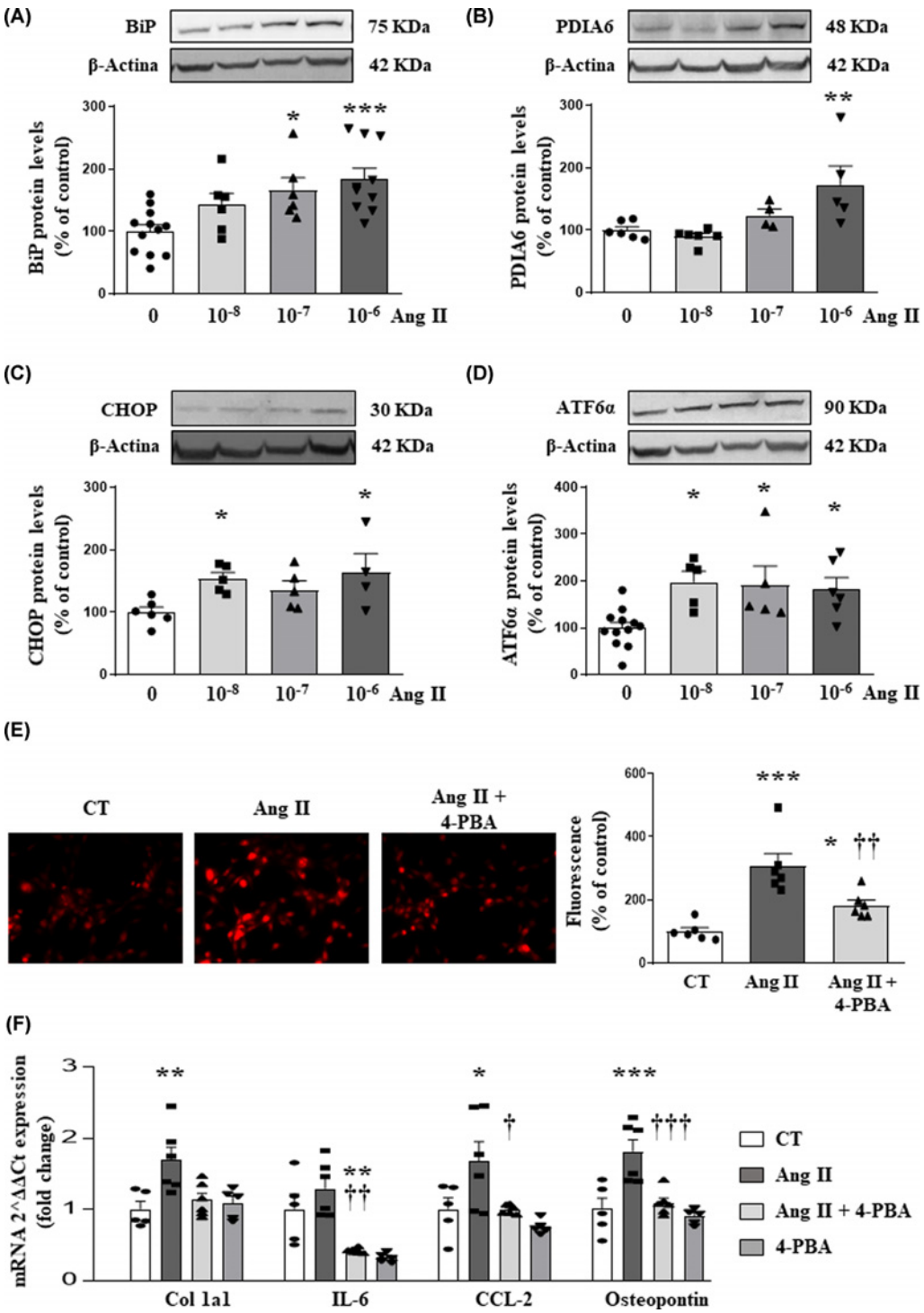


**Figure 5. Endoplasmic reticulum stress mediates the prooxidant, profibrotic and proinflammatory effects of angiotensin II (Ang II) in renal fibroblasts**

Dose–response ($10^{-8}$–$10^{-6}$ M) of Ang II in renal fibroblasts on (**A**) immunoglobulin binding protein (BiP); (**B**) protein disulfide isomerase family A member 6 (PDIA6); (**C**) CCAAT-enhancer-binding protein homologous protein (CHOP) and (**D**) activating transcription factor 6-alpha (ATF6$\alpha$) protein expression. Effects of 4-PBA (4 $\mu$M) on (**E**) superoxide anion production in renal fibroblasts treated with Ang II ($10^{-6}$ M) for 24 h. Representative microphotographs and quantification of cells labelled with the oxidative dye hydroethidine (magnification 40×); (**F**) collagen I, interleukin-6 (IL-6), C-C motif chemokine ligand 2 (CCL-2) and osteopontin mRNA expression in Ang II ($10^{-6}$M) for 24 h. *$P$<0.05; **$P$<0.01; *** $P$<0.001 versus control cells; †$P$<0.05; ††$P$<0.01; †††$P$<0.001 versus Ang II-treated cells.

*Clinical Science* (2021) **135** 143–159
https://doi.org/10.1042/CS20201137

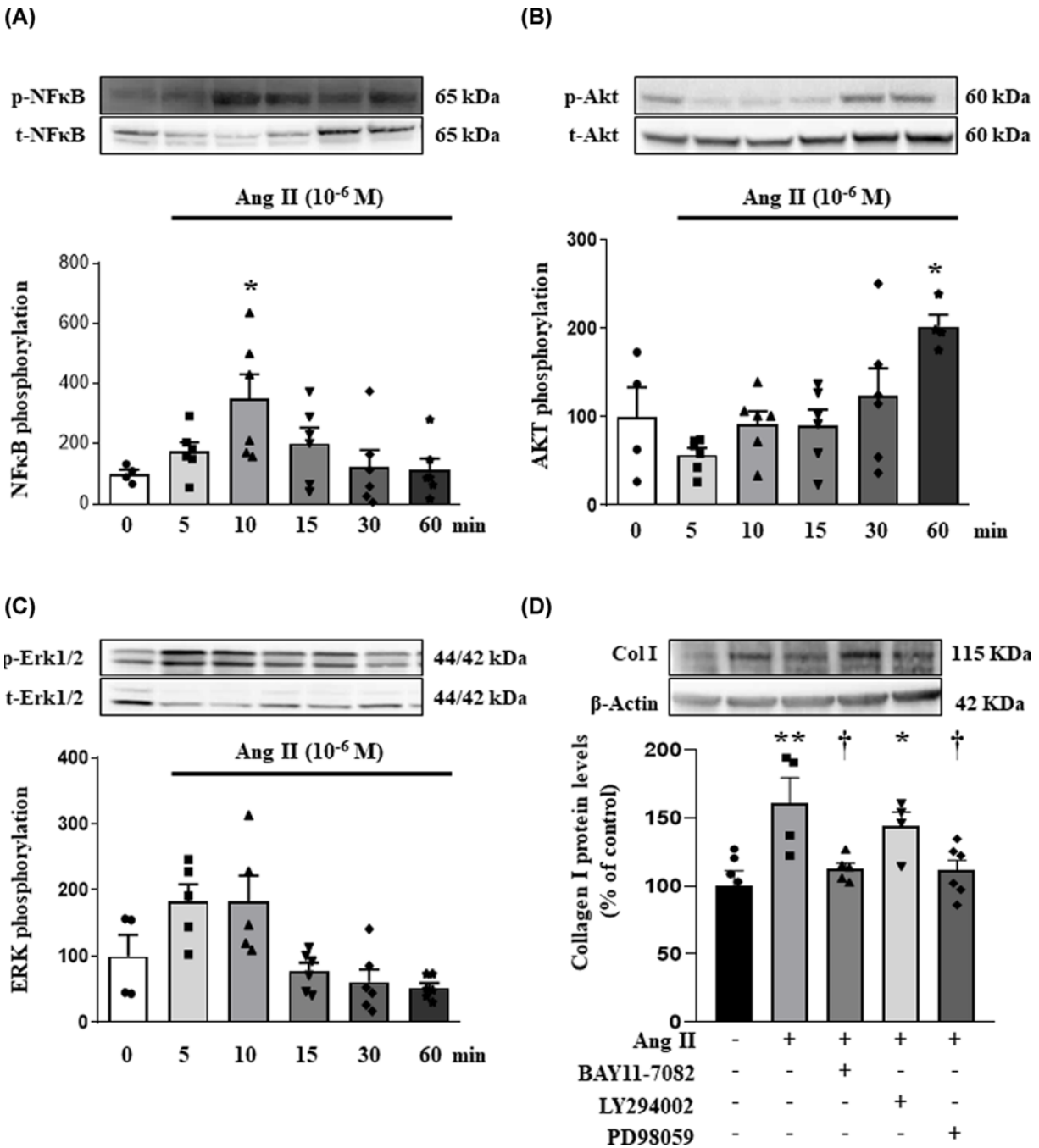


**Figure 6. NFκB and ERK 1/2 mediate the profibrotic actions of angiotensin II (Ang II) in renal fibroblasts**

Phosphorylation of (**A**) NFκB (p-NFκB, nuclear factor-κB; B); (**B**) Akt (p-Akt, protein kinase B) and (**C**) ERK 1/2 (p-ERK1/2, extracellular signal-regulated kinases 1/2) in renal fibroblasts treated with Ang II ($10^{-6}$M) for 24 h. (**D**) Effects of the NFκB inhibitor, BAY 11-7082 ($10^{-6}$ M), AKT inhibitor, LY294002 ($10^{-6}$ M) or ERK 1/2 inhibitor, PD98059 ($10^{-6}$ M) on collagen type I protein synthesis induced by Ang II. Bar graphs represent the mean ± SEM of four to six assays normalized to total NFκB, total Akt, total ERK 1/2 or β-actin; *$P<0.05$; **$P<0.01$ versus control cells; †$P<0.05$ versus Ang II-treated cells.

including heart failure, hypertension or kidney diseases [30–32]. In fact, patients with cardiorenal syndrome present an increase in reactive oxygen species (ROS) [33]. It has been postulated that ROS generation is responsible for IL-6 production linking oxidative stress with inflammation. In line with this, patients with cardiorenal syndrome presented an increase in oxidative stress markers accompanied by higher levels of IL-6 [33]. In agreement with this, MI

rats presented an increase in two inflammatory markers at renal level such as IL-6 and TNF-α. These observations are in agreement with the study performed by Cho et al., which describe that MI is associated with renal macrophages infiltration and TNF-α and IL-6 up-regulation at kidney level in rats subjected to ligation of the left anterior descending coronary artery [10]. In addition, macrophage depletion is able to blunt the development of renal fibrosis in MI rats, thus showing the role of inflammation in kidney fibrosis [10]. Despite the fact that macrophage depletion improved renal fibrosis, it was not able to recover cardiac function after MI induction, indicating the complexity of this pathological situation and supporting the necessity to discover the additional mechanisms involved in the development of fibrosis as well as inflammation in this context.

ER is an organelle essential for protein biosynthesis and post-translational modifications, which is very sensitive to unfolded and misfolded proteins in the lumen of ER. In those situations, ER induces ER stress and activates the UPR to enhance degradation of misfolded proteins [34]. On the other hand, if ER is sustained, it triggers inflammation and apoptosis [35]. Several pathologies have been associated with ER stress activation such as diabetes mellitus [36], cardiovascular disease [37], obesity [38] as well as chronic kidney disease [39]; however, the effect of MI in ER stress activation at renal level is not analyzed. In our study, we observed that ER stress is activated at renal level 4 weeks post-MI showing the possible role of ER stress in ECM production at renal level after MI. Accordingly, several studies have demonstrated the role of ER stress in the development of fibrosis. ER stress has been associated with myocardial fibrosis in different pathological situations such as obesity, pressure overload or hypertension [40–42]. At renal level, it has been also related to fibrosis. The pharmacological inhibition of ER stress was able to prevent fibrosis in an animal model of unilateral ureteral obstruction and the profibrotic effects of TGF-β in tubular cells [43]. Genetic disruption of ATF6α prevented collagen I up-regulation and promoted less tubulointerstitial fibrosis in an animal model of unilateral ischemia reperfusion injury [44]. Similarly, we have observed an increase at renal level in ATF6α levels after MI without modifications in CHOP, which has been described as a mediator of apoptosis [45]. ATF6α has been reported as a key regulator in lipid metabolism antagonizing the activity of sterol regulatory element-binding proteins [46] and its depletion reduces lipid accumulation within the kidneys of mice after ischemia–reperfusion [44]. In this sense, a high intake of saturated fatty acids is considered an important risk factor for coronary heart disease through to its ability to raise low-density lipoprotein cholesterol. It has been demonstrated the relevance of different across types of saturated fatty acids based on the chain-length on cardiovascular diseases and in MI [47]. In this sense, PA (C16:0) is associated with high coronary heart disease while other saturated fatty acids with other carbon chain lengths were not in a prospective cohort study [48]. Martínez-García et al., have demonstrated that lipotoxicity induced by PA, promoted ER stress activation and insulin resistance by disturbing the cytoarchitecture in podocytes [19]; however, the effects of PA on renal fibroblasts are not studied. Several cell types are involved in renal injury and renal fibrosis. It has been previously described that resident tubular epithelial cells, endothelial cells, vascular smooth muscle cells, fibroblasts or inflammatory cells could promote renal fibrosis through different mechanisms such as sources of renal fibroblasts via endothelial-to-mesenchymal transition, prooxidant or proinflammatory effects [49–51]. Renal fibroblasts are one of the cell types responsible for ECM production and the consequent development of renal fibrosis. We have confirmed the role of PA on ER stress activation in renal fibroblasts. In addition, we observed that PA exerts direct profibrotic, prooxidant and proinflammatory actions in renal fibroblasts showing its detrimental role at renal level. ER stress activation seems to play an important role in these modifications since the pharmacological inhibition of ER stress by 4-PBA was able to prevent all the PA effects in renal fibroblasts.

In human proximal tubule epithelial cells, PA has been demonstrated to induce ER stress as well as Ang II in cultured medium. In addition, the blockade of Ang II receptor I with valsartan or the treatment with the renin inhibitor, aliskiren, was able to prevent the ER stress induction by PA in the renal cells [52], supporting that Ang II could mediate the activation of ER stress induced by PA. In renal fibroblasts, Ang II has been shown to increase collagen I and TGF-β protein levels, an effect accompanied by an increase in superoxide anion production [53]. In fact, treatments against renin–angiotensin–aldosterone system are the standard strategies to preserve renal function in chronic kidney diseases [53]. Ang II is recognized as one of the modifiable risk factors involved in several pathologies such as myocardial infarction [54]. Ang II exerts paracrine and autocrine effects increasing the vascular resistance and impairing the correct function of the cardiovascular and renal systems. Activation of the renin–angiotensin system has several haemodynamic and humoral consequences promoting cardiac and renal damage among others [55]. An excess of Ang II promotes sarcolemmic permeability, cell death, an increase in vascular permeability due to the destruction of endothelial cells. All of these events lead to the replacement of contractile tissue by fibrotic one. Different mechanisms have been demonstrated in the detrimental role of Ang II such as tissue hypertrophy [56], oxidative stress [57] or pro-inflammatory activity, which finally trigger the fibrotic response affecting the correct function of the tissue such as heart or kidneys showing that elevated levels of Ang II as a cardiovascular risk factor. In the present study we observed an increase in Ang II plasma levels in MI rats as compared to control ones. In animal models of

*Clinical Science* (2021) **135** 143–159
https://doi.org/10.1042/CS20201137

MI, blockade of receptor type I of Ang II or inhibition of angiotensin converting enzyme has been demonstrated to improve glomerular damage and inflammatory cell infiltration in kidneys [58]; however, its effects on renal fibrosis have not presented a major improvement [8]. Our data show that NFκB and ERK1/2 pathways mediate the profibrotic effects of Ang II. In previous studies, the effects of Ang II on ER stress activation have been described. Ang II is able to induce ER stress in podocytes [59] in macrophages [60] and mesangial cells [61]. In the study, we have corroborated the profibrotic, proinflammatory and prooxidant effects of Ang II in renal fibroblasts. These alterations seem to be mediated by ER stress activation since (i) Ang II was able to induce ER stress and (ii) the presence of 4-PBA in the culture medium prevented the increase in collagen I, superoxide anion production and the inflammatory markers in Ang II-treated fibroblasts.

In summary, we have demonstrated that the renal alterations observed in MI rats were accompanied by ER stress activation. Inhibition of ER stress prevented the increase in ECM proteins, ROS production and inflammatory markers in PA or Ang II-treated renal fibroblasts.

## Limitations

A limitation of our study must be acknowledged regarding the age and that the majority of MI patients were male showing the profile of patients admitted in the emergency room with MI code at the time of inclusion in the study. However, whether these differences in age or gender distribution with the reference group of subjects could impact or influence the interpretation of the clinical data need further work.

## Clinical perspectives

- MI is associated with renal alterations resulting in poor outcomes in patients with MI. Renal fibrosis and inflammation are common features of chronic kidney diseases and play a critical role in renal dysfunction contributing to mortality complications. However, the mechanisms involved in renal alterations in MI are not fully established and there is not an effective treatment, with new strategies being mandatory for treating it.

- In the present study, we demonstrate that MI is associated with renal alterations including ER stress activation. In addition, ER stress is associated with renal interstitial fibrosis in animals with MI. In renal fibroblasts, ER stress mediates the profibrotic, prooxidant and proinflammatory effects of PA and Ang II in these cells.

- Our findings suggest the potential role of ER stress in the renal fibrosis in the context of MI, suggesting new therapeutic approaches in the management of MI for the treatment of kidney dysfunction, as well as in pathological situations with high levels of Ang II or PA (lipotoxicity).

### Data Availability

The data that support the findings of this study are available from the corresponding authors upon reasonable request.

### Competing Interests

The authors declare that there are no competing interests associated with the manuscript.

### Funding

This work was supported by Instituto de Salud Carlos III-Fondo Europeo de Desarrollo Regional (FEDER) [grant numbers PI18/00257; PI15/00742; CIBERCV]. B.D-V was supported by a grant P-FIS [grant number FI19/00277]. E.M-M was supported by a contract from CAM (Atracción de talento) and A.R-M was supported by a contract from CAM (Ayuda de empleo juvenil PEJ-2018-TL/BMD-11906).

### CRediT Author Contribution

**Ernesto Martínez-Martínez:** Conceptualization, Resources, Data curation, Formal analysis, Supervision, Funding acquisition, Investigation, Writing—original draft. **Beatriz Delgado-Valero:** Data curation, Investigation, Writing—review and editing. **Lucía de la Fuente-Chávez:** Data curation, Investigation. **Ana Romero-Miranda:** Investigation. **María Vistación Bartolomé:**

Writing—review and editing. **Bunty Ramachandi:** Investigation, Writing—review and editing. **Fabián Islas:** Investigation, Methodology, Writing—review and editing. **María Luaces:** Investigation, Methodology, Writing—review and editing. **Victoria Cachofeiro:** Conceptualization, Resources, Data curation, Formal analysis, Supervision, Funding acquisition, Investigation, Writing—original draft.

## Acknowledgements

We thank Raquel Jurado-López, Avelina Hidalgo, Virginia Peinado, and Daniel Fernández for their technical help. We thank Anthony DeMarco for his help in editing.

## Abbreviations

α-SMA, alpha-smooth muscle actin; 4-HNE, 4-hydroxynonenal; 4-PBA, 4- phenylbutyric acid; AKT, protein kinase B; Ang II, Angiotensin II; ATF6, activating transcription factor 6; BiP, immunoglobulin binding protein; BMI, body mass index; CCL-2, C-C motif chemokine ligand 2; CHOP, CCAAT-enhancer-binding protein homologous protein; CTGF, connective tissue growth factor; ECM, extracellular matrix; ER, endoplasmic reticulum; ERK 1/2, extracellular signal-regulated kinases 1/2; GAPDH, glyceraldehyde-3-phosphate dehydrogenase; HPRT, hypoxanthine-guanine phosphoribosyltransferase; IL-6, interleukin-6; IRE-1, inositol requiring 1; KIM-1, kidney injury marker-1; LAD, left anterior descendent; MI, myocardial infarction; NFκB, nuclear factor-κB; NGAL, neutrophil gelatinase-associated lipocalin; PA, palmitic acid; PDIA6, protein disulfide isomerase family A member 6; PERK, PKR-like ER kinase; ROS, reactive oxygen species; SBP, systolic blood pressure; TBAR, thiobarbituric acid reactive substance; TFB, renal tube fibroblast; TGF-β, transforming growth factor-beta; TNF-α, tumor necrosis factor-alpha; UPR, unfolded protein response.

# References

1 Ronco, C. and Di Lullo, L. (2014) Cardiorenal syndrome. *Heart Fail. Clin.* **10**, 251–280, https://doi.org/10.1016/j.hfc.2013.12.003
2 Ronco, C. (2011) The Cardiorenal Syndrome: Basis and Common Ground for a Multidisciplinary Patient-Oriented Therapy. *Cardiorenal. Med.* **1**, 3–4, https://doi.org/10.1159/000323352
3 Fabbian, F., Pala, M., De Giorgi, A., Scalone, A., Molino, C., Portaluppi, F. et al. (2011) Clinical features of cardio-renal syndrome in a cohort of consecutive patients admitted to an internal medicine ward. *Open Cardiovasc. Med. J.* **5**, 220–225, https://doi.org/10.2174/1874192401105010220
4 Szymanski, M.K., de Boer, R.A., Navis, G.J., van Gilst, W.H. and Hillege, H.L. (2012) Animal models of cardiorenal syndrome: a review. *Heart Fail. Rev.* **17**, 411–420, https://doi.org/10.1007/s10741-011-9279-6
5 Goldberg, A., Kogan, E., Hammerman, H., Markiewicz, W. and Aronson, D. (2009) The impact of transient and persistent acute kidney injury on long-term outcomes after acute myocardial infarction. *Kidney Int.* **76**, 900–906, https://doi.org/10.1038/ki.2009.295
6 Lekawanvijit, S., Kompa, A.R., Zhang, Y., Wang, B.H., Kelly, D.J. and Krum, H. (2012) Myocardial infarction impairs renal function, induces renal interstitial fibrosis, and increases renal KIM-1 expression: implications for cardiorenal syndrome. *Am. J. Physiol. Heart Circ. Physiol.* **302**, H1884–H1893, https://doi.org/10.1152/ajpheart.00967.2011
7 Ranganathan, P., Jayakumar, C., Tang, Y., Park, K.M., Teoh, J.P., Su, H. et al. (2015) MicroRNA-150 deletion in mice protects kidney from myocardial infarction-induced acute kidney injury. *Am. J. Physiol. Renal. Physiol.* **309**, F551–F558, https://doi.org/10.1152/ajprenal.00076.2015
8 Prakoura, N., Hadchouel, J. and Chatziantoniou, C. (2019) Novel Targets for Therapy of Renal Fibrosis. *J. Histochem. Cytochem.* **67**, 701–715, https://doi.org/10.1369/0022155419849386
9 Nogueira, A., Pires, M.J. and Oliveira, P.A. (2017) Pathophysiological Mechanisms of Renal Fibrosis: A Review of Animal Models and Therapeutic Strategies. *In Vivo* **31**, 1–22, https://doi.org/10.21873/invivo.11019
10 Cho, E., Kim, M., Ko, Y.S., Lee, H.Y., Song, M., Kim, M.G. et al. (2013) Role of inflammation in the pathogenesis of cardiorenal syndrome in a rat myocardial infarction model. *Nephrol. Dial. Transplant.* **28**, 2766–2778, https://doi.org/10.1093/ndt/gft376
11 Kimura, K., Jin, H., Ogawa, M. and Aoe, T. (2008) Dysfunction of the ER chaperone BiP accelerates the renal tubular injury. *Biochem. Biophys. Res. Commun.* **366**, 1048–1053, https://doi.org/10.1016/j.bbrc.2007.12.098
12 Foufelle, F. and Fromenty, B. (2016) Role of endoplasmic reticulum stress in drug-induced toxicity. *Pharmacol. Res. Perspect.* **4**, e00211, https://doi.org/10.1002/prp2.211
13 Zhuang, A. and Forbes, J.M. (2014) Stress in the kidney is the road to pERdition: is endoplasmic reticulum stress a pathogenic mediator of diabetic nephropathy? *J. Endocrinol.* **222**, R97–R111, https://doi.org/10.1530/JOE-13-0517
14 Gao, X., Fu, L., Xiao, M., Xu, C., Sun, L., Zhang, T. et al. (2012) The nephroprotective effect of tauroursodeoxycholic acid on ischaemia/reperfusion-induced acute kidney injury by inhibiting endoplasmic reticulum stress. *Basic Clin. Pharmacol. Toxicol.* **111**, 14–23, https://doi.org/10.1111/j.1742-7843.2011.00854.x
15 Mohammed-Ali, Z., Lu, C., Marway, M.K., Carlisle, R.E., Ask, K., Lukic, D. et al. (2017) Endoplasmic reticulum stress inhibition attenuates hypertensive chronic kidney disease through reduction in proteinuria. *Sci. Rep.* **7**, 41572, https://doi.org/10.1038/srep41572
16 Oslowski, C.M. and Urano, F. (2011) Measuring ER stress and the unfolded protein response using mammalian tissue culture system. *Methods Enzymol.* **490**, 71–92, https://doi.org/10.1016/B978-0-12-385114-7.00004-0
17 Lee, A.S. (2005) The ER chaperone and signaling regulator GRP78/BiP as a monitor of endoplasmic reticulum stress. *Methods* **35**, 373–381, https://doi.org/10.1016/j.ymeth.2004.10.010

18 Song, S., Tan, J., Miao, Y., Li, M. and Zhang, Q. (2017) Crosstalk of autophagy and apoptosis: Involvement of the dual role of autophagy under ER stress. *J. Cell. Physiol.* **232**, 2977–2984, https://doi.org/10.1002/jcp.25785
19 Martinez-Garcia, C., Izquierdo-Lahuerta, A., Vivas, Y., Velasco, I., Yeo, T.K., Chen, S. et al. (2015) Renal Lipotoxicity-Associated Inflammation and Insulin Resistance Affects Actin Cytoskeleton Organization in Podocytes. *PLoS ONE* **10**, e0142291, https://doi.org/10.1371/journal.pone.0142291
20 Thygesen, K., Alpert, J.S., Jaffe, A.S., Simoons, M.L., Chaitman, B.R., White, H.D. et al. (2012) Third universal definition of myocardial infarction. *Eur. Heart J.* **33**, 2551–2567, https://doi.org/10.1093/eurheartj/ehs184
21 Marin-Royo, G., Ortega-Hernandez, A., Martinez-Martinez, E., Jurado-Lopez, R., Luaces, M., Islas, F. et al. (2019) The Impact of Cardiac Lipotoxicity on Cardiac Function and Mirnas Signature in Obese and Non-Obese Rats with Myocardial Infarction. *Sci. Rep.* **9**, 444, https://doi.org/10.1038/s41598-018-36914-y
22 Serafim, V., Tiugan, D.A., Andreescu, N., Mihailescu, A., Paul, C., Velea, I. et al. (2019) Development and Validation of a LC(-)MS/MS-Based Assay for Quantification of Free and Total Omega 3 and 6 Fatty Acids from Human Plasma. *Molecules* **24**, https://doi.org/10.3390/molecules24020360
23 Martinez-Martinez, E., Jurado-Lopez, R., Valero-Munoz, M., Bartolome, M.V., Ballesteros, S., Luaces, M. et al. (2014) Leptin induces cardiac fibrosis through galectin-3, mTOR and oxidative stress: potential role in obesity. *J. Hypertens.* **32**, 1104–1114, discussion 1114, https://doi.org/10.1097/HJH.0000000000000149
24 Zheng, G., Cai, J., Chen, X., Chen, L., Ge, W., Zhou, X. et al. (2017) Relaxin Ameliorates Renal Fibrosis and Expression of Endothelial Cell Transition Markers in Rats of Isoproterenol-Induced Heart Failure. *Biol. Pharm. Bull.* **40**, 960–966, https://doi.org/10.1248/bpb.b16-00882
25 Merdler, I., Rozenfeld, K.L., Zahler, D., Shtark, M., Goldiner, I., Loewenstein, I.S. et al. (2020) Neutrophil Gelatinase-Associated Lipocalin for the Early Prediction of Acute Kidney Injury in ST-Segment Elevation Myocardial Infarction Patients Treated with Primary Percutaneous Coronary Intervention. *Cardiorenal. Med.* **10**, 154–161, https://doi.org/10.1159/000506378
26 Shroff, G.R., Frederick, P.D. and Herzog, C.A. (2012) Renal failure and acute myocardial infarction: clinical characteristics in patients with advanced chronic kidney disease, on dialysis, and without chronic kidney disease. A collaborative project of the United States Renal Data System/National Institutes of Health and the National Registry of Myocardial Infarction. *Am. Heart J.* **163**, 399–406, https://doi.org/10.1016/j.ahj.2011.12.002
27 Lekston, A., Kurek, A. and Tynior, B. (2009) Impaired renal function in acute myocardial infarction. *Cardiol. J.* **16**, 400–406
28 Kumpers, P., Hafer, C., Lukasz, A., Lichtinghagen, R., Brand, K., Fliser, D. et al. (2010) Serum neutrophil gelatinase-associated lipocalin at inception of renal replacement therapy predicts survival in critically ill patients with acute kidney injury. *Crit. Care* **14**, R9, https://doi.org/10.1186/cc8861
29 Efstratiadis, G., Divani, M., Katsioulis, E. and Vergoulas, G. (2009) Renal fibrosis. *Hippokratia* **13**, 224–229
30 Guo, H., Xu, D., Kuroki, M., Lu, Z., Xu, X., Geurts, A. et al. (2020) Kidney failure, arterial hypertension and left ventricular hypertrophy in rats with loss of function mutation of SOD3. *Free Radic. Biol. Med.* **152**, 787–796, https://doi.org/10.1016/j.freeradbiomed.2020.01.023
31 van der Pol, A., van Gilst, W.H., Voors, A.A. and van der Meer, P. (2019) Treating oxidative stress in heart failure: past, present and future. *Eur. J. Heart Fail.* **21**, 425–435, https://doi.org/10.1002/ejhf.1320
32 Matoba, K., Takeda, Y., Nagai, Y., Yokota, T., Utsunomiya, K. and Nishimura, R. (2020) Targeting Redox Imbalance as an Approach for Diabetic Kidney Disease. *Biomedicines* **8**, https://doi.org/10.3390/biomedicines8020040
33 Virzi, M., Clementi, A., de Cal, M., Brocca, A., Day, S., Pastori, S. et al. (2015) Oxidative stress: dual pathway induction in cardiorenal syndrome type 1 pathogenesis. *Oxid. Med. Cell Longev.* **2015**, 391790, https://doi.org/10.1155/2015/391790
34 Liu, Y., Wang, Y., Ding, W. and Wang, Y. (2018) Mito-TEMPO Alleviates Renal Fibrosis by Reducing Inflammation, Mitochondrial Dysfunction, and Endoplasmic Reticulum Stress. *Oxid. Med. Cell Longev.* **2018**, 5828120, https://doi.org/10.1155/2018/5828120
35 Karna, K.K., Shin, Y.S., Choi, B.R., Kim, H.K. and Park, J.K. (2019) The Role of Endoplasmic Reticulum Stress Response in Male Reproductive Physiology and Pathology: A Review. *World J. Mens Health* **38**, https://doi.org/10.5534/wjmh.190038
36 Ghosh, R., Colon-Negron, K. and Papa, F.R. (2019) Endoplasmic reticulum stress, degeneration of pancreatic islet beta-cells, and therapeutic modulation of the unfolded protein response in diabetes. *Mol. Metab.* **27S**, S60–S68, https://doi.org/10.1016/j.molmet.2019.06.012
37 Yang, Y., Zhou, Q., Gao, A., Chen, L. and Li, L. (2020) Endoplasmic reticulum stress and focused drug discovery in cardiovascular disease. *Clin. Chim. Acta* **504**, 125–137, https://doi.org/10.1016/j.cca.2020.01.031
38 Pagliassotti, M.J., Kim, P.Y., Estrada, A.L., Stewart, C.M. and Gentile, C.L. (2016) Endoplasmic reticulum stress in obesity and obesity-related disorders: An expanded view. *Metabolism* **65**, 1238–1246, https://doi.org/10.1016/j.metabol.2016.05.002
39 Ricciardi, C.A. and Gnudi, L. (2019) Endoplasmic Reticulum stress in chronic kidney disease. New molecular targets from bench to the bedside. *G. Ital. Nefrol.* **36**
40 Li, S.J., Liu, C.H., Chu, H.P., Mersmann, H.J., Ding, S.T., Chu, C.H. et al. (2017) The high-fat diet induces myocardial fibrosis in the metabolically healthy obese minipigs-The role of ER stress and oxidative stress. *Clin. Nutr.* **36**, 760–767, https://doi.org/10.1016/j.clnu.2016.06.002
41 Luo, T., Chen, B. and Wang, X. (2015) 4-PBA prevents pressure overload-induced myocardial hypertrophy and interstitial fibrosis by attenuating endoplasmic reticulum stress. *Chem. Biol. Interact.* **242**, 99–106, https://doi.org/10.1016/j.cbi.2015.09.025
42 Kassan, M., Galan, M., Partyka, M., Saifudeen, Z., Henrion, D., Trebak, M. et al. (2012) Endoplasmic reticulum stress is involved in cardiac damage and vascular endothelial dysfunction in hypertensive mice. *Arterioscler. Thromb. Vasc. Biol.* **32**, 1652–1661, https://doi.org/10.1161/ATVBAHA.112.249318
43 Liu, S.H., Yang, C.C., Chan, D.C., Wu, C.T., Chen, L.P., Huang, J.W. et al. (2016) Chemical chaperon 4-phenylbutyrate protects against the endoplasmic reticulum stress-mediated renal fibrosis in vivo and in vitro. *Oncotarget* **7**, 22116–22127, https://doi.org/10.18632/oncotarget.7904
44 Jao, T.M., Nangaku, M., Wu, C.H., Sugahara, M., Saito, H., Maekawa, H. et al. (2019) ATF6alpha downregulation of PPARalpha promotes lipotoxicity-induced tubulointerstitial fibrosis. *Kidney Int.* **95**, 577–589, https://doi.org/10.1016/j.kint.2018.09.023
45 Nishitoh, H. (2012) CHOP is a multifunctional transcription factor in the ER stress response. *J. Biochem.* **151**, 217–219, https://doi.org/10.1093/jb/mvr143
46 Zeng, L., Lu, M., Mori, K., Luo, S., Lee, A.S., Zhu, Y. et al. (2004) ATF6 modulates SREBP2-mediated lipogenesis. *EMBO J.* **23**, 950–958, https://doi.org/10.1038/sj.emboj.7600106

47 Praagman, J., Vissers, L.E.T., Mulligan, A.A., Laursen, A.S.D., Beulens, J.W.J., van der Schouw, Y.T. et al. (2019) Consumption of individual saturated fatty acids and the risk of myocardial infarction in a U.K. and a Danish cohort. *Int. J. Cardiol.* **279**, 18–26, https://doi.org/10.1016/j.ijcard.2018.10.064
48 Praagman, J., de Jonge, E.A., Kiefte-de Jong, J.C., Beulens, J.W., Sluijs, I., Schoufour, J.D. et al. (2016) Dietary Saturated Fatty Acids and Coronary Heart Disease Risk in a Dutch Middle-Aged and Elderly Population. *Arterioscler. Thromb. Vasc. Biol.* **36**, 2011–2018, https://doi.org/10.1161/ATVBAHA.116.307578
49 Yang, L., Besschetnova, T.Y., Brooks, C.R., Shah, J.V. and Bonventre, J.V. (2010) Epithelial cell cycle arrest in G2/M mediates kidney fibrosis after injury. *Nat. Med.* **16**, 535–543, 531p following 143, https://doi.org/10.1038/nm.2144
50 Zeisberg, E.M., Potenta, S.E., Sugimoto, H., Zeisberg, M. and Kalluri, R. (2008) Fibroblasts in kidney fibrosis emerge via endothelial-to-mesenchymal transition. *J. Am. Soc. Nephrol.* **19**, 2282–2287, https://doi.org/10.1681/ASN.2008050513
51 Boor, P., Ostendorf, T. and Floege, J. (2010) Renal fibrosis: novel insights into mechanisms and therapeutic targets. *Nat. Rev. Nephrol.* **6**, 643–656, https://doi.org/10.1038/nrneph.2010.120
52 Li, C., Lin, Y., Luo, R., Chen, S., Wang, F., Zheng, P. et al. (2016) Intrarenal renin-angiotensin system mediates fatty acid-induced ER stress in the kidney. *Am. J. Physiol. Renal. Physiol.* **310**, F351–F363, https://doi.org/10.1152/ajprenal.00223.2015
53 Shen, Y., Miao, N.J., Xu, J.L., Gan, X.X., Xu, D., Zhou, L. et al. (2016) N-acetylcysteine alleviates angiotensin II-mediated renal fibrosis in mouse obstructed kidneys. *Acta Pharmacol. Sin.* **37**, 637–644, https://doi.org/10.1038/aps.2016.12
54 Gavras, I. and Gavras, H. (2002) Angiotensin II as a cardiovascular risk factor. *J. Hum. Hypertens.* **16**, S2–S6, https://doi.org/10.1038/sj.jhh.1001392
55 Reina-Couto, M., Afonso, J., Carvalho, J., Morgado, L., Ronchi, F.A., de Oliveira Leite, A.P. et al. (2020) Interrelationship between renin-angiotensin-aldosterone system and oxidative stress in chronic heart failure patients with or without renal impairment. *Biomed. Pharmacother.* **133**, 110938, https://doi.org/10.1016/j.biopha.2020.110938
56 Kagiyama, S., Eguchi, S., Frank, G.D., Inagami, T., Zhang, Y.C. and Phillips, M.I. (2002) Angiotensin II-induced cardiac hypertrophy and hypertension are attenuated by epidermal growth factor receptor antisense. *Circulation* **106**, 909–912, https://doi.org/10.1161/01.CIR.0000030181.63741.56
57 Ritz, E. and Haxsen, V. (2003) Angiotensin II and oxidative stress: an unholy alliance. *J. Am. Soc. Nephrol.* **14**, 2985–2987, https://doi.org/10.1097/01.ASN.0000096784.86791.21
58 Wen, Z., Cai, M., Mai, Z., Chen, Y., Geng, D. and Wang, J. (2013) Protection of renal impairment by angiotensin II type 1 receptor blocker in rats with post-infarction heart failure. *Ren. Fail.* **35**, 766–775, https://doi.org/10.3109/0886022X.2013.780561
59 Ha, T.S., Park, H.Y., Seong, S.B. and Ahn, H.Y. (2015) Angiotensin II induces endoplasmic reticulum stress in podocyte, which would be further augmented by PI3-kinase inhibition. *Clin. Hypertens* **21**, 13, https://doi.org/10.1186/s40885-015-0018-5
60 Yang, J., Zhang, X., Yu, X., Tang, W. and Gan, H. (2017) Renin-angiotensin system activation accelerates atherosclerosis in experimental renal failure by promoting endoplasmic reticulum stress-related inflammation. *Int. J. Mol. Med.* **39**, 613–621, https://doi.org/10.3892/ijmm.2017.2856
61 Wang, T.N., Chen, X., Li, R., Gao, B., Mohammed-Ali, Z., Lu, C. et al. (2015) SREBP-1 Mediates Angiotensin II-Induced TGF-beta1 Upregulation and Glomerular Fibrosis. *J. Am. Soc. Nephrol.* **26**, 1839–1854, https://doi.org/10.1681/ASN.2013121332

cells

MDPI

*Review*

# Fibrosis, the Bad Actor in Cardiorenal Syndromes: Mechanisms Involved

**Beatriz Delgado-Valero [1], Victoria Cachofeiro [1,2,*] and Ernesto Martínez-Martínez [1,2,*]**

[1] Departamento de Fisiología, Facultad de Medicina, Instituto de Investigación Sanitaria Gregorio Marañón (IiSGM), Universidad Complutense de Madrid, 28040 Madrid, Spain; beadel02@ucm.es
[2] Ciber de Enfermedades Cardiovasculares (CIBERCV), Instituto de Salud Carlos III, 28029 Madrid, Spain
* Correspondence: vcara@ucm.es (V.C.); ernmarti@ucm.es (E.M.-M.); Tel.: +34-913-941-489 (V.C. & E.M.-M.)

**Abstract:** Cardiorenal syndrome is a term that defines the complex bidirectional nature of the interaction between cardiac and renal disease. It is well established that patients with kidney disease have higher incidence of cardiovascular comorbidities and that renal dysfunction is a significant threat to the prognosis of patients with cardiac disease. Fibrosis is a common characteristic of organ injury progression that has been proposed not only as a marker but also as an important driver of the pathophysiology of cardiorenal syndromes. Due to the relevance of fibrosis, its study might give insight into the mechanisms and targets that could potentially be modulated to prevent fibrosis development. The aim of this review was to summarize some of the pathophysiological pathways involved in the fibrotic damage seen in cardiorenal syndromes, such as inflammation, oxidative stress and endoplasmic reticulum stress, which are known to be triggers and mediators of fibrosis.

**Keywords:** cardiorenal syndrome; endoplasmic reticulum stress; fibrosis; heart failure; inflammation; kidney disease; oxidative stress



**Citation:** Delgado-Valero, B.; Cachofeiro, V.; Martínez-Martínez, E. Fibrosis, the Bad Actor in Cardiorenal Syndromes: Mechanisms Involved. *Cells* **2021**, *10*, 1824. https://doi.org/10.3390/cells10071824

Academic Editors: David J. Grieve and Alexander E. Kalyuzhny

Received: 31 May 2021
Accepted: 13 July 2021
Published: 19 July 2021



## 1. Introduction

The existence of a relationship between the heart and the kidney was first described in the XIX century by Robert Bright, who reported structural changes in the heart in patients with advanced kidney disease [1]. Since then, new discoveries have given insight into the interaction between heart and kidney diseases in terms of shared risk factors (such as hypertension, obesity, diabetes and atherosclerosis) and the pathophysiological pathways involved in each [2–4]. Clinically, the shared pathology of the heart and kidneys has a strong impact on the clinical outcome and is associated with increased morbidity and mortality rates [5,6].

The classic definition of cardiorenal syndrome (CRS) was proposed in 2010 by the Acute Dialysis Quality Initiative as a term that gathers the "disorders of the heart and kidneys whereby acute or chronic dysfunction in one organ may induce acute or chronic dysfunction of the other" [7]. In addition, within the term there is further classification into different subtypes according to the primary organ dysfunction and to whether it is an acute or chronic situation [7]. However, the appearance of risk factors that can affect both the heart and the kidney complicate the clinical picture, and with it the causal relationship of one to the other.

## 2. CRS Classification

### *2.1. CRS Type 1 or Acute Cardiorenal Syndrome*

CRS type 1 (CRS-1) is characterized by the worsening of cardiac function leading to acute kidney injury (AKI) and/or dysfunction of both organs [7]. Around 25–30% of patients with acute decompensated heart failure (ADHF) present AKI, often after ischemic or non-ischemic heart disease [8–10]. These patients have higher morbi-mortality and lengthier hospitalization [7]. CRS-1 has a complex pathophysiology, with hemodynamic

and non-hemodynamic alterations for which the treatments show no improvements [10,11], thus demonstrating the need to discover and understand the mechanisms involved.

Faced with a drop in blood pressure levels due to the development of heart failure (HF), the kidney responds to the decrease in cardiac output by retaining sodium and water. Nevertheless, it has been demonstrated that an elevation of the central venous pressure can result in impairment of renal function and congestion of the kidneys [10,12]. In this context, neurohormonal activation through the Renin–Angiotensin–Aldosterone System (RAAS) also has an important role, as it is both an initially compensatory mechanism for the decrease in volume consequence of the ventricular injury, and a long-term initiator of cardiovascular and renal dysfunction [13,14]. Other non-hemodynamic mechanisms, such as inflammation and oxidative stress, have been established as common pathways for cellular dysfunction in heart and kidney failure [9–11,15].

### 2.2. CRS Type 2 or Chronic Cardiorenal Syndrome

CRS type 2 is defined as chronic cardiac dysfunction that leads to progressive appearance of renal impairment that promotes the development of chronic kidney disease (CKD) [6,16,17]. CKD was defined in 2012 by Kidney Disease: Improving Global Outcomes (KDIGO) as an abnormality in kidney function or structure that is present for more than 3 months and has health implications. It is classified based on cause, a glomerular filtration rate (GFR) of <60 mL/min per 1.73 $m^2$ and the degree of albuminuria [18]. A meta-analysis by Damman et al. showed that almost a third (32%) of the total of 1 million HF patients studied presented CKD, and 23% had worsening renal function [19], confirming that renal dysfunction is an important contributor to the comorbidities in HF.

The pathological process implicated in CKD secondary to HF is a consequence of the renal response to preserve the GFR. The combination of renal congestion, hypoperfusion and the increased right atrium pressure promotes renal dysfunction in HF patients [6,11]. It has been suggested that the correct diagnosis of this CRS should be based on HF aetiology, HF with preserved ejection fraction (HFpEF) or with reduced ejection fraction (HFrEF), and on biochemical parameters of renal dysfunction, such as creatinine levels [20]. However, as the interactions between the heart and kidney are bidirectional, is not always easy to assess the inciting event from the secondary damage, thus making it difficult to differentiate CRS type 2 patients from CRS type 4 ones [11,20].

### 2.3. CRS Type 3 or Acute Reno-Cardiac Syndrome

CRS type 3 occurs when there is an acute worsening of kidney function secondary to AKI, ischemia, or glomerulonephritis that leads to acute heart injury and/or dysfunction [6,7,11]. AKI may produce cardiac events as a consequence of the fluid overload, hyperkalaemia, or metabolic acidosis, but the exact cause of the damage is difficult to establish, as there are shared comorbidities and variability in the risk factors for AKI [6,11,21,22].

There are multiple definitions of AKI according to urine output and serum creatinine levels (SCr), all of which have limitations in their clinical application [21,23]. It is due to the differing definitions of AKI that make it difficult to identify this type of CRS. Despite the lacking criteria, the incidence of AKI is increasing in hospitalized patients, and is associated with an 86% increased risk of cardiovascular mortality and a 38% increased risk of major cardiovascular events [24].

### 2.4. CRS Type 4 or Chronic Reno-Cardiac Syndrome

CRS type 4 is characterized by cardiovascular damage in patients with CKD at any stage [7,11]. It is well established that renal dysfunction is an independent risk factor for cardiovascular disease, with the risk for myocardial infection and sudden death being higher in CKD patients [25,26]. Numerous studies have found there is an independent association between the severity of CKD, evaluated by the degree of decline in kidney function, and the subsequent cardiac events [5,27,28], which could suggest that CKD likely accelerates the risk and development of cardiovascular disease [7].

CKD has been demonstrated to be associated with inflammation and other cardiovascular factors, such as hypertension, activation of RAAS, or volume overload, that usually go in parallel with a decline in GFR [26,29]. Pressure and volume overload in CKD patients lead to left ventricular hypertrophy (LVH), which is a common feature that is accompanied by fibrosis and other histological changes. These structural changes consequently cause diastolic dysfunction and increased oxygen demand, which could also explain these patients' predispositions to arrhythmias and sudden death [6,29,30].

### *2.5. CRS Type 5 or Secondary Cardiorenal Syndrome*

CRS type 5 (CRS-5) represents simultaneous injury and/or dysfunction of the heart and kidneys as a result of a systemic condition, such as sepsis, drug toxicity, lupus, cirrhosis or amyloidosis [7,23,31]. Although many pathways have been proposed, it is challenging to identify the mechanisms that are involved in CRS-5 due to the multitude of contributing factors and the sequence of organ involvement [7,31].

CRS-5 has been divided into four stages according to severity: hyperacute (0–72 h after diagnosis), acute (3–7 days), subacute (7–30 days) and chronic (beyond 30 days) [6,23]. Usually, the existing studies of CRS-5 are those of hyperacute or acute stages, as these evaluate the effects of sepsis. Sepsis, defined as a life-threatening organ dysfunction caused by a deregulated host response to infection [32], is one of the most common causes of death among hospitalized patients [33], among whom the prevalence of CRS-5 is high [7,34].

In the early stages of sepsis, microcirculatory changes are developed despite normal systemic haemodynamics [35]. Those alterations, along with inflammation, are important in the cardiac and renal dysfunction given in this type of CRS [11]. For instance, the increase in pro-inflammatory cytokines during sepsis and the decrease in renal blood flow lead to tubular necrosis, reduction in GFR and severe kidney failure [6,23,26]. Sepsis is also related to autonomic nervous system dysfunction and RAAS activation [23,31]. This complex environment makes differentiating between the cardiorenal crosstalk effects and sepsis effects very difficult.

The different CRSs are summarized in Figure 1.

**CRS type 1**

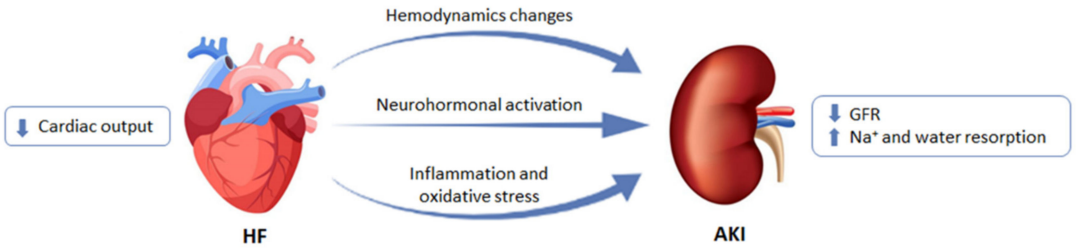


(**a**)

**Figure 1.** *Cont.*

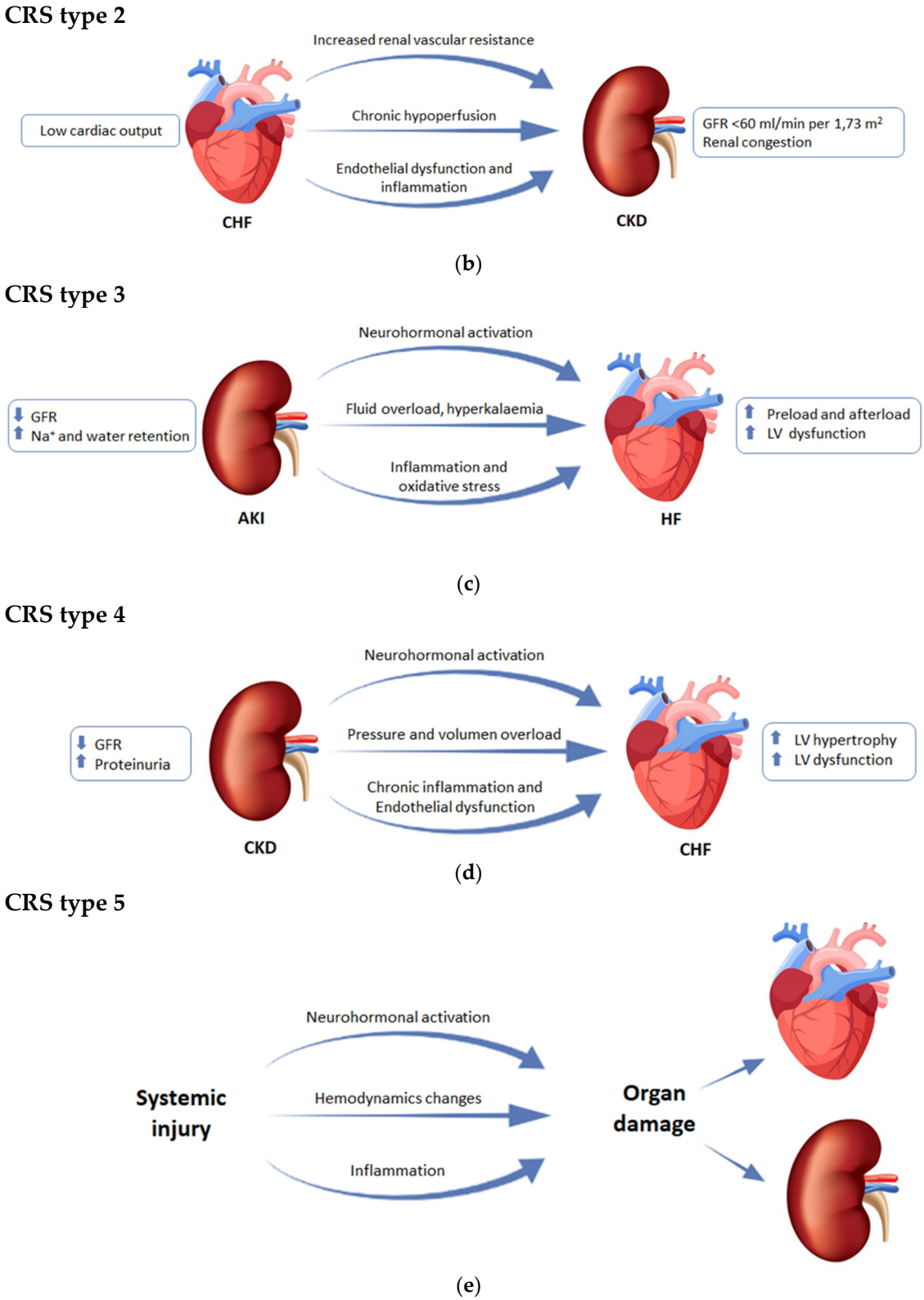


**Figure 1.** Differences among the subtypes of cardiorenal syndrome (CRS). (**a**) CRS type 1 or acute cardiorenal syndrome; (**b**) CRS type 2 or chronic cardiorenal syndrome; (**c**) CRS type 3 or acute reno-cardiac syndrome; (**d**) CRS type 4 or chronic reno-cardiac syndrome; (**e**) CRS type 5 or secondary cardiorenal syndrome. GFR: glomerular filtration rate; LV: left ventricular. Modified from [7].

## 3. Pathophysiology of CRS

Due to the essential role of both the heart and kidney in the maintenance of cardiovascular homeostasis, initial organ damage during a disease state, such as CRS, can induce structural remodelling and functional alterations in the other.

### 3.1. Cardiac Alterations Associated with CKD

As CKD is considered an important complication associated with higher cardiovascular risk and mortality. This increased risk is partially due to common risk factors such as hypertension, obesity or diabetes [36], but not entirely, as the association between CKD and cardiovascular mortality persists after risk factor adjustment [37,38]. Albuminuria- and creatinine-based estimated GFR (eGFR) are currently considered to be useful measurements for cardiovascular risk prediction, as they improve discrimination for cardiovascular mortality among CKD patients beyond traditional risk factors [38,39].

In patients with CKD there is high prevalence of structural and functional heart alterations from the early stages to end-stage renal disease (ESRD), which includes left ventricular (LV) remodelling, valvular sclerosis, reduction of the ejection fraction (EF) and diastolic dysfunction [40–42].

Echocardiographic studies have observed that LV remodelling is prevalent among patients with CKD and has been recognized as an important predictor of poor prognosis [43,44]. There are many factors that influence LV geometry in CKD patients. Pressure overload causes the thickening of the LV walls, which translates into concentric hypertrophy, whereas hypervolemia and anaemia contributes to the development of eccentric hypertrophy [45]. Two studies have reported the existence of associations between LV hypertrophy and renal dysfunction, characterized by low eGFR, which are independent of other risk factors, suggesting that impaired kidney function contributes to LV hypertrophy. In addition, they also describe that LV geometry tends to shift to concentric LV hypertrophy in advanced kidney dysfunction rather than eccentric hypertrophy [44,46]. A recent clinical study showed that the stages are associated with LV remodelling even in milder CKD, as 22% of 90 patients with stages 1 to 3 presented concentric hypertrophy, 19% eccentric hypertrophy and 20% concentric remodelling [47].

Most of the studies that have investigated the association between CKD and cardiac alterations have focused on the assessment of LV mass or hypertrophy, whilst fewer have explored LV function (neither systolic nor diastolic) [48]. In terms of LV systolic function, LVEF has been used in the majority of studies, although subclinical systolic dysfunction can happen in patients with CKD despite normal LVEF [49–51]. Diastolic dysfunction usually coexists with systolic dysfunction during LV remodelling and is common in CKD patients [44,52–54].

Numerous studies have assessed LV function in patients with CKD by trying to find an association between eGFR or albuminuria and systolic or diastolic function alterations. According to the literature, systolic dysfunction seems to be strongly correlated with albuminuria over low eGFR [55–57]. However, there is high variability. Similarly, there seems to be higher association of diastolic dysfunction with albuminuria than eGFR [56–58]. Therefore, some studies have found clear association between low eGFR, LV diastolic dysfunction and LVH [44,59].

Despite the advances made in cardiac damage, the increasing incidence and prevalence of HF makes it an important health problem. For that reason, various potential biomarkers that could contribute to diagnosis have been proposed. The gold standard in chronic HF diagnosis and prognosis is the natriuretic peptides, such as atrial natriuretic peptide (ANP) and brain natriuretic peptide (BNP), which are produced within the heart as a response to myocardial stretch as a consequence of volume or pressure overload [60,61]. HF guidelines currently recommends monitoring of BNP and its precursor, N-terminal-proBNP (NT-proBNP), for CHF progression evaluation. It must be acknowledged, however, that age, body mass, renal failure and pulmonary diseases influence its plasmatic concentrations [62]. Other molecules associated with myocyte necrosis or injury have been evaluated as HF biomarkers, such as cardiac troponins (cTn), which are regulatory proteins involved in contraction. The troponin complex is formed by cardiac troponin C (cTnC), I (cTnI) and T

(cTnT), which dissociates after $Ca^{2+}$ binds to cTnC. cTnI and cTnT are considered a reference marker of myocardial injury as its blood concentrations rise after myocyte damage [63,64].

### 3.2. Renal Alteration Associated to HF

As explained before, CRS-1 and CRS-2 are characterized by progressive kidney damage due to HF. Over 50% of HF patients have been reported to have renal insufficiency [19,65]. Indeed, even a modest reduction in renal function is associated with a higher mortality rate in cardiovascular disease patients [19,66]. The most currently used diagnostic measurements for renal damage are GFR, serum creatinine and urinary output.

The systolic blood pressure and effective arterial volume are reduced once HF develops, which translates into a decrease in renal blood flow as well as GFR [67]. In order to preserve adequate blood flow, the kidneys autoregulate through different mechanisms, including sympathetic nervous system (SNS) and RAAS activation, which would act as vasoconstrictors of the afferent and the efferent arteriole [13,68]. In the long term, this activation or the neurohormonal axis could result in podocyte injury [69,70], loss of mesangial integrity [71,72], tubular and glomerular damage [73–75] and kidney dysfunction [76], which are often associated with CKD and ESRD.

It is common to use the term kidney failure in a clinical setting to refer to a situation where there is a persistent decrease in eGFR in the short term [18]. Another important concept is worsening renal function, which is considered to appear in those patients in which the serum creatinine increases by 25% compared to the basal levels or the eGFR decreases by more than 20% in a period of around 25 weeks [77,78]. AKI is characterized by a rapid loss of kidney function that can happen in HF patients when diuresis decreases <0.5 mL/kg/h in 6–12 h or the basal serum creatinine levels increases $\geq$0.3 mg/dL in 48 h [77,78].

In addition to traditional markers of decreased glomerular filtration, such as creatinine and albuminuria [79,80], other markers, such as cystatin C [81,82] and blood urea nitrogen (BUN) [83,84], also have been proposed as possible biomarkers of tubular damage.

One of these is Neutrophil Gelatinase Associated Lipocalin (NGAL), a small glycoprotein expressed in renal and other cell types to which different functions have been attributed [85]. Its involvement in renal pathologies and its role as a biomarker comes from its rapid release in response to a tubular lesion and its presence in plasma, serum and urine, making it easy to quantify [85,86]. Another proposed molecule is kidney injury molecule-1 (KIM-1), a transmembrane glycoprotein expressed in low levels in healthy kidneys. Shortly after tubular damage, KIM-1 cleavage allows its secretion by the injured cells to the tubule lumen, resulting in detection in the urine, to where it is excreted [87]. Moreover, its role as a biomarker has proved to be associated with inflammation and fibrosis in the injured kidney, which would help monitor the degree of tubular damage [88–90]. Interleukin-18 (IL-18) is a proinflammatory cytokine that is expressed in activated macrophages, renal epithelial cells and others [91]. Urinary IL-18 is considered a marker of both short- and long-term injury in AKI, as it increases within 6 h of the insult or at least a day before serum creatinine increase [91,92].

### 3.3. Fibrosis

Another common structural alteration observed in both heart and kidney remodelling in CRS is fibrosis, which is also considered a key contributor to the progression of cardiac and renal failure [93–95]. Fibrosis is an important process that can be contemplated as aberrant wound healing as a consequence of the misbalance between extracellular matrix (ECM) production and degradation [96]. The fibrotic response to injury can be classified into reparative, when the scar is necessary to stabilize the tissue defect, or reactive, when the mechanical stress and the hormonal mediators facilitate the expansion of connective tissue in a remote non-injured zone, compromising the correct function of the organ [97]. The main fibrosis effectors are the fibroblasts and myofibroblasts, both of which are responsible for the synthesis and accumulation of interstitial ECM proteins. While fibroblasts are mesenchymal cells ubiquitous in tissues and organs, myofibroblasts are differentiated

cells that are rarely found in non-pathological environments [98–100]. The fibrotic scar composition is similar amongst different tissues, predominantly formed by collagens type I and III, fibronectin, proteoglycans and laminin [101–103].

As a response to the damaged heart in cardiac ischemia, myocardial remodelling occurs through the secretion of ECM components by the myofibroblasts. Histopathologically speaking, there are three types of cardiac fibrosis: replacement fibrosis, interstitial fibrosis and perivascular fibrosis. Replacement fibrosis provides structural support, as it consists of the removal of necrotic tissue and generation of a fibrotic scar within the infarcted zone that compensates cardiomyocyte loss [104,105]. On the other hand, the widespread deposition of ECM proteins in the endo and perimysium of remote areas of the infarct is what is known as interstitial fibrosis [106]. The term perivascular fibrosis is used to describe the increase in connective tissue around the cardiac microvasculature [107], both of which are types of fibrotic lesions that could not be a consequence of cardiomyocyte death.

The remodelling that follows after MI happens in different phases that partially overlap: First, there is cell death and an inflammatory response (inflammatory phase); secondly, the resolution of inflammation and fibroblast proliferation (proliferative or reparative phase); and lastly, the scar formation and maturation (maturation or remodelling phase) [108]. During the proliferative phase, which usually coexists with the inflammatory and reparative phases, there is an increase in the number of fibroblasts, which will adopt the proliferatory, secretory and migratory myofibroblast phenotype [109]. Following the proliferative phase of cardiac repair, when the scar has been synthesized, there begins a long process known as maturation, in which an organized fibrotic state is formed due to ECM crosslinking [110] and scar reinforcement by other components of the ECM, such as decorin [111,112] and perlecan [113,114]. In addition, during the maturation phase, the activated fibroblasts go through apoptosis and senescence [115]. The presence of a mature fibrotic scar ultimately leads to an increased ventricular stiffness that compromises cardiac output [116,117]. In addition to the impaired cardiac contractility, fibrosis also interferes with the normal electrical signals within the heart, which predisposes to arrhythmias and fibrillation [118,119]. Overall, fibrosis has thus been proposed as a risk factor in HF as it predisposes to ventricular systolic and diastolic dysfunction [120–122], cardiomyocyte hypertrophy [122–124] and sudden cardiac death [125,126], thereby increasing mortality [127,128].

At the renal level, CKD is characterized by functional loss and deposition of connective tissue that ends up creating a common fibrotic phenotype independently of the initial damage. This happens since tubulointerstitial diseases lead to glomerular injury, and glomerular lesions produce tubulointerstitial damage. Fibrosis is a common manifestation of functional alterations that spreads in response to sustained inflammation and epithelial damage [129–131]. Among the events that induce fibrosis, both diabetes and hypertension are considered to be the leading causes of CKD [132,133], as they elevate the glomerular pressure that gradually leads to glomerular damage, endothelial dysfunction [134,135] and other structural changes, such as alterations of the glomerular basement membrane [136–138], decrease in podocyte number and mesangial distension [136,139,140]. As a result of such damage, the renal tissue would start a response that resembles wound healing in other tissues. The scar created in the early stage is potentially reversible but with the progression of the damage, the cross-linking of the ECM proteins makes it stiff and resistant to proteolysis [141].

During chronic injury to the kidney in CKD, the excessive accumulation of connective tissue and expansion of interstitial fibroblasts during the reparative stage of the fibrotic scar can happen in all compartments of the kidney, including the glomeruli, usually termed glomerulosclerosis, and the tubules, which is referred to as tubulointerstitial fibrosis [142–144]. Such deposition of the fibrotic matrix alters organ structure and function, which could further damage kidney function, as it impairs blood flow in this region of the parenchyma [96,145]. The fibrotic wound is not the only structural change involved since it is usually associated with tubular atrophy, tubular dilation and inflammatory cell infiltration [146–148]. Indeed, as the loss of renal cells and its replacement by ECM are common sequelae of renal damage, expansion of cortical

fibrosis is considered one of the best histologic predictors of kidney dysfunction loss in CKD along with tubular atrophy (IFTA parameter) [148–150]. It is also one of the most common features assessed in biopsies in predicting a progression to ESRD [151,152].

Even though chronic damage to the kidney will naturally converge into histological and functional alterations that are common and lead to glomerulosclerosis and fibrosis, it is important to understand that the fibrotic progression is different depending on where it begins [153]. In glomerular damage, the progression starts with an injury within the Bowman's Capsule that initially leads to glomerular hyperfiltration for a long period of time until it progresses to decrease the total GFR [154,155]. This reduction in the blood flow results in tubular hypoxia and epithelial cell death normally referred to as tubule atrophy [156,157]. In these circumstances, the inflammation initiated by the damaged tubular cells propitiates the formation of a fibrotic scar to fill the void created by epithelial cell death [158,159]. To form that scar, resident fibroblasts differentiate into the myofibroblast phenotype, which can synthesize different extracellular matrix proteins. Among the ECM components produced by myofibroblasts in order to form the fibrotic scar, the main ones in the kidney are collagen type I, III and IV, as well as fibronectin [160–162]. During tubule atrophy, the tubular basement membrane remains, thereby separating the cell death from the interstitium but disappears after the cell-free tubule collapses, at which point we could talk of complete loss of the nephron [163–165].

Epithelial damage is heterogeneous in tubular injury, which can be caused by many factors, such as hemodynamic, inflammatory, toxin-related or metabolic alterations. Some cells will instantly go through necrosis or apoptosis, whereas others will survive with different levels of injury, these being the ones that could proliferate and replace the lost cells of the tubular epithelium [166–168]. In the cases in which the tubules do not recover, inflammation signalling activates and with it the fibroblasts differentiate into myofibroblasts that will lead to tubulointerstitial fibrosis and tubular atrophy [169–171]. Tubulointerstitial fibrosis is the deposition of ECM proteins in the space between the tubular basement membrane and the peritubular capillaries [160], which impairs blood flow and induces ischemic injury in the nephrons of the fibrotic wound [148,172,173].

Inflammation and oxidative stress serve as the initial response to injury although its long-term progression could damage organ structure and function [174,175]. Inflammation is a common process in fibroproliferative diseases that leads to the release of pro-inflammatory mediators that have an important role in tissue damage and could either stimulate or inhibit fibrosis [176,177]. An appropriate level of cytokines and growth factors that mediates the cellular responses is key in normal wound healing. Among the many growth factors involved, transforming growth factor ß (TGF-ß) is considered to be a prototypic profibrotic cytokine that has a central role in organ fibrosis as it binds to its receptors causing the phosphorylation of SMADs, which modulate the expression of the target genes [100,178]. TGF-ß can also activate SMAD-independent pathways in what is called non-canonical signalling [179]. Among the many TGF-ß-mediated responses are cell proliferation and differentiation, ECM production and immune modulation [180–182]. Another important mediator is the connective tissue growth factor (CTGF), a downstream factor of TGF ß that has been reported in fibrosis in different organs such as the heart and kidney [93,183,184]. CTGF promotes the TGF-ß-induced excessive ECM production and fibroblast proliferation [185,186], and its expression appears to correlate with the degree of fibrosis [187].

As previously said, a dynamic balance between production and breakdown of ECM regulates the degree of fibrosis. The degradation of the ECM components is performed by the matrix metalloproteinases (MMPs), whose activity is controlled by the tissue inhibitors of MMPs (TIMPs) in order to maintain the homeostasis. MMPs can be classified according to substrate specificity into collagenases, such as MMP-1, MMP-8 and MMP-13 [188,189]; gelatinases, such as MMP-2 and MMP-9 [190,191]; membrane MMPs, such as MMP-14 [192]; and stromelysins, such as MMP-3, MMP-10 and MMP-11 [193]. Interestingly, MMPs can have both inhibitory and stimulatory effects on fibrosis as some of them promote it [194].

For example, the most frequently studied MMPs in HF and kidney damage are MMP-2 and MMP-9, out of which MMP-9 is believed to have a profibrotic effect [195–197] whereas MMP-2 has antifibrotic effects [198,199].

In recent years, it has been proved that different metabolic alterations stimulate structural and/or functional alterations, such as fibrosis development. Changes in metabolic regulation, such as that occurring in a situation such as lipotoxicity, defined as the accumulation of lipids in non-adipose tissues, is known to promote the development of fibrosis. This fibrosis is due to an upregulation in ECM protein synthesis, promoted by fibroblasts [200,201]. In this sense, we have observed in a recent study that MI is associated with cardiac lipotoxicity in rats, independently of the presence of obesity. This lipotoxicity was accompanied by alterations in the mitochondrial lipid profile and associated with myocardial fibrosis, suggesting that MI promotes an increase in lipid accumulation in the heart through mechanisms that are currently unknown. Similarly, we observed at the renal level the direct profibrotic role of palmitic acid at renal fibroblasts, as it induced an increase in ECM synthesis mediated by activation of ER stress, suggesting its importance in lipotoxicity-induced fibrosis [202]. These observations are in agreement with another study in which the authors proved that accumulation of lipid droplets accelerates tubulointerstitial fibrosis development in an animal model of kidney disease [200].

## 4. Mechanisms Involved in Fibrosis Progression

As a wide variety of diseases converge in fibrosis understanding, the pathogenesis involved is important in order to determine potential therapeutic targets. Despite the efforts to acquire insight into the process, the mechanisms involved are not fully established, and the current therapies are either ineffective or only slightly successful [203,204]. The current clinical strategies for CRS are guided towards the treatment of the general processes, such as diuretics, to treat volume overload, or angiotensin converting enzyme (ACE) inhibitors, Angiotensin II receptor blockers, mineralocorticoid receptor antagonist or β-adrenergic blockers to inhibit RAAS activation [17,205]. Due to the complex pathophysiology of CRS, new therapeutic approaches centred in fibrosis have been proposed. For instance, in a recent study, it has been proved that cardiac shock wave therapy significantly reduces cardiac fibrosis in a rat model of MI through the activation of the PI3K/Akt signalling pathway [206]. Despite this, these new experimental approaches are still required in order to have a comprehensive understanding of the pathophysiological mechanisms underlying fibrosis.

### *4.1. Inflammation*

Inflammation can be defined as a defensive immune response that is triggered by damage to a tissue. The acute inflammatory response can be initiated as a consequence of an infection in which the pattern recognition receptors in the innate immune cells interact with the pathogen-associated molecular patterns (PAMPs), or due to the damage-associated molecular patterns (DAMPs) that are released during physical injury [207]. An acute inflammatory response is characterized by vasodilation, vascular leak and leukocyte emigration and, shortly after its induction, secretion of cytokines and chemokines will happen in order to recruit the immune cells to the damaged or infected region. Among the cells recruited, neutrophils are the first to migrate as a means to engulf the pathogens and secrete pro-inflammatory mediators and vasoactive substances [208,209].

In a normal inflammatory response, the activity is temporally restricted, as it resolves once the threat has been dealt with. However, the presence of a prolonged low-grade activity leads to chronic inflammation, which is characterized by the activation of different immune components that lead to major alterations in tissues, increasing the risk of diseases [210]. The clinical consequences of chronic inflammation include type 2 diabetes [211,212], hypertension [213], cardiovascular disease [214,215], chronic kidney disease [216]) and metabolic syndrome [217] among others.

Since both CHF and CKD are associated with a chronic inflammation response, characterized by an increase in the circulating inflammatory mediators, this process has become of interest in the understanding of CRS. A persistent inflammatory trigger is needed in order to activate the wound-healing process. However, if not eliminated quickly, the inflammatory cells could increase the response, leading to the abnormal wound healing and scarring characteristic of fibrosis. Within the wound-healing mechanism that is activated after injury, the first response is coagulation, in which activated platelets release platelet-derived growth factor (PDGF), acting as a chemoattractant for inflammatory cells, and transforming growth factor ß1 (TGF-ß1), which is one of the main drivers of fibrosis as it stimulates ECM synthesis by the fibroblasts of the tissue that was damaged [218–220].

Inflammation is known to have an important role in the development and progression of chronic diseases. For example, CKD progression into ESRD is characterized by chronic inflammation in the renal parenchyma, concluding in ECM deposition and loss of renal function [221–223]. Independent of the original cause, experimental models and human biopsies have shown that during renal inflammation, cells such as neutrophils and macrophages infiltrate both the glomeruli and tubulointerstitial space in order to remove the cell and matrix components that were damaged during the insult [223–225]. In general, M1 macrophages generate the initial response in the diseased organ by generation of pro-inflammatory cytokines, such as tumour necrosis factor α (TNFα) and interleukin-1 (IL-1), whereas M2 macrophages propitiate tissue repair by secretion of immunosuppressive cytokines during the repair phase [223,226]. It is that transition from the M1 to M2 phenotype that promotes fibrosis, as the production of cytokines, chemokines and growth factors alter the ECM balance between production and degradation [214,227,228].

Cytokines are cell-derived polypeptides that mediate the inflammatory response and can have positive or negative effects. It is well known that not all cytokines are involved at all stages of inflammation, but some of them do mediate both acute and chronic responses. This is the case of TNF-α, IL-1 (α and β) and IL-6 [229], which are some of the most studied ones and have been suggested to have an important role in inflammatory modulation during CRS due to its extremely potent proinflammatory effects [94,230–232].

It is well established that RAAS activation and the sympathetic nervous system (SNS) promotes the inflammatory response both in the heart and kidneys [233]. Angiotensin II (Ang II), one of the main effectors of RAAS activation, induces endothelial dysfunction, upregulation of adhesion molecules and fibrosis [234–236]. These Ang II effects are accompanied by recruitment of infiltrating cells and an increase in proinflammatory cytokines via the angiotensin type 1 (AT1) receptor in cardiorenal disease [230,237]. It has been proved that Ang II produces the accumulation of macrophage in the kidney [238,239], and it was shown in a murine unilateral ureteral obstruction (UUO) model that the macrophages' AT1 receptor activation impedes polarization towards the M1 phenotype and limits the damage and fibrosis [240]. This shows that an increase in M1 macrophage differentiation makes organs more susceptible to damage whereas the M2 phenotype decreases injury [223,241,242]. Nevertheless, neurohormonal activation is not the only proposed source of inflammation in CRS. Both animal and human studies have shown that congestion may lead to endothelial activation and peripheral release of proinflammatory mediators, as venous congestion itself causes an inflammatory response activation in cells [233,243,244].

Inflammation leads to functional and structural damage in the cardiorenal axis, as the different cytokines, especially TNF-α, which plays a central role in organ dysfunction, are involved in inflammation, cell proliferation [245] and apoptosis [246]. During inflammation, TNF-α has been described to be involved in vasodilation, inflammatory cell adhesion, coagulation and reactive oxygen species (ROS) production, among others [247].

Numerous cytokines have been studied due to their profibrotic or antifibrotic effects [248]. Th2-derived cytokines, such as IL-4, IL-5, IL-6, IL-13 and IL-21, are important in the regulation of organ fibrosis [249,250], out of which the most studied one is IL-13, an interleukin whose profibrotic effect can be enhanced by IL-5 and IL-21, and which can increase its production and its receptor expression [251–253]. IL-21 can also promote tissue

fibrosis through the induction of differentiation into Th17 cells [254,255], which produce a well-known profibrotic interleukin, IL-17, and which is involved in the development of fibrosis in various organs [256–258], although a recent study has suggested IL-17 plays an antifibrotic role in tubulointerstitial fibrosis [259]. On the other hand, Th1 cytokines, such as IL-7 [250,260], IL-10 [261,262], IL-12 [263,264] and IL-22 [265,266], along with IFN-γ [267,268], have been shown to have a suppressive effect on fibrosis. For instance, the inflammatory response in IL-10 KO mice resulted in scar formation rather than wound repair, suggesting IL-10 has an important antifibrotic role [269,270].

Chronic, unresolved inflammation damages renal structure and function, thereby leading to CKD, a state characterized by progressive renal fibrosis. In previous studies, it was reported that circulating levels of fibrinogen, TNF-α and a decrease in serum albumin were associated with loss of kidney function, linking the progression of CKD to the inflammatory response [221,271]. Systemic inflammation and function decline can alter the structure of the kidney, creating an environment in which epithelial damage increases and the factors released by infiltrating macrophages lead to fibrotic expansion [272,273]. Indeed, macrophage depletion has proved to reduce renal fibrosis in an animal model of myocardial infarction [274]. In renal fibrosis, the first process involved is the injury itself, followed by the unresolved inflammation. In the tubulointerstitium, pro-inflammatory cytokines, such as IL-6, TNF-α and IL-1β, promote further inflammatory cell infiltration, propitiating activation of profibrotic cells to differentiate into myofibroblasts and local secretion of fibrotic mediators [275–277]. This situation will lead to overproduction and deposition of ECM proteins, disruption of tissue integrity and progressive decline in function. Finally, glomerulosclerosis and tubular atrophy will happen in the latest stages [278,279].

In cardiac injury, as what happens in renal damage, the necrotic cell death within the heart activates tissue cells that will synthetize proinflammatory cytokines to recruit inflammatory cells. In the first phase, the macrophages and neutrophils act to remove the debris and release growth factors and cytokines that propitiate formation of connective tissue. Afterwards, fibroblast activation and cell proliferation will happen in the maturation phase to repair the myocardium by fibrotic wound formation [280,281]. After the phagocytic clearance of the apoptotic cells, macrophages will polarize towards the "reparative" M2 phenotype, releasing anti-inflammatory and profibrotic cytokines such as IL-10 and TGFβ, while proinflammatory cytokines, such as IL-1β or TNF-α, decrease in order to stimulate cardiac fibroblast activation to collagen-secreting myofibroblast [281–283]. Having said that, chronic inflammation entails a change in the inflammatory behaviour towards persistent and exacerbated fibrinogenesis, which is a structural feature in chronic injuries. It is due to that characteristic chronic inflammation for which TNF-α has been proposed as an independent predictor of cardiac and non-cardiac mortality in CHF patients [284]. Nonetheless, there is no consensus on the role of cytokines and chemokines, as some studies suggest its aggravating injury effects and others show that they endanger cardioprotective responses. For example, TNF-α ablation has proved to reduce the infarct size in mice with I/R injury [285], but in other studies TNF receptor deficiency increased the ischemic injury during I/R [286].

### 4.2. Oxidative Stress

Oxidative stress is a general concept that describes the imbalance between the production of ROS and the antioxidant defences. ROS includes both free radicals, which are species with an unpaired electron, such as superoxide anion ($O_2^{\bullet -}$) and hydroxyl radical (·OH), or non-free radical oxygenated molecules, such as hydrogen peroxide ($H_2O_2$) [287,288]. Other reactive species derived from nitrogen or sulphur do exist, but they are less abundant [289,290].

Even in basal conditions, aerobic metabolism involves ROS production, thus making $O_2^{\bullet -}$ and $H_2O_2$ physiological intracellular metabolites. In low quantities, ROS act as signalling molecules involved in different pathways, such as cell proliferation, apoptosis and gene expression [291,292]. However, the fact that an important increase in oxidants

could target almost all substrates implies the impairment and alteration of all biomolecules, resulting in cell damage and death [293,294]. ROS can damage proteins [295] and nucleic acids [296,297], but among all the molecules to undergo oxidation, polyunsaturated fatty acids are the most susceptible, leading to an increase in the markers of lipid peroxidation, such as malondialdehyde or 4-hydroxynonenal [298–300].

The endogenous sources of prooxidant species include organelles where there is high oxygen use, such as the mitochondria, peroxisomes, due to the fatty acid β-oxidation [301,302], and the endoplasmic reticulum (ER) [303], although the mitochondria seem to be the major source of ROS production, as around 95% of the breathed oxygen is reduced in the mitochondrial electron chain. Specifically, there are two major sites in the electron transport chain, the NADH dehydrogenase (complex I) and the ubiquinone cytochrome c reductase (complex III), which transfer electrons to coenzyme Q or ubiquinone, creating reduced forms that will ultimately transfer electrons to the molecular oxygen, generating superoxide radicals [304,305]. Through the action of mitochondrial superoxide dismutase (SOD), the superoxide anion is converted to hydrogen peroxide, which can be detoxified by the catalase and glutathione peroxidase [305,306].

In the outer mitochondrial membrane, the monoamine oxidases are another source of ROS that is not related to respiration [307,308]. In this case, the bivalent reduction of oxygen produces $H_2O_2$. In order to regulate the levels of ROS, the sources colocalize with the antioxidant response, among which there are enzymes, such as superoxide dismutases, catalase and glutathione peroxidase, as well as non-enzymatic antioxidants, such as vitamin A, bilirubin or reduced coenzyme Q [288,309,310].

Both inflammation and oxidative stress are related to chronic diseases, such as diabetes, hypertension, cardiovascular diseases or CKD [175,311–313]. It is known that under chronic damage the inflammatory and hypoxic environment propitiates fibrosis by fibroblast activation and proliferation into myofibroblasts. In this circumstance, ROS formation also occurs, and is considered to have an important role in both inflammation and organ fibrosis [314–316]. The bidirectional link between ROS and TGF-β1 is well established, as ROS production and enhanced ROS formation leads to higher activation and expression of TGF-β1 [317–319]. One of the possible explanations for this link resides in the action of an important ROS source, such as the different NADPH oxidases (NOX). In normal conditions, the NOX-derived ROS act as modulators of cell growth, proliferation, differentiation and apoptosis, but once it is uncontrolled, oxidative stress damages the DNA, proteins and lipids, inducing organ damage and fibrosis [320–322]. Multiple studies have shown the effectiveness of NOX-1 and NOX-4 inhibition in inflammation and fibrosis amelioration in liver and kidney injury [323–325], while different studies in the heart have shown that both NOX-2 and NOX-4 mediate the oxidative stress and cardiac injury following I/R [320,326,327]. Indeed, NOX-4 is considered a well-recognized mediator of the transition from fibroblast to myofibroblast, and its inhibition in in vitro studies with renal cells proved to prevent ROS production and myofibroblast differentiation, which would translate into a decrease in fibrosis during damage [328,329].

Multiple factors seem to participate in order to produce the characteristic multiorgan dysfunction of CRS, among which the increase in proinflammatory cytokines, the dysregulation of apoptosis and the increase in oxidative stress have been proposed as key elements of this complex pathophysiology [232,330,331]. Different animal models have shown that an increase in oxidative stress plays a pivotal role in cardiac and renal damage, independently of the CRS type depicted, through activation of the inflammatory response [15,331–333]. This can also be seen in patients with CRS, who presented an increase in ROS and RNS, which was accompanied by higher inflammatory cytokines, such as IL-6 [15].

### *4.3. Endoplasmic Reticulum Stress*

The ER is an essential organelle for calcium homeostasis, lipid biosynthesis and protein synthesis and post-translational modifications. To ensure correct protein folding, the ER

lumen balance between unfolded and misfolded proteins, and the capability to handle it, must be maintained. Such homeostasis could be altered by both physiological and pathological entities, such as inflammatory cytokines, protein demand or mutant protein expression, which translates into what is called ER stress [334,335].

In response to ER stress, the unfolded protein response (UPR) is initiated by at least one of three different pathways: the ER transmembrane proteins Activating Transcription Factor 6 (ATF6), Inositol-Requiring 1 (IRE1) or PKR-like ER kinase (PERK). In unstressed conditions, the chaperone Immunoglobin Binding Protein (BiP) binds to the luminal domain of ATF6, IRE1 and PERK, keeping them inactive [334,336]. In ER stress conditions, BiP dissociates from the three regulators, activating UPR [337]. Although initially UPR is considered a beneficial adaptive response, if it fails to restore homeostasis, then the UPR pathways guide the damaged cells to apoptosis and the consequent tissue injury [338,339].

Different pathologies, such as diabetes mellitus [340], obesity [341,342], cardiovascular disease [343,344] and CKD [345,346], have been associated with ER stress. In CRS, the activation of ER stress in the heart and kidney could be induced by different factors, such as hemodynamic changes, hormones from the RAAS, inflammation or oxidative stress [346–348]. These pathophysiological mediators could directly induce ER stress in the myocardium or renal parenchyma, resulting in apoptotic cell death due to prolonged UPR activation [349–351] and the consequent fibrotic wound formation, all of which would eventually lead to structural and functional changes [348,352–354]. Our group has recently evaluated the effect of myocardial infarction (MI) at renal level in rats. At 4 weeks post-MI, animals presented renal alterations characterized by tubulointerstitial fibrosis, oxidative stress and upregulation of inflammatory cytokines, such as IL-6 and TNF-α. All these alterations were accompanied by ER stress activation, which correlates with the renal fibrosis, suggesting ER stress relevance in the structural renal damage in CRS type 1 [202].

As ER stress inhibition has proved to ameliorate the fibrotic progression, it has been suggested that its blockade could be a new therapeutic approach for fibrosis [355–357]. One of the possible ways in which ER stress could lead to fibrosis is through fibroblast differentiation and collagen formation by TGF-β upregulation, as PERK and IRE1 activation have been seen to increase TGF-β expression [358–360]. ER stress activation of fibroblasts during injury at the wounded site triggers their differentiation into myoblasts, so as to restore the area by ECM protein synthesis and secretion [361,362]. Different in vitro studies have described ER-mediated differentiation into different cell types, such as renal tubular cells [363], cardiac cells [364], adipocytes [365,366], plasma cells [367,368] and others [369–371]. Additionally, our group's in vitro studies in kidney fibroblasts, stimulated with the well-known profibrotic factor Ang II in presence of the pharmacological inhibitor of ER stress, 4-phenylbutiric acid (4-PBA), proved to be effective in preventing the increase in collagen I, inflammatory markers and superoxide anion production. All of this suggests the important role of ER stress in fibrosis, inflammation and oxidative stress in renal damage [202].

The explained mechanisms involvement in CRS is depicted in Figure 2.

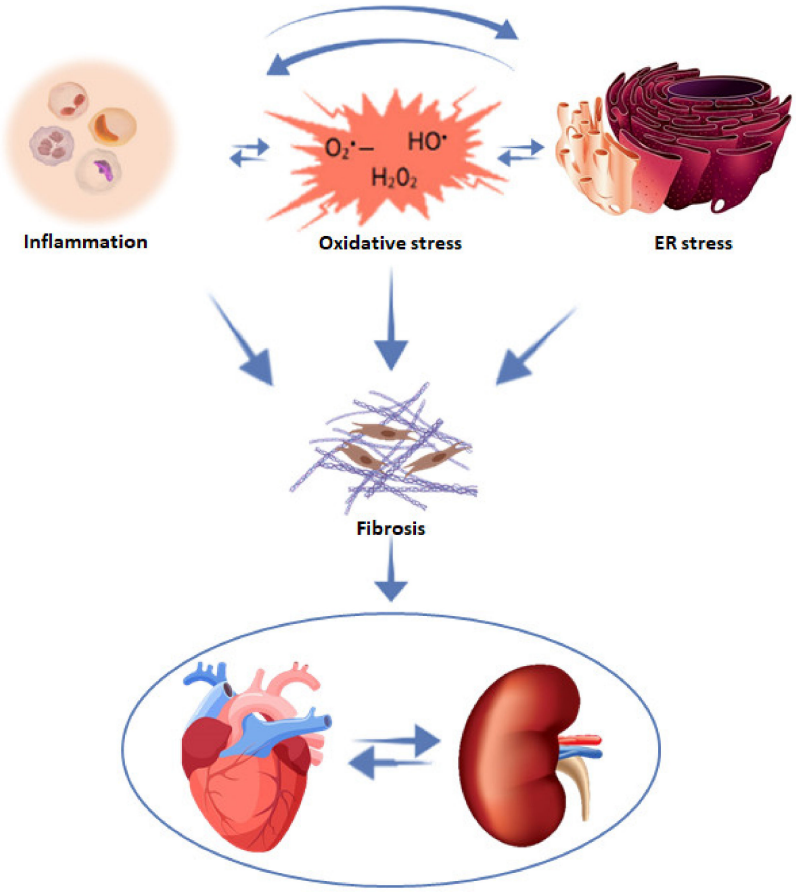


**Figure 2.** Mechanisms involved in the progression of cardiac and renal fibrosis in CRS.

## 5. Conclusions

Due to the pathogenesis of cardiorenal syndromes, numerous efforts have given insight into the different pathways and mediators involved. This review has summarized evidence that the development of a fibrotic wound has proved to play a central role in both cardiac and renal damage progression, in which inflammation, oxidative stress and ER stress could be relevant players. This makes it crucial to understand the pathogenic basis of fibrosis in order to determine therapeutic targets.

**Author Contributions:** Conceptualization: E.M.-M. and V.C.; investigation: B.D.-V., E.M.-M. and V.C.; orgibnal draft preparation: B.D.-V.; review and editing: B.D.-V., E.M.-M. and V.C.; funding acquisition: E.M.-M. and V.C. All authors have read and agreed to the published version of the manuscript.

**Funding:** This research was funded by Instituto de Salud Carlos III-Fondo Europeo de Desarrollo Regional (FEDER) [grant numbers PI18/00257; CIBERCV]. B.D.-V. was supported by a grant P-FIS (FI19/00277) and E.M-M was supported by a contract from CAM (Atracción de talento).

**Institutional Review Board Statement:** Not applicable.

**Informed Consent Statement:** Not applicable.

**Acknowledgments:** We thank Anthony DeMarco for his help in editing.

**Conflicts of Interest:** The authors declare no conflict of interest.

## References


1. Bright, R. Cases and Observations Illustrative of Renal Disease, Accompanied with the Secretion of Albuminous Urine. *Med. Chir. Rev.* **1836**, *25*, 23–35.
2. Zannad, F.; Rossignol, P. Cardiorenal Syndrome Revisited. *Circulation* **2018**, *138*, 929–944. [CrossRef]
3. Cabandugama, P.K.; Gardner, M.J.; Sowers, J.R. The Renin Angiotensin Aldosterone System in Obesity and Hypertension. *Med. Clin. North Am.* **2017**, *101*, 129–137. [CrossRef] [PubMed]
4. Banerjee, S.; Panas, R. Diabetes and Cardiorenal Syndrome: Understanding the "Triple Threat". *Hell. J. Cardiol.* **2017**, *58*, 342–347. [CrossRef] [PubMed]
5. McCullough, P.A.; Jurkovitz, C.T.; Pergola, P.E.; McGill, J.B.; Brown, W.W.; Collins, A.J.; Chen, S.-C.; Li, S.; Singh, A.; Norris, K.C.; et al. Independent Components of Chronic Kidney Disease as a Cardiovascular Risk State. *Arch. Intern. Med.* **2007**, *167*, 1122–1129. [CrossRef]
6. Raina, R.; Nair, N.; Chakraborty, R.; Nemer, L.; Dasgupta, R.; Varian, K. An Update on the Pathophysiology and Treatment of Cardiorenal Syndrome. *Cardiol. Res.* **2020**, *11*, 76–88. [CrossRef] [PubMed]
7. Ronco, C.; McCullough, P.; Anker, S.D.; Anand, I.; Aspromonte, N.; Bagshaw, S.M.; Bellomo, R.; Berl, T.; Bobek, I.; Cruz, D.N.; et al. Cardio-Renal Syndromes: Report from the Consensus Conference of the Acute Dialysis Quality Initiative. *Eur. Heart J.* **2009**, *31*, 703–711. [CrossRef] [PubMed]
8. Heywood, J.T.; Fonarow, G.; Costanzo, M.R.; Mathur, V.S.; Wigneswaran, J.R.; Wynne, J. High Prevalence of Renal Dysfunction and Its Impact on Outcome in 118,465 Patients Hospitalized with Acute Decompensated Heart Failure: A Report from the ADHERE Database. *J. Card. Fail.* **2007**, *13*, 422–430. [CrossRef] [PubMed]
9. Ronco, C.; Cicoira, M.; McCullough, P.A. Cardiorenal Syndrome Type 1. *J. Am. Coll. Cardiol.* **2012**, *60*, 1031–1042. [CrossRef] [PubMed]
10. Prins, K.W.; Thenappan, T.; Markowitz, J.S.; Pritzker, M.R. Cardiorenal Syndrome Type 1: Renal Dysfunction in Acute Decompensated Heart Failure. *J. Clin. Outcomes Manag.* **2015**, *22*, 443–454. [PubMed]
11. Ronco, C.; Bellasi, A.; Di Lullo, L. Cardiorenal Syndrome: An Overview. *Adv. Chronic Kidney Dis.* **2018**, *25*, 382–390. [CrossRef] [PubMed]
12. Mullens, W.; Abrahams, Z.; Francis, G.S.; Sokos, G.; Taylor, D.O.; Starling, R.C.; Young, J.B.; Tang, W.W. Importance of Venous Congestion for Worsening of Renal Function in Advanced Decompensated Heart Failure. *J. Am. Coll. Cardiol.* **2009**, *53*, 589–596. [CrossRef] [PubMed]
13. Ames, M.K.; Atkins, C.E.; Pitt, B. The renin-angiotensin-aldosterone System and Its Suppression. *J. Veter. Intern. Med.* **2019**, *33*, 363–382. [CrossRef] [PubMed]
14. Brewster, U.C.; Perazella, A.M. The Renin-Angiotensin-Aldosterone System and the Kidney: Effects on Kidney Disease. *Am. J. Med.* **2004**, *116*, 263–272. [CrossRef] [PubMed]
15. Virzì, G.M.; Clementi, A.; De Cal, M.; Brocca, A.; Day, S.; Pastori, S.; Bolin, C.; Vescovo, G.; Ronco, C. Oxidative Stress: Dual Pathway Induction in Cardiorenal Syndrome Type 1 Pathogenesis. *Oxidative Med. Cell. Longev.* **2015**, *2015*, 1–9. [CrossRef]
16. Harrison, J.C.; Smart, S.D.G.; Besley, E.M.H.; Kelly, J.R.; Read, M.I.; Yao, Y.; Sammut, I. A Clinically Relevant Functional Model of Type-2 Cardio-Renal Syndrome with Paraventricular Changes Consequent to Chronic Ischaemic Heart Failure. *Sci. Rep.* **2020**, *10*, 1–12. [CrossRef]
17. Rangaswami, J.; Bhalla, V.; Blair, J.E.; Chang, T.I.; Costa, S.; Lentine, K.L.; Lerma, E.; Mezue, K.; Molitch, M.; Mullens, W.; et al. Cardiorenal Syndrome: Classification, Pathophysiology, Diagnosis, and Treatment Strategies: A Scientific Statement from the American Heart Association. *Circulation* **2019**, *139*, e840–e878. [CrossRef]
18. Stevens, P.E.; Levin, A. Kidney Disease: Improving Global Outcomes Chronic Kidney Disease Guideline Development Work Group Members. Evaluation and Management of Chronic Kidney Disease: Synopsis of the Kidney Disease: Improving Global Outcomes 2012 Clinical Practice Guideline. *Ann. Intern. Med.* **2013**, *158*, 825–830. [CrossRef]
19. Damman, K.; Valente, M.A.; Voors, A.A.; O'Connor, C.M.; Van Veldhuisen, D.J.; Hillege, H.L. Renal impairment, worsening renal function, and outcome in patients with heart failure: An updated meta-analysis. *Eur. Heart J.* **2014**, *35*, 455–469. [CrossRef] [PubMed]
20. De Vecchis, R.; Baldi, C. Cardiorenal Syndrome Type 2: From Diagnosis to optimal Management. *Ther. Clin. Risk Manag.* **2014**, *10*, 949–961. [CrossRef]
21. Di Lullo, L.; Reeves, P.B.; Bellasi, A.; Ronco, C. Cardiorenal Syndrome in Acute Kidney Injury. *Semin. Nephrol.* **2019**, *39*, 31–40. [CrossRef] [PubMed]
22. Bagshaw, S.M.; Hoste, E.; Braam, B.; Briguori, C.; Kellum, J.A.; McCullough, P.A.; Ronco, C. Cardiorenal Syndrome Type 3: Pathophysiologic and Epidemiologic Considerations. *Contrib. Nephrol.* **2013**, *182*, 137–157. [CrossRef]
23. Kumar, U.; Wettersten, N.; Garimella, P.S. Cardiorenal Syndrome. *Cardiol. Clin.* **2019**, *37*, 251–265. [CrossRef] [PubMed]
24. Uduman, J. Epidemiology of Cardiorenal Syndrome. *Adv. Chronic Kidney Dis.* **2018**, *25*, 391–399. [CrossRef]
25. Mentzer, R.M.; Oz, M.C.; Sladen, R.N.; Graeve, A.H.; Hebeler, R.F.; Luber, J.M.; Smedira, N.G. Effects of Perioperative Nesiritide in Patients with Left Ventricular Dysfunction Undergoing Cardiac Surgery: The NAPA Trial. *J. Am. Coll. Cardiol.* **2007**, *49*, 716–726. [CrossRef]
26. Di Lullo, L.; Bellasi, A.; Barbera, V.; Russo, D.; Russo, L.; Di Iorio, B.; Cozzolino, M.; Ronco, C. Pathophysiology of the Cardio-Renal Syndromes Types 1–5: An Uptodate. *Indian Heart J.* **2017**, *69*, 255–265. [CrossRef]

27. Hillege, H.L.; Nitsch, D.; Pfeffer, M.A.; Swedberg, K.; McMurray, J.J.; Yusuf, S.; Granger, C.B.; Michelson, E.L.; Ostergren, J.; Cornel, J.; et al. Renal Function as a Predictor of Outcome in a Broad Spectrum of Patients with Heart Failure. *Circulation* **2006**, *113*, 671–678. [CrossRef]
28. Go, A.S.; Chertow, G.M.; Fan, D.; McCulloch, C.E.; Hsu, C.-Y. Chronic Kidney Disease and the Risks of Death, Cardiovascular Events, and Hospitalization. *N. Eng. J. Med.* **2004**, *351*, 1296–1305. [CrossRef]
29. Suresh, H.; Arun, B.S.; Moger, V.; Swamy, M. Cardiorenal Syndrome Type 4: A Study of Cardiovascular Diseases in Chronic Kidney Disease. *Indian Heart J.* **2017**, *69*, 11–16. [CrossRef]
30. Clementi, A.; Virzì, G.M.; Goh, C.Y.; Cruz, D.N.; Granata, A.; Vescovo, G.; Ronco, C. Cardiorenal Syndrome Type 4: A Review. *Cardiorenal Med.* **2013**, *3*, 63–70. [CrossRef] [PubMed]
31. Mehta, R.L.; Rabb, H.; Shaw, A.D.; Singbartl, K.; Ronco, C.; McCullough, P.A.; Kellum, J.A. Cardiorenal Syndrome Type 5: Clinical Presentation, Pathophysiology and Management Strategies from the Eleventh Consensus Conference of the Acute Dialysis Quality Initiative (ADQI). *Contrib. Nephrol.* **2013**, *182*, 174–194. [CrossRef]
32. Singer, M.; Deutschman, C.S.; Seymour, C.W.; Shankar-Hari, M.; Annane, D.; Bauer, M.; Bellomo, R.; Bernard, G.R.; Chiche, J.-D.; Coopersmith, C.M.; et al. The Third International Consensus Definitions for Sepsis and Septic Shock (Sepsis-3). *JAMA* **2016**, *315*, 801–810. [CrossRef] [PubMed]
33. Vincent, J.-L.; Rello, J.; Marshall, J.K.; Silva, E.; Anzueto, A.; Martin, C.D.; Moreno, R.; Lipman, J.; Gomersall, C.; Sakr, Y.; et al. International Study of the Prevalence and Outcomes of Infection in Intensive Care Units. *JAMA* **2009**, *302*, 2323–2329. [CrossRef] [PubMed]
34. Mehta, R.L.; Program to Improve Care in Acute Renal Disease (PICARD) Study Group; Bouchard, J.; Soroko, S.B.; Ikizler, T.; Paganini, E.P.; Chertow, G.M.; Himmelfarb, J. Sepsis as a Cause and Consequence of Acute Kidney Injury: Program to Improve Care in Acute Renal Disease. *Intensiv. Care Med.* **2010**, *37*, 241–248. [CrossRef] [PubMed]
35. Ronco, C.; McCullough, P.A.; Anker, S.D.; Anand, I.; Aspromonte, N.; Bagshaw, S.M.; Bellomo, R.; Berl, T.; Bobek, I.; Cruz, D.N.; et al. Cardiorenal Syndromes: An Executive Summary from the Consensus Conference of the Acute Dialysis Quality Initiative (ADQI). *Contrib. Nephrol.* **2010**, *165*, 54–67. [CrossRef] [PubMed]
36. Evans, M.; Grams, M.E.; Sang, Y.; Astor, B.C.; Blankestijn, P.J.; Brunskill, N.J.; Collins, J.F.; Kalra, P.A.; Kovesdy, C.P.; Levin, A.; et al. Risk Factors for Prognosis in Patients with Severely Decreased GFR. *Kidney Int. Rep.* **2018**, *3*, 625–637. [CrossRef] [PubMed]
37. Matsushita, K.; Van Der Velde, M.; Astor, B.C.; Woodward, M.; Levey, A.S.; De Jong, P.E.; Coresh, J.; Gansevoort, R.T. Association of Estimated Glomerular Filtration Rate and Albuminuria with All-Cause and Cardiovascular Mortality in General Population Cohorts: A Collaborative Meta-Analysis. *Lancet* **2010**, *375*, 2073–2081. [CrossRef]
38. Matsushita, K.; Coresh, J.; Sang, Y.; Chalmers, J.; Fox, C.; Guallar, E.; Jafar, T.; Jassal, S.K.; Landman, G.W.D.; Muntner, P.; et al. Estimated Glomerular Filtration Rate and Albuminuria for Prediction of Cardiovascular Outcomes: A Collaborative Meta-Analysis of Individual Participant Data. *Lancet Diabetes Endocrinol.* **2015**, *3*, 514–525. [CrossRef]
39. James, M.T.; Grams, M.E.; Woodward, M.; Elley, C.R.; Green, J.A.; Wheeler, D.C.; de Jong, P.; Gansevoort, R.T.; Levey, A.S.; Warnock, D.G.; et al. A Meta-Analysis of the Association of Estimated GFR, Albuminuria, Diabetes Mellitus, and Hypertension with Acute Kidney Injury. *Am. J. Kidney Dis.* **2015**, *66*, 602–612. [CrossRef]
40. Matsuo, H.; Dohi, K.; Machida, H.; Takeuchi, H.; Aoki, T.; Nishimura, H.; Yasutomi, M.; Senga, M.; Ichikawa, T.; Kakuta, K.; et al. Echocardiographic Assessment of Cardiac Structural and Functional Abnormalities in Patients with End-Stage Renal Disease Receiving Chronic Hemodialysis. *Circ. J.* **2018**, *82*, 586–595. [CrossRef]
41. Otsuka, T.; Suzuki, M.; Yoshikawa, H.; Sugi, K. Left Ventricular Diastolic Dysfunction in the Early Stage of Chronic Kidney Disease. *J. Cardiol.* **2009**, *54*, 199–204. [CrossRef] [PubMed]
42. Dobre, M.; Roy, J.; Tao, K.; Anderson, A.H.; Bansal, N.; Chen, J.; Deo, R.; Drawz, P.; Feldman, H.I.; Hamm, L.L.; et al. Serum Bicarbonate and Structural and Functional Cardiac Abnormalities in Chronic Kidney Disease - A Report from the Chronic Renal Insufficiency Cohort Study. *Am. J. Nephrol.* **2016**, *43*, 411–420. [CrossRef]
43. Shlipak, M.G.; Fried, L.F.; Cushman, M.; Manolio, T.A.; Peterson, D.; Stehman-Breen, C.; Bleyer, A.; Newman, A.B.; Siscovick, D.; Psaty, B. Cardiovascular Mortality Risk in Chronic Kidney Disease. *JAMA* **2005**, *293*, 1737–1745. [CrossRef] [PubMed]
44. Park, M.; Hsu, C.-Y.; Li, Y.; Mishra, R.K.; Keane, M.; Rosas, S.E.; Dries, D.; Xie, D.; Chen, J.; He, J.; et al. Associations Between Kidney Function and Subclinical Cardiac Abnormalities in CKD. *J. Am. Soc. Nephrol.* **2012**, *23*, 1725–1734. [CrossRef] [PubMed]
45. Taddei, S.; Nami, R.; Bruno, R.M.; Quatrini, I.; Nuti, R. Hypertension, Left Ventricular Hypertrophy and Chronic Kidney Disease. *Heart Fail. Rev.* **2010**, *16*, 615–620. [CrossRef]
46. Matsumoto, M.; Io, H.; Furukawa, M.; Okumura, K.; Masuda, A.; Seto, T.; Takagi, M.; Sato, M.; Nagahama, L.; Omote, K.; et al. Risk Factors Associated with Increased Left Ventricular Mass Index in Chronic Kidney Disease Patients Evaluated Using Echocardiography. *J. Nephrol.* **2012**, *25*, 794–801. [CrossRef] [PubMed]
47. Pluta, A.; Stróżecki, P.; Krintus, M.; Odrowaz-Sypniewska, G.; Manitius, J. Left Ventricular Remodeling and Arterial Remodeling in Patients with Chronic Kidney Disease Stage 1–3. *Ren. Fail.* **2015**, *37*, 1–6. [CrossRef]
48. Matsushita, K.; Ballew, S.; Coresh, J. Influence of Chronic Kidney Disease on Cardiac Structure and Function. *Curr. Hypertens. Rep.* **2015**, *17*, 1–9. [CrossRef]

49. Toida, T.; Toida, R.; Yamashita, R.; Komiya, N.; Uezono, S.; Komatsu, H.; Ishikawa, T.; Kitamura, K.; Sato, Y.; Fujimoto, S. Grading of Left Ventricular Diastolic Dysfunction with Preserved Systolic Function by the 2016 American Society of Echocardiography/European Association of Cardiovascular Imaging Recommendations Contributes to Predicting Cardiovascular Events in Hemodialysis Patients. *Cardiorenal Med.* **2019**, *9*, 190–200. [CrossRef]
50. Escoli, R.; Carvalho, M.J.; Cabrita, A.; Rodrigues, A. Diastolic Dysfunction, an Underestimated New Challenge in Dialysis. *Ther. Apher. Dial.* **2019**, *23*, 108–117. [CrossRef]
51. Cai, Q.-Z.; Lu, X.-Z.; Lu, Y.; Wang, A.Y.-M. Longitudinal Changes of Cardiac Structure and Function in CKD (CASCADE Study). *J. Am. Soc. Nephrol.* **2014**, *25*, 1599–1608. [CrossRef]
52. Franczyk, B.; Gluba, A.; Olszewski, R.; Banach, M.; Rysz, J. Heart Function Disturbances in Chronic Kidney Disease – Echocardiographic Indices. *Arch. Med Sci.* **2014**, *10*, 1109–1116. [CrossRef] [PubMed]
53. Vogel, M.W.; Slusser, J.P.; Hodge, D.O.; Chen, H.H. The Natural History of Preclinical Diastolic Dysfunction. *Circ. Heart Fail.* **2012**, *5*, 144–151. [CrossRef]
54. Shah, S.; Kitzman, D.W.; Borlaug, B.; Van Heerebeek, L.; Zile, M.; Kass, D.A.; Paulus, W.J. Phenotype-Specific Treatment of Heart Failure with Preserved Ejection Fraction. *Circulation* **2016**, *134*, 73–90. [CrossRef] [PubMed]
55. Dekkers, I.A.; De Mutsert, R.; Rabelink, T.J.; Jukema, J.W.; De Roos, A.; Rosendaal, F.R.; Lamb, H.J.; De Vries, A.P. Associations Between Normal Range Albuminuria, Renal Function and Cardiovascular Function in a Population-Based Imaging Study. *Atherosclerosis* **2018**, *272*, 94–100. [CrossRef] [PubMed]
56. Shah, A.M.; Lam, C.S.; Cheng, S.; Verma, A.; Desai, A.S.; Rocha, R.A.; Hilkert, R.; Izzo, J.; Oparil, S.; Pitt, B.; et al. The Relationship Between Renal Impairment and Left Ventricular Structure, Function, and ventricular–arterial Interaction in Hypertension. *J. Hypertens.* **2011**, *29*, 1829–1836. [CrossRef] [PubMed]
57. Matsushita, K.; Kwak, L.; Sang, Y.; Ballew, S.H.; Skali, H.; Shah, A.M.; Coresh, J.; Solomon, S. Kidney Disease Measures and Left Ventricular Structure and Function: The Atherosclerosis Risk in Communities Study. *J. Am. Heart Assoc.* **2017**, *6*, e006259. [CrossRef]
58. Zhou, J.; Cui, X.; Jin, X.; Zhou, J.; Zhang, H.; Tang, B.; Fu, M.; Herlitz, H.; Cui, J.; Zhu, H.; et al. Association of Renal Biochemical Parameters with Left Ventricular Diastolic Dysfunction in a Community-Based Elderly Population in China: A Cross-Sectional Study. *PLoS ONE* **2014**, *9*, e88638. [CrossRef]
59. Kang, E.; Ryu, H.; Kim, J.; Lee, J.; Lee, K.; Chae, D.; Sung, S.A.; Kim, S.W.; Ahn, C.; Oh, K. Association Between High-Sensitivity Cardiac Troponin T and Echocardiographic Parameters in Chronic Kidney Disease: Results from the KNOW-CKD Cohort Study. *J. Am. Heart Assoc.* **2019**, *8*, e013357. [CrossRef]
60. McCullough, P.A.; Jefferies, J.L. Novel Markers and Therapies for Patients with Acute Heart Failure and Renal Dysfunction. *Am. J. Med.* **2015**, *128*, 312-e1–312.e22. [CrossRef]
61. Savic-Radojevic, A.; Pljesa-Ercegovac, M.; Matic, M.; Simic, D.; Radovanovic, S.; Simic, T. Novel Biomarkers of Heart Failure. *Adv. Clin. Chem.* **2017**, *79*, 93–152. [CrossRef] [PubMed]
62. Ponikowski, P.; Voors, A.A.; Anker, S.D.; Bueno, H.; Cleland, J.G.F.; Coats, A.J.S.; Falk, V.; González-Juanatey, J.R.; Harjola, V.-P.; Jankowska, E.A.; et al. 2016 ESC Guidelines for the diagnosis and treatment of acute and chronic heart failure: The Task Force for the diagnosis and treatment of acute and chronic heart failure of the European Society of Cardiology (ESC). Developed with the special contribution of the Heart Failure Association (HFA) of the ESC. *Eur. J. Heart Fail.* **2016**, *18*, 891–975. [CrossRef] [PubMed]
63. Arslan, M.; Dedic, A.; Boersma, E.; A Dubois, E. Serial High-Sensitivity Cardiac Troponin T Measurements to Rule Out Acute Myocardial Infarction and a Single High Baseline Measurement for Swift Rule-In: A Systematic Review and Meta-Analysis. *Eur. Heart J. Acute Cardiovasc. Care* **2020**, *9*, 14–22. [CrossRef]
64. Westermann, D.; Neumann, J.T.; Sörensen, N.A.; Blankenberg, D.W.J.T.N.N.A.S.S. High-Sensitivity Assays for Troponin in Patients with Cardiac Disease. *Nat. Rev. Cardiol.* **2017**, *14*, 472–483. [CrossRef] [PubMed]
65. Hill, N.R.; Fatoba, S.T.; Oke, J.L.; Hirst, J.; O'Callaghan, C.A.; Lasserson, D.; Hobbs, R. Global Prevalence of Chronic Kidney Disease—A Systematic Review and Meta-Analysis. *PLoS ONE* **2016**, *11*, e0158765. [CrossRef] [PubMed]
66. Vogt, L.; Bangalore, S.; Fayyad, R.; Melamed, S.; Hovingh, G.K.; DeMicco, D.A.; Waters, D.D. Atorvastatin Has a Dose-Dependent Beneficial Effect on Kidney Function and Associated Cardiovascular Outcomes: Post Hoc Analysis of 6 Double-Blind Randomized Controlled Trials. *J. Am. Heart Assoc.* **2019**, *8*, e010827. [CrossRef]
67. Dalal, R.; Bruss, Z.S.; Sehdev, J.S. *Physiology, Renal Blood Flow and Filtration*; StatPearls: Treasure Island, FL, USA, 2021.
68. Borovac, J.A.; D'Amario, D.; Bozic, J.; Glavas, D. Sympathetic Nervous System Activation and Heart Failure: Current State of Evidence and the Pathophysiology in the Light of Novel Biomarkers. *World J. Cardiol.* **2020**, *12*, 373–408. [CrossRef]
69. Dlugos, C.P.; Picciotto, C.; Lepa, C.; Krakow, M.; Stöber, A.; Eddy, M.-L.; Weide, T.; Jeibmann, A.; Krahn, M.; Van Marck, V.; et al. Nephrin Signaling Results in Integrin β1 Activation. *J. Am. Soc. Nephrol.* **2019**, *30*, 1006–1019. [CrossRef]
70. Lichtnekert, J.; Kaverina, N.V.; Eng, D.G.; Gross, K.W.; Kutz, J.N.; Pippin, J.W.; Shankland, S.J. Renin-Angiotensin-Aldosterone System Inhibition Increases Podocyte Derivation from Cells of Renin Lineage. *J. Am. Soc. Nephrol.* **2016**, *27*, 3611–3627. [CrossRef]
71. Stoll, D.; Yokota, R.; Aragão, D.S.; Casarini, D.E. Both Aldosterone and Spironolactone Can Modulate the Intracellular ACE/ANG II/AT1 and ACE2/ANG (1-7)/MAS Receptor Axes in Human Mesangial Cells. *Physiol. Rep.* **2019**, *7*, e14105. [CrossRef]
72. Gómez, G.I.; Fernández, P.; Velarde, V.; Sáez, J.C. Angiotensin II-Induced Mesangial Cell Damage Is Preceded by Cell Membrane Permeabilization Due to Upregulation of Non-Selective Channels. *Int. J. Mol. Sci.* **2018**, *19*, 957. [CrossRef]

73. Xu, Z.; Li, W.; Han, J.; Zou, C.; Huang, W.; Yu, W.; Shan, X.; Lum, H.; Li, X.; Liang, G. Angiotensin II Induces Kidney Inflammatory Injury and Fibrosis through Binding to Myeloid Differentiation Protein-2 (MD2). *Sci. Rep.* **2017**, *7*, srep44911. [CrossRef] [PubMed]
74. Brankovic, M.; Akkerhuis, K.M.; Van Boven, N.; Manintveld, O.; Germans, T.; Brugts, J.; Caliskan, K.; Umans, V.; Constantinescu, A.; Kardys, I. Real-Life Use of Neurohormonal Antagonists and Loop Diuretics in Chronic Heart Failure: Analysis of Serial Biomarker Measurements and Clinical Outcome. *Clin. Pharmacol. Ther.* **2017**, *104*, 346–355. [CrossRef] [PubMed]
75. Aggarwal, D.; Singh, G. Effects of Single and Dual RAAS Blockade Therapy on Progressive Kidney Disease Transition to CKD in Rats. *Naunyn-Schmiedeberg's Arch. Pharmacol.* **2019**, *393*, 615–627. [CrossRef]
76. Dörr, O.; Liebetrau, C.; Möllmann, H.; Gaede, L.; Troidl, C.; Wiebe, J.; Renker, M.; Bauer, T.; Hamm, C.; Nef, H. Long-Term Verification of Functional and Structural Renal Damage After Renal Sympathetic Denervation. *Catheter. Cardiovasc. Interv.* **2016**, *87*, 1298–1303. [CrossRef] [PubMed]
77. Damman, K.; Tang, W.W.; Testani, J.M.; McMurray, J.J. Terminology and Definition of Changes Renal Function in Heart Failure. *Eur. Heart J.* **2014**, *35*, 3413–3416. [CrossRef] [PubMed]
78. Damman, K.; Testani, J.M. The Kidney in Heart Failure: An Update. *Eur. Heart J.* **2015**, *36*, 1437–1444. [CrossRef]
79. Norris, K.C.; Smoyer, K.E.; Rolland, C.; Van Der Vaart, J.; Grubb, E.B. Albuminuria, Serum Creatinine, and Estimated Glomerular Filtration Rate as Predictors of Cardio-Renal Outcomes in Patients with Type 2 Diabetes Mellitus and Kidney Disease: A Systematic Literature Review. *BMC Nephrol.* **2018**, *19*, 1–13. [CrossRef] [PubMed]
80. Jackson, C.E.; Solomon, S.D.; Gerstein, H.; Zetterstrand, S.; Olofsson, B.; Michelson, E.L.; Granger, C.B.; Swedberg, K.; A Pfeffer, M.; Yusuf, S.; et al. Albuminuria in Chronic Heart Failure: Prevalence and Prognostic Importance. *Lancet* **2009**, *374*, 543–550. [CrossRef]
81. Yang, Y.; Kim, K.; Hwang, I.; Yim, T.; Do, W.; Kim, M.; Lee, S.; Jung, H.-Y.; Choi, J.-Y.; Park, S.-H.; et al. Cystatin C–Based Equation for Predicting the Glomerular Filtration Rate in Kidney Transplant Recipients. *Transplant. Proc.* **2017**, *49*, 1018–1022. [CrossRef]
82. Wang, D.; Feng, J.-F.; Wang, A.-Q.; Yang, Y.-W.; Liu, Y.-S. Role of Cystatin C and Glomerular Filtration Rate in Diagnosis of Kidney Impairment in Hepatic Cirrhosis Patients. *Medicine* **2017**, *96*, e6949. [CrossRef] [PubMed]
83. Richter, B.; Sulzgruber, P.; Koller, L.; Steininger, M.; El-Hamid, F.; Rothgerber, D.J.; Forster, S.; Goliasch, G.; Silbert, B.I.; Meyer, E.L.; et al. Blood Urea Nitrogen Has Additive Value Beyond Estimated Glomerular Filtration Rate for Prediction of Long-Term Mortality in Patients with Acute Myocardial Infarction. *Eur. J. Intern. Med.* **2019**, *59*, 84–90. [CrossRef] [PubMed]
84. Seki, M.; Nakayama, M.; Sakoh, T.; Yoshitomi, R.; Fukui, A.; Katafuchi, E.; Tsuda, S.; Nakano, T.; Tsuruya, K.; Kitazono, T. Blood Urea Nitrogen Is Independently Associated with Renal Outcomes in Japanese Patients with Stage 3–5 Chronic Kidney Disease: A Prospective Observational Study. *BMC Nephrol.* **2019**, *20*, 115. [CrossRef] [PubMed]
85. Buonafine, M.; Martinez-Martinez, E.; Jaisser, F. More Than a Simple Biomarker: The Role of NGAL in Cardiovascular and Renal Diseases. *Clin. Sci.* **2018**, *132*, 909–923. [CrossRef] [PubMed]
86. Merdler, I.; Rozenfeld, K.-L.; Zahler, D.; Shtark, M.; Goldiner, I.; Loewenstein, I.S.; Fortis, L.; Hochstadt, A.; Keren, G.; Banai, S.; et al. Neutrophil Gelatinase-Associated Lipocalin for the Early Prediction of Acute Kidney Injury in ST-Segment Elevation Myocardial Infarction Patients Treated with Primary Percutaneous Coronary Intervention. *Cardiorenal Med.* **2020**, *10*, 154–161. [CrossRef]
87. Moresco, R.N.; Bochi, G.V.; Stein, C.S.; de Carvalho, J.A.M.; Cembranel, B.M.; Bollick, Y.S. Urinary Kidney Injury Molecule-1 in Renal Disease. *Clin. Chim. Acta* **2018**, *487*, 15–21. [CrossRef] [PubMed]
88. Maydan, O.; McDade, P.G.; Liu, Y.; Wu, X.-R.; Matsell, D.; Eddy, A.A. Uromodulin Deficiency Alters Tubular Injury and Interstitial Inflammation But Not Fibrosis in Experimental Obstructive Nephropathy. *Physiol. Rep.* **2018**, *6*, e13654. [CrossRef]
89. Nogare, A.L.; Veronese, F.V.; Carpio, V.N.; Montenegro, R.M.; Pedroso, J.A.; Pegas, K.L.; Gonçalves, L.F.; Manfro, R.C. Kidney Injury Molecule-1 Expression in Human Kidney Transplants with Interstitial Fibrosis and Tubular Atrophy. *BMC Nephrol.* **2015**, *16*, 19. [CrossRef]
90. Humphreys, B.D.; Xu, F.; Sabbisetti, V.; Grgic, I.; Naini, S.M.; Wang, N.; Chen, D.; Xiao, S.; Patel, D.; Henderson, J.M.; et al. Chronic Epithelial Kidney Injury Molecule-1 Expression Causes Murine Kidney Fibrosis. *J. Clin. Investig.* **2013**, *123*, 4023–4035. [CrossRef]
91. Edelstein, C.L. Biomarkers of Acute Kidney Injury. *Adv. Chronic Kidney Dis.* **2008**, *15*, 222–234. [CrossRef]
92. Parikh, C.R.; Abraham, E.; Ancukiewicz, M.; Edelstein, C.L. Urine IL-18 Is an Early Diagnostic Marker for Acute Kidney Injury and Predicts Mortality in the Intensive Care Unit. *J. Am. Soc. Nephrol.* **2005**, *16*, 3046–3052. [CrossRef]
93. Szabó, Z.; Magga, J.; Alakoski, T.; Ulvila, J.; Piuhola, J.; Vainio, L.; Kivirikko, K.I.; Vuolteenaho, O.; Ruskoaho, H.; Lipson, K.; et al. Connective Tissue Growth Factor Inhibition Attenuates Left Ventricular Remodeling and Dysfunction in Pressure Overload–Induced Heart Failure. *Hypertension* **2014**, *63*, 1235–1240. [CrossRef]
94. Zhao, Y.; Wang, C.; Hong, X.; Miao, J.; Liao, Y.; Hou, F.F.; Zhou, L.; Liu, Y. Wnt/β-Catenin Signaling Mediates Both Heart and Kidney Injury in Type 2 Cardiorenal Syndrome. *Kidney Int.* **2019**, *95*, 815–829. [CrossRef]
95. Lekawanvijit, S.; Kompa, A.R.; Zhang, Y.; Wang, B.H.; Kelly, D.J.; Krum, H. Myocardial Infarction Impairs Renal Function, Induces Renal Interstitial Fibrosis, and Increases Renal KIM-1 Expression: Implications for Cardiorenal Syndrome. *Am. J. Physiol. Circ. Physiol.* **2012**, *302*, H1884–H1893. [CrossRef]
96. Rockey, D.C.; Bell, P.D.; Hill, J.A. Fibrosis—A Common Pathway to Organ Injury and Failure. *N. Engl. J. Med.* **2015**, *372*, 1138–1149. [CrossRef] [PubMed]

97. Weber, K.T.; Brilla, C.G. Factors Associated with Reactive and Reparative Fibrosis of the Myocardium. *Cell. Mol. Alter. Fail. Human Heart* **1992**, *87* (Suppl. S1), 291–301. [CrossRef]
98. Baum, J.; Duffy, H.S. Fibroblasts and Myofibroblasts: What Are We Talking About? *J. Cardiovasc. Pharmacol.* **2011**, *57*, 376–379. [CrossRef] [PubMed]
99. Mack, M.; Yanagita, M. Origin of Myofibroblasts and Cellular Events Triggering Fibrosis. *Kidney Int.* **2015**, *87*, 297–307. [CrossRef]
100. Györfi, A.-H.; Matei, A.-E.; Distler, J.H. Targeting TGF-β Signaling for the Treatment of Fibrosis. *Matrix Biol.* **2018**, *68–69*, 8–27. [CrossRef] [PubMed]
101. Valiente-Alandi, I.; Potter, S.J.; Salvador, A.M.; Schafer, A.E.; Schips, T.; Carrillo-Salinas, F.J.; Gibson, A.M.; Nieman, M.L.; Perkins, C.; Sargent, M.A.; et al. Inhibiting Fibronectin Attenuates Fibrosis and Improves Cardiac Function in a Model of Heart Failure. *Circulation* **2018**, *138*, 1236–1252. [CrossRef] [PubMed]
102. Zheng, Z.; Ma, T.; Lian, X.; Gao, J.; Wang, W.; Weng, W.; Lu, X.; Sun, W.; Cheng, Y.; Fu, Y.; et al. Clopidogrel Reduces Fibronectin Accumulation and Improves Diabetes-Induced Renal Fibrosis. *Int. J. Biol. Sci.* **2019**, *15*, 239–252. [CrossRef]
103. Karsdal, M.A.; Nielsen, S.H.; Leeming, D.J.; Langholm, L.L.; Nielsen, M.J.; Manon-Jensen, T.; Siebuhr, A.; Gudmann, N.S.; Ronnow, S.; Sand, J.M.; et al. The good and the bad collagens of fibrosis—Their role in signaling and organ function. *Adv. Drug Deliv. Rev.* **2017**, *121*, 43–56. [CrossRef] [PubMed]
104. Frangogiannis, N.G. Pathophysiology of Myocardial Infarction. *Compr. Physiol.* **2015**, *5*, 1841–1875. [CrossRef] [PubMed]
105. Frangogiannis, N.G. Cardiac Fibrosis: Cell Biological Mechanisms, Molecular Pathways and Therapeutic Opportunities. *Mol. Asp. Med.* **2019**, *65*, 70–99. [CrossRef]
106. Frangogiannis, N.G. The Extracellular Matrix in Ischemic and Nonischemic Heart Failure. *Circ. Res.* **2019**, *125*, 117–146. [CrossRef]
107. Ytrehus, K.; Hulot, J.-S.; Perrino, C.; Schiattarella, G.; Madonna, R. Perivascular Fibrosis and the Microvasculature of the Heart. Still Hidden Secrets of Pathophysiology? *Vasc. Pharmacol.* **2018**, *107*, 78–83. [CrossRef] [PubMed]
108. Talman, V.; Ruskoaho, H. Cardiac fibrosis in myocardial infarction—from repair and remodeling to regeneration. *Cell Tissue Res.* **2016**, *365*, 563–581. [CrossRef]
109. Shinde, A.V.; Frangogiannis, N.G. Fibroblasts in Myocardial Infarction: A Role in Inflammation and Repair. *J. Mol. Cell. Cardiol.* **2014**, *70*, 74–82. [CrossRef] [PubMed]
110. Schilter, H.; Findlay, A.D.; Perryman, L.; Yow, T.T.; Moses, J.; Zahoor, A.; Turner, C.I.; Deodhar, M.; Foot, J.S.; Zhou, W.; et al. The Lysyl Oxidase Like 2/3 Enzymatic Inhibitor, PXS-5153A, Reduces Crosslinks and Ameliorates Fibrosis. *J. Cell. Mol. Med.* **2018**, *23*, 1759–1770. [CrossRef]
111. Doi, M.; Kusachi, S.; Murakami, T.; Ninomiya, Y.; Murakami, M.; Nakahama, M.; Takeda, K.; Komatsubara, I.; Naito, I.; Tsuji, T. Time-Dependent Changes of Decorin in the Infarct Zone After Experimentally Induced Myocardial Infarction in Rats: Comparison with Biglycan. *Pathol. Res. Pract.* **2000**, *196*, 23–33. [CrossRef]
112. Li, L.; Okada, H.; Takemura, G.; Kosai, K.-I.; Kanamori, H.; Esaki, M.; Takahashi, T.; Goto, K.; Tsujimoto, A.; Maruyama, R.; et al. Postinfarction Gene Therapy with Adenoviral Vector Expressing Decorin Mitigates Cardiac Remodeling and Dysfunction. *Am. J. Physiol. Circ. Physiol.* **2009**, *297*, H1504–H1513. [CrossRef]
113. Nakahama, M.; Murakami, T.; Kusachi, S.; Naito, I.; Takeda, K.; Ohnishi, H.; Komatsubara, I.; Oka, T.; Ninomiya, Y.; Tsuji, T. Expression of Perlecan Proteoglycan in the Infarct Zone of Mouse Myocardial Infarction. *J. Mol. Cell. Cardiol.* **2000**, *32*, 1087–1100. [CrossRef] [PubMed]
114. Sasse, P.; Malan, D.; Fleischmann, M.; Roell, W.; Gustafsson, E.; Bostani, T.; Fan, Y.; Kolbe, T.; Breitbach, M.; Addicks, K.; et al. Perlecan Is Critical for Heart Stability. *Cardiovasc. Res.* **2008**, *80*, 435–444. [CrossRef]
115. Fu, X.; Khalil, H.; Kanisicak, O.; Boyer, J.G.; Vagnozzi, R.J.; Maliken, B.D.; Sargent, M.A.; Prasad, V.; Valiente-Alandi, I.; Blaxall, B.C.; et al. Specialized Fibroblast Differentiated States Underlie Scar Formation in the Infarcted Mouse Heart. *J. Clin. Investig.* **2018**, *128*, 2127–2143. [CrossRef]
116. Woodiwiss, A.J.; Tsotetsi, O.J.; Sprott, S.; Lancaster, E.J.; Mela, T.; Chung, E.S.; Meyer, T.E.; Norton, G. Reduction in Myocardial Collagen Cross-Linking Parallels Left Ventricular Dilatation in Rat Models of Systolic Chamber Dysfunction. *Circulation* **2001**, *103*, 155–160. [CrossRef]
117. Santamaria, J.G.; Villalba, M.; Busnadiego, O.; López-Olañeta, M.M.; Sandoval, P.; Snabel, J.; López-Cabrera, M.; Erler, J.; Hanemaaijer, R.; Lara-Pezzi, E.; et al. Matrix Cross-Linking Lysyl Oxidases Are Induced in Response to Myocardial Infarction and Promote Cardiac Dysfunction. *Cardiovasc. Res.* **2015**, *109*, 67–78. [CrossRef]
118. Siebermair, J.; Suksaranjit, P.; McGann, C.J.; Peterson, K.A.; Kheirkhahan, M.; Baher, A.A.; Damal, K.; Wakili, R.; Marrouche, N.F.; Wilson, B.D. Atrial Fibrosis in non–atrial Fibrillation Individuals and Prediction of Atrial Fibrillation by Use of Late Gadolinium Enhancement Magnetic Resonance Imaging. *J. Cardiovasc. Electrophysiol.* **2019**, *30*, 550–556. [CrossRef] [PubMed]
119. Tan, T.C.; Koutsogeorgis, I.D.; Grapsa, J.; Papadopoulos, C.; Katsivas, A.; Nihoyannopoulos, P. Left Atrium and the Imaging of Atrial Fibrosis: Catch It If You Can! *Eur. J. Clin. Investig.* **2014**, *44*, 872–881. [CrossRef]
120. Yang, J.; Savvatis, K.; Kang, J.S.; Fan, P.; Zhong, H.; Schwartz, K.; Barry, V.; Mikels-Vigdal, A.; Karpinski, S.; Kornyeyev, D.; et al. Targeting LOXL2 for Cardiac Interstitial Fibrosis and Heart Failure Treatment. *Nat. Commun.* **2016**, *7*, 13710. [CrossRef] [PubMed]
121. De Gaspari, M.; Toscano, G.; Bagozzi, L.; Metra, M.; Lombardi, C.; Rizzo, S.; Angelini, A.; Marra, M.P.; Gerosa, G.; Basso, C. Endomyocardial Fibrosis and Myocardial Infarction Leading to Diastolic and Systolic Dysfunction Requiring Transplantation. *Cardiovasc. Pathol. Off. J. Soc. Cardiovasc. Pathol.* **2019**, *38*, 21–24. [CrossRef] [PubMed]

122. Nucifora, G.; Muser, D.; Gianfagna, P.; Morocutti, G.; Proclemer, A. Systolic and Diastolic Myocardial Mechanics in Hypertrophic Cardiomyopathy and Their Link to the Extent of Hypertrophy, Replacement Fibrosis and Interstitial Fibrosis. *Int. J. Cardiovasc. Imaging* **2015**, *31*, 1603–1610. [CrossRef] [PubMed]
123. Shinde, A.V.; Su, Y.; Palanski, B.A.; Fujikura, K.; Garcia, M.J.; Frangogiannis, N.G. Pharmacologic Inhibition of the Enzymatic Effects of Tissue Transglutaminase Reduces Cardiac Fibrosis and Attenuates Cardiomyocyte Hypertrophy Following Pressure Overload. *J. Mol. Cell. Cardiol.* **2018**, *117*, 36–48. [CrossRef] [PubMed]
124. A Beltrami, C.; Finato, N.; Rocco, M.; A Feruglio, G.; Puricelli, C.; Cigola, E.; Quaini, F.; Sonnenblick, E.H.; Olivetti, G.; Anversa, P. Structural Basis of End-Stage Failure in Ischemic Cardiomyopathy in Humans. *Circulation* **1994**, *89*, 151–163. [CrossRef] [PubMed]
125. Shah, N.N.; Ayyadurai, P.; Saad, M.; E Kosmas, C.; Dogar, M.U.; Patel, U.; Vittorio, T.J. Galectin-3 and Soluble ST2 As Complementary Tools to Cardiac MRI for Sudden Cardiac Death Risk Stratification in Heart Failure: A Review. *JRSM Cardiovasc. Dis.* **2020**, *9*. [CrossRef]
126. Kim, E.K.; Chattranukulchai, P.; Klem, I. Cardiac Magnetic Resonance Scar Imaging for Sudden Cardiac Death Risk Stratification in Patients with Non-Ischemic Cardiomyopathy. *Korean J. Radiol.* **2015**, *16*, 683–695. [CrossRef]
127. Kato, S.; Saito, N.; Kirigaya, H.; Gyotoku, D.; Iinuma, N.; Kusakawa, Y.; Iguchi, K.; Nakachi, T.; Fukui, K.; Futaki, M.; et al. Prognostic Significance of Quantitative Assessment of Focal Myocardial Fibrosis in Patients with Heart Failure with Preserved Ejection Fraction. *Int. J. Cardiol.* **2015**, *191*, 314–319. [CrossRef]
128. King, J.B.; Azadani, P.N.; Suksaranjit, P.; Bress, A.P.; Witt, D.M.; Han, F.T.; Chelu, M.; Silver, M.A.; Biskupiak, J.; Wilson, B.D.; et al. Left Atrial Fibrosis and Risk of Cerebrovascular and Cardiovascular Events in Patients with Atrial Fibrillation. *J. Am. Coll. Cardiol.* **2017**, *70*, 1311–1321. [CrossRef] [PubMed]
129. Peddakkulappagari, C.S.; Saifi, M.A.; Khurana, A.; Anchi, P.; Singh, M.; Godugu, C. Withaferin A Ameliorates Renal Injury Due to Its Potent Effect on Inflammatory Signaling. *BioFactors* **2019**, *45*, 750–762. [CrossRef]
130. Tammaro, A.; Florquin, S.; Brok, M.; Claessen, N.; Butter, L.M.; Teske, G.J.D.; de Boer, O.; Vogl, T.; Leemans, J.C.; Dessing, M.C. S100A8/A9 Promotes Parenchymal Damage and Renal Fibrosis in Obstructive Nephropathy. *Clin. Exp. Immunol.* **2018**, *193*, 361–375. [CrossRef]
131. Grande, M.T.; Sanchez-Laorden, B.; López-Blau, C.; De Frutos, C.A.; Boutet, A.; Arévalo, M.; Rowe, R.G.; Weiss, S.J.; López-Novoa, J.M.; Nieto, M.A. Snail1-Induced Partial Epithelial-to-Mesenchymal Transition Drives Renal Fibrosis in Mice and Can Be Targeted to Reverse Established Disease. *Nat. Med.* **2015**, *21*, 989–997. [CrossRef]
132. Xie, K.; Bao, L.; Jiang, X.; Ye, Z.; Bing, J.; Dong, Y.; Gao, D.; Ji, X.; Jiang, T.; Li, J.; et al. The Association of Metabolic Syndrome Components and Chronic Kidney Disease in Patients with Hypertension. *Lipids Health Dis.* **2019**, *18*, 1–6. [CrossRef]
133. Alicic, R.Z.; Rooney, M.T.; Tuttle, K. Diabetic Kidney Disease. *Clin. J. Am. Soc. Nephrol.* **2017**, *12*, 2032–2045. [CrossRef]
134. Mordi, I.; Mordi, N.; Delles, C.; Tzemos, N. Endothelial Dysfunction in Human Essential Hypertension. *J. Hypertens.* **2016**, *34*, 1464–1472. [CrossRef] [PubMed]
135. Shi, Y.; Vanhoutte, P.M. Macro- and Microvascular Endothelial Dysfunction in Diabetes. *J. Diabetes* **2017**, *9*, 434–449. [CrossRef]
136. Moriya, T.; Yamagishi, T.; Matsubara, M.; Ouchi, M. Serial Renal Biopsies in Normo- and Microalbuminuric Patients with Type 2 Diabetes Demonstrate That Loss of Renal Function Is Associated with a Reduction in Glomerular Filtration Surface Secondary to Mesangial Expansion. *J. Diabetes Complicat.* **2019**, *33*, 368–373. [CrossRef] [PubMed]
137. Heintz, B.; Stöcker, G.; Mrowka, C.; Rentz, U.; Melzer, H.; Stickeler, E.; Sieberth, H.-G.; Greiling, H.; Haubeck, H.-D. Decreased Glomerular Basement Membrane Heparan Sulfate Proteoglycan in Essential Hypertension. *Hypertension* **1995**, *25*, 399–407. [CrossRef]
138. Salem, R.M.; Todd, J.N.; Sandholm, N.; Cole, J.B.; Chen, W.-M.; Andrews, D.; Pezzolesi, M.G.; McKeigue, P.M.; Hiraki, L.T.; Qiu, C.; et al. Genome-Wide Association Study of Diabetic Kidney Disease Highlights Biology Involved in Glomerular Basement Membrane Collagen. *J. Am. Soc. Nephrol.* **2019**, *30*, 2000–2016. [CrossRef] [PubMed]
139. Tung, C.-W.; Hsu, Y.-C.; Shih, Y.-H.; Chang, P.-J.; Lin, C.-L. Glomerular Mesangial Cell and Podocyte Injuries in Diabetic Nephropathy. *Nephrology* **2018**, *23*, 32–37. [CrossRef]
140. Puelles, V.G.; Cullen-McEwen, L.; Taylor, G.E.; Li, J.; Hughson, M.D.; Kerr, P.G.; Hoy, W.E.; Bertram, J. Human Podocyte Depletion in Association with Older Age and Hypertension. *Am. J. Physiol. Physiol.* **2016**, *310*, F656–F668. [CrossRef]
141. Liu, Y. Cellular and molecular mechanisms of renal fibrosis. *Nat. Rev. Nephrol.* **2011**, *7*, 684–696. [CrossRef]
142. Conlin, C.C.; Huang, Y.; Gordon, B.A.J.; Zhang, J.L. Quantitative Characterization of Glomerular Fibrosis with Magnetic Resonance Imaging: A Feasibility Study in a Rat Glomerulonephritis Model. *Am. J. Physiol. Physiol.* **2018**, *314*, F747–F752. [CrossRef] [PubMed]
143. Zhou, C.; Lou, K.; Tatum, K.; Funk, J.; Wu, J.; Bartkowiak, T.; Kagan, D.; Lou, Y. Differentiating Glomerular Inflammation from Fibrosis in a Bone Marrow Chimera for Rat Anti-Glomerular Basement Membrane Glomerulonephritis. *Am. J. Nephrol.* **2015**, *42*, 42–53. [CrossRef] [PubMed]
144. Genovese, F.; A Manresa, A.; Leeming, D.J.; Karsdal, M.A.; Boor, P. The Extracellular Matrix in the Kidney: A Source of Novel Non-Invasive Biomarkers of Kidney Fibrosis? *Fibrogenesis Tissue Repair* **2014**, *7*, 4. [CrossRef]
145. Bohle, A.; Mackensen-Haen, S.; Gise, H.V. Significance of Tubulointerstitial Changes in the Renal Cortex for the Excretory Function and Concentration Ability of the Kidney: A Morphometric Contribution. *Am. J. Nephrol.* **1987**, *7*, 421–433. [CrossRef]
146. Tervaert, T.W.C.; Mooyaart, A.; Amann, K.; Cohen, A.H.; Cook, H.T.; Drachenberg, C.B.; Ferrario, F.; Fogo, A.B.; Haas, M.; De Heer, E.; et al. Pathologic Classification of Diabetic Nephropathy. *J. Am. Soc. Nephrol.* **2010**, *21*, 556–563. [CrossRef] [PubMed]

147. Boor, P.; Perkuhn, M.; Ms, M.W.; Zok, S.; Martin, W.; Ms, J.G.; Schoth, F.; Ostendorf, T.; Kuhl, C.; Floege, J. Diffusion-Weighted MRI Does Not Reflect Kidney Fibrosis in a Rat Model of Fibrosis. *J. Magn. Reson. Imaging* **2015**, *42*, 990–998. [CrossRef]
148. Zhao, J.; Wang, Z.; Liu, M.; Zhu, J.; Zhang, X.; Zhang, T.; Li, S.; Li, Y. Assessment of Renal Fibrosis in Chronic Kidney Disease Using Diffusion-Weighted MRI. *Clin. Radiol.* **2014**, *69*, 1117–1122. [CrossRef]
149. Eadon, M.T.; Schwantes-An, T.-H.; Phillips, C.L.; Roberts, A.R.; Greene, C.V.; Hallab, A.; Hart, K.J.; Lipp, S.N.; Perez-Ledezma, C.; Omar, K.O.; et al. Kidney Histopathology and Prediction of Kidney Failure: A Retrospective Cohort Study. *Am. J. Kidney Dis.* **2020**, *76*, 350–360. [CrossRef]
150. Belghasem, M.E.; A'Amar, O.; Roth, D.; Walker, J.; Arinze, N.; Richards, S.M.; Francis, J.M.; Salant, D.J.; Chitalia, V.C.; Bigio, I.J. Towards Minimally-Invasive, Quantitative Assessment of Chronic Kidney Disease Using Optical Spectroscopy. *Sci. Rep.* **2019**, *9*, 7168. [CrossRef] [PubMed]
151. Nath, K.A. Tubulointerstitial Changes As a Major Determinant in the Progression of Renal Damage. *Am. J. Kidney Dis.* **1992**, *20*, 1–17. [CrossRef]
152. Howie, A.J.; Ferreira, M.A.S.; Adu, D. Prognostic Value of Simple Measurement of Chronic Damage in Renal Biopsy Specimens. *Nephrol. Dial. Transplant.* **2001**, *16*, 1163–1169. [CrossRef]
153. Kaissling, B.; LeHir, M.; Kriz, W. Renal Epithelial Injury and Fibrosis. *Biochim. Biophys. Acta Mol. Basis Dis.* **2013**, *1832*, 931–939. [CrossRef]
154. Rosenberg, A.; Kopp, J. Focal Segmental Glomerulosclerosis. *Clin. J. Am. Soc. Nephrol.* **2017**, *12*, 502–517. [CrossRef]
155. Palatini, P. Glomerular Hyperfiltration: A Marker of Early Renal Damage in Pre-Diabetes and Pre-Hypertension. *Nephrol. Dial. Transplant.* **2012**, *27*, 1708–1714. [CrossRef] [PubMed]
156. Kriz, W.; Lehir, M. Pathways to Nephron Loss Starting from Glomerular diseases—Insights from Animal Models. *Kidney Int.* **2005**, *67*, 404–419. [CrossRef] [PubMed]
157. Dong, J.; Li, Y.; Yue, S.; Liu, X.; Wang, L.; Xiong, M.; Wang, G.; Nie, S.; Xu, X. The Profiles of Biopsy-Proven Renal Tubulointerstitial Lesions in Patients with Glomerular Disease. *Ann. Transl. Med.* **2020**, *8*, 1066. [CrossRef] [PubMed]
158. Tang, P.M.K.; Nikolic-Paterson, D.J.; Lan, H.-Y. Macrophages: Versatile Players in Renal Inflammation and Fibrosis. *Nat. Rev. Nephrol.* **2019**, *15*, 144–158. [CrossRef] [PubMed]
159. Zhao, J.-H. Mesangial Cells and Renal Fibrosis. *Adv. Exp. Med. Biol.* **2019**, *1165*, 165–194. [CrossRef]
160. Bülow, R.D.; Boor, P. Extracellular Matrix in Kidney Fibrosis: More Than Just a Scaffold. *J. Histochem. Cytochem.* **2019**, *67*, 643–661. [CrossRef]
161. Müller, G.A.; Rodemann, H.P. Characterization of Human Renal Fibroblasts in Health and Disease: I. Immunophenotyping of Cultured Tubular Epithelial Cells and Fibroblasts Derived from Kidneys with Histologically Proven Interstitial Fibrosis. *Am. J. Kidney Dis.* **1991**, *17*, 680–683. [CrossRef]
162. Rodemann, H.P.; Müller, G.A. Characterization of Human Renal Fibroblasts in Health and Disease: II. In Vitro Growth, Differentiation, and Collagen Synthesis of Fibroblasts from Kidneys with Interstitial Fibrosis. *Am. J. Kidney Dis.* **1991**, *17*, 684–686. [CrossRef]
163. Koesters, R.; Kaissling, B.; LeHir, M.; Picard, N.; Theilig, F.; Gebhardt, R.; Glick, A.B.; Hähnel, B.; Hosser, H.; Gröne, H.-J.; et al. Tubular Overexpression of Transforming Growth Factor-β1 Induces Autophagy and Fibrosis But Not Mesenchymal Transition of Renal Epithelial Cells. *Am. J. Pathol.* **2010**, *177*, 632–643. [CrossRef] [PubMed]
164. Kriz, W.; Hähnel, B.; Hosser, H.; Ostendorf, T.; Gaertner, S.; Kränzlin, B.; Gretz, N.; Shimizu, F.; Floege, J. Pathways to Recovery and Loss of Nephrons in Anti-Thy-1 Nephritis. *J. Am. Soc. Nephrol.* **2003**, *14*, 1904–1926. [CrossRef] [PubMed]
165. Cheng, S.; Pollock, A.S.; Mahimkar, R.; Olson, J.L.; Lovett, D.H. Matrix Metalloproteinase 2 and Basement Membrane Integrity: A Unifying Mechanism for Progressive Renal Injury. *FASEB J.* **2006**, *20*, 1898–1900. [CrossRef] [PubMed]
166. Nadasdy, T.; Laszik, Z.; E Blick, K.; Johnson, L.D.; Silva, F.G. Proliferative Activity of Intrinsic Cell Populations in the Normal Human Kidney. *J. Am. Soc. Nephrol.* **1994**, *4*, 2032–2039. [CrossRef]
167. Humphreys, B.D.; Valerius, M.T.; Kobayashi, A.; Mugford, J.W.; Soeung, S.; Duffield, J.S.; McMahon, A.P.; Bonventre, J.V. Intrinsic Epithelial Cells Repair the Kidney After Injury. *Cell Stem Cell* **2008**, *2*, 284–291. [CrossRef]
168. Yang, L.; Besschetnova, T.Y.; Brooks, C.R.; Shah, J.V.; Bonventre, J.V. Epithelial Cell Cycle Arrest in G2/M Mediates Kidney Fibrosis After Injury. *Nat. Med.* **2010**, *16*, 535–543. [CrossRef]
169. Grgic, I.; Campanholle, G.; Bijol, V.; Wang, C.; Sabbisetti, V.S.; Ichimura, T.; Humphreys, B.D.; Bonventre, J.V. Targeted Proximal Tubule Injury Triggers Interstitial Fibrosis and Glomerulosclerosis. *Kidney Int.* **2012**, *82*, 172–183. [CrossRef]
170. Xu, L.; Sharkey, D.; Cantley, L.G. Tubular GM-CSF Promotes Late MCP-1/CCR2-Mediated Fibrosis and Inflammation After Ischemia/Reperfusion Injury. *J. Am. Soc. Nephrol.* **2019**, *30*, 1825–1840. [CrossRef]
171. Arfian, N.; Wahyudi, D.A.P.; Zulfatina, I.B.; Citta, A.N.; Anggorowati, N.; Multazam, A.; Romi, M.M.; Sari, D.C.R. Chlorogenic Acid Attenuates Kidney Ischemic/Reperfusion Injury via Reducing Inflammation, Tubular Injury, and Myofibroblast Formation. *BioMed Res. Int.* **2019**, *2019*, 1–10. [CrossRef]
172. Jing, W.; Vaziri, N.D.; Nunes, A.C.F.; Suematsu, Y.; Farzaneh, T.; Khazaeli, M.; Moradi, H. LCZ696 (Sacubitril/Valsartan) Ameliorates Oxidative Stress, Inflammation, Fibrosis and Improves Renal Function Beyond Angiotensin Receptor Blockade in CKD. *Am. J. Transl. Res.* **2017**, *9*, 5473–5484.
173. Fortrie, G.; De Geus, H.R.H.; Betjes, M.G.H. The Aftermath of Acute Kidney Injury: A Narrative Review of Long-Term Mortality and Renal Function. *Crit. Care* **2019**, *23*, 1–11. [CrossRef] [PubMed]

174. Stroo, I.; Stokman, G.; Teske, G.J.D.; Raven, A.; Butter, L.M.; Florquin, S.; Leemans, J.C. Chemokine Expression in Renal ischemia/Reperfusion Injury Is Most Profound During the Reparative Phase. *Int. Immunol.* **2010**, *22*, 433–442. [CrossRef]
175. Ali, B.H.; Al-Salam, S.; Al Suleimani, Y.; Al Kalbani, J.; Al Bahlani, S.; Ashique, M.; Manoj, P.; Al Dhahli, B.; Al Abri, N.; Naser, H.T.; et al. Curcumin Ameliorates Kidney Function and Oxidative Stress in Experimental Chronic Kidney Disease. *Basic Clin. Pharmacol. Toxicol.* **2018**, *122*, 65–73. [CrossRef]
176. Fabre, T.; Kared, H.; Friedman, S.L.; Shoukry, N.H. IL-17A Enhances the Expression of Profibrotic Genes through Upregulation of the TGF-β Receptor on Hepatic Stellate Cells in a JNK-Dependent Manner. *J. Immunol.* **2014**, *193*, 3925–3933. [CrossRef]
177. Mack, M. Inflammation and Fibrosis. *Matrix Biol.* **2018**, *68-69*, 106–121. [CrossRef] [PubMed]
178. Massagué, J. TGFβ Signalling in Context. *Nat. Rev. Mol. Cell Biol.* **2012**, *13*, 616–630. [CrossRef]
179. Finnson, K.; Almadani, Y.; Philip, A. Non-Canonical (non-SMAD2/3) TGF-β Signaling in Fibrosis: Mechanisms and Targets. *Semin. Cell Dev. Biol.* **2020**, *101*, 115–122. [CrossRef]
180. Sun, K.-H.; Chang, Y.; Reed, N.I.; Sheppard, D. α-Smooth Muscle Actin Is an Inconsistent Marker of Fibroblasts Responsible for Force-Dependent TGFβ Activation or Collagen Production across Multiple Models of Organ Fibrosis. *Am. J. Physiol. Cell. Mol. Physiol.* **2016**, *310*, L824–L836. [CrossRef] [PubMed]
181. Walker, E.J.; Heydet, D.; Veldre, T.; Ghildyal, R. Transcriptomic Changes During TGF-β-Mediated Differentiation of Airway Fibroblasts to Myofibroblasts. *Sci. Rep.* **2019**, *9*, 1–14. [CrossRef]
182. Chen, W.; Dijke, P.T. Immunoregulation by Members of the TGFβ Superfamily. *Nat. Rev. Immunol.* **2016**, *16*, 723–740. [CrossRef] [PubMed]
183. Gravning, J.; Ørn, S.; Kaasbøll, O.J.; Martinov, V.N.; Manhenke, C.; Dickstein, K.; Edvardsen, T.; Attramadal, H.; Ahmed, M.S. Myocardial Connective Tissue Growth Factor (CCN2/CTGF) Attenuates Left Ventricular Remodeling After Myocardial Infarction. *PLoS ONE* **2012**, *7*, e52120. [CrossRef]
184. Mao, L.; Liu, L.; Zhang, T.; Wu, X.; Zhang, T.; Xu, Y. MKL1 Mediates TGF-β-induced CTGF Transcription to Promote Renal Fibrosis. *J. Cell. Physiol.* **2020**, *235*, 4790–4803. [CrossRef]
185. Mori, T.; Kawara, S.; Shinozaki, M.; Hayashi, N.; Kakinuma, T.; Igarashi, A.; Takigawa, M.; Nakanishi, T.; Takehara, K. Role and in-Teraction of Connective Tissue Growth Factor with Transforming Growth Factor-Beta in Persistent Fibrosis: A Mouse Fibrosis Model. *J. Cell Physiol.* **1999**, *181*, 153–159. [CrossRef]
186. (96) Frazier, K.; Williams, S.; Kothapalli, D.; Klapper, H.; Grotendorst, G.R. Stimulation of Fibroblast Cell Growth, Matrix Production, and Granulation Tissue Formation by Connective Tissue Growth Factor. *J. Investig. Dermatol.* **1996**, *107*, 404–411. [CrossRef] [PubMed]
187. Igarashi, A.; Nashiro, K.; Kikuchi, K.; Sato, S.; Ihn, H.; Fujimoto, M.; Grotendorst, G.R.; Takehara, K. Connective Tissue Growth Factor Gene Expression in Tissue Sections from Localized Scleroderma, Keloid, and Other Fibrotic Skin Disorders. *J. Investig. Dermatol.* **1996**, *106*, 729–733. [CrossRef]
188. Inanc, S.; Keleş, D.; Oktay, G. An Improved Collagen Zymography Approach for Evaluating the Collagenases MMP-1, MMP-8, and MMP-13. *Biotechnology* **2017**, *63*, 174–180. [CrossRef]
189. Falconer, A.M.D.; Chan, C.M.; Gray, J.; Nagashima, I.; Holland, R.A.; Shimizu, H.; Pickford, A.R.; Rowan, A.D.; Wilkinson, D.J. Collagenolytic Matrix Metalloproteinases Antagonize Proteinase-Activated Receptor-2 Activation, Providing Insights into Extracellular Matrix Turnover. *J. Biol. Chem.* **2019**, *294*, 10266–10277. [CrossRef]
190. Toth, M.; Sohail, A.; Fridman, R. Assessment of Gelatinases (MMP-2 and MMP-9) by Gelatin Zymography. In *Metastasis Research Protocols*; Humana Press: Totowa, NJ, USA, 2012; pp. 163–174.
191. Vafashoar, F.; Mousavizadeh, K.; Poormoghim, H.; Tavasoli, A.; Shabestari, T.M.; JavadMoosavi, S.A.; Mojtabavi, N. Gelatinases Increase in Bleomycin-Induced Systemic Sclerosis Mouse Model. *Iran. J. Allergy Asthma Immunol.* **2019**, *18*, 182–189. [CrossRef]
192. Butler, G.S.; Connor, A.R.; Sounni, N.E.; Eckhard, U.; Morrison, C.J.; Noel, A.; Overall, C.M. Degradomic and Yeast 2-Hybrid Inactive Catalytic Domain Substrate Trapping Identifies New Membrane-Type 1 Matrix Metalloproteinase (MMP14) Substrates: CCN3 (Nov) and CCN5 (WISP2). *Matrix Biol.* **2017**, *59*, 23–38. [CrossRef] [PubMed]
193. Mirastschijski, U.; Dinesh, N.; Baskaran, S.; Wedekind, D.; Gavrilovic, J.; Murray, M.Y.; Bevan, D.; Kelm, S. Novel Specific Human and Mouse stromelysin-1 (MMP-3) and stromelysin-2 (MMP-10) Antibodies for Biochemical and Immunohistochemical Analyses. *Wound Repair Regen.* **2019**, *27*, 309–323. [CrossRef] [PubMed]
194. Giannandrea, M.; Parks, W.C. Diverse Functions of Matrix Metalloproteinases During Fibrosis. *Dis. Model. Mech.* **2014**, *7*, 193–203. [CrossRef] [PubMed]
195. Wang, H.; Gao, M.; Li, J.; Sun, J.; Wu, R.; Han, D.; Tan, J.; Wang, J.; Wang, B.; Zhang, L.; et al. MMP-9-positive Neutrophils Are Essential for Establishing Profibrotic Microenvironment in the Obstructed Kidney of UUO Mice. *Acta Physiol.* **2019**, *227*, e13317. [CrossRef]
196. Zhao, Y.; Qiao, X.; Tan, T.K.; Zhao, H.; Zhang, Y.; Liu, L.; Zhang, J.; Wang, L.; Cao, Q.; Wang, Y.; et al. Matrix Metalloproteinase 9-Dependent Notch Signaling Contributes to Kidney Fibrosis through Peritubular Endothelial-Mesenchymal Transition. *Nephrol. Dial. Transplant.* **2016**, *32*, 781–791. [CrossRef] [PubMed]
197. Chiao, Y.A.; Ramirez, T.A.; Zamilpa, R.; Okoronkwo, S.M.; Dai, Q.; Zhang, J.; Jin, Y.-F.; Lindsey, M.L. Matrix Metalloproteinase-9 Deletion Attenuates Myocardial Fibrosis and Diastolic Dysfunction in Ageing Mice. *Cardiovasc. Res.* **2012**, *96*, 444–455. [CrossRef]

198. Altieri, P.; Brunelli, C.; Garibaldi, S.; Nicolino, A.; Ubaldi, S.; Spallarossa, P.; Olivotti, L.; Rossettin, P.; Barsotti, A.; Ghigliotti, G. Metalloproteinases 2 and 9 Are Increased in Plasma of Patients with Heart Failure. *Eur. J. Clin. Investig.* **2003**, *33*, 648–656. [CrossRef]
199. Takamiya, Y.; Fukami, K.; Yamagishi, S.-I.; Kaida, Y.; Nakayama, Y.; Obara, N.; Iwatani, R.; Ando, R.; Koike, K.; Matsui, T.; et al. Experimental Diabetic Nephropathy Is Accelerated in Matrix Metalloproteinase-2 Knockout Mice. *Nephrol. Dial. Transplant.* **2012**, *28*, 55–62. [CrossRef]
200. Jao, T.-M.; Nangaku, M.; Wu, C.-H.; Sugahara, M.; Saito, H.; Maekawa, H.; Ishimoto, Y.; Aoe, M.; Inoue, T.; Tanaka, T.; et al. ATF6α Downregulation of PPARα Promotes Lipotoxicity-Induced Tubulointerstitial Fibrosis. *Kidney Int.* **2019**, *95*, 577–589. [CrossRef]
201. Jiménez-González, S.; Marín-Royo, G.; Jurado-López, R.; Bartolomé, M.V.; Miranda, A.R.; Luaces, M.; Islas, F.; Nieto, M.L.; Martínez-Martínez, E.; Cachofeiro, V. The Crosstalk Between Cardiac Lipotoxicity and Mitochondrial Oxidative Stress in the Cardiac Alterations in Diet-Induced Obesity in Rats. *Cells* **2020**, *9*, 451. [CrossRef]
202. Delgado-Valero, B.; de la Fuente-Chávez, L.; Romero-Miranda, A.; Bartolomé, M.V.; Ramchandani, B.; Islas, F.; Luaces, M.; Cachofeiro, V.; Martínez-Martínez, E. Role of Endoplasmic Reticulum Stress in Renal Damage After Myocardial Infarction. *Clin. Sci.* **2021**, *135*, 143–159. [CrossRef]
203. Nogueira, A.; Pires, M.J.; Oliveira, P.A. Pathophysiological Mechanisms of Renal Fibrosis: A Review of Animal Models and Therapeutic Strategies. *Vivo* **2017**, *31*, 1–22. [CrossRef]
204. Sun, H.-J. Current Opinion for Hypertension in Renal Fibrosis. *Adv. Exp. Med. Biol.* **2019**, *1165*, 37–47. [CrossRef]
205. Rubinstein, J.; Sanford, D. Treatment of Cardiorenal Syndrome. *Cardiol. Clin.* **2019**, *37*, 267–273. [CrossRef]
206. Wang, L.; Tian, X.; Cao, Y.; Ma, X.; Shang, L.; Li, H.; Zhang, X.; Deng, F.; Li, S.; Guo, T.; et al. Cardiac Shock Wave Therapy Improves Ventricular Function by Relieving Fibrosis Through PI3K/Akt Signaling Pathway: Evidence from a Rat Model of Post-Infarction Heart Failure. *Front. Cardiovasc. Med.* **2021**, *8*, 693875. [CrossRef] [PubMed]
207. Zindel, J.; Kubes, P. DAMPs, PAMPs, and LAMPs in Immunity and Sterile Inflammation. *Annu. Rev. Pathol. Mech. Dis.* **2020**, *15*, 493–518. [CrossRef] [PubMed]
208. Abdulkhaleq, L.A.; Assi, M.A.; Abdullah, R.; Zamri-Saad, M.; Taufiq-Yap, Y.H.; Hezmee, M.N.M. The Crucial Roles of Inflammatory Mediators in Inflammation: A Review. *Veter. World* **2018**, *11*, 627–635. [CrossRef] [PubMed]
209. Clark, R.; Kupper, T. Old Meets New: The Interaction Between Innate and Adaptive Immunity. *J. Investig. Dermatol.* **2005**, *125*, 629–637. [CrossRef] [PubMed]
210. Furman, D.; Campisi, J.; Verdin, E.; Carrera-Bastos, P.; Targ, S.; Franceschi, C.; Ferrucci, L.; Gilroy, D.W.; Fasano, A.; Miller, G.W.; et al. Chronic Inflammation in the Etiology of Disease across the Life Span. *Nat. Med.* **2019**, *25*, 1822–1832. [CrossRef]
211. Odegaard, A.O.; Goff, D.R., Jr.; Sanchez, O.A.; Goff, D.C.; Reiner, A.P.; Gross, M.D. Oxidative Stress, Inflammation, Endothelial Dysfunction and Incidence of Type 2 Diabetes. *Cardiovasc. Diabetol.* **2016**, *15*, 1–12. [CrossRef]
212. Kanazawa, I.; Tanaka, S.; Sugimoto, T. The Association Between Osteocalcin and Chronic Inflammation in Patients with Type 2 Diabetes Mellitus. *Calcif. Tissue Int.* **2018**, *103*, 599–605. [CrossRef]
213. Xiao, L.; Harrison, D.G. Inflammation in Hypertension. *Can. J. Cardiol.* **2020**, *36*, 635–647. [CrossRef]
214. Rios, F.; Zou, Z.-G.; Harvey, A.P.; Harvey, K.Y.; Nosalski, R.; Anyfanti, P.; Camargo, L.L.; Lacchini, S.; Ryazanov, A.G.; Ryazanova, L.; et al. Chanzyme TRPM7 Protects Against Cardiovascular Inflammation and Fibrosis. *Cardiovasc. Res.* **2020**, *116*, 721–735. [CrossRef] [PubMed]
215. Ridker, P.M.; Everett, B.M.; Thuren, T.; MacFadyen, J.G.; Chang, W.H.; Ballantyne, C.; Fonseca, F.; Nicolau, J.; Koenig, W.; Anker, S.D.; et al. Antiinflammatory Therapy with Canakinumab for Atherosclerotic Disease. *N. Engl. J. Med.* **2017**, *377*, 1119–1131. [CrossRef]
216. Mihai, S.; Codrici, E.; Popescu, I.D.; Enciu, A.-M.; Albulescu, L.; Necula, L.G.; Mambet, C.; Anton, G.; Tanase, C. Inflammation-Related Mechanisms in Chronic Kidney Disease Prediction, Progression, and Outcome. *J. Immunol. Res.* **2018**, *2018*, 1–16. [CrossRef] [PubMed]
217. Torres, S.; Fabersani, E.; Marquez, A.; Gauffin-Cano, P. Adipose Tissue Inflammation and Metabolic Syndrome. The Proactive Role of Probiotics. *Eur. J. Nutr.* **2018**, *58*, 27–43. [CrossRef] [PubMed]
218. Pierce, G.F.; A Mustoe, T.; Lingelbach, J.; Masakowski, V.R.; Griffin, G.L.; Senior, R.M.; Deuel, T.F. Platelet-Derived Growth Factor and Transforming Growth Factor-Beta Enhance Tissue Repair Activities by Unique Mechanisms. *J. Cell Biol.* **1989**, *109*, 429–440. [CrossRef] [PubMed]
219. Rossaint, J.; Margraf, A.; Zarbock, A. Role of Platelets in Leukocyte Recruitment and Resolution of Inflammation. *Front. Immunol.* **2018**, *9*, 2712. [CrossRef] [PubMed]
220. Lichtman, M.K.; Otero-Vinas, M.; Falanga, V. Transforming Growth Factor Beta (TGF-β) Isoforms in Wound Healing and Fibrosis. *Wound Repair Regen.* **2015**, *24*, 215–222. [CrossRef] [PubMed]
221. Amdur, R.L.; Feldman, H.I.; Gupta, J.; Yang, W.; Kanetsky, P.; Shlipak, M.; Rahman, M.; Lash, J.P.; Townsend, R.R.; Ojo, A.; et al. Inflammation and Progression of CKD: The CRIC Study. *Clin. J. Am. Soc. Nephrol.* **2016**, *11*, 1546–1556. [CrossRef] [PubMed]
222. Greenberg, J.H.; Abraham, A.G.; Xu, Y.; Schelling, J.R.; Feldman, H.I.; Sabbisetti, V.S.; Gonzalez, M.C.; Coca, S.; Schrauben, S.J.; Waikar, S.S.; et al. Plasma Biomarkers of Tubular Injury and Inflammation Are Associated with CKD Progression in Children. *J. Am. Soc. Nephrol.* **2020**, *31*, 1067–1077. [CrossRef]
223. Wen, Y.; Lu, X.; Ren, J.; Privratsky, J.R.; Yang, B.; Rudemiller, N.P.; Zhang, J.; Griffiths, R.; Jain, M.K.; Nedospasov, S.A.; et al. KLF4 in Macrophages Attenuates TNFα-Mediated Kidney Injury and Fibrosis. *J. Am. Soc. Nephrol.* **2019**, *30*, 1925–1938. [CrossRef]

224. Brandt, S.; Ballhause, T.M.; Bernhardt, A.; Becker, A.; Salaru, D.; Le-Deffge, H.M.; Fehr, A.; Fu, Y.; Philipsen, L.; Djudjaj, S.; et al. Fibrosis and Immune Cell Infiltration Are Separate Events Regulated by Cell-Specific Receptor Notch3 Expression. *J. Am. Soc. Nephrol.* **2020**, *31*, 2589–2608. [CrossRef] [PubMed]
225. Wang, Y.-Y.; Jiang, H.; Pan, J.; Huang, X.-R.; Wang, Y.-C.; Huang, H.-F.; To, K.-F.; Nikolic-Paterson, D.J.; Lan, H.-Y.; Chen, J.-H. Macrophage-to-Myofibroblast Transition Contributes to Interstitial Fibrosis in Chronic Renal Allograft Injury. *J. Am. Soc. Nephrol.* **2017**, *28*, 2053–2067. [CrossRef] [PubMed]
226. Kormann, R.; Kavvadas, P.; Placier, S.; Vandermeersch, S.; Dorison, A.; Dussaule, J.-C.; Chadjichristos, C.E.; Prakoura, N.; Chatziantoniou, C. Periostin Promotes Cell Proliferation and Macrophage Polarization to Drive Repair After AKI. *J. Am. Soc. Nephrol.* **2020**, *31*, 85–100. [CrossRef] [PubMed]
227. Simões, F.C.; Cahill, T.J.; Kenyon, A.; Gavriouchkina, D.; Vieira, J.M.; Sun, X.; Pezzolla, D.; Ravaud, C.; Masmanian, E.; Weinberger, M.; et al. Macrophages Directly Contribute Collagen to Scar Formation During Zebrafish Heart Regeneration and Mouse Heart Repair. *Nat. Commun.* **2020**, *11*, 1–17. [CrossRef]
228. Shen, B.; Liu, X.; Fan, Y.; Qiu, J. Macrophages Regulate Renal Fibrosis Through Modulating TGFβ Superfamily Signaling. *Inflammation* **2014**, *37*, 2076–2084. [CrossRef] [PubMed]
229. Wright, T.M. Cytokines in Acute and Chronic Inflammation. *Front. Biosci.* **1997**, *2*, d12–d26. [CrossRef] [PubMed]
230. Panico, K.; Abrahão, M.V.; Sonoda, M.T.; Muzi-Filho, H.; Vieyra, A.; Carneiro-Ramos, M.S. Cardiac Inflammation After Ischemia-Reperfusion of the Kidney: Role of the Sympathetic Nervous System and the Renin-Angiotensin System. *Cell. Physiol. Biochem.* **2019**, *53*, 587–605. [CrossRef]
231. Virzì, G.M.; Breglia, A.; Castellani, C.; Ankawi, G.; Bolin, C.; De Cal, M.; Cianci, V.; Angelini, A.; Vescovo, G.; Ronco, C. Lipopolysaccharide in Systemic Circulation Induces Activation of Inflammatory Response and Oxidative Stress in Cardiorenal Syndrome Type 1. *J. Nephrol.* **2019**, *32*, 803–810. [CrossRef]
232. Virzì, G.M.; Breglia, A.; Brocca, A.; De Cal, M.; Bolin, C.; Vescovo, G.; Ronco, C. Levels of Proinflammatory Cytokines, Oxidative Stress, and Tissue Damage Markers in Patients with Acute Heart Failure with and without Cardiorenal Syndrome Type 1. *Cardiorenal Med.* **2018**, *8*, 321–331. [CrossRef]
233. Colombo, P.C.; Ganda, A.; Lin, J.; Onat, D.; Harxhi, A.; Iyasere, J.E.; Uriel, N.; Cotter, G. Inflammatory Activation: Cardiac, Renal, and Cardio-Renal Interactions in Patients with the Cardiorenal Syndrome. *Heart Fail. Rev.* **2012**, *17*, 177–190. [CrossRef]
234. Li, R.; Mi, X.; Yang, S.; Yang, Y.; Zhang, S.; Hui, R.; Chen, Y.; Zhang, W. Long-Term Stimulation of Angiotensin II Induced Endothelial Senescence and Dysfunction. *Exp. Gerontol.* **2019**, *119*, 212–220. [CrossRef] [PubMed]
235. Du, Y.; Han, J.; Zhang, H.; Xu, J.; Jiang, L.; Ge, W. Kaempferol Prevents Against Ang II-Induced Cardiac Remodeling Through Attenuating Ang II-Induced Inflammation and Oxidative Stress. *J. Cardiovasc. Pharmacol.* **2019**, *74*, 326–335. [CrossRef]
236. Lang, P.-P.; Bai, J.; Zhang, Y.-L.; Yang, X.-L.; Xia, Y.-L.; Lin, Q.-Y.; Li, H.-H. Blockade of Intercellular Adhesion Molecule-1 Prevents Angiotensin II-Induced Hypertension and Vascular Dysfunction. *Lab. Investig.* **2019**, *100*, 378–386. [CrossRef] [PubMed]
237. Kalra, D.; Sivasubramanian, N.; Mann, D.L. Angiotensin II Induces Tumor Necrosis Factor Biosynthesis in the Adult Mammalian Heart Through a Protein Kinase C–Dependent Pathway. *Circulation* **2002**, *105*, 2198–2205. [CrossRef]
238. Ozawa, Y.; Kobori, H.; Suzaki, Y.; Navar, L.G. Sustained Renal Interstitial Macrophage Infiltration Following Chronic Angiotensin II Infusions. *Am. J. Physiol. Physiol.* **2007**, *292*, F330–F339. [CrossRef]
239. Frenay, A.-R.S.; Yazdani, S.; Boersema, M.; Van Der Graaf, A.M.; Waanders, F.; Born, J.V.D.; Navis, G.J.; Van Goor, H. Incomplete Restoration of Angiotensin II - Induced Renal Extracellular Matrix Deposition and Inflammation Despite Complete Functional Recovery in Rats. *PLoS ONE* **2015**, *10*, e0129732. [CrossRef]
240. Zhang, J.-D.; Patel, M.B.; Griffiths, R.; Dolber, P.C.; Ruiz, P.; Sparks, M.A.; Stegbauer, J.; Jin, H.; Gomez, J.A.; Buckley, A.F.; et al. Type 1 Angiotensin Receptors on Macrophages Ameliorate IL-1 receptor–mediated Kidney Fibrosis. *J. Clin. Investig.* **2014**, *124*, 2198–2203. [CrossRef] [PubMed]
241. Wang, D.; Xiong, M.; Chen, C.; Du, L.; Liu, Z.; Shi, Y.; Zhang, M.; Gong, J.; Song, X.; Xiang, R.; et al. Legumain, an Asparaginyl Endopeptidase, Mediates the Effect of M2 Macrophages on Attenuating Renal Interstitial Fibrosis in Obstructive Nephropathy. *Kidney Int.* **2018**, *94*, 91–101. [CrossRef]
242. Witherel, C.E.; Abebayehu, D.; Barker, T.H.; Spiller, K.L. Macrophage and Fibroblast Interactions in Biomaterial-Mediated Fibrosis. *Adv. Health Mater.* **2019**, *8*, e1801451. [CrossRef]
243. Colombo, P.C.; Onat, D.; Harxhi, A.; Demmer, R.T.; Hayashi, Y.; Jelic, S.; LeJemtel, T.H.; Bucciarelli, L.; Kebschull, M.; Papapanou, P.N.; et al. Peripheral Venous Congestion Causes Inflammation, Neurohormonal, and Endothelial Cell Activation. *Eur. Heart J.* **2013**, *35*, 448–454. [CrossRef] [PubMed]
244. Colombo, P.C.; Rastogi, S.; Onat, D.; Zacà, V.; Gupta, R.C.; Jorde, U.P.; Sabbah, H.N. Activation of Endothelial Cells in Conduit Veins of Dogs with Heart Failure and Veins of Normal Dogs After Vascular Stretch by Acute Volume Loading. *J. Card. Fail.* **2009**, *15*, 457–463. [CrossRef] [PubMed]
245. Berguetti, T.S.; Quintaes, L.S.P.; Pereira, T.H.; Robaina, M.C.; Cruz, A.L.S.; Maia, R.C.; De Souza, P.S.; Hancio, T. TNF-α Modulates P-Glycoprotein Expression and Contributes to Cellular Proliferation via Extracellular Vesicles. *Cells* **2019**, *8*, 500. [CrossRef]
246. Chen, T.; Zhang, X.; Zhu, G.; Liu, H.; Chen, J.; Wang, Y.; He, X. Quercetin Inhibits TNF-α Induced HUVECs Apoptosis and Inflammation via Downregulating NF-KB and AP-1 Signaling Pathway in Vitro. *Medicine* **2020**, *99*, e22241. [CrossRef]
247. Zelová, H.; Hošek, J. TNF-α Signalling and Inflammation: Interactions Between Old Acquaintances. *Inflamm. Res.* **2013**, *62*, 641–651. [CrossRef] [PubMed]

248. Sziksz, E.; Pap, D.; Lippai, R.; Béres, N.J.; Fekete, A.; Szabó, A.J.; Vannay, Á. Fibrosis Related Inflammatory Mediators: Role of the IL-10 Cytokine Family. *Mediat. Inflamm.* **2015**, *2015*, 1–15. [CrossRef]
249. Wynn, T.A. Cellular and Molecular Mechanisms of Fibrosis. *J. Pathol.* **2007**, *214*, 199–210. [CrossRef]
250. Shao, D.; Suresh, R.; Vakil, V.; Gomer, R.; Pilling, D. Pivotal Advance: Th-1 Cytokines Inhibit, and Th-2 Cytokines Promote Fibrocyte Differentiation. *J. Leukoc. Biol.* **2008**, *83*, 1323–1333. [CrossRef] [PubMed]
251. Le Floc'H, A.; Allinne, J.; Nagashima, K.; Scott, G.; Birchard, D.; Asrat, S.; Bai, Y.; Lim, W.K.; Martin, J.; Huang, T.; et al. Dual Blockade of IL-4 and IL-13 with Dupilumab, an IL-4Rα Antibody, Is Required to Broadly Inhibit Type 2 Inflammation. *Allergy* **2019**, *75*, 1188–1204. [CrossRef]
252. Reiman, R.M.; Thompson, R.W.; Feng, C.; Hari, D.; Knight, R.; Cheever, A.W.; Rosenberg, H.F.; Wynn, T.A. Interleukin-5 (IL-5) Augments the Progression of Liver Fibrosis by Regulating IL-13 Activity. *Infect. Immun.* **2006**, *74*, 1471–1479. [CrossRef] [PubMed]
253. Pesce, J.; Kaviratne, M.; Ramalingam, T.R.; Thompson, R.W.; Urban, J.; Cheever, A.W.; Young, D.A.; Collins, M.; Grusby, M.J.; Wynn, T.A. The IL-21 Receptor Augments Th2 Effector Function and Alternative Macrophage Activation. *J. Clin. Investig.* **2006**, *116*, 2044–2055. [CrossRef]
254. Korn, T.; Bettelli, E.; Gao, W.; Awasthi, A.; Jäger, A.; Strom, T.B.; Oukka, M.; Kuchroo, V.K. IL-21 Initiates an Alternative Pathway to Induce Proinflammatory TH17 Cells. *Nat. Cell Biol.* **2007**, *448*, 484–487. [CrossRef]
255. Nurieva, R.; Yang, X.O.; Martinez, G.; Zhang, Y.; Panopoulos, A.; Ma, L.; Schluns, K.; Tian, Q.; Watowich, S.S.; Jetten, A.; et al. Essential Autocrine Regulation by IL-21 in the Generation of Inflammatory T Cells. *Nat. Cell Biol.* **2007**, *448*, 480–483. [CrossRef]
256. Lei, L.; Zhao, C.; Qin, F.; He, Z.Y.; Wang, X.; Zhong, X.N. Th17 Cells and IL-17 Promote the Skin and Lung Inflammation and Fibrosis Process in a Bleomycin-Induced Murine Model of Systemic Sclerosis. *Clin. Exp. Rheumatol.* **2016**, *34* (Suppl. S100), 14–22.
257. Wu, L.; Ong, S.; Talor, M.V.; Barin, J.G.; Baldeviano, G.C.; Kass, D.A.; Bedja, D.; Zhang, H.; Sheikh, A.; Margolick, J.B.; et al. Cardiac Fibroblasts Mediate IL-17A–driven Inflammatory Dilated Cardiomyopathy. *J. Exp. Med.* **2014**, *211*, 1449–1464. [CrossRef] [PubMed]
258. Sommerfeld, S.D.; Cherry, C.; Schwab, R.M.; Chung, L.; Maestas, D.R., Jr.; Laffont, P.; Stein, J.E.; Tam, A.; Ganguly, S.; Housseau, F.; et al. Interleukin-36γ–producing Macrophages Drive IL-17–mediated Fibrosis. *Sci. Immunol.* **2019**, *4*, eaax4783. [CrossRef]
259. Ramani, K.; Tan, R.J.; Zhou, D.; Coleman, B.M.; Jawale, C.V.; Liu, Y.; Biswas, P.S. IL-17 Receptor Signaling Negatively Regulates the Development of Tubulointerstitial Fibrosis in the Kidney. *Mediat. Inflamm.* **2018**, *2018*, 1–14. [CrossRef] [PubMed]
260. Huang, M.; Sharma, S.; Zhu, L.X.; Keane, M.P.; Luo, J.; Zhang, L.; Burdick, M.D.; Lin, Y.Q.; Dohadwala, M.; Gardner, B.; et al. IL-7 Inhibits Fibroblast TGF-β Production and Signaling in Pulmonary Fibrosis. *J. Clin. Investig.* **2002**, *109*, 931–937. [CrossRef]
261. Demols, A.; Van Laethem, J.-L.; Quertinmont, E.; Degraef, C.; Delhaye, M.; Geerts, A.; Devière, J. Endogenous Interleukin-10 Modulates Fibrosis and Regeneration in Experimental Chronic Pancreatitis. *Am. J. Physiol. Liver Physiol.* **2002**, *282*, G1105–G1112. [CrossRef] [PubMed]
262. Shamskhou, E.A.; Kratochvil, M.J.; Orcholski, M.E.; Nagy, N.; Kaber, G.; Steen, E.; Balaji, S.; Yuan, K.; Keswani, S.; Danielson, B.; et al. Hydrogel-Based Delivery of Il-10 Improves Treatment of Bleomycin-Induced Lung Fibrosis in Mice. *Biomaterials* **2019**, *203*, 52–62. [CrossRef]
263. Guan, Q.; Weiss, C.R.; Wang, S.; Qing, G.; Yang, X.; Warrington, R.J.; Bernstein, C.N.; Peng, Z. Reversing Ongoing Chronic Intestinal Inflammation and Fibrosis by Sustained Block of IL-12 and IL-23 Using a Vaccine in Mice. *Inflamm. Bowel Dis.* **2018**, *24*, 1941–1952. [CrossRef]
264. Keane, M.P.; Belperio, J.A.; Burdick, M.D.; Strieter, R.M. IL-12 Attenuates Bleomycin-Induced Pulmonary Fibrosis. *Am. J. Physiol. Cell. Mol. Physiol.* **2001**, *281*, L92–L97. [CrossRef] [PubMed]
265. Weidenbusch, M.; Song, S.; Iwakura, T.; Shi, C.; Rodler, S.; Kobold, S.; Mulay, S.R.; Honarpisheh, M.M.; Anders, H.-J. IL-22 Sustains Epithelial Integrity in Progressive Kidney Remodeling and Fibrosis. *Physiol. Rep.* **2018**, *6*, e13817. [CrossRef] [PubMed]
266. Wang, S.; Li, Y.; Fan, J.; Zhang, X.; Luan, J.; Bian, Q.; Ding, T.; Wang, Y.; Wang, Z.; Song, P.; et al. Interleukin-22 Ameliorated Renal Injury and Fibrosis in Diabetic Nephropathy through Inhibition of NLRP3 Inflammasome Activation. *Cell Death Dis.* **2017**, *8*, e2937. [CrossRef]
267. Lee, J.-W.; Oh, J.E.; Rhee, K.-J.; Yoo, B.-S.; Eom, Y.W.; Park, S.W.; Lee, J.H.; Son, J.-W.; Youn, Y.J.; Ahn, M.-S.; et al. Co-Treatment with Interferon-γ and 1-Methyl Tryptophan Ameliorates Cardiac Fibrosis through Cardiac Myofibroblasts Apoptosis. *Mol. Cell. Biochem.* **2019**, *458*, 197–205. [CrossRef] [PubMed]
268. Poosti, F.; Bansal, R.; Yazdani, S.; Prakash, J.; Post, E.; Klok, P.; Born, J.V.D.; de Borst, M.H.; van Goor, H.; Poelstra, K.; et al. Selective Delivery of IFN-γ to Renal Interstitial Myofibroblasts: A Novel Strategy for the Treatment of Renal Fibrosis. *FASEB J.* **2015**, *29*, 1029–1042. [CrossRef]
269. Liechty, K.W.; Kim, H.B.; Adzick, N.; Crombleholme, T.M. Fetal Wound Repair Results in Scar Formation in Interleukin-10–deficient Mice in a Syngeneic Murine Model of Scarless Fetal Wound Repair. *J. Pediatr. Surg.* **2000**, *35*, 866–873. [CrossRef]
270. Lin, W.-R.; Lim, S.-N.; Yen, T.-H.; Alison, M.R. The Influence of Bone Marrow-Secreted IL-10 in a Mouse Model of Cerulein-Induced Pancreatic Fibrosis. *BioMed Res. Int.* **2016**, *2016*, 1–11. [CrossRef]
271. Gupta, J.; Mitra, N.; Kanetsky, P.A.; Devaney, J.; Wing, M.R.; Reilly, M.; Shah, V.O.; Balakrishnan, V.S.; Guzman, N.J.; Girndt, M.; et al. Association Between Albuminuria, Kidney Function, and Inflammatory Biomarker Profile in CKD in CRIC. *Clin. J. Am. Soc. Nephrol.* **2012**, *7*, 1938–1946. [CrossRef]
272. Li, R.; Guo, Y.; Zhang, Y.; Zhang, X.; Zhu, L.; Yan, T. Salidroside Ameliorates Renal Interstitial Fibrosis by Inhibiting the TLR4/NF-κB and MAPK Signaling Pathways. *Int. J. Mol. Sci.* **2019**, *20*, 1103. [CrossRef]

273. Edeling, M.; Ragi, G.; Huang, S.; Pavenstädt, H.; Susztak, K. Developmental Signalling Pathways in Renal Fibrosis: The Roles of Notch, Wnt and Hedgehog. *Nat. Rev. Nephrol.* **2016**, *12*, 426–439. [CrossRef]
274. Cho, E.; Kim, M.; Ko, Y.S.; Lee, H.Y.; Song, M.; Kim, H.-K.; Cho, W.-Y.; Jo, S.-K. Role of Inflammation in the Pathogenesis of Cardiorenal Syndrome in a Rat Myocardial Infarction Model. *Nephrol. Dial. Transplant.* **2013**, *28*, 2766–2778. [CrossRef]
275. Yhee, J.-Y.; Yu, C.-H.; Kim, J.-H.; Sur, J.-H. Effects of T Lymphocytes, Interleukin-1, and Interleukin-6 on Renal Fibrosis in Canine End-Stage Renal Disease. *J. Veter. Diagn. Investig.* **2008**, *20*, 585–592. [CrossRef] [PubMed]
276. Van Linthout, S.; Miteva, K.; Tschöpe, C. Crosstalk Between Fibroblasts and Inflammatory Cells. *Cardiovasc. Res.* **2014**, *102*, 258–269. [CrossRef] [PubMed]
277. Black, L.M.; Lever, J.M.; Agarwal, A. Renal Inflammation and Fibrosis: A Double-Edged Sword. *J. Histochem. Cytochem.* **2019**, *67*, 663–681. [CrossRef] [PubMed]
278. Meng, X.-M. Inflammatory Mediators and Renal Fibrosis. *Adv. Exp. Med. Biol.* **2019**, *1165*, 381–406. [CrossRef]
279. Iwano, M.; Neilson, E.G. Mechanisms of Tubulointerstitial Fibrosis. *Curr. Opin. Nephrol. Hypertens.* **2004**, *13*, 279–284. [CrossRef] [PubMed]
280. Prabhu, S.D.; Frangogiannis, N.G. The Biological Basis for Cardiac Repair After Myocardial Infarction. *Circ. Res.* **2016**, *119*, 91–112. [CrossRef]
281. Sun, K.; Li, Y.-Y.; Jin, J. A Double-Edged Sword of Immuno-Microenvironment in Cardiac Homeostasis and Injury Repair. *Signal Transduct. Target. Ther.* **2021**, *6*, 1–16. [CrossRef]
282. Fadok, V.A.; Bratton, D.L.; Konowal, A.; Freed, P.W.; Westcott, J.Y.; Henson, P.M. Macrophages That Have Ingested Apoptotic Cells In Vitro Inhibit Proinflammatory Cytokine Production through autocrine/Paracrine Mechanisms Involving TGF-Beta, PGE2, and PAF. *J. Clin. Investig.* **1998**, *101*, 890–898. [CrossRef] [PubMed]
283. Song, E.; Ouyang, N.; Hörbelt, M.; Antus, B.; Wang, M.; Exton, M.S. Influence of Alternatively and Classically Activated Macrophages on Fibrogenic Activities of Human Fibroblasts. *Cell. Immunol.* **2000**, *204*, 19–28. [CrossRef]
284. Valgimigli, M.; Ceconi, C.; Malagutti, P.; Merli, E.; Soukhomovskaia, O.; Francolini, G.; Cicchitelli, G.; Olivares, A.; Parrinello, G.; Percoco, G.; et al. Tumor Necrosis Factor-α Receptor 1 Is a Major Predictor of Mortality and New-Onset Heart Failure in Patients with Acute Myocardial Infarction. *Circulation* **2005**, *111*, 863–870. [CrossRef] [PubMed]
285. Maekawa, N.; Wada, H.; Kanda, T.; Niwa, T.; Yamada, Y.; Saito, K.; Fujiwara, H.; Sekikawa, K.; Seishima, M. Improved Myocardial ischemia/Reperfusion Injury in Mice Lacking Tumor Necrosis Factor-α. *J. Am. Coll. Cardiol.* **2002**, *39*, 1229–1235. [CrossRef]
286. Kurrelmeyer, K.M.; Michael, L.H.; Baumgarten, G.; Taffet, G.E.; Peschon, J.J.; Sivasubramanian, N.; Entman, M.L.; Mann, D.L. Endogenous Tumor Necrosis Factor Protects the Adult Cardiac Myocyte Against Ischemic-Induced Apoptosis in a Murine Model of Acute Myocardial Infarction. *Proc. Natl. Acad. Sci. USA* **2000**, *97*, 5456–5461. [CrossRef]
287. Huang, M.; Li, J.-Y. Physiological Regulation of Reactive Oxygen Species in Organisms Based on Their Physicochemical Properties. *Acta Physiol.* **2020**, *228*, e13351. [CrossRef] [PubMed]
288. Pisoschi, A.M.; Pop, A. The Role of Antioxidants in the Chemistry of Oxidative Stress: A Review. *Eur. J. Med. Chem.* **2015**, *97*, 55–74. [CrossRef]
289. Lau, N.; Pluth, M.D. Reactive Sulfur Species (RSS): Persulfides, Polysulfides, Potential, and Problems. *Curr. Opin. Chem. Biol.* **2019**, *49*, 1–8. [CrossRef] [PubMed]
290. Deng, Z.; Hu, J.; Liu, S. Reactive Oxygen, Nitrogen, and Sulfur Species (RONSS)-Responsive Polymersomes for Triggered Drug Release. *Macromol. Rapid Commun.* **2017**, *38*, 10–1002. [CrossRef]
291. Luo, Z.; Xu, X.; Sho, T.; Zhang, J.; Xu, W.; Yao, J.; Xu, J. ROS-Induced Autophagy Regulates Porcine Trophectoderm Cell Apoptosis, Proliferation, and Differentiation. *Am. J. Physiol. Physiol.* **2019**, *316*, C198–C209. [CrossRef]
292. Pei, J.; Wang, F.; Pei, S.; Bai, R.; Cong, X.; Nie, Y.; Chen, X. Hydrogen Sulfide Promotes Cardiomyocyte Proliferation and Heart Regeneration via ROS Scavenging. *Oxidative Med. Cell. Longev.* **2020**, *2020*, 1–11. [CrossRef]
293. Zhang, G.; He, J.; Ye, X.; Zhu, J.; Hu, X.; Shen, M.; Ma, Y.; Mao, Z.; Song, H.; Chen, F. β-Thujaplicin Induces Autophagic Cell Death, Apoptosis, and Cell Cycle Arrest through ROS-Mediated Akt and p38/ERK MAPK Signaling in Human Hepatocellular Carcinoma. *Cell Death Dis.* **2019**, *10*, 1–14. [CrossRef]
294. Kang, R.; Li, R.; Dai, P.; Li, Z.; Li, Y.; Li, C. Deoxynivalenol Induced Apoptosis and Inflammation of IPEC-J2 Cells by Promoting ROS Production. *Environ. Pollut.* **2019**, *251*, 689–698. [CrossRef] [PubMed]
295. Hawkins, C.L.; Davies, M.J. Detection, Identification, and Quantification of Oxidative Protein Modifications. *J. Biol. Chem.* **2019**, *294*, 19683–19708. [CrossRef] [PubMed]
296. Kowalska, M.; Piekut, T.; Prendecki, M.; Sodel, A.; Kozubski, W.; Dorszewska, J. Mitochondrial and Nuclear DNA Oxidative Damage in Physiological and Pathological Aging. *DNA Cell Biol.* **2020**, *39*, 1410–1420. [CrossRef]
297. Salehi, F.; Behboudi, H.; Kavoosi, G.; Ardestani, S.K. Oxidative DNA Damage Induced by ROS-Modulating Agents with the Ability to Target DNA: A Comparison of the Biological Characteristics of Citrus Pectin and Apple Pectin. *Sci. Rep.* **2018**, *8*, 1–16. [CrossRef]
298. Ayala, A.; Muñoz, M.F.; Argüelles, S. Lipid Peroxidation: Production, Metabolism, and Signaling Mechanisms of Malondialdehyde and 4-Hydroxy-2-Nonenal. *Oxid. Med. Cell. Longev.* **2014**, *2014*, 1–31. [CrossRef] [PubMed]
299. Tsikas, D. Assessment of Lipid Peroxidation by Measuring Malondialdehyde (MDA) and Relatives in Biological Samples: Analytical and Biological Challenges. *Anal. Biochem.* **2017**, *524*, 13–30. [CrossRef]

300. Gallo, G.; Sprovierio, P.; Martino, G. 4-Hydroxynonenal and Oxidative Stress in Several Organelles and Its Damaging Effects on Cell Functions. *J. Physiol. Pharmacol. Off. J. Pol. Physiol. Soc.* **2020**, *71*, 10–26402.
301. Schrader, M.; Fahimi, H. Peroxisomes and Oxidative Stress. *Biochim. Biophys. Acta Bioenerg.* **2006**, *1763*, 1755–1766. [CrossRef]
302. Antonenkov, V.D.; Grunau, S.; Ohlmeier, S.; Hiltunen, K. Peroxisomes Are Oxidative Organelles. *Antioxid. Redox Signal* **2010**, *13*, 525–537. [CrossRef]
303. Zeeshan, H.M.A.; Lee, G.H.; Kim, H.-R.; Chae, H.-J. Endoplasmic Reticulum Stress and Associated ROS. *Int. J. Mol. Sci.* **2016**, *17*, 327. [CrossRef] [PubMed]
304. Zhao, R.-Z.; Jiang, S.; Zhang, L.; Yu, Z.-B. Mitochondrial electron transport chain, ROS generation and uncoupling (Review). *Int. J. Mol. Med.* **2019**, *44*, 3–15. [CrossRef] [PubMed]
305. Phaniendra, A.; Jestadi, D.B.; Periyasamy, L. Free Radicals: Properties, Sources, Targets, and Their Implication in Various Diseases. *Ind. J. Clin. Biochem.* **2015**, *30*, 11–26. [CrossRef]
306. Oyewole, A.O.; Birch-Machin, M.A. Mitochondria-targeted Antioxidants. *FASEB J.* **2015**, *29*, 4766–4771. [CrossRef]
307. Iacovino, L.G.; Manzella, N.; Resta, J.; Vanoni, M.A.; Rotilio, L.; Pisani, L.; Edmondson, D.E.; Parini, A.; Mattevi, A.; Mialet-Perez, J.; et al. Rational Redesign of Monoamine Oxidase A into a Dehydrogenase to Probe ROS in Cardiac Aging. *ACS Chem. Biol.* **2020**, *15*, 1795–1800. [CrossRef]
308. Kaludercic, N.; Mialet-Perez, J.; Paolocci, N.; Parini, A.; Di Lisa, F. Monoamine Oxidases As Sources of Oxidants in the Heart. *J. Mol. Cell. Cardiol.* **2014**, *73*, 34–42. [CrossRef]
309. Dey, S.; Sidor, A.; O'Rourke, B. Compartment-Specific Control of Reactive Oxygen Species Scavenging by Antioxidant Pathway Enzymes. *J. Biol. Chem.* **2016**, *291*, 11185–11197. [CrossRef]
310. He, L.; He, T.; Farrar, S.; Ji, L.; Liu, T.; Ma, X. Antioxidants Maintain Cellular Redox Homeostasis by Elimination of Reactive Oxygen Species. *Cell. Physiol. Biochem.* **2017**, *44*, 532–553. [CrossRef] [PubMed]
311. Dinh, Q.N.; Drummond, G.; Sobey, C.G.; Chrissobolis, S. Roles of Inflammation, Oxidative Stress, and Vascular Dysfunction in Hypertension. *BioMed Res. Int.* **2014**, *2014*, 1–11. [CrossRef]
312. Chiba, T.; Peasley, K.D.; Cargill, K.R.; Maringer, K.V.; Bharathi, S.S.; Mukherjee, E.; Zhang, Y.; Holtz, A.; Basisty, N.; Yagobian, S.D.; et al. Sirtuin 5 Regulates Proximal Tubule Fatty Acid Oxidation to Protect Against AKI. *J. Am. Soc. Nephrol.* **2019**, *30*, 2384–2398. [CrossRef]
313. Papinska, A.M.; Rodgers, K.E. Long-Term Administration of Angiotensin (1–7) to db/Db Mice Reduces Oxidative Stress Damage in the Kidneys and Prevents Renal Dysfunction. *Oxidative Med. Cell. Longev.* **2018**, *2018*, 1–10. [CrossRef]
314. Kumar, S.; Wang, G.; Zheng, N.; Cheng, W.; Ouyang, K.; Lin, H.; Liao, Y.; Liu, J. HIMF (Hypoxia-Induced Mitogenic Factor)-IL (Interleukin)-6 Signaling Mediates Cardiomyocyte-Fibroblast Crosstalk to Promote Cardiac Hypertrophy and Fibrosis. *Hypertension* **2019**, *73*, 1058–1070. [CrossRef]
315. He, T.; Guan, X.; Wang, S.; Xiao, T.; Yang, K.; Xu, X.; Wang, J.; Zhao, J. Resveratrol Prevents High Glucose-Induced epithelial–mesenchymal Transition in Renal Tubular Epithelial Cells by Inhibiting NADPH oxidase/ROS/ERK Pathway. *Mol. Cell. Endocrinol.* **2015**, *402*, 13–20. [CrossRef]
316. Carthy, J.M. TGFβ Signaling and the Control of Myofibroblast Differentiation: Implications for Chronic Inflammatory Disorders. *J. Cell. Physiol.* **2017**, *233*, 98–106. [CrossRef] [PubMed]
317. Park, S.-A.; Kim, M.-J.; Park, S.-Y.; Kim, J.-S.; Lee, S.-J.; Woo, H.A.; Kim, D.-K.; Nam, J.-S.; Sheen, Y.Y. EW-7197 Inhibits Hepatic, Renal, and Pulmonary Fibrosis by Blocking TGF-β/Smad and ROS Signaling. *Cell. Mol. Life Sci.* **2014**, *72*, 2023–2039. [CrossRef] [PubMed]
318. Liu, Y.; Yuan, X.; Li, W.; Cao, Q.; Shu, Y. Aspirin-Triggered Resolvin D1 Inhibits TGF-β1-Induced EMT through the Inhibition of the MTOR Pathway by Reducing the Expression of PKM2 and Is Closely Linked to Oxidative Stress. *Int. J. Mol. Med.* **2016**, *38*, 1235–1242. [CrossRef]
319. De Bleser, P.J.; Xu, G.; Rombouts, K.; Rogiers, V.; Geerts, A. Glutathione Levels Discriminate Between Oxidative Stress and Transforming Growth Factor-β Signaling in Activated Rat Hepatic Stellate Cells. *J. Biol. Chem.* **1999**, *274*, 33881–33887. [CrossRef] [PubMed]
320. Matsushima, S.; Kuroda, J.; Ago, T.; Zhai, P.; Ikeda, Y.; Oka, S.; Fong, G.-H.; Tian, R.; Sadoshima, J. Broad Suppression of NADPH Oxidase Activity Exacerbates Ischemia/Reperfusion Injury Through Inadvertent Downregulation of Hypoxia-Inducible Factor-1α and Upregulation of Peroxisome Proliferator–activated Receptor-α. *Circ. Res.* **2013**, *112*, 1135–1149. [CrossRef]
321. Verzola, D.; Ratto, E.; Villaggio, B.; Parodi, E.L.; Pontremoli, R.; Garibotto, G.; Viazzi, F. Uric Acid Promotes Apoptosis in Human Proximal Tubule Cells by Oxidative Stress and the Activation of NADPH Oxidase NOX 4. *PLoS ONE* **2014**, *9*, e115210. [CrossRef] [PubMed]
322. Buvelot, H.; Jaquet, V.; Krause, K.-H. Mammalian NADPH Oxidases. *Methods Mol. Biol.* **2019**, *1982*, 17–36. [CrossRef]
323. Lan, T.; Kisseleva, T.; Brenner, D.A. Deficiency of NOX1 or NOX4 Prevents Liver Inflammation and Fibrosis in Mice through Inhibition of Hepatic Stellate Cell Activation. *PLoS ONE* **2015**, *10*, e0129743. [CrossRef]
324. Muñoz, M.; López-Oliva, M.E.; Rodríguez, C.; Martínez, M.P.; Sáenz-Medina, J.; Sánchez, A.; Climent, B.; Benedito, S.; García-Sacristán, A.; Rivera, L.; et al. Differential Contribution of Nox1, Nox2 and Nox4 to Kidney Vascular Oxidative Stress and Endothelial Dysfunction in Obesity. *Redox Biol.* **2020**, *28*, 101330. [CrossRef] [PubMed]

325. Rajaram, R.D.; Dissard, R.; Faivre, A.; Ino, F.; Delitsikou, V.; Jaquet, V.; Cagarelli, T.; Lindenmeyer, M.; Jansen-Duerr, P.; Cohen, C.; et al. Tubular NOX4 Expression Decreases in Chronic Kidney Disease But Does Not Modify Fibrosis Evolution. *Redox Biol.* **2019**, *26*, 101234. [CrossRef]
326. Braunersreuther, V.; Montecucco, F.; Ashri, M.; Pelli, G.; Galan, K.; Frias, M.; Burger, F.; Quinderé, A.L.G.; Montessuit, C.; Krause, K.-H.; et al. Role of NADPH Oxidase Isoforms NOX1, NOX2 and NOX4 in Myocardial ischemia/Reperfusion Injury. *J. Mol. Cell. Cardiol.* **2013**, *64*, 99–107. [CrossRef] [PubMed]
327. Cai, X.; Yang, C.; Shao, L.; Zhu, H.; Wang, Y.; Huang, X.; Wang, S.; Hong, L. Targeting NOX 4 by Petunidin Improves anoxia/Reoxygenation-Induced Myocardium Injury. *Eur. J. Pharmacol.* **2020**, *888*, 173414. [CrossRef]
328. Bondi, C.D.; Manickam, N.; Lee, D.Y.; Block, K.; Gorin, Y.; Abboud, H.E.; Barnes, J.L. NAD(P)H Oxidase Mediates TGF-β1–Induced Activation of Kidney Myofibroblasts. *J. Am. Soc. Nephrol.* **2009**, *21*, 93–102. [CrossRef] [PubMed]
329. He, T.; Xiong, J.; Nie, L.; Yu, Y.; Guan, X.; Xu, X.; Xiao, T.; Yang, K.; Liu, L.; Zhang, D.; et al. Resveratrol Inhibits Renal Interstitial Fibrosis in Diabetic Nephropathy by Regulating AMPK/NOX4/ROS Pathway. *J. Mol. Med.* **2016**, *94*, 1359–1371. [CrossRef]
330. Breglia, A.; Virzì, G.M.; Pastori, S.; Brocca, A.; De Cal, M.; Bolin, C.; Vescovo, G.; Ronco, C. Determinants of Monocyte Apoptosis in Cardiorenal Syndrome Type 1. *Cardiorenal Med.* **2018**, *8*, 208–216. [CrossRef]
331. Caio-Silva, W.; Dias, D.D.S.; JunHo, C.V.C.; Panico, K.; Neres-Santos, R.S.; Pelegrino, M.T.; Pieretti, J.C.; Seabra, A.B.; De Angelis, K.; Carneiro-Ramos, M.S. Characterization of the Oxidative Stress in Renal Ischemia/Reperfusion-Induced Cardiorenal Syndrome Type 3. *BioMed Res. Int.* **2020**, *2020*, 1–11. [CrossRef]
332. Fox, B.M.; Gil, H.-W.; Kirkbride-Romeo, L.; Bagchi, R.; Wennersten, S.; Haefner, K.R.; Skrypnyk, N.I.; Brown, C.N.; Soranno, D.E.; Gist, K.M.; et al. Metabolomics Assessment Reveals Oxidative Stress and Altered Energy Production in the Heart After Ischemic Acute Kidney Injury in Mice. *Kidney Int.* **2019**, *95*, 590–610. [CrossRef]
333. Guo, H.; Xu, D.; Kuroki, M.; Lu, Z.; Xu, X.; Geurts, A.; Osborn, J.W.; Chen, Y. Kidney Failure, Arterial Hypertension and Left Ventricular Hypertrophy in Rats with Loss of Function Mutation of SOD3. *Free. Radic. Biol. Med.* **2020**, *152*, 787–796. [CrossRef] [PubMed]
334. Oslowski, C.M.; Urano, F. Measuring ER Stress and the Unfolded Protein Response Using Mammalian Tissue Culture System. *Methods Enzymol.* **2011**, *490*, 71–92. [CrossRef] [PubMed]
335. Díaz-Villanueva, J.F.; Díaz-Molina, R.; García-González, V. Protein Folding and Mechanisms of Proteostasis. *Int. J. Mol. Sci.* **2015**, *16*, 17193–17230. [CrossRef]
336. Read, A.; Schröder, M. The Unfolded Protein Response: An Overview. *Biology* **2021**, *10*, 384. [CrossRef]
337. Sanyal, A.; Zbornik, E.A.; Watson, B.G.; Christoffer, C.; Ma, J.; Kihara, D.; Mattoo, S. Kinetic and Structural Parameters Governing Fic-Mediated adenylylation/AMPylation of the Hsp70 Chaperone, BiP/GRP78. *Cell Stress Chaperon* **2021**, 1–18. [CrossRef]
338. Song, S.; Tan, J.; Miao, Y.; Li, M.; Zhang, Q. Crosstalk of Autophagy and Apoptosis: Involvement of the Dual Role of Autophagy under ER Stress. *J. Cell. Physiol.* **2017**, *232*, 2977–2984. [CrossRef] [PubMed]
339. Lam, M.; A Marsters, S.; Ashkenazi, A.; Walter, P. Misfolded Proteins Bind and Activate Death Receptor 5 to Trigger Apoptosis During Unresolved Endoplasmic Reticulum Stress. *eLife* **2020**, *9*, e52291. [CrossRef]
340. Shrestha, N.; De Franco, E.; Arvan, P.; Cnop, M. Pathological β-Cell Endoplasmic Reticulum Stress in Type 2 Diabetes: Current Evidence. *Front. Endocrinol.* **2021**, *12*, 650158. [CrossRef]
341. Parks, S.Z.; Gao, T.; Awuapura, N.J.; Ayathamattam, J.; Chabosseau, P.L.; Kalvakolanu, D.V.; Valdivia, H.H.; Rutter, G.A.; Leclerc, I. The Ca 2+ -binding Protein Sorcin Stimulates Transcriptional Activity of the Unfolded Protein Response Mediator ATF6. *FEBS Lett.* **2021**, *10*. [CrossRef]
342. Baba, B.; Caliskan, M.; Boyuk, G.; Hacisevki, A. Chemical Chaperone PBA Attenuates ER Stress and Upregulates SOCS3 Expression as a Regulator of Leptin Signaling. *Biochemistry* **2021**, *86*, 480–488. [CrossRef]
343. Yang, Y.; Zhou, Q.; Gao, A.; Chen, L.; Li, L. Endoplasmic Reticulum Stress and Focused Drug Discovery in Cardiovascular Disease. *Clin. Chim. Acta* **2020**, *504*, 125–137. [CrossRef] [PubMed]
344. Ajoolabady, A.; Wang, S.; Kroemer, G.; Klionsky, D.J.; Uversky, V.N.; Sowers, J.R.; Aslkhodapasandhokmabad, H.; Bi, Y.; Ge, J.; Ren, J. ER Stress in Cardiometabolic Diseases: From Molecular Mechanisms to Therapeutics. *Endocr. Rev.* **2021**. [CrossRef] [PubMed]
345. Hsu, Y.-H.; Zheng, C.-M.; Chou, C.-L.; Chen, Y.-J.; Lee, Y.-H.; Lin, Y.-F.; Chiu, H.-W. Therapeutic Effect of Endothelin-Converting Enzyme Inhibitor on Chronic Kidney Disease through the Inhibition of Endoplasmic Reticulum Stress and the NLRP3 Inflammasome. *Biomedicine* **2021**, *9*, 398. [CrossRef]
346. Lins, B.B.; Casare, F.A.M.; Fontenele, F.F.; Gonçalves, G.L.; Oliveira-Souza, M. Long-Term Angiotensin II Infusion Induces Oxidative and Endoplasmic Reticulum Stress and Modulates Na+ Transporters Through the Nephron. *Front. Physiol.* **2021**, *12*, 642752. [CrossRef] [PubMed]
347. Dong, Z.; Wu, P.; Li, Y.; Shen, Y.; Xin, P.; Li, S.; Wang, Z.; Dai, X.; Zhu, W.; Wei, M. Myocardial Infarction Worsens Glomerular Injury and Microalbuminuria in Rats with Pre-Existing Renal Impairment Accompanied by the Activation of ER Stress and Inflammation. *Mol. Biol. Rep.* **2014**, *41*, 7911–7921. [CrossRef]
348. Dickhout, J.G.; Carlisle, R.E.; Austin, R.C. Interrelationship Between Cardiac Hypertrophy, Heart Failure, and Chronic Kidney Disease. *Circ. Res.* **2011**, *108*, 629–642. [CrossRef]

349. Olivares-Silva, F.; Espitia-Corredor, J.; Letelier, A.; Vivar, R.; Parra-Flores, P.; Olmedo, I.; Montenegro, J.; Pardo-Jiménez, V.; Díaz-Araya, G. TGF-β1 Decreases CHOP Expression and Prevents Cardiac Fibroblast Apoptosis Induced by Endoplasmic Reticulum Stress. *Toxicol. Vitr.* **2020**, *70*, 105041. [CrossRef]
350. Yamamoto, T.; Endo, J.; Kataoka, M.; Matsuhashi, T.; Katsumata, Y.; Shirakawa, K.; Isobe, S.; Moriyama, H.; Goto, S.; Shimanaka, Y.; et al. Palmitate Induces Cardiomyocyte Death via Inositol Requiring Enzyme-1 (IRE1)-Mediated Signaling Independent of X-Box Binding Protein 1 (XBP1). *Biochem. Biophys. Res. Commun.* **2020**, *526*, 122–127. [CrossRef]
351. Shu, S.; Zhu, J.; Liu, Z.; Tang, C.; Cai, J.; Dong, Z. Endoplasmic Reticulum Stress Is Activated in Post-Ischemic Kidneys to Promote Chronic Kidney Disease. *EBioMedicine* **2018**, *37*, 269–280. [CrossRef]
352. Huang, D.; Yan, M.-L.; Chen, K.-K.; Sun, R.; Dong, Z.-F.; Wu, P.-L.; Li, S.; Zhu, G.-S.; Ma, S.-X.; Pan, Y.-S.; et al. Cardiac-Specific Overexpression of Silent Information Regulator 1 Protects Against Heart and Kidney Deterioration in Cardiorenal Syndrome via Inhibition of Endoplasmic Reticulum Stress. *Cell. Physiol. Biochem.* **2018**, *46*, 9–22. [CrossRef]
353. Liu, Y.; Wang, Y.; Ding, W.; Wang, Y. Mito-TEMPO Alleviates Renal Fibrosis by Reducing Inflammation, Mitochondrial Dysfunction, and Endoplasmic Reticulum Stress. *Oxidative Med. Cell. Longev.* **2018**, *2018*, 1–13. [CrossRef]
354. (66) Luo, T.; Kim, J.K.; Chen, B.; Abdel-Latif, A.; Kitakaze, M.; Yan, L. Attenuation of ER Stress Prevents Post-Infarction-Induced Cardiac Rupture and Remodeling by Modulating Both Cardiac Apoptosis and Fibrosis. *Chem. Interact.* **2015**, *225*, 90–98. [CrossRef] [PubMed]
355. Fan, Y.; Xiao, W.; Lee, K.; Salem, F.; Wen, J.; He, L.; Zhang, J.; Fei, Y.; Cheng, D.; Bao, H.; et al. Inhibition of Reticulon-1A–Mediated Endoplasmic Reticulum Stress in Early AKI Attenuates Renal Fibrosis Development. *J. Am. Soc. Nephrol.* **2017**, *28*, 2007–2021. [CrossRef]
356. Han, J.; Pang, X.; Shi, X.; Zhang, Y.; Peng, Z.; Xing, Y. Ginkgo Biloba Extract EGB761 Ameliorates the Extracellular Matrix Accumulation and Mesenchymal Transformation of Renal Tubules in Diabetic Kidney Disease by Inhibiting Endoplasmic Reticulum Stress. *BioMed Res. Int.* **2021**, *2021*, 1–11. [CrossRef]
357. Qu, J.; Li, M.; Li, D.; Xin, Y.; Li, J.; Lei, S.; Wu, W.; Liu, X. Stimulation of Sigma-1 Receptor Protects Against Cardiac Fibrosis by Alleviating IRE1 Pathway and Autophagy Impairment. *Oxidative Med. Cell. Longev.* **2021**, *2021*, 1–25. [CrossRef] [PubMed]
358. Chen, Y.-T.; Jhao, P.-Y.; Hung, C.-T.; Wu, Y.-F.; Lin, S.-J.; Chiang, W.-C.; Lin, S.-L.; Yang, K.-C. Endoplasmic Reticulum Protein TXNDC5 Promotes Renal Fibrosis by Enforcing TGF-β Signaling in Kidney Fibroblasts. *J. Clin. Investig.* **2021**, *131*. [CrossRef]
359. Liu, S.-H.; Yang, C.-C.; Chan, D.-C.; Wu, C.-T.; Chen, L.-P.; Huang, J.-W.; Hung, K.-Y.; Chiang, C.-K. Chemical Chaperon 4-Phenylbutyrate Protects Against the Endoplasmic Reticulum Stress-Mediated Renal Fibrosis in Vivo and in Vitro. *Oncotarget* **2016**, *7*, 22116–22127. [CrossRef]
360. Park, M.-J.; Oh, K.-S.; Nho, J.-H.; Kim, G.-Y.; Kim, D.-I. Asymmetric Dimethylarginine (ADMA) Treatment Induces Apoptosis in Cultured Rat Mesangial Cells via Endoplasmic Reticulum Stress Activation. *Cell Biol. Int.* **2016**, *40*, 662–670. [CrossRef]
361. Matsuzaki, S.; Hiratsuka, T.; Taniguchi, M.; Shingaki, K.; Kubo, T.; Kiya, K.; Fujiwara, T.; Kanazawa, S.; Kanematsu, R.; Maeda, T.; et al. Physiological ER Stress Mediates the Differentiation of Fibroblasts. *PLoS ONE* **2015**, *10*, e0123578. [CrossRef] [PubMed]
362. Shih, Y.-C.; Chen, C.-L.; Zhang, Y.; Mellor, R.L.; Kanter, E.M.; Fang, Y.; Wang, H.-C.; Hung, C.-T.; Nong, J.-Y.; Chen, H.-J.; et al. Endoplasmic Reticulum Protein TXNDC5 Augments Myocardial Fibrosis by Facilitating Extracellular Matrix Protein Folding and Redox-Sensitive Cardiac Fibroblast Activation. *Circ. Res.* **2018**, *122*, 1052–1068. [CrossRef]
363. Pallet, N.; Bouvier, N.; Bendjallabah, A.; Rabant, M.; Flinois, J.P.; Hertig, A.; Legendre, C.; Beaune, P.; Thervet, E.; Anglicheau, D. Cyclosporine-Induced Endoplasmic Reticulum Stress Triggers Tubular Phenotypic Changes and Death. *Arab. Archaeol. Epigr.* **2008**, *8*, 2283–2296. [CrossRef]
364. Li, Y.; Weng, X.; Wang, P.; He, Z.; Cheng, S.; Wang, D.; Li, X.; Cheng, G.; Li, T. 4-Phenylbutyrate Exerts Stage-Specific Effects on Cardiac Differentiation via HDAC Inhibition. *PLoS ONE* **2021**, *16*, e0250267. [CrossRef]
365. Basseri, S.; Lhoták, Š.; Sharma, A.M.; Austin, R.C. The Chemical Chaperone 4-Phenylbutyrate Inhibits Adipogenesis by Modulating the Unfolded Protein Response. *J. Lipid Res.* **2009**, *50*, 2486–2501. [CrossRef]
366. Akita, S.; Suzuki, K.; Yoshimoto, H.; Ohtsuru, A.; Hirano, A.; Yamashita, S. Cellular Mechanism Underlying Highly-Active or Antiretroviral Therapy-Induced Lipodystrophy: Atazanavir, a Protease Inhibitor, Compromises Adipogenic Conversion of Adipose-Derived Stem/Progenitor Cells through Accelerating ER Stress-Mediated Cell Death in Differentiating Adipocytes. *Int. J. Mol. Sci.* **2021**, *22*, 2114. [CrossRef]
367. Shaffer, A.; Shelef, M.; Iwakoshi, N.N.; Lee, A.-H.; Qian, S.-B.; Zhao, H.; Yu, X.; Yang, L.; Tan, B.K.; Rosenwald, A.; et al. XBP1, Downstream of Blimp-1, Expands the Secretory Apparatus and Other Organelles, and Increases Protein Synthesis in Plasma Cell Differentiation. *Immunity* **2004**, *21*, 81–93. [CrossRef] [PubMed]
368. Gaudette, B.T.; Jones, D.D.; Bortnick, A.; Argon, Y.; Allman, D. MTORC1 Coordinates an Immediate Unfolded Protein Response-Related Transcriptome in Activated B Cells Preceding Antibody Secretion. *Nat. Commun.* **2020**, *11*, 1–16. [CrossRef] [PubMed]
369. Meijer, B.J.; Smit, W.L.; Koelink, P.J.; Westendorp, B.F.; de Boer, R.J.; van der Meer, J.H.M.; Vermeulen, J.L.M.; Paton, J.C.; Paton, A.W.; Qin, J.; et al. Endoplasmic Reticulum Stress Regulates the Intestinal Stem Cell State through CtBP2. *Sci. Rep.* **2021**, *11*, 1–15. [CrossRef] [PubMed]
370. Tanaka, K.-I.; Yamaguchi, T.; Kaji, H.; Kanazawa, I.; Sugimoto, T. Advanced Glycation End Products Suppress Osteoblastic Differentiation of Stromal Cells by Activating Endoplasmic Reticulum Stress. *Biochem. Biophys. Res. Commun.* **2013**, *438*, 463–467. [CrossRef] [PubMed]
371. Moon, J.Y.; Kim, H.S. α-Syntrophin Alleviates ER Stress to Maintain Protein Homeostasis During Myoblast Differentiation. *FEBS Lett.* **2021**, *595*, 1656–1670. [CrossRef]

*Clinical Science* (2021) **135** 143–159
https://doi.org/10.1042/CS20201137

PORTLAND PRESS

Research Article

# Role of endoplasmic reticulum stress in renal damage after myocardial infarction

**Beatriz Delgado-Valero[1], Lucía de la Fuente-Chávez[1], Ana Romero-Miranda[1], María Visitación Bartolomé[2,3], Bunty Ramchandani[4], Fabián Islas[5], María Luaces[5], Victoria Cachofeiro[1,3,*] and Ernesto Martínez-Martínez[1,3,*]**

[1]Departamento de Fisiología, Facultad de Medicina, Universidad Complutense de Madrid-Instituto de Investigación Sanitaria Gregorio Marañón (IiSGM), Madrid, Spain; [2]Departmento de Inmunología, Oftalmología y Otorrinolaringología, Facultad de Psicología, Universidad Complutense Madrid, Spain; [3]Ciber de Enfermedades Cardiovasculares (CIBERCV), Instituto de Salud Carlos III, Madrid, Spain; [4]Servicio de Cirugía Cardiaca Infantil, Hospital La Paz, Madrid, Spain; [5]Servicio de Cardiología, Instituto Cardiovascular, Hospital Clínico San Carlos, Madrid, Spain

**Correspondence:** Victoria Cachofeiro (vcara@ucm.es) or Ernesto Martínez-Martínez (ernmarti@ucm.es)

Myocardial infarction (MI) is associated with renal alterations resulting in poor outcomes in patients with MI. Renal fibrosis is a potent predictor of progression in patients and is often accompanied by inflammation and oxidative stress; however, the mechanisms involved in these alterations are not well established. Endoplasmic reticulum (ER) plays a central role in protein processing and folding. An accumulation of unfolded proteins leads to ER dysfunction, termed ER stress. Since the kidney is the organ with highest protein synthesis fractional rate, we herein investigated the effects of MI on ER stress at renal level, as well as the possible role of ER stress on renal alterations after MI. Patients and MI male Wistar rats showed an increase in the kidney injury marker neutrophil gelatinase-associated lipocalin (NGAL) at circulating level or renal level respectively. Four weeks post-MI rats presented renal fibrosis, oxidative stress and inflammation accompanied by ER stress activation characterized by enhanced immunoglobin binding protein (BiP), protein disulfide-isomerase A6 (PDIA6) and activating transcription factor 6-alpha (ATF6$\alpha$) protein levels. In renal fibroblasts, palmitic acid (PA; 50-200 $\mu$M) and angiotensin II (Ang II; $10^{-8}$ to $10^{-6}$M) promoted extracellular matrix, superoxide anion production and inflammatory markers up-regulation. The presence of the ER stress inhibitor, 4-phenylbutyric acid (4-PBA; 4 $\mu$M), was able to prevent all of these modifications in renal cells. Therefore, the data show that ER stress mediates the deleterious effects of PA and Ang II in renal cells and support the potential role of ER stress on renal alterations associated with MI.

## Introduction

Kidneys and heart are linked since the heart provides nutrients and oxygen to support normal kidney function. Moreover, kidneys regulate fluid, electrolytes and acid-base homeostasis which facilitate heart function [1]. Based on that interaction, Consensus Conference of Acute Dialysis Quality Initiative Group defined cardiorenal syndrome as the different conditions in which kidney and heart dysfunction overlap [2]. The definition of cardiorenal syndrome involves five subtypes, being type 1 defined by renal injury due to a deterioration in cardiac function, the most prevalent in patients diagnosed with cardiorenal syndrome [3].

Several animal models have been described to study cardiorenal syndrome, being myocardial infarction (MI) the most commonly used to evaluate it due to its reproducibility and its relation to human pathophysiology [4]. It has been observed that approximately 20% of MI patients present renal damage which increase mortality as compared with MI patients without renal impairment [5,6]. Experimental studies have

*These authors contributed equally to this work.

Received: 03 September 2020
Revised: 17 December 2020
Accepted: 23 December 2020

Accepted Manuscript online: 23 December 2020
Version of Record published: 08 January 2021

*Clinical Science* (2021) **135** 143–159
https://doi.org/10.1042/CS20201137

demonstrated that MI is associated with development of renal fibrosis accompanied by renal inflammation even in absence of renal dysfunction few weeks post-MI [7]. Chronically, MI is accompanied by renal dysfunction. Although patients with MI usually show a time-course recovery of impaired renal function, an increased mortality rate is observed [5]. Renal fibrosis is a common feature of chronic kidney diseases and plays a critical role in renal dysfunction contributing to mortality complications [8,9]. Renal fibrosis occurs as a consequence in the misbalance between extracellular matrix (ECM) production/degradation. The increase in ECM production could be a trigger for an inflammatory response and myofibroblast proliferation [9]. Several cytokines appear to be major contributors to renal fibrosis as transforming growth factor-beta (TGF-β) which is involved in ECM production, as well as in the inflammatory response. In accordance with that, MI is accompanied by interleukin (IL)-6 overexpression, as well as macrophage infiltration at renal level in rats [6]. The inflammatory response seems to play a critical role in the development of renal fibrosis, since systemic depletion of monocytes/macrophages improves renal fibrosis in an animal model of MI [10]. However, the mechanisms involved in renal fibrosis are not fully established and there is not an effective treatment, with new strategies being mandatory for treating it.

In the last years, it has been described that various types of kidney damage such as kidney aging [11], nephronophthisis [12], diabetic kidney disease [13], acute kidney injury [14] and hypertension-associated kidney disease [15] are associated with endoplasmic reticulum (ER) dysfunction, termed ER stress. ER plays a central role in calcium homeostasis, lipid biosynthesis and protein processing. Different conditions such as high protein demand, viral infections, inflammatory cytokines and mutant protein expression, result in ER stress and the subsequent activation of unfolded protein response (UPR) in order to try to mitigate this pathological situation [16]. UPR response tries to deal with the accumulation of unfolded proteins, activating three different pathways initiated by inositol requiring 1 (IRE1), PKR-like ER kinase (PERK) and activating transcription factor 6 (ATF6) proteins. In unstressed conditions, immunoglobin binding protein (BiP) binds to IRE1, PERK and ATF6 and keep them inactive. Upon undergoing ER stress, BiP dissociates from these master regulators, thereby activating UPR. For this reason, BiP is considered to be a monitor of ER stress [17]. UPR activation is initially considered to be an adaptive response; however, persistent activation of UPR drives damaged cells to apoptosis [18] and is associated with the pathogenesis of a number of diseases.

Therefore, the aim of the present study was to evaluate whether ER stress can participate in the renal fibrosis associated with MI. To achieve this aim, we have evaluated if ER stress is activated at renal level in rats with MI and its association with renal fibrosis. We have also analyzed the impact of the activation of ER stress on ECM components and mediators on renal fibroblasts stimulated with palmitic acid (PA) which has been proven to activate ER stress accompanied by an increase in inflammatory markers in podocytes [19]; however, its effect on renal fibroblasts and the effects of PA on ECM production is not studied. In addition, we used a well-known profibrotic factor such as angiotensin II (Ang II) in renal fibroblasts to study the possible role of ER stress in ECM production.

# Materials and methods

## Subjects

Patients who suffer a first acute myocardial infarction (MI) as defined by "The Third Universal Definition of Myocardial Infarction" [20]: increase in biomarkers in the presence of ischemia, ST-T changes, the appearance of new Q waves, identification of alterations of local contraction by image technique or intracoronary thrombus detected by angiography were recruited from the Cardiology Department of Hospital Clínico San Carlos, Madrid, Spain. The exclusion criterion were a previous MI or myocardial revascularization, hemodynamic instability 12 h previous revascularization, severe chronic kidney disease with a creatinine clearance $<30$ ml/min/1.7m$^2$. Twenty-four to forty-eight hours after hospital admission for MI, patients underwent transthoracic echocardiographic and at the same time blood samples were collected. A group of healthy volunteers were recruited from staff of the hospital. The study protocol was approved by the ethics committee (16/107-E_BS) and all participants signed the informed consent. The present study was conducted in compliance with Good Clinical Practice Guidelines and the ethical principles stated in the Declaration of Helsinki.

## Experimental design and animals

Myocardial infarction was induced in 12-week-old male Wistar rats of 320–350 g (Harlan Ibérica, Barcelona, Spain; $n=8$) anesthetized (2% isofluorane), intubated and ventilated (Inspira Asv, Harvard Instruments) and placed on an adjustable heating pad to maintain a core temperature of 36–37°C by ligation of the left anterior descendent (LAD) coronary artery as previously reported [21]. Rats subjected to Sham operation (the same surgical procedure except that

the suture passing the LAD was not fastened; $n$=8) was included as a reference group (Sham). After surgery, buprenorphine (0.05 mg/kg per 8 h, intramuscular) was given for 48 h. After recovery, the animals were kept in collective cages with free access to food and water in the animal facility of the Universidad Complutense de Madrid. Four-weeks after myocardial infarction, animals were sacrificed. Systolic blood pressure (SBP) was estimated end-of-study through use of a tail-cuff plethysmograph (Narco Bio-Systems) in unrestrained rats. Animals were sacrificed by decapitation. At the end of the experiment, blood was collected in EDTA in food-deprived animals. Kidneys were removed carefully from animals, immediately frozen in liquid nitrogen and stored at −80°C until its use. The Animal Care and Use Committee of Universidad Complutense de Madrid approved all experimental procedures according to the Spanish Policy for Animal Protection RD53/2013, which meets the European Union Directive 2010/63/UE.

## Creatinine measurements

Plasma creatinine levels were measured using spectrophotometric techniques in an autoanalyzer (Vitros 5600, Diagnostics Ortho Clinical, Johnson & Johnson, New Brunswick, NJ, U.S.A.).

## Circulating measurements

Plasma Neutrophil gelatinase-associated lipocalin (NGAL) (R&D Systems; catalogue number: DY1757-05), Ang II (abbex; catalogue number: abx052349) and thiobarbituric acid reactive substances (TBARS) (Sigma Aldrich; catalogue number: MAK085) levels, were measured following the instructions of the manufacturer.

PA was measured as previously reported [22]. Aliquots of 100 μl of plasma were transferred to Eppendorf tubes. The lipids were then extracted with hexane/isopropanol, 3:2 v/v at a 1:10 sample/solvent ratio. The tubes were vortexed and maintained at −20°C for 10 min, then centrifuged at 14,000 ***g*** at 4°C for 5 min. The supernatant was collected, transferred to glass tubes and dried under nitrogen flow. Then, 1 ml of 80% methanol was added, and the tubes were thoroughly mixed.

The liquid chromatography-tandem mass spectrometry (LC-MS/MS) system comprised a Shimadzu UHPLC Nexera X2 system hyphenated to a triple quadrupole mass spectrometer LCMS-8030 (Shimadzu Corporation, Kyoto, Japan). The mass spectrometer was operated with an electrospray ionization (ESI) source in negative mode. The desolvation line and heat block temperatures were set at 250 and 400°C, respectively. The interface voltage was maintained at 3.5 kV. Nitrogen was used as nebulizing and drying gas at a flow of 1.5 and 15 l/min, respectively. Argon was used as collision gas at 230 kPa.

## Morphological and histological evaluation

Renal tissue samples were dehydrated, embedded in paraffin and cut in 4 μm-thick sections that were stained with picrosirius red in order to detect collagen fibers. Other renal tissue samples were embedded in Tissue-Tek® O.C.T™. The area of renal interstitial fibrosis was identified as the ratio of fibrosis or collagen deposition to the total tissue area (after excluding the vessel and glomerular area from the region of interest). For each sample stained with picrosirius red, 30 fields all through the cortex were analysed with a 20× objective under transmitted light microscopy (Leica DM 2000; Leica AG, Germany).

## Cell culture

The renal tube fibroblasts (TFBs) is a murine renal interstitial fibroblast cell line originally isolated from SJL mouse kidney and was a generous gift from Dr Ucero AC. TFBs were maintained in RPMI 1640 medium supplemented with 10% FBS, L-glutamine 1% and penicillin/streptomycin 1%. The cells were seeded in T75 tissue culture flask pretreated with L-polylysine (0.1 mg/ml) and then grown as a monolayer culture. Cells were passaged with 1× trypsin whenever they became confluent. All assays in the present study were done at temperatures of 37°C, 95% sterile air and 5% $CO_2$ in a saturation humidified incubator. Cells were treated with different doses of palmitic acid (PA) with bovine serum albumin (BSA) as a carrier—conjugated to 10% free fatty acids (FFA)-free BSA (PA; 50-200 μM), angiotensin II (Ang II; $10^{-8}$ to $10^{-6}$M) and/or 4-phenylbutyric acid (4-PBA; 2 and 4 μM).

For the intracellular pathways study, cells were treated with Ang II for 5, 10, 15, 30 and 60 min. The following chemical inhibitors were added at $10^{-6}$ M: BAY11-7082 (Sigma Aldrich); LY294002 (Sigma Aldrich) and PD98059 (Sigma Aldrich).

*Clinical Science* (2021) **135** 143–159
https://doi.org/10.1042/CS20201137

## Western blot

Protein extraction was performed from kidneys by mechanic disruption by 0.5 mm zirconium oxide beads in a tissue homogenizer bullet blender (Scientific Instrument Services, MA, U.S.A.) containing 300 μl of lysis buffer (cOmplete Lysis-M; Roche, Risch-Rotkreuz, Suiza, catalogue number 04719956001).

Renal and cellular proteins were separated by SDS-PAGE on polyacrylamide Criterion™ TGX™ Precast Gels (Bio-Rad, California, U.S.A.) and transfered to Hybond-c Extra nitrocellulose membranes (Hybond-P; Amersham Biosciences, Piscataway, NJ). Membranes were probed with primary antibody for α-smooth muscle actin (α-SMA; Biocare medical, California, U.S.A.; dilution 1:200), 4-Hydroxynonenal (4-HNE; Abcam plc, Cambridge, U.K.; dilution 1:250), protein kinase B (Akt, Cell Signaling, Danvers, MA, U.S.A.; dilution 1:1000), Akt, (phospho Ser473, Cell Signaling, Danvers, MA, U.S.A.; dilution 1:1000), activating transcription factor 6-alpha (ATF6α; Santa Cruz, Texas, U.S.A.; dilution 1:250), immunoglobin binding protein (BiP; BD Biosciences, Madrid, Spain; dilution 1:500), CCAAT-enhancer-binding protein homologous protein (CHOP; Cell Signaling Technology, Massachusetts, U.S.A.; dilution 1:500), collagen I (Calbiochem, California, U.S.A.; dilution 1:1000), connective tissue growth factor (CTGF; Sigma-Aldrich, Missouri, U.S.A.; dilution 1:1000), extracellular signal-regulated kinases (Erk1/2, ThermoFisher; Rockford, IL, U.S.A.; dilution 1:1000), Erk1/2 (phospho-p44/42 Thr202/Tyr204, Cell Signaling, Danvers, MA, U.S.A.; dilution 1:1000), nuclear factor-κB p65 (NF-κB, Abcam; Cambridge, U.K.; dilution 1:1000), NF-κB (phospho S536, Abcam; Cambridge, U.K.; dilution 1:1000), protein disulfide-isomerase A6 (PDIA6; Abcam plc, Cambridge, U.K.; dilution 1:1000), transforming growth factor-β (TGF-β; Abcam plc, Cambridge, U.K.; dilution 1:1000), β-actin (Sigma-Aldrich, Missouri, U.S.A.; dilution 1:1000) and glyceraldehyde 3-phosphate dehydrogenase (GAPDH; Cell Signaling Technology, Massachusetts, U.S.A.; dilution 1:5000) as a loading control. Signals were detected using the ECL system (Millipore, Massachusetts; U.S.A.). Results are expressed as an *n*-fold increase over the values of the control group in densitometric arbitrary units.

## Detection of superoxide anion production

The oxidative fluorescent dye dihydroethidium (DHE; $10^{-5}$ M) was used to evaluate superoxide anion ($O^{-2}$) presence at renal level or production in cells as previously described [23]. The fluorescence intensity was determined with Leica application suite (Leica microsystems, Wetzlar, Germany).

## Inmunocytochemistry

Characterization of the cells using immunocytochemistry technical procedure, revealed a consistent expression of vimentin (Supplementary Figure S1) confirming that the cells possessed fibroblasts phenotype. Renal fibroblasts (TFBs) were fixed with Merckofix (Merck KGaA, Darmstadt, Germany) and permeabilized with Triton X-100. Cells were then incubated overnight at 4°C in a solution containing 1:100 antivimentin (GeneTex, California, U.S.A.). After three washings (5 min each) in PBS, the cells were incubated in fluorescein anti-rabbit (Vectastin Vector) 1:200. Images were analysed and photographed at 40× objective with a Leica DMI 3000B microscope.

## Retrotranscription and real-time PCR

Total RNA was isolated using Trizol Reagent (Fisher Scientific, Waltham, MA, U.S.A.) and was reverse transcribed into cDNA using the High-Capacity cDNA Reverse Transcription Kit (Thermo Fisher Scientific Inc, Waltham, MA, U.S.A.). Quantitative PCR analysis was performed with SYBR green PCR technology (Bio-Rad) (Supplementary Tables S1 and S2). Quantification of mRNA levels was performed by real-time PCR using the $\Delta\Delta C_t$ method. Data were normalized to hypoxanthine phosphoribosyltransferase (HPRT).

## Statistical analysis

Continuous variables of patients are expressed as mean ± SD. Categorical variables are expressed in absolute values and percentages. Continuous variables of experimental data are expressed as mean ± SEM. Normality of distributions was verified by means of the Kolmogorov–Smirnov test. Levene's test was used to assess the equality of variances and a Student's *t* test was performed to determine if two sets of data were significantly different from each other. One-way ANOVA was used and followed by Newman–Keuls test or a Dunnett test. Pearson correlation analysis was used to examine association among different variables. A value of $P<0.05$ was used as the cut-off value for defining statistical significance. Data analysis was performed using the statistical program GraphPad Prism 8 (San Diego, CA, U.S.A.).

# Results

## MI is associated with higher NGAL levels in patients

The mean age of patients with MI was higher than that of control subjects (54.8 ± 6.8 vs. 41.6 ± 4.1 years; $P<0.0001$), with there being only males in the group of MI versus 50% in the control one. All MI patients, but only 8.3% of the control subjects, had associated comorbidities, with the most prevalent being hypertension and dyslipidemia. Drug treatment for hypertension included angiotensin converting enzyme inhibitors (or angiotensin II type 1 receptor antagonists), whereas all dyslipidemic patients were placed on statins. Body mass index (BMI) was higher in MI patients than in non-MI subjects (26.4 ± 2.1 vs. 23.04 ± 2.01 kg/m$^2$; $P$=0.005). Plasma creatinine levels in MI patients were higher than those of control subjects (0.88 ± 0.17 vs. 0.73 ± 0.11 mg/dl; $P$=0.0119). Despite the fact that plasma creatinine values were within normal values in both groups, MI group presented an important increase in NGAL, an acute marker of kidney injury, as compared to control subjects (87,873 ± 24,419 vs. 61,941 ± 14,695 pg/ml; $P$=0.0046; Supplementary Table S3).

## MI is associated with renal fibrosis, oxidative stress and inflammation

Animals subjected to ligation of the coronary artery presented several cardiac structural and functional alterations characterized by an increase in left ventricular end-systolic diameter accompanied by a reduction in systolic and diastolic function as compared with Sham group [21]. MI animals also presented an increase in interstitial cardiac fibrosis [21].

As occurs in patients, creatinine serum levels were similar between both groups; however, MI animals presented an increase in two markers of kidney injury NGAL and kidney injury marker-1 (KIM-1), as compared to control animals (Figure 1A). In addition, MI animals showed kidney fibrosis (Figure 1B) which was accompanied by an increase in collagen type I protein levels (Figure 1C). Complementary analysis revealed that the MI group presented a slight increase in α-SMA without signification and enhanced protein levels of the profibrotic mediator TGF-β without modification in CTGF protein levels (Figure 1C).

Oxidative stress was evaluated at renal level in the animals. An increase in TBARs circulating plasma levels was observed in MI animals as compared with control ones (Figure 1D). As shown in Figure 1E, there was an increase in fluorescence intensity in the kidney of MI animals as compared with control ones, suggesting a higher presence of superoxide anion in MI animals. This prooxidant scenario was confirmed by 4-HNE, a major end-product of lipid peroxidation, which was enhanced after MI at renal level (Figure 1F).

MI induced increased levels of pro-inflammatory markers in the kidney, including IL-6 and TNF-α (Figure 1G) mRNA levels as compared with Sham animals.

## Endoplasmic reticulum stress is activated at renal level after MI

At 4 weeks after MI, two markers of ER stress, BiP (Figure 2A) and PDIA6 (Figure 2B) were up-regulated in MI animals as compared with control ones. Analysis of different pathways involved in ER stress activation revealed that ATF6α protein levels were enhanced in MI animals (Figure 2C) in absence of CHOP protein modifications (Figure 2D). This endoplasmic reticulum stress activation was accompanied by a slight increase of PA, which did not reach significant statistically, (Figure 2E) and Ang II plasma levels in MI rats (Figure 2F).

## Activation of ER stress in renal fibroblasts

In order to activate the ER stress in renal tube fibroblasts (TFBs), we exposed the cells to PA that has been demonstrated to activate ER stress accompanied by an increase in inflammatory markers in podocytes [19].

The exposition of TFBs to different doses of PA (50–200 μM) for 24 h was accompanied by activation of ER stress characterized by enhanced PDIA6 protein levels (Figure 3A) and up-regulation of two downstream proteins of ER stress as ATF6α and CHOP (Figure 3B,C). Interestingly, PA-treated cells presented an increase in collagen I protein levels at the dose of 100 μM of PA (Figure 3D) and a protein increase in the profibrotic mediator TGF-β independently of the dose of PA (Figure 3E). This profibrotic effect of PA was accompanied by an enhanced production of superoxide anion production, reaching a maximum effect at 100 μM of PA after 24 h of stimulation (Figure 3F).

## Endoplasmic reticulum stress mediates the prooxidant, profibrotic and proinflammatory effects of PA in renal fibroblasts

In order to explore the possible role of ER stress in the prooxidants and profibrotic effects of PA, TFBs were exposed to PA (100 μM) in presence or absence of the pharmacological inhibitor of ER stress, 4-PBA, for 24 h.

*Clinical Science* (2021) **135** 143–159
https://doi.org/10.1042/CS20201137

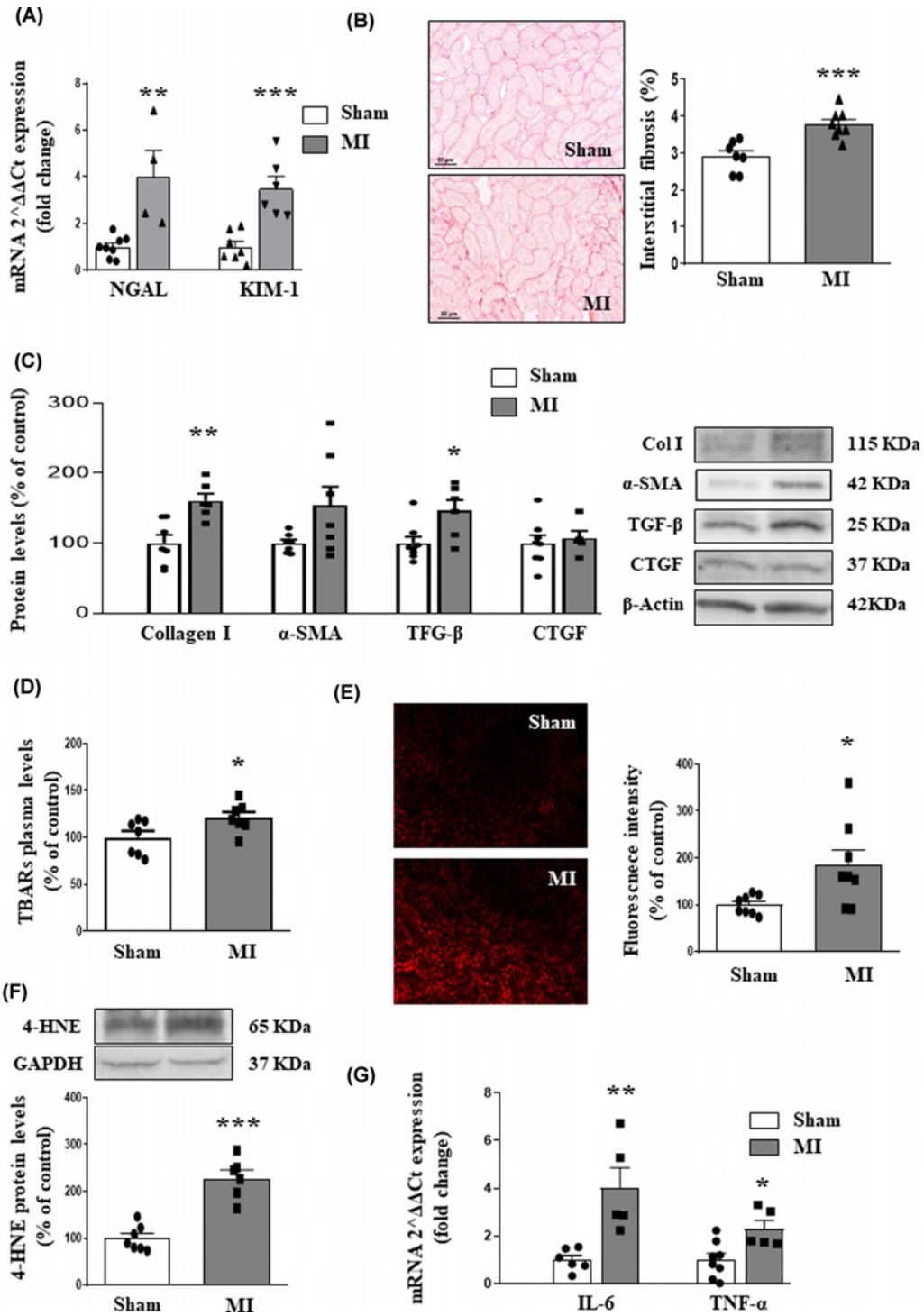


**Figure 1. Impact of MI on renal fibrosis, oxidative stress and inflammation**

(**A**) Neutrophil gelatinase-associated lipocalin (NGAL) and kidney injury marker-1 (KIM-1) mRNA levels. (**B**) Representative microphotographs of renal sections staining with picrosirius red (magnification 20×) and quantification of collagen volume fraction. (**C**) Renal protein levels of collagen type I, alpha-smooth muscle actin (α-SMA), transforming growth factor-beta (TGF-β) and connective tissue growth factor (CTGF). (**D**) Thiobarbituric acid reactive substances (TBARS) plasma. (**E**) Representative images and quantification of renal sections labelled with the oxidative dye hydroethidine (magnification 40×). (**F**) Renal protein levels of 4-hydroxynonenal (4-HNE). (**G**) Renal mRNA levels of interleukin-6 (IL-6) and tumor necrosis factor-alpha (TNF-α) in kidneys from rats after MI or Sham animals. Bar graphs represent the mean ± SEM of 8–10 animals normalized to hypoxanthine-guanine phosphoribosyltransferase (HPRT) or β-actin for cDNA and protein, respectively: *$P<0.05$; **$P<0.01$; ***$P<0.001$ versus Sham group.

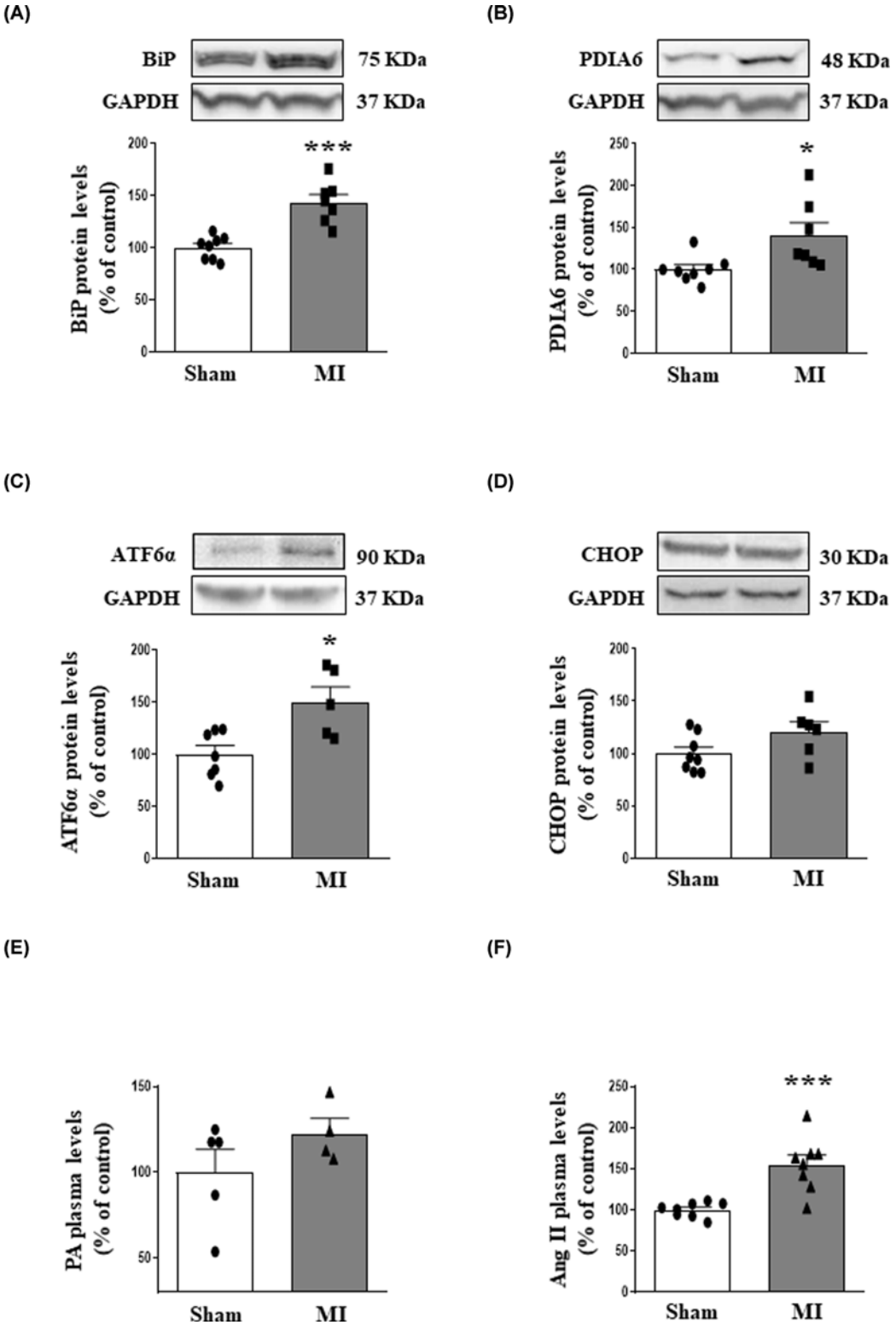


**Figure 2. MI induces endoplasmic reticulum stress at renal level**

Renal protein levels of (**A**) immunoglobulin binding protein (BiP). (**B**) Protein disulfide isomerase family A member 6 (PDIA6). (**C**) Activating transcription factor 6-alpha (ATF6$\alpha$) and (**D**) CCAAT-enhancer-binding protein homologous protein (CHOP) from rats after MI or Sham animals. Plasma levels of (**E**) palmitic acid (PA) and (**F**) Angiotensin II (Ang II) from rats after MI or Sham animals. Bar graphs represent the mean $\pm$ SEM of 8–10 animals normalized to glyceraldehyde-3-phosphate dehydrogenase (GAPDH); $^{*}P<0.05$; $^{***}P<0.001$ versus Sham group.

*Clinical Science* (2021) **135** 143–159
https://doi.org/10.1042/CS20201137

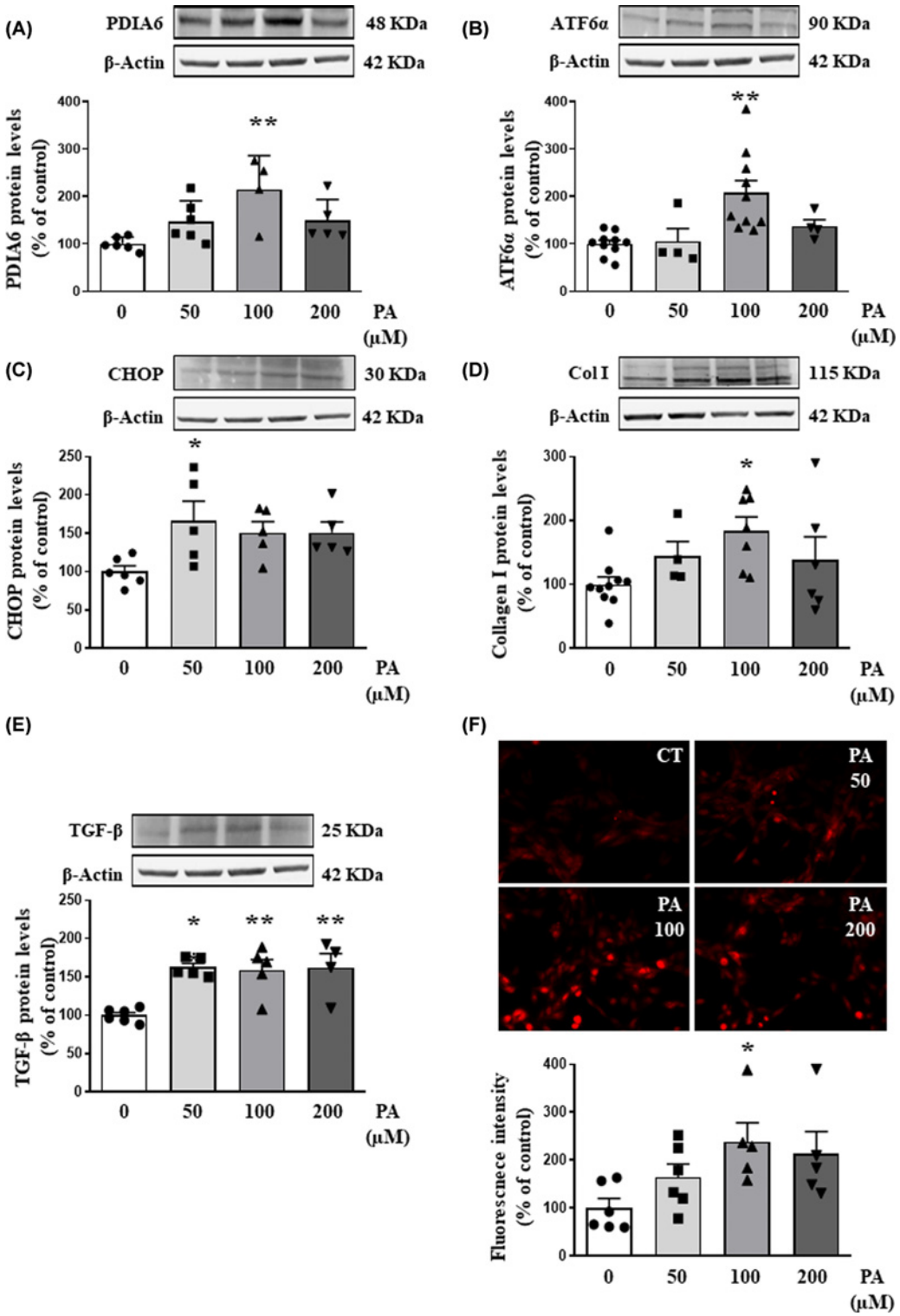


**Figure 3. Palmitic acid (PA) effects on endoplasmic reticulum stress, extracellular matrix proteins and superoxide anion production in renal fibroblasts**

Dose–response (50–200 μM) of PA in renal fibroblasts on (**A**) protein disulfide isomerase family A member 6 (PDIA6); (**B**) activating transcription factor 6-alpha (ATF6α); (**C**) CCAAT-enhancer-binding protein homologous protein (CHOP); (**D**) collagen I; (**E**) transforming growth factor-beta (TGF-β) protein expression and (**F**) representative microphotographs and quantification of cells labeled with the oxidative dye hydroethidine (magnification 40×). Bar graphs represent the mean ± SEM of four to six assays normalized to β-actin; *$P<0.05$, **$P<0.01$ versus control cells.

4-PBA was able to prevent the increase in superoxide anion production induced by PA at two different doses, 2 and 4 μM (Figure 4A). For the next experiments, we used the dose of 4 μM of 4-PBA. At that dose, 4-PBA was able to prevent the activation of ER stress and thus preventing the protein up-regulation of BiP, PDIA6 and ATF6α protein levels induced by PA, showing the efficiency of the treatment (Supplementary Figure S2A–C). In addition, 4-PBA was able to prevent the increase in ECM proteins induced by PA after 24 h of treatment. 4-PBA-treated cells were resistant to the increase in TGF-β (Figure 4B) induced by PA in TFBs. 4-PBA blunted the production of collagen I induced by PA at mRNA levels (Figure 4C).

TFBs treated with PA (100 μM) for 24 h presented and increase in different proinflammatory markers such as IL-6, CCL-2 and osteopontin at mRNA level (Figure 4C). The pharmacological inhibitor of ER stress was able to prevent the proinflammatory response of PA in TFBs (Figure 4C). These effects of 4-PBA were accompanied by a prevention of the up-regulation in the acute kidney injury biomarker, NGAL, induced by PA in the renal cells (Figure 4C).

### Endoplasmic reticulum stress mediates the prooxidant, profibrotic and proinflammatory effects of angiotensin II in renal fibroblasts

We evaluated the possible role of ER stress in a well-known profibrotic factor at renal level. Ang II was able to activate ER stress in a dose dependent-manner characterized by an increase in BiP, PDIA6, CHOP and ATF6α protein levels after 24 h of stimulation (Figure 5A–D). For the next experiments, cells were exposed to Ang II ($10^{-6}$ M) in presence or absence of 4-PBA at 4 μM. The presence of the ER stress inhibitor was able to block the rise in superoxide anion production induced by Ang II (Figure 5E), as well as the increase in collagen I and the inflammatory markers IL-6, CCL-2 and osteopontin at mRNA level in Ang II-treated cells (Figure 5F).

The possible intracellular pathways by which Ang II exerts its profibrotic effects in renal fibroblasts were analysed. Ang II ($10^{-6}$ M) increased NFκB phosphorylation after 10 min of stimulation (Figure 6A), Akt phosphorylation at 60 min (Figure 6B) and enhanced protein levels of ERK phosphorylation at 5 and 10 min (Figure 6C). The presence of LY294002, a specific inhibitor of PI3K/Akt pathway, was not able to modify the increase in collagen I protein levels induced by Ang II (Figure 6D). In contrast, the presence of BAY11-7082, a specific inhibitor of NFκB pathway, or the presence of PD98059, a specific inhibitor of ERK 1/2, prevented the profibrotic effects of Ang II in renal cells (Figure 6D).

## Discussion

The main purpose of the present study was to investigate the role of ER stress in the renal alterations associated with MI. Four weeks post-MI, animals presented renal fibrosis, oxidative stress and inflammation. We show for the first time that these alterations were accompanied by ER stress activation showing its possible role on ECM production. To our knowledge, this is the first study demonstrating that PA is able to exert profibrotic actions as well as ER stress activation. In addition, the pharmacological ER stress inhibition prevented the increase in collagen I, superoxide anion production and inflammatory markers induced by PA or by another profibrotic factor such as Ang II, supporting the role of ER stress in this process. Thus, ER stress emerges as a potential target for treatment of renal fibrosis associated with MI.

Several studies have demonstrated that MI is associated with renal damage [24,25]. This effect was accompanied by the fact that patients with renal alterations experience poor outcomes post-MI [26,27], and make an earlier detection of renal damage in patients mandatory, even in absence of creatinine alterations. Serum NGAL levels have correlated with the severity of renal damage and are associated with an increased risk of mortality in patients [28]. In this line, we have observed an increase in NGAL levels, a marker of acute renal damage, in patients with MI even in the presence of normal creatinine levels. Similarly, 4-week post-MI, animals do not present alterations in creatinine circulating levels as compared with control ones. In fact, serum creatinine levels were not elevated until 60 days post-MI [7]. However, renal NGAL and KIM-1 levels were higher than in Sham rats. This further supports the impact of myocardial ischemia in the kidney.

Renal fibrosis is an alteration that indicates the progression of kidney disease and is related to a decline in renal function in patients and animal models [29]. Different mediators have been postulated as contributors to renal fibrosis with TGF-β being a central one [10]. Our results show an increase in protein levels of this important fibrogenic cytokine in the kidneys of MI animals, which is accompanied by renal fibrosis and collagen I up-regulation. Along with TGF-β and renal fibrosis, oxidative stress and inflammation are other mechanisms described in the progression of renal failure. Our data show that MI animals presented an increase in superoxide anion levels, in 4-HNE, a major end-product of lipid peroxidation, and TBARs confirming oxidative stress at renal level after 4 weeks of MI. A common pathway involved in tissue dysfunction is oxidative stress, which has been associated with different pathologies,

*Clinical Science* (2021) **135** 143–159
https://doi.org/10.1042/CS20201137

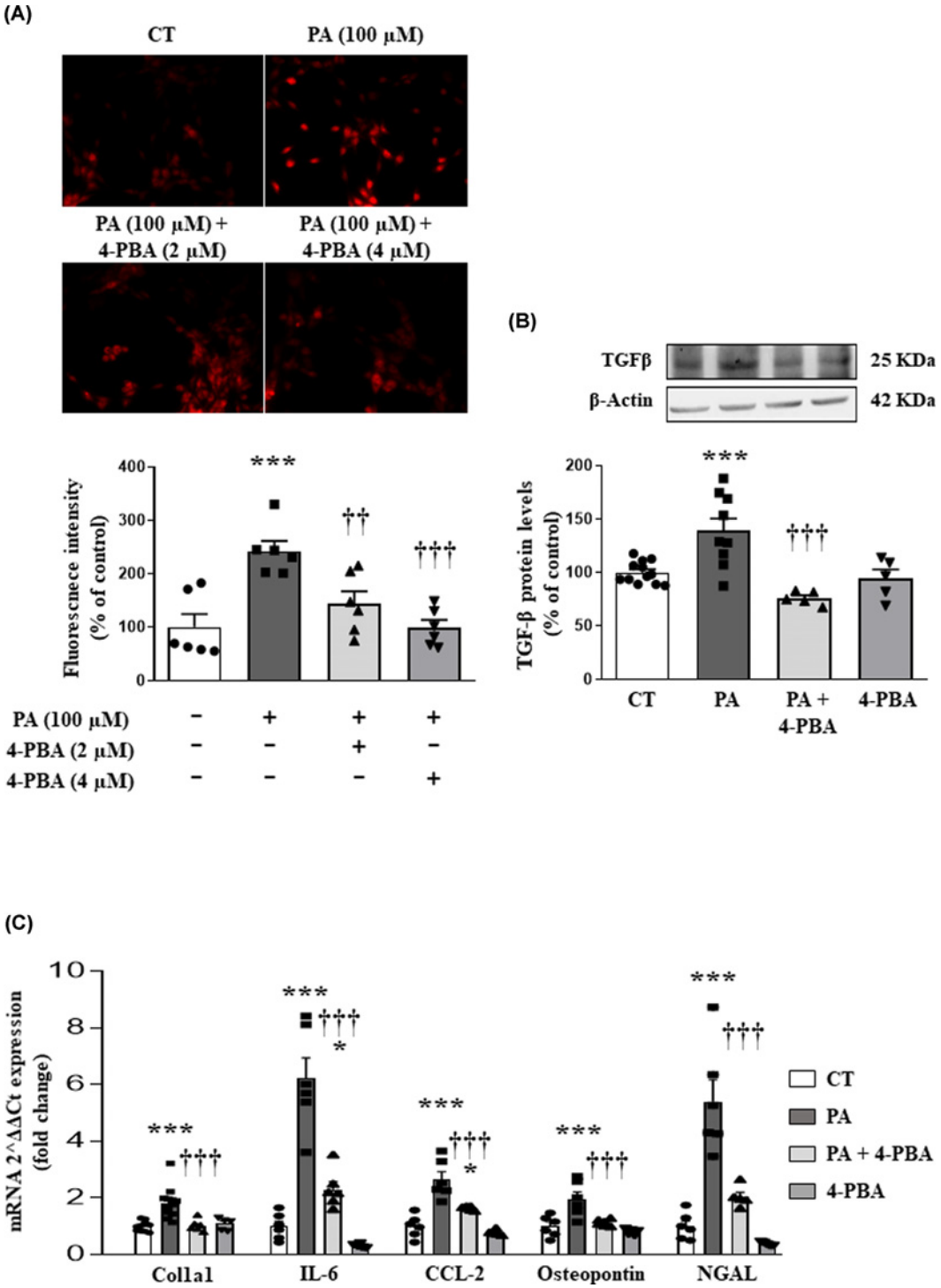


**Figure 4. Endoplasmic reticulum stress mediates the prooxidant, profibrotic and proinflammatory effects of palmitic acid (PA) in renal fibroblasts**

(**A**) Effects of 4-phenylbutyric acid (4-PBA at 2 and 4 μM) on superoxide anion production in renal fibroblasts treated with PA (100 μM) for 24 h. Representative microphotographs and quantification of cells labeled with the oxidative dye hydroethidine (magnification 40×). Effects of 4-PBA (4 μM) on (**B**) transforming growth factor-beta (TGF-β) protein expression; (**C**) collagen I mRNA expression, interleukin-6 (IL-6), C-C motif chemokine ligand 2 (CCL-2), osteopontin and neutrophil gelatinase-associated lipocalin (NGAL) mRNA expression in PA-treated cells (100 μM) for 24 h. Bar graphs represent the mean ± SEM of four to six assays normalized to hypoxanthine-guanine phosphoribosyltransferase (HPRT) or β-actin for cDNA and protein, respectively; *$P<0.05$; ***$P<0.001$ versus control cells; ††$P<0.01$; †††$P<0.001$ versus PA-treated cells.

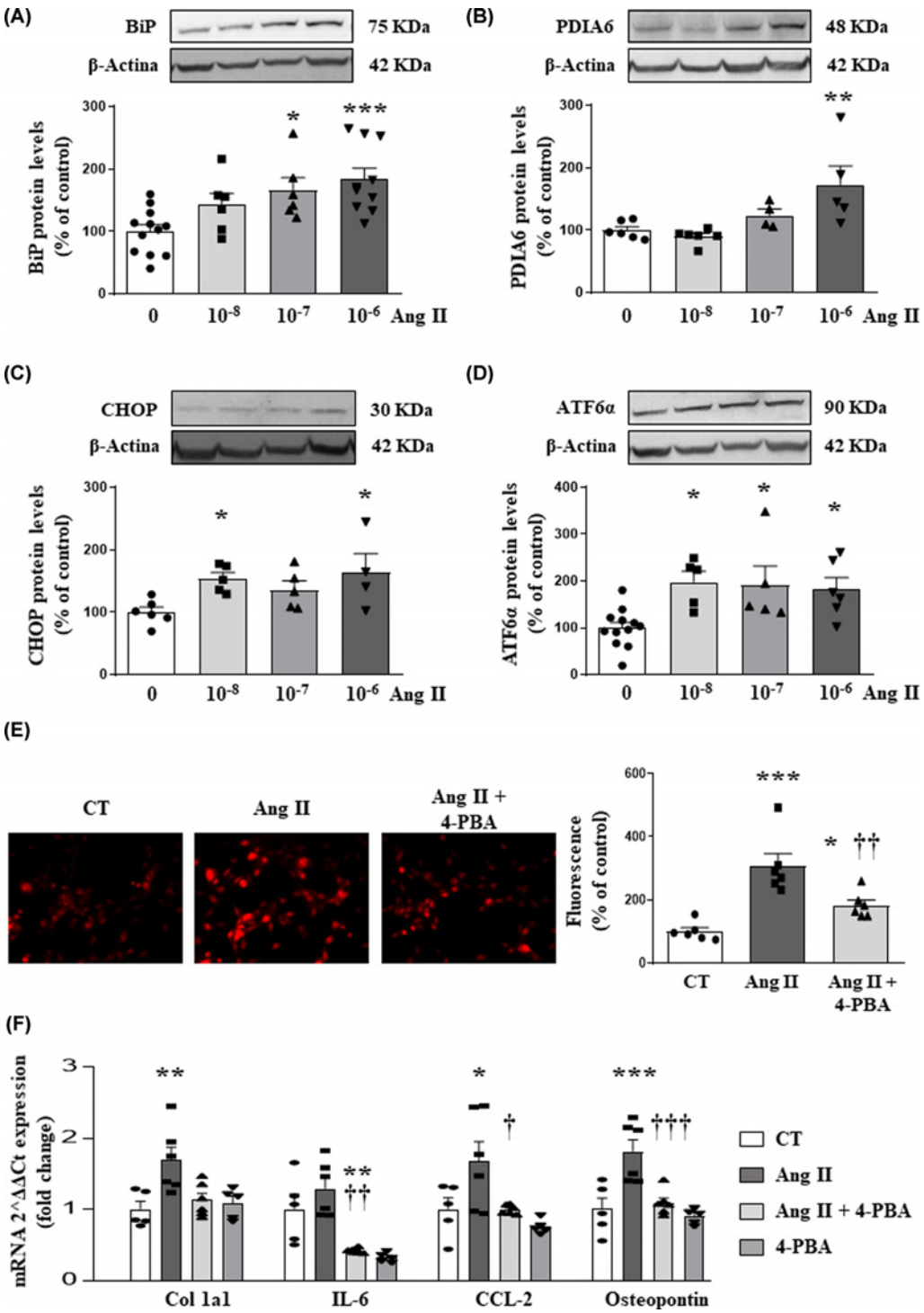


**Figure 5. Endoplasmic reticulum stress mediates the prooxidant, profibrotic and proinflammatory effects of angiotensin II (Ang II) in renal fibroblasts**

Dose–response ($10^{-8}$–$10^{-6}$ M) of Ang II in renal fibroblasts on (**A**) immunoglobulin binding protein (BiP); (**B**) protein disulfide isomerase family A member 6 (PDIA6); (**C**) CCAAT-enhancer-binding protein homologous protein (CHOP) and (**D**) activating transcription factor 6-alpha (ATF6$\alpha$) protein expression. Effects of 4-PBA (4 $\mu$M) on (**E**) superoxide anion production in renal fibroblasts treated with Ang II ($10^{-6}$ M) for 24 h. Representative microphotographs and quantification of cells labelled with the oxidative dye hydroethidine (magnification 40×); (**F**) collagen I, interleukin-6 (IL-6), C-C motif chemokine ligand 2 (CCL-2) and osteopontin mRNA expression in Ang II ($10^{-6}$M) for 24 h. *$P$<0.05; **$P$<0.01; *** $P$<0.001 versus control cells; †$P$<0.05; ††$P$<0.01; †††$P$<0.001 versus Ang II-treated cells.

*Clinical Science* (2021) **135** 143–159
https://doi.org/10.1042/CS20201137

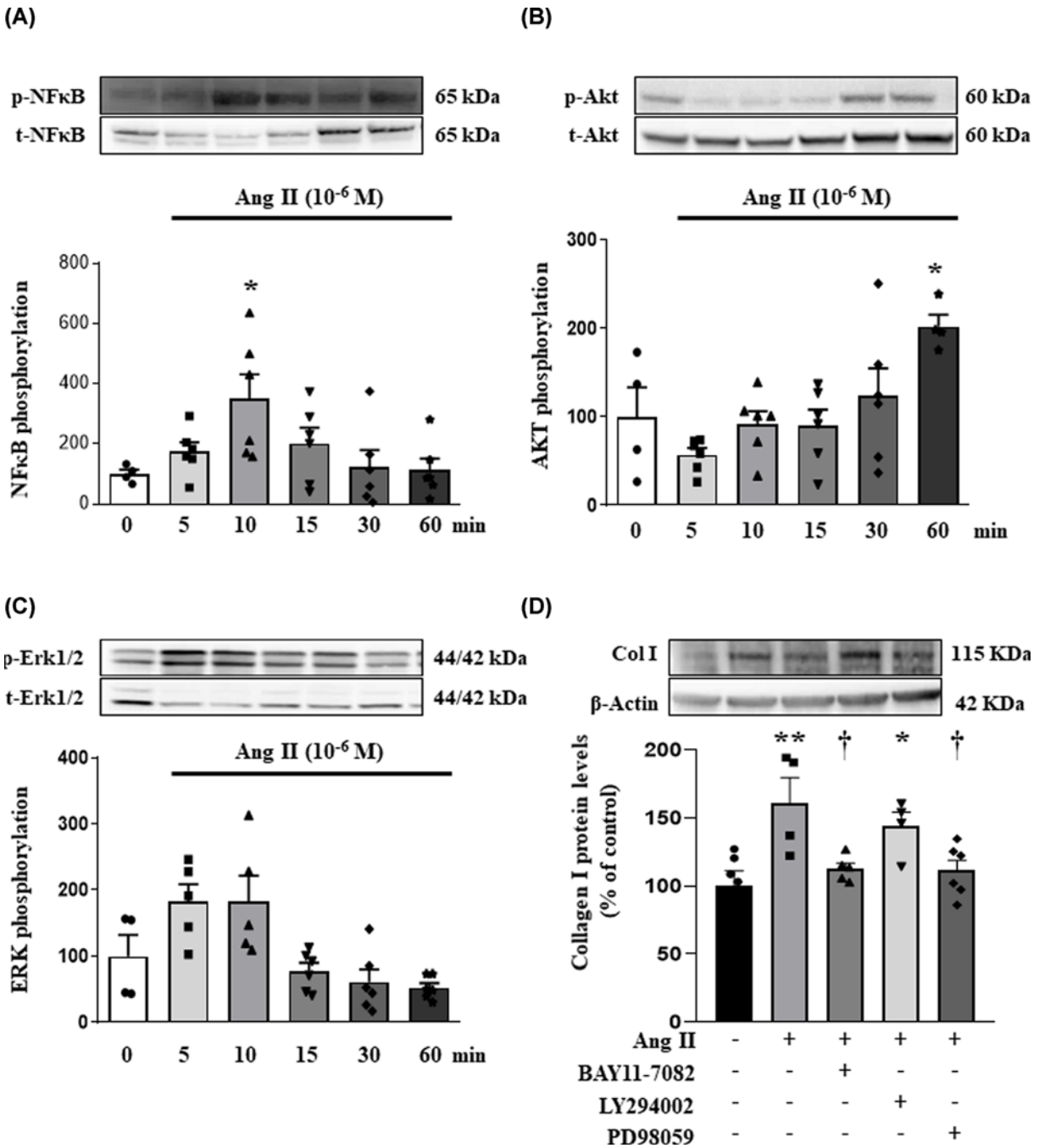


**Figure 6. NFκB and ERK 1/2 mediate the profibrotic actions of angiotensin II (Ang II) in renal fibroblasts**

Phosphorylation of (**A**) NFκB (p-NFκB, nuclear factor-κB; B); (**B**) Akt (p-Akt, protein kinase B) and (**C**) ERK 1/2 (p-ERK1/2, extracellular signal-regulated kinases 1/2) in renal fibroblasts treated with Ang II ($10^{-6}$M) for 24 h. (**D**) Effects of the NFκB inhibitor, BAY 11-7082 ($10^{-6}$ M), AKT inhibitor, LY294002 ($10^{-6}$ M) or ERK 1/2 inhibitor, PD98059 ($10^{-6}$ M) on collagen type I protein synthesis induced by Ang II. Bar graphs represent the mean ± SEM of four to six assays normalized to total NFκB, total Akt, total ERK 1/2 or β-actin; *$P<0.05$; **$P<0.01$ versus control cells; †$P<0.05$ versus Ang II-treated cells.

including heart failure, hypertension or kidney diseases [30–32]. In fact, patients with cardiorenal syndrome present an increase in reactive oxygen species (ROS) [33]. It has been postulated that ROS generation is responsible for IL-6 production linking oxidative stress with inflammation. In line with this, patients with cardiorenal syndrome presented an increase in oxidative stress markers accompanied by higher levels of IL-6 [33]. In agreement with this, MI

rats presented an increase in two inflammatory markers at renal level such as IL-6 and TNF-α. These observations are in agreement with the study performed by Cho et al., which describe that MI is associated with renal macrophages infiltration and TNF-α and IL-6 up-regulation at kidney level in rats subjected to ligation of the left anterior descending coronary artery [10]. In addition, macrophage depletion is able to blunt the development of renal fibrosis in MI rats, thus showing the role of inflammation in kidney fibrosis [10]. Despite the fact that macrophage depletion improved renal fibrosis, it was not able to recover cardiac function after MI induction, indicating the complexity of this pathological situation and supporting the necessity to discover the additional mechanisms involved in the development of fibrosis as well as inflammation in this context.

ER is an organelle essential for protein biosynthesis and post-translational modifications, which is very sensitive to unfolded and misfolded proteins in the lumen of ER. In those situations, ER induces ER stress and activates the UPR to enhance degradation of misfolded proteins [34]. On the other hand, if ER is sustained, it triggers inflammation and apoptosis [35]. Several pathologies have been associated with ER stress activation such as diabetes mellitus [36], cardiovascular disease [37], obesity [38] as well as chronic kidney disease [39]; however, the effect of MI in ER stress activation at renal level is not analyzed. In our study, we observed that ER stress is activated at renal level 4 weeks post-MI showing the possible role of ER stress in ECM production at renal level after MI. Accordingly, several studies have demonstrated the role of ER stress in the development of fibrosis. ER stress has been associated with myocardial fibrosis in different pathological situations such as obesity, pressure overload or hypertension [40–42]. At renal level, it has been also related to fibrosis. The pharmacological inhibition of ER stress was able to prevent fibrosis in an animal model of unilateral ureteral obstruction and the profibrotic effects of TGF-β in tubular cells [43]. Genetic disruption of ATF6α prevented collagen I up-regulation and promoted less tubulointerstitial fibrosis in an animal model of unilateral ischemia reperfusion injury [44]. Similarly, we have observed an increase at renal level in ATF6α levels after MI without modifications in CHOP, which has been described as a mediator of apoptosis [45]. ATF6α has been reported as a key regulator in lipid metabolism antagonizing the activity of sterol regulatory element-binding proteins [46] and its depletion reduces lipid accumulation within the kidneys of mice after ischemia–reperfusion [44]. In this sense, a high intake of saturated fatty acids is considered an important risk factor for coronary heart disease through to its ability to raise low-density lipoprotein cholesterol. It has been demonstrated the relevance of different across types of saturated fatty acids based on the chain-length on cardiovascular diseases and in MI [47]. In this sense, PA (C16:0) is associated with high coronary heart disease while other saturated fatty acids with other carbon chain lengths were not in a prospective cohort study [48]. Martínez-García et al., have demonstrated that lipotoxicity induced by PA, promoted ER stress activation and insulin resistance by disturbing the cytoarchitecture in podocytes [19]; however, the effects of PA on renal fibroblasts are not studied. Several cell types are involved in renal injury and renal fibrosis. It has been previously described that resident tubular epithelial cells, endothelial cells, vascular smooth muscle cells, fibroblasts or inflammatory cells could promote renal fibrosis through different mechanisms such as sources of renal fibroblasts via endothelial-to-mesenchymal transition, prooxidant or proinflammatory effects [49–51]. Renal fibroblasts are one of the cell types responsible for ECM production and the consequent development of renal fibrosis. We have confirmed the role of PA on ER stress activation in renal fibroblasts. In addition, we observed that PA exerts direct profibrotic, prooxidant and proinflammatory actions in renal fibroblasts showing its detrimental role at renal level. ER stress activation seems to play an important role in these modifications since the pharmacological inhibition of ER stress by 4-PBA was able to prevent all the PA effects in renal fibroblasts.

In human proximal tubule epithelial cells, PA has been demonstrated to induce ER stress as well as Ang II in cultured medium. In addition, the blockade of Ang II receptor I with valsartan or the treatment with the renin inhibitor, aliskiren, was able to prevent the ER stress induction by PA in the renal cells [52], supporting that Ang II could mediate the activation of ER stress induced by PA. In renal fibroblasts, Ang II has been shown to increase collagen I and TGF-β protein levels, an effect accompanied by an increase in superoxide anion production [53]. In fact, treatments against renin–angiotensin–aldosterone system are the standard strategies to preserve renal function in chronic kidney diseases [53]. Ang II is recognized as one of the modifiable risk factors involved in several pathologies such as myocardial infarction [54]. Ang II exerts paracrine and autocrine effects increasing the vascular resistance and impairing the correct function of the cardiovascular and renal systems. Activation of the renin–angiotensin system has several haemodynamic and humoral consequences promoting cardiac and renal damage among others [55]. An excess of Ang II promotes sarcolemmic permeability, cell death, an increase in vascular permeability due to the destruction of endothelial cells. All of these events lead to the replacement of contractile tissue by fibrotic one. Different mechanisms have been demonstrated in the detrimental role of Ang II such as tissue hypertrophy [56], oxidative stress [57] or pro-inflammatory activity, which finally trigger the fibrotic response affecting the correct function of the tissue such as heart or kidneys showing that elevated levels of Ang II as a cardiovascular risk factor. In the present study we observed an increase in Ang II plasma levels in MI rats as compared to control ones. In animal models of

*Clinical Science* (2021) **135** 143–159
https://doi.org/10.1042/CS20201137

MI, blockade of receptor type I of Ang II or inhibition of angiotensin converting enzyme has been demonstrated to improve glomerular damage and inflammatory cell infiltration in kidneys [58]; however, its effects on renal fibrosis have not presented a major improvement [8]. Our data show that NFκB and ERK1/2 pathways mediate the profibrotic effects of Ang II. In previous studies, the effects of Ang II on ER stress activation have been described. Ang II is able to induce ER stress in podocytes [59] in macrophages [60] and mesangial cells [61]. In the study, we have corroborated the profibrotic, proinflammatory and prooxidant effects of Ang II in renal fibroblasts. These alterations seem to be mediated by ER stress activation since (i) Ang II was able to induce ER stress and (ii) the presence of 4-PBA in the culture medium prevented the increase in collagen I, superoxide anion production and the inflammatory markers in Ang II-treated fibroblasts.

In summary, we have demonstrated that the renal alterations observed in MI rats were accompanied by ER stress activation. Inhibition of ER stress prevented the increase in ECM proteins, ROS production and inflammatory markers in PA or Ang II-treated renal fibroblasts.

## Limitations

A limitation of our study must be acknowledged regarding the age and that the majority of MI patients were male showing the profile of patients admitted in the emergency room with MI code at the time of inclusion in the study. However, whether these differences in age or gender distribution with the reference group of subjects could impact or influence the interpretation of the clinical data need further work.

## Clinical perspectives

- MI is associated with renal alterations resulting in poor outcomes in patients with MI. Renal fibrosis and inflammation are common features of chronic kidney diseases and play a critical role in renal dysfunction contributing to mortality complications. However, the mechanisms involved in renal alterations in MI are not fully established and there is not an effective treatment, with new strategies being mandatory for treating it.

- In the present study, we demonstrate that MI is associated with renal alterations including ER stress activation. In addition, ER stress is associated with renal interstitial fibrosis in animals with MI. In renal fibroblasts, ER stress mediates the profibrotic, prooxidant and proinflammatory effects of PA and Ang II in these cells.

- Our findings suggest the potential role of ER stress in the renal fibrosis in the context of MI, suggesting new therapeutic approaches in the management of MI for the treatment of kidney dysfunction, as well as in pathological situations with high levels of Ang II or PA (lipotoxicity).

### Data Availability

The data that support the findings of this study are available from the corresponding authors upon reasonable request.

### Competing Interests

The authors declare that there are no competing interests associated with the manuscript.

### Funding

This work was supported by Instituto de Salud Carlos III-Fondo Europeo de Desarrollo Regional (FEDER) [grant numbers PI18/00257; PI15/00742; CIBERCV]. B.D-V was supported by a grant P-FIS [grant number FI19/00277]. E.M-M was supported by a contract from CAM (Atracción de talento) and A.R-M was supported by a contract from CAM (Ayuda de empleo juvenil PEJ-2018-TL/BMD-11906).

### CRediT Author Contribution

**Ernesto Martínez-Martínez:** Conceptualization, Resources, Data curation, Formal analysis, Supervision, Funding acquisition, Investigation, Writing—original draft. **Beatriz Delgado-Valero:** Data curation, Investigation, Writing—review and editing. **Lucía de la Fuente-Chávez:** Data curation, Investigation. **Ana Romero-Miranda:** Investigation. **María Vistación Bartolomé:**

Writing—review and editing. **Bunty Ramachandi:** Investigation, Writing—review and editing. **Fabián Islas:** Investigation, Methodology, Writing—review and editing. **María Luaces:** Investigation, Methodology, Writing—review and editing. **Victoria Cachofeiro:** Conceptualization, Resources, Data curation, Formal analysis, Supervision, Funding acquisition, Investigation, Writing—original draft.

## Acknowledgements

We thank Raquel Jurado-López, Avelina Hidalgo, Virginia Peinado, and Daniel Fernández for their technical help. We thank Anthony DeMarco for his help in editing.

## Abbreviations

α-SMA, alpha-smooth muscle actin; 4-HNE, 4-hydroxynonenal; 4-PBA, 4- phenylbutyric acid; AKT, protein kinase B; Ang II, Angiotensin II; ATF6, activating transcription factor 6; BiP, immunoglobulin binding protein; BMI, body mass index; CCL-2, C-C motif chemokine ligand 2; CHOP, CCAAT-enhancer-binding protein homologous protein; CTGF, connective tissue growth factor; ECM, extracellular matrix; ER, endoplasmic reticulum; ERK 1/2, extracellular signal-regulated kinases 1/2; GAPDH, glyceraldehyde-3-phosphate dehydrogenase; HPRT, hypoxanthine-guanine phosphoribosyltransferase; IL-6, interleukin-6; IRE-1, inositol requiring 1; KIM-1, kidney injury marker-1; LAD, left anterior descendent; MI, myocardial infarction; NFκB, nuclear factor-κB; NGAL, neutrophil gelatinase-associated lipocalin; PA, palmitic acid; PDIA6, protein disulfide isomerase family A member 6; PERK, PKR-like ER kinase; ROS, reactive oxygen species; SBP, systolic blood pressure; TBAR, thiobarbituric acid reactive substance; TFB, renal tube fibroblast; TGF-β, transforming growth factor-beta; TNF-α, tumor necrosis factor-alpha; UPR, unfolded protein response.

# References

1 Ronco, C. and Di Lullo, L. (2014) Cardiorenal syndrome. *Heart Fail. Clin.* **10**, 251–280, https://doi.org/10.1016/j.hfc.2013.12.003
2 Ronco, C. (2011) The Cardiorenal Syndrome: Basis and Common Ground for a Multidisciplinary Patient-Oriented Therapy. *Cardiorenal. Med.* **1**, 3–4, https://doi.org/10.1159/000323352
3 Fabbian, F., Pala, M., De Giorgi, A., Scalone, A., Molino, C., Portaluppi, F. et al. (2011) Clinical features of cardio-renal syndrome in a cohort of consecutive patients admitted to an internal medicine ward. *Open Cardiovasc. Med. J.* **5**, 220–225, https://doi.org/10.2174/1874192401105010220
4 Szymanski, M.K., de Boer, R.A., Navis, G.J., van Gilst, W.H. and Hillege, H.L. (2012) Animal models of cardiorenal syndrome: a review. *Heart Fail. Rev.* **17**, 411–420, https://doi.org/10.1007/s10741-011-9279-6
5 Goldberg, A., Kogan, E., Hammerman, H., Markiewicz, W. and Aronson, D. (2009) The impact of transient and persistent acute kidney injury on long-term outcomes after acute myocardial infarction. *Kidney Int.* **76**, 900–906, https://doi.org/10.1038/ki.2009.295
6 Lekawanvijit, S., Kompa, A.R., Zhang, Y., Wang, B.H., Kelly, D.J. and Krum, H. (2012) Myocardial infarction impairs renal function, induces renal interstitial fibrosis, and increases renal KIM-1 expression: implications for cardiorenal syndrome. *Am. J. Physiol. Heart Circ. Physiol.* **302**, H1884–H1893, https://doi.org/10.1152/ajpheart.00967.2011
7 Ranganathan, P., Jayakumar, C., Tang, Y., Park, K.M., Teoh, J.P., Su, H. et al. (2015) MicroRNA-150 deletion in mice protects kidney from myocardial infarction-induced acute kidney injury. *Am. J. Physiol. Renal. Physiol.* **309**, F551–F558, https://doi.org/10.1152/ajprenal.00076.2015
8 Prakoura, N., Hadchouel, J. and Chatziantoniou, C. (2019) Novel Targets for Therapy of Renal Fibrosis. *J. Histochem. Cytochem.* **67**, 701–715, https://doi.org/10.1369/0022155419849386
9 Nogueira, A., Pires, M.J. and Oliveira, P.A. (2017) Pathophysiological Mechanisms of Renal Fibrosis: A Review of Animal Models and Therapeutic Strategies. *In Vivo* **31**, 1–22, https://doi.org/10.21873/invivo.11019
10 Cho, E., Kim, M., Ko, Y.S., Lee, H.Y., Song, M., Kim, M.G. et al. (2013) Role of inflammation in the pathogenesis of cardiorenal syndrome in a rat myocardial infarction model. *Nephrol. Dial. Transplant.* **28**, 2766–2778, https://doi.org/10.1093/ndt/gft376
11 Kimura, K., Jin, H., Ogawa, M. and Aoe, T. (2008) Dysfunction of the ER chaperone BiP accelerates the renal tubular injury. *Biochem. Biophys. Res. Commun.* **366**, 1048–1053, https://doi.org/10.1016/j.bbrc.2007.12.098
12 Foufelle, F. and Fromenty, B. (2016) Role of endoplasmic reticulum stress in drug-induced toxicity. *Pharmacol. Res. Perspect.* **4**, e00211, https://doi.org/10.1002/prp2.211
13 Zhuang, A. and Forbes, J.M. (2014) Stress in the kidney is the road to pERdition: is endoplasmic reticulum stress a pathogenic mediator of diabetic nephropathy? *J. Endocrinol.* **222**, R97–R111, https://doi.org/10.1530/JOE-13-0517
14 Gao, X., Fu, L., Xiao, M., Xu, C., Sun, L., Zhang, T. et al. (2012) The nephroprotective effect of tauroursodeoxycholic acid on ischaemia/reperfusion-induced acute kidney injury by inhibiting endoplasmic reticulum stress. *Basic Clin. Pharmacol. Toxicol.* **111**, 14–23, https://doi.org/10.1111/j.1742-7843.2011.00854.x
15 Mohammed-Ali, Z., Lu, C., Marway, M.K., Carlisle, R.E., Ask, K., Lukic, D. et al. (2017) Endoplasmic reticulum stress inhibition attenuates hypertensive chronic kidney disease through reduction in proteinuria. *Sci. Rep.* **7**, 41572, https://doi.org/10.1038/srep41572
16 Oslowski, C.M. and Urano, F. (2011) Measuring ER stress and the unfolded protein response using mammalian tissue culture system. *Methods Enzymol.* **490**, 71–92, https://doi.org/10.1016/B978-0-12-385114-7.00004-0
17 Lee, A.S. (2005) The ER chaperone and signaling regulator GRP78/BiP as a monitor of endoplasmic reticulum stress. *Methods* **35**, 373–381, https://doi.org/10.1016/j.ymeth.2004.10.010

18 Song, S., Tan, J., Miao, Y., Li, M. and Zhang, Q. (2017) Crosstalk of autophagy and apoptosis: Involvement of the dual role of autophagy under ER stress. *J. Cell. Physiol.* **232**, 2977–2984, https://doi.org/10.1002/jcp.25785
19 Martinez-Garcia, C., Izquierdo-Lahuerta, A., Vivas, Y., Velasco, I., Yeo, T.K., Chen, S. et al. (2015) Renal Lipotoxicity-Associated Inflammation and Insulin Resistance Affects Actin Cytoskeleton Organization in Podocytes. *PLoS ONE* **10**, e0142291, https://doi.org/10.1371/journal.pone.0142291
20 Thygesen, K., Alpert, J.S., Jaffe, A.S., Simoons, M.L., Chaitman, B.R., White, H.D. et al. (2012) Third universal definition of myocardial infarction. *Eur. Heart J.* **33**, 2551–2567, https://doi.org/10.1093/eurheartj/ehs184
21 Marin-Royo, G., Ortega-Hernandez, A., Martinez-Martinez, E., Jurado-Lopez, R., Luaces, M., Islas, F. et al. (2019) The Impact of Cardiac Lipotoxicity on Cardiac Function and Mirnas Signature in Obese and Non-Obese Rats with Myocardial Infarction. *Sci. Rep.* **9**, 444, https://doi.org/10.1038/s41598-018-36914-y
22 Serafim, V., Tiugan, D.A., Andreescu, N., Mihailescu, A., Paul, C., Velea, I. et al. (2019) Development and Validation of a LC(-)MS/MS-Based Assay for Quantification of Free and Total Omega 3 and 6 Fatty Acids from Human Plasma. *Molecules* **24**, https://doi.org/10.3390/molecules24020360
23 Martinez-Martinez, E., Jurado-Lopez, R., Valero-Munoz, M., Bartolome, M.V., Ballesteros, S., Luaces, M. et al. (2014) Leptin induces cardiac fibrosis through galectin-3, mTOR and oxidative stress: potential role in obesity. *J. Hypertens.* **32**, 1104–1114, discussion 1114, https://doi.org/10.1097/HJH.0000000000000149
24 Zheng, G., Cai, J., Chen, X., Chen, L., Ge, W., Zhou, X. et al. (2017) Relaxin Ameliorates Renal Fibrosis and Expression of Endothelial Cell Transition Markers in Rats of Isoproterenol-Induced Heart Failure. *Biol. Pharm. Bull.* **40**, 960–966, https://doi.org/10.1248/bpb.b16-00882
25 Merdler, I., Rozenfeld, K.L., Zahler, D., Shtark, M., Goldiner, I., Loewenstein, I.S. et al. (2020) Neutrophil Gelatinase-Associated Lipocalin for the Early Prediction of Acute Kidney Injury in ST-Segment Elevation Myocardial Infarction Patients Treated with Primary Percutaneous Coronary Intervention. *Cardiorenal. Med.* **10**, 154–161, https://doi.org/10.1159/000506378
26 Shroff, G.R., Frederick, P.D. and Herzog, C.A. (2012) Renal failure and acute myocardial infarction: clinical characteristics in patients with advanced chronic kidney disease, on dialysis, and without chronic kidney disease. A collaborative project of the United States Renal Data System/National Institutes of Health and the National Registry of Myocardial Infarction. *Am. Heart J.* **163**, 399–406, https://doi.org/10.1016/j.ahj.2011.12.002
27 Lekston, A., Kurek, A. and Tynior, B. (2009) Impaired renal function in acute myocardial infarction. *Cardiol. J.* **16**, 400–406
28 Kumpers, P., Hafer, C., Lukasz, A., Lichtinghagen, R., Brand, K., Fliser, D. et al. (2010) Serum neutrophil gelatinase-associated lipocalin at inception of renal replacement therapy predicts survival in critically ill patients with acute kidney injury. *Crit. Care* **14**, R9, https://doi.org/10.1186/cc8861
29 Efstratiadis, G., Divani, M., Katsioulis, E. and Vergoulas, G. (2009) Renal fibrosis. *Hippokratia* **13**, 224–229
30 Guo, H., Xu, D., Kuroki, M., Lu, Z., Xu, X., Geurts, A. et al. (2020) Kidney failure, arterial hypertension and left ventricular hypertrophy in rats with loss of function mutation of SOD3. *Free Radic. Biol. Med.* **152**, 787–796, https://doi.org/10.1016/j.freeradbiomed.2020.01.023
31 van der Pol, A., van Gilst, W.H., Voors, A.A. and van der Meer, P. (2019) Treating oxidative stress in heart failure: past, present and future. *Eur. J. Heart Fail.* **21**, 425–435, https://doi.org/10.1002/ejhf.1320
32 Matoba, K., Takeda, Y., Nagai, Y., Yokota, T., Utsunomiya, K. and Nishimura, R. (2020) Targeting Redox Imbalance as an Approach for Diabetic Kidney Disease. *Biomedicines* **8**, https://doi.org/10.3390/biomedicines8020040
33 Virzi, M., Clementi, A., de Cal, M., Brocca, A., Day, S., Pastori, S. et al. (2015) Oxidative stress: dual pathway induction in cardiorenal syndrome type 1 pathogenesis. *Oxid. Med. Cell Longev.* **2015**, 391790, https://doi.org/10.1155/2015/391790
34 Liu, Y., Wang, Y., Ding, W. and Wang, Y. (2018) Mito-TEMPO Alleviates Renal Fibrosis by Reducing Inflammation, Mitochondrial Dysfunction, and Endoplasmic Reticulum Stress. *Oxid. Med. Cell Longev.* **2018**, 5828120, https://doi.org/10.1155/2018/5828120
35 Karna, K.K., Shin, Y.S., Choi, B.R., Kim, H.K. and Park, J.K. (2019) The Role of Endoplasmic Reticulum Stress Response in Male Reproductive Physiology and Pathology: A Review. *World J. Mens Health* **38**, https://doi.org/10.5534/wjmh.190038
36 Ghosh, R., Colon-Negron, K. and Papa, F.R. (2019) Endoplasmic reticulum stress, degeneration of pancreatic islet beta-cells, and therapeutic modulation of the unfolded protein response in diabetes. *Mol. Metab.* **27S**, S60–S68, https://doi.org/10.1016/j.molmet.2019.06.012
37 Yang, Y., Zhou, Q., Gao, A., Chen, L. and Li, L. (2020) Endoplasmic reticulum stress and focused drug discovery in cardiovascular disease. *Clin. Chim. Acta* **504**, 125–137, https://doi.org/10.1016/j.cca.2020.01.031
38 Pagliassotti, M.J., Kim, P.Y., Estrada, A.L., Stewart, C.M. and Gentile, C.L. (2016) Endoplasmic reticulum stress in obesity and obesity-related disorders: An expanded view. *Metabolism* **65**, 1238–1246, https://doi.org/10.1016/j.metabol.2016.05.002
39 Ricciardi, C.A. and Gnudi, L. (2019) Endoplasmic Reticulum stress in chronic kidney disease. New molecular targets from bench to the bedside. *G. Ital. Nefrol.* **36**
40 Li, S.J., Liu, C.H., Chu, H.P., Mersmann, H.J., Ding, S.T., Chu, C.H. et al. (2017) The high-fat diet induces myocardial fibrosis in the metabolically healthy obese minipigs-The role of ER stress and oxidative stress. *Clin. Nutr.* **36**, 760–767, https://doi.org/10.1016/j.clnu.2016.06.002
41 Luo, T., Chen, B. and Wang, X. (2015) 4-PBA prevents pressure overload-induced myocardial hypertrophy and interstitial fibrosis by attenuating endoplasmic reticulum stress. *Chem. Biol. Interact.* **242**, 99–106, https://doi.org/10.1016/j.cbi.2015.09.025
42 Kassan, M., Galan, M., Partyka, M., Saifudeen, Z., Henrion, D., Trebak, M. et al. (2012) Endoplasmic reticulum stress is involved in cardiac damage and vascular endothelial dysfunction in hypertensive mice. *Arterioscler. Thromb. Vasc. Biol.* **32**, 1652–1661, https://doi.org/10.1161/ATVBAHA.112.249318
43 Liu, S.H., Yang, C.C., Chan, D.C., Wu, C.T., Chen, L.P., Huang, J.W. et al. (2016) Chemical chaperon 4-phenylbutyrate protects against the endoplasmic reticulum stress-mediated renal fibrosis in vivo and in vitro. *Oncotarget* **7**, 22116–22127, https://doi.org/10.18632/oncotarget.7904
44 Jao, T.M., Nangaku, M., Wu, C.H., Sugahara, M., Saito, H., Maekawa, H. et al. (2019) ATF6alpha downregulation of PPARalpha promotes lipotoxicity-induced tubulointerstitial fibrosis. *Kidney Int.* **95**, 577–589, https://doi.org/10.1016/j.kint.2018.09.023
45 Nishitoh, H. (2012) CHOP is a multifunctional transcription factor in the ER stress response. *J. Biochem.* **151**, 217–219, https://doi.org/10.1093/jb/mvr143
46 Zeng, L., Lu, M., Mori, K., Luo, S., Lee, A.S., Zhu, Y. et al. (2004) ATF6 modulates SREBP2-mediated lipogenesis. *EMBO J.* **23**, 950–958, https://doi.org/10.1038/sj.emboj.7600106

47 Praagman, J., Vissers, L.E.T., Mulligan, A.A., Laursen, A.S.D., Beulens, J.W.J., van der Schouw, Y.T. et al. (2019) Consumption of individual saturated fatty acids and the risk of myocardial infarction in a U.K. and a Danish cohort. *Int. J. Cardiol.* **279**, 18–26, https://doi.org/10.1016/j.ijcard.2018.10.064
48 Praagman, J., de Jonge, E.A., Kiefte-de Jong, J.C., Beulens, J.W., Sluijs, I., Schoufour, J.D. et al. (2016) Dietary Saturated Fatty Acids and Coronary Heart Disease Risk in a Dutch Middle-Aged and Elderly Population. *Arterioscler. Thromb. Vasc. Biol.* **36**, 2011–2018, https://doi.org/10.1161/ATVBAHA.116.307578
49 Yang, L., Besschetnova, T.Y., Brooks, C.R., Shah, J.V. and Bonventre, J.V. (2010) Epithelial cell cycle arrest in G2/M mediates kidney fibrosis after injury. *Nat. Med.* **16**, 535–543, 531p following 143, https://doi.org/10.1038/nm.2144
50 Zeisberg, E.M., Potenta, S.E., Sugimoto, H., Zeisberg, M. and Kalluri, R. (2008) Fibroblasts in kidney fibrosis emerge via endothelial-to-mesenchymal transition. *J. Am. Soc. Nephrol.* **19**, 2282–2287, https://doi.org/10.1681/ASN.2008050513
51 Boor, P., Ostendorf, T. and Floege, J. (2010) Renal fibrosis: novel insights into mechanisms and therapeutic targets. *Nat. Rev. Nephrol.* **6**, 643–656, https://doi.org/10.1038/nrneph.2010.120
52 Li, C., Lin, Y., Luo, R., Chen, S., Wang, F., Zheng, P. et al. (2016) Intrarenal renin-angiotensin system mediates fatty acid-induced ER stress in the kidney. *Am. J. Physiol. Renal. Physiol.* **310**, F351–F363, https://doi.org/10.1152/ajprenal.00223.2015
53 Shen, Y., Miao, N.J., Xu, J.L., Gan, X.X., Xu, D., Zhou, L. et al. (2016) N-acetylcysteine alleviates angiotensin II-mediated renal fibrosis in mouse obstructed kidneys. *Acta Pharmacol. Sin.* **37**, 637–644, https://doi.org/10.1038/aps.2016.12
54 Gavras, I. and Gavras, H. (2002) Angiotensin II as a cardiovascular risk factor. *J. Hum. Hypertens.* **16**, S2–S6, https://doi.org/10.1038/sj.jhh.1001392
55 Reina-Couto, M., Afonso, J., Carvalho, J., Morgado, L., Ronchi, F.A., de Oliveira Leite, A.P. et al. (2020) Interrelationship between renin-angiotensin-aldosterone system and oxidative stress in chronic heart failure patients with or without renal impairment. *Biomed. Pharmacother.* **133**, 110938, https://doi.org/10.1016/j.biopha.2020.110938
56 Kagiyama, S., Eguchi, S., Frank, G.D., Inagami, T., Zhang, Y.C. and Phillips, M.I. (2002) Angiotensin II-induced cardiac hypertrophy and hypertension are attenuated by epidermal growth factor receptor antisense. *Circulation* **106**, 909–912, https://doi.org/10.1161/01.CIR.0000030181.63741.56
57 Ritz, E. and Haxsen, V. (2003) Angiotensin II and oxidative stress: an unholy alliance. *J. Am. Soc. Nephrol.* **14**, 2985–2987, https://doi.org/10.1097/01.ASN.0000096784.86791.21
58 Wen, Z., Cai, M., Mai, Z., Chen, Y., Geng, D. and Wang, J. (2013) Protection of renal impairment by angiotensin II type 1 receptor blocker in rats with post-infarction heart failure. *Ren. Fail.* **35**, 766–775, https://doi.org/10.3109/0886022X.2013.780561
59 Ha, T.S., Park, H.Y., Seong, S.B. and Ahn, H.Y. (2015) Angiotensin II induces endoplasmic reticulum stress in podocyte, which would be further augmented by PI3-kinase inhibition. *Clin. Hypertens* **21**, 13, https://doi.org/10.1186/s40885-015-0018-5
60 Yang, J., Zhang, X., Yu, X., Tang, W. and Gan, H. (2017) Renin-angiotensin system activation accelerates atherosclerosis in experimental renal failure by promoting endoplasmic reticulum stress-related inflammation. *Int. J. Mol. Med.* **39**, 613–621, https://doi.org/10.3892/ijmm.2017.2856
61 Wang, T.N., Chen, X., Li, R., Gao, B., Mohammed-Ali, Z., Lu, C. et al. (2015) SREBP-1 Mediates Angiotensin II-Induced TGF-beta1 Upregulation and Glomerular Fibrosis. *J. Am. Soc. Nephrol.* **26**, 1839–1854, https://doi.org/10.1681/ASN.2013121332

cells

MDPI

*Review*

# Fibrosis, the Bad Actor in Cardiorenal Syndromes: Mechanisms Involved

**Beatriz Delgado-Valero [1], Victoria Cachofeiro [1,2,*] and Ernesto Martínez-Martínez [1,2,*]**

[1] Departamento de Fisiología, Facultad de Medicina, Instituto de Investigación Sanitaria Gregorio Marañón (IiSGM), Universidad Complutense de Madrid, 28040 Madrid, Spain; beadel02@ucm.es
[2] Ciber de Enfermedades Cardiovasculares (CIBERCV), Instituto de Salud Carlos III, 28029 Madrid, Spain
* Correspondence: vcara@ucm.es (V.C.); ernmarti@ucm.es (E.M.-M.); Tel.: +34-913-941-489 (V.C. & E.M.-M.)

**Abstract:** Cardiorenal syndrome is a term that defines the complex bidirectional nature of the interaction between cardiac and renal disease. It is well established that patients with kidney disease have higher incidence of cardiovascular comorbidities and that renal dysfunction is a significant threat to the prognosis of patients with cardiac disease. Fibrosis is a common characteristic of organ injury progression that has been proposed not only as a marker but also as an important driver of the pathophysiology of cardiorenal syndromes. Due to the relevance of fibrosis, its study might give insight into the mechanisms and targets that could potentially be modulated to prevent fibrosis development. The aim of this review was to summarize some of the pathophysiological pathways involved in the fibrotic damage seen in cardiorenal syndromes, such as inflammation, oxidative stress and endoplasmic reticulum stress, which are known to be triggers and mediators of fibrosis.

**Keywords:** cardiorenal syndrome; endoplasmic reticulum stress; fibrosis; heart failure; inflammation; kidney disease; oxidative stress



**Citation:** Delgado-Valero, B.; Cachofeiro, V.; Martínez-Martínez, E. Fibrosis, the Bad Actor in Cardiorenal Syndromes: Mechanisms Involved. *Cells* **2021**, *10*, 1824. https://doi.org/10.3390/cells10071824

Academic Editors: David J. Grieve and Alexander E. Kalyuzhny

Received: 31 May 2021
Accepted: 13 July 2021
Published: 19 July 2021



## 1. Introduction

The existence of a relationship between the heart and the kidney was first described in the XIX century by Robert Bright, who reported structural changes in the heart in patients with advanced kidney disease [1]. Since then, new discoveries have given insight into the interaction between heart and kidney diseases in terms of shared risk factors (such as hypertension, obesity, diabetes and atherosclerosis) and the pathophysiological pathways involved in each [2–4]. Clinically, the shared pathology of the heart and kidneys has a strong impact on the clinical outcome and is associated with increased morbidity and mortality rates [5,6].

The classic definition of cardiorenal syndrome (CRS) was proposed in 2010 by the Acute Dialysis Quality Initiative as a term that gathers the "disorders of the heart and kidneys whereby acute or chronic dysfunction in one organ may induce acute or chronic dysfunction of the other" [7]. In addition, within the term there is further classification into different subtypes according to the primary organ dysfunction and to whether it is an acute or chronic situation [7]. However, the appearance of risk factors that can affect both the heart and the kidney complicate the clinical picture, and with it the causal relationship of one to the other.

## 2. CRS Classification

### *2.1. CRS Type 1 or Acute Cardiorenal Syndrome*

CRS type 1 (CRS-1) is characterized by the worsening of cardiac function leading to acute kidney injury (AKI) and/or dysfunction of both organs [7]. Around 25–30% of patients with acute decompensated heart failure (ADHF) present AKI, often after ischemic or non-ischemic heart disease [8–10]. These patients have higher morbi-mortality and lengthier hospitalization [7]. CRS-1 has a complex pathophysiology, with hemodynamic

and non-hemodynamic alterations for which the treatments show no improvements [10,11], thus demonstrating the need to discover and understand the mechanisms involved.

Faced with a drop in blood pressure levels due to the development of heart failure (HF), the kidney responds to the decrease in cardiac output by retaining sodium and water. Nevertheless, it has been demonstrated that an elevation of the central venous pressure can result in impairment of renal function and congestion of the kidneys [10,12]. In this context, neurohormonal activation through the Renin–Angiotensin–Aldosterone System (RAAS) also has an important role, as it is both an initially compensatory mechanism for the decrease in volume consequence of the ventricular injury, and a long-term initiator of cardiovascular and renal dysfunction [13,14]. Other non-hemodynamic mechanisms, such as inflammation and oxidative stress, have been established as common pathways for cellular dysfunction in heart and kidney failure [9–11,15].

### 2.2. CRS Type 2 or Chronic Cardiorenal Syndrome

CRS type 2 is defined as chronic cardiac dysfunction that leads to progressive appearance of renal impairment that promotes the development of chronic kidney disease (CKD) [6,16,17]. CKD was defined in 2012 by Kidney Disease: Improving Global Outcomes (KDIGO) as an abnormality in kidney function or structure that is present for more than 3 months and has health implications. It is classified based on cause, a glomerular filtration rate (GFR) of <60 mL/min per 1.73 $m^2$ and the degree of albuminuria [18]. A meta-analysis by Damman et al. showed that almost a third (32%) of the total of 1 million HF patients studied presented CKD, and 23% had worsening renal function [19], confirming that renal dysfunction is an important contributor to the comorbidities in HF.

The pathological process implicated in CKD secondary to HF is a consequence of the renal response to preserve the GFR. The combination of renal congestion, hypoperfusion and the increased right atrium pressure promotes renal dysfunction in HF patients [6,11]. It has been suggested that the correct diagnosis of this CRS should be based on HF aetiology, HF with preserved ejection fraction (HFpEF) or with reduced ejection fraction (HFrEF), and on biochemical parameters of renal dysfunction, such as creatinine levels [20]. However, as the interactions between the heart and kidney are bidirectional, is not always easy to assess the inciting event from the secondary damage, thus making it difficult to differentiate CRS type 2 patients from CRS type 4 ones [11,20].

### 2.3. CRS Type 3 or Acute Reno-Cardiac Syndrome

CRS type 3 occurs when there is an acute worsening of kidney function secondary to AKI, ischemia, or glomerulonephritis that leads to acute heart injury and/or dysfunction [6,7,11]. AKI may produce cardiac events as a consequence of the fluid overload, hyperkalaemia, or metabolic acidosis, but the exact cause of the damage is difficult to establish, as there are shared comorbidities and variability in the risk factors for AKI [6,11,21,22].

There are multiple definitions of AKI according to urine output and serum creatinine levels (SCr), all of which have limitations in their clinical application [21,23]. It is due to the differing definitions of AKI that make it difficult to identify this type of CRS. Despite the lacking criteria, the incidence of AKI is increasing in hospitalized patients, and is associated with an 86% increased risk of cardiovascular mortality and a 38% increased risk of major cardiovascular events [24].

### 2.4. CRS Type 4 or Chronic Reno-Cardiac Syndrome

CRS type 4 is characterized by cardiovascular damage in patients with CKD at any stage [7,11]. It is well established that renal dysfunction is an independent risk factor for cardiovascular disease, with the risk for myocardial infection and sudden death being higher in CKD patients [25,26]. Numerous studies have found there is an independent association between the severity of CKD, evaluated by the degree of decline in kidney function, and the subsequent cardiac events [5,27,28], which could suggest that CKD likely accelerates the risk and development of cardiovascular disease [7].

CKD has been demonstrated to be associated with inflammation and other cardiovascular factors, such as hypertension, activation of RAAS, or volume overload, that usually go in parallel with a decline in GFR [26,29]. Pressure and volume overload in CKD patients lead to left ventricular hypertrophy (LVH), which is a common feature that is accompanied by fibrosis and other histological changes. These structural changes consequently cause diastolic dysfunction and increased oxygen demand, which could also explain these patients' predispositions to arrhythmias and sudden death [6,29,30].

### *2.5. CRS Type 5 or Secondary Cardiorenal Syndrome*

CRS type 5 (CRS-5) represents simultaneous injury and/or dysfunction of the heart and kidneys as a result of a systemic condition, such as sepsis, drug toxicity, lupus, cirrhosis or amyloidosis [7,23,31]. Although many pathways have been proposed, it is challenging to identify the mechanisms that are involved in CRS-5 due to the multitude of contributing factors and the sequence of organ involvement [7,31].

CRS-5 has been divided into four stages according to severity: hyperacute (0–72 h after diagnosis), acute (3–7 days), subacute (7–30 days) and chronic (beyond 30 days) [6,23]. Usually, the existing studies of CRS-5 are those of hyperacute or acute stages, as these evaluate the effects of sepsis. Sepsis, defined as a life-threatening organ dysfunction caused by a deregulated host response to infection [32], is one of the most common causes of death among hospitalized patients [33], among whom the prevalence of CRS-5 is high [7,34].

In the early stages of sepsis, microcirculatory changes are developed despite normal systemic haemodynamics [35]. Those alterations, along with inflammation, are important in the cardiac and renal dysfunction given in this type of CRS [11]. For instance, the increase in pro-inflammatory cytokines during sepsis and the decrease in renal blood flow lead to tubular necrosis, reduction in GFR and severe kidney failure [6,23,26]. Sepsis is also related to autonomic nervous system dysfunction and RAAS activation [23,31]. This complex environment makes differentiating between the cardiorenal crosstalk effects and sepsis effects very difficult.

The different CRSs are summarized in Figure 1.

**CRS type 1**

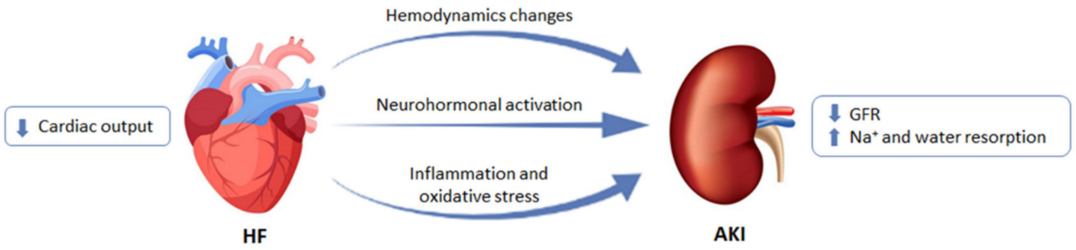


(**a**)

**Figure 1.** *Cont.*

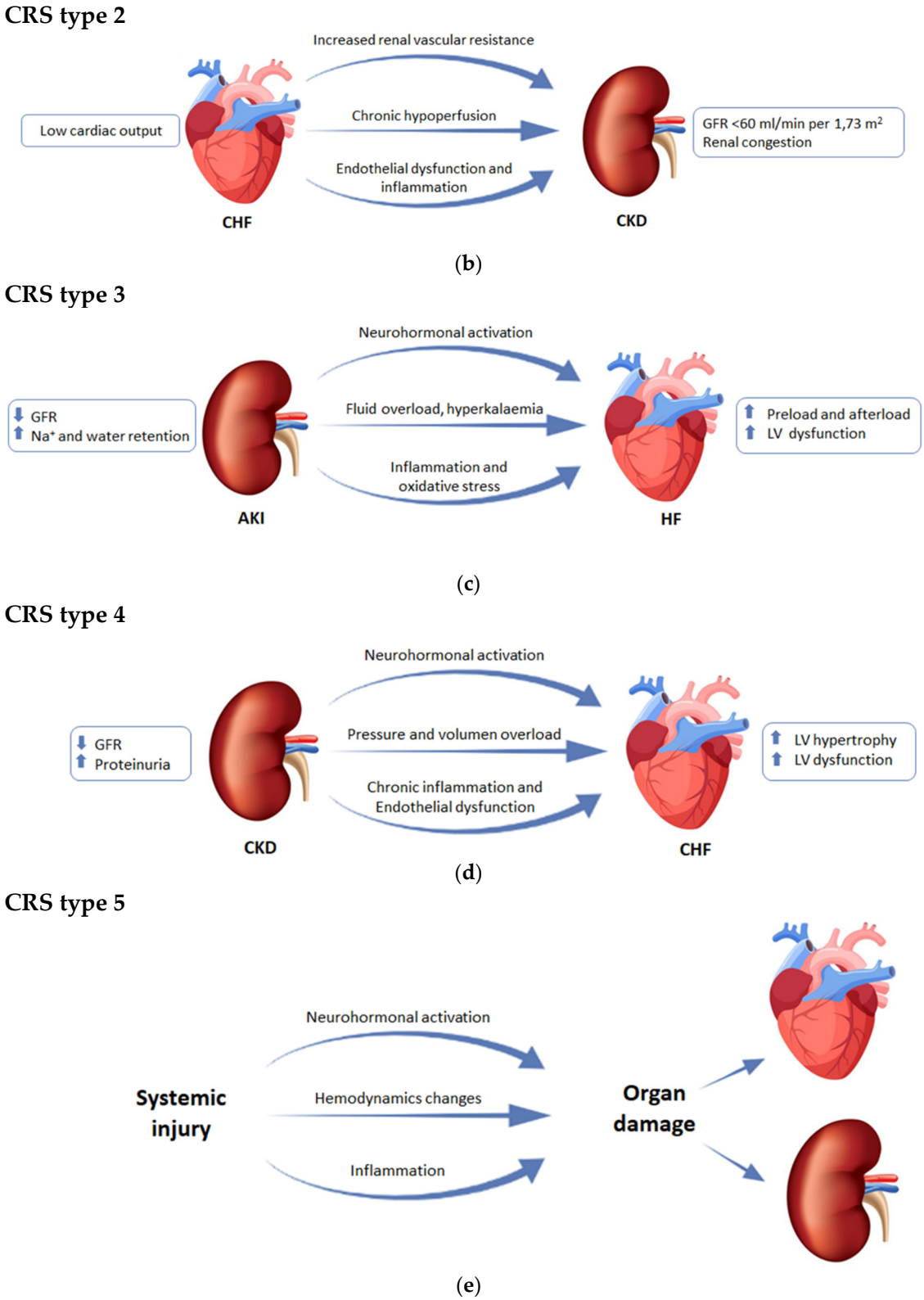


**Figure 1.** Differences among the subtypes of cardiorenal syndrome (CRS). (**a**) CRS type 1 or acute cardiorenal syndrome; (**b**) CRS type 2 or chronic cardiorenal syndrome; (**c**) CRS type 3 or acute reno-cardiac syndrome; (**d**) CRS type 4 or chronic reno-cardiac syndrome; (**e**) CRS type 5 or secondary cardiorenal syndrome. GFR: glomerular filtration rate; LV: left ventricular. Modified from [7].

## 3. Pathophysiology of CRS

Due to the essential role of both the heart and kidney in the maintenance of cardiovascular homeostasis, initial organ damage during a disease state, such as CRS, can induce structural remodelling and functional alterations in the other.

### 3.1. Cardiac Alterations Associated with CKD

As CKD is considered an important complication associated with higher cardiovascular risk and mortality. This increased risk is partially due to common risk factors such as hypertension, obesity or diabetes [36], but not entirely, as the association between CKD and cardiovascular mortality persists after risk factor adjustment [37,38]. Albuminuria- and creatinine-based estimated GFR (eGFR) are currently considered to be useful measurements for cardiovascular risk prediction, as they improve discrimination for cardiovascular mortality among CKD patients beyond traditional risk factors [38,39].

In patients with CKD there is high prevalence of structural and functional heart alterations from the early stages to end-stage renal disease (ESRD), which includes left ventricular (LV) remodelling, valvular sclerosis, reduction of the ejection fraction (EF) and diastolic dysfunction [40–42].

Echocardiographic studies have observed that LV remodelling is prevalent among patients with CKD and has been recognized as an important predictor of poor prognosis [43,44]. There are many factors that influence LV geometry in CKD patients. Pressure overload causes the thickening of the LV walls, which translates into concentric hypertrophy, whereas hypervolemia and anaemia contributes to the development of eccentric hypertrophy [45]. Two studies have reported the existence of associations between LV hypertrophy and renal dysfunction, characterized by low eGFR, which are independent of other risk factors, suggesting that impaired kidney function contributes to LV hypertrophy. In addition, they also describe that LV geometry tends to shift to concentric LV hypertrophy in advanced kidney dysfunction rather than eccentric hypertrophy [44,46]. A recent clinical study showed that the stages are associated with LV remodelling even in milder CKD, as 22% of 90 patients with stages 1 to 3 presented concentric hypertrophy, 19% eccentric hypertrophy and 20% concentric remodelling [47].

Most of the studies that have investigated the association between CKD and cardiac alterations have focused on the assessment of LV mass or hypertrophy, whilst fewer have explored LV function (neither systolic nor diastolic) [48]. In terms of LV systolic function, LVEF has been used in the majority of studies, although subclinical systolic dysfunction can happen in patients with CKD despite normal LVEF [49–51]. Diastolic dysfunction usually coexists with systolic dysfunction during LV remodelling and is common in CKD patients [44,52–54].

Numerous studies have assessed LV function in patients with CKD by trying to find an association between eGFR or albuminuria and systolic or diastolic function alterations. According to the literature, systolic dysfunction seems to be strongly correlated with albuminuria over low eGFR [55–57]. However, there is high variability. Similarly, there seems to be higher association of diastolic dysfunction with albuminuria than eGFR [56–58]. Therefore, some studies have found clear association between low eGFR, LV diastolic dysfunction and LVH [44,59].

Despite the advances made in cardiac damage, the increasing incidence and prevalence of HF makes it an important health problem. For that reason, various potential biomarkers that could contribute to diagnosis have been proposed. The gold standard in chronic HF diagnosis and prognosis is the natriuretic peptides, such as atrial natriuretic peptide (ANP) and brain natriuretic peptide (BNP), which are produced within the heart as a response to myocardial stretch as a consequence of volume or pressure overload [60,61]. HF guidelines currently recommends monitoring of BNP and its precursor, N-terminal-proBNP (NT-proBNP), for CHF progression evaluation. It must be acknowledged, however, that age, body mass, renal failure and pulmonary diseases influence its plasmatic concentrations [62]. Other molecules associated with myocyte necrosis or injury have been evaluated as HF biomarkers, such as cardiac troponins (cTn), which are regulatory proteins involved in contraction. The troponin complex is formed by cardiac troponin C (cTnC), I (cTnI) and T

(cTnT), which dissociates after $Ca^{2+}$ binds to cTnC. cTnI and cTnT are considered a reference marker of myocardial injury as its blood concentrations rise after myocyte damage [63,64].

### 3.2. Renal Alteration Associated to HF

As explained before, CRS-1 and CRS-2 are characterized by progressive kidney damage due to HF. Over 50% of HF patients have been reported to have renal insufficiency [19,65]. Indeed, even a modest reduction in renal function is associated with a higher mortality rate in cardiovascular disease patients [19,66]. The most currently used diagnostic measurements for renal damage are GFR, serum creatinine and urinary output.

The systolic blood pressure and effective arterial volume are reduced once HF develops, which translates into a decrease in renal blood flow as well as GFR [67]. In order to preserve adequate blood flow, the kidneys autoregulate through different mechanisms, including sympathetic nervous system (SNS) and RAAS activation, which would act as vasoconstrictors of the afferent and the efferent arteriole [13,68]. In the long term, this activation or the neurohormonal axis could result in podocyte injury [69,70], loss of mesangial integrity [71,72], tubular and glomerular damage [73–75] and kidney dysfunction [76], which are often associated with CKD and ESRD.

It is common to use the term kidney failure in a clinical setting to refer to a situation where there is a persistent decrease in eGFR in the short term [18]. Another important concept is worsening renal function, which is considered to appear in those patients in which the serum creatinine increases by 25% compared to the basal levels or the eGFR decreases by more than 20% in a period of around 25 weeks [77,78]. AKI is characterized by a rapid loss of kidney function that can happen in HF patients when diuresis decreases <0.5 mL/kg/h in 6–12 h or the basal serum creatinine levels increases $\geq$0.3 mg/dL in 48 h [77,78].

In addition to traditional markers of decreased glomerular filtration, such as creatinine and albuminuria [79,80], other markers, such as cystatin C [81,82] and blood urea nitrogen (BUN) [83,84], also have been proposed as possible biomarkers of tubular damage.

One of these is Neutrophil Gelatinase Associated Lipocalin (NGAL), a small glycoprotein expressed in renal and other cell types to which different functions have been attributed [85]. Its involvement in renal pathologies and its role as a biomarker comes from its rapid release in response to a tubular lesion and its presence in plasma, serum and urine, making it easy to quantify [85,86]. Another proposed molecule is kidney injury molecule-1 (KIM-1), a transmembrane glycoprotein expressed in low levels in healthy kidneys. Shortly after tubular damage, KIM-1 cleavage allows its secretion by the injured cells to the tubule lumen, resulting in detection in the urine, to where it is excreted [87]. Moreover, its role as a biomarker has proved to be associated with inflammation and fibrosis in the injured kidney, which would help monitor the degree of tubular damage [88–90]. Interleukin-18 (IL-18) is a proinflammatory cytokine that is expressed in activated macrophages, renal epithelial cells and others [91]. Urinary IL-18 is considered a marker of both short- and long-term injury in AKI, as it increases within 6 h of the insult or at least a day before serum creatinine increase [91,92].

### 3.3. Fibrosis

Another common structural alteration observed in both heart and kidney remodelling in CRS is fibrosis, which is also considered a key contributor to the progression of cardiac and renal failure [93–95]. Fibrosis is an important process that can be contemplated as aberrant wound healing as a consequence of the misbalance between extracellular matrix (ECM) production and degradation [96]. The fibrotic response to injury can be classified into reparative, when the scar is necessary to stabilize the tissue defect, or reactive, when the mechanical stress and the hormonal mediators facilitate the expansion of connective tissue in a remote non-injured zone, compromising the correct function of the organ [97]. The main fibrosis effectors are the fibroblasts and myofibroblasts, both of which are responsible for the synthesis and accumulation of interstitial ECM proteins. While fibroblasts are mesenchymal cells ubiquitous in tissues and organs, myofibroblasts are differentiated

cells that are rarely found in non-pathological environments [98–100]. The fibrotic scar composition is similar amongst different tissues, predominantly formed by collagens type I and III, fibronectin, proteoglycans and laminin [101–103].

As a response to the damaged heart in cardiac ischemia, myocardial remodelling occurs through the secretion of ECM components by the myofibroblasts. Histopathologically speaking, there are three types of cardiac fibrosis: replacement fibrosis, interstitial fibrosis and perivascular fibrosis. Replacement fibrosis provides structural support, as it consists of the removal of necrotic tissue and generation of a fibrotic scar within the infarcted zone that compensates cardiomyocyte loss [104,105]. On the other hand, the widespread deposition of ECM proteins in the endo and perimysium of remote areas of the infarct is what is known as interstitial fibrosis [106]. The term perivascular fibrosis is used to describe the increase in connective tissue around the cardiac microvasculature [107], both of which are types of fibrotic lesions that could not be a consequence of cardiomyocyte death.

The remodelling that follows after MI happens in different phases that partially overlap: First, there is cell death and an inflammatory response (inflammatory phase); secondly, the resolution of inflammation and fibroblast proliferation (proliferative or reparative phase); and lastly, the scar formation and maturation (maturation or remodelling phase) [108]. During the proliferative phase, which usually coexists with the inflammatory and reparative phases, there is an increase in the number of fibroblasts, which will adopt the proliferatory, secretory and migratory myofibroblast phenotype [109]. Following the proliferative phase of cardiac repair, when the scar has been synthesized, there begins a long process known as maturation, in which an organized fibrotic state is formed due to ECM crosslinking [110] and scar reinforcement by other components of the ECM, such as decorin [111,112] and perlecan [113,114]. In addition, during the maturation phase, the activated fibroblasts go through apoptosis and senescence [115]. The presence of a mature fibrotic scar ultimately leads to an increased ventricular stiffness that compromises cardiac output [116,117]. In addition to the impaired cardiac contractility, fibrosis also interferes with the normal electrical signals within the heart, which predisposes to arrhythmias and fibrillation [118,119]. Overall, fibrosis has thus been proposed as a risk factor in HF as it predisposes to ventricular systolic and diastolic dysfunction [120–122], cardiomyocyte hypertrophy [122–124] and sudden cardiac death [125,126], thereby increasing mortality [127,128].

At the renal level, CKD is characterized by functional loss and deposition of connective tissue that ends up creating a common fibrotic phenotype independently of the initial damage. This happens since tubulointerstitial diseases lead to glomerular injury, and glomerular lesions produce tubulointerstitial damage. Fibrosis is a common manifestation of functional alterations that spreads in response to sustained inflammation and epithelial damage [129–131]. Among the events that induce fibrosis, both diabetes and hypertension are considered to be the leading causes of CKD [132,133], as they elevate the glomerular pressure that gradually leads to glomerular damage, endothelial dysfunction [134,135] and other structural changes, such as alterations of the glomerular basement membrane [136–138], decrease in podocyte number and mesangial distension [136,139,140]. As a result of such damage, the renal tissue would start a response that resembles wound healing in other tissues. The scar created in the early stage is potentially reversible but with the progression of the damage, the cross-linking of the ECM proteins makes it stiff and resistant to proteolysis [141].

During chronic injury to the kidney in CKD, the excessive accumulation of connective tissue and expansion of interstitial fibroblasts during the reparative stage of the fibrotic scar can happen in all compartments of the kidney, including the glomeruli, usually termed glomerulosclerosis, and the tubules, which is referred to as tubulointerstitial fibrosis [142–144]. Such deposition of the fibrotic matrix alters organ structure and function, which could further damage kidney function, as it impairs blood flow in this region of the parenchyma [96,145]. The fibrotic wound is not the only structural change involved since it is usually associated with tubular atrophy, tubular dilation and inflammatory cell infiltration [146–148]. Indeed, as the loss of renal cells and its replacement by ECM are common sequelae of renal damage, expansion of cortical

fibrosis is considered one of the best histologic predictors of kidney dysfunction loss in CKD along with tubular atrophy (IFTA parameter) [148–150]. It is also one of the most common features assessed in biopsies in predicting a progression to ESRD [151,152].

Even though chronic damage to the kidney will naturally converge into histological and functional alterations that are common and lead to glomerulosclerosis and fibrosis, it is important to understand that the fibrotic progression is different depending on where it begins [153]. In glomerular damage, the progression starts with an injury within the Bowman's Capsule that initially leads to glomerular hyperfiltration for a long period of time until it progresses to decrease the total GFR [154,155]. This reduction in the blood flow results in tubular hypoxia and epithelial cell death normally referred to as tubule atrophy [156,157]. In these circumstances, the inflammation initiated by the damaged tubular cells propitiates the formation of a fibrotic scar to fill the void created by epithelial cell death [158,159]. To form that scar, resident fibroblasts differentiate into the myofibroblast phenotype, which can synthesize different extracellular matrix proteins. Among the ECM components produced by myofibroblasts in order to form the fibrotic scar, the main ones in the kidney are collagen type I, III and IV, as well as fibronectin [160–162]. During tubule atrophy, the tubular basement membrane remains, thereby separating the cell death from the interstitium but disappears after the cell-free tubule collapses, at which point we could talk of complete loss of the nephron [163–165].

Epithelial damage is heterogeneous in tubular injury, which can be caused by many factors, such as hemodynamic, inflammatory, toxin-related or metabolic alterations. Some cells will instantly go through necrosis or apoptosis, whereas others will survive with different levels of injury, these being the ones that could proliferate and replace the lost cells of the tubular epithelium [166–168]. In the cases in which the tubules do not recover, inflammation signalling activates and with it the fibroblasts differentiate into myofibroblasts that will lead to tubulointerstitial fibrosis and tubular atrophy [169–171]. Tubulointerstitial fibrosis is the deposition of ECM proteins in the space between the tubular basement membrane and the peritubular capillaries [160], which impairs blood flow and induces ischemic injury in the nephrons of the fibrotic wound [148,172,173].

Inflammation and oxidative stress serve as the initial response to injury although its long-term progression could damage organ structure and function [174,175]. Inflammation is a common process in fibroproliferative diseases that leads to the release of pro-inflammatory mediators that have an important role in tissue damage and could either stimulate or inhibit fibrosis [176,177]. An appropriate level of cytokines and growth factors that mediates the cellular responses is key in normal wound healing. Among the many growth factors involved, transforming growth factor ß (TGF-ß) is considered to be a prototypic profibrotic cytokine that has a central role in organ fibrosis as it binds to its receptors causing the phosphorylation of SMADs, which modulate the expression of the target genes [100,178]. TGF-ß can also activate SMAD-independent pathways in what is called non-canonical signalling [179]. Among the many TGF-ß-mediated responses are cell proliferation and differentiation, ECM production and immune modulation [180–182]. Another important mediator is the connective tissue growth factor (CTGF), a downstream factor of TGF ß that has been reported in fibrosis in different organs such as the heart and kidney [93,183,184]. CTGF promotes the TGF-ß-induced excessive ECM production and fibroblast proliferation [185,186], and its expression appears to correlate with the degree of fibrosis [187].

As previously said, a dynamic balance between production and breakdown of ECM regulates the degree of fibrosis. The degradation of the ECM components is performed by the matrix metalloproteinases (MMPs), whose activity is controlled by the tissue inhibitors of MMPs (TIMPs) in order to maintain the homeostasis. MMPs can be classified according to substrate specificity into collagenases, such as MMP-1, MMP-8 and MMP-13 [188,189]; gelatinases, such as MMP-2 and MMP-9 [190,191]; membrane MMPs, such as MMP-14 [192]; and stromelysins, such as MMP-3, MMP-10 and MMP-11 [193]. Interestingly, MMPs can have both inhibitory and stimulatory effects on fibrosis as some of them promote it [194].

For example, the most frequently studied MMPs in HF and kidney damage are MMP-2 and MMP-9, out of which MMP-9 is believed to have a profibrotic effect [195–197] whereas MMP-2 has antifibrotic effects [198,199].

In recent years, it has been proved that different metabolic alterations stimulate structural and/or functional alterations, such as fibrosis development. Changes in metabolic regulation, such as that occurring in a situation such as lipotoxicity, defined as the accumulation of lipids in non-adipose tissues, is known to promote the development of fibrosis. This fibrosis is due to an upregulation in ECM protein synthesis, promoted by fibroblasts [200,201]. In this sense, we have observed in a recent study that MI is associated with cardiac lipotoxicity in rats, independently of the presence of obesity. This lipotoxicity was accompanied by alterations in the mitochondrial lipid profile and associated with myocardial fibrosis, suggesting that MI promotes an increase in lipid accumulation in the heart through mechanisms that are currently unknown. Similarly, we observed at the renal level the direct profibrotic role of palmitic acid at renal fibroblasts, as it induced an increase in ECM synthesis mediated by activation of ER stress, suggesting its importance in lipotoxicity-induced fibrosis [202]. These observations are in agreement with another study in which the authors proved that accumulation of lipid droplets accelerates tubulointerstitial fibrosis development in an animal model of kidney disease [200].

## 4. Mechanisms Involved in Fibrosis Progression

As a wide variety of diseases converge in fibrosis understanding, the pathogenesis involved is important in order to determine potential therapeutic targets. Despite the efforts to acquire insight into the process, the mechanisms involved are not fully established, and the current therapies are either ineffective or only slightly successful [203,204]. The current clinical strategies for CRS are guided towards the treatment of the general processes, such as diuretics, to treat volume overload, or angiotensin converting enzyme (ACE) inhibitors, Angiotensin II receptor blockers, mineralocorticoid receptor antagonist or β-adrenergic blockers to inhibit RAAS activation [17,205]. Due to the complex pathophysiology of CRS, new therapeutic approaches centred in fibrosis have been proposed. For instance, in a recent study, it has been proved that cardiac shock wave therapy significantly reduces cardiac fibrosis in a rat model of MI through the activation of the PI3K/Akt signalling pathway [206]. Despite this, these new experimental approaches are still required in order to have a comprehensive understanding of the pathophysiological mechanisms underlying fibrosis.

### *4.1. Inflammation*

Inflammation can be defined as a defensive immune response that is triggered by damage to a tissue. The acute inflammatory response can be initiated as a consequence of an infection in which the pattern recognition receptors in the innate immune cells interact with the pathogen-associated molecular patterns (PAMPs), or due to the damage-associated molecular patterns (DAMPs) that are released during physical injury [207]. An acute inflammatory response is characterized by vasodilation, vascular leak and leukocyte emigration and, shortly after its induction, secretion of cytokines and chemokines will happen in order to recruit the immune cells to the damaged or infected region. Among the cells recruited, neutrophils are the first to migrate as a means to engulf the pathogens and secrete pro-inflammatory mediators and vasoactive substances [208,209].

In a normal inflammatory response, the activity is temporally restricted, as it resolves once the threat has been dealt with. However, the presence of a prolonged low-grade activity leads to chronic inflammation, which is characterized by the activation of different immune components that lead to major alterations in tissues, increasing the risk of diseases [210]. The clinical consequences of chronic inflammation include type 2 diabetes [211,212], hypertension [213], cardiovascular disease [214,215], chronic kidney disease [216]) and metabolic syndrome [217] among others.

Since both CHF and CKD are associated with a chronic inflammation response, characterized by an increase in the circulating inflammatory mediators, this process has become of interest in the understanding of CRS. A persistent inflammatory trigger is needed in order to activate the wound-healing process. However, if not eliminated quickly, the inflammatory cells could increase the response, leading to the abnormal wound healing and scarring characteristic of fibrosis. Within the wound-healing mechanism that is activated after injury, the first response is coagulation, in which activated platelets release platelet-derived growth factor (PDGF), acting as a chemoattractant for inflammatory cells, and transforming growth factor ß1 (TGF-ß1), which is one of the main drivers of fibrosis as it stimulates ECM synthesis by the fibroblasts of the tissue that was damaged [218–220].

Inflammation is known to have an important role in the development and progression of chronic diseases. For example, CKD progression into ESRD is characterized by chronic inflammation in the renal parenchyma, concluding in ECM deposition and loss of renal function [221–223]. Independent of the original cause, experimental models and human biopsies have shown that during renal inflammation, cells such as neutrophils and macrophages infiltrate both the glomeruli and tubulointerstitial space in order to remove the cell and matrix components that were damaged during the insult [223–225]. In general, M1 macrophages generate the initial response in the diseased organ by generation of pro-inflammatory cytokines, such as tumour necrosis factor α (TNFα) and interleukin-1 (IL-1), whereas M2 macrophages propitiate tissue repair by secretion of immunosuppressive cytokines during the repair phase [223,226]. It is that transition from the M1 to M2 phenotype that promotes fibrosis, as the production of cytokines, chemokines and growth factors alter the ECM balance between production and degradation [214,227,228].

Cytokines are cell-derived polypeptides that mediate the inflammatory response and can have positive or negative effects. It is well known that not all cytokines are involved at all stages of inflammation, but some of them do mediate both acute and chronic responses. This is the case of TNF-α, IL-1 (α and β) and IL-6 [229], which are some of the most studied ones and have been suggested to have an important role in inflammatory modulation during CRS due to its extremely potent proinflammatory effects [94,230–232].

It is well established that RAAS activation and the sympathetic nervous system (SNS) promotes the inflammatory response both in the heart and kidneys [233]. Angiotensin II (Ang II), one of the main effectors of RAAS activation, induces endothelial dysfunction, upregulation of adhesion molecules and fibrosis [234–236]. These Ang II effects are accompanied by recruitment of infiltrating cells and an increase in proinflammatory cytokines via the angiotensin type 1 (AT1) receptor in cardiorenal disease [230,237]. It has been proved that Ang II produces the accumulation of macrophage in the kidney [238,239], and it was shown in a murine unilateral ureteral obstruction (UUO) model that the macrophages' AT1 receptor activation impedes polarization towards the M1 phenotype and limits the damage and fibrosis [240]. This shows that an increase in M1 macrophage differentiation makes organs more susceptible to damage whereas the M2 phenotype decreases injury [223,241,242]. Nevertheless, neurohormonal activation is not the only proposed source of inflammation in CRS. Both animal and human studies have shown that congestion may lead to endothelial activation and peripheral release of proinflammatory mediators, as venous congestion itself causes an inflammatory response activation in cells [233,243,244].

Inflammation leads to functional and structural damage in the cardiorenal axis, as the different cytokines, especially TNF-α, which plays a central role in organ dysfunction, are involved in inflammation, cell proliferation [245] and apoptosis [246]. During inflammation, TNF-α has been described to be involved in vasodilation, inflammatory cell adhesion, coagulation and reactive oxygen species (ROS) production, among others [247].

Numerous cytokines have been studied due to their profibrotic or antifibrotic effects [248]. Th2-derived cytokines, such as IL-4, IL-5, IL-6, IL-13 and IL-21, are important in the regulation of organ fibrosis [249,250], out of which the most studied one is IL-13, an interleukin whose profibrotic effect can be enhanced by IL-5 and IL-21, and which can increase its production and its receptor expression [251–253]. IL-21 can also promote tissue

fibrosis through the induction of differentiation into Th17 cells [254,255], which produce a well-known profibrotic interleukin, IL-17, and which is involved in the development of fibrosis in various organs [256–258], although a recent study has suggested IL-17 plays an antifibrotic role in tubulointerstitial fibrosis [259]. On the other hand, Th1 cytokines, such as IL-7 [250,260], IL-10 [261,262], IL-12 [263,264] and IL-22 [265,266], along with IFN-γ [267,268], have been shown to have a suppressive effect on fibrosis. For instance, the inflammatory response in IL-10 KO mice resulted in scar formation rather than wound repair, suggesting IL-10 has an important antifibrotic role [269,270].

Chronic, unresolved inflammation damages renal structure and function, thereby leading to CKD, a state characterized by progressive renal fibrosis. In previous studies, it was reported that circulating levels of fibrinogen, TNF-α and a decrease in serum albumin were associated with loss of kidney function, linking the progression of CKD to the inflammatory response [221,271]. Systemic inflammation and function decline can alter the structure of the kidney, creating an environment in which epithelial damage increases and the factors released by infiltrating macrophages lead to fibrotic expansion [272,273]. Indeed, macrophage depletion has proved to reduce renal fibrosis in an animal model of myocardial infarction [274]. In renal fibrosis, the first process involved is the injury itself, followed by the unresolved inflammation. In the tubulointerstitium, pro-inflammatory cytokines, such as IL-6, TNF-α and IL-1β, promote further inflammatory cell infiltration, propitiating activation of profibrotic cells to differentiate into myofibroblasts and local secretion of fibrotic mediators [275–277]. This situation will lead to overproduction and deposition of ECM proteins, disruption of tissue integrity and progressive decline in function. Finally, glomerulosclerosis and tubular atrophy will happen in the latest stages [278,279].

In cardiac injury, as what happens in renal damage, the necrotic cell death within the heart activates tissue cells that will synthetize proinflammatory cytokines to recruit inflammatory cells. In the first phase, the macrophages and neutrophils act to remove the debris and release growth factors and cytokines that propitiate formation of connective tissue. Afterwards, fibroblast activation and cell proliferation will happen in the maturation phase to repair the myocardium by fibrotic wound formation [280,281]. After the phagocytic clearance of the apoptotic cells, macrophages will polarize towards the "reparative" M2 phenotype, releasing anti-inflammatory and profibrotic cytokines such as IL-10 and TGFβ, while proinflammatory cytokines, such as IL-1β or TNF-α, decrease in order to stimulate cardiac fibroblast activation to collagen-secreting myofibroblast [281–283]. Having said that, chronic inflammation entails a change in the inflammatory behaviour towards persistent and exacerbated fibrinogenesis, which is a structural feature in chronic injuries. It is due to that characteristic chronic inflammation for which TNF-α has been proposed as an independent predictor of cardiac and non-cardiac mortality in CHF patients [284]. Nonetheless, there is no consensus on the role of cytokines and chemokines, as some studies suggest its aggravating injury effects and others show that they endanger cardioprotective responses. For example, TNF-α ablation has proved to reduce the infarct size in mice with I/R injury [285], but in other studies TNF receptor deficiency increased the ischemic injury during I/R [286].

### 4.2. Oxidative Stress

Oxidative stress is a general concept that describes the imbalance between the production of ROS and the antioxidant defences. ROS includes both free radicals, which are species with an unpaired electron, such as superoxide anion ($O_2^{\bullet -}$) and hydroxyl radical (·OH), or non-free radical oxygenated molecules, such as hydrogen peroxide ($H_2O_2$) [287,288]. Other reactive species derived from nitrogen or sulphur do exist, but they are less abundant [289,290].

Even in basal conditions, aerobic metabolism involves ROS production, thus making $O_2^{\bullet -}$ and $H_2O_2$ physiological intracellular metabolites. In low quantities, ROS act as signalling molecules involved in different pathways, such as cell proliferation, apoptosis and gene expression [291,292]. However, the fact that an important increase in oxidants

could target almost all substrates implies the impairment and alteration of all biomolecules, resulting in cell damage and death [293,294]. ROS can damage proteins [295] and nucleic acids [296,297], but among all the molecules to undergo oxidation, polyunsaturated fatty acids are the most susceptible, leading to an increase in the markers of lipid peroxidation, such as malondialdehyde or 4-hydroxynonenal [298–300].

The endogenous sources of prooxidant species include organelles where there is high oxygen use, such as the mitochondria, peroxisomes, due to the fatty acid β-oxidation [301,302], and the endoplasmic reticulum (ER) [303], although the mitochondria seem to be the major source of ROS production, as around 95% of the breathed oxygen is reduced in the mitochondrial electron chain. Specifically, there are two major sites in the electron transport chain, the NADH dehydrogenase (complex I) and the ubiquinone cytochrome c reductase (complex III), which transfer electrons to coenzyme Q or ubiquinone, creating reduced forms that will ultimately transfer electrons to the molecular oxygen, generating superoxide radicals [304,305]. Through the action of mitochondrial superoxide dismutase (SOD), the superoxide anion is converted to hydrogen peroxide, which can be detoxified by the catalase and glutathione peroxidase [305,306].

In the outer mitochondrial membrane, the monoamine oxidases are another source of ROS that is not related to respiration [307,308]. In this case, the bivalent reduction of oxygen produces $H_2O_2$. In order to regulate the levels of ROS, the sources colocalize with the antioxidant response, among which there are enzymes, such as superoxide dismutases, catalase and glutathione peroxidase, as well as non-enzymatic antioxidants, such as vitamin A, bilirubin or reduced coenzyme Q [288,309,310].

Both inflammation and oxidative stress are related to chronic diseases, such as diabetes, hypertension, cardiovascular diseases or CKD [175,311–313]. It is known that under chronic damage the inflammatory and hypoxic environment propitiates fibrosis by fibroblast activation and proliferation into myofibroblasts. In this circumstance, ROS formation also occurs, and is considered to have an important role in both inflammation and organ fibrosis [314–316]. The bidirectional link between ROS and TGF-β1 is well established, as ROS production and enhanced ROS formation leads to higher activation and expression of TGF-β1 [317–319]. One of the possible explanations for this link resides in the action of an important ROS source, such as the different NADPH oxidases (NOX). In normal conditions, the NOX-derived ROS act as modulators of cell growth, proliferation, differentiation and apoptosis, but once it is uncontrolled, oxidative stress damages the DNA, proteins and lipids, inducing organ damage and fibrosis [320–322]. Multiple studies have shown the effectiveness of NOX-1 and NOX-4 inhibition in inflammation and fibrosis amelioration in liver and kidney injury [323–325], while different studies in the heart have shown that both NOX-2 and NOX-4 mediate the oxidative stress and cardiac injury following I/R [320,326,327]. Indeed, NOX-4 is considered a well-recognized mediator of the transition from fibroblast to myofibroblast, and its inhibition in in vitro studies with renal cells proved to prevent ROS production and myofibroblast differentiation, which would translate into a decrease in fibrosis during damage [328,329].

Multiple factors seem to participate in order to produce the characteristic multiorgan dysfunction of CRS, among which the increase in proinflammatory cytokines, the dysregulation of apoptosis and the increase in oxidative stress have been proposed as key elements of this complex pathophysiology [232,330,331]. Different animal models have shown that an increase in oxidative stress plays a pivotal role in cardiac and renal damage, independently of the CRS type depicted, through activation of the inflammatory response [15,331–333]. This can also be seen in patients with CRS, who presented an increase in ROS and RNS, which was accompanied by higher inflammatory cytokines, such as IL-6 [15].

### *4.3. Endoplasmic Reticulum Stress*

The ER is an essential organelle for calcium homeostasis, lipid biosynthesis and protein synthesis and post-translational modifications. To ensure correct protein folding, the ER

lumen balance between unfolded and misfolded proteins, and the capability to handle it, must be maintained. Such homeostasis could be altered by both physiological and pathological entities, such as inflammatory cytokines, protein demand or mutant protein expression, which translates into what is called ER stress [334,335].

In response to ER stress, the unfolded protein response (UPR) is initiated by at least one of three different pathways: the ER transmembrane proteins Activating Transcription Factor 6 (ATF6), Inositol-Requiring 1 (IRE1) or PKR-like ER kinase (PERK). In unstressed conditions, the chaperone Immunoglobin Binding Protein (BiP) binds to the luminal domain of ATF6, IRE1 and PERK, keeping them inactive [334,336]. In ER stress conditions, BiP dissociates from the three regulators, activating UPR [337]. Although initially UPR is considered a beneficial adaptive response, if it fails to restore homeostasis, then the UPR pathways guide the damaged cells to apoptosis and the consequent tissue injury [338,339].

Different pathologies, such as diabetes mellitus [340], obesity [341,342], cardiovascular disease [343,344] and CKD [345,346], have been associated with ER stress. In CRS, the activation of ER stress in the heart and kidney could be induced by different factors, such as hemodynamic changes, hormones from the RAAS, inflammation or oxidative stress [346–348]. These pathophysiological mediators could directly induce ER stress in the myocardium or renal parenchyma, resulting in apoptotic cell death due to prolonged UPR activation [349–351] and the consequent fibrotic wound formation, all of which would eventually lead to structural and functional changes [348,352–354]. Our group has recently evaluated the effect of myocardial infarction (MI) at renal level in rats. At 4 weeks post-MI, animals presented renal alterations characterized by tubulointerstitial fibrosis, oxidative stress and upregulation of inflammatory cytokines, such as IL-6 and TNF-α. All these alterations were accompanied by ER stress activation, which correlates with the renal fibrosis, suggesting ER stress relevance in the structural renal damage in CRS type 1 [202].

As ER stress inhibition has proved to ameliorate the fibrotic progression, it has been suggested that its blockade could be a new therapeutic approach for fibrosis [355–357]. One of the possible ways in which ER stress could lead to fibrosis is through fibroblast differentiation and collagen formation by TGF-β upregulation, as PERK and IRE1 activation have been seen to increase TGF-β expression [358–360]. ER stress activation of fibroblasts during injury at the wounded site triggers their differentiation into myoblasts, so as to restore the area by ECM protein synthesis and secretion [361,362]. Different in vitro studies have described ER-mediated differentiation into different cell types, such as renal tubular cells [363], cardiac cells [364], adipocytes [365,366], plasma cells [367,368] and others [369–371]. Additionally, our group's in vitro studies in kidney fibroblasts, stimulated with the well-known profibrotic factor Ang II in presence of the pharmacological inhibitor of ER stress, 4-phenylbutiric acid (4-PBA), proved to be effective in preventing the increase in collagen I, inflammatory markers and superoxide anion production. All of this suggests the important role of ER stress in fibrosis, inflammation and oxidative stress in renal damage [202].

The explained mechanisms involvement in CRS is depicted in Figure 2.

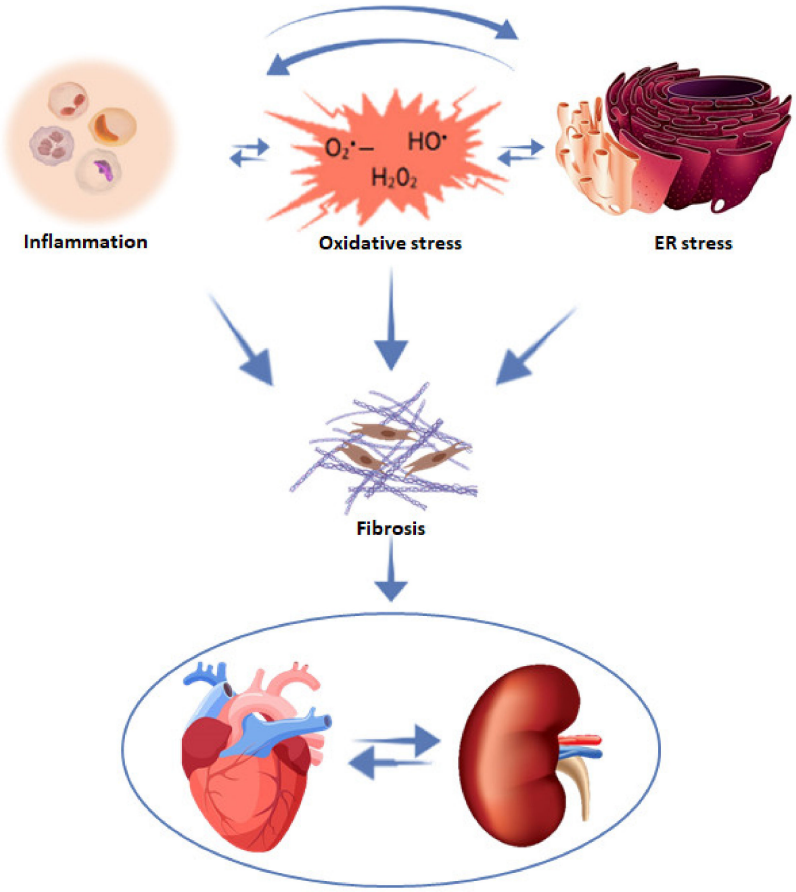


**Figure 2.** Mechanisms involved in the progression of cardiac and renal fibrosis in CRS.

## 5. Conclusions

Due to the pathogenesis of cardiorenal syndromes, numerous efforts have given insight into the different pathways and mediators involved. This review has summarized evidence that the development of a fibrotic wound has proved to play a central role in both cardiac and renal damage progression, in which inflammation, oxidative stress and ER stress could be relevant players. This makes it crucial to understand the pathogenic basis of fibrosis in order to determine therapeutic targets.

**Author Contributions:** Conceptualization: E.M.-M. and V.C.; investigation: B.D.-V., E.M.-M. and V.C.; orgibnal draft preparation: B.D.-V.; review and editing: B.D.-V., E.M.-M. and V.C.; funding acquisition: E.M.-M. and V.C. All authors have read and agreed to the published version of the manuscript.

**Funding:** This research was funded by Instituto de Salud Carlos III-Fondo Europeo de Desarrollo Regional (FEDER) [grant numbers PI18/00257; CIBERCV]. B.D.-V. was supported by a grant P-FIS (FI19/00277) and E.M-M was supported by a contract from CAM (Atracción de talento).

**Institutional Review Board Statement:** Not applicable.

**Informed Consent Statement:** Not applicable.

**Acknowledgments:** We thank Anthony DeMarco for his help in editing.

**Conflicts of Interest:** The authors declare no conflict of interest.

## References


1. Bright, R. Cases and Observations Illustrative of Renal Disease, Accompanied with the Secretion of Albuminous Urine. *Med. Chir. Rev.* **1836**, *25*, 23–35.
2. Zannad, F.; Rossignol, P. Cardiorenal Syndrome Revisited. *Circulation* **2018**, *138*, 929–944. [CrossRef]
3. Cabandugama, P.K.; Gardner, M.J.; Sowers, J.R. The Renin Angiotensin Aldosterone System in Obesity and Hypertension. *Med. Clin. North Am.* **2017**, *101*, 129–137. [CrossRef] [PubMed]
4. Banerjee, S.; Panas, R. Diabetes and Cardiorenal Syndrome: Understanding the "Triple Threat". *Hell. J. Cardiol.* **2017**, *58*, 342–347. [CrossRef] [PubMed]
5. McCullough, P.A.; Jurkovitz, C.T.; Pergola, P.E.; McGill, J.B.; Brown, W.W.; Collins, A.J.; Chen, S.-C.; Li, S.; Singh, A.; Norris, K.C.; et al. Independent Components of Chronic Kidney Disease as a Cardiovascular Risk State. *Arch. Intern. Med.* **2007**, *167*, 1122–1129. [CrossRef]
6. Raina, R.; Nair, N.; Chakraborty, R.; Nemer, L.; Dasgupta, R.; Varian, K. An Update on the Pathophysiology and Treatment of Cardiorenal Syndrome. *Cardiol. Res.* **2020**, *11*, 76–88. [CrossRef] [PubMed]
7. Ronco, C.; McCullough, P.; Anker, S.D.; Anand, I.; Aspromonte, N.; Bagshaw, S.M.; Bellomo, R.; Berl, T.; Bobek, I.; Cruz, D.N.; et al. Cardio-Renal Syndromes: Report from the Consensus Conference of the Acute Dialysis Quality Initiative. *Eur. Heart J.* **2009**, *31*, 703–711. [CrossRef] [PubMed]
8. Heywood, J.T.; Fonarow, G.; Costanzo, M.R.; Mathur, V.S.; Wigneswaran, J.R.; Wynne, J. High Prevalence of Renal Dysfunction and Its Impact on Outcome in 118,465 Patients Hospitalized with Acute Decompensated Heart Failure: A Report from the ADHERE Database. *J. Card. Fail.* **2007**, *13*, 422–430. [CrossRef] [PubMed]
9. Ronco, C.; Cicoira, M.; McCullough, P.A. Cardiorenal Syndrome Type 1. *J. Am. Coll. Cardiol.* **2012**, *60*, 1031–1042. [CrossRef] [PubMed]
10. Prins, K.W.; Thenappan, T.; Markowitz, J.S.; Pritzker, M.R. Cardiorenal Syndrome Type 1: Renal Dysfunction in Acute Decompensated Heart Failure. *J. Clin. Outcomes Manag.* **2015**, *22*, 443–454. [PubMed]
11. Ronco, C.; Bellasi, A.; Di Lullo, L. Cardiorenal Syndrome: An Overview. *Adv. Chronic Kidney Dis.* **2018**, *25*, 382–390. [CrossRef] [PubMed]
12. Mullens, W.; Abrahams, Z.; Francis, G.S.; Sokos, G.; Taylor, D.O.; Starling, R.C.; Young, J.B.; Tang, W.W. Importance of Venous Congestion for Worsening of Renal Function in Advanced Decompensated Heart Failure. *J. Am. Coll. Cardiol.* **2009**, *53*, 589–596. [CrossRef] [PubMed]
13. Ames, M.K.; Atkins, C.E.; Pitt, B. The renin-angiotensin-aldosterone System and Its Suppression. *J. Veter. Intern. Med.* **2019**, *33*, 363–382. [CrossRef] [PubMed]
14. Brewster, U.C.; Perazella, A.M. The Renin-Angiotensin-Aldosterone System and the Kidney: Effects on Kidney Disease. *Am. J. Med.* **2004**, *116*, 263–272. [CrossRef] [PubMed]
15. Virzì, G.M.; Clementi, A.; De Cal, M.; Brocca, A.; Day, S.; Pastori, S.; Bolin, C.; Vescovo, G.; Ronco, C. Oxidative Stress: Dual Pathway Induction in Cardiorenal Syndrome Type 1 Pathogenesis. *Oxidative Med. Cell. Longev.* **2015**, *2015*, 1–9. [CrossRef]
16. Harrison, J.C.; Smart, S.D.G.; Besley, E.M.H.; Kelly, J.R.; Read, M.I.; Yao, Y.; Sammut, I. A Clinically Relevant Functional Model of Type-2 Cardio-Renal Syndrome with Paraventricular Changes Consequent to Chronic Ischaemic Heart Failure. *Sci. Rep.* **2020**, *10*, 1–12. [CrossRef]
17. Rangaswami, J.; Bhalla, V.; Blair, J.E.; Chang, T.I.; Costa, S.; Lentine, K.L.; Lerma, E.; Mezue, K.; Molitch, M.; Mullens, W.; et al. Cardiorenal Syndrome: Classification, Pathophysiology, Diagnosis, and Treatment Strategies: A Scientific Statement from the American Heart Association. *Circulation* **2019**, *139*, e840–e878. [CrossRef]
18. Stevens, P.E.; Levin, A. Kidney Disease: Improving Global Outcomes Chronic Kidney Disease Guideline Development Work Group Members. Evaluation and Management of Chronic Kidney Disease: Synopsis of the Kidney Disease: Improving Global Outcomes 2012 Clinical Practice Guideline. *Ann. Intern. Med.* **2013**, *158*, 825–830. [CrossRef]
19. Damman, K.; Valente, M.A.; Voors, A.A.; O'Connor, C.M.; Van Veldhuisen, D.J.; Hillege, H.L. Renal impairment, worsening renal function, and outcome in patients with heart failure: An updated meta-analysis. *Eur. Heart J.* **2014**, *35*, 455–469. [CrossRef] [PubMed]
20. De Vecchis, R.; Baldi, C. Cardiorenal Syndrome Type 2: From Diagnosis to optimal Management. *Ther. Clin. Risk Manag.* **2014**, *10*, 949–961. [CrossRef]
21. Di Lullo, L.; Reeves, P.B.; Bellasi, A.; Ronco, C. Cardiorenal Syndrome in Acute Kidney Injury. *Semin. Nephrol.* **2019**, *39*, 31–40. [CrossRef] [PubMed]
22. Bagshaw, S.M.; Hoste, E.; Braam, B.; Briguori, C.; Kellum, J.A.; McCullough, P.A.; Ronco, C. Cardiorenal Syndrome Type 3: Pathophysiologic and Epidemiologic Considerations. *Contrib. Nephrol.* **2013**, *182*, 137–157. [CrossRef]
23. Kumar, U.; Wettersten, N.; Garimella, P.S. Cardiorenal Syndrome. *Cardiol. Clin.* **2019**, *37*, 251–265. [CrossRef] [PubMed]
24. Uduman, J. Epidemiology of Cardiorenal Syndrome. *Adv. Chronic Kidney Dis.* **2018**, *25*, 391–399. [CrossRef]
25. Mentzer, R.M.; Oz, M.C.; Sladen, R.N.; Graeve, A.H.; Hebeler, R.F.; Luber, J.M.; Smedira, N.G. Effects of Perioperative Nesiritide in Patients with Left Ventricular Dysfunction Undergoing Cardiac Surgery: The NAPA Trial. *J. Am. Coll. Cardiol.* **2007**, *49*, 716–726. [CrossRef]
26. Di Lullo, L.; Bellasi, A.; Barbera, V.; Russo, D.; Russo, L.; Di Iorio, B.; Cozzolino, M.; Ronco, C. Pathophysiology of the Cardio-Renal Syndromes Types 1–5: An Uptodate. *Indian Heart J.* **2017**, *69*, 255–265. [CrossRef]

27. Hillege, H.L.; Nitsch, D.; Pfeffer, M.A.; Swedberg, K.; McMurray, J.J.; Yusuf, S.; Granger, C.B.; Michelson, E.L.; Ostergren, J.; Cornel, J.; et al. Renal Function as a Predictor of Outcome in a Broad Spectrum of Patients with Heart Failure. *Circulation* **2006**, *113*, 671–678. [CrossRef]
28. Go, A.S.; Chertow, G.M.; Fan, D.; McCulloch, C.E.; Hsu, C.-Y. Chronic Kidney Disease and the Risks of Death, Cardiovascular Events, and Hospitalization. *N. Eng. J. Med.* **2004**, *351*, 1296–1305. [CrossRef]
29. Suresh, H.; Arun, B.S.; Moger, V.; Swamy, M. Cardiorenal Syndrome Type 4: A Study of Cardiovascular Diseases in Chronic Kidney Disease. *Indian Heart J.* **2017**, *69*, 11–16. [CrossRef]
30. Clementi, A.; Virzì, G.M.; Goh, C.Y.; Cruz, D.N.; Granata, A.; Vescovo, G.; Ronco, C. Cardiorenal Syndrome Type 4: A Review. *Cardiorenal Med.* **2013**, *3*, 63–70. [CrossRef] [PubMed]
31. Mehta, R.L.; Rabb, H.; Shaw, A.D.; Singbartl, K.; Ronco, C.; McCullough, P.A.; Kellum, J.A. Cardiorenal Syndrome Type 5: Clinical Presentation, Pathophysiology and Management Strategies from the Eleventh Consensus Conference of the Acute Dialysis Quality Initiative (ADQI). *Contrib. Nephrol.* **2013**, *182*, 174–194. [CrossRef]
32. Singer, M.; Deutschman, C.S.; Seymour, C.W.; Shankar-Hari, M.; Annane, D.; Bauer, M.; Bellomo, R.; Bernard, G.R.; Chiche, J.-D.; Coopersmith, C.M.; et al. The Third International Consensus Definitions for Sepsis and Septic Shock (Sepsis-3). *JAMA* **2016**, *315*, 801–810. [CrossRef] [PubMed]
33. Vincent, J.-L.; Rello, J.; Marshall, J.K.; Silva, E.; Anzueto, A.; Martin, C.D.; Moreno, R.; Lipman, J.; Gomersall, C.; Sakr, Y.; et al. International Study of the Prevalence and Outcomes of Infection in Intensive Care Units. *JAMA* **2009**, *302*, 2323–2329. [CrossRef] [PubMed]
34. Mehta, R.L.; Program to Improve Care in Acute Renal Disease (PICARD) Study Group; Bouchard, J.; Soroko, S.B.; Ikizler, T.; Paganini, E.P.; Chertow, G.M.; Himmelfarb, J. Sepsis as a Cause and Consequence of Acute Kidney Injury: Program to Improve Care in Acute Renal Disease. *Intensiv. Care Med.* **2010**, *37*, 241–248. [CrossRef] [PubMed]
35. Ronco, C.; McCullough, P.A.; Anker, S.D.; Anand, I.; Aspromonte, N.; Bagshaw, S.M.; Bellomo, R.; Berl, T.; Bobek, I.; Cruz, D.N.; et al. Cardiorenal Syndromes: An Executive Summary from the Consensus Conference of the Acute Dialysis Quality Initiative (ADQI). *Contrib. Nephrol.* **2010**, *165*, 54–67. [CrossRef] [PubMed]
36. Evans, M.; Grams, M.E.; Sang, Y.; Astor, B.C.; Blankestijn, P.J.; Brunskill, N.J.; Collins, J.F.; Kalra, P.A.; Kovesdy, C.P.; Levin, A.; et al. Risk Factors for Prognosis in Patients with Severely Decreased GFR. *Kidney Int. Rep.* **2018**, *3*, 625–637. [CrossRef] [PubMed]
37. Matsushita, K.; Van Der Velde, M.; Astor, B.C.; Woodward, M.; Levey, A.S.; De Jong, P.E.; Coresh, J.; Gansevoort, R.T. Association of Estimated Glomerular Filtration Rate and Albuminuria with All-Cause and Cardiovascular Mortality in General Population Cohorts: A Collaborative Meta-Analysis. *Lancet* **2010**, *375*, 2073–2081. [CrossRef]
38. Matsushita, K.; Coresh, J.; Sang, Y.; Chalmers, J.; Fox, C.; Guallar, E.; Jafar, T.; Jassal, S.K.; Landman, G.W.D.; Muntner, P.; et al. Estimated Glomerular Filtration Rate and Albuminuria for Prediction of Cardiovascular Outcomes: A Collaborative Meta-Analysis of Individual Participant Data. *Lancet Diabetes Endocrinol.* **2015**, *3*, 514–525. [CrossRef]
39. James, M.T.; Grams, M.E.; Woodward, M.; Elley, C.R.; Green, J.A.; Wheeler, D.C.; de Jong, P.; Gansevoort, R.T.; Levey, A.S.; Warnock, D.G.; et al. A Meta-Analysis of the Association of Estimated GFR, Albuminuria, Diabetes Mellitus, and Hypertension with Acute Kidney Injury. *Am. J. Kidney Dis.* **2015**, *66*, 602–612. [CrossRef]
40. Matsuo, H.; Dohi, K.; Machida, H.; Takeuchi, H.; Aoki, T.; Nishimura, H.; Yasutomi, M.; Senga, M.; Ichikawa, T.; Kakuta, K.; et al. Echocardiographic Assessment of Cardiac Structural and Functional Abnormalities in Patients with End-Stage Renal Disease Receiving Chronic Hemodialysis. *Circ. J.* **2018**, *82*, 586–595. [CrossRef]
41. Otsuka, T.; Suzuki, M.; Yoshikawa, H.; Sugi, K. Left Ventricular Diastolic Dysfunction in the Early Stage of Chronic Kidney Disease. *J. Cardiol.* **2009**, *54*, 199–204. [CrossRef] [PubMed]
42. Dobre, M.; Roy, J.; Tao, K.; Anderson, A.H.; Bansal, N.; Chen, J.; Deo, R.; Drawz, P.; Feldman, H.I.; Hamm, L.L.; et al. Serum Bicarbonate and Structural and Functional Cardiac Abnormalities in Chronic Kidney Disease - A Report from the Chronic Renal Insufficiency Cohort Study. *Am. J. Nephrol.* **2016**, *43*, 411–420. [CrossRef]
43. Shlipak, M.G.; Fried, L.F.; Cushman, M.; Manolio, T.A.; Peterson, D.; Stehman-Breen, C.; Bleyer, A.; Newman, A.B.; Siscovick, D.; Psaty, B. Cardiovascular Mortality Risk in Chronic Kidney Disease. *JAMA* **2005**, *293*, 1737–1745. [CrossRef] [PubMed]
44. Park, M.; Hsu, C.-Y.; Li, Y.; Mishra, R.K.; Keane, M.; Rosas, S.E.; Dries, D.; Xie, D.; Chen, J.; He, J.; et al. Associations Between Kidney Function and Subclinical Cardiac Abnormalities in CKD. *J. Am. Soc. Nephrol.* **2012**, *23*, 1725–1734. [CrossRef] [PubMed]
45. Taddei, S.; Nami, R.; Bruno, R.M.; Quatrini, I.; Nuti, R. Hypertension, Left Ventricular Hypertrophy and Chronic Kidney Disease. *Heart Fail. Rev.* **2010**, *16*, 615–620. [CrossRef]
46. Matsumoto, M.; Io, H.; Furukawa, M.; Okumura, K.; Masuda, A.; Seto, T.; Takagi, M.; Sato, M.; Nagahama, L.; Omote, K.; et al. Risk Factors Associated with Increased Left Ventricular Mass Index in Chronic Kidney Disease Patients Evaluated Using Echocardiography. *J. Nephrol.* **2012**, *25*, 794–801. [CrossRef] [PubMed]
47. Pluta, A.; Stróżecki, P.; Krintus, M.; Odrowaz-Sypniewska, G.; Manitius, J. Left Ventricular Remodeling and Arterial Remodeling in Patients with Chronic Kidney Disease Stage 1–3. *Ren. Fail.* **2015**, *37*, 1–6. [CrossRef]
48. Matsushita, K.; Ballew, S.; Coresh, J. Influence of Chronic Kidney Disease on Cardiac Structure and Function. *Curr. Hypertens. Rep.* **2015**, *17*, 1–9. [CrossRef]

49. Toida, T.; Toida, R.; Yamashita, R.; Komiya, N.; Uezono, S.; Komatsu, H.; Ishikawa, T.; Kitamura, K.; Sato, Y.; Fujimoto, S. Grading of Left Ventricular Diastolic Dysfunction with Preserved Systolic Function by the 2016 American Society of Echocardiography/European Association of Cardiovascular Imaging Recommendations Contributes to Predicting Cardiovascular Events in Hemodialysis Patients. *Cardiorenal Med.* **2019**, *9*, 190–200. [CrossRef]
50. Escoli, R.; Carvalho, M.J.; Cabrita, A.; Rodrigues, A. Diastolic Dysfunction, an Underestimated New Challenge in Dialysis. *Ther. Apher. Dial.* **2019**, *23*, 108–117. [CrossRef]
51. Cai, Q.-Z.; Lu, X.-Z.; Lu, Y.; Wang, A.Y.-M. Longitudinal Changes of Cardiac Structure and Function in CKD (CASCADE Study). *J. Am. Soc. Nephrol.* **2014**, *25*, 1599–1608. [CrossRef]
52. Franczyk, B.; Gluba, A.; Olszewski, R.; Banach, M.; Rysz, J. Heart Function Disturbances in Chronic Kidney Disease – Echocardiographic Indices. *Arch. Med Sci.* **2014**, *10*, 1109–1116. [CrossRef] [PubMed]
53. Vogel, M.W.; Slusser, J.P.; Hodge, D.O.; Chen, H.H. The Natural History of Preclinical Diastolic Dysfunction. *Circ. Heart Fail.* **2012**, *5*, 144–151. [CrossRef]
54. Shah, S.; Kitzman, D.W.; Borlaug, B.; Van Heerebeek, L.; Zile, M.; Kass, D.A.; Paulus, W.J. Phenotype-Specific Treatment of Heart Failure with Preserved Ejection Fraction. *Circulation* **2016**, *134*, 73–90. [CrossRef] [PubMed]
55. Dekkers, I.A.; De Mutsert, R.; Rabelink, T.J.; Jukema, J.W.; De Roos, A.; Rosendaal, F.R.; Lamb, H.J.; De Vries, A.P. Associations Between Normal Range Albuminuria, Renal Function and Cardiovascular Function in a Population-Based Imaging Study. *Atherosclerosis* **2018**, *272*, 94–100. [CrossRef] [PubMed]
56. Shah, A.M.; Lam, C.S.; Cheng, S.; Verma, A.; Desai, A.S.; Rocha, R.A.; Hilkert, R.; Izzo, J.; Oparil, S.; Pitt, B.; et al. The Relationship Between Renal Impairment and Left Ventricular Structure, Function, and ventricular–arterial Interaction in Hypertension. *J. Hypertens.* **2011**, *29*, 1829–1836. [CrossRef] [PubMed]
57. Matsushita, K.; Kwak, L.; Sang, Y.; Ballew, S.H.; Skali, H.; Shah, A.M.; Coresh, J.; Solomon, S. Kidney Disease Measures and Left Ventricular Structure and Function: The Atherosclerosis Risk in Communities Study. *J. Am. Heart Assoc.* **2017**, *6*, e006259. [CrossRef]
58. Zhou, J.; Cui, X.; Jin, X.; Zhou, J.; Zhang, H.; Tang, B.; Fu, M.; Herlitz, H.; Cui, J.; Zhu, H.; et al. Association of Renal Biochemical Parameters with Left Ventricular Diastolic Dysfunction in a Community-Based Elderly Population in China: A Cross-Sectional Study. *PLoS ONE* **2014**, *9*, e88638. [CrossRef]
59. Kang, E.; Ryu, H.; Kim, J.; Lee, J.; Lee, K.; Chae, D.; Sung, S.A.; Kim, S.W.; Ahn, C.; Oh, K. Association Between High-Sensitivity Cardiac Troponin T and Echocardiographic Parameters in Chronic Kidney Disease: Results from the KNOW-CKD Cohort Study. *J. Am. Heart Assoc.* **2019**, *8*, e013357. [CrossRef]
60. McCullough, P.A.; Jefferies, J.L. Novel Markers and Therapies for Patients with Acute Heart Failure and Renal Dysfunction. *Am. J. Med.* **2015**, *128*, 312-e1–312.e22. [CrossRef]
61. Savic-Radojevic, A.; Pljesa-Ercegovac, M.; Matic, M.; Simic, D.; Radovanovic, S.; Simic, T. Novel Biomarkers of Heart Failure. *Adv. Clin. Chem.* **2017**, *79*, 93–152. [CrossRef] [PubMed]
62. Ponikowski, P.; Voors, A.A.; Anker, S.D.; Bueno, H.; Cleland, J.G.F.; Coats, A.J.S.; Falk, V.; González-Juanatey, J.R.; Harjola, V.-P.; Jankowska, E.A.; et al. 2016 ESC Guidelines for the diagnosis and treatment of acute and chronic heart failure: The Task Force for the diagnosis and treatment of acute and chronic heart failure of the European Society of Cardiology (ESC). Developed with the special contribution of the Heart Failure Association (HFA) of the ESC. *Eur. J. Heart Fail.* **2016**, *18*, 891–975. [CrossRef] [PubMed]
63. Arslan, M.; Dedic, A.; Boersma, E.; A Dubois, E. Serial High-Sensitivity Cardiac Troponin T Measurements to Rule Out Acute Myocardial Infarction and a Single High Baseline Measurement for Swift Rule-In: A Systematic Review and Meta-Analysis. *Eur. Heart J. Acute Cardiovasc. Care* **2020**, *9*, 14–22. [CrossRef]
64. Westermann, D.; Neumann, J.T.; Sörensen, N.A.; Blankenberg, D.W.J.T.N.N.A.S.S. High-Sensitivity Assays for Troponin in Patients with Cardiac Disease. *Nat. Rev. Cardiol.* **2017**, *14*, 472–483. [CrossRef] [PubMed]
65. Hill, N.R.; Fatoba, S.T.; Oke, J.L.; Hirst, J.; O'Callaghan, C.A.; Lasserson, D.; Hobbs, R. Global Prevalence of Chronic Kidney Disease—A Systematic Review and Meta-Analysis. *PLoS ONE* **2016**, *11*, e0158765. [CrossRef] [PubMed]
66. Vogt, L.; Bangalore, S.; Fayyad, R.; Melamed, S.; Hovingh, G.K.; DeMicco, D.A.; Waters, D.D. Atorvastatin Has a Dose-Dependent Beneficial Effect on Kidney Function and Associated Cardiovascular Outcomes: Post Hoc Analysis of 6 Double-Blind Randomized Controlled Trials. *J. Am. Heart Assoc.* **2019**, *8*, e010827. [CrossRef]
67. Dalal, R.; Bruss, Z.S.; Sehdev, J.S. *Physiology, Renal Blood Flow and Filtration*; StatPearls: Treasure Island, FL, USA, 2021.
68. Borovac, J.A.; D'Amario, D.; Bozic, J.; Glavas, D. Sympathetic Nervous System Activation and Heart Failure: Current State of Evidence and the Pathophysiology in the Light of Novel Biomarkers. *World J. Cardiol.* **2020**, *12*, 373–408. [CrossRef]
69. Dlugos, C.P.; Picciotto, C.; Lepa, C.; Krakow, M.; Stöber, A.; Eddy, M.-L.; Weide, T.; Jeibmann, A.; Krahn, M.; Van Marck, V.; et al. Nephrin Signaling Results in Integrin β1 Activation. *J. Am. Soc. Nephrol.* **2019**, *30*, 1006–1019. [CrossRef]
70. Lichtnekert, J.; Kaverina, N.V.; Eng, D.G.; Gross, K.W.; Kutz, J.N.; Pippin, J.W.; Shankland, S.J. Renin-Angiotensin-Aldosterone System Inhibition Increases Podocyte Derivation from Cells of Renin Lineage. *J. Am. Soc. Nephrol.* **2016**, *27*, 3611–3627. [CrossRef]
71. Stoll, D.; Yokota, R.; Aragão, D.S.; Casarini, D.E. Both Aldosterone and Spironolactone Can Modulate the Intracellular ACE/ANG II/AT1 and ACE2/ANG (1-7)/MAS Receptor Axes in Human Mesangial Cells. *Physiol. Rep.* **2019**, *7*, e14105. [CrossRef]
72. Gómez, G.I.; Fernández, P.; Velarde, V.; Sáez, J.C. Angiotensin II-Induced Mesangial Cell Damage Is Preceded by Cell Membrane Permeabilization Due to Upregulation of Non-Selective Channels. *Int. J. Mol. Sci.* **2018**, *19*, 957. [CrossRef]

73. Xu, Z.; Li, W.; Han, J.; Zou, C.; Huang, W.; Yu, W.; Shan, X.; Lum, H.; Li, X.; Liang, G. Angiotensin II Induces Kidney Inflammatory Injury and Fibrosis through Binding to Myeloid Differentiation Protein-2 (MD2). *Sci. Rep.* **2017**, *7*, srep44911. [CrossRef] [PubMed]
74. Brankovic, M.; Akkerhuis, K.M.; Van Boven, N.; Manintveld, O.; Germans, T.; Brugts, J.; Caliskan, K.; Umans, V.; Constantinescu, A.; Kardys, I. Real-Life Use of Neurohormonal Antagonists and Loop Diuretics in Chronic Heart Failure: Analysis of Serial Biomarker Measurements and Clinical Outcome. *Clin. Pharmacol. Ther.* **2017**, *104*, 346–355. [CrossRef] [PubMed]
75. Aggarwal, D.; Singh, G. Effects of Single and Dual RAAS Blockade Therapy on Progressive Kidney Disease Transition to CKD in Rats. *Naunyn-Schmiedeberg's Arch. Pharmacol.* **2019**, *393*, 615–627. [CrossRef]
76. Dörr, O.; Liebetrau, C.; Möllmann, H.; Gaede, L.; Troidl, C.; Wiebe, J.; Renker, M.; Bauer, T.; Hamm, C.; Nef, H. Long-Term Verification of Functional and Structural Renal Damage After Renal Sympathetic Denervation. *Catheter. Cardiovasc. Interv.* **2016**, *87*, 1298–1303. [CrossRef] [PubMed]
77. Damman, K.; Tang, W.W.; Testani, J.M.; McMurray, J.J. Terminology and Definition of Changes Renal Function in Heart Failure. *Eur. Heart J.* **2014**, *35*, 3413–3416. [CrossRef] [PubMed]
78. Damman, K.; Testani, J.M. The Kidney in Heart Failure: An Update. *Eur. Heart J.* **2015**, *36*, 1437–1444. [CrossRef]
79. Norris, K.C.; Smoyer, K.E.; Rolland, C.; Van Der Vaart, J.; Grubb, E.B. Albuminuria, Serum Creatinine, and Estimated Glomerular Filtration Rate as Predictors of Cardio-Renal Outcomes in Patients with Type 2 Diabetes Mellitus and Kidney Disease: A Systematic Literature Review. *BMC Nephrol.* **2018**, *19*, 1–13. [CrossRef] [PubMed]
80. Jackson, C.E.; Solomon, S.D.; Gerstein, H.; Zetterstrand, S.; Olofsson, B.; Michelson, E.L.; Granger, C.B.; Swedberg, K.; A Pfeffer, M.; Yusuf, S.; et al. Albuminuria in Chronic Heart Failure: Prevalence and Prognostic Importance. *Lancet* **2009**, *374*, 543–550. [CrossRef]
81. Yang, Y.; Kim, K.; Hwang, I.; Yim, T.; Do, W.; Kim, M.; Lee, S.; Jung, H.-Y.; Choi, J.-Y.; Park, S.-H.; et al. Cystatin C–Based Equation for Predicting the Glomerular Filtration Rate in Kidney Transplant Recipients. *Transplant. Proc.* **2017**, *49*, 1018–1022. [CrossRef]
82. Wang, D.; Feng, J.-F.; Wang, A.-Q.; Yang, Y.-W.; Liu, Y.-S. Role of Cystatin C and Glomerular Filtration Rate in Diagnosis of Kidney Impairment in Hepatic Cirrhosis Patients. *Medicine* **2017**, *96*, e6949. [CrossRef] [PubMed]
83. Richter, B.; Sulzgruber, P.; Koller, L.; Steininger, M.; El-Hamid, F.; Rothgerber, D.J.; Forster, S.; Goliasch, G.; Silbert, B.I.; Meyer, E.L.; et al. Blood Urea Nitrogen Has Additive Value Beyond Estimated Glomerular Filtration Rate for Prediction of Long-Term Mortality in Patients with Acute Myocardial Infarction. *Eur. J. Intern. Med.* **2019**, *59*, 84–90. [CrossRef] [PubMed]
84. Seki, M.; Nakayama, M.; Sakoh, T.; Yoshitomi, R.; Fukui, A.; Katafuchi, E.; Tsuda, S.; Nakano, T.; Tsuruya, K.; Kitazono, T. Blood Urea Nitrogen Is Independently Associated with Renal Outcomes in Japanese Patients with Stage 3–5 Chronic Kidney Disease: A Prospective Observational Study. *BMC Nephrol.* **2019**, *20*, 115. [CrossRef] [PubMed]
85. Buonafine, M.; Martinez-Martinez, E.; Jaisser, F. More Than a Simple Biomarker: The Role of NGAL in Cardiovascular and Renal Diseases. *Clin. Sci.* **2018**, *132*, 909–923. [CrossRef] [PubMed]
86. Merdler, I.; Rozenfeld, K.-L.; Zahler, D.; Shtark, M.; Goldiner, I.; Loewenstein, I.S.; Fortis, L.; Hochstadt, A.; Keren, G.; Banai, S.; et al. Neutrophil Gelatinase-Associated Lipocalin for the Early Prediction of Acute Kidney Injury in ST-Segment Elevation Myocardial Infarction Patients Treated with Primary Percutaneous Coronary Intervention. *Cardiorenal Med.* **2020**, *10*, 154–161. [CrossRef]
87. Moresco, R.N.; Bochi, G.V.; Stein, C.S.; de Carvalho, J.A.M.; Cembranel, B.M.; Bollick, Y.S. Urinary Kidney Injury Molecule-1 in Renal Disease. *Clin. Chim. Acta* **2018**, *487*, 15–21. [CrossRef] [PubMed]
88. Maydan, O.; McDade, P.G.; Liu, Y.; Wu, X.-R.; Matsell, D.; Eddy, A.A. Uromodulin Deficiency Alters Tubular Injury and Interstitial Inflammation But Not Fibrosis in Experimental Obstructive Nephropathy. *Physiol. Rep.* **2018**, *6*, e13654. [CrossRef]
89. Nogare, A.L.; Veronese, F.V.; Carpio, V.N.; Montenegro, R.M.; Pedroso, J.A.; Pegas, K.L.; Gonçalves, L.F.; Manfro, R.C. Kidney Injury Molecule-1 Expression in Human Kidney Transplants with Interstitial Fibrosis and Tubular Atrophy. *BMC Nephrol.* **2015**, *16*, 19. [CrossRef]
90. Humphreys, B.D.; Xu, F.; Sabbisetti, V.; Grgic, I.; Naini, S.M.; Wang, N.; Chen, D.; Xiao, S.; Patel, D.; Henderson, J.M.; et al. Chronic Epithelial Kidney Injury Molecule-1 Expression Causes Murine Kidney Fibrosis. *J. Clin. Investig.* **2013**, *123*, 4023–4035. [CrossRef]
91. Edelstein, C.L. Biomarkers of Acute Kidney Injury. *Adv. Chronic Kidney Dis.* **2008**, *15*, 222–234. [CrossRef]
92. Parikh, C.R.; Abraham, E.; Ancukiewicz, M.; Edelstein, C.L. Urine IL-18 Is an Early Diagnostic Marker for Acute Kidney Injury and Predicts Mortality in the Intensive Care Unit. *J. Am. Soc. Nephrol.* **2005**, *16*, 3046–3052. [CrossRef]
93. Szabó, Z.; Magga, J.; Alakoski, T.; Ulvila, J.; Piuhola, J.; Vainio, L.; Kivirikko, K.I.; Vuolteenaho, O.; Ruskoaho, H.; Lipson, K.; et al. Connective Tissue Growth Factor Inhibition Attenuates Left Ventricular Remodeling and Dysfunction in Pressure Overload–Induced Heart Failure. *Hypertension* **2014**, *63*, 1235–1240. [CrossRef]
94. Zhao, Y.; Wang, C.; Hong, X.; Miao, J.; Liao, Y.; Hou, F.F.; Zhou, L.; Liu, Y. Wnt/β-Catenin Signaling Mediates Both Heart and Kidney Injury in Type 2 Cardiorenal Syndrome. *Kidney Int.* **2019**, *95*, 815–829. [CrossRef]
95. Lekawanvijit, S.; Kompa, A.R.; Zhang, Y.; Wang, B.H.; Kelly, D.J.; Krum, H. Myocardial Infarction Impairs Renal Function, Induces Renal Interstitial Fibrosis, and Increases Renal KIM-1 Expression: Implications for Cardiorenal Syndrome. *Am. J. Physiol. Circ. Physiol.* **2012**, *302*, H1884–H1893. [CrossRef]
96. Rockey, D.C.; Bell, P.D.; Hill, J.A. Fibrosis—A Common Pathway to Organ Injury and Failure. *N. Engl. J. Med.* **2015**, *372*, 1138–1149. [CrossRef] [PubMed]

97. Weber, K.T.; Brilla, C.G. Factors Associated with Reactive and Reparative Fibrosis of the Myocardium. *Cell. Mol. Alter. Fail. Human Heart* **1992**, *87* (Suppl. S1), 291–301. [CrossRef]
98. Baum, J.; Duffy, H.S. Fibroblasts and Myofibroblasts: What Are We Talking About? *J. Cardiovasc. Pharmacol.* **2011**, *57*, 376–379. [CrossRef] [PubMed]
99. Mack, M.; Yanagita, M. Origin of Myofibroblasts and Cellular Events Triggering Fibrosis. *Kidney Int.* **2015**, *87*, 297–307. [CrossRef]
100. Györfi, A.-H.; Matei, A.-E.; Distler, J.H. Targeting TGF-β Signaling for the Treatment of Fibrosis. *Matrix Biol.* **2018**, *68–69*, 8–27. [CrossRef] [PubMed]
101. Valiente-Alandi, I.; Potter, S.J.; Salvador, A.M.; Schafer, A.E.; Schips, T.; Carrillo-Salinas, F.J.; Gibson, A.M.; Nieman, M.L.; Perkins, C.; Sargent, M.A.; et al. Inhibiting Fibronectin Attenuates Fibrosis and Improves Cardiac Function in a Model of Heart Failure. *Circulation* **2018**, *138*, 1236–1252. [CrossRef] [PubMed]
102. Zheng, Z.; Ma, T.; Lian, X.; Gao, J.; Wang, W.; Weng, W.; Lu, X.; Sun, W.; Cheng, Y.; Fu, Y.; et al. Clopidogrel Reduces Fibronectin Accumulation and Improves Diabetes-Induced Renal Fibrosis. *Int. J. Biol. Sci.* **2019**, *15*, 239–252. [CrossRef]
103. Karsdal, M.A.; Nielsen, S.H.; Leeming, D.J.; Langholm, L.L.; Nielsen, M.J.; Manon-Jensen, T.; Siebuhr, A.; Gudmann, N.S.; Ronnow, S.; Sand, J.M.; et al. The good and the bad collagens of fibrosis—Their role in signaling and organ function. *Adv. Drug Deliv. Rev.* **2017**, *121*, 43–56. [CrossRef] [PubMed]
104. Frangogiannis, N.G. Pathophysiology of Myocardial Infarction. *Compr. Physiol.* **2015**, *5*, 1841–1875. [CrossRef] [PubMed]
105. Frangogiannis, N.G. Cardiac Fibrosis: Cell Biological Mechanisms, Molecular Pathways and Therapeutic Opportunities. *Mol. Asp. Med.* **2019**, *65*, 70–99. [CrossRef]
106. Frangogiannis, N.G. The Extracellular Matrix in Ischemic and Nonischemic Heart Failure. *Circ. Res.* **2019**, *125*, 117–146. [CrossRef]
107. Ytrehus, K.; Hulot, J.-S.; Perrino, C.; Schiattarella, G.; Madonna, R. Perivascular Fibrosis and the Microvasculature of the Heart. Still Hidden Secrets of Pathophysiology? *Vasc. Pharmacol.* **2018**, *107*, 78–83. [CrossRef] [PubMed]
108. Talman, V.; Ruskoaho, H. Cardiac fibrosis in myocardial infarction—from repair and remodeling to regeneration. *Cell Tissue Res.* **2016**, *365*, 563–581. [CrossRef]
109. Shinde, A.V.; Frangogiannis, N.G. Fibroblasts in Myocardial Infarction: A Role in Inflammation and Repair. *J. Mol. Cell. Cardiol.* **2014**, *70*, 74–82. [CrossRef] [PubMed]
110. Schilter, H.; Findlay, A.D.; Perryman, L.; Yow, T.T.; Moses, J.; Zahoor, A.; Turner, C.I.; Deodhar, M.; Foot, J.S.; Zhou, W.; et al. The Lysyl Oxidase Like 2/3 Enzymatic Inhibitor, PXS-5153A, Reduces Crosslinks and Ameliorates Fibrosis. *J. Cell. Mol. Med.* **2018**, *23*, 1759–1770. [CrossRef]
111. Doi, M.; Kusachi, S.; Murakami, T.; Ninomiya, Y.; Murakami, M.; Nakahama, M.; Takeda, K.; Komatsubara, I.; Naito, I.; Tsuji, T. Time-Dependent Changes of Decorin in the Infarct Zone After Experimentally Induced Myocardial Infarction in Rats: Comparison with Biglycan. *Pathol. Res. Pract.* **2000**, *196*, 23–33. [CrossRef]
112. Li, L.; Okada, H.; Takemura, G.; Kosai, K.-I.; Kanamori, H.; Esaki, M.; Takahashi, T.; Goto, K.; Tsujimoto, A.; Maruyama, R.; et al. Postinfarction Gene Therapy with Adenoviral Vector Expressing Decorin Mitigates Cardiac Remodeling and Dysfunction. *Am. J. Physiol. Circ. Physiol.* **2009**, *297*, H1504–H1513. [CrossRef]
113. Nakahama, M.; Murakami, T.; Kusachi, S.; Naito, I.; Takeda, K.; Ohnishi, H.; Komatsubara, I.; Oka, T.; Ninomiya, Y.; Tsuji, T. Expression of Perlecan Proteoglycan in the Infarct Zone of Mouse Myocardial Infarction. *J. Mol. Cell. Cardiol.* **2000**, *32*, 1087–1100. [CrossRef] [PubMed]
114. Sasse, P.; Malan, D.; Fleischmann, M.; Roell, W.; Gustafsson, E.; Bostani, T.; Fan, Y.; Kolbe, T.; Breitbach, M.; Addicks, K.; et al. Perlecan Is Critical for Heart Stability. *Cardiovasc. Res.* **2008**, *80*, 435–444. [CrossRef]
115. Fu, X.; Khalil, H.; Kanisicak, O.; Boyer, J.G.; Vagnozzi, R.J.; Maliken, B.D.; Sargent, M.A.; Prasad, V.; Valiente-Alandi, I.; Blaxall, B.C.; et al. Specialized Fibroblast Differentiated States Underlie Scar Formation in the Infarcted Mouse Heart. *J. Clin. Investig.* **2018**, *128*, 2127–2143. [CrossRef]
116. Woodiwiss, A.J.; Tsotetsi, O.J.; Sprott, S.; Lancaster, E.J.; Mela, T.; Chung, E.S.; Meyer, T.E.; Norton, G. Reduction in Myocardial Collagen Cross-Linking Parallels Left Ventricular Dilatation in Rat Models of Systolic Chamber Dysfunction. *Circulation* **2001**, *103*, 155–160. [CrossRef]
117. Santamaria, J.G.; Villalba, M.; Busnadiego, O.; López-Olañeta, M.M.; Sandoval, P.; Snabel, J.; López-Cabrera, M.; Erler, J.; Hanemaaijer, R.; Lara-Pezzi, E.; et al. Matrix Cross-Linking Lysyl Oxidases Are Induced in Response to Myocardial Infarction and Promote Cardiac Dysfunction. *Cardiovasc. Res.* **2015**, *109*, 67–78. [CrossRef]
118. Siebermair, J.; Suksaranjit, P.; McGann, C.J.; Peterson, K.A.; Kheirkhahan, M.; Baher, A.A.; Damal, K.; Wakili, R.; Marrouche, N.F.; Wilson, B.D. Atrial Fibrosis in non–atrial Fibrillation Individuals and Prediction of Atrial Fibrillation by Use of Late Gadolinium Enhancement Magnetic Resonance Imaging. *J. Cardiovasc. Electrophysiol.* **2019**, *30*, 550–556. [CrossRef] [PubMed]
119. Tan, T.C.; Koutsogeorgis, I.D.; Grapsa, J.; Papadopoulos, C.; Katsivas, A.; Nihoyannopoulos, P. Left Atrium and the Imaging of Atrial Fibrosis: Catch It If You Can! *Eur. J. Clin. Investig.* **2014**, *44*, 872–881. [CrossRef]
120. Yang, J.; Savvatis, K.; Kang, J.S.; Fan, P.; Zhong, H.; Schwartz, K.; Barry, V.; Mikels-Vigdal, A.; Karpinski, S.; Kornyeyev, D.; et al. Targeting LOXL2 for Cardiac Interstitial Fibrosis and Heart Failure Treatment. *Nat. Commun.* **2016**, *7*, 13710. [CrossRef] [PubMed]
121. De Gaspari, M.; Toscano, G.; Bagozzi, L.; Metra, M.; Lombardi, C.; Rizzo, S.; Angelini, A.; Marra, M.P.; Gerosa, G.; Basso, C. Endomyocardial Fibrosis and Myocardial Infarction Leading to Diastolic and Systolic Dysfunction Requiring Transplantation. *Cardiovasc. Pathol. Off. J. Soc. Cardiovasc. Pathol.* **2019**, *38*, 21–24. [CrossRef] [PubMed]

122. Nucifora, G.; Muser, D.; Gianfagna, P.; Morocutti, G.; Proclemer, A. Systolic and Diastolic Myocardial Mechanics in Hypertrophic Cardiomyopathy and Their Link to the Extent of Hypertrophy, Replacement Fibrosis and Interstitial Fibrosis. *Int. J. Cardiovasc. Imaging* **2015**, *31*, 1603–1610. [CrossRef] [PubMed]
123. Shinde, A.V.; Su, Y.; Palanski, B.A.; Fujikura, K.; Garcia, M.J.; Frangogiannis, N.G. Pharmacologic Inhibition of the Enzymatic Effects of Tissue Transglutaminase Reduces Cardiac Fibrosis and Attenuates Cardiomyocyte Hypertrophy Following Pressure Overload. *J. Mol. Cell. Cardiol.* **2018**, *117*, 36–48. [CrossRef] [PubMed]
124. A Beltrami, C.; Finato, N.; Rocco, M.; A Feruglio, G.; Puricelli, C.; Cigola, E.; Quaini, F.; Sonnenblick, E.H.; Olivetti, G.; Anversa, P. Structural Basis of End-Stage Failure in Ischemic Cardiomyopathy in Humans. *Circulation* **1994**, *89*, 151–163. [CrossRef] [PubMed]
125. Shah, N.N.; Ayyadurai, P.; Saad, M.; E Kosmas, C.; Dogar, M.U.; Patel, U.; Vittorio, T.J. Galectin-3 and Soluble ST2 As Complementary Tools to Cardiac MRI for Sudden Cardiac Death Risk Stratification in Heart Failure: A Review. *JRSM Cardiovasc. Dis.* **2020**, *9*. [CrossRef]
126. Kim, E.K.; Chattranukulchai, P.; Klem, I. Cardiac Magnetic Resonance Scar Imaging for Sudden Cardiac Death Risk Stratification in Patients with Non-Ischemic Cardiomyopathy. *Korean J. Radiol.* **2015**, *16*, 683–695. [CrossRef]
127. Kato, S.; Saito, N.; Kirigaya, H.; Gyotoku, D.; Iinuma, N.; Kusakawa, Y.; Iguchi, K.; Nakachi, T.; Fukui, K.; Futaki, M.; et al. Prognostic Significance of Quantitative Assessment of Focal Myocardial Fibrosis in Patients with Heart Failure with Preserved Ejection Fraction. *Int. J. Cardiol.* **2015**, *191*, 314–319. [CrossRef]
128. King, J.B.; Azadani, P.N.; Suksaranjit, P.; Bress, A.P.; Witt, D.M.; Han, F.T.; Chelu, M.; Silver, M.A.; Biskupiak, J.; Wilson, B.D.; et al. Left Atrial Fibrosis and Risk of Cerebrovascular and Cardiovascular Events in Patients with Atrial Fibrillation. *J. Am. Coll. Cardiol.* **2017**, *70*, 1311–1321. [CrossRef] [PubMed]
129. Peddakkulappagari, C.S.; Saifi, M.A.; Khurana, A.; Anchi, P.; Singh, M.; Godugu, C. Withaferin A Ameliorates Renal Injury Due to Its Potent Effect on Inflammatory Signaling. *BioFactors* **2019**, *45*, 750–762. [CrossRef]
130. Tammaro, A.; Florquin, S.; Brok, M.; Claessen, N.; Butter, L.M.; Teske, G.J.D.; de Boer, O.; Vogl, T.; Leemans, J.C.; Dessing, M.C. S100A8/A9 Promotes Parenchymal Damage and Renal Fibrosis in Obstructive Nephropathy. *Clin. Exp. Immunol.* **2018**, *193*, 361–375. [CrossRef]
131. Grande, M.T.; Sanchez-Laorden, B.; López-Blau, C.; De Frutos, C.A.; Boutet, A.; Arévalo, M.; Rowe, R.G.; Weiss, S.J.; López-Novoa, J.M.; Nieto, M.A. Snail1-Induced Partial Epithelial-to-Mesenchymal Transition Drives Renal Fibrosis in Mice and Can Be Targeted to Reverse Established Disease. *Nat. Med.* **2015**, *21*, 989–997. [CrossRef]
132. Xie, K.; Bao, L.; Jiang, X.; Ye, Z.; Bing, J.; Dong, Y.; Gao, D.; Ji, X.; Jiang, T.; Li, J.; et al. The Association of Metabolic Syndrome Components and Chronic Kidney Disease in Patients with Hypertension. *Lipids Health Dis.* **2019**, *18*, 1–6. [CrossRef]
133. Alicic, R.Z.; Rooney, M.T.; Tuttle, K. Diabetic Kidney Disease. *Clin. J. Am. Soc. Nephrol.* **2017**, *12*, 2032–2045. [CrossRef]
134. Mordi, I.; Mordi, N.; Delles, C.; Tzemos, N. Endothelial Dysfunction in Human Essential Hypertension. *J. Hypertens.* **2016**, *34*, 1464–1472. [CrossRef] [PubMed]
135. Shi, Y.; Vanhoutte, P.M. Macro- and Microvascular Endothelial Dysfunction in Diabetes. *J. Diabetes* **2017**, *9*, 434–449. [CrossRef]
136. Moriya, T.; Yamagishi, T.; Matsubara, M.; Ouchi, M. Serial Renal Biopsies in Normo- and Microalbuminuric Patients with Type 2 Diabetes Demonstrate That Loss of Renal Function Is Associated with a Reduction in Glomerular Filtration Surface Secondary to Mesangial Expansion. *J. Diabetes Complicat.* **2019**, *33*, 368–373. [CrossRef] [PubMed]
137. Heintz, B.; Stöcker, G.; Mrowka, C.; Rentz, U.; Melzer, H.; Stickeler, E.; Sieberth, H.-G.; Greiling, H.; Haubeck, H.-D. Decreased Glomerular Basement Membrane Heparan Sulfate Proteoglycan in Essential Hypertension. *Hypertension* **1995**, *25*, 399–407. [CrossRef]
138. Salem, R.M.; Todd, J.N.; Sandholm, N.; Cole, J.B.; Chen, W.-M.; Andrews, D.; Pezzolesi, M.G.; McKeigue, P.M.; Hiraki, L.T.; Qiu, C.; et al. Genome-Wide Association Study of Diabetic Kidney Disease Highlights Biology Involved in Glomerular Basement Membrane Collagen. *J. Am. Soc. Nephrol.* **2019**, *30*, 2000–2016. [CrossRef] [PubMed]
139. Tung, C.-W.; Hsu, Y.-C.; Shih, Y.-H.; Chang, P.-J.; Lin, C.-L. Glomerular Mesangial Cell and Podocyte Injuries in Diabetic Nephropathy. *Nephrology* **2018**, *23*, 32–37. [CrossRef]
140. Puelles, V.G.; Cullen-McEwen, L.; Taylor, G.E.; Li, J.; Hughson, M.D.; Kerr, P.G.; Hoy, W.E.; Bertram, J. Human Podocyte Depletion in Association with Older Age and Hypertension. *Am. J. Physiol. Physiol.* **2016**, *310*, F656–F668. [CrossRef]
141. Liu, Y. Cellular and molecular mechanisms of renal fibrosis. *Nat. Rev. Nephrol.* **2011**, *7*, 684–696. [CrossRef]
142. Conlin, C.C.; Huang, Y.; Gordon, B.A.J.; Zhang, J.L. Quantitative Characterization of Glomerular Fibrosis with Magnetic Resonance Imaging: A Feasibility Study in a Rat Glomerulonephritis Model. *Am. J. Physiol. Physiol.* **2018**, *314*, F747–F752. [CrossRef] [PubMed]
143. Zhou, C.; Lou, K.; Tatum, K.; Funk, J.; Wu, J.; Bartkowiak, T.; Kagan, D.; Lou, Y. Differentiating Glomerular Inflammation from Fibrosis in a Bone Marrow Chimera for Rat Anti-Glomerular Basement Membrane Glomerulonephritis. *Am. J. Nephrol.* **2015**, *42*, 42–53. [CrossRef] [PubMed]
144. Genovese, F.; A Manresa, A.; Leeming, D.J.; Karsdal, M.A.; Boor, P. The Extracellular Matrix in the Kidney: A Source of Novel Non-Invasive Biomarkers of Kidney Fibrosis? *Fibrogenesis Tissue Repair* **2014**, *7*, 4. [CrossRef]
145. Bohle, A.; Mackensen-Haen, S.; Gise, H.V. Significance of Tubulointerstitial Changes in the Renal Cortex for the Excretory Function and Concentration Ability of the Kidney: A Morphometric Contribution. *Am. J. Nephrol.* **1987**, *7*, 421–433. [CrossRef]
146. Tervaert, T.W.C.; Mooyaart, A.; Amann, K.; Cohen, A.H.; Cook, H.T.; Drachenberg, C.B.; Ferrario, F.; Fogo, A.B.; Haas, M.; De Heer, E.; et al. Pathologic Classification of Diabetic Nephropathy. *J. Am. Soc. Nephrol.* **2010**, *21*, 556–563. [CrossRef] [PubMed]

147. Boor, P.; Perkuhn, M.; Ms, M.W.; Zok, S.; Martin, W.; Ms, J.G.; Schoth, F.; Ostendorf, T.; Kuhl, C.; Floege, J. Diffusion-Weighted MRI Does Not Reflect Kidney Fibrosis in a Rat Model of Fibrosis. *J. Magn. Reson. Imaging* **2015**, *42*, 990–998. [CrossRef]
148. Zhao, J.; Wang, Z.; Liu, M.; Zhu, J.; Zhang, X.; Zhang, T.; Li, S.; Li, Y. Assessment of Renal Fibrosis in Chronic Kidney Disease Using Diffusion-Weighted MRI. *Clin. Radiol.* **2014**, *69*, 1117–1122. [CrossRef]
149. Eadon, M.T.; Schwantes-An, T.-H.; Phillips, C.L.; Roberts, A.R.; Greene, C.V.; Hallab, A.; Hart, K.J.; Lipp, S.N.; Perez-Ledezma, C.; Omar, K.O.; et al. Kidney Histopathology and Prediction of Kidney Failure: A Retrospective Cohort Study. *Am. J. Kidney Dis.* **2020**, *76*, 350–360. [CrossRef]
150. Belghasem, M.E.; A'Amar, O.; Roth, D.; Walker, J.; Arinze, N.; Richards, S.M.; Francis, J.M.; Salant, D.J.; Chitalia, V.C.; Bigio, I.J. Towards Minimally-Invasive, Quantitative Assessment of Chronic Kidney Disease Using Optical Spectroscopy. *Sci. Rep.* **2019**, *9*, 7168. [CrossRef] [PubMed]
151. Nath, K.A. Tubulointerstitial Changes As a Major Determinant in the Progression of Renal Damage. *Am. J. Kidney Dis.* **1992**, *20*, 1–17. [CrossRef]
152. Howie, A.J.; Ferreira, M.A.S.; Adu, D. Prognostic Value of Simple Measurement of Chronic Damage in Renal Biopsy Specimens. *Nephrol. Dial. Transplant.* **2001**, *16*, 1163–1169. [CrossRef]
153. Kaissling, B.; LeHir, M.; Kriz, W. Renal Epithelial Injury and Fibrosis. *Biochim. Biophys. Acta Mol. Basis Dis.* **2013**, *1832*, 931–939. [CrossRef]
154. Rosenberg, A.; Kopp, J. Focal Segmental Glomerulosclerosis. *Clin. J. Am. Soc. Nephrol.* **2017**, *12*, 502–517. [CrossRef]
155. Palatini, P. Glomerular Hyperfiltration: A Marker of Early Renal Damage in Pre-Diabetes and Pre-Hypertension. *Nephrol. Dial. Transplant.* **2012**, *27*, 1708–1714. [CrossRef] [PubMed]
156. Kriz, W.; Lehir, M. Pathways to Nephron Loss Starting from Glomerular diseases—Insights from Animal Models. *Kidney Int.* **2005**, *67*, 404–419. [CrossRef] [PubMed]
157. Dong, J.; Li, Y.; Yue, S.; Liu, X.; Wang, L.; Xiong, M.; Wang, G.; Nie, S.; Xu, X. The Profiles of Biopsy-Proven Renal Tubulointerstitial Lesions in Patients with Glomerular Disease. *Ann. Transl. Med.* **2020**, *8*, 1066. [CrossRef] [PubMed]
158. Tang, P.M.K.; Nikolic-Paterson, D.J.; Lan, H.-Y. Macrophages: Versatile Players in Renal Inflammation and Fibrosis. *Nat. Rev. Nephrol.* **2019**, *15*, 144–158. [CrossRef] [PubMed]
159. Zhao, J.-H. Mesangial Cells and Renal Fibrosis. *Adv. Exp. Med. Biol.* **2019**, *1165*, 165–194. [CrossRef]
160. Bülow, R.D.; Boor, P. Extracellular Matrix in Kidney Fibrosis: More Than Just a Scaffold. *J. Histochem. Cytochem.* **2019**, *67*, 643–661. [CrossRef]
161. Müller, G.A.; Rodemann, H.P. Characterization of Human Renal Fibroblasts in Health and Disease: I. Immunophenotyping of Cultured Tubular Epithelial Cells and Fibroblasts Derived from Kidneys with Histologically Proven Interstitial Fibrosis. *Am. J. Kidney Dis.* **1991**, *17*, 680–683. [CrossRef]
162. Rodemann, H.P.; Müller, G.A. Characterization of Human Renal Fibroblasts in Health and Disease: II. In Vitro Growth, Differentiation, and Collagen Synthesis of Fibroblasts from Kidneys with Interstitial Fibrosis. *Am. J. Kidney Dis.* **1991**, *17*, 684–686. [CrossRef]
163. Koesters, R.; Kaissling, B.; LeHir, M.; Picard, N.; Theilig, F.; Gebhardt, R.; Glick, A.B.; Hähnel, B.; Hosser, H.; Gröne, H.-J.; et al. Tubular Overexpression of Transforming Growth Factor-β1 Induces Autophagy and Fibrosis But Not Mesenchymal Transition of Renal Epithelial Cells. *Am. J. Pathol.* **2010**, *177*, 632–643. [CrossRef] [PubMed]
164. Kriz, W.; Hähnel, B.; Hosser, H.; Ostendorf, T.; Gaertner, S.; Kränzlin, B.; Gretz, N.; Shimizu, F.; Floege, J. Pathways to Recovery and Loss of Nephrons in Anti-Thy-1 Nephritis. *J. Am. Soc. Nephrol.* **2003**, *14*, 1904–1926. [CrossRef] [PubMed]
165. Cheng, S.; Pollock, A.S.; Mahimkar, R.; Olson, J.L.; Lovett, D.H. Matrix Metalloproteinase 2 and Basement Membrane Integrity: A Unifying Mechanism for Progressive Renal Injury. *FASEB J.* **2006**, *20*, 1898–1900. [CrossRef] [PubMed]
166. Nadasdy, T.; Laszik, Z.; E Blick, K.; Johnson, L.D.; Silva, F.G. Proliferative Activity of Intrinsic Cell Populations in the Normal Human Kidney. *J. Am. Soc. Nephrol.* **1994**, *4*, 2032–2039. [CrossRef]
167. Humphreys, B.D.; Valerius, M.T.; Kobayashi, A.; Mugford, J.W.; Soeung, S.; Duffield, J.S.; McMahon, A.P.; Bonventre, J.V. Intrinsic Epithelial Cells Repair the Kidney After Injury. *Cell Stem Cell* **2008**, *2*, 284–291. [CrossRef]
168. Yang, L.; Besschetnova, T.Y.; Brooks, C.R.; Shah, J.V.; Bonventre, J.V. Epithelial Cell Cycle Arrest in G2/M Mediates Kidney Fibrosis After Injury. *Nat. Med.* **2010**, *16*, 535–543. [CrossRef]
169. Grgic, I.; Campanholle, G.; Bijol, V.; Wang, C.; Sabbisetti, V.S.; Ichimura, T.; Humphreys, B.D.; Bonventre, J.V. Targeted Proximal Tubule Injury Triggers Interstitial Fibrosis and Glomerulosclerosis. *Kidney Int.* **2012**, *82*, 172–183. [CrossRef]
170. Xu, L.; Sharkey, D.; Cantley, L.G. Tubular GM-CSF Promotes Late MCP-1/CCR2-Mediated Fibrosis and Inflammation After Ischemia/Reperfusion Injury. *J. Am. Soc. Nephrol.* **2019**, *30*, 1825–1840. [CrossRef]
171. Arfian, N.; Wahyudi, D.A.P.; Zulfatina, I.B.; Citta, A.N.; Anggorowati, N.; Multazam, A.; Romi, M.M.; Sari, D.C.R. Chlorogenic Acid Attenuates Kidney Ischemic/Reperfusion Injury via Reducing Inflammation, Tubular Injury, and Myofibroblast Formation. *BioMed Res. Int.* **2019**, *2019*, 1–10. [CrossRef]
172. Jing, W.; Vaziri, N.D.; Nunes, A.C.F.; Suematsu, Y.; Farzaneh, T.; Khazaeli, M.; Moradi, H. LCZ696 (Sacubitril/Valsartan) Ameliorates Oxidative Stress, Inflammation, Fibrosis and Improves Renal Function Beyond Angiotensin Receptor Blockade in CKD. *Am. J. Transl. Res.* **2017**, *9*, 5473–5484.
173. Fortrie, G.; De Geus, H.R.H.; Betjes, M.G.H. The Aftermath of Acute Kidney Injury: A Narrative Review of Long-Term Mortality and Renal Function. *Crit. Care* **2019**, *23*, 1–11. [CrossRef] [PubMed]

174. Stroo, I.; Stokman, G.; Teske, G.J.D.; Raven, A.; Butter, L.M.; Florquin, S.; Leemans, J.C. Chemokine Expression in Renal ischemia/Reperfusion Injury Is Most Profound During the Reparative Phase. *Int. Immunol.* **2010**, *22*, 433–442. [CrossRef]
175. Ali, B.H.; Al-Salam, S.; Al Suleimani, Y.; Al Kalbani, J.; Al Bahlani, S.; Ashique, M.; Manoj, P.; Al Dhahli, B.; Al Abri, N.; Naser, H.T.; et al. Curcumin Ameliorates Kidney Function and Oxidative Stress in Experimental Chronic Kidney Disease. *Basic Clin. Pharmacol. Toxicol.* **2018**, *122*, 65–73. [CrossRef]
176. Fabre, T.; Kared, H.; Friedman, S.L.; Shoukry, N.H. IL-17A Enhances the Expression of Profibrotic Genes through Upregulation of the TGF-β Receptor on Hepatic Stellate Cells in a JNK-Dependent Manner. *J. Immunol.* **2014**, *193*, 3925–3933. [CrossRef]
177. Mack, M. Inflammation and Fibrosis. *Matrix Biol.* **2018**, *68-69*, 106–121. [CrossRef] [PubMed]
178. Massagué, J. TGFβ Signalling in Context. *Nat. Rev. Mol. Cell Biol.* **2012**, *13*, 616–630. [CrossRef]
179. Finnson, K.; Almadani, Y.; Philip, A. Non-Canonical (non-SMAD2/3) TGF-β Signaling in Fibrosis: Mechanisms and Targets. *Semin. Cell Dev. Biol.* **2020**, *101*, 115–122. [CrossRef]
180. Sun, K.-H.; Chang, Y.; Reed, N.I.; Sheppard, D. α-Smooth Muscle Actin Is an Inconsistent Marker of Fibroblasts Responsible for Force-Dependent TGFβ Activation or Collagen Production across Multiple Models of Organ Fibrosis. *Am. J. Physiol. Cell. Mol. Physiol.* **2016**, *310*, L824–L836. [CrossRef] [PubMed]
181. Walker, E.J.; Heydet, D.; Veldre, T.; Ghildyal, R. Transcriptomic Changes During TGF-β-Mediated Differentiation of Airway Fibroblasts to Myofibroblasts. *Sci. Rep.* **2019**, *9*, 1–14. [CrossRef]
182. Chen, W.; Dijke, P.T. Immunoregulation by Members of the TGFβ Superfamily. *Nat. Rev. Immunol.* **2016**, *16*, 723–740. [CrossRef] [PubMed]
183. Gravning, J.; Ørn, S.; Kaasbøll, O.J.; Martinov, V.N.; Manhenke, C.; Dickstein, K.; Edvardsen, T.; Attramadal, H.; Ahmed, M.S. Myocardial Connective Tissue Growth Factor (CCN2/CTGF) Attenuates Left Ventricular Remodeling After Myocardial Infarction. *PLoS ONE* **2012**, *7*, e52120. [CrossRef]
184. Mao, L.; Liu, L.; Zhang, T.; Wu, X.; Zhang, T.; Xu, Y. MKL1 Mediates TGF-β-induced CTGF Transcription to Promote Renal Fibrosis. *J. Cell. Physiol.* **2020**, *235*, 4790–4803. [CrossRef]
185. Mori, T.; Kawara, S.; Shinozaki, M.; Hayashi, N.; Kakinuma, T.; Igarashi, A.; Takigawa, M.; Nakanishi, T.; Takehara, K. Role and in-Teraction of Connective Tissue Growth Factor with Transforming Growth Factor-Beta in Persistent Fibrosis: A Mouse Fibrosis Model. *J. Cell Physiol.* **1999**, *181*, 153–159. [CrossRef]
186. (96) Frazier, K.; Williams, S.; Kothapalli, D.; Klapper, H.; Grotendorst, G.R. Stimulation of Fibroblast Cell Growth, Matrix Production, and Granulation Tissue Formation by Connective Tissue Growth Factor. *J. Investig. Dermatol.* **1996**, *107*, 404–411. [CrossRef] [PubMed]
187. Igarashi, A.; Nashiro, K.; Kikuchi, K.; Sato, S.; Ihn, H.; Fujimoto, M.; Grotendorst, G.R.; Takehara, K. Connective Tissue Growth Factor Gene Expression in Tissue Sections from Localized Scleroderma, Keloid, and Other Fibrotic Skin Disorders. *J. Investig. Dermatol.* **1996**, *106*, 729–733. [CrossRef]
188. Inanc, S.; Keleş, D.; Oktay, G. An Improved Collagen Zymography Approach for Evaluating the Collagenases MMP-1, MMP-8, and MMP-13. *Biotechnology* **2017**, *63*, 174–180. [CrossRef]
189. Falconer, A.M.D.; Chan, C.M.; Gray, J.; Nagashima, I.; Holland, R.A.; Shimizu, H.; Pickford, A.R.; Rowan, A.D.; Wilkinson, D.J. Collagenolytic Matrix Metalloproteinases Antagonize Proteinase-Activated Receptor-2 Activation, Providing Insights into Extracellular Matrix Turnover. *J. Biol. Chem.* **2019**, *294*, 10266–10277. [CrossRef]
190. Toth, M.; Sohail, A.; Fridman, R. Assessment of Gelatinases (MMP-2 and MMP-9) by Gelatin Zymography. In *Metastasis Research Protocols*; Humana Press: Totowa, NJ, USA, 2012; pp. 163–174.
191. Vafashoar, F.; Mousavizadeh, K.; Poormoghim, H.; Tavasoli, A.; Shabestari, T.M.; JavadMoosavi, S.A.; Mojtabavi, N. Gelatinases Increase in Bleomycin-Induced Systemic Sclerosis Mouse Model. *Iran. J. Allergy Asthma Immunol.* **2019**, *18*, 182–189. [CrossRef]
192. Butler, G.S.; Connor, A.R.; Sounni, N.E.; Eckhard, U.; Morrison, C.J.; Noel, A.; Overall, C.M. Degradomic and Yeast 2-Hybrid Inactive Catalytic Domain Substrate Trapping Identifies New Membrane-Type 1 Matrix Metalloproteinase (MMP14) Substrates: CCN3 (Nov) and CCN5 (WISP2). *Matrix Biol.* **2017**, *59*, 23–38. [CrossRef] [PubMed]
193. Mirastschijski, U.; Dinesh, N.; Baskaran, S.; Wedekind, D.; Gavrilovic, J.; Murray, M.Y.; Bevan, D.; Kelm, S. Novel Specific Human and Mouse stromelysin-1 (MMP-3) and stromelysin-2 (MMP-10) Antibodies for Biochemical and Immunohistochemical Analyses. *Wound Repair Regen.* **2019**, *27*, 309–323. [CrossRef] [PubMed]
194. Giannandrea, M.; Parks, W.C. Diverse Functions of Matrix Metalloproteinases During Fibrosis. *Dis. Model. Mech.* **2014**, *7*, 193–203. [CrossRef] [PubMed]
195. Wang, H.; Gao, M.; Li, J.; Sun, J.; Wu, R.; Han, D.; Tan, J.; Wang, J.; Wang, B.; Zhang, L.; et al. MMP-9-positive Neutrophils Are Essential for Establishing Profibrotic Microenvironment in the Obstructed Kidney of UUO Mice. *Acta Physiol.* **2019**, *227*, e13317. [CrossRef]
196. Zhao, Y.; Qiao, X.; Tan, T.K.; Zhao, H.; Zhang, Y.; Liu, L.; Zhang, J.; Wang, L.; Cao, Q.; Wang, Y.; et al. Matrix Metalloproteinase 9-Dependent Notch Signaling Contributes to Kidney Fibrosis through Peritubular Endothelial-Mesenchymal Transition. *Nephrol. Dial. Transplant.* **2016**, *32*, 781–791. [CrossRef] [PubMed]
197. Chiao, Y.A.; Ramirez, T.A.; Zamilpa, R.; Okoronkwo, S.M.; Dai, Q.; Zhang, J.; Jin, Y.-F.; Lindsey, M.L. Matrix Metalloproteinase-9 Deletion Attenuates Myocardial Fibrosis and Diastolic Dysfunction in Ageing Mice. *Cardiovasc. Res.* **2012**, *96*, 444–455. [CrossRef]

198. Altieri, P.; Brunelli, C.; Garibaldi, S.; Nicolino, A.; Ubaldi, S.; Spallarossa, P.; Olivotti, L.; Rossettin, P.; Barsotti, A.; Ghigliotti, G. Metalloproteinases 2 and 9 Are Increased in Plasma of Patients with Heart Failure. *Eur. J. Clin. Investig.* **2003**, *33*, 648–656. [CrossRef]
199. Takamiya, Y.; Fukami, K.; Yamagishi, S.-I.; Kaida, Y.; Nakayama, Y.; Obara, N.; Iwatani, R.; Ando, R.; Koike, K.; Matsui, T.; et al. Experimental Diabetic Nephropathy Is Accelerated in Matrix Metalloproteinase-2 Knockout Mice. *Nephrol. Dial. Transplant.* **2012**, *28*, 55–62. [CrossRef]
200. Jao, T.-M.; Nangaku, M.; Wu, C.-H.; Sugahara, M.; Saito, H.; Maekawa, H.; Ishimoto, Y.; Aoe, M.; Inoue, T.; Tanaka, T.; et al. ATF6α Downregulation of PPARα Promotes Lipotoxicity-Induced Tubulointerstitial Fibrosis. *Kidney Int.* **2019**, *95*, 577–589. [CrossRef]
201. Jiménez-González, S.; Marín-Royo, G.; Jurado-López, R.; Bartolomé, M.V.; Miranda, A.R.; Luaces, M.; Islas, F.; Nieto, M.L.; Martínez-Martínez, E.; Cachofeiro, V. The Crosstalk Between Cardiac Lipotoxicity and Mitochondrial Oxidative Stress in the Cardiac Alterations in Diet-Induced Obesity in Rats. *Cells* **2020**, *9*, 451. [CrossRef]
202. Delgado-Valero, B.; de la Fuente-Chávez, L.; Romero-Miranda, A.; Bartolomé, M.V.; Ramchandani, B.; Islas, F.; Luaces, M.; Cachofeiro, V.; Martínez-Martínez, E. Role of Endoplasmic Reticulum Stress in Renal Damage After Myocardial Infarction. *Clin. Sci.* **2021**, *135*, 143–159. [CrossRef]
203. Nogueira, A.; Pires, M.J.; Oliveira, P.A. Pathophysiological Mechanisms of Renal Fibrosis: A Review of Animal Models and Therapeutic Strategies. *Vivo* **2017**, *31*, 1–22. [CrossRef]
204. Sun, H.-J. Current Opinion for Hypertension in Renal Fibrosis. *Adv. Exp. Med. Biol.* **2019**, *1165*, 37–47. [CrossRef]
205. Rubinstein, J.; Sanford, D. Treatment of Cardiorenal Syndrome. *Cardiol. Clin.* **2019**, *37*, 267–273. [CrossRef]
206. Wang, L.; Tian, X.; Cao, Y.; Ma, X.; Shang, L.; Li, H.; Zhang, X.; Deng, F.; Li, S.; Guo, T.; et al. Cardiac Shock Wave Therapy Improves Ventricular Function by Relieving Fibrosis Through PI3K/Akt Signaling Pathway: Evidence from a Rat Model of Post-Infarction Heart Failure. *Front. Cardiovasc. Med.* **2021**, *8*, 693875. [CrossRef] [PubMed]
207. Zindel, J.; Kubes, P. DAMPs, PAMPs, and LAMPs in Immunity and Sterile Inflammation. *Annu. Rev. Pathol. Mech. Dis.* **2020**, *15*, 493–518. [CrossRef] [PubMed]
208. Abdulkhaleq, L.A.; Assi, M.A.; Abdullah, R.; Zamri-Saad, M.; Taufiq-Yap, Y.H.; Hezmee, M.N.M. The Crucial Roles of Inflammatory Mediators in Inflammation: A Review. *Veter. World* **2018**, *11*, 627–635. [CrossRef] [PubMed]
209. Clark, R.; Kupper, T. Old Meets New: The Interaction Between Innate and Adaptive Immunity. *J. Investig. Dermatol.* **2005**, *125*, 629–637. [CrossRef] [PubMed]
210. Furman, D.; Campisi, J.; Verdin, E.; Carrera-Bastos, P.; Targ, S.; Franceschi, C.; Ferrucci, L.; Gilroy, D.W.; Fasano, A.; Miller, G.W.; et al. Chronic Inflammation in the Etiology of Disease across the Life Span. *Nat. Med.* **2019**, *25*, 1822–1832. [CrossRef]
211. Odegaard, A.O.; Goff, D.R., Jr.; Sanchez, O.A.; Goff, D.C.; Reiner, A.P.; Gross, M.D. Oxidative Stress, Inflammation, Endothelial Dysfunction and Incidence of Type 2 Diabetes. *Cardiovasc. Diabetol.* **2016**, *15*, 1–12. [CrossRef]
212. Kanazawa, I.; Tanaka, S.; Sugimoto, T. The Association Between Osteocalcin and Chronic Inflammation in Patients with Type 2 Diabetes Mellitus. *Calcif. Tissue Int.* **2018**, *103*, 599–605. [CrossRef]
213. Xiao, L.; Harrison, D.G. Inflammation in Hypertension. *Can. J. Cardiol.* **2020**, *36*, 635–647. [CrossRef]
214. Rios, F.; Zou, Z.-G.; Harvey, A.P.; Harvey, K.Y.; Nosalski, R.; Anyfanti, P.; Camargo, L.L.; Lacchini, S.; Ryazanov, A.G.; Ryazanova, L.; et al. Chanzyme TRPM7 Protects Against Cardiovascular Inflammation and Fibrosis. *Cardiovasc. Res.* **2020**, *116*, 721–735. [CrossRef] [PubMed]
215. Ridker, P.M.; Everett, B.M.; Thuren, T.; MacFadyen, J.G.; Chang, W.H.; Ballantyne, C.; Fonseca, F.; Nicolau, J.; Koenig, W.; Anker, S.D.; et al. Antiinflammatory Therapy with Canakinumab for Atherosclerotic Disease. *N. Engl. J. Med.* **2017**, *377*, 1119–1131. [CrossRef]
216. Mihai, S.; Codrici, E.; Popescu, I.D.; Enciu, A.-M.; Albulescu, L.; Necula, L.G.; Mambet, C.; Anton, G.; Tanase, C. Inflammation-Related Mechanisms in Chronic Kidney Disease Prediction, Progression, and Outcome. *J. Immunol. Res.* **2018**, *2018*, 1–16. [CrossRef] [PubMed]
217. Torres, S.; Fabersani, E.; Marquez, A.; Gauffin-Cano, P. Adipose Tissue Inflammation and Metabolic Syndrome. The Proactive Role of Probiotics. *Eur. J. Nutr.* **2018**, *58*, 27–43. [CrossRef] [PubMed]
218. Pierce, G.F.; A Mustoe, T.; Lingelbach, J.; Masakowski, V.R.; Griffin, G.L.; Senior, R.M.; Deuel, T.F. Platelet-Derived Growth Factor and Transforming Growth Factor-Beta Enhance Tissue Repair Activities by Unique Mechanisms. *J. Cell Biol.* **1989**, *109*, 429–440. [CrossRef] [PubMed]
219. Rossaint, J.; Margraf, A.; Zarbock, A. Role of Platelets in Leukocyte Recruitment and Resolution of Inflammation. *Front. Immunol.* **2018**, *9*, 2712. [CrossRef] [PubMed]
220. Lichtman, M.K.; Otero-Vinas, M.; Falanga, V. Transforming Growth Factor Beta (TGF-β) Isoforms in Wound Healing and Fibrosis. *Wound Repair Regen.* **2015**, *24*, 215–222. [CrossRef] [PubMed]
221. Amdur, R.L.; Feldman, H.I.; Gupta, J.; Yang, W.; Kanetsky, P.; Shlipak, M.; Rahman, M.; Lash, J.P.; Townsend, R.R.; Ojo, A.; et al. Inflammation and Progression of CKD: The CRIC Study. *Clin. J. Am. Soc. Nephrol.* **2016**, *11*, 1546–1556. [CrossRef] [PubMed]
222. Greenberg, J.H.; Abraham, A.G.; Xu, Y.; Schelling, J.R.; Feldman, H.I.; Sabbisetti, V.S.; Gonzalez, M.C.; Coca, S.; Schrauben, S.J.; Waikar, S.S.; et al. Plasma Biomarkers of Tubular Injury and Inflammation Are Associated with CKD Progression in Children. *J. Am. Soc. Nephrol.* **2020**, *31*, 1067–1077. [CrossRef]
223. Wen, Y.; Lu, X.; Ren, J.; Privratsky, J.R.; Yang, B.; Rudemiller, N.P.; Zhang, J.; Griffiths, R.; Jain, M.K.; Nedospasov, S.A.; et al. KLF4 in Macrophages Attenuates TNFα-Mediated Kidney Injury and Fibrosis. *J. Am. Soc. Nephrol.* **2019**, *30*, 1925–1938. [CrossRef]

224. Brandt, S.; Ballhause, T.M.; Bernhardt, A.; Becker, A.; Salaru, D.; Le-Deffge, H.M.; Fehr, A.; Fu, Y.; Philipsen, L.; Djudjaj, S.; et al. Fibrosis and Immune Cell Infiltration Are Separate Events Regulated by Cell-Specific Receptor Notch3 Expression. *J. Am. Soc. Nephrol.* **2020**, *31*, 2589–2608. [CrossRef] [PubMed]
225. Wang, Y.-Y.; Jiang, H.; Pan, J.; Huang, X.-R.; Wang, Y.-C.; Huang, H.-F.; To, K.-F.; Nikolic-Paterson, D.J.; Lan, H.-Y.; Chen, J.-H. Macrophage-to-Myofibroblast Transition Contributes to Interstitial Fibrosis in Chronic Renal Allograft Injury. *J. Am. Soc. Nephrol.* **2017**, *28*, 2053–2067. [CrossRef] [PubMed]
226. Kormann, R.; Kavvadas, P.; Placier, S.; Vandermeersch, S.; Dorison, A.; Dussaule, J.-C.; Chadjichristos, C.E.; Prakoura, N.; Chatziantoniou, C. Periostin Promotes Cell Proliferation and Macrophage Polarization to Drive Repair After AKI. *J. Am. Soc. Nephrol.* **2020**, *31*, 85–100. [CrossRef] [PubMed]
227. Simões, F.C.; Cahill, T.J.; Kenyon, A.; Gavriouchkina, D.; Vieira, J.M.; Sun, X.; Pezzolla, D.; Ravaud, C.; Masmanian, E.; Weinberger, M.; et al. Macrophages Directly Contribute Collagen to Scar Formation During Zebrafish Heart Regeneration and Mouse Heart Repair. *Nat. Commun.* **2020**, *11*, 1–17. [CrossRef]
228. Shen, B.; Liu, X.; Fan, Y.; Qiu, J. Macrophages Regulate Renal Fibrosis Through Modulating TGFβ Superfamily Signaling. *Inflammation* **2014**, *37*, 2076–2084. [CrossRef] [PubMed]
229. Wright, T.M. Cytokines in Acute and Chronic Inflammation. *Front. Biosci.* **1997**, *2*, d12–d26. [CrossRef] [PubMed]
230. Panico, K.; Abrahão, M.V.; Sonoda, M.T.; Muzi-Filho, H.; Vieyra, A.; Carneiro-Ramos, M.S. Cardiac Inflammation After Ischemia-Reperfusion of the Kidney: Role of the Sympathetic Nervous System and the Renin-Angiotensin System. *Cell. Physiol. Biochem.* **2019**, *53*, 587–605. [CrossRef]
231. Virzì, G.M.; Breglia, A.; Castellani, C.; Ankawi, G.; Bolin, C.; De Cal, M.; Cianci, V.; Angelini, A.; Vescovo, G.; Ronco, C. Lipopolysaccharide in Systemic Circulation Induces Activation of Inflammatory Response and Oxidative Stress in Cardiorenal Syndrome Type 1. *J. Nephrol.* **2019**, *32*, 803–810. [CrossRef]
232. Virzì, G.M.; Breglia, A.; Brocca, A.; De Cal, M.; Bolin, C.; Vescovo, G.; Ronco, C. Levels of Proinflammatory Cytokines, Oxidative Stress, and Tissue Damage Markers in Patients with Acute Heart Failure with and without Cardiorenal Syndrome Type 1. *Cardiorenal Med.* **2018**, *8*, 321–331. [CrossRef]
233. Colombo, P.C.; Ganda, A.; Lin, J.; Onat, D.; Harxhi, A.; Iyasere, J.E.; Uriel, N.; Cotter, G. Inflammatory Activation: Cardiac, Renal, and Cardio-Renal Interactions in Patients with the Cardiorenal Syndrome. *Heart Fail. Rev.* **2012**, *17*, 177–190. [CrossRef]
234. Li, R.; Mi, X.; Yang, S.; Yang, Y.; Zhang, S.; Hui, R.; Chen, Y.; Zhang, W. Long-Term Stimulation of Angiotensin II Induced Endothelial Senescence and Dysfunction. *Exp. Gerontol.* **2019**, *119*, 212–220. [CrossRef] [PubMed]
235. Du, Y.; Han, J.; Zhang, H.; Xu, J.; Jiang, L.; Ge, W. Kaempferol Prevents Against Ang II-Induced Cardiac Remodeling Through Attenuating Ang II-Induced Inflammation and Oxidative Stress. *J. Cardiovasc. Pharmacol.* **2019**, *74*, 326–335. [CrossRef]
236. Lang, P.-P.; Bai, J.; Zhang, Y.-L.; Yang, X.-L.; Xia, Y.-L.; Lin, Q.-Y.; Li, H.-H. Blockade of Intercellular Adhesion Molecule-1 Prevents Angiotensin II-Induced Hypertension and Vascular Dysfunction. *Lab. Investig.* **2019**, *100*, 378–386. [CrossRef] [PubMed]
237. Kalra, D.; Sivasubramanian, N.; Mann, D.L. Angiotensin II Induces Tumor Necrosis Factor Biosynthesis in the Adult Mammalian Heart Through a Protein Kinase C–Dependent Pathway. *Circulation* **2002**, *105*, 2198–2205. [CrossRef]
238. Ozawa, Y.; Kobori, H.; Suzaki, Y.; Navar, L.G. Sustained Renal Interstitial Macrophage Infiltration Following Chronic Angiotensin II Infusions. *Am. J. Physiol. Physiol.* **2007**, *292*, F330–F339. [CrossRef]
239. Frenay, A.-R.S.; Yazdani, S.; Boersema, M.; Van Der Graaf, A.M.; Waanders, F.; Born, J.V.D.; Navis, G.J.; Van Goor, H. Incomplete Restoration of Angiotensin II - Induced Renal Extracellular Matrix Deposition and Inflammation Despite Complete Functional Recovery in Rats. *PLoS ONE* **2015**, *10*, e0129732. [CrossRef]
240. Zhang, J.-D.; Patel, M.B.; Griffiths, R.; Dolber, P.C.; Ruiz, P.; Sparks, M.A.; Stegbauer, J.; Jin, H.; Gomez, J.A.; Buckley, A.F.; et al. Type 1 Angiotensin Receptors on Macrophages Ameliorate IL-1 receptor–mediated Kidney Fibrosis. *J. Clin. Investig.* **2014**, *124*, 2198–2203. [CrossRef] [PubMed]
241. Wang, D.; Xiong, M.; Chen, C.; Du, L.; Liu, Z.; Shi, Y.; Zhang, M.; Gong, J.; Song, X.; Xiang, R.; et al. Legumain, an Asparaginyl Endopeptidase, Mediates the Effect of M2 Macrophages on Attenuating Renal Interstitial Fibrosis in Obstructive Nephropathy. *Kidney Int.* **2018**, *94*, 91–101. [CrossRef]
242. Witherel, C.E.; Abebayehu, D.; Barker, T.H.; Spiller, K.L. Macrophage and Fibroblast Interactions in Biomaterial-Mediated Fibrosis. *Adv. Health Mater.* **2019**, *8*, e1801451. [CrossRef]
243. Colombo, P.C.; Onat, D.; Harxhi, A.; Demmer, R.T.; Hayashi, Y.; Jelic, S.; LeJemtel, T.H.; Bucciarelli, L.; Kebschull, M.; Papapanou, P.N.; et al. Peripheral Venous Congestion Causes Inflammation, Neurohormonal, and Endothelial Cell Activation. *Eur. Heart J.* **2013**, *35*, 448–454. [CrossRef] [PubMed]
244. Colombo, P.C.; Rastogi, S.; Onat, D.; Zacà, V.; Gupta, R.C.; Jorde, U.P.; Sabbah, H.N. Activation of Endothelial Cells in Conduit Veins of Dogs with Heart Failure and Veins of Normal Dogs After Vascular Stretch by Acute Volume Loading. *J. Card. Fail.* **2009**, *15*, 457–463. [CrossRef] [PubMed]
245. Berguetti, T.S.; Quintaes, L.S.P.; Pereira, T.H.; Robaina, M.C.; Cruz, A.L.S.; Maia, R.C.; De Souza, P.S.; Hancio, T. TNF-α Modulates P-Glycoprotein Expression and Contributes to Cellular Proliferation via Extracellular Vesicles. *Cells* **2019**, *8*, 500. [CrossRef]
246. Chen, T.; Zhang, X.; Zhu, G.; Liu, H.; Chen, J.; Wang, Y.; He, X. Quercetin Inhibits TNF-α Induced HUVECs Apoptosis and Inflammation via Downregulating NF-KB and AP-1 Signaling Pathway in Vitro. *Medicine* **2020**, *99*, e22241. [CrossRef]
247. Zelová, H.; Hošek, J. TNF-α Signalling and Inflammation: Interactions Between Old Acquaintances. *Inflamm. Res.* **2013**, *62*, 641–651. [CrossRef] [PubMed]

248. Sziksz, E.; Pap, D.; Lippai, R.; Béres, N.J.; Fekete, A.; Szabó, A.J.; Vannay, Á. Fibrosis Related Inflammatory Mediators: Role of the IL-10 Cytokine Family. *Mediat. Inflamm.* **2015**, *2015*, 1–15. [CrossRef]
249. Wynn, T.A. Cellular and Molecular Mechanisms of Fibrosis. *J. Pathol.* **2007**, *214*, 199–210. [CrossRef]
250. Shao, D.; Suresh, R.; Vakil, V.; Gomer, R.; Pilling, D. Pivotal Advance: Th-1 Cytokines Inhibit, and Th-2 Cytokines Promote Fibrocyte Differentiation. *J. Leukoc. Biol.* **2008**, *83*, 1323–1333. [CrossRef] [PubMed]
251. Le Floc'H, A.; Allinne, J.; Nagashima, K.; Scott, G.; Birchard, D.; Asrat, S.; Bai, Y.; Lim, W.K.; Martin, J.; Huang, T.; et al. Dual Blockade of IL-4 and IL-13 with Dupilumab, an IL-4Rα Antibody, Is Required to Broadly Inhibit Type 2 Inflammation. *Allergy* **2019**, *75*, 1188–1204. [CrossRef]
252. Reiman, R.M.; Thompson, R.W.; Feng, C.; Hari, D.; Knight, R.; Cheever, A.W.; Rosenberg, H.F.; Wynn, T.A. Interleukin-5 (IL-5) Augments the Progression of Liver Fibrosis by Regulating IL-13 Activity. *Infect. Immun.* **2006**, *74*, 1471–1479. [CrossRef] [PubMed]
253. Pesce, J.; Kaviratne, M.; Ramalingam, T.R.; Thompson, R.W.; Urban, J.; Cheever, A.W.; Young, D.A.; Collins, M.; Grusby, M.J.; Wynn, T.A. The IL-21 Receptor Augments Th2 Effector Function and Alternative Macrophage Activation. *J. Clin. Investig.* **2006**, *116*, 2044–2055. [CrossRef]
254. Korn, T.; Bettelli, E.; Gao, W.; Awasthi, A.; Jäger, A.; Strom, T.B.; Oukka, M.; Kuchroo, V.K. IL-21 Initiates an Alternative Pathway to Induce Proinflammatory TH17 Cells. *Nat. Cell Biol.* **2007**, *448*, 484–487. [CrossRef]
255. Nurieva, R.; Yang, X.O.; Martinez, G.; Zhang, Y.; Panopoulos, A.; Ma, L.; Schluns, K.; Tian, Q.; Watowich, S.S.; Jetten, A.; et al. Essential Autocrine Regulation by IL-21 in the Generation of Inflammatory T Cells. *Nat. Cell Biol.* **2007**, *448*, 480–483. [CrossRef]
256. Lei, L.; Zhao, C.; Qin, F.; He, Z.Y.; Wang, X.; Zhong, X.N. Th17 Cells and IL-17 Promote the Skin and Lung Inflammation and Fibrosis Process in a Bleomycin-Induced Murine Model of Systemic Sclerosis. *Clin. Exp. Rheumatol.* **2016**, *34* (Suppl. S100), 14–22.
257. Wu, L.; Ong, S.; Talor, M.V.; Barin, J.G.; Baldeviano, G.C.; Kass, D.A.; Bedja, D.; Zhang, H.; Sheikh, A.; Margolick, J.B.; et al. Cardiac Fibroblasts Mediate IL-17A–driven Inflammatory Dilated Cardiomyopathy. *J. Exp. Med.* **2014**, *211*, 1449–1464. [CrossRef] [PubMed]
258. Sommerfeld, S.D.; Cherry, C.; Schwab, R.M.; Chung, L.; Maestas, D.R., Jr.; Laffont, P.; Stein, J.E.; Tam, A.; Ganguly, S.; Housseau, F.; et al. Interleukin-36γ–producing Macrophages Drive IL-17–mediated Fibrosis. *Sci. Immunol.* **2019**, *4*, eaax4783. [CrossRef]
259. Ramani, K.; Tan, R.J.; Zhou, D.; Coleman, B.M.; Jawale, C.V.; Liu, Y.; Biswas, P.S. IL-17 Receptor Signaling Negatively Regulates the Development of Tubulointerstitial Fibrosis in the Kidney. *Mediat. Inflamm.* **2018**, *2018*, 1–14. [CrossRef] [PubMed]
260. Huang, M.; Sharma, S.; Zhu, L.X.; Keane, M.P.; Luo, J.; Zhang, L.; Burdick, M.D.; Lin, Y.Q.; Dohadwala, M.; Gardner, B.; et al. IL-7 Inhibits Fibroblast TGF-β Production and Signaling in Pulmonary Fibrosis. *J. Clin. Investig.* **2002**, *109*, 931–937. [CrossRef]
261. Demols, A.; Van Laethem, J.-L.; Quertinmont, E.; Degraef, C.; Delhaye, M.; Geerts, A.; Devière, J. Endogenous Interleukin-10 Modulates Fibrosis and Regeneration in Experimental Chronic Pancreatitis. *Am. J. Physiol. Liver Physiol.* **2002**, *282*, G1105–G1112. [CrossRef] [PubMed]
262. Shamskhou, E.A.; Kratochvil, M.J.; Orcholski, M.E.; Nagy, N.; Kaber, G.; Steen, E.; Balaji, S.; Yuan, K.; Keswani, S.; Danielson, B.; et al. Hydrogel-Based Delivery of Il-10 Improves Treatment of Bleomycin-Induced Lung Fibrosis in Mice. *Biomaterials* **2019**, *203*, 52–62. [CrossRef]
263. Guan, Q.; Weiss, C.R.; Wang, S.; Qing, G.; Yang, X.; Warrington, R.J.; Bernstein, C.N.; Peng, Z. Reversing Ongoing Chronic Intestinal Inflammation and Fibrosis by Sustained Block of IL-12 and IL-23 Using a Vaccine in Mice. *Inflamm. Bowel Dis.* **2018**, *24*, 1941–1952. [CrossRef]
264. Keane, M.P.; Belperio, J.A.; Burdick, M.D.; Strieter, R.M. IL-12 Attenuates Bleomycin-Induced Pulmonary Fibrosis. *Am. J. Physiol. Cell. Mol. Physiol.* **2001**, *281*, L92–L97. [CrossRef] [PubMed]
265. Weidenbusch, M.; Song, S.; Iwakura, T.; Shi, C.; Rodler, S.; Kobold, S.; Mulay, S.R.; Honarpisheh, M.M.; Anders, H.-J. IL-22 Sustains Epithelial Integrity in Progressive Kidney Remodeling and Fibrosis. *Physiol. Rep.* **2018**, *6*, e13817. [CrossRef] [PubMed]
266. Wang, S.; Li, Y.; Fan, J.; Zhang, X.; Luan, J.; Bian, Q.; Ding, T.; Wang, Y.; Wang, Z.; Song, P.; et al. Interleukin-22 Ameliorated Renal Injury and Fibrosis in Diabetic Nephropathy through Inhibition of NLRP3 Inflammasome Activation. *Cell Death Dis.* **2017**, *8*, e2937. [CrossRef]
267. Lee, J.-W.; Oh, J.E.; Rhee, K.-J.; Yoo, B.-S.; Eom, Y.W.; Park, S.W.; Lee, J.H.; Son, J.-W.; Youn, Y.J.; Ahn, M.-S.; et al. Co-Treatment with Interferon-γ and 1-Methyl Tryptophan Ameliorates Cardiac Fibrosis through Cardiac Myofibroblasts Apoptosis. *Mol. Cell. Biochem.* **2019**, *458*, 197–205. [CrossRef] [PubMed]
268. Poosti, F.; Bansal, R.; Yazdani, S.; Prakash, J.; Post, E.; Klok, P.; Born, J.V.D.; de Borst, M.H.; van Goor, H.; Poelstra, K.; et al. Selective Delivery of IFN-γ to Renal Interstitial Myofibroblasts: A Novel Strategy for the Treatment of Renal Fibrosis. *FASEB J.* **2015**, *29*, 1029–1042. [CrossRef]
269. Liechty, K.W.; Kim, H.B.; Adzick, N.; Crombleholme, T.M. Fetal Wound Repair Results in Scar Formation in Interleukin-10–deficient Mice in a Syngeneic Murine Model of Scarless Fetal Wound Repair. *J. Pediatr. Surg.* **2000**, *35*, 866–873. [CrossRef]
270. Lin, W.-R.; Lim, S.-N.; Yen, T.-H.; Alison, M.R. The Influence of Bone Marrow-Secreted IL-10 in a Mouse Model of Cerulein-Induced Pancreatic Fibrosis. *BioMed Res. Int.* **2016**, *2016*, 1–11. [CrossRef]
271. Gupta, J.; Mitra, N.; Kanetsky, P.A.; Devaney, J.; Wing, M.R.; Reilly, M.; Shah, V.O.; Balakrishnan, V.S.; Guzman, N.J.; Girndt, M.; et al. Association Between Albuminuria, Kidney Function, and Inflammatory Biomarker Profile in CKD in CRIC. *Clin. J. Am. Soc. Nephrol.* **2012**, *7*, 1938–1946. [CrossRef]
272. Li, R.; Guo, Y.; Zhang, Y.; Zhang, X.; Zhu, L.; Yan, T. Salidroside Ameliorates Renal Interstitial Fibrosis by Inhibiting the TLR4/NF-κB and MAPK Signaling Pathways. *Int. J. Mol. Sci.* **2019**, *20*, 1103. [CrossRef]

273. Edeling, M.; Ragi, G.; Huang, S.; Pavenstädt, H.; Susztak, K. Developmental Signalling Pathways in Renal Fibrosis: The Roles of Notch, Wnt and Hedgehog. *Nat. Rev. Nephrol.* **2016**, *12*, 426–439. [CrossRef]
274. Cho, E.; Kim, M.; Ko, Y.S.; Lee, H.Y.; Song, M.; Kim, H.-K.; Cho, W.-Y.; Jo, S.-K. Role of Inflammation in the Pathogenesis of Cardiorenal Syndrome in a Rat Myocardial Infarction Model. *Nephrol. Dial. Transplant.* **2013**, *28*, 2766–2778. [CrossRef]
275. Yhee, J.-Y.; Yu, C.-H.; Kim, J.-H.; Sur, J.-H. Effects of T Lymphocytes, Interleukin-1, and Interleukin-6 on Renal Fibrosis in Canine End-Stage Renal Disease. *J. Veter. Diagn. Investig.* **2008**, *20*, 585–592. [CrossRef] [PubMed]
276. Van Linthout, S.; Miteva, K.; Tschöpe, C. Crosstalk Between Fibroblasts and Inflammatory Cells. *Cardiovasc. Res.* **2014**, *102*, 258–269. [CrossRef] [PubMed]
277. Black, L.M.; Lever, J.M.; Agarwal, A. Renal Inflammation and Fibrosis: A Double-Edged Sword. *J. Histochem. Cytochem.* **2019**, *67*, 663–681. [CrossRef] [PubMed]
278. Meng, X.-M. Inflammatory Mediators and Renal Fibrosis. *Adv. Exp. Med. Biol.* **2019**, *1165*, 381–406. [CrossRef]
279. Iwano, M.; Neilson, E.G. Mechanisms of Tubulointerstitial Fibrosis. *Curr. Opin. Nephrol. Hypertens.* **2004**, *13*, 279–284. [CrossRef] [PubMed]
280. Prabhu, S.D.; Frangogiannis, N.G. The Biological Basis for Cardiac Repair After Myocardial Infarction. *Circ. Res.* **2016**, *119*, 91–112. [CrossRef]
281. Sun, K.; Li, Y.-Y.; Jin, J. A Double-Edged Sword of Immuno-Microenvironment in Cardiac Homeostasis and Injury Repair. *Signal Transduct. Target. Ther.* **2021**, *6*, 1–16. [CrossRef]
282. Fadok, V.A.; Bratton, D.L.; Konowal, A.; Freed, P.W.; Westcott, J.Y.; Henson, P.M. Macrophages That Have Ingested Apoptotic Cells In Vitro Inhibit Proinflammatory Cytokine Production through autocrine/Paracrine Mechanisms Involving TGF-Beta, PGE2, and PAF. *J. Clin. Investig.* **1998**, *101*, 890–898. [CrossRef] [PubMed]
283. Song, E.; Ouyang, N.; Hörbelt, M.; Antus, B.; Wang, M.; Exton, M.S. Influence of Alternatively and Classically Activated Macrophages on Fibrogenic Activities of Human Fibroblasts. *Cell. Immunol.* **2000**, *204*, 19–28. [CrossRef]
284. Valgimigli, M.; Ceconi, C.; Malagutti, P.; Merli, E.; Soukhomovskaia, O.; Francolini, G.; Cicchitelli, G.; Olivares, A.; Parrinello, G.; Percoco, G.; et al. Tumor Necrosis Factor-α Receptor 1 Is a Major Predictor of Mortality and New-Onset Heart Failure in Patients with Acute Myocardial Infarction. *Circulation* **2005**, *111*, 863–870. [CrossRef] [PubMed]
285. Maekawa, N.; Wada, H.; Kanda, T.; Niwa, T.; Yamada, Y.; Saito, K.; Fujiwara, H.; Sekikawa, K.; Seishima, M. Improved Myocardial ischemia/Reperfusion Injury in Mice Lacking Tumor Necrosis Factor-α. *J. Am. Coll. Cardiol.* **2002**, *39*, 1229–1235. [CrossRef]
286. Kurrelmeyer, K.M.; Michael, L.H.; Baumgarten, G.; Taffet, G.E.; Peschon, J.J.; Sivasubramanian, N.; Entman, M.L.; Mann, D.L. Endogenous Tumor Necrosis Factor Protects the Adult Cardiac Myocyte Against Ischemic-Induced Apoptosis in a Murine Model of Acute Myocardial Infarction. *Proc. Natl. Acad. Sci. USA* **2000**, *97*, 5456–5461. [CrossRef]
287. Huang, M.; Li, J.-Y. Physiological Regulation of Reactive Oxygen Species in Organisms Based on Their Physicochemical Properties. *Acta Physiol.* **2020**, *228*, e13351. [CrossRef] [PubMed]
288. Pisoschi, A.M.; Pop, A. The Role of Antioxidants in the Chemistry of Oxidative Stress: A Review. *Eur. J. Med. Chem.* **2015**, *97*, 55–74. [CrossRef]
289. Lau, N.; Pluth, M.D. Reactive Sulfur Species (RSS): Persulfides, Polysulfides, Potential, and Problems. *Curr. Opin. Chem. Biol.* **2019**, *49*, 1–8. [CrossRef] [PubMed]
290. Deng, Z.; Hu, J.; Liu, S. Reactive Oxygen, Nitrogen, and Sulfur Species (RONSS)-Responsive Polymersomes for Triggered Drug Release. *Macromol. Rapid Commun.* **2017**, *38*, 10–1002. [CrossRef]
291. Luo, Z.; Xu, X.; Sho, T.; Zhang, J.; Xu, W.; Yao, J.; Xu, J. ROS-Induced Autophagy Regulates Porcine Trophectoderm Cell Apoptosis, Proliferation, and Differentiation. *Am. J. Physiol. Physiol.* **2019**, *316*, C198–C209. [CrossRef]
292. Pei, J.; Wang, F.; Pei, S.; Bai, R.; Cong, X.; Nie, Y.; Chen, X. Hydrogen Sulfide Promotes Cardiomyocyte Proliferation and Heart Regeneration via ROS Scavenging. *Oxidative Med. Cell. Longev.* **2020**, *2020*, 1–11. [CrossRef]
293. Zhang, G.; He, J.; Ye, X.; Zhu, J.; Hu, X.; Shen, M.; Ma, Y.; Mao, Z.; Song, H.; Chen, F. β-Thujaplicin Induces Autophagic Cell Death, Apoptosis, and Cell Cycle Arrest through ROS-Mediated Akt and p38/ERK MAPK Signaling in Human Hepatocellular Carcinoma. *Cell Death Dis.* **2019**, *10*, 1–14. [CrossRef]
294. Kang, R.; Li, R.; Dai, P.; Li, Z.; Li, Y.; Li, C. Deoxynivalenol Induced Apoptosis and Inflammation of IPEC-J2 Cells by Promoting ROS Production. *Environ. Pollut.* **2019**, *251*, 689–698. [CrossRef] [PubMed]
295. Hawkins, C.L.; Davies, M.J. Detection, Identification, and Quantification of Oxidative Protein Modifications. *J. Biol. Chem.* **2019**, *294*, 19683–19708. [CrossRef] [PubMed]
296. Kowalska, M.; Piekut, T.; Prendecki, M.; Sodel, A.; Kozubski, W.; Dorszewska, J. Mitochondrial and Nuclear DNA Oxidative Damage in Physiological and Pathological Aging. *DNA Cell Biol.* **2020**, *39*, 1410–1420. [CrossRef]
297. Salehi, F.; Behboudi, H.; Kavoosi, G.; Ardestani, S.K. Oxidative DNA Damage Induced by ROS-Modulating Agents with the Ability to Target DNA: A Comparison of the Biological Characteristics of Citrus Pectin and Apple Pectin. *Sci. Rep.* **2018**, *8*, 1–16. [CrossRef]
298. Ayala, A.; Muñoz, M.F.; Argüelles, S. Lipid Peroxidation: Production, Metabolism, and Signaling Mechanisms of Malondialdehyde and 4-Hydroxy-2-Nonenal. *Oxid. Med. Cell. Longev.* **2014**, *2014*, 1–31. [CrossRef] [PubMed]
299. Tsikas, D. Assessment of Lipid Peroxidation by Measuring Malondialdehyde (MDA) and Relatives in Biological Samples: Analytical and Biological Challenges. *Anal. Biochem.* **2017**, *524*, 13–30. [CrossRef]

300. Gallo, G.; Sprovierio, P.; Martino, G. 4-Hydroxynonenal and Oxidative Stress in Several Organelles and Its Damaging Effects on Cell Functions. *J. Physiol. Pharmacol. Off. J. Pol. Physiol. Soc.* **2020**, *71*, 10–26402.
301. Schrader, M.; Fahimi, H. Peroxisomes and Oxidative Stress. *Biochim. Biophys. Acta Bioenerg.* **2006**, *1763*, 1755–1766. [CrossRef]
302. Antonenkov, V.D.; Grunau, S.; Ohlmeier, S.; Hiltunen, K. Peroxisomes Are Oxidative Organelles. *Antioxid. Redox Signal* **2010**, *13*, 525–537. [CrossRef]
303. Zeeshan, H.M.A.; Lee, G.H.; Kim, H.-R.; Chae, H.-J. Endoplasmic Reticulum Stress and Associated ROS. *Int. J. Mol. Sci.* **2016**, *17*, 327. [CrossRef] [PubMed]
304. Zhao, R.-Z.; Jiang, S.; Zhang, L.; Yu, Z.-B. Mitochondrial electron transport chain, ROS generation and uncoupling (Review). *Int. J. Mol. Med.* **2019**, *44*, 3–15. [CrossRef] [PubMed]
305. Phaniendra, A.; Jestadi, D.B.; Periyasamy, L. Free Radicals: Properties, Sources, Targets, and Their Implication in Various Diseases. *Ind. J. Clin. Biochem.* **2015**, *30*, 11–26. [CrossRef]
306. Oyewole, A.O.; Birch-Machin, M.A. Mitochondria-targeted Antioxidants. *FASEB J.* **2015**, *29*, 4766–4771. [CrossRef]
307. Iacovino, L.G.; Manzella, N.; Resta, J.; Vanoni, M.A.; Rotilio, L.; Pisani, L.; Edmondson, D.E.; Parini, A.; Mattevi, A.; Mialet-Perez, J.; et al. Rational Redesign of Monoamine Oxidase A into a Dehydrogenase to Probe ROS in Cardiac Aging. *ACS Chem. Biol.* **2020**, *15*, 1795–1800. [CrossRef]
308. Kaludercic, N.; Mialet-Perez, J.; Paolocci, N.; Parini, A.; Di Lisa, F. Monoamine Oxidases As Sources of Oxidants in the Heart. *J. Mol. Cell. Cardiol.* **2014**, *73*, 34–42. [CrossRef]
309. Dey, S.; Sidor, A.; O'Rourke, B. Compartment-Specific Control of Reactive Oxygen Species Scavenging by Antioxidant Pathway Enzymes. *J. Biol. Chem.* **2016**, *291*, 11185–11197. [CrossRef]
310. He, L.; He, T.; Farrar, S.; Ji, L.; Liu, T.; Ma, X. Antioxidants Maintain Cellular Redox Homeostasis by Elimination of Reactive Oxygen Species. *Cell. Physiol. Biochem.* **2017**, *44*, 532–553. [CrossRef] [PubMed]
311. Dinh, Q.N.; Drummond, G.; Sobey, C.G.; Chrissobolis, S. Roles of Inflammation, Oxidative Stress, and Vascular Dysfunction in Hypertension. *BioMed Res. Int.* **2014**, *2014*, 1–11. [CrossRef]
312. Chiba, T.; Peasley, K.D.; Cargill, K.R.; Maringer, K.V.; Bharathi, S.S.; Mukherjee, E.; Zhang, Y.; Holtz, A.; Basisty, N.; Yagobian, S.D.; et al. Sirtuin 5 Regulates Proximal Tubule Fatty Acid Oxidation to Protect Against AKI. *J. Am. Soc. Nephrol.* **2019**, *30*, 2384–2398. [CrossRef]
313. Papinska, A.M.; Rodgers, K.E. Long-Term Administration of Angiotensin (1–7) to db/Db Mice Reduces Oxidative Stress Damage in the Kidneys and Prevents Renal Dysfunction. *Oxidative Med. Cell. Longev.* **2018**, *2018*, 1–10. [CrossRef]
314. Kumar, S.; Wang, G.; Zheng, N.; Cheng, W.; Ouyang, K.; Lin, H.; Liao, Y.; Liu, J. HIMF (Hypoxia-Induced Mitogenic Factor)-IL (Interleukin)-6 Signaling Mediates Cardiomyocyte-Fibroblast Crosstalk to Promote Cardiac Hypertrophy and Fibrosis. *Hypertension* **2019**, *73*, 1058–1070. [CrossRef]
315. He, T.; Guan, X.; Wang, S.; Xiao, T.; Yang, K.; Xu, X.; Wang, J.; Zhao, J. Resveratrol Prevents High Glucose-Induced epithelial–mesenchymal Transition in Renal Tubular Epithelial Cells by Inhibiting NADPH oxidase/ROS/ERK Pathway. *Mol. Cell. Endocrinol.* **2015**, *402*, 13–20. [CrossRef]
316. Carthy, J.M. TGFβ Signaling and the Control of Myofibroblast Differentiation: Implications for Chronic Inflammatory Disorders. *J. Cell. Physiol.* **2017**, *233*, 98–106. [CrossRef] [PubMed]
317. Park, S.-A.; Kim, M.-J.; Park, S.-Y.; Kim, J.-S.; Lee, S.-J.; Woo, H.A.; Kim, D.-K.; Nam, J.-S.; Sheen, Y.Y. EW-7197 Inhibits Hepatic, Renal, and Pulmonary Fibrosis by Blocking TGF-β/Smad and ROS Signaling. *Cell. Mol. Life Sci.* **2014**, *72*, 2023–2039. [CrossRef] [PubMed]
318. Liu, Y.; Yuan, X.; Li, W.; Cao, Q.; Shu, Y. Aspirin-Triggered Resolvin D1 Inhibits TGF-β1-Induced EMT through the Inhibition of the MTOR Pathway by Reducing the Expression of PKM2 and Is Closely Linked to Oxidative Stress. *Int. J. Mol. Med.* **2016**, *38*, 1235–1242. [CrossRef]
319. De Bleser, P.J.; Xu, G.; Rombouts, K.; Rogiers, V.; Geerts, A. Glutathione Levels Discriminate Between Oxidative Stress and Transforming Growth Factor-β Signaling in Activated Rat Hepatic Stellate Cells. *J. Biol. Chem.* **1999**, *274*, 33881–33887. [CrossRef] [PubMed]
320. Matsushima, S.; Kuroda, J.; Ago, T.; Zhai, P.; Ikeda, Y.; Oka, S.; Fong, G.-H.; Tian, R.; Sadoshima, J. Broad Suppression of NADPH Oxidase Activity Exacerbates Ischemia/Reperfusion Injury Through Inadvertent Downregulation of Hypoxia-Inducible Factor-1α and Upregulation of Peroxisome Proliferator–activated Receptor-α. *Circ. Res.* **2013**, *112*, 1135–1149. [CrossRef]
321. Verzola, D.; Ratto, E.; Villaggio, B.; Parodi, E.L.; Pontremoli, R.; Garibotto, G.; Viazzi, F. Uric Acid Promotes Apoptosis in Human Proximal Tubule Cells by Oxidative Stress and the Activation of NADPH Oxidase NOX 4. *PLoS ONE* **2014**, *9*, e115210. [CrossRef] [PubMed]
322. Buvelot, H.; Jaquet, V.; Krause, K.-H. Mammalian NADPH Oxidases. *Methods Mol. Biol.* **2019**, *1982*, 17–36. [CrossRef]
323. Lan, T.; Kisseleva, T.; Brenner, D.A. Deficiency of NOX1 or NOX4 Prevents Liver Inflammation and Fibrosis in Mice through Inhibition of Hepatic Stellate Cell Activation. *PLoS ONE* **2015**, *10*, e0129743. [CrossRef]
324. Muñoz, M.; López-Oliva, M.E.; Rodríguez, C.; Martínez, M.P.; Sáenz-Medina, J.; Sánchez, A.; Climent, B.; Benedito, S.; García-Sacristán, A.; Rivera, L.; et al. Differential Contribution of Nox1, Nox2 and Nox4 to Kidney Vascular Oxidative Stress and Endothelial Dysfunction in Obesity. *Redox Biol.* **2020**, *28*, 101330. [CrossRef] [PubMed]

325. Rajaram, R.D.; Dissard, R.; Faivre, A.; Ino, F.; Delitsikou, V.; Jaquet, V.; Cagarelli, T.; Lindenmeyer, M.; Jansen-Duerr, P.; Cohen, C.; et al. Tubular NOX4 Expression Decreases in Chronic Kidney Disease But Does Not Modify Fibrosis Evolution. *Redox Biol.* **2019**, *26*, 101234. [CrossRef]
326. Braunersreuther, V.; Montecucco, F.; Ashri, M.; Pelli, G.; Galan, K.; Frias, M.; Burger, F.; Quinderé, A.L.G.; Montessuit, C.; Krause, K.-H.; et al. Role of NADPH Oxidase Isoforms NOX1, NOX2 and NOX4 in Myocardial ischemia/Reperfusion Injury. *J. Mol. Cell. Cardiol.* **2013**, *64*, 99–107. [CrossRef] [PubMed]
327. Cai, X.; Yang, C.; Shao, L.; Zhu, H.; Wang, Y.; Huang, X.; Wang, S.; Hong, L. Targeting NOX 4 by Petunidin Improves anoxia/Reoxygenation-Induced Myocardium Injury. *Eur. J. Pharmacol.* **2020**, *888*, 173414. [CrossRef]
328. Bondi, C.D.; Manickam, N.; Lee, D.Y.; Block, K.; Gorin, Y.; Abboud, H.E.; Barnes, J.L. NAD(P)H Oxidase Mediates TGF-β1–Induced Activation of Kidney Myofibroblasts. *J. Am. Soc. Nephrol.* **2009**, *21*, 93–102. [CrossRef] [PubMed]
329. He, T.; Xiong, J.; Nie, L.; Yu, Y.; Guan, X.; Xu, X.; Xiao, T.; Yang, K.; Liu, L.; Zhang, D.; et al. Resveratrol Inhibits Renal Interstitial Fibrosis in Diabetic Nephropathy by Regulating AMPK/NOX4/ROS Pathway. *J. Mol. Med.* **2016**, *94*, 1359–1371. [CrossRef]
330. Breglia, A.; Virzì, G.M.; Pastori, S.; Brocca, A.; De Cal, M.; Bolin, C.; Vescovo, G.; Ronco, C. Determinants of Monocyte Apoptosis in Cardiorenal Syndrome Type 1. *Cardiorenal Med.* **2018**, *8*, 208–216. [CrossRef]
331. Caio-Silva, W.; Dias, D.D.S.; JunHo, C.V.C.; Panico, K.; Neres-Santos, R.S.; Pelegrino, M.T.; Pieretti, J.C.; Seabra, A.B.; De Angelis, K.; Carneiro-Ramos, M.S. Characterization of the Oxidative Stress in Renal Ischemia/Reperfusion-Induced Cardiorenal Syndrome Type 3. *BioMed Res. Int.* **2020**, *2020*, 1–11. [CrossRef]
332. Fox, B.M.; Gil, H.-W.; Kirkbride-Romeo, L.; Bagchi, R.; Wennersten, S.; Haefner, K.R.; Skrypnyk, N.I.; Brown, C.N.; Soranno, D.E.; Gist, K.M.; et al. Metabolomics Assessment Reveals Oxidative Stress and Altered Energy Production in the Heart After Ischemic Acute Kidney Injury in Mice. *Kidney Int.* **2019**, *95*, 590–610. [CrossRef]
333. Guo, H.; Xu, D.; Kuroki, M.; Lu, Z.; Xu, X.; Geurts, A.; Osborn, J.W.; Chen, Y. Kidney Failure, Arterial Hypertension and Left Ventricular Hypertrophy in Rats with Loss of Function Mutation of SOD3. *Free. Radic. Biol. Med.* **2020**, *152*, 787–796. [CrossRef] [PubMed]
334. Oslowski, C.M.; Urano, F. Measuring ER Stress and the Unfolded Protein Response Using Mammalian Tissue Culture System. *Methods Enzymol.* **2011**, *490*, 71–92. [CrossRef] [PubMed]
335. Díaz-Villanueva, J.F.; Díaz-Molina, R.; García-González, V. Protein Folding and Mechanisms of Proteostasis. *Int. J. Mol. Sci.* **2015**, *16*, 17193–17230. [CrossRef]
336. Read, A.; Schröder, M. The Unfolded Protein Response: An Overview. *Biology* **2021**, *10*, 384. [CrossRef]
337. Sanyal, A.; Zbornik, E.A.; Watson, B.G.; Christoffer, C.; Ma, J.; Kihara, D.; Mattoo, S. Kinetic and Structural Parameters Governing Fic-Mediated adenylylation/AMPylation of the Hsp70 Chaperone, BiP/GRP78. *Cell Stress Chaperon* **2021**, 1–18. [CrossRef]
338. Song, S.; Tan, J.; Miao, Y.; Li, M.; Zhang, Q. Crosstalk of Autophagy and Apoptosis: Involvement of the Dual Role of Autophagy under ER Stress. *J. Cell. Physiol.* **2017**, *232*, 2977–2984. [CrossRef] [PubMed]
339. Lam, M.; A Marsters, S.; Ashkenazi, A.; Walter, P. Misfolded Proteins Bind and Activate Death Receptor 5 to Trigger Apoptosis During Unresolved Endoplasmic Reticulum Stress. *eLife* **2020**, *9*, e52291. [CrossRef]
340. Shrestha, N.; De Franco, E.; Arvan, P.; Cnop, M. Pathological β-Cell Endoplasmic Reticulum Stress in Type 2 Diabetes: Current Evidence. *Front. Endocrinol.* **2021**, *12*, 650158. [CrossRef]
341. Parks, S.Z.; Gao, T.; Awuapura, N.J.; Ayathamattam, J.; Chabosseau, P.L.; Kalvakolanu, D.V.; Valdivia, H.H.; Rutter, G.A.; Leclerc, I. The Ca 2+ -binding Protein Sorcin Stimulates Transcriptional Activity of the Unfolded Protein Response Mediator ATF6. *FEBS Lett.* **2021**, *10*. [CrossRef]
342. Baba, B.; Caliskan, M.; Boyuk, G.; Hacisevki, A. Chemical Chaperone PBA Attenuates ER Stress and Upregulates SOCS3 Expression as a Regulator of Leptin Signaling. *Biochemistry* **2021**, *86*, 480–488. [CrossRef]
343. Yang, Y.; Zhou, Q.; Gao, A.; Chen, L.; Li, L. Endoplasmic Reticulum Stress and Focused Drug Discovery in Cardiovascular Disease. *Clin. Chim. Acta* **2020**, *504*, 125–137. [CrossRef] [PubMed]
344. Ajoolabady, A.; Wang, S.; Kroemer, G.; Klionsky, D.J.; Uversky, V.N.; Sowers, J.R.; Aslkhodapasandhokmabad, H.; Bi, Y.; Ge, J.; Ren, J. ER Stress in Cardiometabolic Diseases: From Molecular Mechanisms to Therapeutics. *Endocr. Rev.* **2021**. [CrossRef] [PubMed]
345. Hsu, Y.-H.; Zheng, C.-M.; Chou, C.-L.; Chen, Y.-J.; Lee, Y.-H.; Lin, Y.-F.; Chiu, H.-W. Therapeutic Effect of Endothelin-Converting Enzyme Inhibitor on Chronic Kidney Disease through the Inhibition of Endoplasmic Reticulum Stress and the NLRP3 Inflammasome. *Biomedicine* **2021**, *9*, 398. [CrossRef]
346. Lins, B.B.; Casare, F.A.M.; Fontenele, F.F.; Gonçalves, G.L.; Oliveira-Souza, M. Long-Term Angiotensin II Infusion Induces Oxidative and Endoplasmic Reticulum Stress and Modulates Na+ Transporters Through the Nephron. *Front. Physiol.* **2021**, *12*, 642752. [CrossRef] [PubMed]
347. Dong, Z.; Wu, P.; Li, Y.; Shen, Y.; Xin, P.; Li, S.; Wang, Z.; Dai, X.; Zhu, W.; Wei, M. Myocardial Infarction Worsens Glomerular Injury and Microalbuminuria in Rats with Pre-Existing Renal Impairment Accompanied by the Activation of ER Stress and Inflammation. *Mol. Biol. Rep.* **2014**, *41*, 7911–7921. [CrossRef]
348. Dickhout, J.G.; Carlisle, R.E.; Austin, R.C. Interrelationship Between Cardiac Hypertrophy, Heart Failure, and Chronic Kidney Disease. *Circ. Res.* **2011**, *108*, 629–642. [CrossRef]

349. Olivares-Silva, F.; Espitia-Corredor, J.; Letelier, A.; Vivar, R.; Parra-Flores, P.; Olmedo, I.; Montenegro, J.; Pardo-Jiménez, V.; Díaz-Araya, G. TGF-β1 Decreases CHOP Expression and Prevents Cardiac Fibroblast Apoptosis Induced by Endoplasmic Reticulum Stress. *Toxicol. Vitr.* **2020**, *70*, 105041. [CrossRef]
350. Yamamoto, T.; Endo, J.; Kataoka, M.; Matsuhashi, T.; Katsumata, Y.; Shirakawa, K.; Isobe, S.; Moriyama, H.; Goto, S.; Shimanaka, Y.; et al. Palmitate Induces Cardiomyocyte Death via Inositol Requiring Enzyme-1 (IRE1)-Mediated Signaling Independent of X-Box Binding Protein 1 (XBP1). *Biochem. Biophys. Res. Commun.* **2020**, *526*, 122–127. [CrossRef]
351. Shu, S.; Zhu, J.; Liu, Z.; Tang, C.; Cai, J.; Dong, Z. Endoplasmic Reticulum Stress Is Activated in Post-Ischemic Kidneys to Promote Chronic Kidney Disease. *EBioMedicine* **2018**, *37*, 269–280. [CrossRef]
352. Huang, D.; Yan, M.-L.; Chen, K.-K.; Sun, R.; Dong, Z.-F.; Wu, P.-L.; Li, S.; Zhu, G.-S.; Ma, S.-X.; Pan, Y.-S.; et al. Cardiac-Specific Overexpression of Silent Information Regulator 1 Protects Against Heart and Kidney Deterioration in Cardiorenal Syndrome via Inhibition of Endoplasmic Reticulum Stress. *Cell. Physiol. Biochem.* **2018**, *46*, 9–22. [CrossRef]
353. Liu, Y.; Wang, Y.; Ding, W.; Wang, Y. Mito-TEMPO Alleviates Renal Fibrosis by Reducing Inflammation, Mitochondrial Dysfunction, and Endoplasmic Reticulum Stress. *Oxidative Med. Cell. Longev.* **2018**, *2018*, 1–13. [CrossRef]
354. (66) Luo, T.; Kim, J.K.; Chen, B.; Abdel-Latif, A.; Kitakaze, M.; Yan, L. Attenuation of ER Stress Prevents Post-Infarction-Induced Cardiac Rupture and Remodeling by Modulating Both Cardiac Apoptosis and Fibrosis. *Chem. Interact.* **2015**, *225*, 90–98. [CrossRef] [PubMed]
355. Fan, Y.; Xiao, W.; Lee, K.; Salem, F.; Wen, J.; He, L.; Zhang, J.; Fei, Y.; Cheng, D.; Bao, H.; et al. Inhibition of Reticulon-1A–Mediated Endoplasmic Reticulum Stress in Early AKI Attenuates Renal Fibrosis Development. *J. Am. Soc. Nephrol.* **2017**, *28*, 2007–2021. [CrossRef]
356. Han, J.; Pang, X.; Shi, X.; Zhang, Y.; Peng, Z.; Xing, Y. Ginkgo Biloba Extract EGB761 Ameliorates the Extracellular Matrix Accumulation and Mesenchymal Transformation of Renal Tubules in Diabetic Kidney Disease by Inhibiting Endoplasmic Reticulum Stress. *BioMed Res. Int.* **2021**, *2021*, 1–11. [CrossRef]
357. Qu, J.; Li, M.; Li, D.; Xin, Y.; Li, J.; Lei, S.; Wu, W.; Liu, X. Stimulation of Sigma-1 Receptor Protects Against Cardiac Fibrosis by Alleviating IRE1 Pathway and Autophagy Impairment. *Oxidative Med. Cell. Longev.* **2021**, *2021*, 1–25. [CrossRef] [PubMed]
358. Chen, Y.-T.; Jhao, P.-Y.; Hung, C.-T.; Wu, Y.-F.; Lin, S.-J.; Chiang, W.-C.; Lin, S.-L.; Yang, K.-C. Endoplasmic Reticulum Protein TXNDC5 Promotes Renal Fibrosis by Enforcing TGF-β Signaling in Kidney Fibroblasts. *J. Clin. Investig.* **2021**, *131*. [CrossRef]
359. Liu, S.-H.; Yang, C.-C.; Chan, D.-C.; Wu, C.-T.; Chen, L.-P.; Huang, J.-W.; Hung, K.-Y.; Chiang, C.-K. Chemical Chaperon 4-Phenylbutyrate Protects Against the Endoplasmic Reticulum Stress-Mediated Renal Fibrosis in Vivo and in Vitro. *Oncotarget* **2016**, *7*, 22116–22127. [CrossRef]
360. Park, M.-J.; Oh, K.-S.; Nho, J.-H.; Kim, G.-Y.; Kim, D.-I. Asymmetric Dimethylarginine (ADMA) Treatment Induces Apoptosis in Cultured Rat Mesangial Cells via Endoplasmic Reticulum Stress Activation. *Cell Biol. Int.* **2016**, *40*, 662–670. [CrossRef]
361. Matsuzaki, S.; Hiratsuka, T.; Taniguchi, M.; Shingaki, K.; Kubo, T.; Kiya, K.; Fujiwara, T.; Kanazawa, S.; Kanematsu, R.; Maeda, T.; et al. Physiological ER Stress Mediates the Differentiation of Fibroblasts. *PLoS ONE* **2015**, *10*, e0123578. [CrossRef] [PubMed]
362. Shih, Y.-C.; Chen, C.-L.; Zhang, Y.; Mellor, R.L.; Kanter, E.M.; Fang, Y.; Wang, H.-C.; Hung, C.-T.; Nong, J.-Y.; Chen, H.-J.; et al. Endoplasmic Reticulum Protein TXNDC5 Augments Myocardial Fibrosis by Facilitating Extracellular Matrix Protein Folding and Redox-Sensitive Cardiac Fibroblast Activation. *Circ. Res.* **2018**, *122*, 1052–1068. [CrossRef]
363. Pallet, N.; Bouvier, N.; Bendjallabah, A.; Rabant, M.; Flinois, J.P.; Hertig, A.; Legendre, C.; Beaune, P.; Thervet, E.; Anglicheau, D. Cyclosporine-Induced Endoplasmic Reticulum Stress Triggers Tubular Phenotypic Changes and Death. *Arab. Archaeol. Epigr.* **2008**, *8*, 2283–2296. [CrossRef]
364. Li, Y.; Weng, X.; Wang, P.; He, Z.; Cheng, S.; Wang, D.; Li, X.; Cheng, G.; Li, T. 4-Phenylbutyrate Exerts Stage-Specific Effects on Cardiac Differentiation via HDAC Inhibition. *PLoS ONE* **2021**, *16*, e0250267. [CrossRef]
365. Basseri, S.; Lhoták, Š.; Sharma, A.M.; Austin, R.C. The Chemical Chaperone 4-Phenylbutyrate Inhibits Adipogenesis by Modulating the Unfolded Protein Response. *J. Lipid Res.* **2009**, *50*, 2486–2501. [CrossRef]
366. Akita, S.; Suzuki, K.; Yoshimoto, H.; Ohtsuru, A.; Hirano, A.; Yamashita, S. Cellular Mechanism Underlying Highly-Active or Antiretroviral Therapy-Induced Lipodystrophy: Atazanavir, a Protease Inhibitor, Compromises Adipogenic Conversion of Adipose-Derived Stem/Progenitor Cells through Accelerating ER Stress-Mediated Cell Death in Differentiating Adipocytes. *Int. J. Mol. Sci.* **2021**, *22*, 2114. [CrossRef]
367. Shaffer, A.; Shelef, M.; Iwakoshi, N.N.; Lee, A.-H.; Qian, S.-B.; Zhao, H.; Yu, X.; Yang, L.; Tan, B.K.; Rosenwald, A.; et al. XBP1, Downstream of Blimp-1, Expands the Secretory Apparatus and Other Organelles, and Increases Protein Synthesis in Plasma Cell Differentiation. *Immunity* **2004**, *21*, 81–93. [CrossRef] [PubMed]
368. Gaudette, B.T.; Jones, D.D.; Bortnick, A.; Argon, Y.; Allman, D. MTORC1 Coordinates an Immediate Unfolded Protein Response-Related Transcriptome in Activated B Cells Preceding Antibody Secretion. *Nat. Commun.* **2020**, *11*, 1–16. [CrossRef] [PubMed]
369. Meijer, B.J.; Smit, W.L.; Koelink, P.J.; Westendorp, B.F.; de Boer, R.J.; van der Meer, J.H.M.; Vermeulen, J.L.M.; Paton, J.C.; Paton, A.W.; Qin, J.; et al. Endoplasmic Reticulum Stress Regulates the Intestinal Stem Cell State through CtBP2. *Sci. Rep.* **2021**, *11*, 1–15. [CrossRef] [PubMed]
370. Tanaka, K.-I.; Yamaguchi, T.; Kaji, H.; Kanazawa, I.; Sugimoto, T. Advanced Glycation End Products Suppress Osteoblastic Differentiation of Stromal Cells by Activating Endoplasmic Reticulum Stress. *Biochem. Biophys. Res. Commun.* **2013**, *438*, 463–467. [CrossRef] [PubMed]
371. Moon, J.Y.; Kim, H.S. α-Syntrophin Alleviates ER Stress to Maintain Protein Homeostasis During Myoblast Differentiation. *FEBS Lett.* **2021**, *595*, 1656–1670. [CrossRef]